

SYNTHESIS AND BIOLOGICAL ACTIVITIES OF CHALCONE DERIVATIVES



A Dissertation Submitted in Partial Fulfillment of the Requirements
for the Degree of Doctor of Philosophy in Chemistry

Department of Chemistry

FACULTY OF SCIENCE

Chulalongkorn University

Academic Year 2021

Copyright of Chulalongkorn University

การสังเคราะห์และฤทธิ์ทางชีวภาพของอนุพันธ์แคลโคเน



วิทยานิพนธ์นี้เป็นส่วนหนึ่งของการศึกษาตามหลักสูตรปริญญาวิทยาศาสตรดุษฎีบัณฑิต
สาขาวิชาเคมี ภาควิชาเคมี
คณะวิทยาศาสตร์ จุฬาลงกรณ์มหาวิทยาลัย
ปีการศึกษา 2564
ลิขสิทธิ์ของจุฬาลงกรณ์มหาวิทยาลัย

อะเด ดาโนวา : การสังเคราะห์และฤทธิ์ทางชีวภาพของอนุพันธ์แคลโคเน. (SYNTHESIS AND BIOLOGICAL ACTIVITIES OF CHALCONE DERIVATIVES) อ.ที่ปรึกษาหลัก : วรินทร์ ชวศิริ

แคลโคเนเป็นกลุ่มสารที่ได้รับความสนใจเนื่องจากโครงสร้างที่ง่ายและมีฤทธิ์ทางชีวภาพที่หลากหลาย โดยมีโครงสร้างแกนประกอบด้วยวงแหวน เฮอร์ลสองวงเชื่อมต่อกันด้วยหมู่ α,β -unsaturated ketone และสามารถเตรียมได้ด้วยปฏิกิริยาคอนเดนเซชันแบบ Claisen-Schmidt งานวิจัยนี้ได้สังเคราะห์แคลโคเนและอนุพันธ์ร่วมหนึ่งร้อยแปดตัว พบว่าสารยี่สิบห้าตัวเป็นสารใหม่ ได้ตรวจสอบโครงสร้างของแคลโคเนที่สังเคราะห์ได้ทั้งหมดด้วยวิธีทางสเปกโทรสโกปีและประเมินฤทธิ์ต้านมะเร็งปอด A549 ฤทธิ์ต้านอักเสบและการเป็นตัวยับยั้งแอลฟา-กลูโคซิเดส สำหรับฤทธิ์ต้านมะเร็งพบว่าหมู่ 3',4',5'-trimethoxyphenyl บนวงแหวน A และหมู่ไฮดรอกซีและเมทอกซีบนวงแหวน B แสดงฤทธิ์ยับยั้งมะเร็งปอด A549 อย่างมีศักยภาพ สาร 4, 6 และ 7 เป็นสารที่มีศักยภาพสำหรับฤทธิ์ต้านการอักเสบ สารเดี่ยวได้แก่ 2'-hydroxychalcone (34, 35, 42, 43, 45, 48) และ 4'-aminochalcone (54, 55, 57, 58, 59) แสดงฤทธิ์ยับยั้ง NO ที่มีศักยภาพโดยไม่เป็นพิษต่อเซลล์แมคโครฟาจ RAW 264.7 ที่ถูกชักนำด้วย LPS สำหรับการเป็นตัวยับยั้งแอลฟา-กลูโคซิเดสพบว่า N-monoalkyl-4'-aminochalcone ที่มีหมู่ไฮดรอกซีที่ตำแหน่ง *meta* และหมู่เมทอกซีที่ตำแหน่ง *para* บนวงแหวน B (89, 91, 92) แสดงฤทธิ์ยับยั้งแอลฟา-กลูโคซิเดสที่สูงด้วยรูปแบบการยับยั้งแบบไม่แข่งขัน นอกจากนี้ ได้ศึกษาสารในกลุ่ม E-arylidene steroid พบว่าสารสามตัว (107, 108, 110) เป็นตัวยับยั้งแอลฟา-กลูโคซิเดสด้วยรูปแบบการยับยั้งแบบผสม ปราศจากการแข่งขันและแบบแข่งขันตามลำดับ

จุฬาลงกรณ์มหาวิทยาลัย
CHULALONGKORN UNIVERSITY

สาขาวิชา เคมี
ปีการศึกษา 2564

ลายมือชื่อนิสิต

ลายมือชื่อ อ.ที่ปรึกษาหลัก

6172911323 : MAJOR CHEMISTRY

KEYWORD: chalcones anticancer anti-inflammatory α -glucosidase inhibitors

Ade Danova : SYNTHESIS AND BIOLOGICAL ACTIVITIES OF CHALCONE DERIVATIVES. Advisor: WARINTHORN CHAVASIRI

Chalcones have drawn attention due to the simple structures and wide spectra of biological activities. Their core structure bearing diaryl rings with α,β -unsaturated ketone was generated easily using Claisen-Schmidt condensation. In this study, one hundred and eight chalcones and their derivatives were synthesized; among them, twenty-five were disclosed as new compounds. All synthesized chalcones were well-characterized by means of spectroscopy and evaluated for their anti-cancer (A549) and anti-inflammatory activities, and α -glucosidase inhibition. For anti-cancer activity, 3',4',5'-trimethoxyphenyl on the A ring, and hydroxy and methoxy groups on the B ring exhibited high potent inhibitory activity against A549 with three best potent compounds (4, 6, and 7). For anti-inflammatory activity, lead compounds including 2'-hydroxychalcone (34, 35, 42, 43, 45, and 48) and six 4'-aminochalcones (54, 55, 57, 58, 59, 70) showed high potent NO inhibitory activity without toxicity in LPS-induced RAW 264.7 macrophage cells. For α -glucosidase inhibitors, *N*-monoalkyl-4'-aminochalcones with the hydroxy group at *meta* and the methoxy at *para* position on the B ring (89, 91, 92) exhibited high α -glucosidase inhibitory activity with an uncompetitive inhibition mode. Moreover, *E*-arylidene steroids were investigated and three compounds (107, 108, 110) exhibited high potency as α -glucosidase inhibitors with mixed, noncompetitive, and competitive inhibition mode, respectively.

Field of Study: Chemistry

Student's Signature

Academic Year: 2021

Advisor's Signature

ACKNOWLEDGEMENTS

Assalammu'alaikum Warahmatullahi Wabarakatuh

“Peace be upon you and God's Mercy and Blessings”

The author would like to convey his sincere gratitude towards Allah the almighty for all the grace and wonderful life. He also would like to convey high appreciation to his advisor Assistant Professor Dr. Warinthorn Chavasiri for his guiding and encouragement throughout the entire period of his research.

He would like to thank to Royal Golden Jubilee-PhD program scholarship for ASEAN student countries, Thailand Research Fund, National Research Council of Thailand for supporting financially, and the 90th years anniversary of Chulalongkorn University for research funding.

Sincere gratitude would like to be expressed to all committee Dr. Poonsakdi Ploypradith, Professor Dr. Mongkol Sukwattanasinitt, Professor Dr. Buncha Pulpoka, and Professor Dr. Sirichai Adisakwattana for their valuable comments, discussion, and suggestions.

The author would like to thank Dr. Asshaima Paramita Devi, Dr. Franxisca Mariani, Dr. Edwin Risky Sukandar, Mr. Duy Vun Nguyen M.Sc, Ms. Riho Toyoda, Mrs. Le Thi Thu Huong M.Sc, Dr. Truong Tuong Lam, Rita Hairani M. Sc, I Putu Sukanadi M.Sc, and all members in Center of Excellence in Natural Product Chemistry, Department of Chemistry, Faculty of Science, Chulalongkorn University for all advices and help.

Finally, the author would like to convey his deepest appreciation and gratefulness to his parents and all family members who have been praying and encouragement to achieve this goal.

Ade Danova

TABLE OF CONTENTS

| | Page |
|---|------|
| | iii |
| ABSTRACT (THAI)..... | iii |
| | iv |
| ABSTRACT (ENGLISH)..... | iv |
| ACKNOWLEDGEMENTS..... | v |
| TABLE OF CONTENTS..... | vi |
| TABLE OF FIGURES..... | vi |
| TABLE OF TABLES..... | ix |
| TABLE OF SCHEMES..... | x |
| LIST OF ABBREVIATIONS..... | xi |
| CHAPTER I..... | 1 |
| INTRODUCTION..... | 1 |
| CHAPTER II..... | 3 |
| SYNTHESIS, CYTOTOXIC EVALUATION, AND MOLECULAR DOCKING OF..... | 3 |
| 3',4',5'-TRIMETHOXY AND 3,4-DIMETHOXYCHALCONES AGAINST LUNG CANCER CELL EXPRESSING EGFR..... | 3 |
| 2.1 INTRODUCTION..... | 3 |
| 2.2 MATERIALS AND METHODS..... | 7 |
| 2.2.1 MATERIALS..... | 7 |
| 2.2.2 METHODS..... | 7 |
| 2.2.2.1 GENERAL PROCEDURE FOR THE SYNTHESIS OF 3',4',5'-TRIMETHOXYCHALCONE SERIES (2-6, 9-15, 18-22)..... | 7 |

| | |
|--|----|
| 2.2.2.2 GENERAL PROCEDURE FOR THE SYNTHESIS OF 3',4',5'- TRIMETHOXYCHALCONE SERIES (1, 7-8) | 11 |
| 2.2.2.3 PROCEDURE FOR THE SYNTHESIS OF 16 AND 17 | 12 |
| 2.2.2.4 PROCEDURE FOR THE SYNTHESIS OF 23 | 13 |
| 2.2.2.4 GENERAL PROCEDURE FOR THE SYNTHESIS OF 3,4- DIMETHOXYCHALCONE SERIES (24-33) | 14 |
| 2.2.2.5 <i>IN VITRO</i> ANTI-CANCER A549 ASSAY | 17 |
| 2.2.2.6 MOLECULAR DOCKING | 17 |
| 2.3 RESULTS AND DISCUSSION | 17 |
| 2.3.1 SYNTHESIS OF TWO SELECTED CHALCONE SERIES | 17 |
| 2.3.2 DISCUSSION | 22 |
| 2.3.3 MOLECULAR DOCKING | 26 |
| CHAPTER III | 31 |
| SYNTHESIS AND EVALUATION OF 3,4-DIMETHOXYCHALCONES, 2'-HYDROXYOCHALCONES, AND 4'-AMINOCHALCONES AS POTENT NITRIC OXIDE INHIBITOR IN LPS-INDUCED RAW 264.7 MACROPHAGE CELLS | 31 |
| 3.1 INTRODUCTION | 31 |
| 3.2 MATERIALS AND METHODS | 34 |
| 3.2.1 MATERIALS | 34 |
| 3.2.2 METHODS | 34 |
| 3.2.2.1 SYNTHESIS OF 3,4-DIMETHOXYCHALCONE SERIES (24-28, 33) AND 4'- AMINOCHALCONE SERIES (53-70) | 34 |
| 3.2.2.2 SYNTHESIS OF 2'-HYDROXYCHALCONE SERIES (34-52) | 40 |
| 3.2.2.3 SYNTHESIS OF 2'-HYDROXYCHALCONE DERIVATIVES (51 AND 52) | 44 |
| 3.2.2.3 BIOLOGICAL ASSAY METHOD | 45 |

| | |
|--|----|
| 3.2.2.3.1 CELL VIABILITY ASSAY METHOD | 45 |
| 3.2.2.3.2 ANTI-INFLAMMATORY ASSAY METHOD | 45 |
| 3.3 RESULTS AND DISCUSSION | 45 |
| 3.3.1 SYNTHESIS OF THREE CHALCONE SERIES | 45 |
| 3.3.2 BIOLOGICAL EVALUATION | 50 |
| 3.3.2.1 EFFECTS OF CHALCONES ON CELL VIABILITY IN RAW 264.7 CELLS ... | 50 |
| 3.3.2.2 EFFECTS OF CHALCONES ON NO INHIBITION IN LPS-INDUCED RAW 264.7 CELLS | 52 |
| CHAPTER IV | 54 |
| SYNTHESIS AND BIOLOGICAL ACTIVITY OF 4'-AMINOCHALCONES AND <i>E</i> -ARYLIDENE STEROIDS AS ALPHA-GLUCOSIDASE INHIBITORS | 54 |
| 4.1 INTRODUCTION | 54 |
| 4.2 SYNTHESIS AND BIOLOGICAL EVALUATION OF 4'-AMINOCHALCONES AND THEIR DERIVATIVES AS ALPHA-GLUCOSIDASE INHIBITORS | 56 |
| 4.2.1 MATERIALS AND METHODS | 56 |
| 4.2.1.1 MATERIALS | 56 |
| 4.2.2 METHODS | 56 |
| 4.2.2.1 SYNTHESIS OF 4'-AMINOCHALCONE SERIES (53-81) | 56 |
| 4.2.2.2 SYNTHESIS OF 4'- <i>N</i> -ACETYLAMINOCHALCONE (84) | 62 |
| 4.2.2.3 SYNTHESIS OF 4'- <i>N</i> -(DI)ALKYLAMINOCHALCONE (85, 86, 89, 90) | 63 |
| 4.2.2.4 SYNTHESIS OF 4'- <i>N</i> -ALKYLAMINOCHALCONE (91, 92) | 64 |
| 4.2.2.5 ALPHA-GLUCOSIDASE ASSAY | 68 |
| 4.2.2 RESULTS AND DISCUSSION | 70 |
| 4.2.2.1 SYNTHESIS OF 4'-AMINOCHALCONES AND THEIR DERIVATIVES | 70 |

| | |
|--|-----|
| 4.2.2.2 BIOLOGICAL EVALUATION | 71 |
| 4.3 SYNTHESIS, BIOACTIVITY EVALUATION, AND MOLECULAR DOCKING STUDY OF <i>E</i> -ARYLIDENE STEROID DERIVATIVES AS ALPHA-GLUCOSIDASE INHIBITORS..... | 79 |
| 4.3.1 MATERIALS AND METHODS..... | 79 |
| 4.3.1.1 MATERIALS..... | 79 |
| 4.3.2 METHODS | 79 |
| 4.3.2.1 GENERAL PROCEDURE OF THE SYNTHESIS OF <i>E</i> -ARYLIDENE AND ITS DERIVATIVES (93-112)..... | 79 |
| 4.3.2.2 <i>IN VITRO</i> ALPHA-GLUCOSIDASE ASSAY..... | 87 |
| 4.3.2.3 MOLECULAR MODELING..... | 87 |
| 4.3.2 RESULTS AND DISCUSSION | 87 |
| 4.3.2.1 SYNTHESIS OF <i>E</i> -ARYLIDENE STEROID | 87 |
| 4.3.2.2 <i>IN VITRO</i> ALPHA-GLUCOSIDASE ACTIVITY | 92 |
| 4.3.2.3 MOLECULAR MODELING | 96 |
| CHAPTER V..... | 100 |
| CONCLUSION..... | 100 |
| REFERENCES..... | 102 |
| APPENDIX | 122 |
| VITA..... | 255 |

TABLE OF FIGURES

| | |
|--|----|
| Figure 1.1 Chalcone Structure..... | 1 |
| Figure 1.2 Clinically approved chalcones..... | 1 |
| Figure 2.1 Data of patient cancer cases and mortality in 2018 | 3 |
| Figure 2.2 Chalcones with potent anticancer | 4 |
| Figure 2.3 Natural products conatining trimethoxyphenyl moiety with anticancer activity | 5 |
| Figure 2.4 Synthetic of 3',4',5'-trimethoxychalcones and its derivatives | 6 |
| Figure 2.5 Numbering and structures of 9 and 27 | 19 |
| Figure 2.6 The ¹ H NMR Spectra (CDCl ₃ , 400 MHz) of 9 | 20 |
| Figure 2.7 The ¹³ C NMR Spectra (CDCl ₃ , 100 MHz) of 9 | 20 |
| Figure 2.8 The ¹ H NMR Spectra (CDCl ₃ , 400 MHz) of 27 | 21 |
| Figure 2.9 The ¹³ C NMR Spectra (CDCl ₃ , 100 MHz) of 27 | 22 |
| Figure2.10 Screening of 3',4',5'-trimethoxychalcones (1-23), and 3,4-dimethoxychalcone series (24-33) against A549..... | 23 |
| Figure 2.11 Cytotoxic activity of 1, 2, 4-11, 13, 15, 20 , and erlotinib against A549..... | 24 |
| Figure 2.12 Three best potent compounds as anti-lung cancer..... | 26 |
| Figure 2.13 Structures of 7, 10, 14 , and erlotinib docked with EGFR-TK..... | 27 |
| Figure 2.14 Superimposition of docked 7, 10, 14 , and erlotinib at the ATP-binding pocket of EGFR-TK..... | 27 |
| Figure 2.15 2D interaction diagram of (A) 7 , (B) 10 , (C) 14 , and (D) erlotinib in complex with EGFR-TK..... | 29 |
| Figure 3.1 Nitric oxide (NO) production and its biological activity..... | 31 |
| Figure 3.2 Natural anti-inflammatory chalcones | 32 |
| Figure 3. 3 Synthetic anti-inflammatory chalcones | 33 |
| Figure 3.4 The ¹ H NMR Spectra (CDCl ₃ , 400 MHz) of 47 | 48 |

| | |
|---|----|
| Figure 3.5 The ^{13}C NMR Spectra (CDCl_3 , 100 MHz) of 47 | 48 |
| Figure 3.6 The ^1H NMR Spectra acetone- d_6 , 500 MHz) of 59 | 49 |
| Figure 3.7 The ^{13}C NMR Spectra (acetone- d_6 , 125 MHz) of 59 | 50 |
| Figure 3.8 1) Viability of RAW 264.7 macrophage cells treated with three chalcone series (24-70).. | 51 |
| Figure 3.9 NO inhibition of selected chalcones in LPS-induced RAW 264.7 macrophage cells.. | 52 |
| Figure 3.10 Seven lead compounds with high potent anti-inflammatory without toxicity | 53 |
| Figure 4.1 Design of the structures of two target compounds | 55 |
| Figure 4.2 The ^1H NMR Spectra (acetone- d_6 , 500 MHz) of 91 | 66 |
| Figure 4.3 The ^{13}C NMR Spectra (acetone- d_6 , 125 MHz) of 91 | 66 |
| Figure 4.4 The ^1H NMR Spectra (acetone- d_6 , 500 MHz) of 92 | 68 |
| Figure 4.5 The ^{13}C NMR Spectra (acetone- d_6 , 125 MHz) of 92 | 68 |
| Figure 4.6 The effect of monosubstituent (53-57 , 74-79) on Alpha-glucosidase inhibition | 73 |
| Figure 4.7 The effect of di- and trisubstituent (58-73 , 80) and naphthyl (81) on alpha- glucosidase inhibition..... | 74 |
| Figure 4.8 The effect of <i>N</i> -substituted-4'-aminochalcones against alpha-glucosidase inhibition..... | 75 |
| Figure 4.9 Lineweaver-Burk plots of the kinetic study of alpha-glucosidase inhibition by 85 (A) , 89 (B) , 91 (C) , and 92 (D) | 77 |
| Figure 4.10 Structure-Activity Relationship of 4'-Aminochalcones | 78 |
| Figure 4. 11 The ^1H NMR Spectra (CDCl_3 , 500 MHz) of 93 | 89 |
| Figure 4.12 The ^{13}C NMR Spectra (CDCl_3 , 125 MHz) of 93 | 90 |
| Figure 4.13 The ^1H NMR Spectra (CDCl_3 , 500 MHz) of 108 | 91 |
| Figure 4.14 The ^{13}C NMR Spectra (CDCl_3 , 125 MHz) of 108 | 91 |

| | |
|---|----|
| Figure 4.15 Lineweaver-Burk Plots for compounds 93 (A), 107 (B), 108 (C), and 110 (D). | 94 |
| Figure 4.16 (A.) The predicted binding pockets of alpha-glucosidase homology model | 97 |
| Figure 4.17 The prediction of binding pocket interactions of alpha-glucosidase with 93 (3a), 107 (5a), 108 (5b), and 110 (5d). | 98 |



TABLE OF TABLES

| | |
|--|----|
| Table 2.1 IC_{50} of selected chalcones against A549 | 25 |
| Table 2.2 Analysis of molecular interaction of 7 , 10 , 14 and erlotinib in complex with residues of EGFR-TK..... | 29 |
| Table 2.3 Docking interaction energy (kcal/mol) and H-bond interaction of 7 , 10 , 14 and erlotinib in complex with EGFR-TK..... | 30 |
| Table 4. 1 <i>In vitro</i> Alpha-glucosidase inhibitory activities of 53-81 | 72 |
| Table 4.2 <i>In vitro</i> alpha-glucosidase inhibitory activities of 84-86 , 89 , and 90-92 | 74 |
| Table 4.3 Kinetic study of 84 , 85 , 89 , 91 , and 92 | 76 |
| Table 4.4 Evaluation of the first series of tested compounds 93-106 against alpha-glucosidase..... | 93 |
| Table 4.5 Evaluation of the second series of tested compounds 107-110 , 111 , 112 against Alpha-glucosidase | 93 |
| Table 4.6 Kinetic study of the <i>E</i> -arylidene steroids 93 , 107 , 108 , and 110 against alpha-glucosidase..... | 95 |
| Table 4.7 The binding interaction score (kcal/mol) of the <i>E</i> -arylidene steroids..... | 99 |

TABLE OF SCHEMES

| | |
|--|----|
| Scheme 2.1 Synthesis of 3',4',5'-trimethoxychalcones (1-15, 18-22)..... | 18 |
| Scheme 2.2 Synthesis of 3',4',5'-trimethoxychalcones (16, 17, 23)..... | 18 |
| Scheme 2.3 Synthesis of 3,4-dimethoxychalcone series (24-33). | 19 |
| Scheme 3.1 Synthesis of 3,4-dimethoxychalcones | 46 |
| Scheme 3.2 Synthesis of 2'-hydroxychalcones..... | 46 |
| Scheme 3.3 Synthesis of 4'-aminochalcones..... | 47 |
| Scheme 4.1 Reagents and conditions. | 70 |
| Scheme 4.2 Synthesis of <i>E</i> -arylidene <i>epi</i> -androsterones 93-106 | 88 |
| Scheme 4.3 Synthesis of <i>E</i> -arylidene dehydro- <i>epi</i> -androsterones 107-110 | 88 |
| Scheme 4.4 Synthesis of <i>E</i> -arylidene estrones 111 | 88 |
| Scheme 4.5 Synthesis of <i>E</i> -arylidene androsterone 112..... | 88 |

LIST OF ABBREVIATIONS

| | |
|----------------------|--------------------------------------|
| ABS1 | first allosteric binding site |
| ABS2 | second allosteric binding site |
| μg | microgram(s) |
| μL | microliter(s) |
| μM | micromolar(s) |
| δ | chemical shift |
| $^{\circ}\text{C}$ | degree Celsius |
| ^{13}C -NMR | carbon-13 nuclear magnetic resonance |
| ^1H -NMR | proton nuclear magnetic resonance |
| acetone- <i>d</i> 6 | deuterated acetone |
| C | carbon |
| calcd | calculated |
| CC | column chromatography |
| CDCl_3 | deuterate chloroform |
| d | doublet |
| DCM | dichloromethane |
| dd | doublet of doublet |
| ddd | doublet of doublet of doublet |
| DMSO- <i>d</i> 6 | deuterated dimethylsulfoxide |
| EtOAc | ethyl acetate |

| | |
|------------------|--|
| EtOH | ethanol |
| g | gram(s) |
| HR-ESI-MS | high resonance electrospray ionization mass spectroscopy |
| IC ₅₀ | half maximal inhibition concentration |
| J | coupling constant |
| Hz | hertz |
| M | molar(s) |
| MHz | megahertz |
| MeOH | methanol |
| mg | milligram(s) |
| mL | milliliter(s) |
| mm | millimeter(s) |
| mM | millimolar(s) |
| nM | nanomolar(s) |
| NMR | nuclear magnetic resonance |
| OBS | orthosteric binding site (active site) |
| ppm | part per million |
| ROS | reactive oxygen species |
| R ² | regression |
| s | singlet |

SD standard deviation

U unit

UV ultraviolet



CHAPTER I INTRODUCTION

Chalcones (from Greek “*chalcos*” or “bronze”) naturally distribute in many plants such as vegetables, fruits, teas, and others.¹⁻⁴ They have a simple structure as 1,3-diarylpropenone (Figure 1.1) whose *E* and *Z* isomers, thermodynamically the former is more stable.^{5, 6}

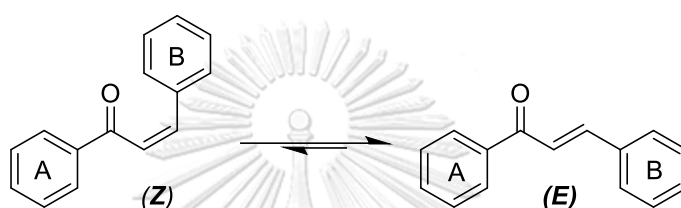


FIGURE 1.1 CHALCONE STRUCTURES

Chalcones and their derivatives have attracted much attention due to their broad-spectra biological activities and ease of structural modification. Application of chalcones in medicine has been utilized since a thousand of years through herbs for anticancer, anti-inflammatory, and antidiabetic properties.^{4, 7} For example, metochalcone and sofalcone (Figure 1.2) have been available in the market and used as anticholeretic, antiulcer and mucoprotective agents.^{2, 5}

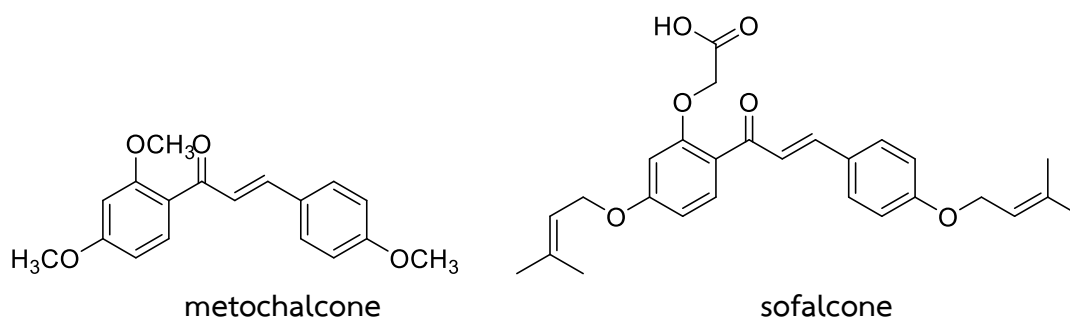
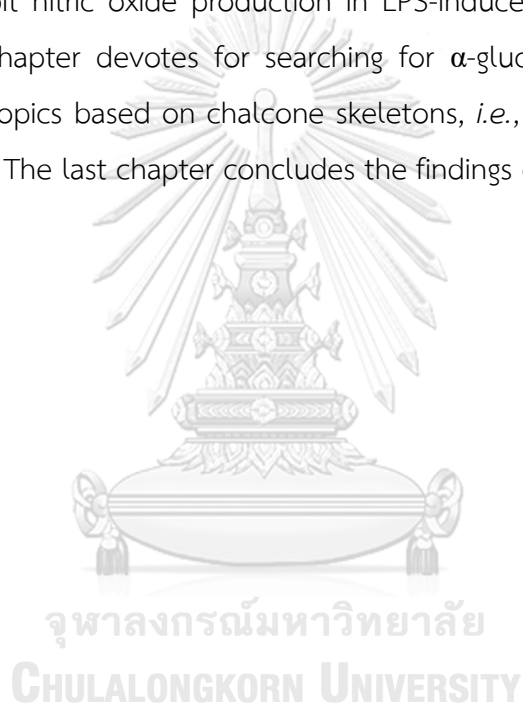


FIGURE 1.2 CLINICALLY APPROVED CHALCONES

As their vast biological activities and promising candidates, this study aims to develop chalcones as a core model for determining structure-activity relationships to

achieve new potent bioactive compounds with anticancer and anti-inflammatory, and as α -glucosidase inhibitor.

This dissertation comprises of five chapters. The first chapter describes about chalcones. The second chapter focuses on the exploration of two chalcone series including 3',4',5'-trimethoxy and 3,4-dimethoxychalcones against lung cancer cell lines (A549) and molecular docking study of selected chalcones with EGFR-TK. The third chapter aims to evaluate the cytotoxic activity of three chalcone series namely 3,4-dimethoxychalcones, 2'-hydroxy-chalcones, and 4'-aminochalcones as well as their potencies to inhibit nitric oxide production in LPS-induced RAW 264.7 macrophage cells. The fourth chapter devotes for searching for α -glucosidase inhibitor which is divided into two topics based on chalcone skeletons, *i.e.*, 4'-aminochalcones and *E*-arylidene steroids. The last chapter concludes the findings of the studies.



CHAPTER II

SYNTHESIS, CYTOTOXIC EVALUATION, AND MOLECULAR DOCKING OF 3',4',5'-TRIMETHOXY AND 3,4-DIMETHOXYCHALCONES AGAINST LUNG CANCER CELL EXPRESSING EGFR

2.1 INTRODUCTION

Cancer is a well-known disease which causes death worldwide.⁸ A lung cancer is the most common with 11.6% new cases and 18.4% deaths annually as shown in Figure 2.1.⁹ To date, the available main therapy for cancer is largely chemotherapy. However, this usage has several limitations including adverse effects and low selectivity.¹⁰ Therefore, the development of new candidate drugs with minimum adverse effects and more selectivity is the most necessary.

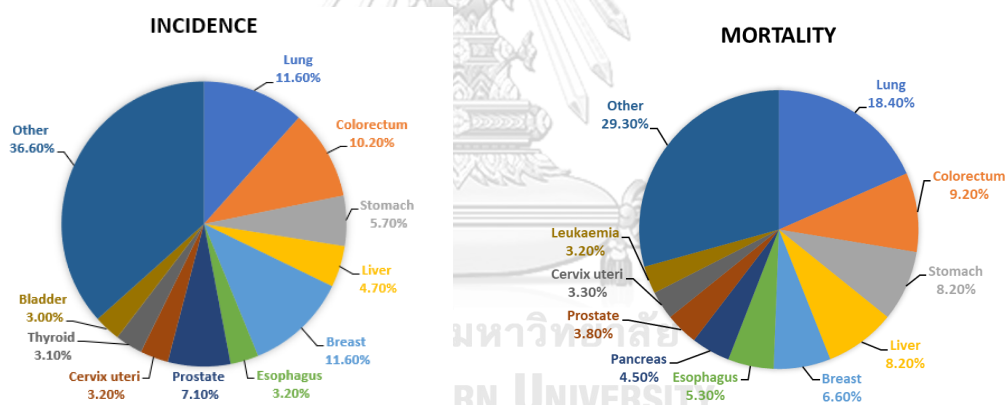


FIGURE 2.1 DATA OF PATIENT CANCER CASES AND MORTALITY IN 2018⁹

Lung cancer mainly derives from out-control-cellular proliferation that triggers normal cells to be cancer cells.¹¹ Epidermal growth factor receptor (EGFR) has been affirmed as an important protein inducing lung cancer.¹² Secreted growth factors transfer biochemical signal from EGFR into lung cancer cells because of their failure to get in membrane cells through signal transduction activated with autocrine or paracrine or both.^{13, 14} EGFR-receptor tyrosine kinases (EGFR-TK) is a crucial target in inducing and producing signal reaction for both non-small cell lung cancer (NSCLC) and small cell lung cancer (SCLC). EGFR has been urged as a cancer target treatment for

chemotherapy method.^{15, 16} To date, EGFR-TK inhibitors are available in market including gefitinib,¹⁷ erlotinib,¹⁸ lapatinib,¹⁹ afatinib,²⁰ and dacomitinib.²¹

Chalcones are intermediates in the biosynthesis of flavonoids and their derivatives. With simple and open-chain structures, chalcones possess two arene rings attached to α,β -unsaturated ketone which are easily modified.²² Chalcones show diverse biological activities, for example antibacterial,²² anti-inflammatory,^{23, 24} antifungal,²⁵⁻²⁷ anti-tumor,²⁸⁻³² anticancer,³³⁻³⁵ and antihypertensive.³⁶ As shown in Figure 2.2, chalcones and isoliquiritigenin revealed as potent chemotherapy agents to inhibit some cancer cell lines, such as lung, breast, prostate, and colorectal cancers.³⁷⁻⁴⁰ Flavokawain A inhibited the growth of bladder tumor cell lines in a nude mice model.⁴¹ Moreover, butein significantly showed an inhibition activity of EGFR-TK with IC_{50} value of $8.50 \mu M$.⁴²

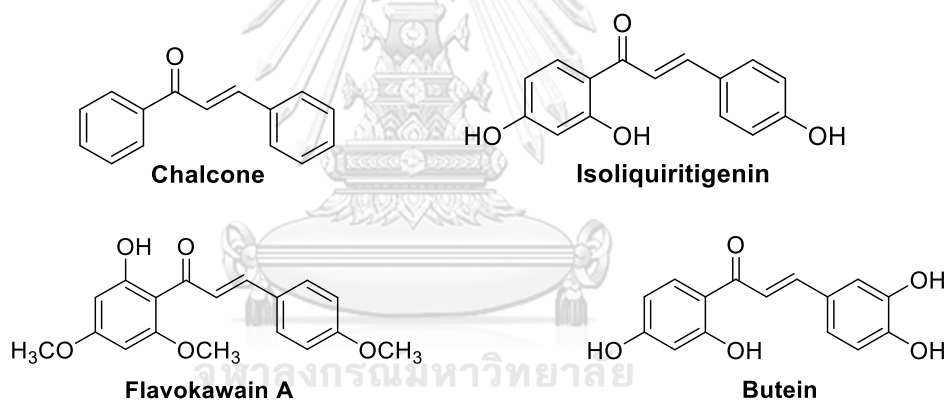


FIGURE 2.2 CHALCONES WITH POTENT ANTICANCER

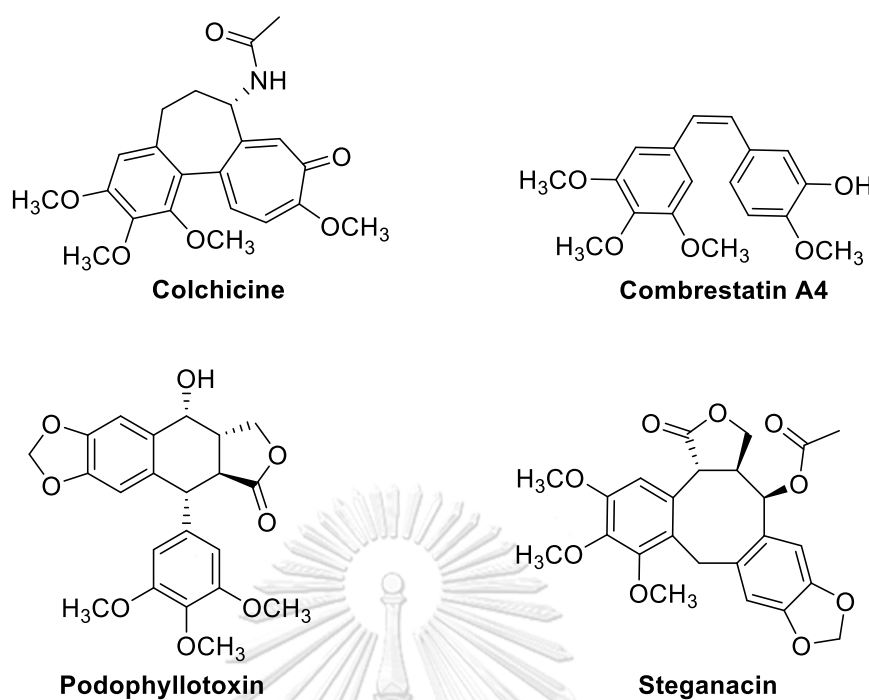


FIGURE 2.3 NATURAL PRODUCTS CONTAINING TRIMETHOXYPHENYL MOIETY WITH ANTICANCER ACTIVITY

Trimethoxyphenyl moiety is an important part exhibiting anticancer activity in many natural products and their derivatives such as colchicine,⁴³ combretastatin A4,⁴⁴⁻⁴⁷ podophyllotoxin,⁴⁷ and steganacin⁴⁷ (Figure 2.3). Romagnoli *et al.* reported that 3',4',5'-trimethoxychalcones and thiophene derivatives showed potency as mitotic inhibitors in five cancer cell lines (L1210, FM3A, Molt/4 and CEM, HeLa). Thiophene derivatives were more cytotoxic against five cancer cell lines and inhibited tubulin assembly when compared with 3',4',5'-trimethoxychalcone analogues. Moreover, active compounds of thiophene derivatives were evaluated in the cell cycle using flow cytometry that led to cell accumulation in the G2/M phase because inhibitors have cellular impact property of agents which bind to tubulin. This study found that methoxy group at *ortho* position on the B ring inhibited significantly against five cancer cell lines at micromolar concentration as presented in Figure 2.4.⁴⁸

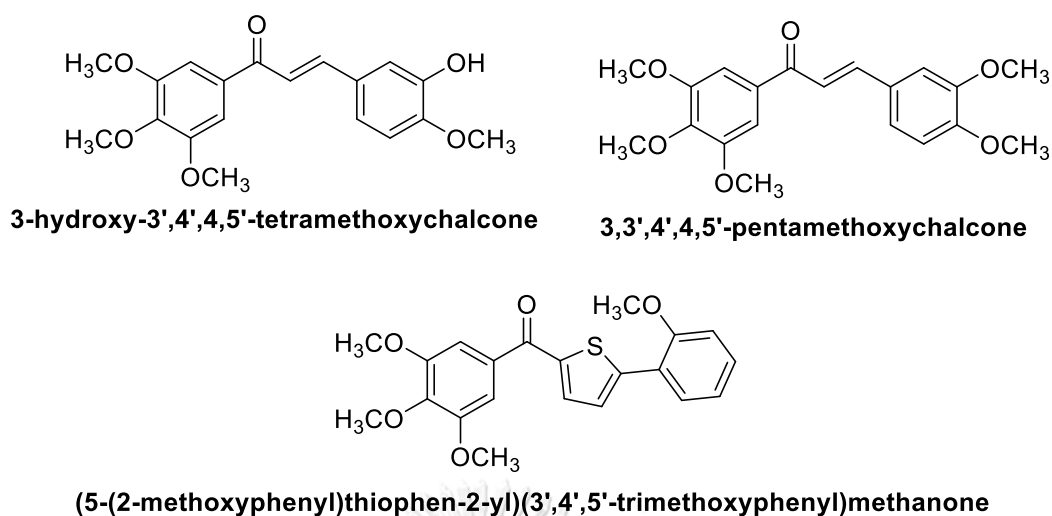


FIGURE 2.4 SYNTHETIC 3',4',5'-TRIMETHOXYCHALCONES AND ITS DERIVATIVES

Moreover, Rao *et al.* reported that the same chalcone series showed that 3',4',5'-trimethoxychalcone series expressed high potency to inhibit NO production and two cancer cell lines, such as Hep G2 (liver cancer cells), and colon 205 (colon cancer cells). This study obtained that the methoxy group at *meta* position on the B ring exhibited more potency against Hep G2 and colon 205, while dimethoxy at *meta* and *para* position on the B ring was found to be more selective in inhibiting Hep G2 cell lines and NO production.²⁴ Lawrence *et al.* also found that 3',4',5'-trimethoxychalcone with dimethoxy at *meta* and *para* position on the B ring expressed anticancer activities with $IC_{50} < 3 \mu M$ against human leukemia cells (K562), human breast cancer cells (MCF7, BT20), and human ovarian cancer cells (A2780, A2780/ADR). 3',4',5'-Trimethoxychalcones also showed anti-estrogenic type II activity against ovarian cancer cell lines (OVCA 433) and a strong binding to tubulin assembly, where molecular docking study showed that 3',4',5'-trimethoxychalcones had a similar structure and conformation to combrestatin A-4 and podophylotoxin.⁴⁹ Srinivasan *et al.* addressed that 3',4',5'-trimethoxychalcones expressed high NF- κ B inhibitory activity and anti-cancer activity against two lung cancer cell lines (H2009, A549) at low micromolar concentration. This result suggested that 3',4',5'-trimethoxychalcones with disubstituents at *m*-OH and *p*-OCH₃ positions on the B ring inhibited growth of lung cancer cells *in vivo* at 1 mg/mouse/day dose with no side effects.³⁴ Salum *et al.* investigated that 3',4',5'-trimethoxyphenyl neighboring with carbonyl, 3',4',5'-

trimethoxychalcones, demonstrated high inhibitory activity against murine acute lymphoblastic leukemia cells (L-1210) and tubulin assembly as potent as colchicine and more selective to cancer cell lines compared with non-tumorigenic cells.⁵⁰ Kumar *et al.* delineated the mechanism of trimethoxyphenyl moiety to possess the binding site similar to that of colchicine.⁵¹ This site is a crucial moiety for anticancer activity.

This study aims to further explore the pharmacophores of chalcones against EGFR-expressing lung cancer cell line A549. To obtain this target, the chalcone core structures including 3',4',5'-trimethoxyphenyl on the A ring and 3,4-dimethoxyphenyl on the B ring have been designed to provide the relationship between their structures and anticancer activity against A549. Molecular docking was then conducted to address the binding site of selected chalcones with EGFR-TK.

2.2 MATERIALS AND METHODS

2.2.1 MATERIALS

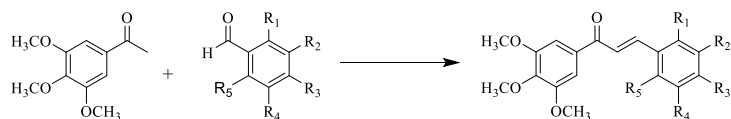
All chemicals were purchased from TCI, Sigma Aldrich, and Merck. Silica gel for column chromatograph (CC, 0.063–0.200 mm), was a product of Merck. TLC was performed on Merck TLC plates (0.23 mm thickness). The compounds were visualized by UV light and/or vanillin in EtOH and then heated on a hot plate. The NMR spectra were measured on Bruker Avance 400 MHz. Chemical shifts are given in ppm using deuterated solvents.

2.2.2 METHODS

2.2.2.1 GENERAL PROCEDURE FOR THE SYNTHESIS OF 3',4',5'-TRIMETHOXYCHALCONE SERIES (2-6, 9-15, 18-22)

3',4',5'-Trimethoxyacetophenone (420 mg, 2 mmol) and substituted benzaldehyde (2-3 mmols) were mixed in MeOH (10 mL) and stirred. A solution of 6 M NaOH (0.8 mL, 4.8 mmol) was added dropwise over a period of 40 min at room temperature and continued stirring for additional 48 hours. The crude product was kept in ice-water and 10% HCl was added until pH 3-4. The solution was extracted with EtOAc, then the organic layer was filtered and evaporated using rotary evaporator

to dryness. The crude mixture was further separated by column chromatography using hexane: EtOAc (9:1-8:2).



- 2: R₁ = H, R₂ = OH, R₃, R₄, R₅ = H
 3: R₁ = H, R₂ = H, R₃ = OH, R₄, R₅ = H
 4: R₁ = OH, R₂ = OCH₃, R₃, R₄, R₅ = H
 5: R₁ = OCH₃, R₂ = OCH₃, R₃, R₄, R₅ = H
 6: R_{1,2} = OCH₂O, R₃, R₄, R₅ = H
 9: R₁ = H, R₂ = OH, R₃ = OCH₃, R₄, R₅ = H
 10: R₁ = H, R₂ = OCH₃, R₃ = OCH₃, R₄, R₅ = H
 11: R₁ = H, R_{2,3} = OCH₂O, R₄, R₅ = H
 12: R₁ = OCH₃, R₂ = H, R₃ = OCH₃, R₄, R₅ = H
 13: R₁ = H, R₂ = OCH₃, R₄ = OCH₃, R₃, R₅ = H
 14: R₁ = OCH₃, R₂, R₃, R₄ = H, R₅ = OCH₃
 15: R₁ = OCH₃, R₂, R₃ = H, R₄ = OCH₃, R₅ = H
 18: R₁ = H, R₂ = Br, R₃ = OCH₃, R₄, R₅ = H
 19: R₁ = OCH₃, R₂ = OCH₃, R₃ = OCH₃, R₄, R₅ = H
 20: R₁ = H, R₂ = OCH₃, R₃ = OCH₃, R₄ = OCH₃, R₅ = H
 21: R₁ = OCH₃, R₂ = H, R₃ = OCH₃, R₄ = OCH₃, R₅ = H
 22: R₁ = OCH₃, R₂ = H, R₃ = OCH₃, R₄ = H, R₅ = OCH₃

(*E*)-3-(3-hydroxyphenyl)-1-(3',4',5'-trimethoxyphenyl)prop-2-en-1-one (**2**): Pale yellow powder; yield 34%. ¹H NMR (400 MHz, DMSO-*d*₆): δ = 9.61 (s, 1H), 7.82 (d, *J* = 15.6 Hz, 1H), 7.62 (d, *J* = 15.2 Hz, 1H), 7.38 (s, 2H), 7.29 (d, *J* = 7.6 Hz, 1H), 7.22 (dd, *J* = 7.6, 2.0 Hz, 2H), 6.85 (d, *J* = 8.0 Hz, 1H), 3.87 (s, 6H), 3.73 (s, 3H). ¹³C NMR (100 MHz, DMSO-*d*₆): δ = 187.9, 157.6, 152.8, 144.1, 142.0, 135.9, 132.9, 129.7, 121.8, 119.9, 117.7, 115.3, 106.2, 60.1, 56.2.

(*E*)-3-(4-hydroxyphenyl)-1-(3',4',5'-trimethoxyphenyl)prop-2-en-1-one (**3**): Yellow powder; yield 15%. ¹H NMR (400 MHz, acetone-*d*₆): δ = 8.98 (s, 1H), 7.71 (m, 4 H), 7.44 (s, 2H), 6.92 (d, *J* = 8.8 Hz, 2H), 3.93 (s, 6H), 3.82 (s, 3H). ¹³C NMR (100 MHz, acetone-*d*₆): δ = 188.7, 160.8, 154.3, 144.8, 134.8, 131.5, 127.7, 119.7, 116.7, 107.1, 60.7, 56.7.

(*E*)-3-(2-hydroxy-3-methoxyphenyl)-1-(3',4',5'-trimethoxyphenyl)prop-2-en-1-one (**4**): Brown-yellow powder; yield 6%. ¹H NMR (500 MHz, CDCl₃) δ = 8.01 (d, *J* = 15.5 Hz, 1H), 7.68 (d, *J* = 15.5 Hz, 1H), 7.29 (s, 2H), 7.18 (dd, *J* = 6.5, 3.0 Hz, 1H), 6.88 (dd, *J* = 8.0, 2.5 Hz, 2H), 3.94 (s, 6H), 3.93 (s, 3H), 3.92 (s, 3H). ¹³C NMR (125 MHz, CDCl₃) δ = 190.3, 153.2, 146.9, 145.9, 142.3, 140.2, 133.8, 123.6, 121.8, 121.4, 119.8, 112.1, 106.3, 61.1, 56.4, 56.3.

(*E*)-3-(2,3-dimethoxyphenyl)-1-(3',4',5'-trimethoxyphenyl)prop-2-en-1-one (**5**): Yellow powder; yield 84%. ¹H NMR (400 MHz, CDCl₃): δ = 8.08 (d, *J* = 16.0 Hz, 1H), 7.57 (d, *J* =

15.6 Hz, 1H), 7.31 (s, 1H), 7.12 (dd, $J = 8.0, 7.6$ Hz, 2H), 6.99 (d, $J = 8.0$ Hz, 2H), 3.96 (s, 9H), 3.91 (s, 3H), 3.90 (s, 3H). ^{13}C NMR (100 MHz, CDCl_3): $\delta = 189.8, 153.3, 149.0, 142.6, 139.8, 133.7, 129.3, 124.3, 123.8, 120.0, 114.3, 106.4, 61.3, 61.1, 56.5, 56.1$.

(*E*)-3-(benzo[d][1,3]dioxol-4-yl)-1-(3',4',5'-trimethoxyphenyl)prop-2-en-1-one (**6**): White-yellow powder; yield 43%. ^1H NMR (400 MHz, CDCl_3): $\delta = 7.75$ (d, $J = 15.6$, 1H), 7.71 (d, $J = 15.6$ Hz, 1H), 7.30 (s, 2H), 7.04 (dd, $J = 6.4, 2.8$ Hz, 1H), 6.88 (dd, $J = 6.4, 3.6$ Hz, 2H), 6.13 (s, 2H), 3.96 (s, 6H), 3.95 (s, 3H). ^{13}C NMR (100 MHz, CDCl_3): $\delta = 189.3, 152.9, 147.8, 146.5, 142.5, 138.8, 133.3, 124.3, 122.9, 121.7, 117.8, 109.8, 106.2, 101.3, 60.8, 56.3$. MS (ESI, m/z): 365.1 $[\text{M} + \text{Na}]^+$, HRMS calcd for $\text{C}_{19}\text{H}_{18}\text{O}_6$: 342.1103, Found: 342.1102.

(*E*)-3-(3-hydroxy-4-methoxyphenyl)-1-(3',4',5'-trimethoxyphenyl)prop-2-en-1-one (**9**): Pale yellow powder; yield 62%. ^1H NMR (400 MHz, CDCl_3): $\delta = 7.76$ (d, $J = 15.6$ Hz, 1H), 7.37 (d, $J = 15.6$ Hz, 1H), 7.32 (d, $J = 2.0$ Hz, 1H), 7.29 (s, 2H), 7.15 (dd, $J = 8.4, 2.4$ Hz, 1H), 6.89 (d, $J = 8.4$ Hz, 1H), 5.84 (br s, 1H), 3.96 (s, 6H), 3.95 (s, 6H). ^{13}C NMR (100 MHz, CDCl_3): $\delta = 189.3, 153.3, 149.0, 146.1, 144.8, 142.6, 133.8, 128.7, 123.0, 120.0, 112.9, 110.8, 106.2, 61.1, 56.5, 56.2$.

(*E*)-3-(3,4-dimethoxyphenyl)-1-(3',4',5'-trimethoxyphenyl)prop-2-en-1-one (**10**): Pale yellow powder; yield 87%. ^1H NMR (500 MHz, CDCl_3): $\delta = 7.74$ (d, $J = 15.5$ Hz, 1H), 7.31 (d, $J = 16.0$ Hz, 1H), 7.24 (dd, $J = 8.0, 2.0$ Hz, 3H), 7.13 (d, $J = 2.0$ Hz, 1H), 6.88 (d, $J = 8.5$ Hz, 1H), 3.93 (s, 3H), 3.92 (s, 6H), 3.91 (s, 6H). ^{13}C NMR (125 MHz, CDCl_3): $\delta = 189.5, 153.2, 151.5, 149.3, 145.1, 142.4, 133.9, 127.9, 123.0, 119.9, 111.2, 110.6, 106.2, 61.1, 56.5, 56.1$.

(*E*)-3-(benzo[d][1,3]dioxol-5-yl)-1-(3',4',5'-trimethoxyphenyl)prop-2-en-1-one (**11**): Pale yellow powder; yield 85%. ^1H NMR (400 MHz, CDCl_3): $\delta = 7.74$ (d, $J = 15.2$ Hz, 1H), 7.31 (d, $J = 15.6$ Hz, 1H), 7.16 (d, $J = 1.6$ Hz, 1H), 7.13 (dd, $J = 8.0, 1.6$ Hz, 1H), 6.85 (d, $J = 8.0$ Hz, 1H), 6.03 (s, 2H), 3.95 (s, 6H), 3.93 (s, 3H). ^{13}C NMR (100 MHz, CDCl_3): $\delta = 189.5, 153.6, 150.4, 148.8, 145.0, 134.1, 129.8, 125.6, 120.2, 109.1, 107.1, 106.6, 102.1, 61.4, 56.8$.

(*E*)-3-(2,4-dimethoxyphenyl)-1-(3',4',5'-trimethoxyphenyl)prop-2-en-1-one (**12**): Yellow powder; yield 57%. ^1H NMR (400 MHz, CDCl_3): δ = 8.06 (d, J = 15.6 Hz, 1H), 7.59 (d, J = 8.8 Hz, 1H), 7.49 (d, J = 15.6 Hz, 1H), 7.28 (s, 2H), 6.55 (dd, J = 8.4, 2.0 Hz, 2H), 6.49 (d, J = 2.4 Hz, 1H), 3.95 (s, 6H), 3.94 (s, 3H), 3.91 (s, 3H), 3.86 (s, 3H). ^{13}C NMR (100 MHz, CDCl_3): δ = 189.8, 162.8, 160.1, 152.8, 140.2, 133.9, 130.6, 120.1, 116.9, 105.9, 105.3, 98.3, 60.7, 56.1, 55.3.

(*E*)-3-(3,5-dimethoxyphenyl)-1-(3',4',5'-trimethoxyphenyl)prop-2-en-1-one (**13**): White yellow powder; yield 78%. ^1H NMR (400 MHz, CDCl_3): δ = 7.74 (d, J = 15.6 Hz, 1H), 7.44 (d, J = 15.6 Hz, 1H), 7.28 (s, 2H), 6.80 (d, J = 2.4 Hz, 2H), 6.55 (dd, J = 2.4, 2.0 Hz), 3.96 (s, 9 H), 3.86 (s, 6H). ^{13}C NMR (100 MHz, CDCl_3): δ = 189.0, 160.9, 152.9, 144.5, 142.5, 136.6, 133.2, 122.2, 106.3, 106.1, 102.3, 60.8, 56.3, 55.3.

(*E*)-3-(2,6-dimethoxyphenyl)-1-(3',4',5'-trimethoxyphenyl)prop-2-en-1-one (**14**): Yellow powder; yield 87%. ^1H NMR (400 MHz, CDCl_3): δ = 8.25 (d, J = 15.6 Hz, 1H), 7.95 (d, J = 15.6 Hz, 1H), 7.31 (s, 2H), 6.61 (d, J = 8.4 Hz, 3H), 3.96 (s, 6H), 3.95 (s, 3H), 3.93 (s, 6H). ^{13}C NMR (100 MHz, CDCl_3): δ = 191.06, 160.12, 152.80, 141.82, 135.52, 134.12, 131.27, 124.96, 112.80, 106.05, 103.65, 77.16, 60.73, 56.08, 55.67.

(*E*)-3-(2,5-dimethoxyphenyl)-1-(3',4',5'-trimethoxyphenyl)prop-2-en-1-one (**15**): Yellow powder; yield 64%. ^1H NMR (400 MHz, CDCl_3): δ = 8.07 (d, J = 15, 2 Hz, 1H), 7.52 (d, J = 15.6 Hz, 1H), 7.28 (s, 2H), 7.18 (d, J = 2.8 Hz, 1H), 6.95 (dd, J = 8.8, 3.2 Hz, 1H), 6.89 (d, J = 9.2 Hz, 1H), 3.96 (s, 9H), 3.88 (s, 3H), 3.83 (s, 3H). ^{13}C NMR (100 MHz, CDCl_3): δ = 189.8, 153.3, 153.1, 152.8, 142.1, 139.8, 133.5, 124.4, 122.9, 116.7, 113.8, 112.2, 106.0, 60.7, 56.1, 55.9, 55.6.

(*E*)-3-(3-bromo-4-methoxyphenyl)-1-(3',4',5'-trimethoxyphenyl)prop-2-en-1-one (**18**): Pale yellow powder; yield 35%. ^1H NMR (400 MHz, CDCl_3): δ = 7.90 (s, 1H), 7.72 (d, J = 15.6 Hz, 1H), 7.55 (dd, J = 8.4, 2.0 Hz, 1H), 7.37 (d, J = 15.6 Hz, 1H), 7.28 (s, 2H), 6.94 (d, J = 8.4 Hz, 1H), 3.97 (s, 6H), 3.95 (s, 6H). ^{13}C NMR (100 MHz, CDCl_3): δ = 188.6, 157.4, 152.9, 142.7, 133.3, 132.4, 129.6, 128.8, 120.3, 112.2, 111.7, 105.9, 60.7, 56.3.

(*E*)-3-(2,3,4-trimethoxyphenyl)-1-(3',4',5'-trimethoxyphenyl)prop-2-en-1-one (**19**): Yellow powder; yield 79%. ^1H NMR (400 MHz, CDCl_3): δ = 7.99 (d, J = 16.0 Hz, 1H), 7.52

(d, $J = 15.6$ Hz, 1H), 7.39 (d, $J = 8.8$ Hz, 1H), 7.29 (s, 2H), 6.74 (d, $J = 8.8$ Hz, 1H), 3.96 (s, 3H), 3.95 (s, 6H), 3.94 (s, 3H), 3.92 (s, 3H), 3.91 (s, 3H). ^{13}C NMR (100 MHz, CDCl_3): $\delta = 189.5, 155.6, 153.5, 152.9, 142.3, 139.9, 133.7, 123.7, 121.8, 121.1, 107.5, 105.9, 61.1, 60.7, 56.2, 55.9$.

(*E*)-1,3-bis(3,4,5-trimethoxyphenyl)prop-2-en-1-one (**20**): Yellow powder; yield 43%. ^1H NMR (400 MHz, CDCl_3): $\delta = 7.70$ (d, $J = 15.6$ Hz, 1H), 7.32 (d, $J = 15.6$ Hz, 1H), 7.25 (s, 2H), 6.85 (s, 2H), 3.94 (s, 6H), 3.93 (s, 3H), 3.91 (s, 6H), 3.89 (s, 3H). ^{13}C NMR (100 MHz, CDCl_3): $\delta = 189.5, 153.7, 153.3, 145.0, 133.7, 130.5, 121.5, 106.5, 106.0, 61.1, 56.6, 56.4$.

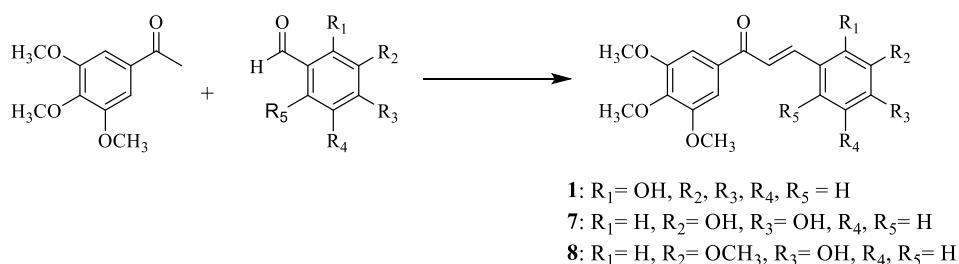
(*E*)-3-(2,4,5-trimethoxyphenyl)-1-(3',4',5'-trimethoxyphenyl)prop-2-en-1-one (**21**): Yellow powder; yield 97%. ^1H NMR (400 MHz, CDCl_3): $\delta = 8.05$ (d, $J = 15.6$ Hz, 1H), 7.38 (d, $J = 16$ Hz, 1H), 7.25 (s, 2H), 7.11 (s, 1H), 6.52 (s, 1H), 3.93 (s, 9H), 3.92 (s, 3H), 3.89 (s, 3H), 3.88 (s, 3H). ^{13}C NMR (100 MHz, CDCl_3): $\delta = 190.3, 154.8, 153.2, 152.7, 143.5, 140.3, 134.3, 120.6, 115.7, 112.1, 106.4, 97.1, 61.1, 56.8, 56.5, 56.5, 56.2$.

(*E*)-3-(2,4,6-trimethoxyphenyl)-1-(3',4',5'-trimethoxyphenyl)prop-2-en-1-one (**22**): Yellow powder; yield 87%. ^1H NMR (400 MHz, CDCl_3): $\delta = 8.23$ (d, $J = 15.6$ Hz, 1H), 7.82 (d, $J = 16.0$ Hz, 1H), 7.28 (s, 2H), 6.14 (s, 2H), 3.94 (s, 6H), 3.93 (s, 3H), 3.90 (s, 6H), 3.86 (s, 3H). ^{13}C NMR (100 MHz, CDCl_3): $\delta = 190.9, 162.9, 161.4, 152.7, 141.6, 135.8, 134.4, 121.8, 106.4, 105.9, 90.4, 60.7, 56.0, 55.6, 55.2$.

จุฬาลงกรณ์มหาวิทยาลัย
CHULALONGKORN UNIVERSITY

2.2.2.2 GENERAL PROCEDURE FOR THE SYNTHESIS OF 3',4',5'-TRIMETHOXYCHALCONE SERIES (1, 7-8)

3',4',5'-Trimethoxyacetophenone (420 mg, 2 mmol) and 3,4-dihydroxybenzaldehyde (456 mg, 3 mmol) were mixed in MeOH (10 mL) and stirred. The concentrated H_2SO_4 (0.5 mL) was added to this mixture slowly at room temperature and refluxed for 24 hours. The crude product was extracted using EtOAc, then evaporated, and separated by column chromatography using hexane:EtOAc (3:2) to obtain a pure product.



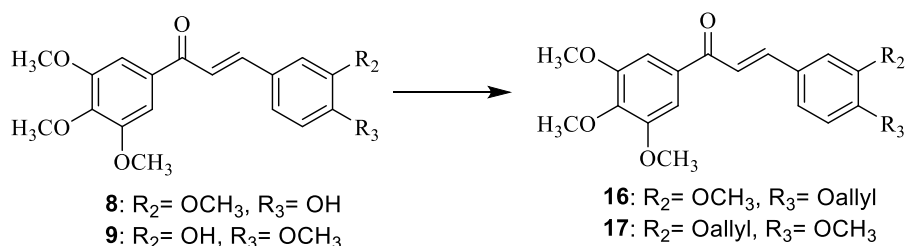
(*E*)-3-(2-hydroxyphenyl)-1-(3',4',5'-trimethoxyphenyl)prop-2-en-1-one (**1**): Yellow powder; yield 14%. ^1H NMR (400 MHz, CDCl_3): δ = 8.20 (d, J = 16.0 Hz, 1H), 7.72 (brs, 1H), 7.64 (d, J = 16.0 Hz, 1H), 7.57 (dd, J = 8.0, 1.2 Hz, 1H), 7.28 (s, 2H), 7.25 (td, J = 8.8, 1.6 Hz, 1H), 6.96 (d, J = 8.4 Hz, 1H), 6.92 (t, J = 8.0 Hz, 1H), 3.93 (s, 3H), 3.91 (s, 6H). ^{13}C NMR (100 MHz, CDCl_3): δ = 191.3, 156.5, 153.2, 142.6, 141.6, 133.7, 132.0, 129.5, 122.3, 122.3, 120.7, 116.8, 106.6, 61.1, 56.5.

(*E*)-3-(3,4-dihydroxyphenyl)-1-(3',4',5'-trimethoxyphenyl)prop-2-en-1-one (**7**): Yellow powder; yield 49%. ^1H NMR (400 MHz, CDCl_3): δ = 7.73 (d, J = 15.6 Hz, 1H), 7.31 (d, J = 16.0 Hz, 1H), 7.254 (s, 3H), 7.11 (dd, J = 8.0, 2.0 Hz, 1H), 6.93 (d, J = 8.4 Hz, 1H), 3.95 (s, 3H), 3.93 (s, 6H). ^{13}C NMR (100 MHz, CDCl_3): δ = 190.5, 153.3, 147.4, 146.0, 144.5, 142.7, 133.7, 127.8, 123.0, 119.5, 115.7, 115.0, 106.4, 61.12, 56.6.

(*E*)-3-(4-hydroxy-3-methoxyphenyl)-1-(3',4',5'-trimethoxyphenyl)prop-2-en-1-one (**8**): Yellow liquid; yield 52%. ^1H NMR (400 MHz, CDCl_3): δ = 7.75 (d, J = 15.6 Hz, 1H), 7.31 (d, J = 15.6 Hz, 1H), 7.24 (dd, J = 8.0, 2.0 Hz, 3H), 7.11 (d, J = 2.0 Hz, 1H), 6.96 (d, J = 8.4 Hz, 1H), 6.03 (br s, 1H), 3.96 (s, 3H), 3.95 (s, 6H), 3.94 (s, 3H). ^{13}C NMR (100 MHz, CDCl_3): δ = 189.6, 153.3, 148.5, 147.0, 145.3, 142.6, 133.9, 127.7, 123.1, 119.8, 115.1, 110.7, 106.4, 61.1, 56.6, 56.2.

2.2.2.3 PROCEDURE FOR THE SYNTHESIS OF 16 AND 17

The mixtures of either **8** or **9** (100 mg, 0.3 mmol) and K_2CO_3 (0.3 mmol) in acetone (10 mL) were stirred at room temperature. After 5 min, allyl bromide (26 μL , 0.3 mmol) was added and the mixture was refluxed for 24 hours. The complete reaction was monitored by TLC. The mixture of products was filtered, evaporated, and then purified by column chromatography using hexane:EtOAc (3:2).

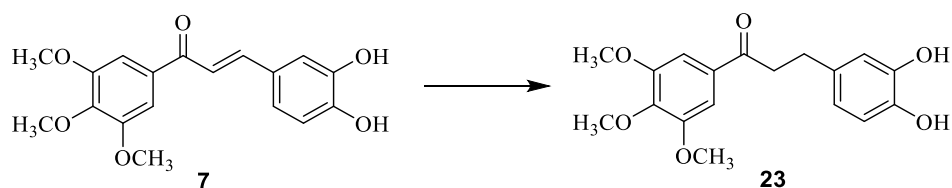


(*E*)-3-(4-(allyloxy)-3-methoxyphenyl)-1-(3',4',5'-trimethoxyphenyl)prop-2-en-1-one (**16**): Yellow liquid; yield 42%. ¹H NMR (400 MHz, CDCl₃): δ = 7.73 (d, *J* = 15.6 Hz, 1H), 7.31 (d, *J* = 15.6 Hz, 1H), 7.24 (s, 2H), 7.19 (dd, *J* = 8.4, 1.6 Hz, 1H), 7.14 (d, *J* = 2.0 Hz, 1H), 6.06 (ddt, *J* = 17.6, 10.8, 5.2 Hz, 1H), 5.41 (dd, *J* = 17.2, 1.2 Hz, 1H), 5.30 (dd, *J* = 10.8, 1.2 Hz, 1H), 4.64 (dt, *J* = 5.2, 1.6 Hz, 1H), 3.92 (s, 9H), 3.91 (s, 3H). ¹³C NMR (100 MHz, CDCl₃): δ = 189.5, 153.2, 150.6, 149.7, 144.9, 133.9, 132.8, 128.2, 122.7, 120.1, 118.4, 114.5, 113.2, 111.2, 106.4, 69.8, 61.0, 56.5, 56.2.

(*E*)-3-(3-(allyloxy)-4-methoxyphenyl)-1-(3',4',5'-trimethoxyphenyl)prop-2-en-1-one (**17**): Yellow liquid; yield 58%. ¹H NMR (400 MHz, CDCl₃): δ = 7.74 (d, *J* = 15.6 Hz, 1H), 7.31 (d, *J* = 15.6 Hz, 1H), 7.26 (s, 3H), 7.18 (s, 1H), 6.92 (d, *J* = 8.4 Hz, 1H), 6.11 (ddt, *J* = 17.2, 10.8, 5.6 Hz, 1H), 5.45 (d, *J* = 17.2 Hz, 1H), 5.33 (d, *J* = 10.4 Hz, 1H), 4.68 (d, *J* = 5.6 Hz, 2H), 3.95 (s, 6H), 3.94 (s, 3H), 3.93 (s, 3H). ¹³C NMR (100 MHz, CDCl₃): δ = 189.7, 153.3, 152.2, 148.4, 145.0, 142.6, 133.3, 127.9, 123.3, 120.1, 118.3, 113.2, 111.7, 106.4, 70.3, 61.1, 56.6, 56.2. MS (ESI, *m/z*): 407.1472 [M + Na]⁺, HRMS calcd for C₂₂H₂₄O₆: 384.1573, Found: 384.1574.

2.2.2.4 PROCEDURE FOR THE SYNTHESIS OF 23

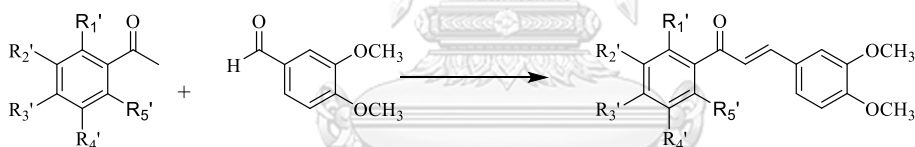
Compound **7** (166 mg, 0.5 mmol) was mixed with 10% Pd/C (16.6 mg) in EtOAc (20 mL) and stirred. Into the mixture then was flowed H₂ gas (balloon) at room temperature for 24 hours. The reaction mixture was filtered, evaporated, and then separated to obtain pure product by column chromatography (hexane:EtOAc = 3:2).



3-(3,4-dihydroxyphenyl)-1-(3',4',5'-trimethoxyphenyl)propan-1-one (**23**): Brown powder; yield 74%. ^1H NMR (400 MHz, $\text{DMSO}-d_6$): δ = 8.59 (br s, 2H), 7.13 (s, 2H), 6.55 (dd, J = 9.2, 2.4 Hz, 2H) 6.42 (d, J = 8.0 Hz, 1H), 3.74 (s, 6H), 3.64 (s, 3H), 3.16 (t, J = 7.2 Hz, 2H), 2.66 (t, J = 7.2 Hz, 2H). ^{13}C NMR (100 MHz, $\text{DMSO}-d_6$): δ = 198.4, 152.7, 144.9, 143.3, 132.1, 119.0, 115.9, 115.4, 105.6, 60.2, 56.1, 39.7, 39.5, 29.2. MS (ESI, m/z): 355.1162 [$\text{M} + \text{Na}$] $^+$, HRMS calcd for $\text{C}_{18}\text{H}_{20}\text{O}_6$: 332.1260, Found: 332.1264.

2.2.2.4 GENERAL PROCEDURE FOR THE SYNTHESIS OF 3,4-DIMETHOXYCHALCONE SERIES (24-33)

A method similar to that for 2.2.2.1 was also employed.



- 24:** $\text{R}_1' = \text{OCH}_3$, R_2' , R_3' , R_4' , $\text{R}_5' = \text{H}$
25: $\text{R}_1' = \text{H}$, $\text{R}_2' = \text{OCH}_3$, R_3' , R_4' , $\text{R}_5' = \text{H}$
26: $\text{R}_1' = \text{H}$, $\text{R}_2' = \text{H}$, $\text{R}_3' = \text{OCH}_3$, R_4' , $\text{R}_5' = \text{H}$
27: $\text{R}_1' = \text{OH}$, $\text{R}_3' = \text{OCH}_3$, R_4' , $\text{R}_5' = \text{H}$
28: $\text{R}_1' = \text{OH}$, R_2' , R_3' , $\text{R}_4' = \text{H}$, $\text{R}_5' = \text{OCH}_3$
29: $\text{R}_1' = \text{OCH}_3$, $\text{R}_2' = \text{H}$, $\text{R}_3' = \text{OCH}_3$, R_4' , $\text{R}_5' = \text{H}$
30: $\text{R}_1' = \text{OCH}_3$, R_2' , $\text{R}_3' = \text{H}$, $\text{R}_4' = \text{OCH}_3$, $\text{R}_5' = \text{H}$
31: $\text{R}_1' = \text{H}$, $\text{R}_2' = \text{OCH}_3$, $\text{R}_3' = \text{OCH}_3$, R_4' , $\text{R}_5' = \text{H}$
32: $\text{R}_1' = \text{OCH}_3$, $\text{R}_2' = \text{OCH}_3$, $\text{R}_3' = \text{OCH}_3$, R_4' , $\text{R}_5' = \text{H}$
33: $\text{R}_1' = \text{OH}$, $\text{R}_2' = \text{H}$, $\text{R}_3' = \text{OCH}_3$, $\text{R}_4' = \text{H}$, $\text{R}_5' = \text{OCH}_3$

(*E*)-3-(3,4-dimethoxyphenyl)-1-(2'-methoxyphenyl)prop-2-en-1-one (**24**): Yellow liquid; yield 89%. ^1H NMR (400 MHz, CDCl_3): δ = 7.57 (dd, J = 7.6, 1.6 Hz, 1H), 7.53 (d, J = 15.6 Hz, 1H), 7.45 (td, J = 8.8, 2.0 Hz, 1H), 7.20 (d, J = 15.6 Hz, 1H), 7.16 (dd, J = 8.0, 1.6 Hz, 1H), 7.01 (s, 1H), 7.04 (t, J = 8.0 Hz, 1H), 7.00 (d, J = 8.4 Hz, 1H), 6.86 (d, J = 8.4 Hz, 1H), 3.91 (s, 6H), 3.88 (s, 3H). ^{13}C NMR (100 MHz, CDCl_3): δ = 193.3, 158.0, 151.4, 149.3, 143.9, 132.6, 130.2, 129.7, 128.2, 125.4, 123.0, 120.8, 111.8, 111.3, 110.4, 56.1, 56.0, 55.9.

(*E*)-3-(3,4-dimethoxyphenyl)-1-(3'-methoxyphenyl)prop-2-en-1-one (**25**): Yellow liquid; yield 82%. ^1H NMR (400 MHz, CDCl_3): δ = 7.76 (d, J = 15.6 Hz, 1H), 7.59 (d, J = 8.8 Hz, 1H), 7.53 (s, 1H), 7.40 (t, J = 8.0 Hz, 1H), 7.36 (d, J = 15.6 Hz, 1H), 7.22 (dd, J = 8.4, 2.0 Hz, 1H), 7.15 (d, J = 2.0 Hz, 1H), 7.11 (dd, J = 8.0, 1.6 Hz, 1H), 6.89 (d, J = 8.4 Hz, 1H), 3.94 (s, 3H), 3.92 (s, 3H), 3.87 (s, 3H). ^{13}C NMR (100 MHz, CDCl_3): δ = 190.4, 160.0, 151.6, 149.4, 145.2, 140.0, 129.6, 128.0, 123.3, 121.1, 120.3, 119.1, 113.1, 111.3, 110.4, 56.1, 55.6.

(*E*)-3-(3,4-dimethoxyphenyl)-1-(4'-methoxyphenyl)prop-2-en-1-one (**26**): Yellow liquid; yield 99%. ^1H NMR (400 MHz, CDCl_3): δ = 8.02 (d, J = 8.8 Hz, 2H), 7.74 (d, J = 15.6 Hz, 1H), 7.39 (d, J = 14.8 Hz, 1H), 7.21 (dd, J = 8.4, 2.0 Hz), 7.14 (s, 1H), 6.96 (d, J = 8.8 Hz, 2H), 6.87 (d, J = 8.0 Hz, 1H), 3.93 (s, 3H), 3.90 (s, 3H), 3.86 (s, 3H). ^{13}C NMR (100 MHz, CDCl_3): δ = 188.8, 163.4, 151.4, 149.4, 144.2, 131.4, 130.8, 128.2, 123.0, 119.9, 113.9, 111.3, 110.3, 56.1, 55.5.

(*E*)-3-(3,4-dimethoxyphenyl)-1-(2'-hydroxy-4'-methoxyphenyl)prop-2-en-1-one (**27**): Yellow powder; yield 12%. ^1H NMR (400 MHz, CDCl_3): δ = 13.54 (br s, OH), 7.84 (d, J = 14.8, 8.8 Hz, 2H), 7.42 (d, J = 15.2 Hz, 1H), 7.24 (dd, J = 8.4, 2.0, 1H), 7.15 (d, J = 2.0 Hz, 1H), 6.89 (d, J = 8.0 Hz, 1H), 6.48 (dd, J = 8.4, 2.0 Hz, 2H), 3.95 (s, 3H), 3.93 (s, 3H), 3.85 (s, 3H). ^{13}C NMR (100 MHz, CDCl_3): δ = 191.9, 166.8, 166.2, 151.7, 149.5, 144.7, 131.2, 127.9, 123.4, 118.2, 114.3, 111.4, 110.5, 107.7, 101.2, 56.2, 55.7.

(*E*)-3-(3,4-dimethoxyphenyl)-1-(2'-hydroxy-6'-methoxyphenyl)prop-2-en-1-one (**28**): Orange powder; yield 36%. ^1H NMR (400 MHz, CDCl_3): δ = 13.24 (br s, OH), 7.79 (d, J = 15.6, 1H), 7.78 (d, J = 15.2 Hz, 1H), 7.34 (t, J = 8.4 Hz, 1H), 7.22 (dd, J = 8.0, 2.0 Hz, 1H), 7.13 (d, J = 2.0, 1H), 6.90 (d, J = 8.0 Hz, 1H), 6.61 (d, J = 8.0 Hz, 1H), 6.42 (d, J = 8.0 Hz, 1H), 3.94 (s, 9H). ^{13}C NMR (101 MHz, CDCl_3): δ = 194.3, 164.9, 161.0, 151.5, 149.3, 143.4, 135.7, 128.5, 125.6, 122.9, 112.2, 111.4, 111.1, 110.7, 101.7, 56.1, 56.0.

(*E*)-1-(2',4'-dimethoxyphenyl)-3-(3,4-dimethoxyphenyl)prop-2-en-1-one (**29**): Green-yellow powder; yield 72%. ^1H NMR (400 MHz, CDCl_3): δ = 7.72 (d, J = 8.4 Hz, 1H), 7.60 (d, J = 15.6 Hz, 1H), 7.35 (d, J = 15.6 Hz, 1H), 7.17 (dd, J = 8.4, 2.0 Hz, 1H), 7.11 (d, J = 2.0 Hz, 1H), 6.87 (d, J = 8.4 Hz, 1H), 6.55 (dd, J = 8.4, 2.4 Hz, 1H), 6.49 (d, J = 2.4 Hz,

1H), 3.91 (s, 3H), 3.90 (s, 3H), 3.88 (s, 3H), 3.86 (s, 3H). ¹³C NMR (100 MHz, CDCl₃): δ = 190.8, 164.0, 160.3, 151.1, 149.3, 142.5, 132.7, 128.6, 125.5, 122.7, 111.3, 110.5, 105.3, 98.8, 56.1, 56.0, 55.8, 55.6.

(*E*)-1-(2',5'-dimethoxyphenyl)-3-(3,4-dimethoxyphenyl)prop-2-en-1-one (**30**): Yellow liquid; yield 76%. ¹H NMR (400 MHz, CDCl₃): δ = 7.58 (d, *J* = 15.6 Hz, 1H), 7.26 (d, *J* = 16.0 Hz, 1H), 7.19 (dd, *J* = 8.4, 2.0 Hz, 1H), 7.17 (d, *J* = 3.2 Hz, 1H), 7.13 (d, *J* = 2.0 Hz, 1H), 7.02 (dd, *J* = 9.2, 3.2 Hz, 1H), 6.96 (d, *J* = 9.2 Hz, 1H), 6.89 (d, *J* = 8.0 Hz, 1H), 3.93 (s, 6H), 3.86 (s, 3H), 3.82 (s, 3H). ¹³C NMR (100 MHz, CDCl₃): δ = 192.7, 153.8, 152.4, 151.4, 149.4, 143.9, 130.2, 128.2, 125.2, 123.0, 118.7, 114.6, 113.6, 111.3, 110.4, 56.7, 56.1, 56.0, 55.9.

(*E*)-1,3-bis(3,4-dimethoxyphenyl)prop-2-en-1-one (**31**): Yellow powder; yield 90%. ¹H NMR (400 MHz, CDCl₃): δ = 7.77 (d, *J* = 15.6 Hz, 1H), 7.69 (dd, *J* = 8.4, 2.0 Hz, 1H), 7.63 (s, 1H), 7.42 (d, *J* = 15.2 Hz, 1H), 7.26 (t, *J* = 8.0 Hz, 1H), 7.17 (s, 1H), 6.95 (d, *J* = 8.4 Hz, 1H), 6.91 (d, *J* = 8.4 Hz, 1H), 3.98 (s, 3H), 3.97 (s, 3H), 3.96 (s, 3H), 3.93 (s, 3H). ¹³C NMR (100 MHz, CDCl₃): δ = 188.8, 153.3, 151.4, 149.4, 144.3, 131.7, 128.2, 122.9, 119.8, 111.3, 111.1, 110.5, 110.1, 56.2, 56.1.

(*E*)-3-(3,4-dimethoxyphenyl)-1-(2',3',4'-trimethoxyphenyl)prop-2-en-1-one (**32**): Yellow liquid; yield 85%. ¹H NMR (400 MHz, CDCl₃): δ = 7.61 (d, *J* = 16.0 Hz, 1H), 7.44 (d, *J* = 8.4 Hz, 1H), 7.33 (d, *J* = 15.6 Hz, 1H), 7.18 (dd, *J* = 8.0, 2.0 Hz, 1H), 7.12 (d, *J* = 2.0 Hz, 1H), 6.87 (d, *J* = 8.4 Hz, 1H), 6.74 (d, *J* = 8.4 Hz, 1H), 3.91 (s, 15H). ¹³C NMR (100 MHz, CDCl₃): δ = 191.1, 156.9, 153.6, 151.3, 149.4, 143.5, 142.3, 128.3, 127.2, 125.7, 124.8, 122.9, 111.3, 110.4, 107.5, 62.2, 61.2, 56.2, 56.1, 56.0.

(*E*)-3-(3,4-dimethoxyphenyl)-1-(2'-hydroxy-4',6'-dimethoxyphenyl)prop-2-en-1-one (**33**): Orange powder; yield 21%. ¹H NMR (400 MHz, CDCl₃): δ = 7.77 (d, *J* = 15.2 Hz, 7.76 (d, *J* = 15.6 Hz, 1H), 7.20 (d, *J* = 8.4, 2.0 Hz, 1H), 7.11 (d, *J* = 2.0 Hz, 1H), 6.88 (d, *J* = 8.4 Hz, 1H), 6.09 (d, *J* = 2.4 Hz, 1H), 5.95 (d, *J* = 2.4 Hz, 1H), 3.93 (s, 3H), 3.91 (s, 3H), 3.89 (s, 3H), 3.82 (s, 3H). ¹³C NMR (100 MHz, CDCl₃): δ = 192.5, 168.5, 166.2, 162.5, 151.2, 149.3, 142.7, 128.7, 125.6, 122.7, 111.4, 110.7, 106.5, 94.0, 91.4, 56.1, 55.9, 55.9, 55.6.

2.2.2.5 *IN VITRO* ANTI-CANCER A549 ASSAY

This assay was conducted under the collaboration with Department of Pharmacology, Faculty of Medicine, Chulalongkorn University. An assay was performed as previously described.⁵² A549 cells were seeded into 96-well plates at 5×10^3 cells/well. After overnight incubation, cells were treated with the synthesized compounds or erlotinib at concentrations of 0.1, 1, 10, and 100 μM or 0.2% DMSO (vehicle control) for 48 hours. 3-(4,5-Dimethylthiazol-2-yl)-2,5-diphenyl-2H-tetrazolium bromide (MTT) solution was added and incubated for additional 4 h. The medium was removed and 200 μL of DMSO was added to each well. The absorbance of the converted dye was measured at 570 nm using a microplate reading spectrophotometer. IC_{50} values were calculated using GraphPad Prism 7 Software.

2.2.2.6 MOLECULAR DOCKING

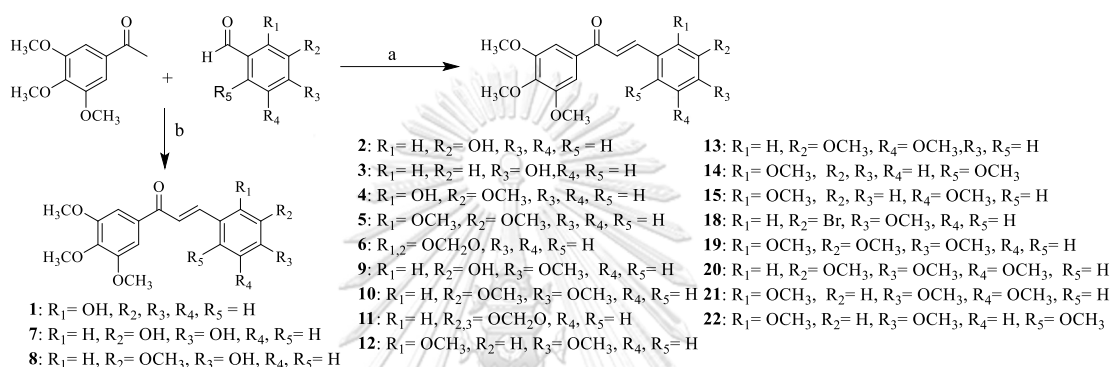
The molecular docking analysis was carried out under the collaborative project with Department of Biochemistry, Faculty of Science, Chulalongkorn University. The 3D structure of EGFR-TK in complex with erlotinib was downloaded from Protein Data Bank (PDB ID: 1M17). According to the standard protocols,^{53, 54} the initial structures of **7**, **10**, and **14** were created and optimized using the Gaussian09 program.⁵⁵ The protein-ligand complexes were generated using the CDOCKER module⁵⁶ implemented in the Accelrys Discovery Studio 2.5 program (with 100 independent docking runs) using a sphere radius of 15 Å.

2.3 RESULTS AND DISCUSSION

2.3.1 SYNTHESIS OF TWO SELECTED CHALCONE SERIES

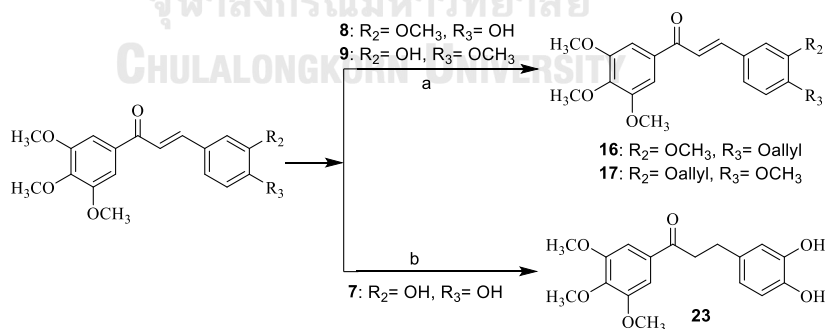
Two chalcone series were prepared using Claisen-Schmidt condensation reaction.⁵⁷ The first series with 3',4',5'-trimethoxyphenyl on the A ring and various substituents on the B ring (**1-23**) was synthesized with two conditions (basic and acid) as presented in Schemes 2.1 and 2.2. In basic condition (Scheme 2.1A), the products were obtained in moderate to high yield (40-90%), but compounds **1**, **7**, and **8** were

not formed in basic condition due to conjugation electron in benzaldehyde ring leading to reduce reactivity of carbonyl group. Thus, compounds **1**, **7**, and **8** succeeded to be obtained in moderate yield (40-50%) when the condition was changed to acid condition using concentrated sulphuric acid. **23** was derived from the hydrogenation of **7** using H_2 in the presence of Pd/C catalyst. Williamson ether reaction was performed for the synthesis of **16** and **17** from **8** and **9** in the presence of allyl bromide under basic and reflux conditions as presented in Scheme 2.2.



Reagents and conditions: (a) 6 M NaOH, MeOH, substituted benzaldehydes, rt, 24 h. (b) conc. H_2SO_4 , MeOH, substituted benzaldehydes, reflux, 24 h.

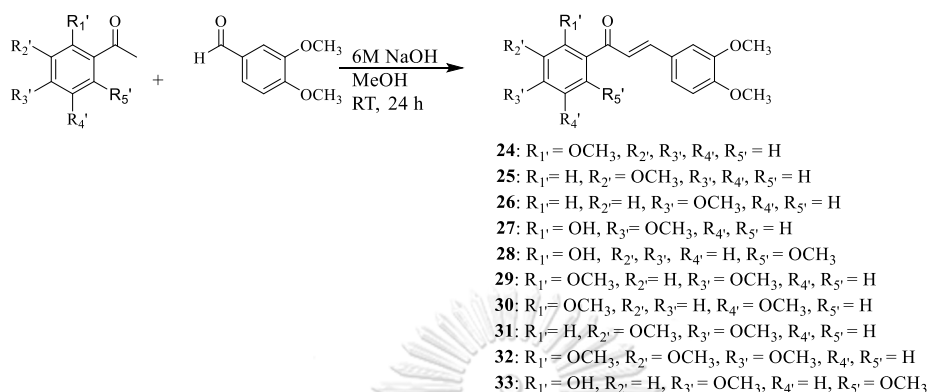
SCHEME 2.1 SYNTHESIS OF 3',4',5'-TRIMETHOXYCHALCONES (**1-15** AND **18-22**).



Reagents and conditions: (a) K_2CO_3 , acetone, allyl bromide, reflux, 24 h. (b) H_2 , 10% Pd/C, EtOAc, rt, 24 h.

SCHEME 2.2 SYNTHESIS OF 3',4',5'-TRIMETHOXYCHALCONES (**16**, **17** AND **23**).

The second series (**24-33**) containing 3,4-dimethoxyphenyl on the B ring with various hydroxy and methoxy substituents on the A ring were conducted as shown in Scheme 2.3.



SCHEME 2.3 SYNTHESIS OF 3,4-DIMETHOXYCHALCONE SERIES (**24-33**).

All compounds were characterized using ¹H and ¹³C NMR spectroscopic methods. To explain the structural elucidation of two chalcone series, **9** and **27** were selected as representatives (Figure 2.5).

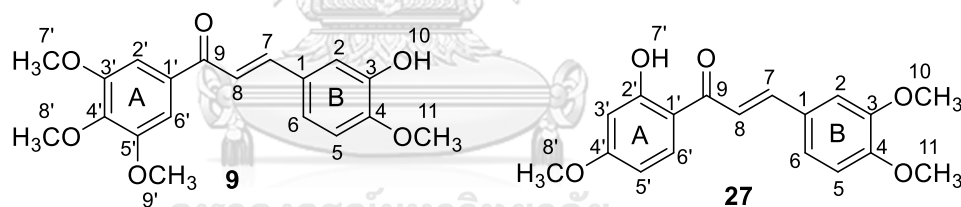


FIGURE 2.5 NUMBERING AND STRUCTURES OF **9** AND **27**.

The ¹H NMR Spectra of **9** (Figure 2.6) shows two signals for *trans*-protons at δ_{H} 7.76 (d, $J = 15.6$ Hz, H-7) and 7.37 (d, $J = 15.6$ Hz, H-8). The proton signal at δ_{H} 7.32 (d, $J = 2.0$ Hz, H-2) and two proton signals at δ_{H} 7.15 (dd, $J = 8.4, 2.4$ Hz, H-6) and 6.89 (d, $J = 8.4$ Hz, H-5) were belonged to those on the B ring, while two singlets at δ_{H} 7.29 (s, H-2' and H-6') were belonged to those on the A ring. A broad singlet signal at δ_{H} 5.84 (br s, H-10) could be assigned for the hydroxy group on the B ring. The signals at δ_{H} 3.96 (s, 11-OCH₃, 8'-OCH₃-) and 3.95 (s, 7'-OCH₃, 9'-OCH₃) displayed twelve protons of four methoxy groups. The ¹³C NMR Spectra of **9** (Figure 2.7) displays a characteristic carbonyl chalcone carbon signal at δ_{C} 189.3. Four signals of oxygenated aromatic

carbons were observed at δ_C 153.3-144.8, while nine aromatic carbon signals could be detected at δ_C 144.8-106.2. In addition, three signals of the methoxy groups were observed at δ_C 61.1 (8'-OCH₃), 56.5 (7'-OCH₃, 9'-OCH₃), and 56.2 (11-OCH₃).

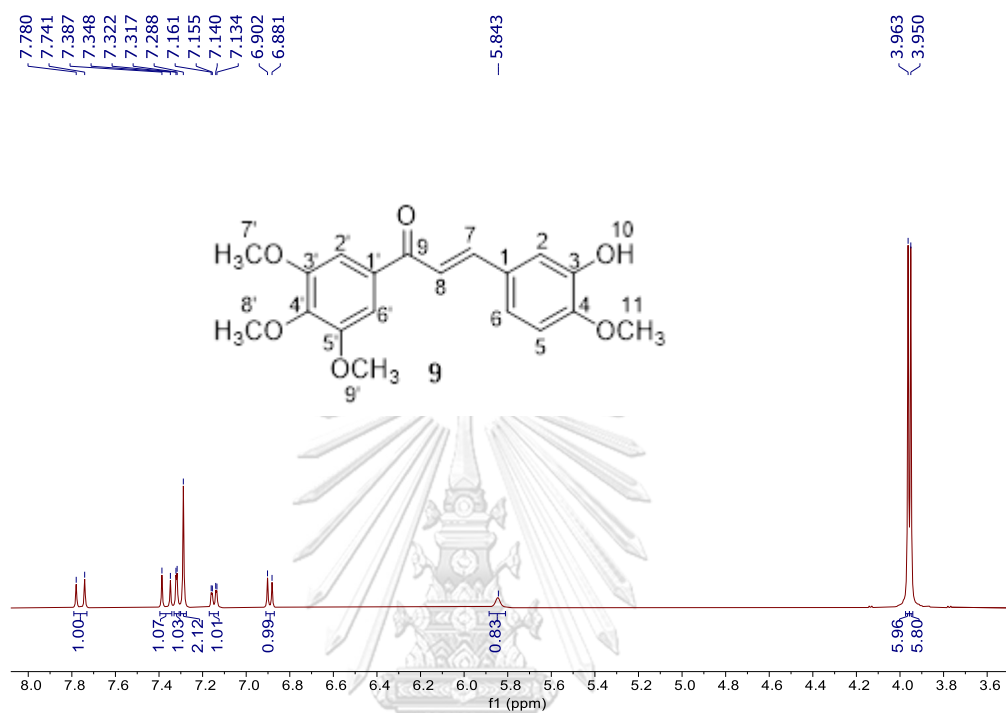


FIGURE 2.6 THE ¹H NMR SPECTRA (CDCl₃, 400 MHZ) OF 9.

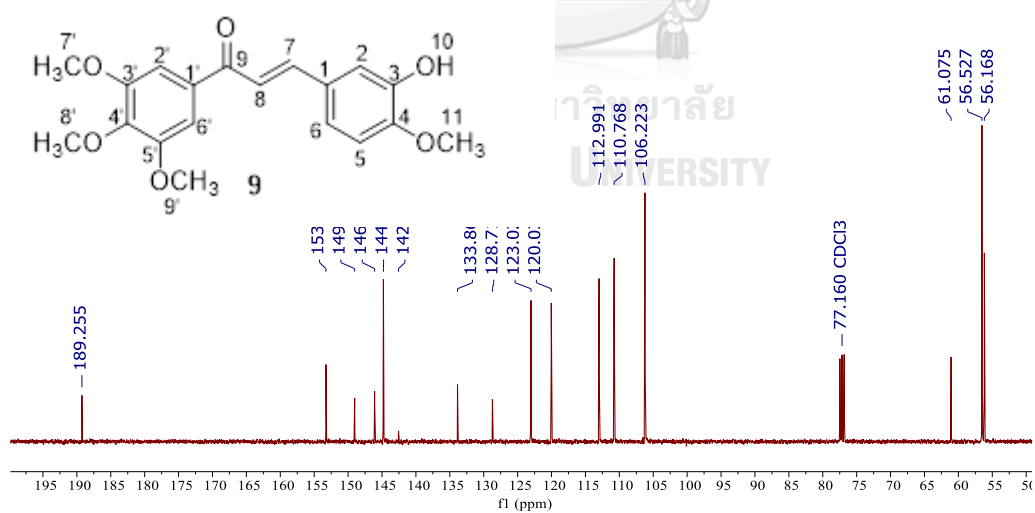


FIGURE 2.7 THE ¹³C NMR SPECTRA (CDCl₃, 100 MHZ) OF 9

The ^1H NMR Spectra of **27** (Figure 2.8) exhibited two protons signals at δ_{H} 7.84 (dd, $J = 14.8, 8.8$ Hz, H-5, and H-7) and a proton (H-8) at δ_{H} 7.42 (d, $J = 15.2$ Hz, H-8). A broad singlet proton (H-7') at δ_{H} 13.54 could be assigned for the chelated hydroxy proton. Two proton signals at δ_{H} 7.24 (dd, $J = 8.4, 2.0$ Hz, H-6) and 7.15 (d, $J = 2.0$ Hz, H-2) belonged to those on the B ring, while two signals at δ_{H} 6.89 (d, $J = 8.0$ Hz, H-6') and 6.48 (dd, $J = 8.4, 2.0$ Hz, H-3' and H-5') were those on the A ring. The three singlet signals at δ_{H} 3.95, 3.95, and 3.85 showed nine protons of the three methoxy groups. The ^{13}C NMR Spectra of **27** (Figure 2.9) showed the unique of carbonyl group attached to olefinic carbon at δ_{C} 191.9. The signals of oxygenated aromatic carbons were detected at δ_{C} 166.8-149.5, while ten signals of aromatic carbons were observed at δ_{C} 144.7-101.2. Moreover, two signals of methoxy groups were visible at δ_{C} 56.2 (10-OCH₃, 11-OCH₃) and 55.7 (8'-OCH₃).

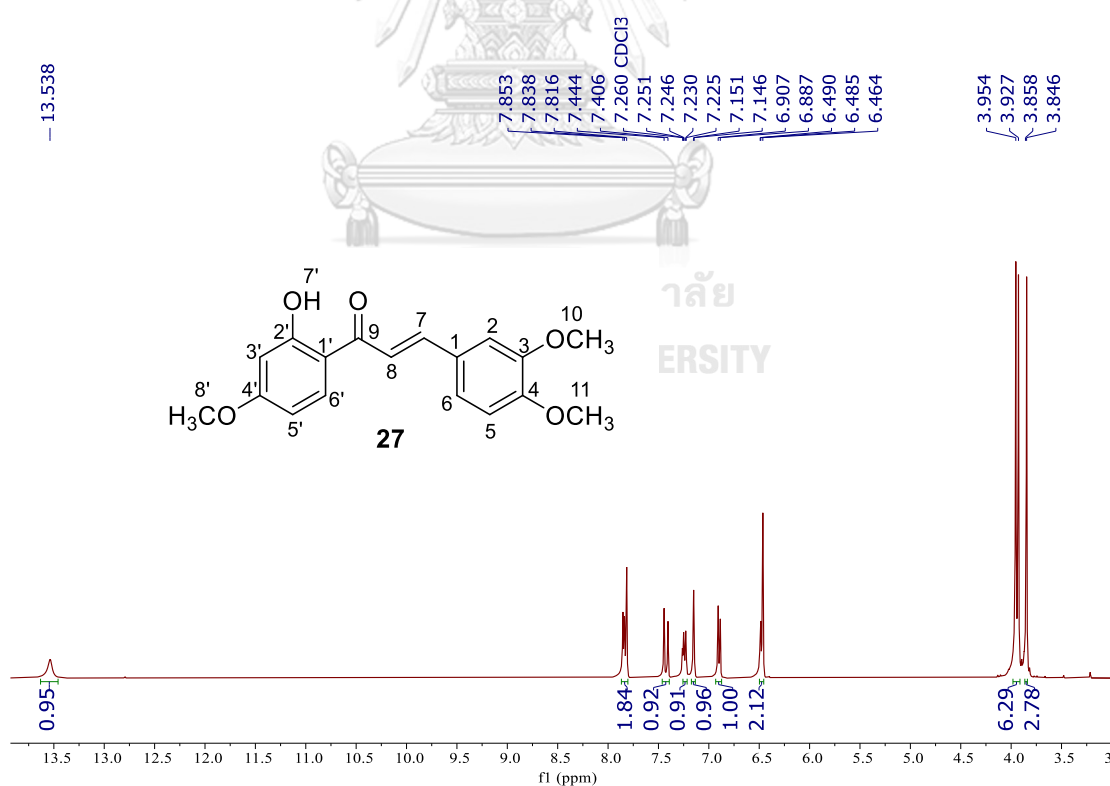


FIGURE 2.8 THE ^1H NMR SPECTRA (CDCl₃, 400 MHz) OF **27**.

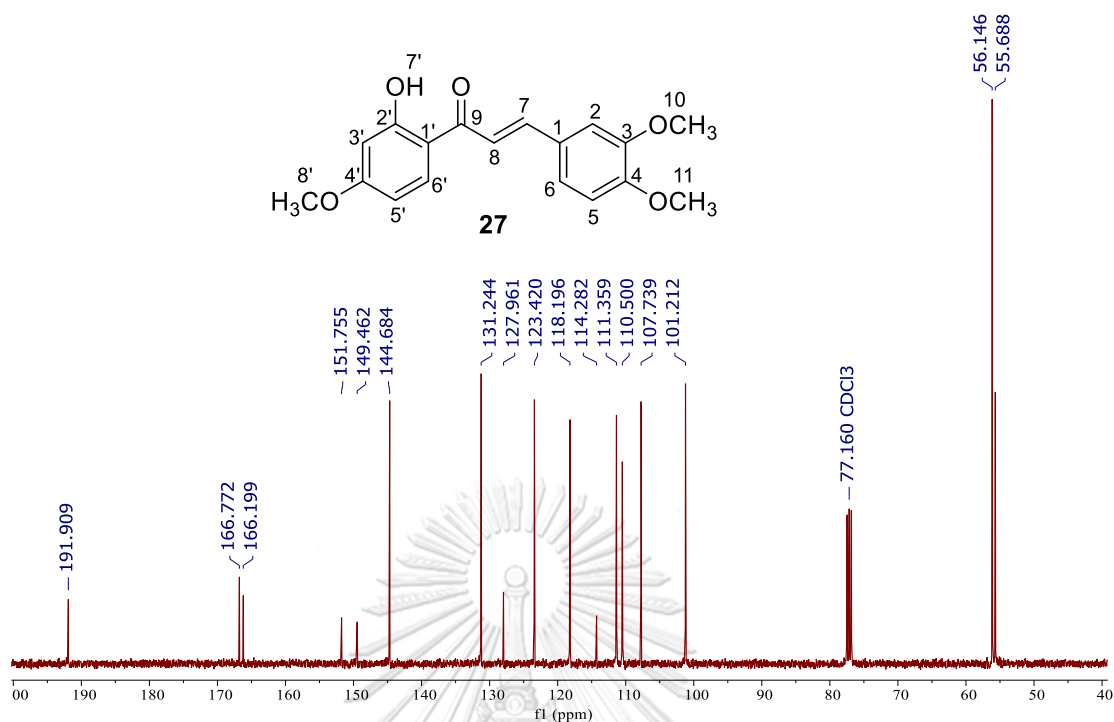


FIGURE 2.9 THE ^{13}C NMR SPECTRA (CDCl₃, 100 MHz) OF 27.

2.3.2 DISCUSSION

Twenty-three 3',4',5'-trimethoxychalcones (1-23) and ten 3,4-dimethoxychalcones (24-33) were evaluated for their anti-cancer activity against A549 using MTT assay as presented in Figure 2.10. For screening, all compounds were tested at 10 μM because erlotinib (drug standard) showed cytotoxic activity at $12.50 \pm 1.05 \mu\text{M}$.

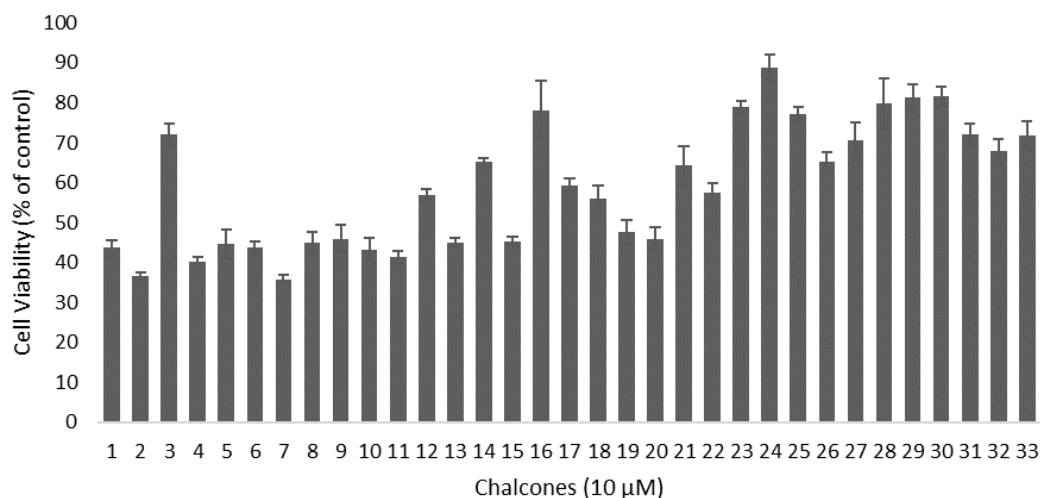


FIGURE 2.10 SCREENING OF 3',4',5'-TRIMETHOXYCHALCONES (1-23), AND 3,4-DIMETHOXYCHALCONE SERIES (24-33) AGAINST A549. DATA ARE EXPRESSED AS MEAN \pm SD IN TRIPLICATE FROM THREE DIFFERENT EXPERIMENTS.

According to the results presented, two groups of compounds could be divided, *i.e.*, those with high activity (% cell viability less than 50%) and inactive compounds (% cell viability more than 50%). Only thirteen 3',4',5'-trimethoxychalcones (1-2, 4-11, 13, 15, 20) expressed high activity against A549, whereas 3,4-dimethoxychalcones in the second series (24-33) showed that the alteration of substituents on the A ring led to significant decrease in anti-cancer activity with percentage of cell viability more than 50% at 10 μ M as presented in Figure 2.10. Inhibition concentration of a half-maximal drug (IC_{50}) is often widely applied to measure drug efficacy. This result demonstrates about the effectiveness of drug usage to inhibit a biological reaction by fifty percent that provides an informative measure of a potency drug in pharmacological field.⁵⁸ Thus, these compounds were further evaluated for IC_{50} values by varying concentration of compounds as presented in Figure 2.11 and IC_{50} values were listed in Table 2.1.

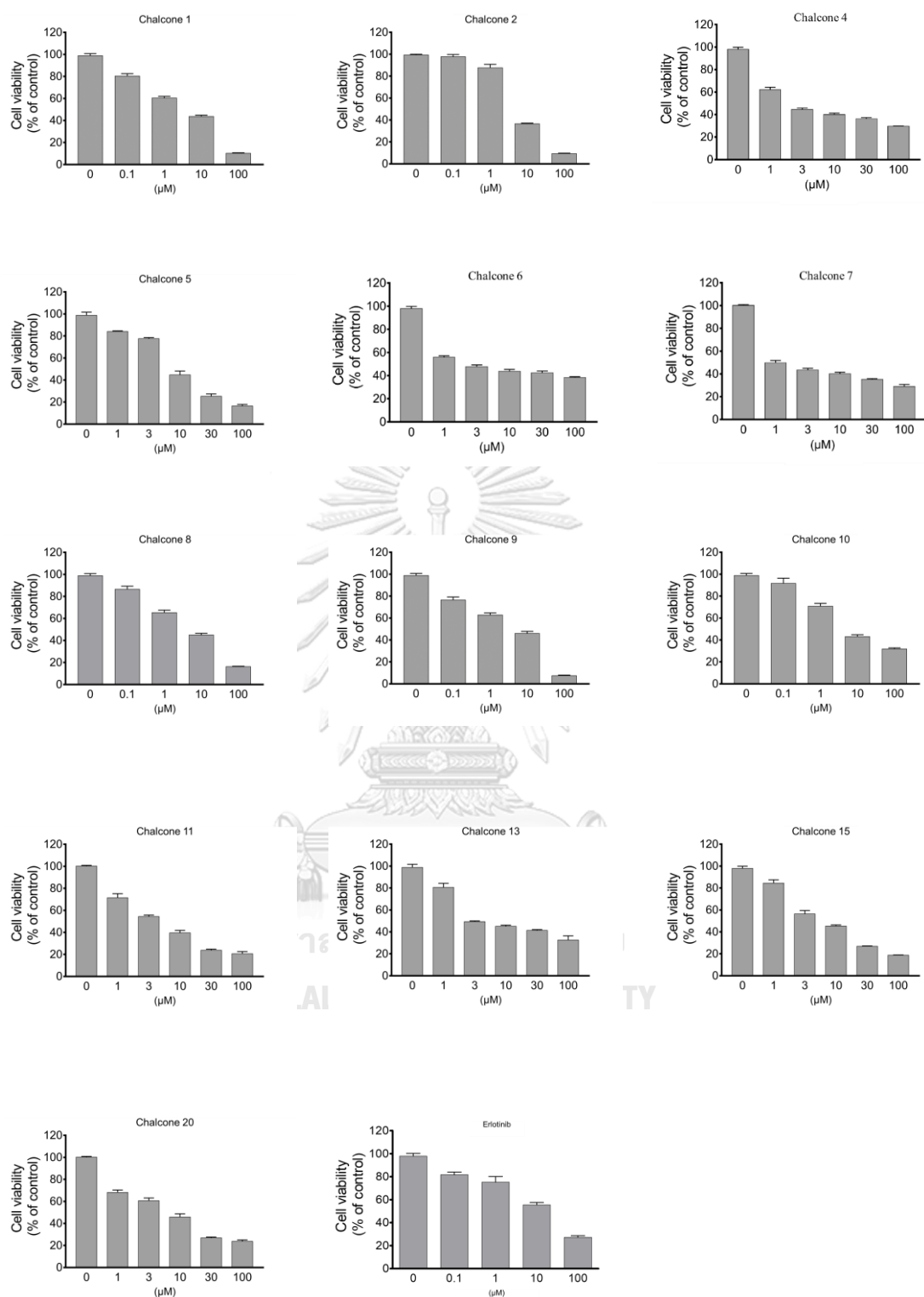


FIGURE 2.11 CYTOTOXIC ACTIVITY OF 1, 2, 4-11, 13, 15, 20, AND ERLOTINIB AGAINST A549

TABLE 2.1 IC₅₀ OF SELECTED CHALCONES AGAINST A549

| Compound | IC ₅₀ (μM) ^a | Compound | IC ₅₀ (μM) ^a |
|----------|------------------------------------|-----------|------------------------------------|
| 1 | 4.62±1.22 | 9 | 4.57±0.93 |
| 2 | 6.16±0.42 | 10 | 5.34±0.48 |
| 4 | 3.03±0.72 | 11 | 4.66±0.67 |
| 5 | 9.31±1.04 | 13 | 9.24±1.83 |
| 6 | 2.93±1.16 | 15 | 7.01±0.49 |
| 7 | 0.91±0.09 | 20 | 6.07±0.81 |
| 8 | 5.51±0.88 | erlotinib | 12.50±1.05 |

^aIC₅₀ values are expressed as mean ± SD of three independent experiments.

Derived from low IC₅₀ values of monohydroxy substituent on the B ring (**1**, **2**, except **3**) as 4.62 and 6.16 μM, the exploration of disubstituents on the B ring was conducted. Compound **4** with hydroxy and methoxy groups on the B ring also revealed high anti-cancer activity with IC₅₀ value of 3.03 μM as well as **6** bearing a methylenedioxy group with IC₅₀ value of 2.93 μM. The introduction of dimethoxy or methylenedioxy groups on the B ring at R₂ and R₃ positions (**10-11**) also showed high anti-cancer activity with IC₅₀ values of 5.34 and 4.66 μM. In addition, compounds **8-9** bearing hydroxy and methoxy groups, respectively exhibited the IC₅₀ values of 5.51 and 4.57 μM. The alteration of hydroxy to allyloxy group in **8-9** decreased their anti-cancer activity for compounds **16** and **17**. This was also observed for **18** possessing bromine and methoxy groups at R₂ and R₃ positions possibly due to steric hindrance and inductive effects. Among chalcones studied, **7** possessing dihydroxy groups at R₂ and R₃ positions exhibited the highest anti-cancer activity with IC₅₀ value of 0.91 μM; nonetheless, the activity of the hydrogenated analog (**23**) was decreased sharply (Figure 2.10), where this result was believed that inhibition mechanism is likely *via* nucleophilic addition (Michael reaction) from protein candidate(s) (like SH from cysteine) to α,β-unsaturated on chalcones.³⁴ Therefore, the presence of α,β-unsaturated ketone is vital to maintain anti-cancer activity. Among trisubstituents on the B ring (**19-22**), only **20** exhibited high potent anti-cancer activities.

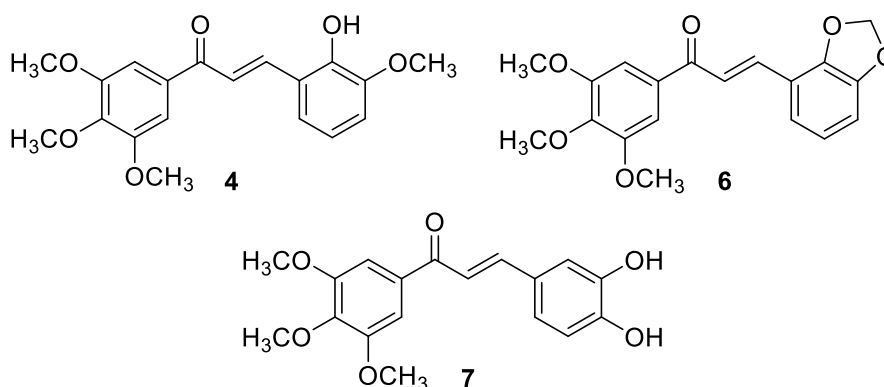


FIGURE 2.12 THREE BEST POTENT COMPOUNDS AS ANTI-LUNG CANCER

Among two chalcone series investigated, structure-activity relationship was conducted based on the substituent variables both on the A and B rings. Thirteen chalcones (**1-2**, **4-11**, **13**, **15**, **20**) exhibited high potent anti-cancer activity, where three best potent chalcones were **4**, **6**, and **7** (Figure 2.12). These findings showed that 3',4',5'-trimethoxyphenyl group on the A ring, α,β -unsaturated ketone with mono, and disubstituent on the B ring are key factors responsible to maintain anti-cancer activity against A549.

2.3.3 MOLECULAR DOCKING

Two high potent (**7** and **10**) and one less potent (**14**) anti-cancer candidates including erlotinib (Figure 2.13) as a drug standard were selected to investigate under the collaborative project with Department of Biochemistry, Faculty of Science, Chulalongkorn University, to delineate the binding mechanism against EGFR-TK (Figure 2.14). The 3D structure of EGFR-TK complex with erlotinib was obtained from Protein Data Bank (PDB: 1M17). The structure optimizations of **7**, **10**, and **14** were generated using Gaussian09 program and continued to be docked against EGFR-TK using CDOCKER application in the Accelrys Discovery Studio 2.5 program while the result of binding affinity was compared with erlotinib as reference.

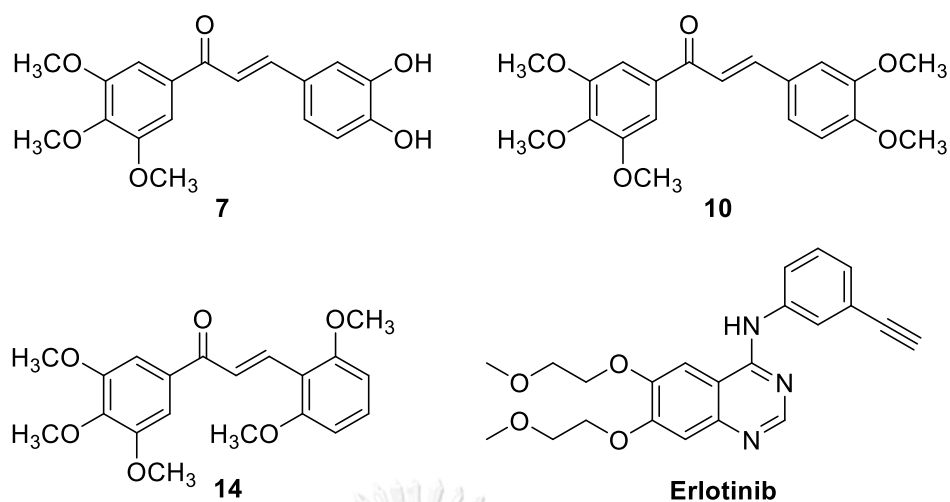


FIGURE 2.13 STRUCTURES OF 7, 10, 14, AND ERLOTINIB USED FOR DOCKING WITH EGFR-TK.

Based on the binding patterns and interactions, the B rings of all selected chalcones were observed to enter the ATP-binding pocket, whereas their trimethoxy groups on A ring located near the solvent-exposed surface in a manner like erlotinib (Figure 2.14).

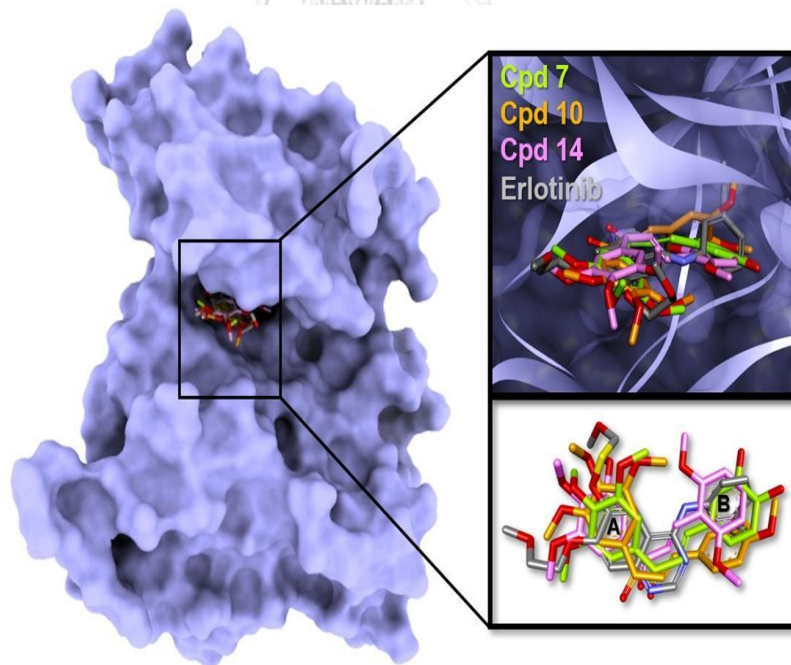


FIGURE 2.14 SUPERIMPOSITION OF DOCKED 7, 10, 14, AND ERLOTINIB AT THE ATP-BINDING POCKET OF EGFR-TK.

The molecular docking in EGFR-TK showed that all selected compounds (**7**, **10**, **14**) and erlotinib possessed one or more H-bond, hydrophobic, π -lone pair, π -alkyl, and π -sulfur interaction (Table 2.2). Compound **7** generated one H-bond between carbonyl and MET793 residue, while the A ring showed two π -alkyl interactions with LEU718, LEU844, and the B ring showed three H-bonds between two hydroxy groups with LYS745, GLU762, and ASP855 and one π -sulfur interaction with MET766 (Figure 2.13A). Compound **10** showed two H-bonds, namely carbonyl group with MET793, and the oxygen atom of the methoxy group on the B ring at R₃ position with CYS775. Moreover, the A ring of compound **10** formed two π -alkyl interactions with LEU718, LEU844, and two π -sulfur interactions with MET766, CYS775, while the B ring showed only one π -alkyl interaction with ALA743 (Figure 2.13B). Compound **14** showed one H-bond interaction between the carbonyl group and MET793, one π -alkyl of A ring with LEU718, while B ring showed one π -sulfur interaction with LYS745 and a steric clash with CYS775 due to the dimethoxy group at R₁ position (Figure 2.13C), leading to decrease in the inhibitory activity as observed for compounds **5**, **12**, **15**, **19**, **21**, and **22** all of which with an attached methoxy group at R₁ position (Figure 2.10). These results demonstrated that the hydroxy groups on the B ring at R₂ and R₃ positions were important to inhibit EGFR-TK. The hydrophobic residues (i) LYS745 and (ii) LEU718 and LEU844 were found to respectively stabilize the A and B rings of chalcones *via* π -alkyl interactions, similar to the erlotinib binding. Notably, (i) only compounds **7** and **10** were stabilized by MET766 *via* π -sulfur interaction and (ii) the α,β -unsaturated ketone group of all docked chalcones generated H-bond with MET793, whereas the N1 atom of quinazoline ring of erlotinib was stabilized by this residue instead.

TABLE 2.2 ANALYSIS OF MOLECULAR INTERACTION OF 7, 10, 14 AND ERLOTINIB IN COMPLEX WITH RESIDUES OF EGFR-TK.

| Comp. | H-bond | Alkyl | π -Alkyl | π -Sulfur | π -Lone pair |
|-----------|---|-------------------|---|-------------------|------------------|
| 7 | MET793, ASP855, GLU762, LYS745 | - | LEU718, LEU844, LYS745 | MET766 | - |
| 10 | MET793, CYS775 | - | LEU718, LEU844, ALA743 | MET766, CYS775 | THR790 |
| 14 | MET793 | - | LEU718, LYS745 | - | - |
| erlotinib | MET793 | LYS745, LEU788 | LYS745, ALA743, LEU844, LEU718 | - | - |

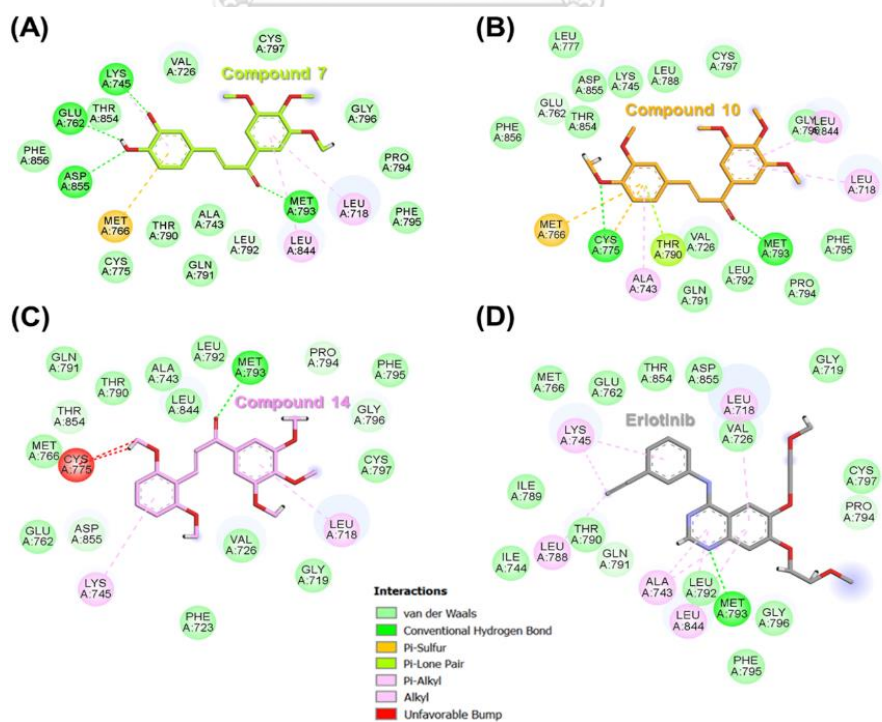


FIGURE 2.15 2D INTERACTION DIAGRAM OF (A) 7, (B) 10, (C) 14, AND (D) ERLOTINIB IN COMPLEX WITH EGFR-TK.

TABLE 2.3 DOCKING INTERACTION ENERGY (KCAL/MOL) AND H-BOND INTERACTION OF 7, 10, 14 AND ERLOTINIB IN COMPLEX WITH EGFR-TK.

| Comp. | Docking interaction energy (kcal/mol) | #H-bonding |
|------------------|--|------------|
| 7 | -48.34 | 4 |
| 10 | -45.89 | 2 |
| 14 | -43.12 | 1 |
| erlotinib | -45.52 | 1 |

Overall, the *van der Waals* contacts and H-bond interactions were key factors between chalcones and EGFR-TK complexations, and the low H-bonding and the absence of π -sulfur interaction instigated the decrease in binding affinity (Table 2.3) and cytotoxic activity of **14** against A549 (Figure 2.10). As shown in Table 2.3, the binding affinity of **7** (-48.34 kcal/mol) was significantly higher than those of **10** (-45.89 kcal/mol), **14** (-43.12 kcal/mol), and erlotinib (-45.52 kcal/mol) against EGFR-TK. The more interaction, the more stable the complex system between inhibitor and EGFR-TK was followed by the lower interaction energy, the higher binding affinity. Thus, H-bond and hydrophobic interaction via π -alkyl, and π -sulfur could be crucial molecular interactions to enhance binding affinity in inhibitor/EGFR-TK complex.^{59, 60} Thus, these results suggested that **7** has a potent ATP-competitive inhibitor against EGFR-TK. This should indicate that the docking interaction energies were in line with the IC₅₀ values (Table 2.1).

CHAPTER III

SYNTHESIS AND EVALUATION OF 3,4-DIMETHOXYCHALCONES, 2'-HYDROXYCHALCONES, AND 4'-AMINOCHALCONES AS POTENT NITRIC OXIDE INHIBITOR IN LPS-INDUCED RAW 264.7 MACROPHAGE CELLS

3.1 INTRODUCTION

Inflammation is a reaction of cells in the human body to protect itself due to infection, wounded cell, or pain. This inflammation may lead to the other effects (arthritis, cancer, and diabetes) caused by releasing various chemical initiators such as nitric oxide (NO), prostaglandins (PG), vasoactive amines (histamine and serotonin), leukotrienes (LT), and cytokines (Figure 3.1).⁶¹

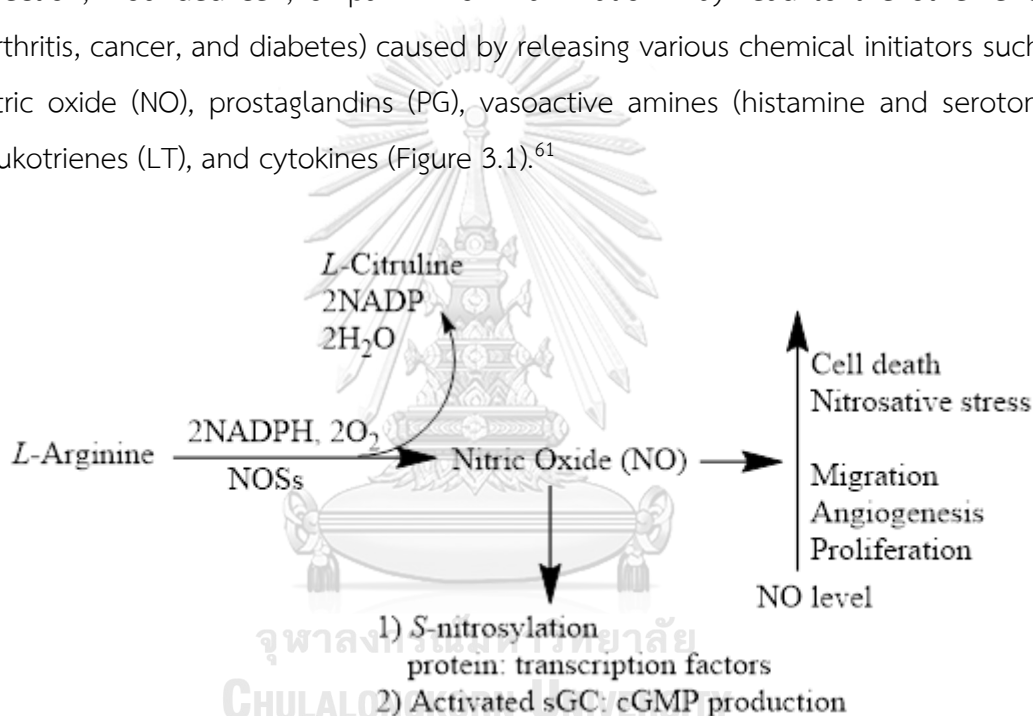


FIGURE 3.1 NITRIC OXIDE (NO) PRODUCTION AND ITS BIOLOGICAL ACTIVITY. NITRIC OXIDE SYNTHASES NOSs (ENOS, NNOS, INOS), SOLUBLE GUANYLATE CYCLASE (SGC), CYCLIC GUANIDINE MONOPHOSPHATE (CGMP), NICOTINAMIDE ADENINE DINUCLEOTIDE PHOSPHATE (NADPH).⁶²

Macrophages are important players in the inflammation system. Lipopolysaccharide (LPS) contained in macrophages is an irritant mainly from Gram-negative bacteria induced signal transduction such as inhibitor activation of κ B kinase (IKK) proteins that cause NF- κ B activation which controls the inflammatory expression series obtained from inducible enzyme syntheses such as COX-2 (cyclooxygenase-2)

and iNOSs (inducible nitric oxide synthase).⁶³ L-arginine generates NO catalyzed by nitric oxide synthases (NOSs), where NO is very necessary for host innate immune feedback to pathogens, such as bacteria, viruses, fungi, and parasites.⁶⁴ However, over production of NO causes cell damage and toxic to the host that is recognized to induce diseases, such as septic shock, autoimmune diseases, cerebral infarction, and diabetes mellitus.^{65, 66} Therefore, the inhibition of NO production is proposed as the potential target to discovery anti-inflammatory candidates. The usage of non-steroidal anti-inflammatory (NSAIDs) for inflammatory therapy has been approved. However, NSAIDs still cause adverse effect for long-term treatment.⁶⁷

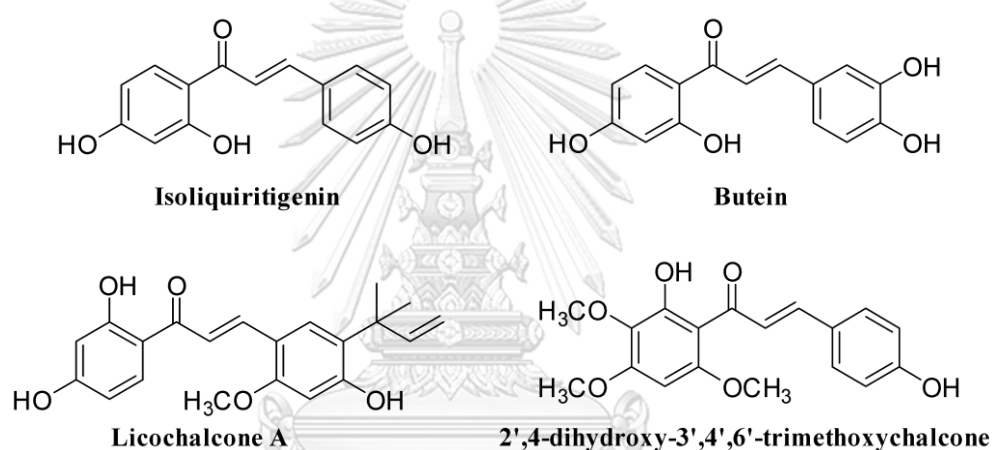


FIGURE 3.2 NATURAL ANTI-INFLAMMATORY CHALCONES

Several chalcones have shown potency as anti-inflammatory agents such as isoliquiritigenin, butein, licochalcone A, and 2',4-dihydroxy-3',4',6'-trimethoxychalcone (Figure 3.2).⁶⁸⁻⁷¹ 4'-Aminochalcones exhibited an edema effect in carrageenan-induced rat paw,⁷² while isoindoline chalcones and pyrazole derivatives also showed COX-2 inhibitory activity and anti-edema in formalin-induced rat paw assay.⁷³ Bist *et al* reported that the hydroxy group on the A ring and the trifluoromethoxy group on the B ring attached on the chalcone structure presented a strong inhibitory activity in LPS-induced ROS (reactive oxygen species) production in RAW 264.7 macrophages.⁷⁴ Moreover, Shrestha *et al* investigated 2-benzylidene-indanones; the results showed that the hydroxy group on the indanone moiety and the halogen group on the arene

ring strongly inhibited ROS production in LPS-induced RAW 264.7 macrophages through modulation of NADPH oxidase.⁷⁵ Boshra *et al* reported that 2'-hydroxychalcone-triazole hybrids expressed a double inhibition of COX-2 and 15-LOX and anti-edema effect in carrageenan-induced rat paw assay.⁷⁶ Yang *et al* reported that 2'-hydroxy-4',6'-dimethoxychalcone derivatives containing morpholine moiety displayed potency as NO inhibitors through down-regulator module of inducible nitric oxide synthase (iNOS) with low cytotoxicity.⁷⁷ The list of compounds was presented in Figure 3.3.

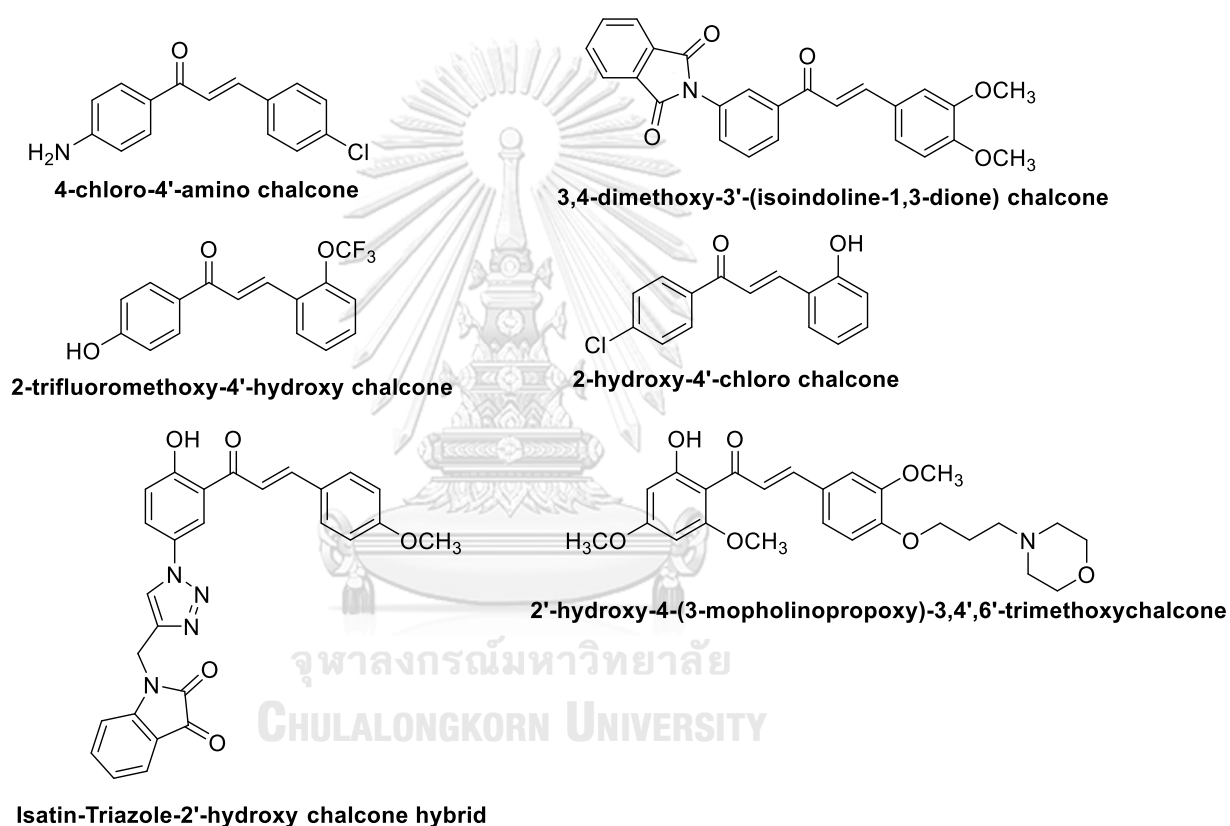


FIGURE 3. 3 SYNTHETIC ANTI-INFLAMMATORY CHALCONES

Thus, the objective of this study was to evaluate three chalcone series, namely 3,4-dimethoxychalcones, 2'-hydroxychalcones, and 4'-aminochalcones regarding NO inhibition in lipopolysaccharide (LPS)-stimulated RAW 264.7 macrophage cells and their cytotoxicity. The structure-activity relationship exploration was conducted to obtain a clue for important pharmacophore as anti-inflammatory candidates.

3.2 MATERIALS AND METHODS

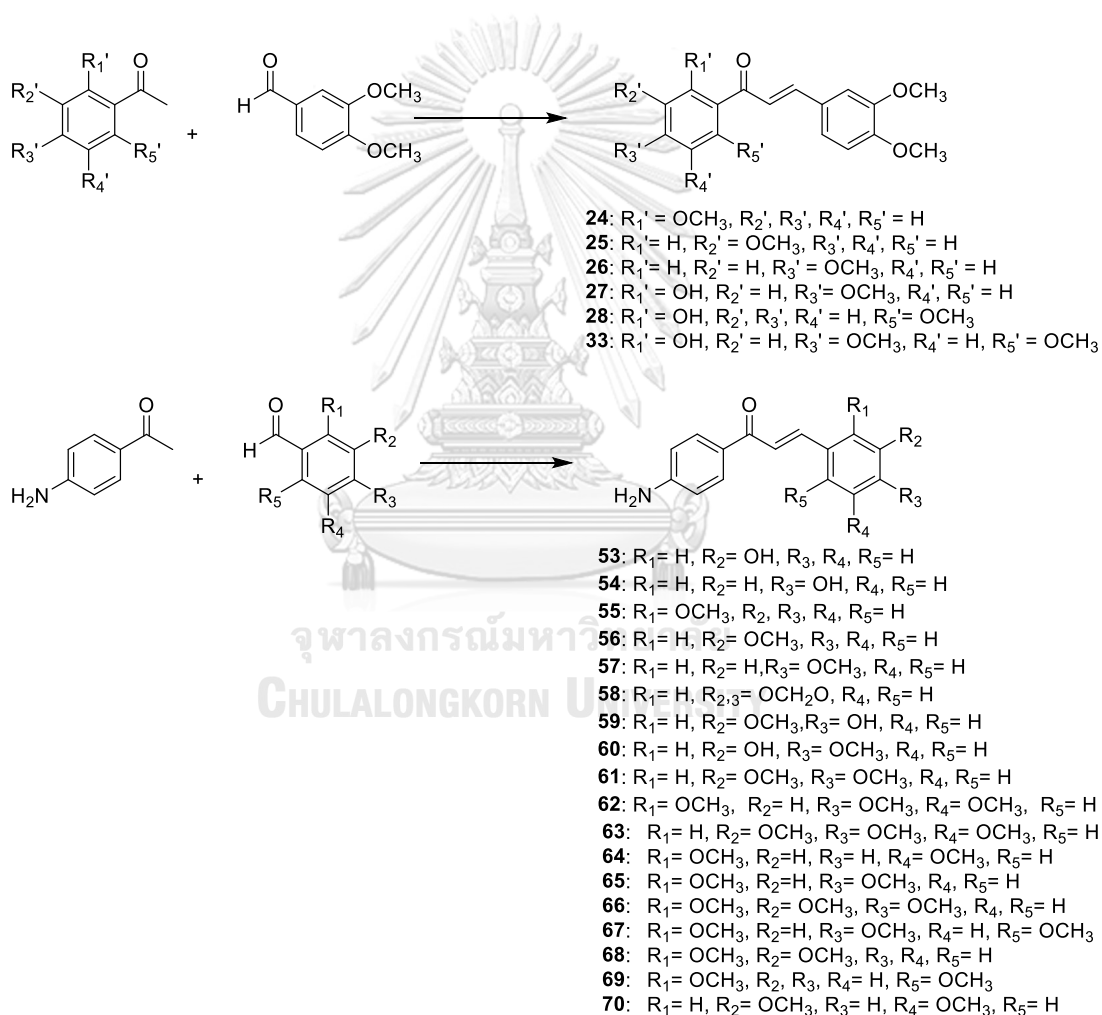
3.2.1 MATERIALS

Equipments and chemicals used are the same as those described in Chapter 2.

3.2.2 METHODS

3.2.2.1 SYNTHESIS OF 3,4-DIMETHOXYCHALCONE SERIES (24-28, 33) AND 4'-AMINOCHALCONE SERIES (53-70)

A method similar to that for 2.2.2.1 was also employed.



(*E*)-3-(3,4-dimethoxyphenyl)-1-(2-methoxyphenyl)prop-2-en-1-one (**24**)

Yellow liquid; yield 89%. ^1H NMR (400 MHz, CDCl_3) δ = 7.57 (dd, J = 7.6, 1.6 Hz, 1H), 7.53 (d, J = 15.6 Hz, 1H), 7.45 (td, J = 8.8, 2.0 Hz, 1H), 7.20 (d, J = 15.6 Hz, 1H), 7.16 (dd, J = 8.0, 1.6 Hz, 1H), 7.01 (s, 1H), 7.04 (t, J = 8.0 Hz, 1H), 7.00 (d, J = 8.4 Hz, 1H), 6.86 (d,

$J = 8.4$ Hz, 1H), 3.91 (s, 6H), 3.88 (s, 3H). ^{13}C NMR (100 MHz, CDCl_3) $\delta = 193.3, 158.0, 151.4, 149.3, 143.9, 132.6, 130.2, 129.7, 128.2, 125.4, 123.0, 120.8, 111.8, 111.3, 110.4, 56.1, 56.0, 55.9$.

(*E*)-3-(3,4-dimethoxyphenyl)-1-(3-methoxyphenyl)prop-2-en-1-one (**25**)

Yellow liquid; yield 82%. ^1H NMR (400 MHz, CDCl_3) $\delta = 7.76$ (d, $J = 15.6$ Hz, 1H), 7.59 (d, $J = 8.8$ Hz, 1H), 7.53 (s, 1H), 7.40 (t, $J = 8.0$ Hz, 1H), 7.36 (d, $J = 15.6$ Hz, 1H), 7.22 (dd, $J = 8.4, 2.0$ Hz, 1H), 7.15 (d, $J = 2.0$ Hz, 1H), 7.11 (dd, $J = 8.0, 1.6$ Hz, 1H), 6.89 (d, $J = 8.4$ Hz, 1H), 3.94 (s, 3H), 3.92 (s, 3H), 3.87 (s, 3H). ^{13}C NMR (100 MHz, CDCl_3) $\delta = 190.4, 160.0, 151.6, 149.4, 145.2, 140.0, 129.6, 128.0, 123.3, 121.1, 120.3, 119.1, 113.1, 111.3, 110.4, 56.1, 55.6$.

(*E*)-3-(3,4-dimethoxyphenyl)-1-(4-methoxyphenyl)prop-2-en-1-one (**26**)

Yellow liquid; yield 99%. ^1H NMR (400 MHz, CDCl_3) $\delta = 8.02$ (d, $J = 8.8$ Hz, 2H), 7.74 (d, $J = 15.6$ Hz, 1H), 7.39 (d, $J = 14.8$ Hz, 1H), 7.21 (dd, $J = 8.4, 2.0$ Hz), 7.14 (s, 1H), 6.96 (d, $J = 8.8$ Hz, 2H), 6.87 (d, $J = 8.0$ Hz, 1H), 3.93 (s, 3H), 3.90 (s, 3H), 3.86 (s, 3H). ^{13}C NMR (100 MHz, CDCl_3) $\delta = 188.8, 163.4, 151.4, 149.4, 144.2, 131.4, 130.8, 128.2, 123.0, 119.9, 113.9, 111.3, 110.3, 56.1, 55.5$.

(*E*)-3-(3,4-dimethoxyphenyl)-1-(2-hydroxy-4-methoxyphenyl)prop-2-en-1-one (**27**)

Yellow powder; yield 12%. ^1H NMR (400 MHz, CDCl_3) $\delta = 13.54$ (br s, OH), 7.84 (d, $J = 14.8, 8.8$ Hz, 2H), 7.42 (d, $J = 15.2$ Hz, 1H), 7.24 (dd, $J = 8.4, 2.0$, 1H), 7.15 (d, $J = 2.0$ Hz, 1H), 6.89 (d, $J = 8.0$ Hz, 1H), 6.48 (dd, $J = 8.4, 2.0$ Hz, 2H), 3.95 (s, 3H), 3.93 (s, 3H), 3.85 (s, 3H). ^{13}C NMR (100 MHz, CDCl_3) $\delta = 191.9, 166.8, 166.2, 151.7, 149.5, 144.7, 131.2, 127.9, 123.4, 118.2, 114.3, 111.4, 110.5, 107.7, 101.2, 56.2, 55.7$.

(*E*)-3-(3,4-dimethoxyphenyl)-1-(2-hydroxy-6-methoxyphenyl)prop-2-en-1-one (**28**)

Orange powder; yield 36%. ^1H NMR (400 MHz, CDCl_3) $\delta = 13.24$ (br s, OH), 7.79 (d, $J = 15.6$, 1H), 7.78 (d, $J = 15.2$ Hz, 1H), 7.34 (t, $J = 8.4$ Hz, 1H), 7.22 (dd, $J = 8.0, 2.0$ Hz, 1H), 7.13 (d, $J = 2.0$, 1H), 6.90 (d, $J = 8.0$ Hz, 1H), 6.61 (d, $J = 8.0$ Hz, 1H), 6.42 (d, $J = 8.0$ Hz, 1H), 3.93 (t, 9H). ^{13}C NMR (101 MHz, CDCl_3) $\delta = 194.3, 164.9, 161.0, 151.5, 149.3, 143.4, 135.7, 128.5, 125.6, 122.9, 112.2, 111.4, 111.1, 110.7, 101.7, 56.1, 56.0$.

(*E*)-3-(3,4-dimethoxyphenyl)-1-(2-hydroxy-4,6-dimethoxyphenyl)prop-2-en-1-one (**33**)

Orange powder; yield 21%. ^1H NMR (400 MHz, CDCl_3) $\delta = 7.77$ (d, $J = 15.2$ Hz), 7.76 (d, $J = 15.6$ Hz, 1H), 7.20 (d, $J = 8.4, 2.0$ Hz, 1H), 7.11 (d, $J = 2.0$ Hz, 1H), 6.88 (d, $J = 8.4$ Hz,

1H), 6.09 (d, $J = 2.4$ Hz, 1H), 5.95 (d, $J = 2.4$ Hz, 1H), 3.93 (s, 3H), 3.91 (s, 3H), 3.89 (s, 3H), 3.82 (s, 3H). ^{13}C NMR (100 MHz, CDCl_3) $\delta = 192.5, 168.5, 166.2, 162.5, 151.2, 149.3, 142.7, 128.7, 125.6, 122.7, 111.4, 110.7, 106.5, 94.0, 91.4, 56.1, 55.9, 55.9, 55.6$.

(*E*)-1-(4-aminophenyl)-3-(3-hydroxyphenyl)prop-2-en-1-one (**53**)

Orange powder; yield 47%. ^1H NMR (400 MHz, $\text{DMSO}-d_6$) $\delta = 9.50$ (s, 1H), 7.82 (d, $J = 8.4$ Hz, 2H), 7.67 (d, $J = 15.6$ Hz, 1H), 7.44 (d, $J = 15.6$ Hz, 1H), 7.16 (d, $J = 7.2$ Hz, 2H), 7.09 (s, 1H), 6.55 (d, $J = 8.8$ Hz, 2H), 6.06 (s, 2H). ^{13}C NMR (100 MHz, $\text{DMSO}-d_6$) $\delta = 185.9, 157.6, 153.8, 141.6, 136.4, 131.0, 129.8, 125.4, 122.3, 119.4, 117.1, 114.9, 112.7$.

(*E*)-1-(4-aminophenyl)-3-(4-hydroxyphenyl)prop-2-en-1-one (**54**)

Yellow powder; yield 3%. ^1H NMR (400 MHz, acetone- d_6) $\delta = 9.15$ (s, OH), 7.94 (d, $J = 8.8$ Hz, 2H), 7.65 (dd, $J = 8.4, 3.2$ Hz, 4H), 6.90 (d, $J = 8.8$ Hz, 2H), 6.73 (d, $J = 8.4$ Hz, 2H). ^{13}C NMR (100 MHz, acetone- d_6) $\delta = 187.4, 160.4, 154.1, 142.9, 131.6, 131.0, 128.1, 119.9, 116.7, 114.0$.

(*E*)-1-(4-aminophenyl)-3-(2-methoxyphenyl)prop-2-en-1-one (**55**)

Yellow powder; yield 85%. ^1H NMR (400 MHz, $\text{DMSO}-d_6$) $\delta = 7.89$ (d, $J = 15.6$ Hz, 1H), 7.85 (dd, $J = 8.8, 2.4$ Hz, 2H), 7.75 (d, $J = 15.6$ Hz, 1H), 7.35 (td, $J = 8.4, 1.6$ Hz, 1H), 7.03 (d, $J = 8.4$ Hz, 1H), 6.96 (t, $J = 7.6$ Hz, 1H), 6.58 (d, $J = 8.4$ Hz, 2H), 6.07 (s, 2H), 3.83 (s, 3H). ^{13}C NMR (100 MHz, $\text{DMSO}-d_6$) $\delta = 186.1, 157.9, 153.7, 135.9, 131.5, 130.9, 128.1, 125.5, 123.5, 122.3, 120.6, 112.7, 111.7, 55.6$.

(*E*)-1-(4-aminophenyl)-3-(3-methoxyphenyl)prop-2-en-1-one (**56**)

Yellow powder; yield 67%. ^1H NMR (500 MHz, $\text{DMSO}-d_6$) $\delta = 7.95$ (d, $J = 8.5$ Hz, 2H), 7.87 (d, $J = 15.5$ Hz, 1H), 7.59 (d, $J = 15.5$ Hz, 1H), 7.43 (s, 1H), 7.38 (d, $J = 8.0$ Hz, 2H), 7.34 (t, $J = 8.0$ Hz, 1H), 6.99 (dd, $J = 2.5, 1.0$ Hz, 1H), 6.97 (dd, $J = 2.5, 1.0$ Hz, 1H), 6.64 (d, $J = 8.5$ Hz, 2H), 3.82 (s, 3H). ^{13}C NMR (125 MHz, $\text{DMSO}-d_6$) $\delta = 185.9, 159.7, 153.7, 141.5, 136.6, 131.2, 129.8, 125.5, 122.7, 121.3, 116.1, 113.0, 112.9, 55.3$.

(*E*)-1-(4-aminophenyl)-3-(4-methoxyphenyl)prop-2-en-1-one (**57**)

Yellow powder; yield 84%. ^1H NMR (400 MHz, $\text{DMSO}-d_6$) $\delta = 7.86$ (d, $J = 8.8$ Hz, 2H), 7.73 (d, $J = 8.8$ Hz, 2H), 7.67 (d, $J = 15.6$ Hz, 1H), 7.54 (d, $J = 15.6$ Hz, 1H), 6.94 (d, $J = 8.8$ Hz, 2H), 6.57 (d, $J = 8.8$ Hz, 2H), 6.05 (s, 2H), 3.75 (s, 3H). ^{13}C NMR (100 MHz, $\text{DMSO}-d_6$) $\delta = 185.9, 160.8, 153.6, 141.3, 130.9, 130.2, 127.8, 125.6, 119.9, 114.3, 112.7, 55.3$.

(*E*)-1-(4-aminophenyl)-3-(benzo[d][1,3]dioxol-5-yl)prop-2-en-1-one (**58**)

Yellow powder; yield 61%. ^1H NMR (400 MHz, $\text{DMSO-}d_6$) δ = 7.87 (d, J = 8.4 Hz, 1H), 7.68 (d, J = 15.2 Hz, 1H), 7.54 (s, 1H), 7.49 (d, J = 15.6 Hz, 1H), 7.19 (d, J = 8.4 Hz, 1H), 6.90 (d, J = 8.0 Hz, 1H), 6.56 (d, J = 8.4 Hz, 2H), 6.05 (s, 2H), 6.03 (s, 2H). ^{13}C NMR (100 MHz, $\text{DMSO-}d_6$) δ = 185.7, 153.5, 147.8, 141.2, 130.8, 129.5, 125.3, 124.8, 120.3, 112.5, 108.2, 106.5, 101.3, 49.0.

(*E*)-1-(4-aminophenyl)-3-(4-hydroxy-3-methoxyphenyl)prop-2-en-1-one (**59**)

Brown powder; yield 7%. ^1H NMR (500 MHz, acetone- d_6) δ = 7.93 (d, J = 9.0 Hz, 2H), 7.69 (d, J = 15.0 Hz, 1H), 7.64 (d, J = 15.5 Hz, 1H), 7.45 (d, J = 2.0 Hz, 1H), 7.25 (dd, J = 8.0, 2.5 Hz, 1H), 6.88 (d, J = 8.0 Hz, 1H), 6.73 (d, J = 9.0 Hz, 2H), 5.50 (s, 2H), 3.93 (s, 3H). ^{13}C NMR (125 MHz, acetone- d_6) δ = 187.2, 154.1, 149.8, 148.7, 143.3, 131.6, 128.6, 128.1, 123.9, 120.2, 116.1, 113.9, 111.7, 56.4.

(*E*)-1-(4-aminophenyl)-3-(3-hydroxy-4-methoxyphenyl)prop-2-en-1-one (**60**)

Yellow powder; yield 42%. ^1H NMR (400 MHz, $\text{DMSO-}d_6$) δ = 9.06 (s, 1H), 7.84 (d, J = 8.4 Hz, 2H), 7.56 (d, J = 15.6 Hz, 1H), 7.44 (d, J = 15.2 Hz, 1H), 7.22 (s, 1H), 7.17 (d, J = 8.4 Hz, 1H), 6.91 (d, J = 8.4 Hz, 1H), 6.56 (d, J = 8.4 Hz, 2H), 6.04 (s, 2H), 3.77 (s, 3H). ^{13}C NMR (100 MHz, $\text{DMSO-}d_6$) δ = 185.9, 153.6, 149.7, 146.6, 141.8, 130.8, 128.1, 125.6, 121.3, 119.8, 114.6, 112.7, 111.9, 55.7.

(*E*)-1-(4-aminophenyl)-3-(3,4-dimethoxyphenyl)prop-2-en-1-one (**61**)

Yellow powder; yield 46%. ^1H NMR (400 MHz, $\text{DMSO-}d_6$) δ = 7.90 (d, J = 8.4 Hz, 2H), 7.72 (d, J = 15.6 Hz, 1H), 7.54 (d, J = 15.6 Hz, 1H), 7.45 (s, 1H), 7.27 (d, J = 8.4 Hz, 1H), 6.95 (d, J = 8.4 Hz, 1H), 6.59 (d, J = 8.4 Hz, 2H), 6.06 (s, 2H), 3.82 (s, 3H), 3.76 (s, 3H). ^{13}C NMR (100 MHz, $\text{DMSO-}d_6$) δ = 185.9, 153.6, 150.7, 149.0, 141.8, 130.9, 128.0, 125.6, 123.2, 120.0, 112.7, 111.6, 110.6, 55.7, 55.6.

(*E*)-1-(4-aminophenyl)-3-(2,4,5-trimethoxyphenyl)prop-2-en-1-one (**62**)

Orange powder; yield 69%. ^1H NMR (400 MHz, $\text{DMSO-}d_6$) δ = 7.85 (dd, J = 15.6 Hz, 8.8 Hz, 3H), 7.62 (d, J = 15.6 Hz, 1H), 7.40 (s, 1H), 6.65 (s, 1H), 6.55 (d, J = 8.4 Hz, 2H), 3.80 (s, 3H), 3.78 (s, 3H), 3.74 (s, 3H). ^{13}C NMR (100 MHz, $\text{DMSO-}d_6$) δ = 186.2, 153.7, 153.5, 152.2, 143.1, 136.0, 130.8, 125.8, 119.3, 114.9, 112.7, 111.0, 97.7, 56.4, 55.8.

(*E*)-1-(4-aminophenyl)-3-(3,4,5-trimethoxyphenyl)prop-2-en-1-one (**63**)

Orange powder; yield: 99%. ^1H NMR (400 MHz, CDCl_3) δ = 7.92 (d, J = 8.8 Hz, 2H), 7.68 (d, J = 15.6 Hz, 1H), 7.43 (d, J = 15.6 Hz, 1H), 6.84 (s, 2H), 6.69 (d, J = 8.4 Hz, 2H), 3.91

(s, 6H), 3.88 (s, 3H). ^{13}C NMR (100 MHz, CDCl_3) δ = 188.2, 153.6, 151.3, 143.4, 131.2, 130.9, 128.6, 121.5, 114.0, 105.7, 61.1, 56.4.

(*E*)-1-(4-aminophenyl)-3-(2,5-dimethoxyphenyl)prop-2-en-1-one (**64**)

Yellow liquid; yield 42%. ^1H NMR (500 MHz, CDCl_3) δ = 8.04 (d, J = 16.0 Hz, 1H), 7.91 (d, J = 9.0 Hz, 2H), 7.15 (d, J = 16.0 Hz, 1H), 7.15 (d, J = 3.0 Hz, 1H), 6.91 (dd, J = 9.0, 3.0 Hz, 1H), 6.85 (d, J = 9.0 Hz, 1H), 6.71 (dt, J = 9.0 Hz, 2H), 3.84 (s, 3H), 3.80 (s, 3H). ^{13}C NMR (125 MHz, CDCl_3) δ = 188.8, 153.6, 153.3, 138.6, 131.2, 125.0, 123.2, 116.8, 114.3, 113.8, 112.6, 56.2, 55.9.

(*E*)-1-(4-aminophenyl)-3-(2,4-dimethoxyphenyl)prop-2-en-1-one (**65**)

Orange powder; yield 36%. ^1H NMR (500 MHz, $\text{DMSO}-d_6$) δ = 7.89 (d, J = 5.0 Hz, 1H), 7.86 (dd, J = 8.5, 2.0 Hz, 3H), 7.68 (d, J = 15.5 Hz, 1H), 6.63 (d, J = 8.5 Hz, 3H), 6.60 (dd, J = 8.5, 2.0 Hz, 1H), 3.88 (s, 3H), 3.82 (s, 3H). ^{13}C NMR (125 MHz, $\text{DMSO}-d_6$) δ = 186.2, 162.5, 159.6, 153.3, 136.3, 130.8, 129.6, 125.9, 119.5, 116.4, 113.0, 106.2, 98.3, 55.8, 55.5.

(*E*)-1-(4-aminophenyl)-3-(2,3,4-trimethoxyphenyl)prop-2-en-1-one (**66**)

Yellow liquid; yield 34%. ^1H NMR (500 MHz, CDCl_3) δ = 7.95 (d, J = 15.5 Hz, 1H), 7.91 (d, J = 8.5 Hz, 2H), 7.55 (d, J = 15.5 Hz, 1H), 7.36 (d, J = 8.5 Hz, 1H), 6.71 (q, J = 8.5 Hz, 3H), 3.92 (s, 3H), 3.89 (s, 3H), 3.88 (s, 3H). ^{13}C NMR (125 MHz, CDCl_3) δ = 188.7, 155.5, 153.7, 150.6, 142.6, 138.6, 131.1, 129.1, 123.8, 122.5, 121.5, 114.3, 107.7, 61.5, 61.04, 56.2.

(*E*)-1-(4-aminophenyl)-3-(2,4,6-trimethoxyphenyl)prop-2-en-1-one (**67**)

Orange powder; yield 91%. ^1H NMR (500 MHz, $\text{DMSO}-d_6$) δ = 7.97 (d, J = 16.0 Hz, 1H), 7.86 (d, J = 15.5 Hz, 1H), 7.75 (d, J = 8.5 Hz, 2H), 6.61 (d, J = 8.5 Hz, 2H), 6.31 (s, 2H), 6.04 (s, 2H), 3.91 (s, 6H), 3.85 (s, 3H). ^{13}C NMR (125 MHz, $\text{DMSO}-d_6$) δ = 187.1, 162.6, 161.0, 153.4, 132.7, 130.5, 126.1, 120.9, 112.8, 105.4, 91.0, 56.0, 55.5.

(*E*)-1-(4-aminophenyl)-3-(2,3-dimethoxyphenyl)prop-2-en-1-one (**68**)

Yellow powder; yield 44%. ^1H NMR (500 MHz, CDCl_3) δ = 8.05 (d, J = 16.0 Hz, 1H), 7.92 (d, J = 8.5 Hz, 2H), 7.60 (d, J = 16.0 Hz, 1H), 7.26 (d, J = 9.0 Hz, 1H), 7.08 (t, J = 8.0 Hz, 1H), 6.94 (dd, J = 8.0, 1.0 Hz, 1H), 6.71 (d, J = 8.5 Hz, 2H), 3.87 (s, 3H), 3.86 (s, 3H). ^{13}C NMR (125 MHz, CDCl_3) δ = 188.6, 153.3, 150.8, 148.8, 138.1, 131.2, 129.6, 128.9, 124.3, 123.7, 119.7, 114.3, 113.8, 61.4, 55.9.

(*E*)-1-(4-aminophenyl)-3-(2,6-dimethoxyphenyl)prop-2-en-1-one (**69**)

Yellow powder; yield 57%. ^1H NMR (500 MHz, $\text{DMSO-}d_6$) δ = 7.99 (d, J = 16.0 Hz, 1H), 7.98 (d, J = 16.0 Hz, 1H), 7.77 (d, J = 8.5 Hz, 1H), 7.35 (t, J = 8.5 Hz, 1H), 6.73 (d, J = 8.5 Hz, 2H), 6.63 (d, J = 8.5 Hz, 2H), 6.11 (s, 2H), 3.90 (s, 6H). ^{13}C NMR (125 MHz, $\text{DMSO-}d_6$) δ = 187.1, 159.7, 153.6, 132.4, 131.5, 130.7, 125.8, 124.1, 112.8, 111.9, 104.2, 56.0.

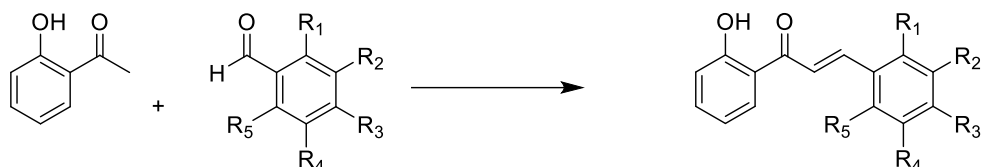
(*E*)-1-(4-aminophenyl)-3-(3,5-dimethoxyphenyl)prop-2-en-1-one (**70**)

Yellow powder; yield 11%. ^1H NMR (500 MHz, $\text{DMSO-}d_6$) δ = 7.94 (d, J = 8.5 Hz, 2H), 7.86 (d, J = 15.5 Hz, 1H), 7.54 (d, J = 15.5 Hz, 1H), 7.01 (d, J = 2.5 Hz, 2H), 6.62 (d, J = 9.0 Hz, 2H), 6.54 (t, J = 2.0 Hz, 1H), 6.2 (s, 2H), 3.80 (s, 6H). ^{13}C NMR (125 MHz, $\text{DMSO-}d_6$) δ = 185.8, 160.7, 153.9, 141.6, 137.2, 131.2, 125.3, 122.9, 112.7, 106.4, 102.3, 55.4.



3.2.2.2 SYNTHESIS OF 2'-HYDROXYCHALCONE SERIES (34-52)

A method similar to that for 2.2.2.1 was also employed.



- 34:** R₁= H, R₂= OCH₃, R₃= OC₃H₇, R₄, R₅= H
35: R₁= OCH₃, R₂= H, R₃= OCH₃, R₄= OCH₃, R₅= H
36: R₁= H, R₂= OCH₃, R₃= OCH₃, R₄= OCH₃, R₅= H
37: R₁= Oallyl, R₂= H, R₃= Oallyl, R₄= Oallyl, R₅= H
38: R₁= H, R₂= OCH₃, R₃= OCH₂OCH₃, R₄, R₅= H
39: R₁= H, R₂= OH, R₃= OH, R₄, R₅= H
40: R₁= OH, R₂, R₃, R₄, R₅= H
41: R₁= H, R₂= H, R₃= OH, R₄, R₅= H
42: R₁= OCH₃, R₂, R₃, R₄, R₅= H
43: R₁= H, R₂= H, R₃= OCH₃, R₄, R₅= H
44: R₁= H, R_{2,3}= OCH₂O, R₄, R₅= H
45: R₁= H, R₂= OCH₃, R₃= OCH₃, R₄, R₅= H
46: R₁= H, R₂= OCH₃, R₃, R₄, R₅= H
47: R₁= H, R₂= OH, R₃= OCH₃, R₄, R₅= H
48: R₁= H, R₂= OCH₃, R₃= OC₂H₅, R₄, R₅= H
49: R₁, R₂, R₃, R₄, R₅= H
50: R₁= H, R₂= OH, R₃, R₄, R₅= H

(*E*)-1-(2-hydroxyphenyl)-3-(3-methoxy-4-propoxyphenyl)prop-2-en-1-one (**34**)

Yellow powder. ¹H-NMR (400 MHz, CDCl₃) δ = 12.96 (s, 1H), 7.91 (dd, *J* = 8.4, 1.6 Hz, 1H), 7.85 (d, *J* = 15.2 Hz, 1H), 7.49 (d, *J* = 15.2 Hz, 1H), 7.45 (td, *J* = 8.4, 1.6 Hz, 1H), 7.21 (dd, *J* = 8.4, 2.0 Hz, 1H), 7.15 (d, *J* = 2.0 Hz, 1H), 7.00 (dd, *J* = 8.4, 0.8 Hz, 1H), 6.90 (td, *J* = 8.0, 0.8 Hz, 1H), 6.87 (d, *J* = 8.4 Hz, 1H), 4.00 (t, *J* = 6.8 Hz, 2H), 3.92 (s, 3H), 1.88 (sextet, *J* = 7.6 Hz, 2H), 1.04 (t, *J* = 7.6 Hz, 3H). ¹³C-NMR (100 MHz, CDCl₃) δ = 193.6, 163.6, 151.6, 149.7, 145.8, 136.1, 129.6, 127.4, 123.6, 120.1, 118.7, 118.6, 117.6, 112.5, 111.0, 70.5, 56.2, 22.4, 10.4. HR-MS (ESI) for C₁₉H₂₀O₄Na [M+Na]⁺ calcd 335.12593 found 335.12410.

(*E*)-1-(2-hydroxyphenyl)-3-(2,4,5-trimethoxyphenyl)prop-2-en-1-one (**35**)

Yellow powder. ¹H-NMR (400 MHz, CDCl₃) δ = 13.07 (s, 1H), 8.20 (d, *J* = 15.6 Hz, 1H), 7.92 (dd, *J* = 8.0, 1.2 Hz, 1H), 7.61 (d, *J* = 15.2 Hz, 1H), 7.46 (td, *J* = 8.4, 1.2 Hz, 1H), 7.12 (s, 1H), 7.00 (dd, *J* = 8.0, 0.8 Hz, 1H), 6.92 (t, *J* = 8.0, 0.8 Hz, 1H), 6.52 (s, 1H), 3.95 (s, 3H), 3.92 (s, 3H), 3.91 (s, 3H). ¹³C-NMR (100 MHz, CDCl₃) δ = 194.2, 163.6, 155.3, 153.2, 143.5, 141.0, 136.0, 129.7, 120.4, 118.7, 118.6, 118.0, 115.4, 112.1, 97.0, 56.8, 56.5, 56.2.

(*E*)-1-(2-hydroxyphenyl)-3-(3,4,5-trimethoxyphenyl)prop-2-en-1-one (**36**)

Yellow powder. $^1\text{H-NMR}$ (400 MHz, CDCl_3) δ = 12.83 (s, 1H), 7.92 (dd, J = 8.4 Hz, J = 1.2 Hz, 1H), 7.84 (d, J = 15.6 Hz, 1H), 7.53 (d, J = 15.2 Hz, 1H), 7.50 (td, J = 7.2 Hz, J = 1.6 Hz, 1H), 7.02 (dd, J = 8.4 Hz, J = 0.8 Hz, 1H), 6.94 (td, J = 8.0 Hz, J = 0.8 Hz, 1H), 6.88 (s, 2H), 3.93 (s, 6H), 3.91 (s, 3H). $^{13}\text{C-NMR}$ (100 MHz, CDCl_3) δ = 193.7, 163.7, 153.7, 145.8, 141.1, 136.5, 130.2, 129.7, 120.2, 119.4, 118.9, 118.8, 106.2, 61.1, 56.4.

(*E*)-1-(2-hydroxyphenyl)-3-(2,4,5-tris(allyloxy)phenyl)prop-2-en-1-one (**37**)

Yellow powder. $^1\text{H-NMR}$ (400 MHz, $\text{DMSO-}d_6$) δ = 12.87 (s, 1H), 8.24 (d, J = 8.0 Hz, 1H), 8.20 (d, J = 15.6 Hz, 1H), 7.87 (d, J = 15.2 Hz, 1H), 7.61 (s, 1H), 7.55 (t, J = 8.0 Hz, 1H), 7.00 (t, J = 7.6 Hz, 1H), 6.98 (d, J = 8.4 Hz, 1H), 6.78 (s, 1H), 6.09 (m, 3H), 5.44 (d, J = 17.2 Hz, 3H), 5.32 (d, J = 10.4 Hz, 1H), 5.30 (d, J = 11.2 Hz, 1H), 5.27 (d, J = 10.8 Hz, 1H), 4.68 (d, J = 4.8 Hz, 4H), 4.62 (d, J = 5.2 Hz, 2H). $^{13}\text{C-NMR}$ (100 MHz, $\text{DMSO-}d_6$) δ = 193.6, 162.2, 153.6, 152.6, 142.2, 139.5, 136.0, 134.0, 133.4, 133.2, 130.5, 120.5, 118.9, 118.1, 118.0, 117.8, 117.7, 117.4, 114.9, 113.7, 100.2, 70.0, 69.6, 69.1. HR-MS (ESI) for $\text{C}_{24}\text{H}_{24}\text{O}_5\text{Na}$ $[\text{M}+\text{Na}]^+$ calcd 415.15214 found 415.14970.

(*E*)-1-(2-hydroxyphenyl)-3-(3-methoxy-4-(methoxymethoxy)phenyl)prop-2-en-1-one

(**38**). Yellow powder. $^1\text{H-NMR}$ (400 MHz, CDCl_3) δ = 12.91 (s, 1H), 7.93 (dd, J = 8.0, 1.2 Hz, 1H), 7.87 (d, J = 15.6 Hz, 1H), 7.51 (d, J = 15.2 Hz, 1H), 7.49 (td, J = 7.8, 1.6 Hz, 1H), 7.50 (s, 1H), 7.32 (dd, J = 8.4, 2.0 Hz, 1H), 7.02 (dd, J = 8.0, 0.4 Hz, 1H), 6.95 (td, J = 8.0, 0.8 Hz, 1H), 6.94 (d, J = 8.4 Hz, 1H), 5.30 (s, 2H), 3.94 (s, 3H), 3.56 (s, 3H). $^{13}\text{C-NMR}$ (100 MHz, CDCl_3) δ = 193.8, 163.7, 152.6, 147.1, 145.6, 136.3, 129.8, 128.0, 125.0, 120.3, 118.9, 118.7, 118.3, 115.8, 111.9, 95.8, 56.5, 56.2. HR-MS (ESI) for $\text{C}_{18}\text{H}_{18}\text{O}_5\text{Na}$ $[\text{M}+\text{Na}]^+$ calcd 337.10519 found 337.10480.

(*E*)-3-(3,4-dihydroxyphenyl)-1-(2-hydroxyphenyl)prop-2-en-1-one (**39**)

Yellow powder. $^1\text{H-NMR}$ (400 MHz, $\text{acetone-}d_6$) δ = 13.08 (s, 1H), 8.43 (s, 2H), 8.22 (dd, J = 8.4, 1.6 Hz, 1H), 7.85 (d, J = 15.2 Hz, 1H), 7.79 (d, J = 15.2 Hz, 1H), 7.53 (td, J = 8.4, 1.6 Hz, 1H), 7.40 (d, J = 2.0 Hz, 1H), 7.27 (dd, J = 8.0, 2.0 Hz, 1H), 6.97 (td, J = 8.4, 1.2 Hz, 1H), 6.96 (dd, J = 8.4, 1.2 Hz, 1H), 6.93 (d, J = 8.0 Hz, 1H). $^{13}\text{C-NMR}$ (100 MHz, $\text{Acetone-}d_6$) δ = 194.8, 164.4, 149.6, 147.0, 146.4, 137.0, 131.1, 128.1, 123.9, 121.0, 119.7, 118.9, 118.1, 116.5, 116.2.

(*E*)-1,3-bis(2-hydroxyphenyl)prop-2-en-1-one (**40**)

Yellow powder. $^1\text{H-NMR}$ (400 MHz, acetone- d_6) δ = 13.03 (s, 1H), 9.51 (s, 1H), 8.33 (d, J = 15.6 Hz, 1H), 8.19 (dd, J = 8.0, 1.2 Hz, 1H), 8.07 (d, J = 15.6 Hz, 1H), 7.85 (dd, J = 7.6, 1.2 Hz, 1H), 7.55 (td, J = 8.4, 1.6 Hz, 1H), 7.31 (td, J = 8.4, 1.6 Hz, 1H), 7.03 (d, J = 8.0 Hz, 1H), 6.99 (t, J = 7.2 Hz, 1H), 6.97 (t, J = 6.4 Hz, 1H), 6.92 (d, J = 7.2 Hz, 1H). $^{13}\text{C-NMR}$ (100 MHz, Acetone- d_6) δ = 195.1, 164.2, 158.2, 141.8, 136.9, 133.0, 130.9, 130.1, 122.5, 120.8, 120.7, 120.5, 119.5, 118.7, 117.0.

(*E*)-1-(2-hydroxyphenyl)-3-(4-hydroxyphenyl)prop-2-en-1-one (**41**)

Yellow powder. $^1\text{H-NMR}$ (400 MHz, acetone- d_6) δ = 13.08 (s, 1H), 9.27 (s, 1H), 8.23 (dd, J = 8.4, 1.6 Hz, 1H), 7.91 (d, J = 15.6 Hz, 1H), 7.85 (d, J = 15.2 Hz, 1H), 7.77 (d, J = 8.8 Hz, 2H), 7.54 (td, J = 8.4, 1.6 Hz, 1H), 6.96 (m, 4H). $^{13}\text{C-NMR}$ (100 MHz, acetone- d_6) δ = 194.7, 164.3, 161.3, 146.5, 136.8, 131.9, 130.9, 127.1, 120.8, 119.5, 118.7, 117.8, 116.7.

(*E*)-1-(2-hydroxyphenyl)-3-(2-methoxyphenyl)prop-2-en-1-one (**42**)

Yellow powder. $^1\text{H-NMR}$ (400 MHz, CDCl_3) δ = 12.95 (s, 1H), 8.23 (d, J = 15.6 Hz, 1H), 7.92 (dd, J = 8.0, 1.2 Hz, 1H), 7.78 (d, J = 15.6 Hz, 1H), 7.65 (dd, J = 7.6, 0.8 Hz, 1H), 7.49 (td, J = 8.4, 1.2 Hz, 1H), 7.40 (td, J = 8.4, 1.2 Hz, 1H), 7.03 (d, J = 8.4 Hz, 1H), 7.02 (t, J = 8.0 Hz, 1H), 6.96 (d, J = 8.0 Hz, 1H), 6.94 (t, J = 7.6 Hz, 1H), 3.94 (s, 3H). $^{13}\text{C-NMR}$ (100 MHz, CDCl_3) δ = 194.5, 163.7, 159.2, 141.3, 136.2, 132.3, 129.8, 129.7, 123.8, 121.0, 120.9, 120.4, 118.9, 118.7, 111.5, 55.7.

(*E*)-1-(2-hydroxyphenyl)-3-(4-methoxyphenyl)prop-2-en-1-one (**43**)

Yellow powder. $^1\text{H-NMR}$ (400 MHz, CDCl_3) δ = 12.95 (s, 1H), 7.91 (dd, J = 8.0, 1.2 Hz, 1H), 7.90 (d, J = 15.6 Hz, 1H), 7.62 (d, J = 8.0 Hz, 2H), 7.53 (d, J = 15.2 Hz, 1H), 7.48 (td, J = 8.4, 1.6 Hz, 1H), 7.02 (d, J = 8.4 Hz, 1H), 6.95 (d, J = 8.8 Hz, 2H), 6.94 (t, J = 7.6 Hz, 1H), 3.86 (s, 3H). $^{13}\text{C-NMR}$ (100 MHz, CDCl_3) δ = 193.8, 163.7, 162.2, 145.5, 136.2, 130.6, 129.6, 127.5, 120.3, 118.9, 118.7, 117.8, 114.6, 55.6.

(*E*)-3-(benzo[d][1,3]dioxol-5-yl)-1-(2-hydroxyphenyl)prop-2-en-1-one (**44**)

Yellow powder. $^1\text{H-NMR}$ (400 MHz, CDCl_3) δ = 12.92 (s, 1H), 7.91 (dd, J = 8.0, 0.8 Hz, 1H), 7.86 (d, J = 15.2 Hz, 1H), 7.51 (td, J = 8.0, 1.6 Hz, 1H), 7.50 (d, J = 15.2 Hz, 1H), 7.19 (d, J = 1.2 Hz, 1H), 7.16 (d, J = 8.0 Hz, 1H), 7.04 (d, J = 8.0 Hz, 1H), 6.95 (t, J = 8.0 Hz, 1H), 6.87 (d, J = 8.0 Hz, 1H), 6.05 (s, 2H). $^{13}\text{C-NMR}$ (100 MHz, CDCl_3) δ = 193.6, 163.6, 150.3, 148.5, 145.3, 136.2, 129.5, 129.1, 125.7, 120.1, 118.8, 118.6, 118.0, 108.8, 106.8, 101.8.

(*E*)-3-(3,4-dimethoxyphenyl)-1-(2-hydroxyphenyl)prop-2-en-1-one (**45**)

Yellow powder. $^1\text{H-NMR}$ (400 MHz, CDCl_3) δ = 12.92 (s, 1H), 7.92 (dd, J = 8.0, 0.8 Hz, 1H), 7.87 (d, J = 15.6 Hz, 1H), 7.51 (d, J = 15.2 Hz, 1H), 7.48 (td, J = 7.2, 1.6 Hz, 1H), 7.26 (dd, J = 8.4, 1.6 Hz, 1H), 7.16 (d, J = 1.6 Hz, 1H), 7.01 (d, J = 8.4 Hz, 1H), 6.94 (dd, J = 7.2, 0.8 Hz, 1H), 6.91 (t, J = 8.4 Hz, 1H), 3.96 (s, 3H), 3.93 (s, 3H). $^{13}\text{C-NMR}$ (100 MHz, CDCl_3) δ = 193.7, 163.7, 152.0, 149.5, 145.8, 136.3, 129.6, 127.8, 123.7, 120.2, 118.8, 118.7, 118.0, 111.4, 110.6, 56.2.

(*E*)-1-(2-hydroxyphenyl)-3-(3-methoxyphenyl)prop-2-en-1-one (**46**)

Yellow powder. $^1\text{H-NMR}$ (400 MHz, CDCl_3) δ = 12.83 (s, 1H), 7.94 (d, J = 8.4 Hz, 1H), 7.91 (d, J = 16.0 Hz, 1H), 7.66 (d, J = 15.6 Hz, 1H), 7.53 (td, J = 8.0, 1.2 Hz, 1H), 7.38 (t, J = 7.6 Hz, 1H), 7.29 (d, J = 7.2 Hz, 1H), 7.19 (s, 1H), 7.06 (d, J = 8.4 Hz, 1H), 7.01 (dd, J = 8.4, 2.0 Hz, 1H), 6.97 (t, J = 7.6 Hz, 1H), 3.89 (s, 3H). $^{13}\text{C-NMR}$ (100 MHz, CDCl_3) δ = 193.7, 163.6, 160.0, 145.4, 136.4, 136.0, 130.0, 129.7, 121.3, 120.5, 120.0, 118.8, 118.6, 116.6, 113.8, 55.4.

(*E*)-3-(3-hydroxy-4-methoxyphenyl)-1-(2-hydroxyphenyl)prop-2-en-1-one (**47**)

Yellow powder. $^1\text{H-NMR}$ (400 MHz, CDCl_3) δ = 12.93 (s, 1H), 7.92 (d, J = 8.0 Hz, 1H), 7.87 (d, J = 15.2 Hz, 1H), 7.50 (d, J = 15.2 Hz, 1H), 7.48 (td, J = 7.8, 1.6 Hz, 1H), 7.25 (dd, J = 8.0, 1.2 Hz, 1H), 7.14 (s, 1H), 7.02 (d, J = 8.4 Hz, 1H), 6.97 (d, J = 8.4 Hz, 1H), 6.93 (t, J = 7.2 Hz, 1H), 6.04 (s, 1H), 3.97 (s, 3H). $^{13}\text{C-NMR}$ (100 MHz, CDCl_3) δ = 193.8, 163.7, 148.9, 147.0, 146.0, 136.3, 129.7, 127.4, 123.8, 120.3, 118.9, 118.7, 117.7, 115.2, 110.5, 56.2.

(*E*)-3-(4-ethoxy-3-methoxyphenyl)-1-(2-hydroxyphenyl)prop-2-en-1-one (**48**)

Yellow powder. $^1\text{H-NMR}$ (400 MHz, CDCl_3) δ = 12.92 (s, 1H), 7.93 (dd, J = 8.0, 1.6 Hz, 1H), 7.89 (d, J = 15.2 Hz, 1H), 7.52 (d, J = 15.6 Hz, 1H), 7.49 (td, J = 8.8, 1.6 Hz, 1H), 7.25 (dd, J = 8.4, 2.0 Hz, 1H), 7.18 (d, J = 1.6 Hz, 1H), 7.03 (d, J = 8.0 Hz, 1H), 6.94 (td, J = 8.0, 0.8 Hz, 1H), 6.91 (d, J = 8.4 Hz, 1H), 4.17 (tetra, J = 7.2 Hz, 2H), 3.96 (s, 3H), 1.50 (t, J = 7.2 Hz, 3H). $^{13}\text{C-NMR}$ (100 MHz, CDCl_3) δ = 193.8, 163.7, 151.5, 149.7, 145.9, 136.3, 129.7, 127.6, 123.7, 120.3, 118.9, 118.8, 117.9, 112.5, 111.0, 64.6, 56.3, 14.8.

(*E*)-1-(2-hydroxyphenyl)-3-phenylprop-2-en-1-one (**49**)

Yellow powder. $^1\text{H-NMR}$ (500 MHz, CDCl_3) δ = 7.93 (d, J = 15.5 Hz, 1H), 7.93 (dd, J = 8.0, 1.5 Hz, 1H), 7.67 (d, J = 15.0 Hz, 1H), 7.67 (m, 2H), 7.51 (ddd, J = 8.5, 7.0, 1.5 Hz, 1H), 7.45 (t, J = 3.0 Hz, 3H), 7.04 (dd, J = 8.0, 1.0 Hz, 1H), 6.96 (ddd, J = 8.5, 7.0, 1.5 Hz,

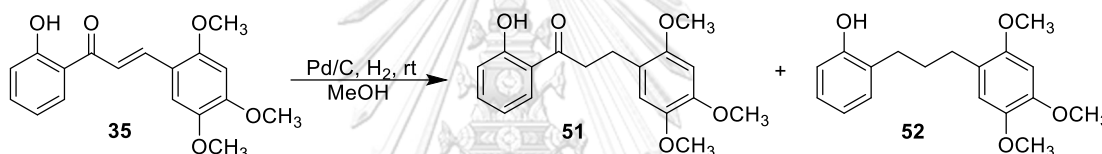
1H). ^{13}C NMR (125 MHz, CDCl_3) δ = 193.88, 163.73, 145.61, 136.56, 134.72, 131.07, 129.79, 129.18, 128.80, 120.23, 120.15, 119.00, 118.77.

(*E*)-1-(2-hydroxyphenyl)-3-(3-hydroxyphenyl)prop-2-en-1-one (**50**)

Yellow powder. ^1H -NMR (400 MHz, CDCl_3) δ = 12.79 (s, 1H), 7.92 (d, J = 8.0 Hz, 1H), 7.86 (d, J = 15.6 Hz, 1H), 7.63 (d, J = 15.6 Hz, 1H), 7.51 (t, J = 8.0 Hz, 1H), 7.31 (t, J = 7.6 Hz, 1H), 7.24 (d, J = 7.6 Hz, 1H), 7.14 (s, 1H), 7.04 (d, J = 8.0 Hz, 1H), 6.95 (t, J = 7.6 Hz, 1H), 6.92 (d, J = 7.6 Hz, 1H). ^{13}C -NMR (100 MHz, CDCl_3) δ = 193.9, 163.7, 156.2, 145.2, 136.6, 136.4, 130.4, 129.8, 121.7, 120.8, 120.2, 119.1, 118.8, 118.2, 115.0.

3.2.2.3 SYNTHESIS OF 2'-HYDROXYCHALCONE DERIVATIVES (**51** AND **52**)

A method similar to that for 2.2.2.4 was also employed.



(*E*)-1-(2-hydroxyphenyl)-3-(2,4,5-trimethoxyphenyl)propan-1-one (**51**)

^1H -NMR (400 MHz, CDCl_3) δ = 12.38 (s, 1H), 7.77 (dd, J = 8.0, 0.8 Hz, 1H), 7.45 (td, J = 8.0, 1.2 Hz, 1H), 6.98 (d, J = 8.0 Hz, 1H), 6.86 (t, J = 7.6 Hz, 1H), 6.75 (s, 1H), 6.52 (s, 1H), 3.88 (s, 3H), 3.82 (s, 3H), 3.80 (s, 3H), 3.24 (t, J = 8.0 Hz, 2H), 2.98 (t, J = 8.0 Hz, 2H). ^{13}C -NMR (100 MHz, CDCl_3) δ = 206.6, 162.6, 151.8, 148.4, 143.1, 136.3, 130.2, 120.5, 119.6, 118.9, 118.6, 114.8, 97.2, 56.9, 56.5, 56.2, 39.2, 25.8. HR-MS (ESI) for $\text{C}_{18}\text{H}_{20}\text{O}_5\text{Na}$ [$\text{M}+\text{Na}$]⁺ requires 339.12084 found 339.1204.

(*E*)-2-(3-(2,4,5-trimethoxyphenyl)propyl)phenol (**52**)

^1H -NMR (400 MHz, $\text{DMSO}-d_6$) δ = 9.24 (s, 1H), 7.03 (dd, J = 7.6, 0.8 Hz, 1H), 6.96 (td, J = 7.6, 1.2 Hz, 1H), 6.76 (d, J = 8.0 Hz, 1H), 6.74 (s, 1H), 6.69 (t, J = 7.6 Hz, 1H), 6.62 (s, 1H), 3.75 (s, 3H), 3.73 (s, 3H), 3.67 (s, 3H), 2.51 (m, 4H), 1.74 (pentet, J = 8.0 Hz, 2H). ^{13}C -NMR (100 MHz, $\text{DMSO}-d_6$) δ = 155.1, 151.2, 147.6, 142.5, 129.6, 128.3, 126.6, 121.6, 118.8, 114.8, 114.7, 98.7, 56.4, 56.2, 55.9, 29.9, 29.5, 29.0. HR-MS (ESI) for $\text{C}_{18}\text{H}_{22}\text{O}_4\text{Na}$ [$\text{M}+\text{Na}$]⁺ requires 325.14158 found 325.1395.

3.2.2.3 BIOLOGICAL ASSAY METHOD

3.2.2.3.1 CELL VIABILITY ASSAY METHOD

Cell viability was conducted under the collaborative project with Department of Microbiology, Faculty of Science, Chulalongkorn University. The assay was conducted using MTT assay method. MTT solution in PBS (0.5 mg/mL, final concentration) was added to each well and further incubated for 4 hours. The medium was discarded, and 0.04 N HCl in isopropanol (100 μ L) was added to dissolve the formazan crystals. The absorbance was measured at 540 nm, and the percent survival was determined by comparison with a control group.⁷⁸

3.2.2.3.2 ANTI-INFLAMMATORY ASSAY METHOD

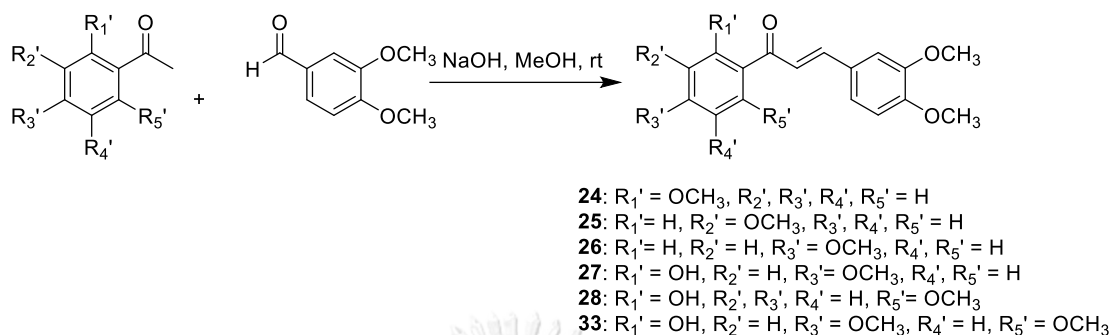
Anti-inflammatory was conducted under the collaborative project with Department of Microbiology, Faculty of Science, Chulalongkorn University. Since NO is extremely unstable and undergoes rapid oxidative degradation to nitrite (NO_2^-) and nitrate (NO_3^-), followed by the conversion of nitrate to nitrite, the amount of NO was thus indirectly determined by measuring the amount of nitrite in the cell culture supernatant using Griess reagent.⁷⁹ RAW 264.7 cells were seeded in 96-well plates at a density of 1×10^4 cells/well in 100 μ L and were incubated overnight at 37 $^\circ\text{C}$ and 5% CO_2 . Subsequently, cells were treated by various concentrations of the test compounds and vehicle (DMSO) for 2 hours, followed by LPS (100 ng/mL) and $\text{IFN}\gamma$ (10 ng/mL). After an additional 24 hours of incubation, the nitrite released in culture medium was reacted with Griess reagent, followed by incubation for 10 min under dark conditions at room temperature. The absorbance was measured at 540 nm, and the inhibitory activities were calculated from a standard calibration curve obtained from different concentrations of sodium nitrite.⁷⁸

3.3 RESULTS AND DISCUSSION

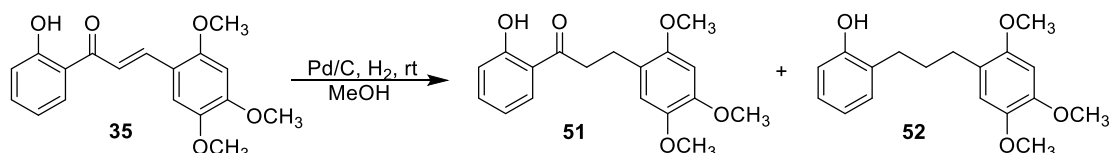
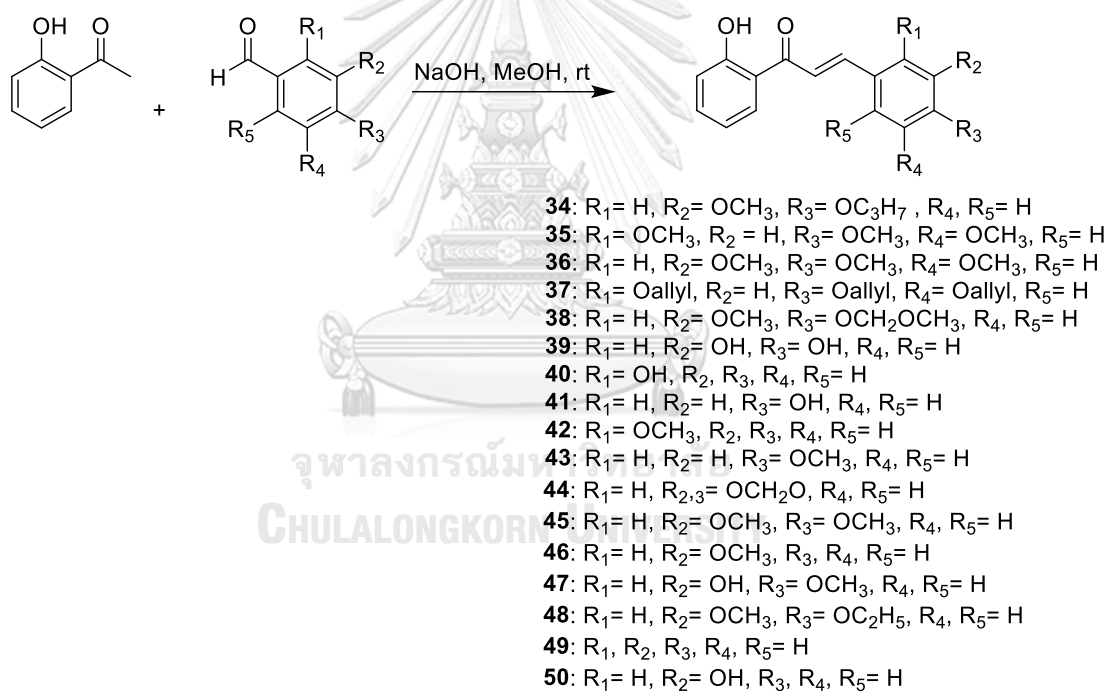
3.3.1 SYNTHESIS OF THREE CHALCONE SERIES

The synthesis of three chalcone series, namely 3,4-dimethoxychalcones (**24-28** and **33**), 2'-hydroxychalcones (**34-50**) and 4'-aminochalcones (**53-70**) were conducted using Claisen-Schmidt condensation under basic conditions as shown in Schemes 3.1-

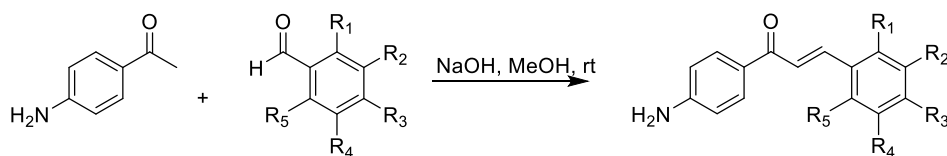
3.3. Hydrogenation of **35** catalyzed by Pd/C at room temperature was conducted and further purified by column chromatography to yield the target compounds **51** and **52**.



SCHEME 3.1 SYNTHESIS OF 3,4-DIMETHOXYCHALCONES



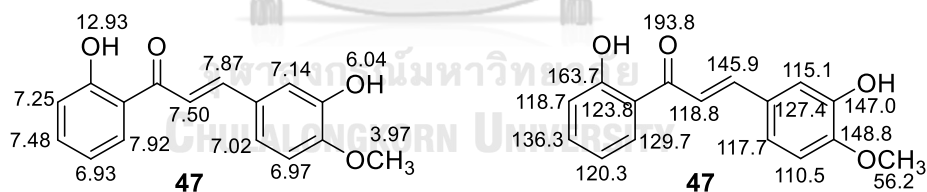
SCHEME 3.2 SYNTHESIS OF 2'-HYDROXYCHALCONES



- 53:** R₁= H, R₂= OH, R₃, R₄, R₅= H
54: R₁= H, R₂= H, R₃= OH, R₄, R₅= H
55: R₁= OCH₃, R₂, R₃, R₄, R₅= H
56: R₁= H, R₂= OCH₃, R₃, R₄, R₅= H
57: R₁= H, R₂= H, R₃= OCH₃, R₄, R₅= H
58: R₁= H, R_{2,3}= OCH₂O, R₄, R₅= H
59: R₁= H, R₂= OCH₃, R₃= OH, R₄, R₅= H
60: R₁= H, R₂= OH, R₃= OCH₃, R₄, R₅= H
61: R₁= H, R₂= OCH₃, R₃= OCH₃, R₄, R₅= H
62: R₁= OCH₃, R₂= H, R₃= OCH₃, R₄= OCH₃, R₅= H
63: R₁= H, R₂= OCH₃, R₃= OCH₃, R₄= OCH₃, R₅= H
64: R₁= OCH₃, R₂=H, R₃= H, R₄= OCH₃, R₅= H
65: R₁= OCH₃, R₂=H, R₃= OCH₃, R₄, R₅= H
66: R₁= OCH₃, R₂= OCH₃, R₃= OCH₃, R₄, R₅= H
67: R₁= OCH₃, R₂=H, R₃= OCH₃, R₄= H, R₅= OCH₃
68: R₁= OCH₃, R₂= OCH₃, R₃, R₄, R₅= H
69: R₁= OCH₃, R₂, R₃, R₄= H, R₅= OCH₃
70: R₁= H, R₂= OCH₃, R₃= H, R₄= OCH₃, R₅= H

SCHEME 3.3 SYNTHESIS OF 4'-AMINOCHALCONES

All compounds were characterized using ¹H and ¹³C NMR spectroscopic methods. To describe the structural elucidation of chalcones, **47** and **59** were selected as representatives and numbering system as in 2.3.1 section.



The ¹H NMR Spectra of **47** (Figure 3.4) showed the signal of chelated proton (H-7') at δ_{H} 12.93 (s, 1H). Four proton signals at δ_{H} 7.92 (d, J = 8.0 Hz, 1H), 7.48 (td, J = 7.8, 1.6 Hz, 1H), 7.25 (dd, J = 8.0, 1.2 Hz, 1H), and 6.93 (t, J = 7.2 Hz, 1H) belonged to those on the A ring, while three proton signals at δ_{H} 7.14 (s, 1H), 7.02 (d, J = 8.4 Hz, 1H), and 6.97 (d, J = 8.4 Hz, 1H) were on the B ring. Two doublet signals clearly revealed *trans* geometry of olefinic bond (H-7, H-8) at δ_{H} 7.87 (d, J = 15.2 Hz, 1H), and 7.50 (d, J = 15.2 Hz, 1H). The hydroxy proton on the B ring exhibited more up field at δ_{H} 6.04 (s, 1H) compared with the chelate proton (H-7') on the A ring due to the proximity to the carbonyl group, hence hydrogen bond forming. The methoxy protons were observed

at δ_{H} 3.97 (s, 3H). The ^{13}C NMR Spectra of **47** (Figure 3.5) revealed the carbonyl carbon signale at at δ_{C} 193.8, while three signals of oxygenated carbon aromatics were observed more down field at δ_{C} 163.7, 148.8, and 147.0, compared with eleven signals of sp^2 carbon at δ_{C} 145.8-110.6 and one methoxy carbon signal at δ_{C} 56.2.

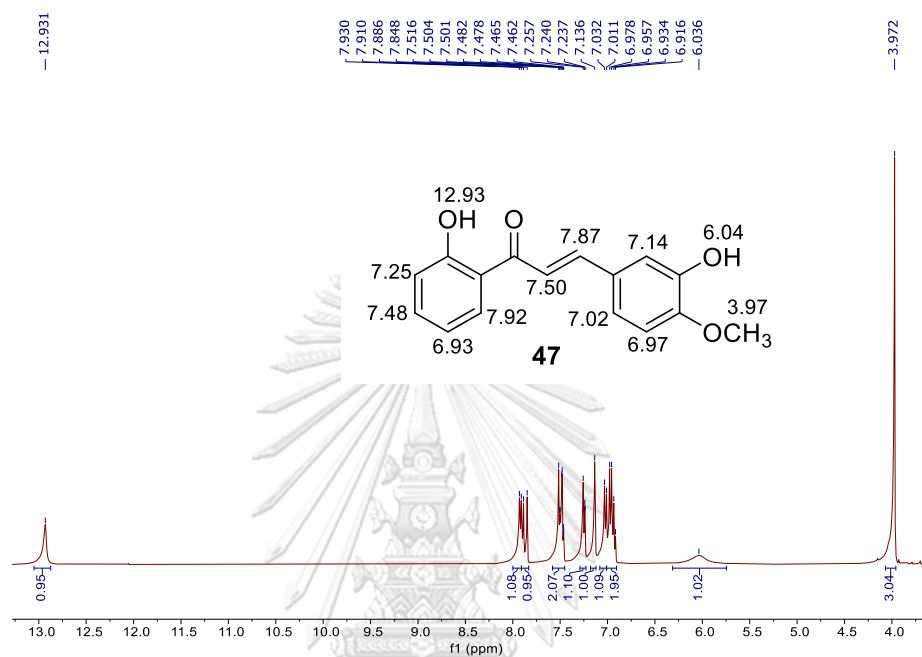


FIGURE 3.4 THE ^1H NMR SPECTRA (CDCl_3 , 400 MHZ) OF **47**

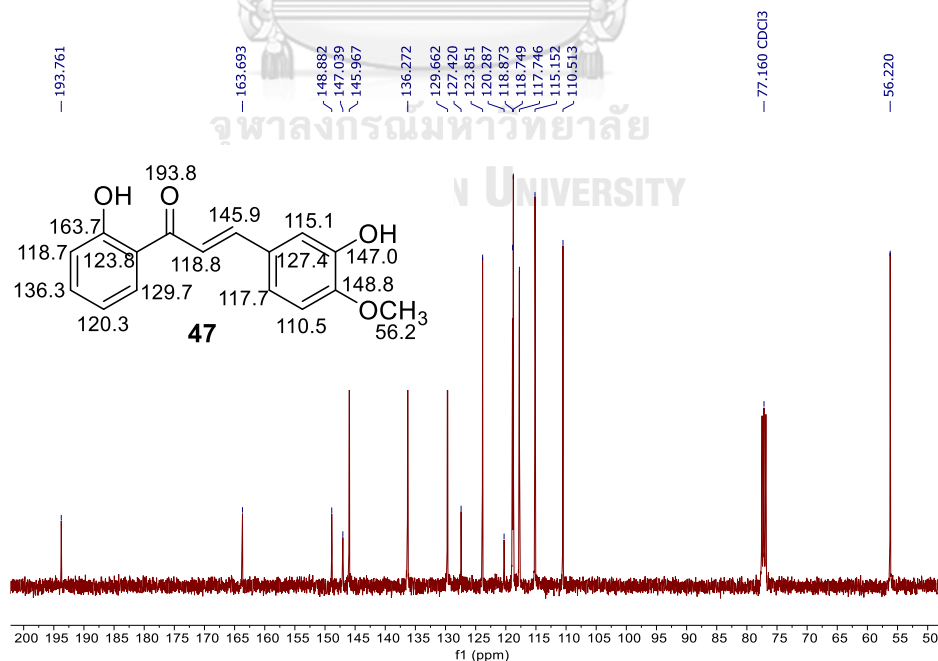
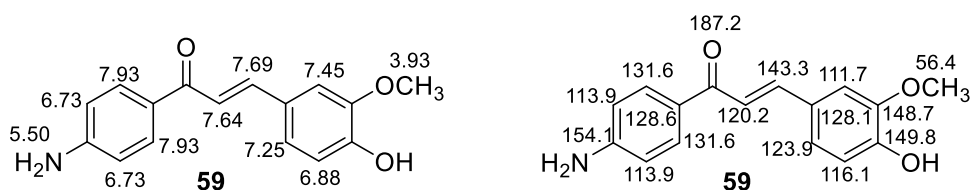


FIGURE 3.5 THE ^{13}C NMR SPECTRA (CDCl_3 , 100 MHZ) OF **47**



The ¹H NMR Spectra of of **59** (Figure 3.6) displayed *trans*-protons (H-7, H-8) at δ_H 7.69 (d, *J* = 15.0 Hz, 1H), and 7.64 (d, *J* = 15.5 Hz, 1H). Two signals were observed at δ_H 7.93 (d, *J* = 9.0 Hz, 2H), and 6.73 (d, *J* = 9.0 Hz, 2H) belonging to those on the A ring, while three signals at δ_H 7.45 (d, *J* = 2.0 Hz, 1H), 7.25 (dd, *J* = 8.0, 2.5 Hz, 1H), and 6.88 (d, *J* = 8.0 Hz, 1H) belonged to those on the B ring. Two signals were shown at δ_H 5.50 (s, 2H), and 3.93 (s, 3H) belonged to amino and methoxy groups. The ¹³C NMR Spectra of **59** (Figure 3.7) displayed the carbonyl carbon signal at δ_C 187.2. Two signals of oxygenated aromatic carbons were displayed at δ_C 149.8, and 148.7, while aromatic carbon attached to amino group on the A ring was detected more down field at δ_C 154.1. Nine sp² carbon signals were observed at δ_C 143.3-111.7, while the methoxy carbon was visualized at δ_C 56.4.

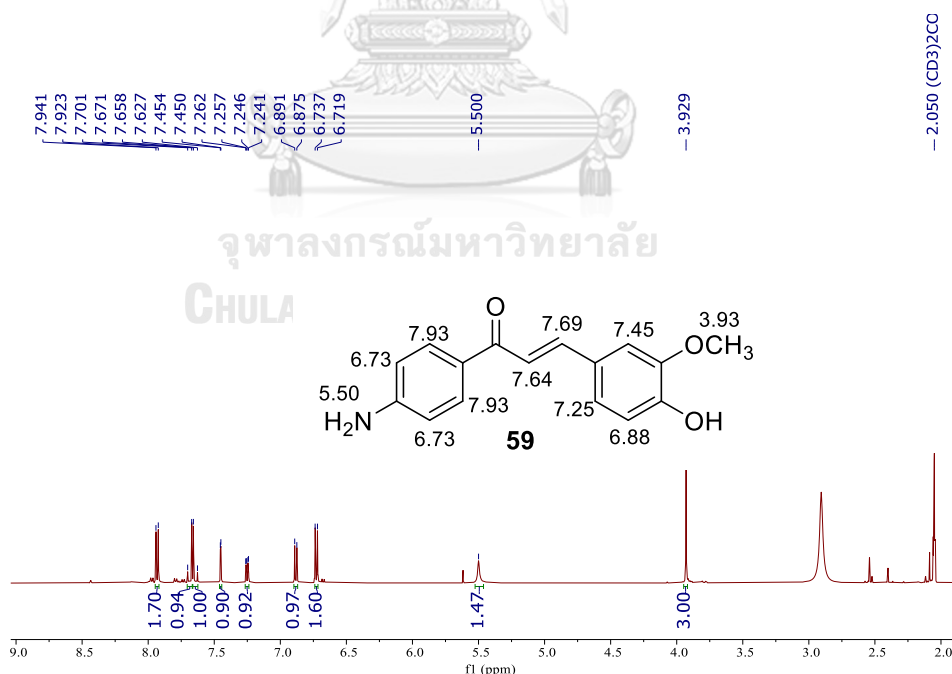


FIGURE 3.6 THE ¹H NMR SPECTRA ACETONE-*D*₆, 500 MHZ) OF **59**

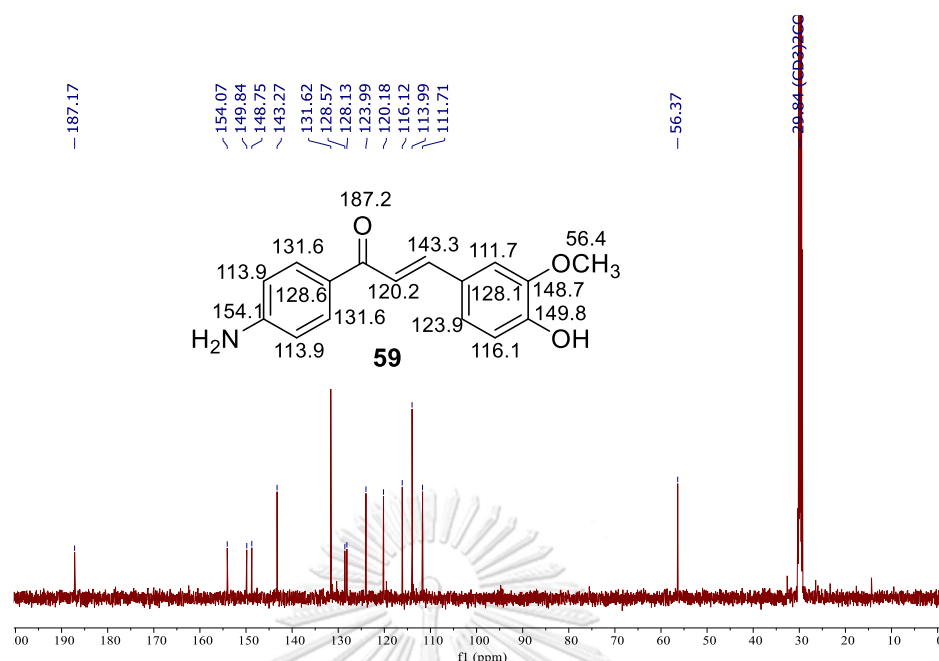


FIGURE 3.7 THE ^{13}C NMR SPECTRA (ACETONE- D_6 , 125 MHZ) OF 59

3.3.2 BIOLOGICAL EVALUATION

3.3.2.1 EFFECTS OF CHALCONES ON CELL VIABILITY IN RAW 264.7 CELLS

Cell viability is the amount of healthy cell in a sample. This assay is often used to measure cell growth in a population by the time repeatedly. In addition, the evaluation of cell death mechanism was studied by detecting whether the cell death was caused by apoptosis or necrosis. Apoptosis is responsible for cell death program to release undesired cells during normal cell growth due to cells lifespan, damage, virus infection, or stress. Necrosis is a cell death mechanism that is more premature due to infection, poison, or physical pain.⁸⁰

The cell viability activity of three chalcone series was conducted under the collaborative project with Department of Microbiology, Faculty of Science, Chulalongkorn University. Forty-three synthesized chalcones (**24-70**) were evaluated by incubating in RAW 264.7 cells at low (5 μM) and high concentrations (50 μM) to determine % cell viability using MTT assay to ensure that the NO inhibition was not due to cytotoxicity activity, respectively (Figure 3.8). This assay used LPS at 100 ng/mL for the best condition to avoid the cytotoxicity.

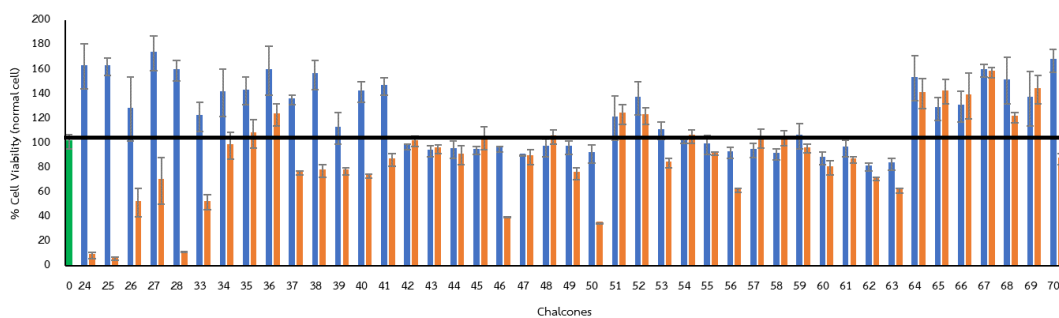


FIGURE 3.8 1) VIABILITY OF RAW 264.7 MACROPHAGE CELLS TREATED WITH THREE CHALCONE SERIES (24-70) (■ = UNTREATED CELLS, ■ = 5 μ M, ■ = 50 μ M). THE DATA WERE MEASURED AS PERCENTAGE OF CELL VIABILITY (MEAN \pm SD IN TRIPLICATE).

The figure 3.8 showed three effects of three chalcone series (24-70) on the RAW 264.7 macrophage cells, such as cytotoxic activity (<95 %), less cytotoxic activity (95-110%), and proliferation activity (> 110%).^{81, 82} Thirty-six chalcones showed cytotoxic activity including thirteen compounds (43-45, 47, 49, 50, 56-58 and 60-63) at 5 μ M and twenty-three compounds (24-28, 33, 37-41, 44, 46-47, 49, 50, 53, 59-56, 60, 62, 63 and 70) at 50 μ M. Seventeen compounds showed less cytotoxic activity including seven compounds (42, 46, 48, 54, 55, 59 and 61) at 5 μ M and ten compounds (34, 35, 42, 43, 45, 48, 54 and 57-59) at 50 μ M. Moreover, thirty-one compounds including twenty-one compounds (24-28, 33-41 and 64-70) at 5 μ M and ten compounds at 50 μ M (36, 51-53 and 64-69) had proliferative effect on the RAW 264.7 macrophage cells. In this study, the percentage of cell viability between 95-110% at 5 and 50 μ M was desirable to further determine NO inhibition due to less cytotoxicity and less proliferation activity. This finding showed that seven teen chalcones may be potent for cytoprotective in normal cells at both concentrations. Seven teen chalcones including seven compounds (42, 46, 48, 54, 55, 59 and 61) at 5 and ten compounds (34, 35, 42, 43, 45, 48, 54 and 57-59) at 50 μ M were further evaluated for anti-inflammatory activity in inhibiting NO production in LPS-induced RAW 264.7 macrophage cells.

3.3.2.2 EFFECTS OF CHALCONES ON NO INHIBITION IN LPS-INDUCED RAW 264.7 CELLS

NO is a free radical with a short half-life as chemical messenger for many physiological and pathological systems.⁸³ Thus, the overproduction of NO has been associated with cell damages.⁶⁵ The RAW 264.7 cells are from Abelson leukemia virus transformed cell line derived from BALB/c mice and have been recognized as an appropriate model of macrophage that has an ability to perform pinocytosis and phagocytosis.⁸⁴ Lipopolysaccharide (LPS) is a major component in the outer membrane of Gram-negative bacteria which may serve as the prototypical endotoxin and it connects to the Toll-like receptor 4 (TLR4) while stimulating the secretion of proinflammatory cytokines in many kinds of cells, particularly in macrophage.⁸⁵ Thus, LPS can stimulate RAW 264.7 to increase NO production and phagocytosis, where these cells have a capability to damage target cells by antibody-dependent cytotoxicity.⁸⁴ Seven teen chalcones including seven compounds (**42**, **46**, **48**, **54**, **55**, **59** and **61**) at 5 and ten compounds (**34**, **35**, **42**, **43**, **45**, **48**, **54** and **57-59**) at 50 μM were selected to study their NO inhibition activity due to less cytotoxicity and less proliferation activity (Figure 3.8). The percentage of NO inhibition of greater than 80% was deemed as desirable. The result of NO inhibition activity is presented in Figure 3.9.

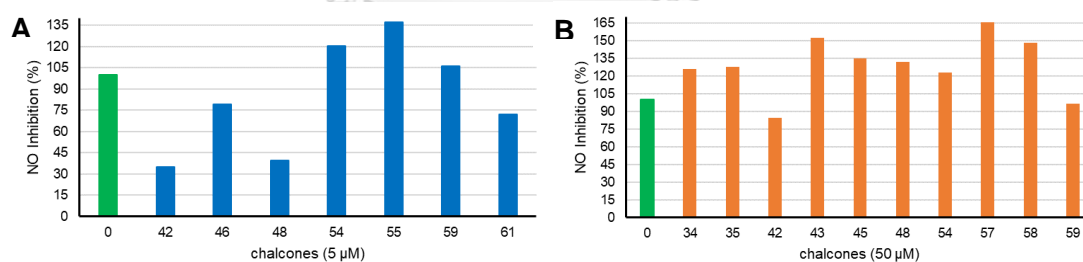


FIGURE 3.9 NITRIC OXIDE (NO) INHIBITION OF SELECTED CHALCONES IN LPS-INDUCED RAW 264.7 MACROPHAGE CELLS (■ = UNTREATED CELLS, ■ = 5 μM , ■ = 50 μM). THE DATA WERE MEASURED AS PERCENTAGE OF CELL VIABILITY (MEAN \pm SD IN TRIPPLICATE).

The evaluation of NO inhibition at 5 μM (figure 3.9) showed that three 2'-hydroxychalcones (**42**, **46** and **48**) and one 4'-aminochalcones (**61**) did not have potency for NO inhibition activity, while three 4'-aminochalcones (**54**, **55** and **59**) inhibited NO production more than 80%. Moreover, the evaluation of NO inhibition at

50 μM (figure 3.9) showed that six 2'-hydroxychalcones (**34**, **35**, **42**, **43**, **45** and **48**) and four 4'-aminochalcones (**54**, **57**, **58** and **59**) showed NO inhibition activity more than 80%. From this result demonstrated that 2'-hydroxychalcones showed NO inhibition activity at high concentration, while 4'-aminochalcones displayed NO inhibition activity at both concentrations.

Based on the results, six 2'-hydroxychalcones (**34**, **35**, **42**, **43**, **45** and **48**) only exhibited NO inhibition activity at high concentration. The result showed that most methoxy groups on the B ring including unsaturated ketone as bridge are important moieties to enhance NO inhibition activity. This result suggested that the inhibition mechanism of inflammation was caused by Michael addition (such as thiol from cysteine) to α,β -unsaturated ketone (chalcones).⁸⁶⁻⁸⁸ This result indicated that 2'-hydroxychalcones may be good candidate for further study to investigate the inhibition mechanism.

Moreover, three 4'-aminochalcones (**54**, **55** and **59**) at low concentration and four 4'-aminochalcones (**54**, **57**, **58** and **59**) at high concentration showed NO inhibition activity. This result proposed that the *p*-amino group on the A ring and monohydroxy group at *para* position and disubstituent (OH and OCH₃) on the B ring are key factors for NO inhibition activity with cytoprotective activity.

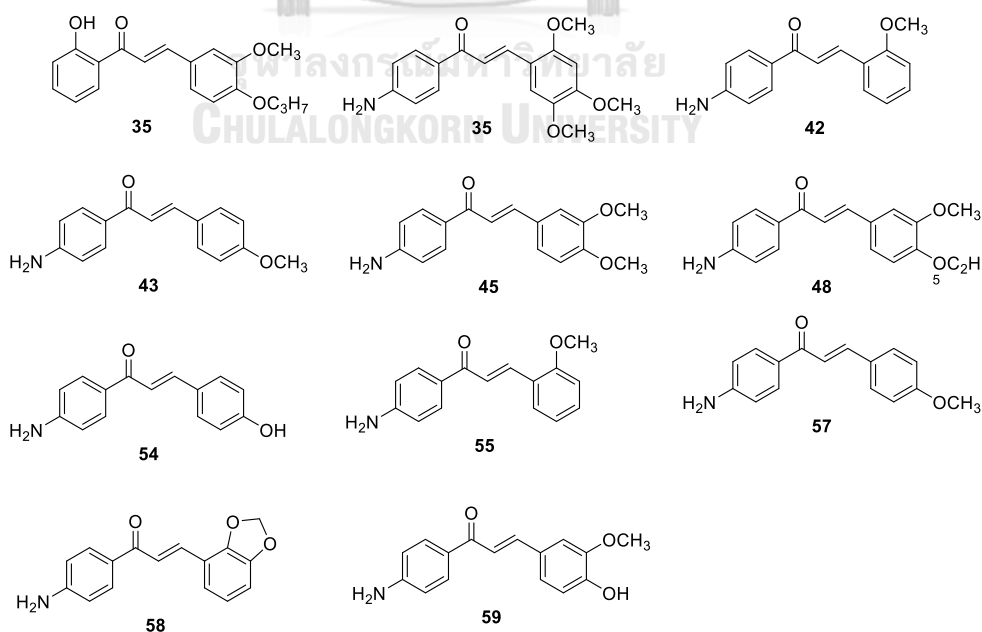


FIGURE 3.10 LEAD COMPOUNDS WITH HIGH POTENT ANTI-INFLAMMATORY WITHOUT CYTOTOXICITY.

CHAPTER IV

SYNTHESIS AND BIOLOGICAL ACTIVITY OF 4'-AMINOCHALCONES AND *E*-ARYLIDENE STEROIDS AS ALPHA-GLUCOSIDASE INHIBITORS

4.1 INTRODUCTION

Diabetes mellitus is a metabolic disease caused by hyperglycemia due to insufficient insulin or insulin cannot be used properly in the human body.⁸ In 2017, the number of diabetes was approximated around 451 million people in the world. This number is projected raise to around 693 million people by 2045.⁸⁹ Diabetes mellitus is divided into three types including type 1 and type 2 diabetes mellitus, and gestational diabetes.⁸ Type 2 diabetes mellitus (T2DM) is a common metabolic disorder.^{8, 90} α -Glucosidase is a vital enzyme in the small intestine to hydrolyze α -1,4-glycosidic bond of disaccharide to form monosaccharide.⁹¹ In humans, there are two complex enzymes of mucosal α -glucosidases in the small intestine membrane, such as maltase-glucoamylase (MGAM) and sucrase-isomaltase (SI). MGAM and SI have two catalytic sites, which are C-terminal domain (Ct-MGAM and Ct-SI) and N-terminal domain (Nt-MGAM and Nt-SI) in the enzymes, respectively.^{92, 93} Two complex enzymes exhibit a wide catalytic property in the breakdown α -1,4-glycosidic bond on various substrates.^{94, 95} MGAM possesses high hydrolysis activity to digest maltose and the other larger starch, such as oligosaccharides and polysaccharides.⁹⁶⁻⁹⁸ The number of SI protein is higher around 40-50 times than MGAM, so SI has high contribution for maltase activity in the small intestine membrane.^{96, 97} Thus, α -glucosidase inhibitors are very necessary to control glucose level.^{99, 100} In the market, α -glucosidase inhibitors are commercially available such as acarbose, voglibose, and miglitol.^{99, 101} Acarbose has shown inhibitory potency against α -glucosidase by the order, as follows: glucoamylase > sucrase > maltase > isomaltase. Thus, acarbose has an ability to suspend hydrolysis of sucrose to monosaccharide by retarding sucrase, whereas starch digestion process is suspended by inhibiting glucoamylase, maltase, and isomaltase.¹⁰² Nevertheless, the side effects of those inhibitors include diarrhea, abdominal pain, and flatulence.¹⁰¹

Steroids possess tetracyclic ring as a core structure.¹⁰³ They represent a potential drug candidate for treating various diseases such as anticancer,¹⁰³⁻¹⁰⁶

leukaemia,¹⁰⁷ autoimmune,¹⁰⁸ and α -glucosidase inhibitors.^{109, 110} Steroid derivatives were exploited for treatment of menopausal symptoms and preventing of osteoporosis, which was used for hormone replacement therapy (HRT) caused by glucose metabolism in non-diabetic obesity.^{109, 111-113}

Chalcones have been addressed for their potent bioactivities such as anti-cancer,^{29, 30, 32, 33} anti-diabetic,¹¹⁴⁻¹¹⁸ antioxidant,^{23, 119-121} and anti-inflammatory.²⁴ According to previous studies, 4'-aminochalcones,^{114, 122} sulfonamide chalcones,¹¹⁴ and phenylthiourea chalcones¹²³ displayed high potency as anti-diabetic. 4'-Amino chalcones¹²⁴ bearing α -bromoacryl,¹²⁵ acetyl,¹²⁶ *N*-acyl homoserine lactones,¹²⁷ maleimides,¹²⁸ and coumarin¹²⁹ on the amino group revealed prominent anti-cancer activity. Moreover, 4'-aminochalcones containing coumarin,¹²⁹ acridinyl,¹³⁰ and benzene sulfonyl¹³¹ exhibited antimalarial activity. 4'-Amino chalcones⁷² with benzenesulfonyl,¹³² and phenylsulfonylurenyl¹³³ presented potent anti-inflammatory activity. The introduction of pyrazole,¹³⁴ and benzothiazole¹³⁵ on 4'-aminochalcones demonstrated better tyrosinase inhibitory activity, while phenylurenyl, and phenylthiourenyl moieties attached on 4'-aminochalcones were reported to express anti-carbonic anhydrase I and II activity.¹³⁶ In addition, other 4'-aminochalcone derivatives were claimed for anti-HIV,¹³⁷ anti-Alzheimer's,¹³⁸ and anti-microbial.^{139, 140}

Based on the literature reviews of chalcones and steroids, the evaluation and determination for structure-activity relationship of chalcones, steroids and their analogues as α -glucosidase inhibitors should be worth performing. This chapter was divided into two topics to search for α -glucosidase inhibitors through the synthesis, biological activity test and structure-activity relationship of 4'-aminochalcones and *E*-arylidene steroid (steroid-chalcone hybrid) derivatives (Figure 4.1).

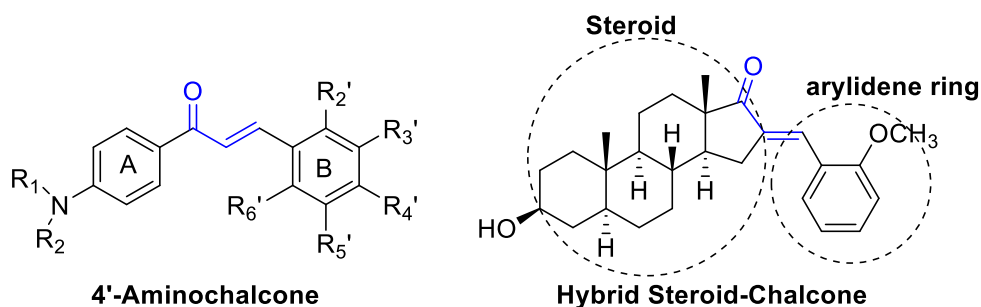


FIGURE 4.1 THE STRUCTURES OF TWO DESIGNED TARGET COMPOUNDS

To address structure-activity relationship, the synthesis of 4'-aminochalcone was divided into two parts: 1) the inhibitory effect of α -glucosidase activity with various substituents on B ring, and 2) that with acyl and alkyl attached on amino group on the A ring. The same synthesis for *E*-arylidene steroid derivatives was applied. In this study, steroid-chalcone hybrids were synthesized and evaluated for the inhibitory effects of various substituents on arylidene ring and steroid structures.

4.2 SYNTHESIS AND BIOLOGICAL EVALUATION OF 4'-AMINOCHALCONES AND THEIR DERIVATIVES AS ALPHA-GLUCOSIDASE INHIBITORS

4.2.1 MATERIALS AND METHODS

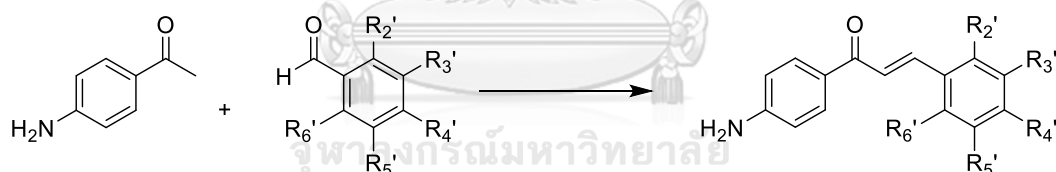
4.2.1.1 MATERIALS

Equipment and chemicals were used the same as those described in Chapter 2.

4.2.2 METHODS

4.2.2.1 SYNTHESIS OF 4'-AMINOCHALCONE SERIES (53-81)

A method similar to that for 2.2.2.1 was also employed.



- | | |
|---|--|
| 53: R ₃ '= OH, R ₂ ', R ₄ ', R ₅ ', R ₆ '= H | 71: R ₂ ', ₃ '= OCH ₂ O, R ₄ ', R ₅ ', R ₆ '= H |
| 54: R ₄ '= OH, R ₂ ', R ₃ ', R ₅ ', R ₆ '= H | 72: R ₂ '= OH, R ₃ '= OCH ₃ , R ₄ ', R ₅ ', R ₆ '= H |
| 55: R ₂ '= OCH ₃ , R ₃ ', R ₄ ', R ₅ ', R ₆ '= H | 73: R ₂ '= CH ₃ , R ₄ '= CH ₃ , R ₆ '= CH ₃ , R ₃ ', R ₅ '= H |
| 56: R ₃ '= OCH ₃ , R ₂ ', R ₄ ', R ₅ ', R ₆ '= H | 74: R ₂ '= F, R ₃ ', R ₄ ', R ₅ ', R ₆ '= H |
| 57: R ₄ '= OCH ₃ , R ₂ ', R ₃ ', R ₅ ', R ₆ '= H | 75: R ₂ '= F, R ₃ ', R ₄ ', R ₅ ', R ₆ '= H |
| 58: R ₃ ', ₄ '= OCH ₂ O, R ₂ ', R ₅ ', R ₆ '= H | 76: R ₂ '= F, R ₃ ', R ₄ ', R ₅ ', R ₆ '= H |
| 59: R ₃ '= OCH ₃ , R ₄ '= OH, R ₂ ', R ₅ ', R ₆ '= H | 77: R ₂ '= Br, R ₃ ', R ₄ ', R ₅ ', R ₆ '= H |
| 60: R ₃ '= OH, R ₄ '= OCH ₃ , R ₂ ', R ₅ ', R ₆ '= H | 78: R ₂ '= Br, R ₃ ', R ₄ ', R ₅ ', R ₆ '= H |
| 61: R ₃ '= OCH ₃ , R ₄ '= OCH ₃ , R ₂ ', R ₅ ', R ₆ '= H | 79: R ₂ '= Br, R ₃ ', R ₄ ', R ₅ ', R ₆ '= H |
| 62: R ₂ '= OCH ₃ , R ₄ '= OCH ₃ , R ₅ '= OCH ₃ , R ₃ ', R ₆ '= H | 80: R ₂ '= Cl, R ₆ '= Cl, R ₃ ', R ₄ ', R ₅ '= H |
| 63: R ₃ '= OCH ₃ , R ₄ '= OCH ₃ , R ₅ '= OCH ₃ , R ₂ ', R ₆ '= H | 81: Naphthyl |
| 64: R ₂ '= OCH ₃ , R ₅ '= OCH ₃ , R ₃ ', R ₄ ', R ₆ '= H | |
| 65: R ₂ '= OCH ₃ , R ₄ '= OCH ₃ , R ₃ ', R ₅ ', R ₆ '= H | |
| 66: R ₂ '= OCH ₃ , R ₃ '= OCH ₃ , R ₄ '= OCH ₃ , R ₅ ', R ₆ '= H | |
| 67: R ₂ '= OCH ₃ , R ₄ '= OCH ₃ , R ₆ '= OCH ₃ , R ₃ ', R ₅ '= H | |
| 68: R ₂ '= OCH ₃ , R ₃ '= OCH ₃ , R ₄ ', R ₅ ', R ₆ '= H | |
| 69: R ₂ '= OCH ₃ , R ₆ '= OCH ₃ , R ₃ ', R ₄ ', R ₅ '= H | |
| 70: R ₃ '= OCH ₃ , R ₅ '= OCH ₃ , R ₂ ', R ₄ ', R ₆ '= H | |

(*E*)-1-(4-aminophenyl)-3-(3-hydroxyphenyl)prop-2-en-1-one (**53**)

Orange powder; yield 47%. ^1H NMR (400 MHz, DMSO- d_6) δ = 9.50 (s, 1H), 7.82 (d, J = 8.4 Hz, 2H), 7.67 (d, J = 15.6 Hz, 1H), 7.44 (d, J = 15.6 Hz, 1H), 7.16 (d, J = 7.2 Hz, 2H), 7.09 (s, 1H), 6.55 (d, J = 8.8 Hz, 2H), 6.06 (s, 2H). ^{13}C NMR (100 MHz, DMSO- d_6) δ = 185.9, 157.6, 153.8, 141.6, 136.4, 131.0, 129.8, 125.4, 122.3, 119.4, 117.1, 114.9, 112.7.

(*E*)-1-(4-aminophenyl)-3-(4-hydroxyphenyl)prop-2-en-1-one (**54**)

Yellow powder; yield 3%. ^1H NMR (400 MHz, acetone- d_6) δ = 9.15 (s, OH), 7.94 (d, J = 8.8 Hz, 2H), 7.65 (dd, J = 8.4, 3.2 Hz, 4H), 6.90 (d, J = 8.8 Hz, 2H), 6.73 (d, J = 8.4 Hz, 2H). ^{13}C NMR (100 MHz, acetone- d_6) δ = 187.4, 160.4, 154.1, 142.9, 131.6, 131.0, 128.1, 119.9, 116.7, 114.0.

(*E*)-1-(4-aminophenyl)-3-(2-methoxyphenyl)prop-2-en-1-one (**55**)

Yellow powder; yield 85%. ^1H NMR (400 MHz, DMSO- d_6) δ = 7.89 (d, J = 15.6 Hz, 1H), 7.85 (dd, J = 8.8, 2.4 Hz, 2H), 7.75 (d, J = 15.6 Hz, 1H), 7.35 (td, J = 8.4, 1.6 Hz, 1H), 7.03 (d, J = 8.4 Hz, 1H), 6.96 (t, J = 7.6 Hz, 1H), 6.58 (d, J = 8.4 Hz, 2H), 6.07 (s, 2H), 3.83 (s, 3H). ^{13}C NMR (100 MHz, DMSO- d_6) δ = 186.1, 157.9, 153.7, 135.9, 131.5, 130.9, 128.1, 125.5, 123.5, 122.3, 120.6, 112.7, 111.7, 55.6.

(*E*)-1-(4-aminophenyl)-3-(3-methoxyphenyl)prop-2-en-1-one (**56**)

Yellow powder; yield 67%. ^1H NMR (500 MHz, DMSO- d_6) δ = 7.95 (d, J = 8.5 Hz, 2H), 7.87 (d, J = 15.5 Hz, 1H), 7.59 (d, J = 15.5 Hz, 1H), 7.43 (s, 1H), 7.38 (d, J = 8.0 Hz, 2H), 7.34 (t, J = 8.0 Hz, 1H), 6.99 (dd, J = 2.5, 1.0 Hz, 1H), 6.97 (dd, J = 2.5, 1.0 Hz, 1H), 6.64 (d, J = 8.5 Hz, 2H), 3.82 (s, 3H). ^{13}C NMR (125 MHz, DMSO- d_6) δ = 185.9, 159.7, 153.7, 141.5, 136.6, 131.2, 129.8, 125.5, 122.7, 121.3, 116.1, 113.0, 112.9, 55.3.

(*E*)-1-(4-aminophenyl)-3-(4-methoxyphenyl)prop-2-en-1-one (**57**)

Yellow powder; yield 84%. ^1H NMR (400 MHz, DMSO- d_6) δ = 7.86 (d, J = 8.8 Hz, 2H), 7.73 (d, J = 8.8 Hz, 2H), 7.67 (d, J = 15.6 Hz, 1H), 7.54 (d, J = 15.6 Hz, 1H), 6.94 (d, J = 8.8 Hz, 2H), 6.57 (d, J = 8.8 Hz, 2H), 6.05 (s, 2H), 3.75 (s, 3H). ^{13}C NMR (100 MHz, DMSO- d_6) δ = 185.9, 160.8, 153.6, 141.3, 130.9, 130.2, 127.8, 125.6, 119.9, 114.3, 112.7, 55.3.

(*E*)-1-(4-aminophenyl)-3-(benzo[d][1,3]dioxol-5-yl)prop-2-en-1-one (**58**)

Yellow powder; yield 61%. ^1H NMR (400 MHz, DMSO- d_6) δ = 7.87 (d, J = 8.4 Hz, 1H), 7.68 (d, J = 15.2 Hz, 1H), 7.54 (s, 1H), 7.49 (d, J = 15.6 Hz, 1H), 7.19 (d, J = 8.4 Hz, 1H), 6.90 (d, J = 8.0 Hz, 1H), 6.56 (d, J = 8.4 Hz, 2H), 6.05 (s, 2H), 6.03 (s, 2H). ^{13}C NMR (100

MHz, DMSO- d_6) δ = 185.7, 153.5, 147.8, 141.2, 130.8, 129.5, 125.3, 124.8, 120.3, 112.5, 108.2, 106.5, 101.3, 49.0.

(*E*)-1-(4-aminophenyl)-3-(4-hydroxy-3-methoxyphenyl) prop-2-en-1-one (**59**)

Brown powder; yield 7%. ^1H NMR (500 MHz, acetone- d_6) δ = 7.93 (d, J = 9.0 Hz, 2H), 7.69 (d, J = 15.0 Hz, 1H), 7.64 (d, J = 15.5 Hz, 1H), 7.45 (d, J = 2.0 Hz, 1H), 7.25 (dd, J = 8.0, 2.5 Hz, 1H), 6.88 (d, J = 8.0 Hz, 1H), 6.73 (d, J = 9.0 Hz, 2H), 3.93 (s, 3H). ^{13}C NMR (125 MHz, acetone- d_6) δ = 187.2, 154.1, 149.8, 148.7, 143.3, 131.6, 128.6, 128.1, 123.9, 120.2, 116.1, 113.9, 111.7, 56.4.

(*E*)-1-(4-aminophenyl)-3-(3-hydroxy-4-methoxyphenyl)prop-2-en-1-one (**60**)

Yellow powder; yield 42%. ^1H NMR (400 MHz, DMSO- d_6) δ = 9.06 (s, 1H), 7.84 (d, J = 8.4 Hz, 2H), 7.56 (d, J = 15.6 Hz, 1H), 7.44 (d, J = 15.2 Hz, 1H), 7.22 (s, 1H), 7.17 (d, J = 8.4 Hz, 1H), 6.91 (d, J = 8.4 Hz, 1H), 6.56 (d, J = 8.4 Hz, 2H), 6.04 (s, 2H), 3.77 (s, 3H). ^{13}C NMR (100 MHz, DMSO- d_6) δ = 185.9, 153.6, 149.7, 146.6, 141.8, 130.8, 128.1, 125.6, 121.3, 119.8, 114.6, 112.7, 111.9, 55.7.

(*E*)-1-(4-aminophenyl)-3-(3,4-dimethoxyphenyl)prop-2-en-1-one (**61**)

Yellow powder; yield 46%. ^1H NMR (400 MHz, DMSO- d_6) δ = 7.90 (d, J = 8.4 Hz, 2H), 7.72 (d, J = 15.6 Hz, 1H), 7.54 (d, J = 15.6 Hz, 1H), 7.45 (s, 1H), 7.27 (d, J = 8.4 Hz, 1H), 6.95 (d, J = 8.4 Hz, 1H), 6.59 (d, J = 8.4 Hz, 2H), 6.06 (s, 2H), 3.82 (s, 3H), 3.76 (s, 3H). ^{13}C NMR (100 MHz, DMSO- d_6) δ = 185.9, 153.6, 150.7, 149.0, 141.8, 130.9, 128.0, 125.6, 123.2, 120.0, 112.7, 111.6, 110.6, 55.7, 55.6.

(*E*)-1-(4-aminophenyl)-3-(2,4,5-trimethoxyphenyl)prop-2-en-1-one (**62**)

Orange powder; yield 69%. ^1H NMR (400 MHz, DMSO- d_6) δ = 7.85 (dd, J = 15.6 Hz, 8.8 Hz, 3H), 7.62 (d, J = 15.6 Hz, 1H), 7.40 (s, 1H), 6.65 (s, 1H), 6.55 (d, J = 8.4 Hz, 2H), 3.80 (s, 3H), 3.78 (s, 3H), 3.74 (s, 3H). ^{13}C NMR (100 MHz, DMSO- d_6) δ = 186.2, 153.7, 153.5, 152.2, 143.1, 136.0, 130.8, 125.8, 119.3, 114.9, 112.7, 111.0, 97.7, 56.4, 55.8.

(*E*)-1-(4-aminophenyl)-3-(3,4,5-trimethoxyphenyl) prop-2-en-1-one (**63**)

Orange powder; yield 99%. ^1H NMR (400 MHz, CDCl_3) δ = 7.92 (d, J = 8.8 Hz, 2H), 7.68 (d, J = 15.6 Hz, 1H), 7.43 (d, J = 15.6 Hz, 1H), 6.84 (s, 2H), 6.69 (d, J = 8.4 Hz, 2H), 3.91 (s, 6H), 3.88 (s, 3H). ^{13}C NMR (100 MHz, CDCl_3) δ = 188.2, 153.6, 151.3, 143.4, 131.2, 130.9, 128.6, 121.5, 114.0, 105.7, 61.1, 56.4.

(*E*)-1-(4-aminophenyl)-3-(2,5-dimethoxyphenyl)prop-2-en-1-one (**64**)

Yellow liquid; yield 42%. ^1H NMR (500 MHz, CDCl_3) δ = 8.04 (d, J = 16.0 Hz, 1H), 7.91 (d, J = 9.0 Hz, 2H), 7.15 (d, J = 16.0 Hz, 1H), 7.15 (d, J = 3.0 Hz, 1H), 6.91 (dd, J = 9.0, 3.0 Hz, 1H), 6.85 (d, J = 9.0 Hz, 1H), 6.71 (dt, J = 9.0 Hz, 2H), 3.84 (s, 3H), 3.80 (s, 3H). ^{13}C NMR (125 MHz, CDCl_3) δ = 188.8, 153.6, 153.3, 138.6, 131.2, 125.0, 123.2, 116.8, 114.3, 113.8, 112.6, 56.2, 55.9.

(*E*)-1-(4-aminophenyl)-3-(2,4-dimethoxyphenyl)prop-2-en-1-one (**65**)

Orange powder; yield 36%. ^1H NMR (500 MHz, $\text{DMSO-}d_6$) δ = 7.89 (d, J = 5.0 Hz, 1H), 7.86 (dd, J = 8.5, 2.0 Hz, 3H), 7.68 (d, J = 15.5 Hz, 1H), 6.63 (d, J = 8.5 Hz, 3H), 6.60 (dd, J = 8.5, 2.0 Hz, 1H), 3.88 (s, 3H), 3.82 (s, 3H). ^{13}C NMR (125 MHz, $\text{DMSO-}d_6$) δ = 186.2, 162.5, 159.6, 153.3, 136.3, 130.8, 129.6, 125.9, 119.5, 116.4, 113.0, 106.2, 98.3, 55.8, 55.5.

(*E*)-1-(4-aminophenyl)-3-(2,3,4-trimethoxyphenyl)prop-2-en-1-one (**66**)

Yellow liquid; yield 34%. ^1H NMR (500 MHz, CDCl_3) δ = 7.95 (d, J = 15.5 Hz, 1H), 7.91 (d, J = 8.5 Hz, 2H), 7.55 (d, J = 15.5 Hz, 1H), 7.36 (d, J = 8.5 Hz, 1H), 6.71 (q, J = 8.5 Hz, 3H), 3.92 (s, 3H), 3.89 (s, 3H), 3.88 (s, 3H). ^{13}C NMR (125 MHz, CDCl_3) δ = 188.7, 155.5, 153.7, 150.6, 142.6, 138.6, 131.1, 129.1, 123.8, 122.5, 121.5, 114.3, 107.7, 61.5, 61.04, 56.2.

(*E*)-1-(4-aminophenyl)-3-(2,4,6-trimethoxyphenyl)prop-2-en-1-one (**67**)

Orange powder; yield 91%. ^1H NMR (500 MHz, $\text{DMSO-}d_6$) δ = 7.97 (d, J = 16.0 Hz, 1H), 7.86 (d, J = 15.5 Hz, 1H), 7.75 (d, J = 8.5 Hz, 2H), 6.61 (d, J = 8.5 Hz, 2H), 6.31 (s, 2H), 6.04 (s, 2H), 3.91 (s, 6H), 3.85 (s, 3H). ^{13}C NMR (125 MHz, $\text{DMSO-}d_6$) δ = 187.1, 162.6, 161.0, 153.4, 132.7, 130.5, 126.1, 120.9, 112.8, 105.4, 91.0, 56.0, 55.5.

(*E*)-1-(4-aminophenyl)-3-(2,3-dimethoxyphenyl)prop-2-en-1-one (**68**)

Yellow powder; yield 44%. ^1H NMR (500 MHz, CDCl_3) δ = 8.05 (d, J = 16.0 Hz, 1H), 7.92 (d, J = 8.5 Hz, 2H), 7.60 (d, J = 16.0 Hz, 1H), 7.26 (d, J = 9.0 Hz, 1H), 7.08 (t, J = 8.0 Hz, 1H), 6.94 (dd, J = 8.0, 1.0 Hz, 1H), 6.71 (d, J = 8.5 Hz, 2H), 3.87 (s, 3H), 3.86 (s, 3H). ^{13}C NMR (125 MHz, CDCl_3) δ = 188.6, 153.3, 150.8, 148.8, 138.1, 131.2, 129.6, 128.9, 124.3, 123.7, 119.7, 114.3, 113.8, 61.4, 55.9.

(*E*)-1-(4-aminophenyl)-3-(2,6-dimethoxyphenyl)prop-2-en-1-one (**69**)

Yellow powder; yield 57%. ^1H NMR (500 MHz, $\text{DMSO-}d_6$) δ = 7.99 (d, J = 16.0 Hz, 1H), 7.98 (d, J = 16.0 Hz, 1H), 7.77 (d, J = 8.5 Hz, 1H), 7.35 (t, J = 8.5 Hz, 1H), 6.73 (d, J = 8.5

Hz, 2H), 6.63 (d, $J = 8.5$ Hz, 2H), 6.11 (s, 2H), 3.90 (s, 6H). ^{13}C NMR (125 MHz, $\text{DMSO-}d_6$) $\delta = 187.1, 159.7, 153.6, 132.4, 131.5, 130.7, 125.8, 124.1, 112.8, 111.9, 104.2, 56.0$.

(*E*)-1-(4-aminophenyl)-3-(3,5-dimethoxyphenyl)prop-2-en-1-one (**70**)

Yellow powder; yield 11%. ^1H NMR (500 MHz, $\text{DMSO-}d_6$) $\delta = 7.94$ (d, $J = 8.5$ Hz, 2H), 7.86 (d, $J = 15.5$ Hz, 1H), 7.54 (d, $J = 15.5$ Hz, 1H), 7.01 (d, $J = 2.5$ Hz, 2H), 6.62 (d, $J = 9.0$ Hz, 2H), 6.54 (t, $J = 2.0$ Hz, 1H), 6.2 (s, 2H), 3.80 (s, 6H). ^{13}C NMR (125 MHz, $\text{DMSO-}d_6$) $\delta = 185.8, 160.7, 153.9, 141.6, 137.2, 131.2, 125.3, 122.9, 112.7, 106.4, 102.3, 55.4$.

(*E*)-1-(4-aminophenyl)-3-(benzo[d][1,3]dioxol-4-yl)prop-2-en-1-one (**71**)

Yellow powder; yield 99%. ^1H NMR (500 MHz, $\text{DMSO-}d_6$) $\delta = 7.84$ (d, $J = 16.0$ Hz, 1H), 7.84 (d, $J = 8.5$ Hz, 2H), 7.58 (d, $J = 15.5$ Hz, 1H), 7.29 (d, $J = 7.5$ Hz, 1H), 6.96 (d, $J = 7.5$ Hz, 1H), 6.89 (d, $J = 8.0$ Hz, 1H), 6.63 (d, $J = 8.5$ Hz, 2H), 6.19 (s, 2H), 6.17 (s, 2H). ^{13}C NMR (125 MHz, $\text{DMSO-}d_6$) $\delta = 185.7, 154.0, 147.6, 146.3, 135.2, 131.0, 125.1, 124.1, 121.9, 117.6, 112.8, 109.6, 101.6, 39.7$.

(*E*)-1-(4-aminophenyl)-3-(2-hydroxy-3-methoxyphenyl)prop-2-en-1-one (**72**)

Yellow powder; yield 42%. ^1H NMR (500 MHz, $\text{DMSO-}d_6$) $\delta = 8.11$ (d, $J = 8.5$ Hz, 2H), 7.99 (dd, $J = 5.5, 3.0$ Hz, 2H), 7.93 (dd, $J = 5.5, 3.0$ Hz, 2H), 7.61 (d, $J = 8.5$ Hz, 2H), 2.63 (s, 3H). ^{13}C NMR (125 MHz, $\text{DMSO-}d_6$) $\delta = 197.4, 166.7, 136.0, 135.8, 134.9, 131.5, 128.8, 127.1, 123.6, 26.9$.

(*E*)-1-(4-aminophenyl)-3-mesitylprop-2-en-1-one (**73**)

Pale yellow powder; yield 42%. ^1H NMR (500 MHz, $\text{DMSO-}d_6$) $\delta = 7.83$ (d, $J = 8.5$ Hz, 2H), 7.70 (d, $J = 15.5$ Hz, 1H), 7.29 (d, $J = 16.0$ Hz, 1H), 6.92 (s, 2H), 6.61 (d, $J = 8.5$ Hz, 2H), 6.15 (s, 2H), 2.32 (s, 6H), 2.24 (s, 3H). ^{13}C NMR (125 MHz, $\text{DMSO-}d_6$) $\delta = 185.91, 153.91, 139.34, 137.41, 136.56, 131.63, 131.08, 129.00, 127.24, 125.19, 112.81, 20.89, 20.70$.

(*E*)-1-(4-aminophenyl)-3-(2-fluorophenyl)prop-2-en-1-one (**74**)

Yellow powder; yield 69%. ^1H NMR (500 MHz, $\text{DMSO-}d_6$) $\delta = 8.07$ (td, $J = 8.0, 1.5$ Hz, 1H), 7.91 (dd, $J = 15.0, 8.5$ Hz, 3H), 7.73 (d, $J = 16.0$ Hz, 1H), 7.47 (qd, $J = 7.5, 2.0$ Hz, 1H), 7.30 (d, $J = 7.0$ Hz, 1H), 7.28 (d, $J = 7.5$ Hz, 1H), 6.63 (d, $J = 8.5$ Hz, 2H), 6.21 (s, 2H). ^{13}C NMR (125 MHz, $\text{DMSO-}d_6$) $\delta = 185.6, 160.7, 154.1, 132.6, 131.9, 131.3, 128.8, 125.1, 124.7, 122.8, 116.0, 112.8$.

(*E*)-1-(4-aminophenyl)-3-(3-fluorophenyl)prop-2-en-1-one (**75**)

Orange powder; yield 60%. ^1H NMR (500 MHz, $\text{DMSO-}d_6$) δ = 7.95 (d, J = 9.0 Hz, 2H), 7.94 (d, J = 15.5 Hz, 1H), 7.80 (d, J = 10.5 Hz, 1H), 7.64 (d, J = 8.0 Hz, 1H), 7.61 (d, J = 15.5 Hz, 1H), 7.47 (q, J = 8.5 Hz, 1H), 7.24 (td, J = 8.5, 2.5 Hz, 1H), 6.63 (d, J = 9.0 Hz, 2H), 6.19 (s, 2H). ^{13}C NMR (125 MHz, $\text{DMSO-}d_6$) δ = 185.7, 162.6, 154.1, 140.0, 137.8, 131.3, 130.8, 125.2, 123.9, 116.5, 114.3, 112.8.

(*E*)-1-(4-aminophenyl)-3-(4-fluorophenyl)prop-2-en-1-one (**76**)

Yellow powder; yield 57%. ^1H NMR (500 MHz, $\text{DMSO-}d_6$) δ = 7.93 (d, J = 8.5 Hz, 2H), 7.90 (dd, J = 8.5, 3.0 Hz, 2H), 7.83 (d, J = 15.5 Hz, 1H), 7.61 (d, J = 15.5 Hz, 1H), 7.26 (t, J = 8.5 Hz, 2H), 6.63 (d, J = 8.5 Hz, 2H), 6.16 (s, 2H). ^{13}C NMR (125 MHz, $\text{DMSO-}d_6$) δ = 185.8, 163.1, 153.9, 140.2, 131.8, 131.2, 125.3, 122.4, 115.8, 112.8.

(*E*)-1-(4-aminophenyl)-3-(2-bromophenyl)prop-2-en-1-one (**77**)

Orange powder; yield 32%. ^1H NMR (500 MHz, $\text{DMSO-}d_6$) δ = 8.14 (d, J = 8.0 Hz, 1H), 7.94 (d, J = 8.5 Hz, 2H), 7.88 (ABq, J = 15.5 Hz, 2H), 7.71 (d, J = 8.0 Hz, 1H), 7.46 (t, J = 7.5 Hz, 1H), 7.34 (td, J = 8.0, 1.5 Hz, 1H), 6.63 (d, J = 9.0 Hz, 2H), 6.22 (s, 2H). ^{13}C NMR (125 MHz, $\text{DMSO-}d_6$) δ = 185.50, 154.18, 138.88, 134.50, 133.23, 131.59, 131.37, 128.54, 128.19, 125.42, 125.06, 112.80.

(*E*)-1-(4-aminophenyl)-3-(3-bromophenyl)prop-2-en-1-one (**78**)

Yellow powder; yield 96%. ^1H NMR (500 MHz, $\text{DMSO-}d_6$) δ = 8.16 (s, 1H), 7.96 (d, J = 8.5 Hz, 2H), 7.95 (d, J = 15.5 Hz, 1H), 7.80 (d, J = 7.5 Hz, 1H), 7.59 (dq, J = 7.7, 0.5 Hz, 2H), 7.58 (d, J = 16.0 Hz, 1H), 7.38 (t, J = 8.0 Hz, 1H), 6.63 (d, J = 8.5 Hz, 2H), 6.20 (s, 2H). ^{13}C NMR (125 MHz, $\text{DMSO-}d_6$) δ = 185.7, 154.1, 139.7, 137.7, 132.4, 131.3, 130.9, 130.5, 127.9, 125.2, 124.0, 122.4, 112.7.

(*E*)-1-(4-aminophenyl)-3-(4-bromophenyl)prop-2-en-1-one (**79**)

Yellow powder; yield 23%. ^1H NMR (500 MHz, $\text{DMSO-}d_6$) δ = 7.93 (d, J = 8.5 Hz, 2H), 7.90 (d, J = 15.5 Hz, 1H), 7.80 (d, J = 8.5 Hz, 2H), 7.66 (d, J = 9.0 Hz, 1H), 7.62 (d, J = 8.5 Hz, 2H), 7.58 (d, J = 15.5 Hz, 1H), 6.62 (d, J = 8.5 Hz, 2H), 6.56 (d, J = 9.0 Hz, 1H), 6.18 (s, 2H). ^{13}C NMR (125 MHz, $\text{DMSO-}d_6$) δ = 185.7, 154.0, 140.1, 134.5, 131.8, 131.2, 130.6, 130.5, 125.2, 123.2, 112.8, 112.5.

(E)-1-(4-aminophenyl)-3-(2,6-dichlorophenyl)prop-2-en-1-one (80)

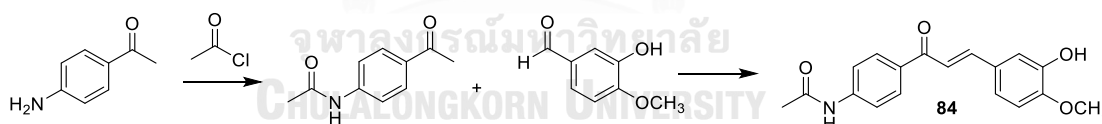
White powder; yield 78%. ^1H NMR (500 MHz, $\text{DMSO-}d_6$) δ = 7.82 (d, J = 9.0 Hz, 2H), 7.72 (d, J = 16.0 Hz, 1H), 7.58 (d, J = 15.5 Hz, 1H), 7.57 (d, J = 8.5 Hz, 2H), 7.41 (t, J = 8.0 Hz, 1H), 6.62 (d, J = 9.0 Hz, 2H), 6.27 (s, 2H). ^{13}C NMR (125 MHz, $\text{DMSO-}d_6$) δ = 185.3, 154.4, 134.36, 134.03, 132.66, 131.30, 130.91, 130.62, 129.08, 124.62, 112.90, 39.52.

(E)-1-(4-aminophenyl)-3-(naphthalen-2-yl)prop-2-en-1-one (81)

Yellow powder; yield 88%. ^1H NMR (500 MHz, $\text{DMSO-}d_6$) δ = 8.45 (d, J = 15.5 Hz, 1H), 8.26 (d, J = 8.0 Hz, 1H), 8.18 (d, J = 7.0 Hz, 1H), 7.98 (m, 5H), 7.60 (m, 3H), 6.65 (d, J = 8.5 Hz, 2H), 6.20 (s, 2). ^{13}C NMR (125 MHz, $\text{DMSO-}d_6$) δ = 185.8, 154.0, 137.4, 133.4, 131.9, 131.3, 131.2, 130.2, 128.8, 127.1, 126.2, 125.7, 125.2, 125.1, 123.0, 112.8.

4.2.2.2 SYNTHESIS OF 4'-N-ACETYLAMINOCHALCONE (84)

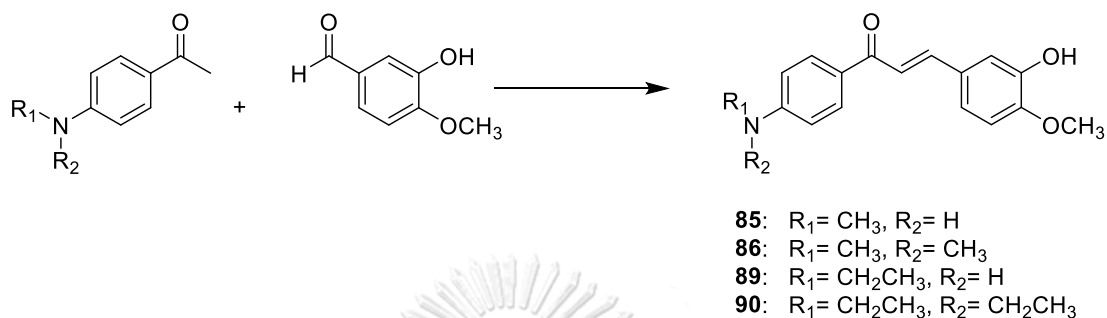
Acetyl chloride (1.5 eq) was added into the mixture of acetophenone (1.0 eq) in dichloromethane and TEA and stirred at 0 °C and continued to room temperature for 24 hours. The pH of the mixture was adjusted by adding 50% HCl until pH = 7. The product was extracted using dichloromethane, evaporated, and separated by silica gel column using hexane:EtOAc (4:1). The pure product was reacted with isovanillin using method described in 4.2.2.1.

**(E)-N-(4-(3-(3-hydroxy-4-methoxyphenyl)acryloyl)phenyl)acetamide (84)**

Yellow powder; yield 24%. ^1H NMR (500 MHz, $\text{DMSO-}d_6$) δ = 10.31 (s, 1H), 9.21 (s, 1H), 8.10 (d, J = 9.0 Hz, 2H), 7.75 (d, J = 9.0 Hz, 2H), 7.68 (d, J = 15.5 Hz, 1H), 7.59 (d, J = 15.5 Hz, 1H), 7.31 (d, J = 2.0 Hz, 1H), 7.27 (dd, J = 8.0, 2.0 Hz, 1H), 6.99 (d, J = 8.5 Hz, 1H), 3.83 (s, 3H), 2.09 (s, 3H). ^{13}C NMR (125 MHz, $\text{DMSO-}d_6$) δ = 187.54, 169.13, 150.31, 146.73, 143.94, 143.58, 132.52, 129.81, 127.79, 122.10, 119.39, 118.40, 114.83, 112.01, 55.77, 24.26. MS(ESI, m/z): 334.10579 $[\text{M} + \text{Na}]^+$. HRMS calcd for $\text{C}_{16}\text{H}_{13}\text{NO}_3$: 311.1158, Found: 311.10579.

4.2.2.3 SYNTHESIS OF 4'-N-(DI)ALKYLAMINOCHALCONE (85, 86, 89, 90)

The 4'-N-alkylaminocetophenone was reacted with isovanillin as that mentioned in 4.2.2.1.



(E)-3-(3-hydroxy-4-methoxyphenyl)-1-(4-(methylamino)phenyl)prop-2-en-1-one (**85**)

Yellow solid; yield 7%. ¹H NMR (500 MHz, acetone-*d*₆) δ = 8.02 (d, *J* = 9.0 Hz, 2H), 7.88 (s, 1H), 7.67 (d, *J* = 15.5 Hz, 1H), 7.63 (d, *J* = 15.0 Hz, 1H), 7.33 (d, *J* = 2.5 Hz, 1H), 7.20 (dd, *J* = 8.5, 2.5 Hz, 1H), 6.98 (d, *J* = 8.5 Hz, 1H), 6.67 (d, *J* = 8.5 Hz, 2H), 3.89 (s, 3H), 2.88 (d, *J* = 4.5 Hz, 3H). ¹³C NMR (125 MHz, acetone-*d*₆) δ = 187.10, 154.76, 150.39, 147.77, 142.80, 131.60, 129.81, 127.57, 122.58, 120.82, 114.59, 112.27, 111.73, 56.28, 29.92. MS(ESI, *m/z*): 306.11223 [M + Na]⁺. HRMS calcd for C₁₆H₁₃NO₃: 283.1208, found: 283.11223.

(E)-1-(4-(dimethylamino)phenyl)-3-(3-hydroxy-4-methoxyphenyl)prop-2-en-1-one (**86**)

Yellow solid; yield 6%. ¹H NMR (500 MHz, acetone-*d*₆) δ = 8.06 (d, *J* = 8.5 Hz, 2H), 7.89 (s, 1H), 7.69 (d, *J* = 15.5 Hz, 1H), 7.62 (d, *J* = 15.5 Hz, 1H), 7.33 (d, *J* = 2.5 Hz, 1H), 7.20 (dd, *J* = 8.5, 2.5 Hz, 1H), 7.00 (d, *J* = 8.0 Hz, 1H), 6.78 (d, *J* = 9.0 Hz, 2H), 3.89 (s, 3H), 3.07 (s, 3H). ¹³C NMR (125 MHz, acetone-*d*₆) δ = 187.16, 154.40, 150.43, 147.78, 142.89, 131.32, 129.78, 127.13, 122.61, 120.78, 114.60, 112.28, 111.71, 56.28, 40.07.

(E)-1-(4-(ethylamino)phenyl)-3-(3-hydroxy-4-methoxyphenyl)prop-2-en-1-one (**89**)

Yellow solid; yield 16%. ¹H NMR (500 MHz, acetone-*d*₆) δ = 8.00 (d, *J* = 8.5 Hz, 2H), 7.88 (s, 1H), 7.67 (d, *J* = 15.5 Hz, 1H), 7.62 (d, *J* = 15.5 Hz, 1H), 7.31 (d, *J* = 2.5 Hz, 1H), 7.20 (dd, *J* = 8.0, 2.0 Hz, 1H), 6.99 (d, *J* = 8.5 Hz, 1H), 6.68 (d, *J* = 9.0 Hz, 1H), 3.88 (s, 3H), 3.24 (q, *J* = 7.0 Hz, 2H), 1.24 (t, *J* = 7.5 Hz, 3H). ¹³C NMR (125 MHz, acetone-*d*₆) δ = 187.05, 153.85, 150.38, 147.75, 142.79, 131.64, 129.79, 127.50, 122.56, 120.80, 114.58,

112.26, 111.99, 56.26, 38.20, 14.63. MS(ESI, m/z): 320.12811 $[M + Na]^+$. HRMS calcd for $C_{16}H_{13}NO_3$: 297.1365, found: 297.12811

(*E*)-1-(4-(diethylamino)phenyl)-3-(3-hydroxy-4-methoxyphenyl)prop-2-en-1-one (**90**)

Yellow liquid; yield 15%. 1H NMR (500 MHz, acetone- d_6) δ = 8.01 (d, J = 7.5 Hz, 2H), 7.65 (d, J = 15.5 Hz, 1H), 7.60 (d, J = 15.5 Hz, 1H), 7.31 (s, 1H), 7.17 (d, J = 8.5 Hz, 1H), 6.95 (dd, J = 8.5, 4.0 Hz, 1H), 6.71 (d, J = 9.0 Hz, 2H), 3.847 (s, 3H), 3.45 (qui, J = 7.5 Hz, 4H), 1.15 (q, J = 7.0 Hz, 6H). ^{13}C NMR (125 MHz, acetone- d_6) δ = 186.87, 151.99, 150.36, 147.76, 142.70, 131.70, 129.84, 126.48, 122.56, 120.83, 114.57, 112.27, 111.23, 56.28, 45.01, 12.80. MS(ESI, m/z): 348.15743 $[M + Na]^+$. HRMS calcd for $C_{16}H_{13}NO_3$: 325.1678, found: 325.1676.

4.2.2.4 SYNTHESIS OF 4'-*N*-ALKYLAMINOCHALCONE (**91**, **92**)

Isobutyraldehyde or 2-ethylbutyraldehyde (6.0 mmol) was added into the mixture of **60** (0.4 mmol) in MeOH (10 mL), AcOH (100 μ L), $NaBH_3CN$ (3.0 mmol), and stirred at room temperature for 6 days. The crude product was extracted using EtOAc, evaporated, and separated by silica gel column using hexane:EtOAc (3:2).



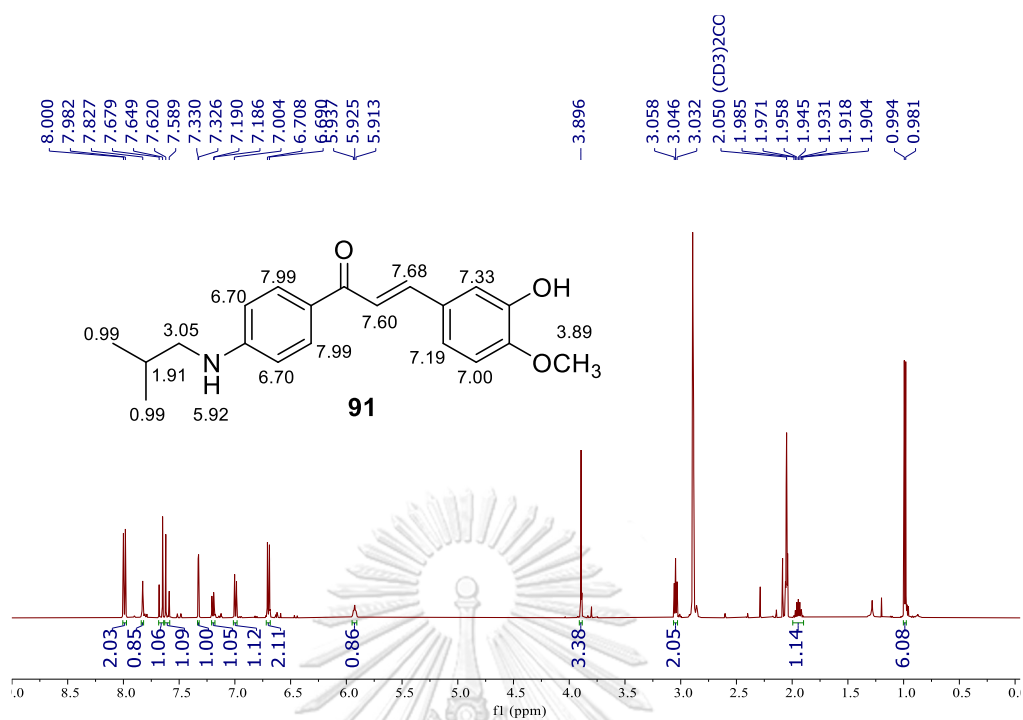
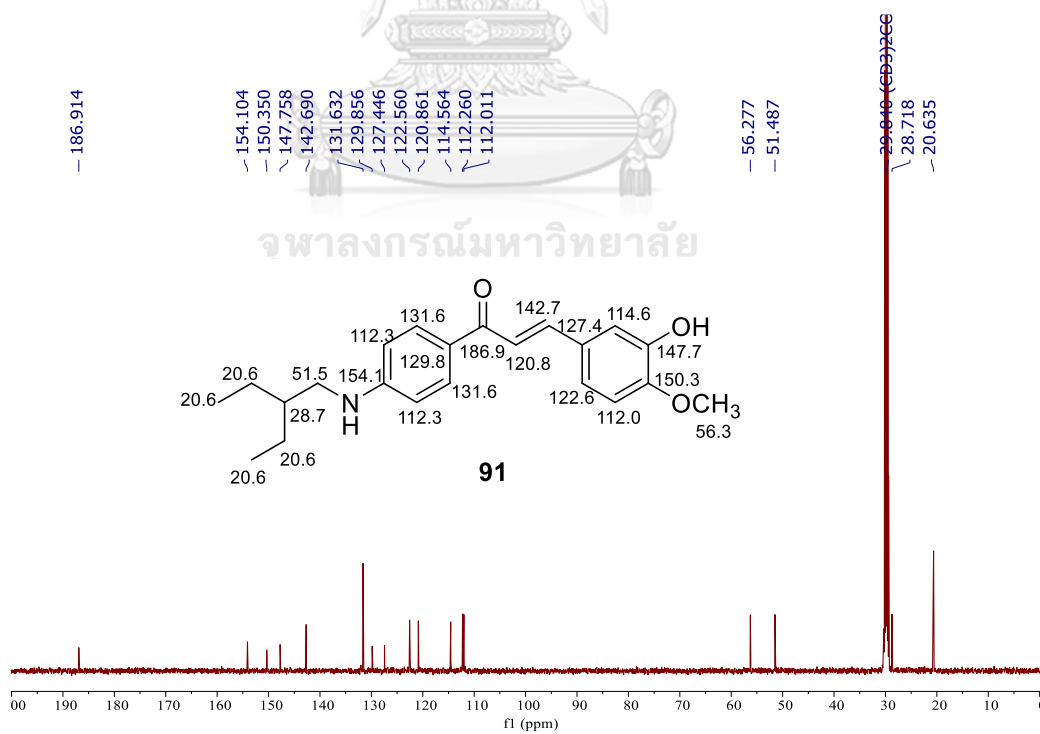
(*E*)-3-(3-hydroxy-4-methoxyphenyl)-1-(4-(isobutylamino)phenyl)prop-2-en-1-one (**91**)

Yellow liquid; yield 0.1%. 1H NMR (500 MHz, acetone- d_6) δ = 7.99 (d, J = 9.0 Hz, 2H), 7.83 (s, 1H), 7.68 (d, J = 15.0 Hz, 1H), 7.60 (d, J = 15.5 Hz, 1H), 7.33 (d, J = 2.0 Hz, 1H), 7.19 (d, J = 8.5, 2.0 Hz, 1H), 7.00 (d, J = 8.0 Hz, 1H), 6.70 (d, J = 9.0 Hz, 2H), 5.92 (t, J = 6.0 Hz, 1H), 3.89 (s, 3H), 3.05 (t, J = 6.0 Hz, 2H), 1.91 (m, 1H), 0.99 (d, J = 6.5 Hz, 6H). ^{13}C NMR (125 MHz, acetone- d_6) δ = 186.9, 154.1, 150.3, 147.7, 142.7, 131.6, 129.8, 127.4, 122.6, 120.8, 114.6, 112.3, 112.0, 56.3, 51.5, 20.6. MS(ESI, m/z): 348.15807 $[M + Na]^+$. HRMS calcd for $C_{16}H_{13}NO_3$: 325.1678, found: 325.15807.

(*E*)-1-(4-((2-ethylbutyl)amino)phenyl)-3-(3-hydroxy-4-methoxyphenyl)prop-2-en-1-one (**92**). Yellow liquid; yield 0.1%. ^1H NMR (500 MHz, acetone- d_6) δ = 8.00 (d, J = 8.5 Hz, 2H), 7.83 (s, 1H), 7.67 (d, J = 15.0 Hz, 1H), 7.61 (d, J = 15.5 Hz, 1H), 7.33 (d, J = 2.0 Hz, 1H), 7.20 (d, J = 8.5, 2.5 Hz, 1H), 6.99 (d, J = 8.0 Hz, 1H), 6.71 (d, J = 9.0 Hz, 2H), 3.89 (s, 3H), 3.14 (t, J = 6.0 Hz, 2H), 1.59 (heptet, J = 6.0 Hz, 1H), 1.45 (m, 4H), 0.92 (t, J = 7.0 Hz, 6H). ^{13}C NMR (125 MHz, acetone- d_6) δ = 186.9, 154.2, 150.3, 147.7, 142.7, 131.6, 129.8, 127.4, 122.5, 120.8, 114.5, 112.2, 111.9, 56.3, 46.6, 41.2, 24.4, 11.2. MS(ESI, m/z): 376.18882 [M + Na] $^+$. HRMS calcd for $\text{C}_{16}\text{H}_{13}\text{NO}_3$: 353.1991, found: 353.199.

All compounds were characterized using ^1H and ^{13}C NMR spectroscopy. For new compounds, the molecular ion was determined by HRMS. Two compounds, **91** and **92**, were selected to address the structural elucidation.

The ^1H NMR Spectra of **91** (Figure 4.2) showed two *trans*-olefinic protons at δ_{H} 7.68 (d, J = 15.0 Hz, 1H), and 7.60 (d, J = 15.5 Hz, 1H). Two doublet signals belonged to the A ring at δ_{H} 7.99 (d, J = 9.0 Hz, 2H), and 6.70 (d, J = 9.0 Hz, 2H), while two doublet signals at δ_{H} 7.33 (d, J = 2.0 Hz, 1H), 7.00 (d, J = 8.0 Hz, 1H), and one doublet of doublet signal at δ_{H} 7.19 (dd, J = 8.5, 2.0 Hz, 1H) showed an ABX system assigned for proton on the B ring. The triplet signal at δ_{H} 3.05 (t, J = 6.0 Hz, 2H) was methylene (CH_2) and more downfield due to attach to nitrogen, while multiplet signals at δ_{H} 1.91 (m, 1H) was methine (CH) neighboring with two methyl and methylene, and doublet signal at δ_{H} 0.99 (d, J = 6.5 Hz, 6H) was assigned for two methyl groups attached with methine. The ^{13}C NMR Spectra of **91** (Figure 4.3) showed a characteristic of carbonyl signal at δ_{C} 186.9 (C=O) more down field due to have a conjugation system compared with acetone more than δ_{C} 200.0. The aromatic carbon attached to an amino group on the A ring was detected at δ_{C} 154.1 (=C-N) more down field compared with oxygenated aromatic carbons on the B ring at δ_{C} 150.3 (=C-OCH $_3$) and 147.7 (=C-OH). Moreover, the sp^2 carbon signals were displayed at δ_{C} 142.7-112.0, and those of sp^3 carbon were observed at δ_{C} 56.3 (OCH $_3$), 51.5 (CH $_2$), 28.7 (CH), and 20.6 (2CH $_3$).

FIGURE 4.2 THE ^1H NMR SPECTRA (ACETONE- D_6 , 500 MHZ) OF **91**FIGURE 4.3 THE ^{13}C NMR SPECTRA (ACETONE- D_6 , 125 MHZ) OF **91**

The ^1H NMR Spectra of **92** (Figure 4.4) displayed two doublet signals at δ_{H} 7.67 (d, $J = 15.0$ Hz, 1H), and 7.61 (d, $J = 15.5$ Hz, 1H) belonged to *trans*-olefinic proton. Two doublet signals on A ring showed at δ_{H} 8.00 (d, $J = 8.5$ Hz, 2H), and 6.71 (d, $J = 9.0$ Hz, 2H) due to symmetry structure, while three signals on B ring had an ABX pattern at δ_{H} 7.33 (d, $J = 2.0$ Hz, 1H), 7.20 (dd, $J = 8.5, 2.5$ Hz, 1H), and 6.99 (d, $J = 8.0$ Hz, 1H). The triplet signal on amino group (NH) was detected at δ_{H} 5.84 (t, $J = 6.0$ Hz, 1H) due to neighboring with methylene (CH_2), and the methoxy group (OCH_3) was appeared as a singlet signal at δ_{H} 3.89 (s, 3H). The methylene group signal was observed more down field at δ_{H} 3.14 (t, $J = 6.0$ Hz, 2H) due to attach with NH, compared with the other aliphatic signals at δ_{H} 1.59 (heptet, $J = 6.0$ Hz, 1H), 1.45 (m, 4H), and 0.92 (t, $J = 7.0$ Hz, 6H). The ^{13}C NMR Spectra of **92** (Figure 4.5) presented a carbonyl signal at δ_{C} 186.9 (C=O) was more down field because of conjugation electron from olefinic to carbonyl, while an aromatic carbon signal (=C-N) at δ_{C} 154.2, and two signals of oxygenated carbon aromatic at δ_{C} 150.3 (=C- OCH_3), and 147.7 (=C-OH) were observed. The sp^2 carbon signals were visualized at δ_{C} 142.7-111.9 including aromatic and olefinic carbons, while sp^3 carbon presented at δ_{C} 56.3 (OCH_3), 46.6 (CH_2), 41.2 (CH), 24.4 (2CH_2), 11.2 (2CH_3).

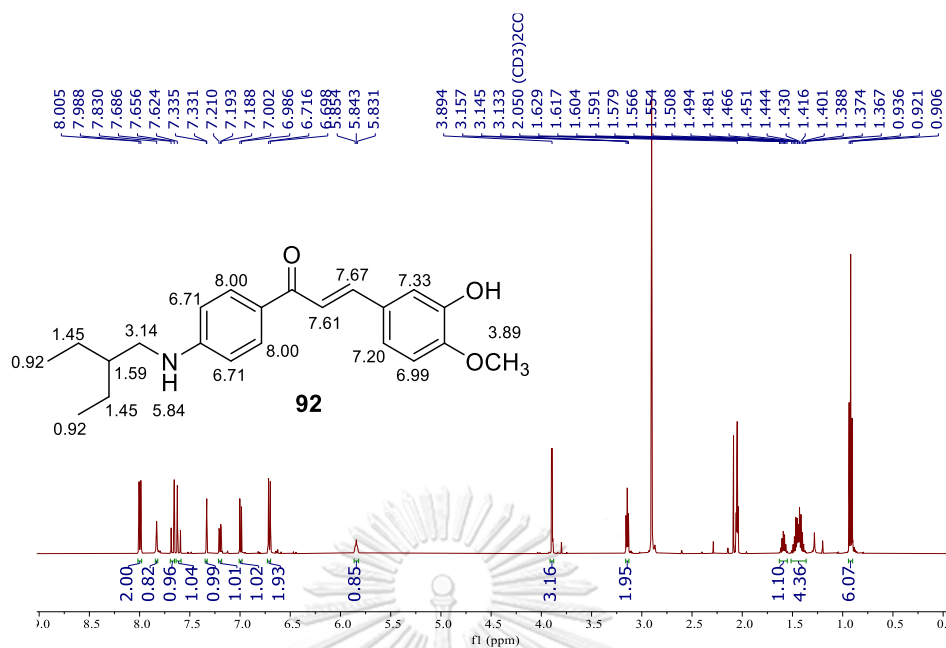


FIGURE 4.4 THE ^1H NMR SPECTRA (ACETONE- D_6 , 500 MHZ) OF **92**

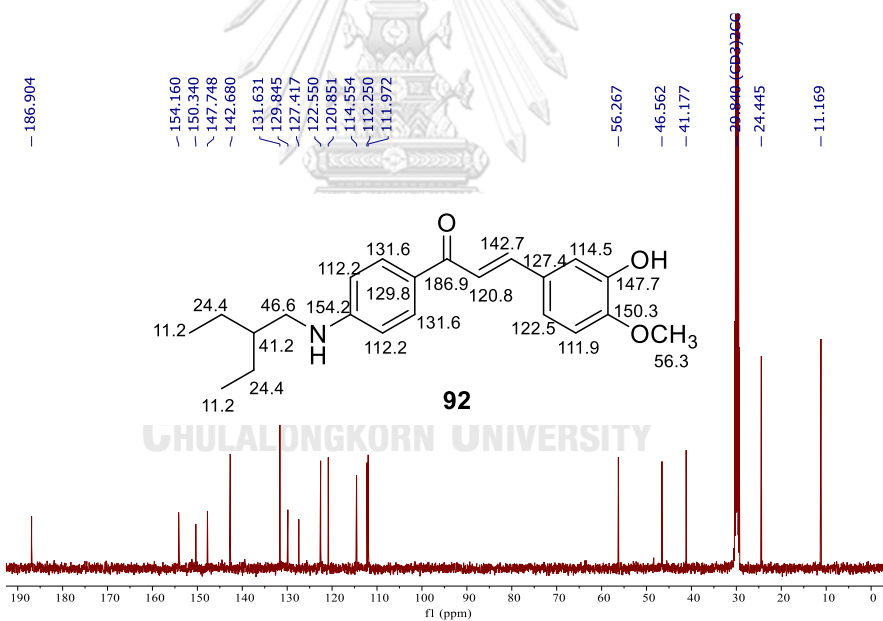


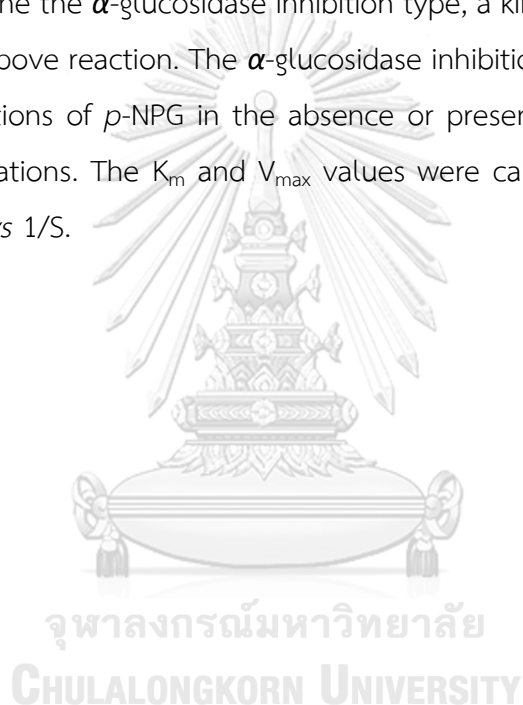
FIGURE 4.5 THE ^{13}C NMR SPECTRA (ACETONE- D_6 , 125 MHZ) OF **92**

4.2.2.5 ALPHA-GLUCOSIDASE ASSAY

The α -glucosidase (0.1 U/mL) and *p*-nitrophenyl- α -*D*-glucopyranoside, *p*-NPG (substrate, 1 mM) were dissolved in 0.1 M phosphate buffer (pH 6.9). A test sample (10 μL) was pre-incubated with α -glucosidase (40 μL) at 37 $^\circ\text{C}$ for 10 min. The substrate

solution (50 μL) was then added to the reaction mixture and incubated at 37 $^{\circ}\text{C}$ for an additional 20 min and terminated by adding 1 M Na_2CO_3 solution (100 μL). Enzymatic activity was quantified by measuring the absorbance at 405 nm (ALLSHENG AMR-100 microplate reader). The percentage inhibition of activity was calculated as follows: % Inhibition = $[(A_0 - A_1)/A_0] \times 100$, where: A_0 is the absorbance without the sample; A_1 is the absorbance with the sample. The IC_{50} value was deduced from the plot of % inhibition vs concentration of test sample. Acarbose was used as a standard control and the experiment was performed in triplicate.

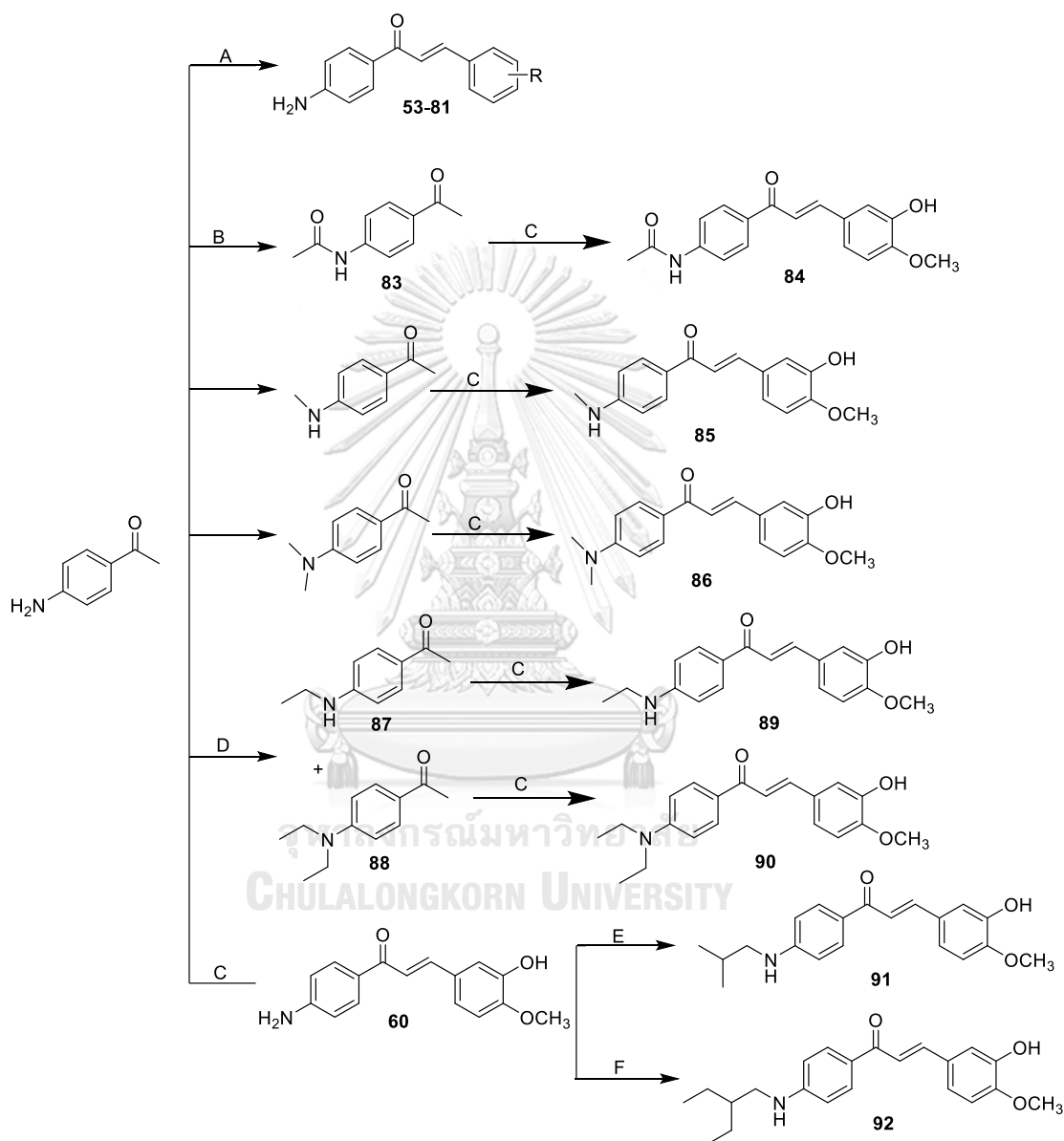
To determine the α -glucosidase inhibition type, a kinetic study was conducted according to the above reaction. The α -glucosidase inhibition type was determined at various concentrations of *p*-NPG in the absence or presence of test compounds at different concentrations. The K_m and V_{max} values were calculated from Lineweaver-Burk plots of $1/V$ vs $1/S$.



4.2.2 RESULTS AND DISCUSSION

4.2.2.1 SYNTHESIS OF 4'-AMINOCHALCONES AND THEIR DERIVATIVES

Thirty-six 4'-aminochalcones including their derivatives were synthesized as shown in Scheme 4.1.



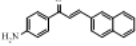
SCHEME 4.1 REAGENTS AND CONDITIONS: A) 6 M NaOH, MeOH, ROOM TEMPERATURE. B) ACETYL CHLORIDE, DCM, TEA, ROOM TEMPERATURE. C) ISOVANILLIN, 6 M NaOH, MeOH, ROOM TEMPERATURE. D) ETHYL IODIDE, ACETONE, K_2CO_3 , ROOM TEMPERATURE. E) ISOBUTYRALDEHYDE, $NaBH_3CN$, MeOH, ROOM TEMPERATURE. F) 2-ETHYL BUTYRALDEHYDE, $NaBH_3CN$, MeOH, ROOM TEMPERATURE.

4'-Aminochalcones (**53-81**) and their derivatives (**84, 85, 86, 89-92**) are presented in Scheme 4.1. 4'-Aminoacetophenone reacted with different substituted benzaldehydes in the presence of 6 M NaOH in MeOH at room temperature to obtain 4'-aminochalcones (**53-81**). **83** was obtained from the reaction of 4'-aminoacetophenone and acetyl chloride in dichloromethane and TEA at room temperature. **84** was synthesized from the treatment of **83** with isovanillin and 6 M NaOH in MeOH at room temperature. **85** and **86** were obtained from the reactions of *N*-methyl- and *N,N'*-dimethyl-4'-aminoacetophenones and isovanillin and 6 M NaOH in MeOH at room temperature. To attain **87** and **88**, 4'-aminoacetophenone reacted with excess ethyl iodide in acetone and K₂CO₃. **89** and **90** were obtained from the reactions of **87** and **88** with isovanillin with 6 M NaOH in MeOH. In this condition, *N*-alkyl(acetyl) aminoacetophenones was reacted with isovanillin in basic condition using Claisen-Schmidt condensation to synthesize compounds (**84, 85, 86, 89, 90**) which obtained the product in low yield (6-24%). This result may be due to different polarity when compared with compound **60** (yield 45%). **91** and **92** were synthesized from **60** with isobutyraldehyde and 2-ethyl butyraldehyde in MeOH to form imine and *in situ* reduced by NaBH₃CN at room temperature. Unfortunately, using reductive amination method, the **91** and **92** were obtained in very low yield (0.1%). This result was due to low reactivity of aliphatic aldehyde to form imine. Therefore, the product of reductive amination may obtain in very low yield.

4.2.2.2 BIOLOGICAL EVALUATION

To evaluate inhibitory activity of 4'-aminochalcones and their derivatives, thirty-six synthesized compounds (**53-92**) were evaluated for α -glucosidase inhibitory activity and their kinetic study as previous described.¹⁴¹ The results are shown in Tables 4.1 and 4.2. In this study, four levels of inhibition were categorized according to the IC₅₀ values compared with acarbose, *i.e.*, weak (>100-200 μ M), moderate (>50-100 μ M), strong (>10-50 μ M), and very strong (<10 μ M).

TABLE 4. 1 *IN VITRO* ALPHA-GLUCOSIDASE INHIBITORY ACTIVITIES OF 53-81

| Comp. | R | IC ₅₀ (μM) ^a | Comp. | R | IC ₅₀ (μM) ^a |
|-------|---|------------------------------------|-------|---|------------------------------------|
| 53 | 3'-OH | 32.78 ± 1.79 | 68 | 2'-OCH ₃ , 3'-OCH ₃ | >200 |
| 54 | 4'-OH | 41.0 ³⁵ | 69 | 2'-OCH ₃ , 6'-OCH ₃ | 75.27 ± 1.56 |
| 55 | 2'-OCH ₃ | 127.92 ± 8.98 | 70 | 3'-OCH ₃ , 5'-OCH ₃ | 168.34 ± 2.08 |
| 56 | 3'-OCH ₃ | 99.06 ± 7.62 | 71 | 2', 3'-(OCH ₂ O) | 150.46 ± 0.54 |
| 57 | 4'-OCH ₃ | 78.06 ± 6.16 | 72 | 2'-OH, 3'-OCH ₃ | 146.73 ± 2.86 |
| 58 | 3', 4'-(OCH ₂ O) | >200 | 73 | 2'-CH ₃ , 4'-CH ₃ , 6'-CH ₃ | >200 |
| 59 | 3'-OCH ₃ , 4'-OH | 89.35 ± 4.11 | 74 | 2'-F | 109.67 ± 0.11 |
| 60 | 3'-OH, 4'-OCH ₃ | 21.39 ± 1.06 | 75 | 3'-F | 59.12 ± 3.58 |
| 61 | 3'-OCH ₃ , 4'-OCH ₃ | >200 | 76 | 4'-F | 90.84 ± 6.09 |
| 62 | 2'-OCH ₃ , 4'-OCH ₃ , 5'-OCH ₃ | >200 | 77 | 2'-Br | 135.12 ± 9.61 |
| 63 | 3'-OCH ₃ , 4'-OCH ₃ , 5'-OCH ₃ | >200 | 78 | 3'-Br | >200 |
| 64 | 2'-OCH ₃ , 5'-OCH ₃ | 138.76 ± 3.54 | 79 | 4'-Br | 133.57 ± 3.23 |
| 65 | 2'-OCH ₃ , 4'-OCH ₃ | 103.87 ± 1.71 | 80 | 2'-Cl, 6'-Cl | >200 |
| 66 | 2'-OCH ₃ , 3'-OCH ₃ , 4'-OCH ₃ | >200 | 81 |  | >200 |
| 67 | 2'-OCH ₃ , 4'-OCH ₃ , 6'-OCH ₃ | 101.88 ± 0.79 | 82 | Acarbose | 93.63 ± 0.49 |

^aData are expressed as mean ± SD in triplicate

As shown in Table 4.1, 4'-aminochalcones displayed potent α -glucosidase inhibitors with IC₅₀ values of 21.39 – 90.84 μM. To determine structure-activity relationships, firstly, the introduction of monosubstituent on the B ring significantly inhibited α -glucosidase.⁹⁰ Monohydroxy (-OH) group on the B ring (**53** and **54**) exhibited stronger activity than acarbose. Nevertheless, monomethoxy (-OCH₃) group on the B ring (**55** and **56**) showed weak inhibitory activity, except **57** at *para* position being moderate with IC₅₀ value of 78.06 μM. These results showed that the hydroxy group was more important to the α -glucosidase inhibition perhaps due to its possibility more H-bonding interaction with α -glucosidase compared with the methoxy group.^{142, 143} The presence of halogen groups on the B ring (**74-80**) showed weak to moderate α -glucosidase inhibition with IC₅₀ values from 59.12 to more than 200 μM. Among halogen substituents studied, fluorine group revealed the most active halogen, especially at *meta* position (**75**). This data suggested that a less bulky fluorine atom provided a binding interaction between inhibitors and enzyme.^{144, 145} The effect of monosubstituent on α -glucosidase inhibition is summarized as presented in Figure 4.6.

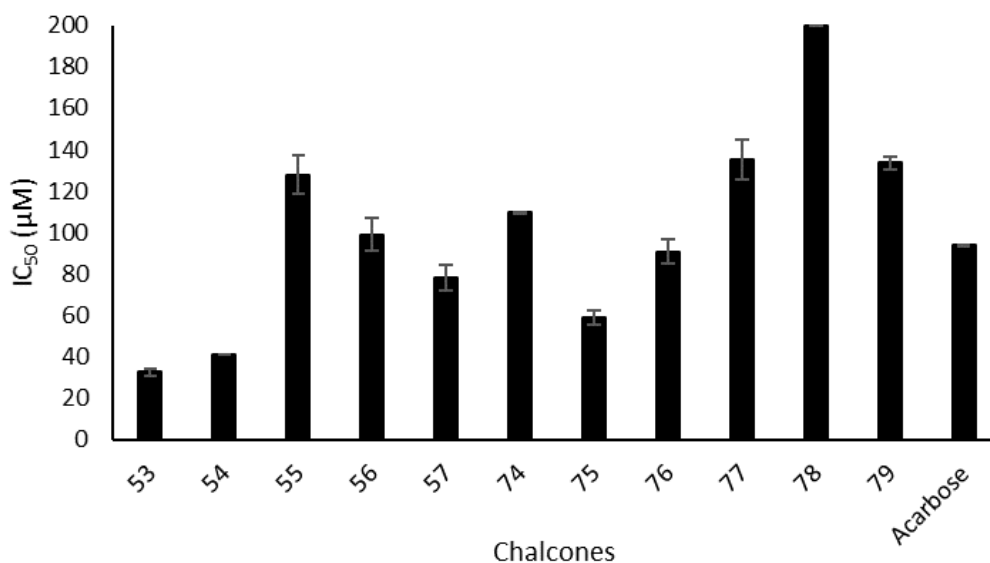


FIGURE 4.6 THE EFFECT OF MONOSUBSTITUENT (53-57, 74-79) ON ALPHA-GLUCOSIDASE INHIBITION

Further studies were carried out for di-, and trisubstituents on the B ring (58-73, 80). Dimethoxy ((-OCH₃)₂) and methylenedioxy (-OCH₂O-) decreased an inhibitory activity. Surprisingly, 69 with dimethoxy group at 2' and 6' positions displayed moderate inhibition with IC₅₀ value of 75.27 µM, whereas additional of methoxy group on 69 at 4' position, like 67 decreased an inhibitory activity. Moreover, 60, which possessed hydroxy group at *meta* and methoxy group *para* positions revealed strong α-glucosidase inhibitory activity around 4.4-fold compared with acarbose, when removing a methoxy group at *para* position decreased slightly inhibition activity, such as 32. In addition, 59 with a methoxy at *meta* and hydroxy at *para* position showed a moderate inhibition. Hence, these results showed that disubstituent contained hydroxy and methoxy group on the B ring increased an inhibitory activity due to hydroxy group, especially at *meta* position, which easily formed H-bonding with enzyme, whereas methoxy and methylenedioxy groups decreased an inhibition activity due to the lack of H-bonding with enzyme. Meanwhile, the trimethoxy group displayed a weak inhibitory activity; similarly, the hydrophobic group (73 and 81) also showed weak inhibitory activity. This data suggested that H-bonding formation on the B ring would be pivotal to enhance inhibitory activity.¹⁴⁶ The effect of di- and tri-substituent on α-glucosidase inhibition is accumulated as shown in Figure 4.7.

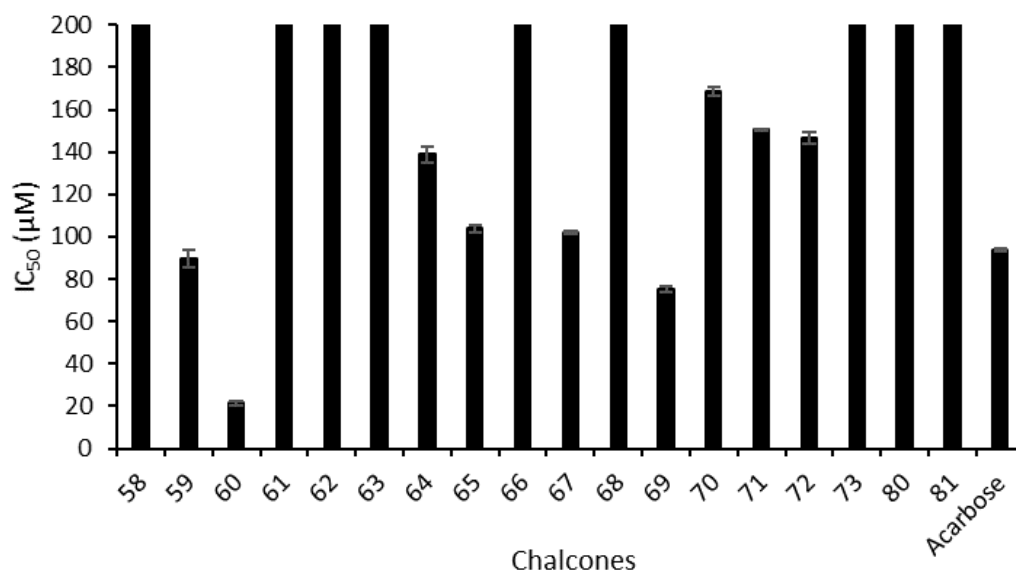


FIGURE 4.7 THE EFFECT OF DI- AND TRISUBSTITUENT (58-73, 80) AND NAPHTHYL (81) ON ALPHA-GLUCOSIDASE INHIBITION

TABLE 4.2 *IN VITRO* ALPHA-GLUCOSIDASE INHIBITORY ACTIVITIES OF 84-86, 89, AND 90-92

| Comp. | IC ₅₀ (µM) ^a | Comp. | IC ₅₀ (µM) ^a |
|-------|------------------------------------|----------|------------------------------------|
| 84 | 21.16 ± 2.68 | 90 | 37.78 ± 2.17 |
| 85 | 16.49 ± 0.86 | 91 | 1.81 ± 0.33 |
| 86 | 138.83 ± 4.64 | 92 | 0.14 ± 0.02 |
| 89 | 2.33 ± 0.14 | acarbose | 93.63 ± 0.49 |

^aData are expressed as mean ± SD in triplicate.

To determine the effect of *N*-substituted moiety on the A ring (**60**), a series of compounds was synthesized and then evaluated for their inhibitory activity as shown in Table 4.2. The acetylation of amino group (**84**) showed inhibitory activity comparable with **60**. Surprisingly, the introduction of monomethyl (**85**) or monoethyl (**89**) to the amino group significantly increased α -glucosidase inhibition with IC₅₀ values of 16.49 ± 0.86 and 2.33 ± 0.14 µM, respectively. However, the presence of the *N,N*-dimethyl group (**86**) decreased the activity significantly around 7-fold when compared with **60**. This phenomenon was also observed with *N,N*-diethyl (**90**) substituent which decreased the activity with IC₅₀ value of 37.78 ± 2.17 µM. This indicated that monoalkyl

and hydrogen on amino group would prefer to bind with amino residues through hydrophobic and H- bonding interaction.

Moreover, the investigation of mono *N*-alkyl substituent was conducted with branched alkyl to determine the steric effect and hydrophobicity. Surprisingly, isobutyl (**91**) and 2-ethyl butyl (**92**) on the amino group showed strong α -glucosidase inhibition with IC_{50} values of 1.81 ± 0.33 and $0.14 \pm 0.02 \mu\text{M}$, respectively. This suggested that more hydrophobic interaction on the A ring be a key factor binding with amino residues in α -glucosidase.^{147, 148} The effect of *N*-substituted 4'-aminochalcones against α -glucosidase inhibition is presented in Figure 4.8.

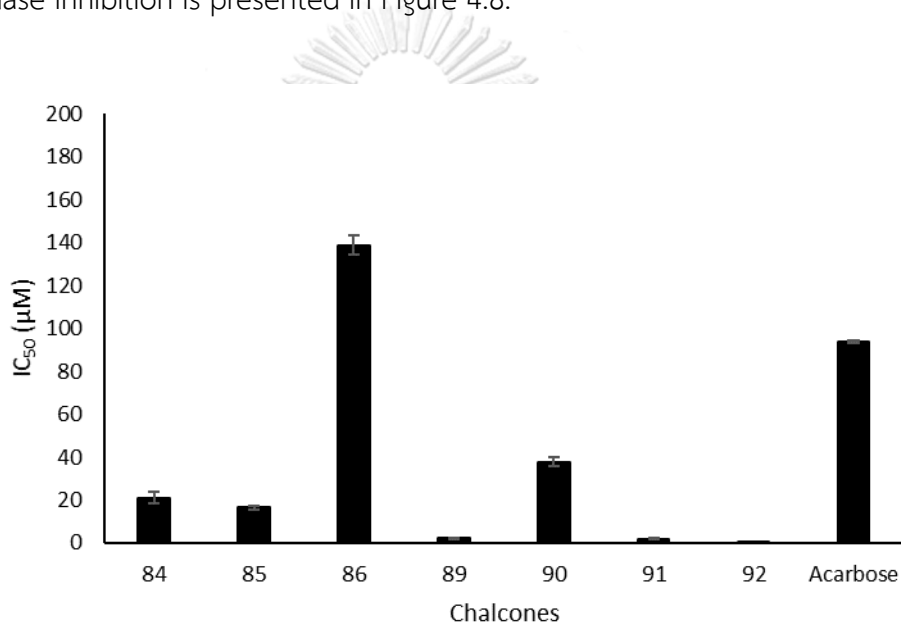


FIGURE 4.8 THE EFFECT OF *N*-SUBSTITUTED-4'-AMINOCHALCONES AGAINST ALPHA-GLUCOSIDASE INHIBITION

The inhibition modes of **84**, **85**, **89**, **91**, and **92** were evaluated from Lineweaver-Burk plots to investigate the inhibition mechanism of the α -glucosidase inhibitors using the previously published method.¹⁴¹ The results are presented in Table 4.3 and Figure 4.9.

TABLE 4.3 KINETIC STUDY OF 84, 85, 89, 91, AND 92

| Comp. | Concentration of Inhibitor (μM) | K_m (mM) ^a | V_{max} ($\Delta\text{OD}_{405}/\text{min}$) ^a | Mode of Inhibition |
|-------|--|-------------------------|---|--------------------|
| 84 | 0 | 0.22 | 0.24 | Uncompetitive |
| | 21.00 | 0.10 | 0.10 | |
| | 42.00 | 0.08 | 0.08 | |
| 85 | 0 | 0.19 | 0.18 | Mixed |
| | 11.00 | 0.26 | 0.13 | |
| | 33.00 | 0.19 | 0.07 | |
| 89 | 0 | 0.25 | 0.23 | Uncompetitive |
| | 1.60 | 0.18 | 0.15 | |
| | 4.70 | 0.11 | 0.07 | |
| 91 | 0 | 0.54 | 0.26 | Uncompetitive |
| | 1.80 | 0.09 | 0.05 | |
| | 3.60 | 0.06 | 0.03 | |
| 92 | 0 | 0.44 | 0.19 | Uncompetitive |
| | 0.14 | 0.24 | 0.11 | |
| | 0.28 | 0.14 | 0.06 | |

^aThe kinetic study was conducted in triplicate.

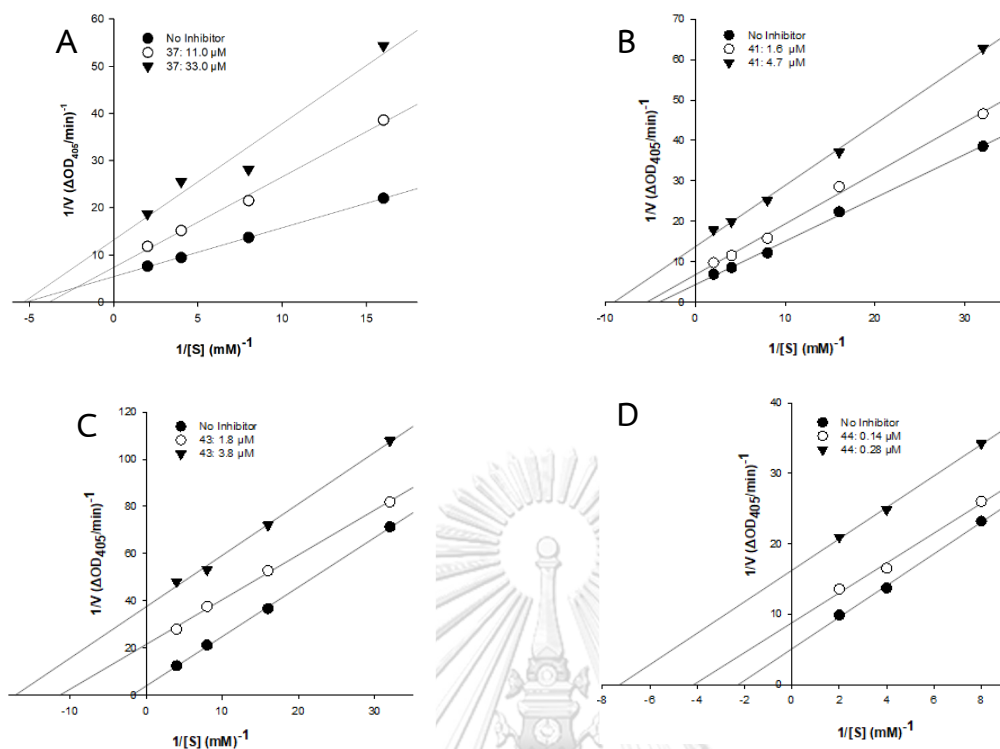


FIGURE 4.9 LINEWEAVER-BURK PLOTS OF THE KINETIC STUDY OF ALPHA-GLUCOSIDASE INHIBITION BY **85** (A), **89** (B), **91** (C), AND **92** (D)

As shown in Table 4.3, the data showed that **84**, **89**, **91**, and **92** demonstrated an uncompetitive inhibition as evident by the reduced K_m and V_{max} values with increasing inhibitor concentrations. These data revealed that **84**, **89**, **91**, and **92** were preferred to bind with enzyme-substrate complex rather than the free enzyme. Meanwhile, **85** with monomethyl on amino group showed an intersection of lines in the second quadrant on the Lineweaver-Burk plots as shown in Figure 4.9. These data suggested that **85** showed mixed-mode inhibitions with K_i values of 29.72 and 21.61 μM .

According to all results, the representative picture of structure-activity relationships (SARs) could be drawn as shown in Figure 4.10.

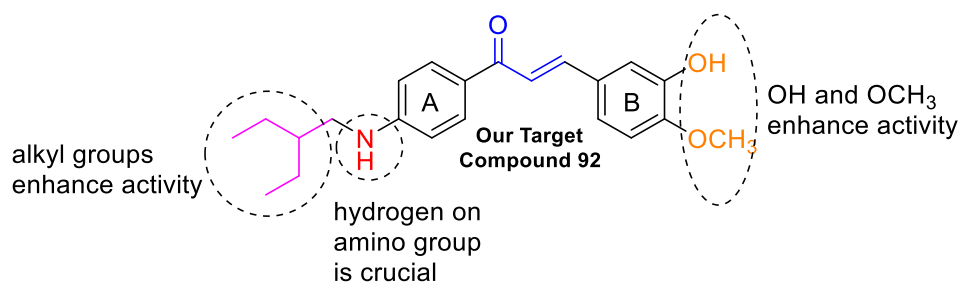


FIGURE 4.10 STRUCTURE-ACTIVITY RELATIONSHIP OF 4'-AMINOCHALCONES

The presence of the hydroxy group at *meta* position and the methoxy group at *para* position on the B ring are crucial to enhance inhibitory activity by providing hydrogen interaction, while *N*-monoalkyl group on A ring and hydrogen atom on the amino group are very necessary to enhance inhibitory activity by forming hydrophobic interaction with the enzyme. This study found that 4'-aminochalcones could have hydrogen bonding interaction on the B ring and hydrophobic interaction on the A ring to enhance α -glucosidase inhibitory activity.

4.3 SYNTHESIS, BIOACTIVITY EVALUATION, AND MOLECULAR DOCKING STUDY OF *E*-ARYLIDENE STEROID DERIVATIVES AS ALPHA-GLUCOSIDASE INHIBITORS

4.3.1 MATERIALS AND METHODS

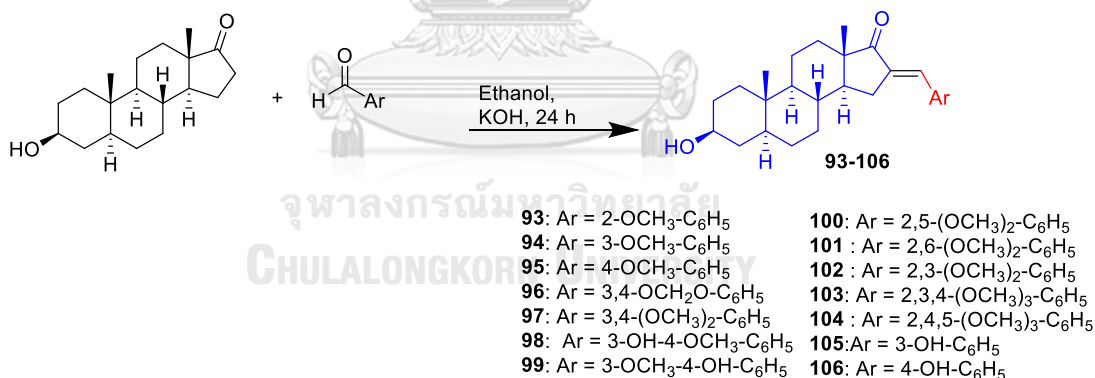
4.3.1.1 MATERIALS

Chemicals and equipment used were the same as described in Chapter 2.

4.3.2 METHODS

4.3.2.1 GENERAL PROCEDURE OF THE SYNTHESIS OF *E*-ARYLIDENE AND ITS DERIVATIVES (93-112)

Steroids (0.7 mmol) were added into the reaction flask along with ethanol (10 mL) at room temperature. 10 M KOH (1 mL) and substituted benzaldehyde (1.4 mmol) were added and the reaction was stirred at room temperature for 24 hours. Afterwards, 10% HCl was added to adjust the pH until around 3-4. The reaction mixture was extracted using EtOAc and evaporated to provide a crude product. The separation was performed with silica gel column using hexane and EtOAc (4:1).



(3*S*,5*S*,8*R*,9*S*,10*S*,13*S*,14*S*)-3-hydroxy-16-((*E*)-2-methoxybenzylidene)-10,13-dimethylhexadecahydro-17*H*-cyclopenta[*a*]phenanthren-17-one (**93**): Pale yellow powder; yield 99%. ¹H NMR (500 MHz, CDCl₃) δ = 7.83 (s, 1H), 7.48 (dd, *J* = 7.5, 2.0 Hz, 1H), 7.31 (dd, *J* = 7.5, 2.0 Hz, 1H), 6.97 (t, *J* = 7.5 Hz, 1H), 6.90 (d, *J* = 8.0 Hz, 1H), 3.85 (s, 3H), 3.58 (m, 1H), 2.76 (ddd, *J* = 8.0, 6.0, 1.5 Hz, 1H), 2.38 (ddd, *J* = 16.0, 13.0, 3.0 Hz, 1H), 1.63-1.85 (m, 8H), 1.26-1.42 (m, 7H), 1.09-1.16 (m, 1H), 0.97-1.02 (m, 1H), 0.95 (s, 3H), 0.85 (s, 3H), 0.69-0.75 (m, 1H). ¹³C NMR (125 MHz, CDCl₃) δ = 209.9, 158.8, 136.2,

130.7, 129.7, 127.8, 124.8, 120.3, 110.9, 71.3, 55.6, 54.6, 49.8, 47.8, 44.9, 38.2, 36.9, 35.8, 34.8, 31.8, 31.6, 31.2, 29.5, 28.5, 20.7, 14.6, 12.5.

(3*S*,5*S*,8*R*,9*S*,10*S*,13*S*,14*S*)-3-hydroxy-16-((*E*)-3-methoxybenzylidene)-10,13-

dimethylhexadecahydro-17*H*-cyclopenta[*a*]phenanthren-17-one (**94**): White powder; yield 98%. ¹H NMR (500 MHz, CDCl₃) δ = 7.38 (s, 1H), 7.32 (t, *J* = 8.0 Hz, 1H), 7.05 (s, 1H), 6.90 (dd, *J* = 8.0, 2.0 Hz, 1H), 3.83 (s, 3H), 3.59 (m, 1H), 2.86 (ddd, *J* = 8.5, 6.5, 2.0 Hz, 1H), 2.39 (ddd, *J* = 15.5, 12.5, 3.0 Hz, 1H), 1.80-1.93 (m, 5H), 1.65-1.74 (m, 3H), 1.29-1.42 (m, 6H), 1.11-1.17 (m, 1H), 0.96-1.03 (m, 2H), 0.95 (s, 3H), 0.86 (s, 3H), 0.71-0.77 (m, 1H). ¹³C NMR (125 MHz, CDCl₃) δ = 210.0, 159.7, 137.1, 136.6, 132.9, 129.7, 122.9, 115.8, 114.8, 71.3, 55.4, 54.6, 49.6, 47.7, 44.9, 38.1, 36.9, 35.8, 34.8, 31.8, 31.5, 31.2, 29.4, 28.5, 20.7, 14.6, 12.5. HRMS (ESI⁺): *m/z* calcd for C₂₇H₃₆O₃Na [M + Na]⁺ : 431.2562, found: 431.2554

(3*S*,5*S*,8*R*,9*S*,10*S*,13*S*,14*S*)-3-hydroxy-16-((*E*)-4-methoxybenzylidene)-10,13-

dimethylhexadecahydro-17*H*-cyclopenta[*a*]phenanthren-17-one (**95**): Pale yellow powder; yield 90%. ¹H NMR (500 MHz, CDCl₃) δ = 7.49 (d, *J* = 9.0 Hz, 2H), 7.37 (s, 1H), 6.93 (d, *J* = 9.0 Hz, 2H), 3.83 (s, 3H), 3.59 (m, 1H), 2.83 (ddd, *J* = 9.0, 7.0, 2.5 Hz, 1H), 2.36 (ddd, *J* = 15.5, 12.5, 3.0 Hz, 1H), 1.79-1.92 (m, 3H), 1.63-1.74 (m, 5H), 1.31-1.43 (m, 6H), 1.11-1.17 (m, 1H), 0.96-1.02 (m, 2H), 0.96 (s, 3H), 0.86 (s, 3H), 0.72 (m, 1H). ¹³C NMR (125 MHz, CDCl₃) δ = 210.2, 160.5, 133.9, 132.8, 132.2, 128.5, 114.3, 71.3, 55.5, 54.7, 49.7, 47.6, 44.9, 38.2, 36.9, 35.8, 34.8, 31.8, 31.6, 31.3, 29.4, 28.5, 20.7, 14.7, 12.5.

(3*S*,5*S*,8*R*,9*S*,10*S*,13*S*,14*S*,*E*)-16-(benzo[*d*][1,3]dioxol-5-ylmethylene)-3-hydroxy-10,13-

dimethylhexadecahydro-17*H*-cyclopenta[*a*]phenanthren-17-one (**96**): Brown powder; yield 91%. ¹H NMR (500 MHz, CDCl₃) δ = 7.32 (s, 1H), 7.04 (dd, *J* = 7.0, 2.0 Hz, 1H), 7.03 (s, 1H), 6.84 (d, *J* = 8.5 Hz, 1H), 6.0 (q, *J* = 1.5 Hz, 2H), 3.59 (m, 1H), 2.81 (ddd, *J* = 8.5, 6.5, 2.0 Hz, 1H), 2.34 (ddd, *J* = 15.5, 12.5, 3.0 Hz, 1H), 1.79-1.92 (m, 3H), 1.67-1.74 (m, 5H), 1.32-1.42 (m, 6H), 1.11-1.17 (m, 1H), 0.95-1.04 (m, 2H), 0.92 (s, 3H), 0.86 (s, 3H), 0.71-0.76 (m, 1H). ¹³C NMR (125 MHz, CDCl₃) δ = 210.1, 148.1, 134.3, 132.9, 130.1, 126.2, 109.5, 108.7, 101.6, 71.3, 54.7, 49.7, 47.7, 44.9, 38.1, 36.9, 35.8, 34.8, 31.8, 31.5, 31.3, 29.4, 28.5, 20.7, 14.7, 12.5.

(3*S*,5*S*,8*R*,9*S*,10*S*,13*S*,14*S*)-16-((*E*)-3,4-dimethoxybenzylidene)-3-hydroxy-10,13-dimethylhexadecahydro-17*H*-cyclopenta[*a*]phenanthren-17-one (**97**): Pale yellow powder; yield 92%. ¹H NMR (500 MHz, CDCl₃) δ = 7.36 (s, 1H), 7.15 (dd, *J* = 8.5, 2.0 Hz, 1H), 7.05 (d, *J* = 1.5 Hz, 1H), 6.9 (d, *J* = 8.5 Hz, 1H), 3.91 (s, 3H), 3.89 (s, 3H), 3.59 (m, 1H), 2.85 (ddd, *J* = 15.5, 7.0, 2.0 Hz, 1H), 2.38 (ddd, *J* = 16.0, 12.5, 3.5 Hz, 1H), 1.63–1.86 (m, 8H), 1.29–1.42 (m, 7H), 1.11–1.17 (m, 1H), 0.96–1.02 (m, 2H), 0.93 (s, 3H), 0.86 (s, 3H), 0.71–0.77 (m, 1H). ¹³C NMR (125 MHz, CDCl₃) δ = 210.1, 150.2, 148.9, 134.2, 133.1, 128.7, 124.0, 113.3, 111.2, 71.2, 56.1, 54.6, 49.7, 47.7, 44.9, 38.2, 36.9, 35.8, 34.8, 31.8, 31.5, 31.2, 31.0, 29.8, 29.4, 28.5, 20.7, 14.7, 12.4. HRMS (ESI⁺): *m/z* calcd for C₂₈H₃₈O₄Na [M + Na]⁺ : 461.2668, found: 461.2667

(3*S*,5*S*,8*R*,9*S*,10*S*,13*S*,14*S*)-3-hydroxy-16-((*E*)-3-hydroxy-4-methoxybenzylidene)-10,13-dimethylhexadecahydro-17*H*-cyclopenta[*a*]phenanthren-17-one (**98**): Yellow powder; yield 93%. ¹H NMR (500 MHz, CDCl₃) δ = 7.32 (s, 1H), 7.16 (d, *J* = 2.0 Hz, 1H), 7.05 (dd, *J* = 9.0, 2.5 Hz, 1H), 6.87 (d, *J* = 8.5 Hz, 1H), 3.92 (s, 3H), 3.59 (m, 1H), 2.84 (ddd, *J* = 16.0, 6.5, 2.0 Hz, 1H), 2.35 (ddd, *J* = 15.5, 12.5, 2.5 Hz, 1H), 1.64–1.89 (m, 8H), 1.27–1.38 (m, 7H), 1.10–1.15 (m, 1H), 0.96–1.02 (m, 2H), 0.92 (s, 3H), 0.85 (s, 3H), 0.70–0.76 (m, 1H). ¹³C NMR (125 MHz, CDCl₃) δ = 210.3, 147.7, 145.7, 134.3, 133.1, 129.3, 124.2, 115.7, 110.7, 71.3, 56.1, 54.7, 49.7, 47.6, 44.9, 38.1, 36.9, 35.8, 34.8, 31.8, 31.5, 31.3, 29.3, 28.5, 20.7, 14.7, 12.5. HRMS (ESI⁺): *m/z* calcd for C₂₇H₃₆O₄Na [M + Na]⁺ : 447.2511, found: 447.2499

(3*S*,5*S*,8*R*,9*S*,10*S*,13*S*,14*S*)-3-hydroxy-16-((*E*)-4-hydroxy-3-methoxybenzylidene)-10,13-dimethylhexadecahydro-17*H*-cyclopenta[*a*]phenanthren-17-one (**99**): Pale yellow powder; yield 25%. ¹H NMR (500 MHz, DMSO-*d*₆) δ = 9.61 (s, 1H), 7.19 (s, 1H), 7.15 (s, 1H), 7.09 (d, *J* = 8.5 Hz, 1H), 6.84 (d, *J* = 8.0 Hz, 1H), 3.79 (s, 3H), 2.74 (d, *J* = 9.0 Hz, 1H), 2.39–2.45 (m, 1H), 1.58–1.83 (m, 7H), 1.18–1.33 (m, 8H), 0.89–1.08 (m, 3H), 0.83 (s, 3H), 0.78 (s, 3H), 0.66–0.72 (m, 1H). ¹³C NMR (125 MHz, DMSO-*d*₆) δ = 208.7, 148.4, 147.6, 133.0, 132.6, 126.7, 124.2, 115.8, 114.4, 69.3, 55.6, 53.9, 49.1, 46.9, 44.4, 38.2, 36.6, 35.4, 34.2, 31.5, 30.6, 28.8, 28.2, 20.2, 14.3, 12.2.

(3*S*,5*S*,8*R*,9*S*,10*S*,13*S*,14*S*)-16-((*E*)-2,5-dimethoxybenzylidene)-3-hydroxy-10,13-dimethylhexadecahydro-17*H*-cyclopenta[*a*]phenanthren-17-one (**100**): Orange powder; yield 94%. ¹H NMR (500 MHz, CDCl₃) δ = 7.78 (dd, *J* = 3.0, 2.0 Hz, 1H), 7.04 (d, *J* = 3.0 Hz, 1H), 6.87 (dd, *J* = 9.0, 3.0 Hz, 1H), 6.83 (d, *J* = 9.0 Hz, 1H), 3.81 (s, 3H), 3.79 (s, 3H), 3.58 (m, 1H), 2.78 (ddd, *J* = 16.0, 6.5, 2.0 Hz, 1H), 2.38 (ddd, *J* = 15.5, 12.5, 3.0 Hz, 1H), 1.66-1.84 (m, 1H), 1.28-1.42 (m, 7H), 1.09-1.16 (m, 1H), 0.96-1.01 (m, 2H), 0.95 (s, 3H), 0.85 (s, 3H), 0.69-0.75 (m, 1H). ¹³C NMR (125 MHz, CDCl₃) δ = 209.8, 153.4, 153.1, 136.5, 127.7, 125.5, 115.7, 115.2, 111.8, 71.3, 56.2, 55.9, 54.6, 49.7, 47.8, 44.9, 38.1, 36.9, 35.8, 34.8, 31.8, 31.5, 31.3, 29.4, 28.5, 20.7, 14.6, 12.4. HRMS (ESI⁺): *m/z* calcd for C₂₈H₃₈O₄Na [M + Na]⁺ : 461.2668, found: 461.2669

(3*S*,5*S*,8*R*,9*S*,10*S*,13*S*,14*S*)-16-((*E*)-2,6-dimethoxybenzylidene)-3-hydroxy-10,13-dimethylhexadecahydro-17*H*-cyclopenta[*a*]phenanthren-17-one (**101**): White powder; yield 93%. ¹H NMR (500 MHz, CDCl₃) δ = 7.52 (s, 1H), 7.27 (t, *J* = 8.5 Hz, 1H), 6.56 (d, *J* = 8.0 Hz, 2H), 3.83 (s, 6H), 3.58 (m, 1H), 2.29 (ddd, *J* = 16.0, 6.5, 2.0 Hz, 1H), 2.17 (ddd, *J* = 16.0, 13.0, 3.0 Hz, 1H), 1.65-1.82 (m, 8H), 1.22-1.41 (m, 8H), 1.07-1.13 (m, 1H), 0.97 (s, 3H), 0.84 (s, 3H), 0.67-0.72 (m, 1H). ¹³C NMR (125 MHz, CDCl₃) δ = 209.8, 158.7, 139.5, 130.4, 125.6, 113.7, 103.7, 71.3, 55.8, 54.7, 48.6, 48.1, 44.9, 38.2, 36.9, 35.8, 34.8, 31.8, 31.6, 31.2, 30.0, 28.6, 20.7, 14.7, 12.5. HRMS (ESI⁺): *m/z* calcd for C₂₈H₃₈O₄Na [M + Na]⁺ : 461.2668, found: 461.2668

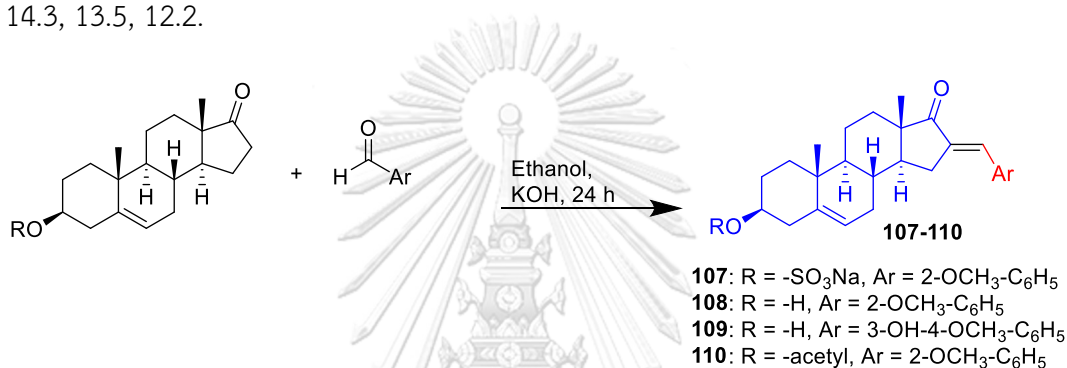
(3*S*,5*S*,8*R*,9*S*,10*S*,13*S*,14*S*)-16-((*E*)-2,3-dimethoxybenzylidene)-3-hydroxy-10,13-dimethylhexadecahydro-17*H*-cyclopenta[*a*]phenanthren-17-one (**102**): Orange powder; yield 70%. ¹H NMR (500 MHz, CDCl₃) δ = 7.75 (s, 1H), 7.12 (dd, *J* = 8.0, 2.0 Hz, 1H), 7.07 (t, *J* = 8.0 Hz, 1H), 6.93 (dd, *J* = 8.0, 1.5 Hz, 1H), 3.87 (s, 3H), 3.83 (s, 3H), 3.58 (m, 1H), 2.76 (ddd, *J* = 16.0, 6.5, 2.0 Hz, 1H), 2.36 (ddd, *J* = 15.5, 12.5, 3.0 Hz, 1H), 1.64-1.85 (m, 7H), 1.28-1.44 (m, 7H), 1.09-1.16 (m, 1H), 0.96-1.02 (m, 2H), 0.94 (s, 3H), 0.85 (s, 3H), 0.70-0.76 (m, 1H). ¹³C NMR (125 MHz, CDCl₃) δ = 209.8, 153.1, 149.2, 137.3, 130.1, 127.7, 123.8, 121.5, 113.4, 71.3, 61.5, 55.9, 54.6, 49.6, 47.8, 44.9, 38.1, 36.9, 35.8, 34.8, 31.8, 31.5, 31.2, 29.5, 28.5, 20.7, 14.6, 12.5. HRMS (ESI⁺): *m/z* calcd for C₂₈H₃₈O₄Na [M + Na]⁺ : 461.2668, found: 461.2684

(3*S*,5*S*,8*R*,9*S*,10*S*,13*S*,14*S*)-16-((*E*)-2,3,4-trimethoxybenzylidene)-3-hydroxy-10,13-dimethylhexadecahydro-17*H*-cyclopenta[*a*]phenanthren-17-one (**103**): Yellow powder; yield 90%. ¹H NMR (500 MHz, CDCl₃) δ = 7.69 (s, 1H), 7.25 (d, *J* = 9.0 Hz, 1H), 6.70 (d, *J* = 8.5 Hz, 1H), 3.89 (s, 3H), 3.88 (s, 3H), 3.86 (s, 3H), 3.58 (m, 1H), 2.75 (dd, *J* = 15.5, 6.5 Hz, 1H), 2.34 (ddd, *J* = 16.0, 12.5, 3.5 Hz, 1H), 1.67-1.82 (m, 7H), 1.27-1.42 (m, 7H), 1.09-1.15 (m, 1H), 0.96-1.02 (m, 2H), 0.93 (s, 3H), 0.85 (s, 3H), 0.70-0.76 (m, 1H). ¹³C NMR (125 MHz, CDCl₃) δ = 209.9, 154.9, 154.1, 142.4, 135.1, 127.4, 124.7, 122.8, 107.1, 71.2, 61.8, 61.0, 56.1, 54.6, 49.8, 47.7, 44.9, 38.1, 36.9, 35.8, 34.8, 31.8, 31.6, 31.3, 31.0, 29.8, 28.5, 20.7, 14.7, 12.5. HRMS (ESI⁺): *m/z* calcd for C₂₉H₄₀O₅H [M + H]⁺ : 469.2954, found: 469.2954

(3*S*,5*S*,8*R*,9*S*,10*S*,13*S*,14*S*)-16-((*E*)-2,4,5-trimethoxybenzylidene)-3-hydroxy-10,13-dimethylhexadecahydro-17*H*-cyclopenta[*a*]phenanthren-17-one (**104**): Yellow powder; yield 97%. ¹H NMR (500 MHz, CDCl₃) δ = 7.80 (s, 1H), 7.07 (s, 1H), 6.51 (s, 1H), 3.92 (s, 3H), 3.84 (s, 3H), 3.58 (m, 1H), 2.78 (ddd, *J* = 8.5, 6.5, 2.0 Hz, 1H), 2.37 (ddd, *J* = 15.5, 12.5, 3.0 Hz, 1H), 1.72-1.82 (m, 7H), 1.28-1.39 (m, 7H), 1.11-1.16 (m, 1H), 0.97-1.01 (m, 2H), 0.94 (s, 3H), 0.85 (s, 3H), 0.69-0.75 (m, 1H). ¹³C NMR (125 MHz, CDCl₃) δ = 209.9, 154.7, 151.5, 142.7, 133.6, 127.7, 116.4, 113.2, 96.9, 71.3, 56.8, 56.5, 56.1, 54.6, 49.8, 47.7, 44.9, 38.2, 36.9, 35.8, 34.8, 31.8, 31.5, 31.2, 29.5, 28.5, 20.7, 14.7, 12.4. HRMS (ESI⁺): *m/z* calcd for C₂₉H₄₀O₅H [M + H]⁺ : 469.2954, found: 469.2955

(3*S*,5*S*,8*R*,9*S*,10*S*,13*S*,14*S*)-3-hydroxy-16-((*E*)-3-hydroxybenzylidene)-10,13-dimethylhexadecahydro-17*H*-cyclopenta[*a*]phenanthren-17-one (**105**): Brown powder; yield 75%. ¹H NMR (500 MHz, DMSO-*d*₆) δ = 9.63 (s, 1H), 7.24 (t, *J* = 8.5 Hz, 1H), 7.16 (s, 1H), 7.03 (d, *J* = 8.0 Hz, 1H), 7.01 (d, *J* = 2.5 Hz, 1H), 6.80 (dd, *J* = 8.0, 3.0 Hz, 1H), 3.34 (m, 1H), 2.75 (ddd, *J* = 8.5, 6.5, 2.0 Hz, 1H), 2.41 (ddd, *J* = 16.0, 13.0, 3.0 Hz, 1H), 1.72-1.81 (m, 2H), 1.58-1.65 (m, 4H), 1.20-1.36 (m, 7H), 1.02-1.08 (m, 1H), 0.87-0.99 (m, 1H), 0.84 (s, 3H), 0.79 (s, 3H), 0.66-0.72 (m, 1H). ¹³C NMR (125 MHz, DMSO-*d*₆) δ = 208.7, 157.6, 136.4, 136.2, 132.1, 129.9, 121.6, 116.7, 116.6, 69.4, 53.9, 48.8, 47.0, 44.4, 38.1, 36.6, 35.4, 34.2, 31.4, 30.8, 30.7, 28.9, 28.2, 20.2, 14.2, 12.2. HRMS (ESI⁺): *m/z* calcd for C₂₆H₃₄O₃Na [M + Na]⁺ : 417.2406, found: 417.2405

(3*S*,5*S*,8*R*,9*S*,10*S*,13*S*,14*S*)-3-hydroxy-16-((*E*)-4-hydroxybenzylidene)-10,13-dimethylhexadecahydro-17*H*-cyclopenta[*a*]phenanthren-17-one (**106**): Pale yellow powder; yield 45%. ¹H NMR (500 MHz, DMSO-*d*₆) δ = 10.02 (s, 1H), 7.46 (d, *J* = 9.0 Hz, 2H), 7.18 (s, 1H), 6.83 (d, *J* = 8.5 Hz, 2H), 3.34 (m, 1H), 2.71 (ddd, *J* = 8.5, 6.5, 2.0 Hz, 1H), 2.37 (m, 1H), 1.79-1.83 (m, 1H), 1.71-1.74 (m, 1H), 1.56-1.65 (m, 5H), 1.21-1.33 (m, 7H), 1.02-1.08 (m, 1H), 0.86-0.97 (m, 2H), 0.82 (s, 3H), 0.78 (s, 3H), 0.66-0.72 (m, 1H). ¹³C NMR (125 MHz, DMSO-*d*₆) δ = 208.7, 158.9, 132.8, 132.4, 132.2, 126.2, 115.8, 69.4, 53.9, 50.7, 49.1, 47.2, 46.9, 44.5, 38.2, 36.6, 35.4, 34.2, 31.5, 31.4, 30.7, 28.9, 28.2, 21.4, 20.2, 14.3, 13.5, 12.2.



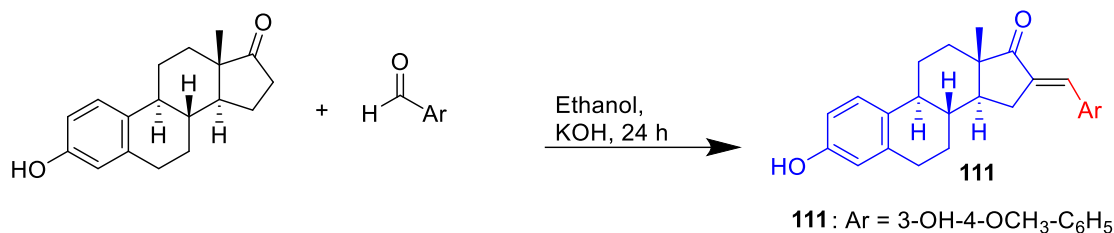
sodium (3*S*,8*R*,9*S*,10*R*,13*S*,14*S*)-16-((*E*)-2-methoxybenzylidene)-10,13-dimethyl-17-oxo-2,3,4,7,8,9,10,11,12,13,14,15,16,17-tetradecahydro-1*H*-cyclopenta[*a*]phenanthren-3-yl sulfate (**107**): Brown powder; yield 20%. ¹H NMR (500 MHz, CDCl₃) δ = 7.61 (s, 1H), 7.56 (d, *J* = 8.0 Hz, 1H), 7.39 (t, *J* = 8.0 Hz, 1H), 7.07 (d, *J* = 8.5 Hz, 1H), 7.02 (t, *J* = 8.0 Hz, 1H), 5.32 (d, *J* = 5.5 Hz, 1H), 3.83 (s, 3H), 2.68 (dd, *J* = 16.0, 6.0 Hz, 1H), 2.40 (dd, *J* = 15.0, 7.0 Hz, 1H), 2.18 (t, *J* = 13.0 Hz, 1H), 2.10 (d, *J* = 17.0 Hz, 1H), 1.89 (d, *J* = 15.5 Hz, 1H), 1.80 (d, *J* = 13.0 Hz, 2H), 1.61-1.72 (m, 3H), 1.38-1.53 (m, 3H), 1.26-1.33 (m, 3H), 0.98-1.03 (m, 3H), 0.88 (s, 3H). ¹³C NMR (125 MHz, DMSO-*d*₆) δ = 208.4, 158.2, 140.8, 135.9, 131.1, 129.4, 126.2, 123.6, 120.8, 120.4, 111.3, 75.3, 55.6, 49.7, 49.1, 46.8, 36.8, 36.3, 31.2, 30.6, 30.2, 28.8, 19.9, 19.1, 13.9. HRMS (ESI⁺): *m/z* calcd for C₂₇H₃₃NaO₆SNa [M + Na]⁺ : 531.1793, found: 531.1786

(3*S*,8*R*,9*S*,10*R*,13*S*,14*S*)-3-hydroxy-16-((*E*)-2-methoxybenzylidene)-10,13-dimethyl-1,2,3,4,7,8,9,10,11,12,13,14,15,16-tetradecahydro-17*H*-cyclopenta[*a*]phenanthren-17-one (**108**): Orange powder; yield 61%. ¹H NMR (500 MHz, CDCl₃) δ = 7.85 (s, 1H), 7.49 (d, *J* = 7.5 Hz, 1H), 7.33 (t, *J* = 7.0 Hz, 1H), 6.98 (t, *J* = 7.5 Hz, 1H), 6.91 (d, *J* = 8.0 Hz,

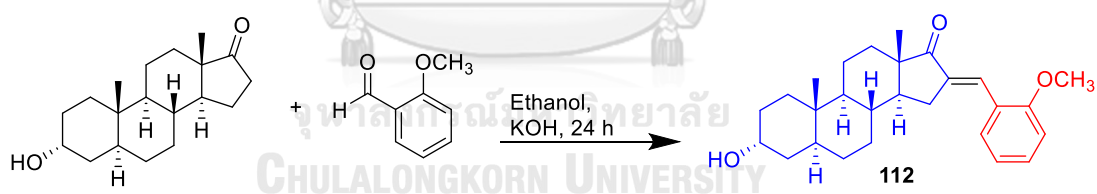
1H), 5.37 (d, $J = 5.5$ Hz, 1H), 3.86 (s, 3H), 3.52 (m, 1H), 2.78 (dd, $J = 15.5, 6.0$ Hz, 1H), 2.42 (ddd, $J = 16.0, 13.0, 3.5$ Hz, 1H), 2.22-2.34 (m, 3H), 2.12-2.16 (m, 2H), 1.96-1.98 (m, 2H), 1.83-1.88 (m, 2H), 1.47-1.66 (m, 4H), 1.29-1.42 (m, 3H), 1.06 (s, 3H), 0.98 (s, 3H). ^{13}C NMR (125 MHz, CDCl_3) $\delta = 209.7, 158.8, 141.2, 135.9, 130.8, 129.7, 127.9, 124.7, 121.0, 120.3, 110.9, 71.7, 62.2, 55.6, 55.4, 50.4, 50.1, 47.5, 42.3, 37.2, 36.8, 31.7, 31.7, 31.3, 31.0, 29.8, 29.5, 20.5, 19.6, 14.3$. HRMS (ESI⁺): m/z calcd for $\text{C}_{27}\text{H}_{34}\text{O}_3\text{SNa}$ $[\text{M} + \text{Na}]^+$: 429.2406, found: 429.2409

(3*S*,8*R*,9*S*,10*R*,13*S*,14*S*)-3-hydroxy-16-((*E*)-3-hydroxy-4-methoxybenzylidene)-10,13-dimethyl-1,2,3,4,7,8,9,10,11,12,13,14,15,16-tetradecahydro-17*H*-cyclopenta[*a*]phenanthren-17-one (**109**): Yellow powder; yield 90%. ^1H NMR (500 MHz, CDCl_3) $\delta = 7.34$ (s, 1H), 7.17 (s, 1H), 7.05 (d, $J = 8.0$ Hz, 1H), 6.88 (d, $J = 8.5$ Hz, 1H), 5.39 (d, $J = 5.5$ Hz, 1H), 3.92 (s, 3H), 3.53 (m, 1H), 2.87 (dd, $J = 16.0, 6.5$ Hz, 1H), 2.16-2.42 (m, 5H), 1.96 (d, $J = 14.5$ Hz, 1H), 1.85-1.88 (m, 2H), 1.63-1.79 (m, 4H), 1.47-1.60 (m, 2H), 1.31-1.41 (m, 2H), 1.06 (s, 3H), 0.95 (s, 3H). ^{13}C NMR (125 MHz, CDCl_3) $\delta = 210.1, 147.8, 145.7, 141.2, 134.1, 133.2, 129.3, 124.3, 121.0, 115.7, 110.7, 71.7, 56.1, 50.5, 50.0, 47.4, 42.3, 37.2, 36.8, 31.7, 31.3, 31.1, 29.4, 20.5, 19.6, 14.4$. HRMS (ESI⁺): m/z calcd for $\text{C}_{27}\text{H}_{34}\text{O}_4\text{Na}$ $[\text{M} + \text{Na}]^+$: 445.2355, found: 445.2363

(3*S*,8*R*,9*S*,10*R*,13*S*,14*S*)-16-((*E*)-2-methoxybenzylidene)-10,13-dimethyl-17-oxo-2,3,4,7,8,9,10,11,12,13,14,15,16,17-tetradecahydro-1*H*-cyclopenta[*a*]phenanthren-3-yl acetate (**110**): Orange powder; yield 99%. ^1H NMR (500 MHz, CDCl_3) $\delta = 7.85$ (s, 1H), 7.49 (dd, $J = 8.0, 2.0$ Hz, 1H), 7.33 (td, $J = 8.5, 1.5$ Hz, 1H), 6.98 (t, $J = 7.5$ Hz, 1H), 6.91 (d, $J = 8.5$ Hz, 1H), 5.37 (d, $J = 5.5$ Hz, 1H), 3.85 (s, 3H), 3.52 (m, 1H), 2.78 (ddd, $J = 8.0, 6.5, 2.0$ Hz, 1H), 2.41 (ddd, $J = 15.5, 12.5, 3.0$ Hz, 1H), 2.22-2.33 (m, 2H), 2.16 (s, 3H), 1.95-1.99 (m, 3H), 1.83-1.88 (m, 2H), 1.47-1.72 (m, 4H), 1.29-1.42 (m, 2H), 1.01-1.12 (m, 2H), 1.06 (s, 3H), 0.98 (s, 3H). ^{13}C NMR (125 MHz, CDCl_3) $\delta = 209.7, 158.8, 141.2, 135.9, 130.8, 129.7, 127.9, 124.7, 121.0, 120.3, 110.9, 71.7, 55.6, 50.4, 50.1, 47.5, 42.3, 37.2, 36.8, 31.7, 31.7, 31.3, 31.0, 29.5, 20.5, 19.6, 14.3$. HRMS (ESI⁺): m/z calcd for $\text{C}_{29}\text{H}_{35}\text{O}_4$ $[\text{M} - \text{H}]$: 447.2541, found: 447.2489



(8*R*,9*S*,13*S*,14*S*)-3-hydroxy-16-((*E*)-3-hydroxy-4-methoxybenzylidene)-13-methyl-6,7,8,9,11,12,13,14,15,16-decahydro-17*H*-cyclopenta[*a*]phenanthren-17-one (**111**): Brown powder; yield 90%. ¹H NMR (500 MHz, DMSO-*d*₆) δ = 9.21 (s, 1H), 9.02 (s, 1H), 7.15 (s, 1H), 7.10 (d, *J* = 2.0 Hz, 1H), 7.04 (dd, *J* = 10.5, 2.0 Hz, 1H), 7.01 (d, *J* = 8.5 Hz, 1H), 6.95 (d, *J* = 8.5 Hz, 1H), 6.50 (dd, *J* = 8.5, 3.0 Hz, 1H), 6.44 (d, *J* = 3.0 Hz, 1H), 3.77 (s, 3H), 2.84-2.69 (m, 3H), 2.44-2.41 (m, 1H), 2.30-2.28 (m, 1H), 2.17-2.11 (m, 1H), 1.97-1.92 (m, 1H), 1.83-1.80 (m, 1H), 1.59-1.52 (m, 1H), 1.47-1.29 (m, 4H), 0.84 (s, 3H). ¹³C NMR (125 MHz, DMSO-*d*₆) δ = 196.9, 145.4, 139.5, 136.8, 127.5, 123.8, 122.7, 120.4, 118.3, 116.4, 113.6, 106.9, 105.4, 103.2, 102.4, 45.9, 38.2, 37.4, 33.8, 27.9, 21.8, 21.1, 19.4, 18.9, 16.7, 15.9. HRMS (ESI⁺): *m/z* calcd for C₂₆H₂₆O₄Na [M + Na]⁺ : 411.1936, found: 411.1939.



(3*R*,5*S*,8*R*,9*S*,10*S*,13*S*,14*S*)-3-hydroxy-16-((*E*)-2-methoxybenzylidene)-10,13-dimethylhexadecahydro-17*H*-cyclopenta[*a*]phenanthren-17-one (**112**): Yellow powder; yield 80%. ¹H NMR (500 MHz, CDCl₃) δ = 7.83 (s, 1H), 7.48 (dd, *J* = 8.0, 2.0 Hz, 1H), 7.32 (td, *J* = 8.5, 2.0 Hz, 1H), 6.96 (td, *J* = 7.5, 1.0 Hz, 1H), 6.90 (dd, *J* = 8.5, 1.0 Hz, 1H), 4.04 (t, *J* = 2.5 Hz, 1H), 3.85 (s, 3H), 2.77 (ddd, *J* = 8.5, 6.5, 2.0 Hz, 1H), 2.37 (ddd, *J* = 18.0, 12.5, 3.0 Hz, 1H), 1.90-1.93 (m, 1H), 1.82-1.85 (m, 1H), 1.57-1.72 (m, 7H), 1.25-1.38 (m, 7H), 0.98-1.06 (m, 1H), 0.95 (s, 3H), 0.84-0.87 (m, 1H), 0.83 (s, 3H). ¹³C NMR (126 MHz, CDCl₃) δ = 210.0, 158.8, 136.2, 130.7, 129.7, 127.7, 124.8, 120.3, 110.8, 66.5, 55.6, 54.6, 49.8, 47.8, 39.2, 36.5, 35.9, 34.8, 32.2, 31.8, 31.2, 29.5, 29.1, 28.4, 20.2, 14.6, 11.3. HRMS (ESI⁺): *m/z* calcd for C₂₇H₃₆O₃Na [M + Na]⁺ : 431.2562, found: 431.2557.

4.3.2.2 *IN VITRO* ALPHA-GLUCOSIDASE ASSAY

The α -glucosidase assay method was described the same as 4.2.2.2.

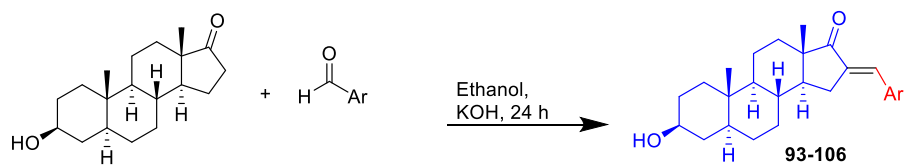
4.3.2.3 MOLECULAR MODELING

Molecular modelling was performed under the collaborative project with Department of Biochemistry, Faculty of Science, Chulalongkorn University and Center for Computational Sciences, University of Tsukuba. The amino sequence of α -glucosidase from *Saccharomyces cerevisiae* (uniport ID: P38158 and P53341)¹⁴⁹ was used to build the protein structure through homology modeling using SWISS-MODEL webserver¹⁵⁰ due to the lack of crystal structure in Protein Databank. Hydrogen atoms were then added to this protein structure and further optimized using ff14SB AMBER force field implemented in AMBER20.¹⁵¹ The 3D structures of selected *E*-arylidene and its derivatives were prepared on GaussView 6.0.16 and optimized by gaussian16 using HF/6-31G+ (d, p) basis. To perform the molecular docking using AutoDock Vina,¹⁵² protein structures and ligands were charged and converted to PDBQT format using AutoDockTools.¹⁵³ The *E*-arylidene and its derivatives were docked to the original receptor binding site (OBS)¹⁵⁴ of α -glucosidase and allosteric site predicted by POCASA 1.1 using roll algorithm.¹⁵⁵ The binding free energy of each ligand was ranked and compared to the known α -glucosidase inhibitor, acarbose.¹⁵⁶

4.3.2 RESULTS AND DISCUSSION

4.3.2.1 SYNTHESIS OF *E*-ARYLIDENE STEROID

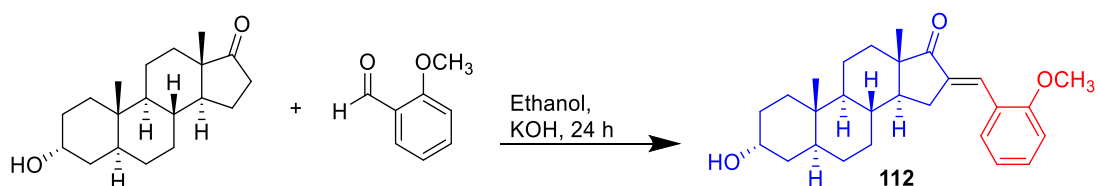
Twenty synthesized *E*-arylidene steroids were obtained using Claisen-Schmidt condensation as shown in Schemes 4.3-4.6.¹⁵⁷ Most compounds were obtained in high yield around 70-99%, while compound **107** obtained in low yield (20%) in reflux condition due to high polarity of steroid compound compared with others.



- | | |
|---|--|
| 93: Ar = 2-OCH ₃ -C ₆ H ₅ | 100: Ar = 2,5-(OCH ₃) ₂ -C ₆ H ₅ |
| 94: Ar = 3-OCH ₃ -C ₆ H ₅ | 101: Ar = 2,6-(OCH ₃) ₂ -C ₆ H ₅ |
| 95: Ar = 4-OCH ₃ -C ₆ H ₅ | 102: Ar = 2,3-(OCH ₃) ₂ -C ₆ H ₅ |
| 96: Ar = 3,4-OCH ₂ O-C ₆ H ₅ | 103: Ar = 2,3,4-(OCH ₃) ₃ -C ₆ H ₅ |
| 97: Ar = 3,4-(OCH ₃) ₂ -C ₆ H ₅ | 104: Ar = 2,4,5-(OCH ₃) ₃ -C ₆ H ₅ |
| 98: Ar = 3-OH-4-OCH ₃ -C ₆ H ₅ | 105: Ar = 3-OH-C ₆ H ₅ |
| 99: Ar = 3-OCH ₃ -4-OH-C ₆ H ₅ | 106: Ar = 4-OH-C ₆ H ₅ |

SCHEME 4.2 SYNTHESIS OF *E*-ARYLIDENE *EPI*-ANDROSTERONES 93-106

- | |
|---|
| 107: R = -SO ₃ Na, Ar = 2-OCH ₃ -C ₆ H ₅ |
| 108: R = -H, Ar = 2-OCH ₃ -C ₆ H ₅ |
| 109: R = -H, Ar = 3-OH-4-OCH ₃ -C ₆ H ₅ |
| 110: R = -acetyl, Ar = 2-OCH ₃ -C ₆ H ₅ |

SCHEME 4.3 SYNTHESIS OF *E*-ARYLIDENE DEHYDRO-*EPI*-ANDROSTERONES 107-110SCHEME 4.4 SYNTHESIS OF *E*-ARYLIDENE ESTRONES 111SCHEME 4.5 SYNTHESIS OF *E*-ARYLIDENE ANDROSTERONE 112

The structures of twenty compounds were determined using ¹H and ¹³C NMR spectroscopic methods. To describe the structural elucidation, **93** and **108** were selected as representatives. Structural elucidations of *E*-arylidene steroids had been reported as previous reference.^{103, 158}

The Spectra of ^1H NMR of **93** (Figure 4.11) shows a singlet signal of H-7' at δ_{H} 7.83 (s, 1H). Four signals of aromatic protons at δ_{H} 7.48 (dd, $J = 7.5, 2.0$ Hz, H-6', 1H), 7.31 (dd, $J = 7.5, 2.0$ Hz, H-4', 1H), 6.97 (t, $J = 7.5$ Hz, H-5', 1H), and 6.90 (d, $J = 8.0$ Hz, H-3', 1H) and a singlet signal of methoxy group at δ_{H} 3.85 (s, H-8', 3H). On the steroid structure, two signals of methyl groups were observed at δ_{H} 0.95 (s, H-18', 3H), and 0.85 (s, H-19', 3H) and the proton signal on the tetracyclic ring was visible at δ_{H} 3.58 (m, 1H), 2.76 (ddd, $J = 8.0, 6.0, 1.5$ Hz, 1H), 2.38 (ddd, $J = 16.0, 13.0, 3.0$ Hz, 1H), 1.63-1.85 (m, 8H), 1.26-1.42 (m, 7H), 1.09-1.16 (m, 1H), 0.97-1.02 (m, 1H), and 0.69-0.75 (m, 1H). The ^{13}C NMR Spectra of **93** (Figure 4.12) displays a carbonyl signal at δ_{C} 209.9 (C-17), and two signals of carbon sp^2 at δ_{C} 130.7 (C-16), and 136.2 (C-7'). Six signals of aromatic carbons were observed at δ_{C} 158.8, 129.7, 127.8, 124.8, 120.3, and 110.9. Moreover, the sp^3 carbon of tetracyclic ring was detected at δ_{C} 71.3 – 20.7, with two methyl groups at δ_{C} 12.5 (C-19), and 14.6 (C-18).

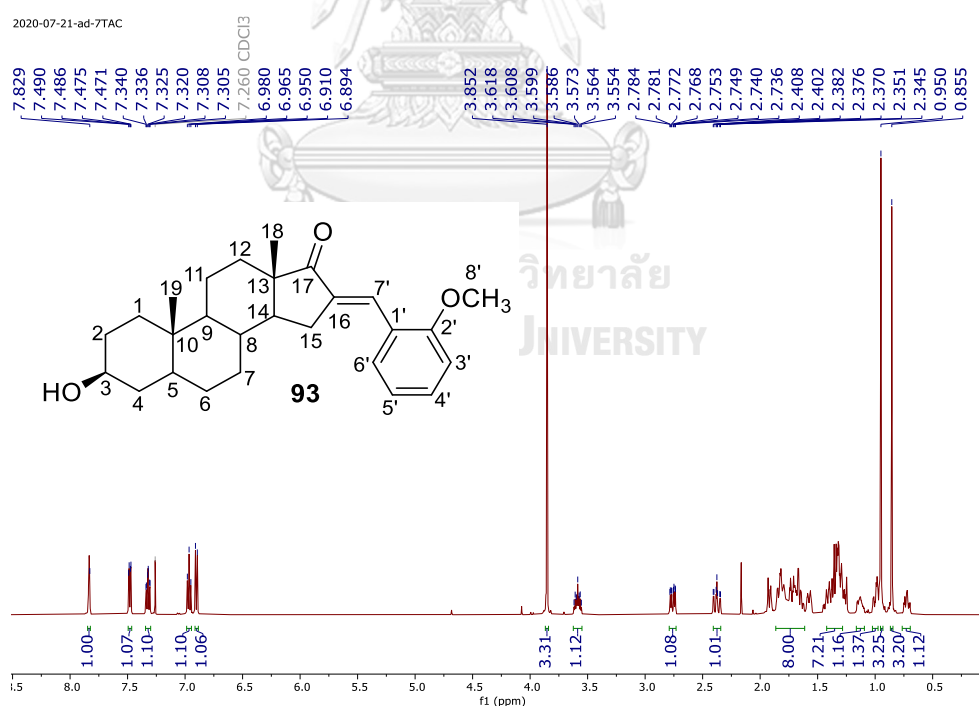


FIGURE 4. 11 THE ^1H NMR SPECTRA (CDCl_3 , 500 MHZ) OF **93**

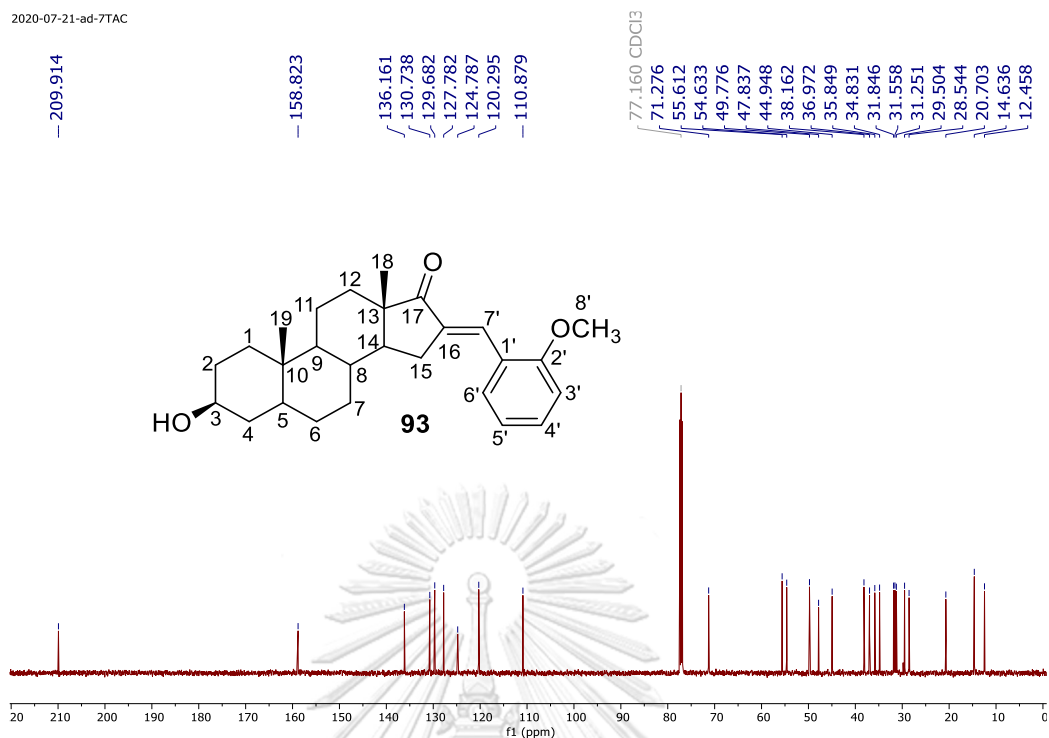
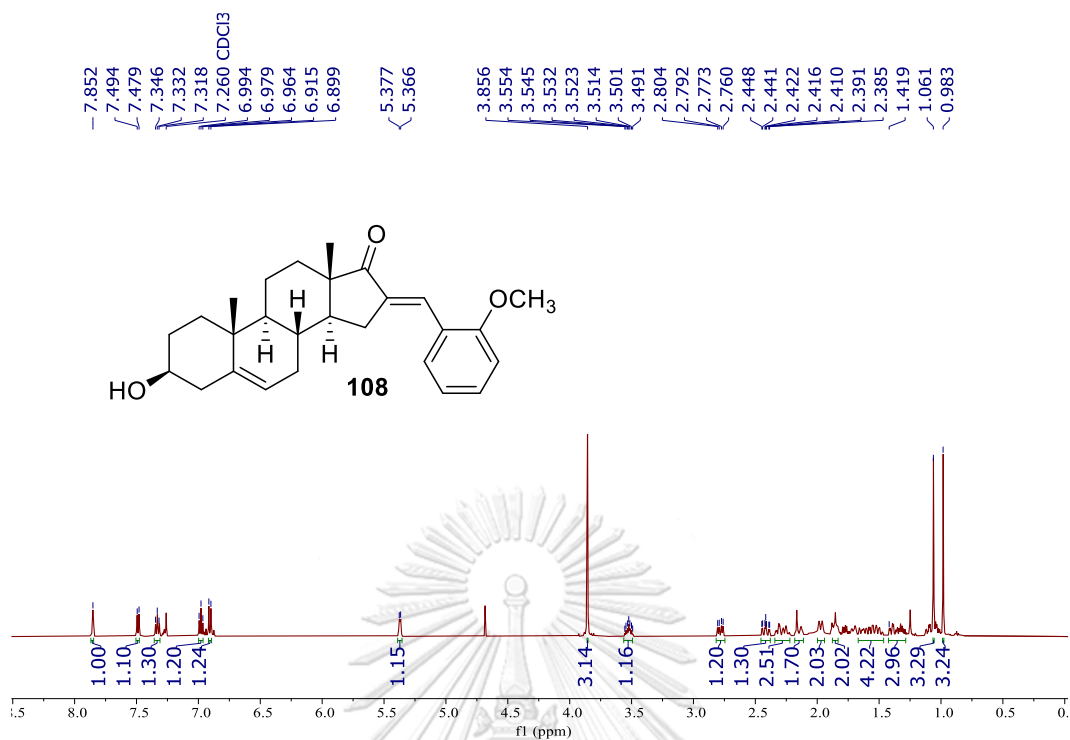
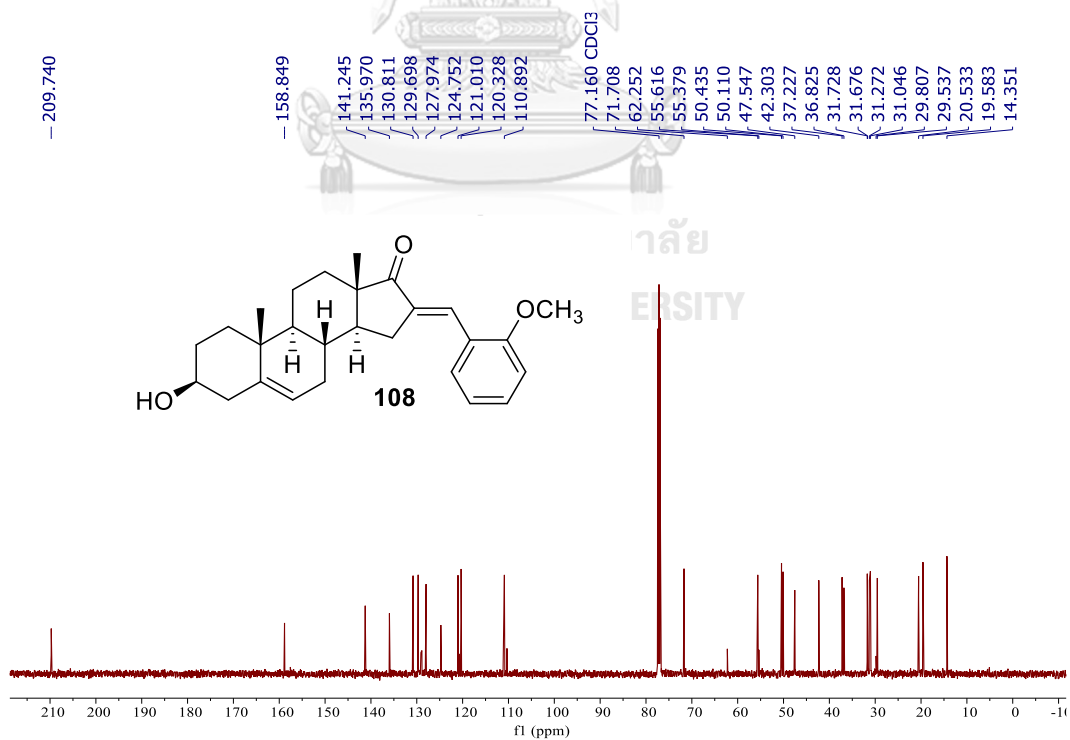


FIGURE 4.12 THE ¹³C NMR SPECTRA (CDCl₃, 125 MHZ) OF 93

The Spectra of ¹H NMR of **108** (Figure 4.13) showed a proton singlet signal at δ_{H} 7.85 (s, H-7', 1H), and four aromatic proton signals at δ_{H} 7.49 (d, $J = 7.5$ Hz, H-6', 1H), 7.33 (t, $J = 7.0$ Hz, H-4', 1H), 6.98 (t, $J = 7.5$ Hz, H-5', 1H), and 6.91 (d, $J = 8.0$ Hz, H-3', 1H). The sp^2 proton on the tetracyclic ring was detected at δ_{H} 5.37 (d, $J = 5.5$ Hz, H-6, 1H). Two methyl signals were displayed at δ_{H} 1.06 (s, 3H), and 0.98 (s, 3H). The sp^3 proton signal of tetracyclic ring was shown at δ_{H} 3.52-1.42. The ¹³C NMR Spectra of **108** (Figure 4.14) displays a carbonyl group at δ_{C} 209.7 (C-17). The aromatic carbons were observed at δ_{C} 158.8, 129.7, 128.0, 124.8, 120.3, and 110.9. The sp^2 carbon signals on C-16 and C-7' were shown at δ_{C} 121.0, and 141.2. On the steroid structure, the carbon signals were visualized at δ_{C} 121.0 (C-6), and 141.2 (C-5) for sp^2 ; 14.3 (C-19), and 19.6 (C-18) for two methyl groups; 71.7-20.5 for sp^3 carbons on the tetracyclic ring.

FIGURE 4.13 THE ¹H NMR SPECTRA (CDCl₃, 500 MHZ) OF 108FIGURE 4.14 THE ¹³C NMR SPECTRA (CDCl₃, 125 MHZ) OF 108

4.3.2.2 IN VITRO ALPHA-GLUCOSIDASE ACTIVITY

Steroid exhibited α -glucosidase inhibition activity.^{109, 110} Thus, *in vitro* α -glucosidase assay was conducted to investigate the inhibitory activity of *E*-arylidene steroids as presented in Tables 4.4 and 4.5. Acarbose was used as a positive control and IC_{50} was calculated from concentration of inhibitors vs percentage of inhibition. As shown in Table 4.4, the first series of fourteen *E*-arylidene *epi*-androsterones (**93-106**) was investigated for their inhibitory activity. The obtained results exhibited that most *E*-arylidene steroids (**93-106**) displayed better inhibitory activity compared with *trans*-androsterone itself and acarbose, especially **93** with IC_{50} value of $9.25 \pm 2.53 \mu\text{M}$. This result demonstrated that C-16 at steroid structure and monomethoxy (-OCH₃) at *ortho* position on aryl moiety could increase the α -glucosidase inhibition activity. Monohydroxy or monomethoxy benzaldehyde (**93-95, 105, 106**) exhibited a better inhibition activity compared with *trans*-androsterone itself, except **95**, but the inhibitory activities of **93** and **94** increased 3.5-10-fold when compared with acarbose. In addition, disubstituted benzaldehydes exhibited α -glucosidase inhibition activity better than acarbose, except five compounds (**99** and **101-104**). Nevertheless, *E*-arylidene steroid with trisubstituted benzaldehyde (**103, 104**) exhibited weak inhibitory α -glucosidase activity compared with acarbose.

TABLE 4.4 EVALUATION OF THE FIRST SERIES OF TESTED COMPOUNDS 93-106 AGAINST ALPHA-GLUCOSIDASE

| Compound | IC ₅₀ (μM) ^a | Compound | IC ₅₀ (μM) ^a |
|----------------------------|------------------------------------|-----------------------|------------------------------------|
| <i>Trans</i> -androsterone | 167.67±9.43 | 100 | 29.2±2.51 |
| 93 | 9.25±2.53 | 101 | 147.74±7.28 |
| 94 | 28.28±3.2 | 102 | 168.61±10.67 |
| 95 | >200 | 103 | 103.6±1.8 |
| 96 | 66.47±3.84 | 104 | 117.12±21.42 |
| 97 | 71.68±2.22 | 105 | 124.77±5.26 |
| 98 | 27.83±0.32 | 106 | 121.72±5.78 |
| 99 | 109.21±0.98 | acarbose [®] | 93.63±0.49 |

^aData are expressed as mean±S.D in triplicate

TABLE 4.5 EVALUATION OF THE SECOND SERIES OF TESTED COMPOUNDS 107-110, 111, 112 AGAINST ALPHA-GLUCOSIDASE

| Compound | IC ₅₀ (μM) ^a | Compound | IC ₅₀ (μM) ^a |
|----------|------------------------------------|-----------------------|------------------------------------|
| 107 | 1.84±0.28 | 111 | 26.99±2.27 |
| 108 | 4.71±0.39 | 112 | 101.68±1.63 |
| 109 | 21.38±6.01 | acarbose [®] | 93.63±0.49 |
| 110 | 3.47±1.09 | | |

^aData are expressed as mean±S.D in triplicate

To determine the structure-activity relationship of **93** and **98** was conducted by altering with the other steroids. Five of the total second series exhibited better inhibitory activity with IC₅₀ values of 1.84±0.28 - 26.99±2.27 μM compared with a positive control as shown in Table 4.5. **107** was the most potent among α-glucosidase inhibitors with IC₅₀ value of 1.84±0.28 μM. This finding showed that the double bond and sulfate moieties on the steroid structure would be the key factors to enhance the inhibitory activity. However, **112** possessing *R* configuration of OH at C-3 position on the steroid structure showed decrease of 10-fold inhibition when compared with **93**

possessing *S* configuration of OH at C-3 position. This finding showed that epimers might show different inhibitory activities.^{144, 159}

Kinetic study was conducted to explain the inhibition types of inhibitors with Lineweaver-Burk plots (Figure 4.15) for selected compounds that showed potency for α -glucosidase inhibitors such as **93**, **107**, **108**, and **110**.

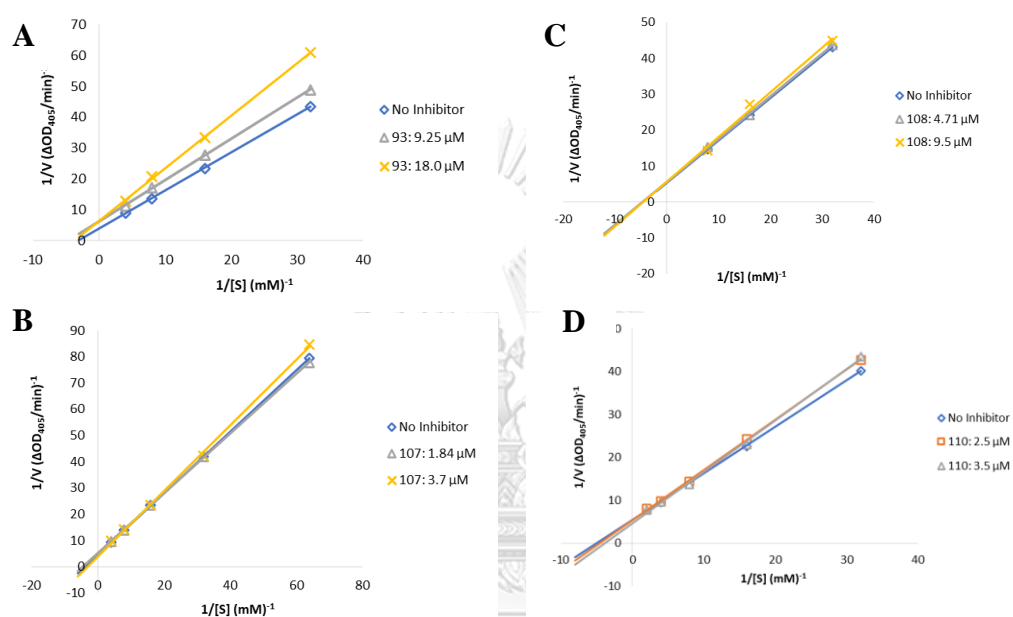


FIGURE 4.15 LINEWEAVER-BURK PLOTS FOR COMPOUNDS **93** (A), **107** (B), **108** (C), AND **110** (D).

TABLE 4.6 KINETIC STUDY OF THE *E*-ARYLIDENE STEROIDS 93, 107, 108, AND 110 AGAINST ALPHA-GLUCOSIDASE

| Comp. | Concentration of Inhibitor (μM) | K_m (mM) ^a | V_{max} ($\Delta\text{OD}_{405}/\text{min}$) ^a | Mode of Inhibition |
|------------|--|-------------------------|---|--------------------|
| | 0 | 0.32 | 0.26 | |
| 93 | 9.25 | 0.22 | 0.16 | Uncompetitive |
| | 18.0 | 0.27 | 0.16 | |
| | 0 | 0.26 | 0.22 | |
| 107 | 1.84 | 0.22 | 0.19 | Mixed |
| | 3.7 | 0.32 | 0.26 | |
| | 0 | 0.22 | 0.18 | |
| 108 | 4.71 | 0.22 | 0.18 | Noncompetitive |
| | 9.5 | 0.23 | 0.18 | |
| | 0 | 0.19 | 0.18 | |
| 110 | 2.5 | 0.22 | 0.19 | Competitive |
| | 7.0 | 0.26 | 0.21 | |

^aData are expressed in triplicate

As shown in Table 4.6, the increase concentration of **93** decreased K_m and V_{max} values through uncompetitive inhibition. Moreover, **107** showed a mixed-type inhibition, because K_m and V_{max} values fluctuated. The increase in concentration of **108** inhibited α -glucosidase through noncompetitive manner which did not alter V_{max} value, but K_m value increased. Compound **110** demonstrated competitive inhibition as evident by increase in both K_m and V_{max} values. This finding demonstrated that **93**, **107**, and **108** could inhibit α -glucosidase through allosteric site, and **110** could bind at the active site.

4.3.2.3 MOLECULAR MODELING

Four best compounds: **93**, **107**, **108**, and **110**, were selected to further study on the interactions of inhibitors including the effects of hydroxy, acetyl, and sodium sulfate groups at C-3 with binding pockets of α -glucosidase.

Molecular docking was performed under the collaborative project with Department of Biochemistry, Faculty of Science, Chulalongkorn University and Center for Computational Sciences, University of Tsukuba. The crystal structure of α -glucosidase is unknown, so the homology modeling technique is used to construct this protein structure by SWISS-model webserver.¹⁵⁰ The possible binding sites of this protein were predicted using POCASA 1.1, which is evaluated the binding site in terms of size and volume using roll algorithm.¹⁵⁵ The top three possible binding pockets of α -glucosidase structure are the active (OBS) and two allosteric (ABS1 and ABS2) sites as shown in Figure 4.16. The active site of α -glucosidase, OBS displayed the largest pocket volume with 481 Å³, while ABS1 and ABS2 were 106 Å³ and 213 Å³, respectively. According to previous study,¹⁶⁰ the prediction of binding pockets may have slightly similar. To investigate the possibility of binding inhibition mechanism, **93**, **107**, **108**, and **110** with the most potent α -glucosidase inhibitors were docked to the OBS, ABS1 and ABS2 sites using AutoDock Vina.¹⁵² Inhibition types of the inhibitors can be differentiated by studying of ligand binding sites. Unlike competitive inhibitors which inhibited through OBS site, the inhibition mechanisms of noncompetitive and uncompetitive inhibitors were bound to the ABS site. Therefore, **93**, **107**, and **108** were docked to ABS pockets, while **110** and acarbose were docked to OBS site.

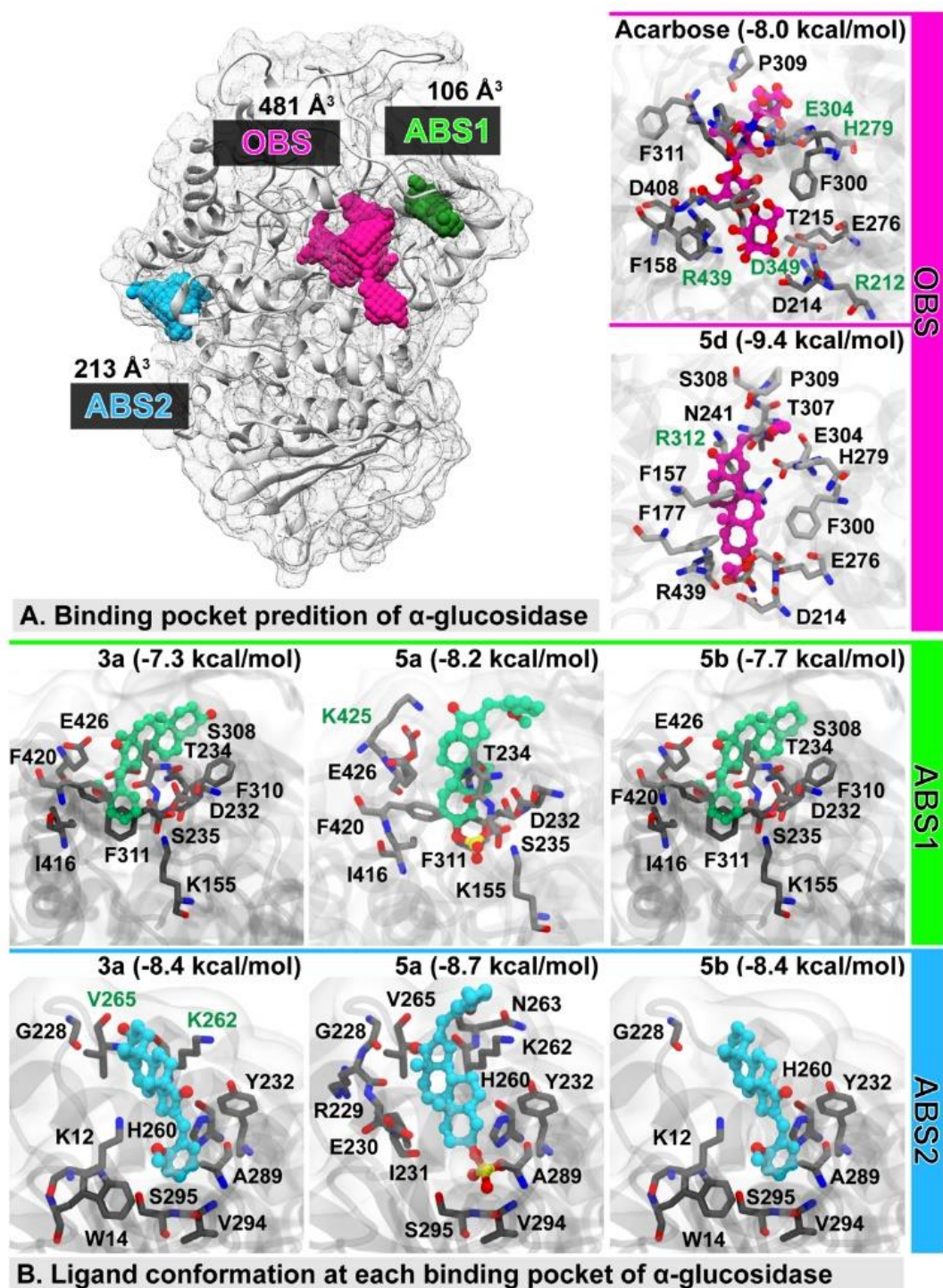


FIGURE 4.16 (A.) THE PREDICTED BINDING POCKETS OF ALPHA-GLUCOSIDASE HOMOLOGY MODEL; OBS (PINK), ABS1 (GREEN), AND ABS2 (BLUE). (B) THE CONFORMATION OF *E*-ARYLIDENE STEROIDS 93 (3A), 107 (5A), 108 (5B), AND 110 (5D) BOUND TO EACH BINDING SITE OF ALPHA-GLUCOSIDASE. HYDROGEN BOND INTERACTED RESIDUES WAS REPRESENTED BY GREEN LABEL THAT CONSISTENCE TO FIGURE 4.15.

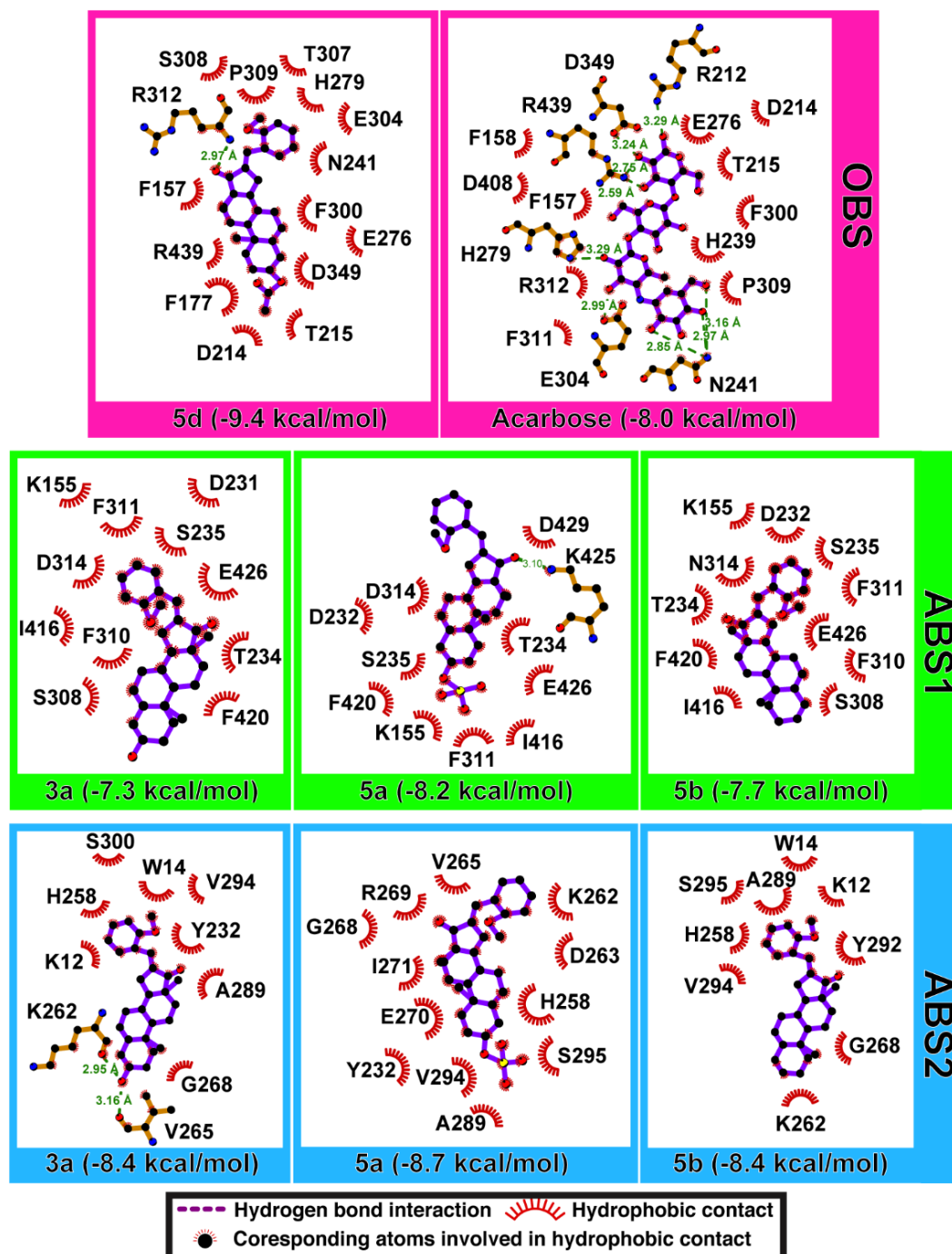


FIGURE 4.17 THE PREDICTION OF BINDING POCKET INTERACTIONS OF ALPHA-GLUCOSIDASE WITH 93 (3A), 107 (5A), 108 (5B), AND 110 (5D).

TABLE 4.7 THE BINDING INTERACTION SCORE (KCAL/MOL) OF THE *E*-ARYLIDENE STEROIDS **93**, **107**, **108**, AND **110** AGAINST ALPHA-GLUCOSIDASE AT THE ACTIVE (OBS) AND ALLOSTERIC BINDING SITES (ABS1, ABS2).

| Compound | OBS | ABS1 | ABS2 |
|-----------------|------|------|------|
| 93 | - | -7.3 | -8.4 |
| 107 | - | -8.2 | -8.7 |
| 108 | - | -7.7 | -8.4 |
| 110 | -9.4 | - | - |
| Acarbose | -8.0 | - | - |

According to the molecular docking study, **110** and Acarbose showed the best binding interaction score, which was bound to the OBS as shown in Table 4.7. Hydrophobic interaction is important for **110**, while acarbose formed the hydrogen bond interaction to nearby residues in this pocket congruent to the previous study¹⁶⁰ as shown in Figure 4.17. These compounds showed the similar binding conformation, the valienamine ring of Acarbose inserted to the center of OBS, which was the maltose binding site.¹⁶¹ Moreover, **110** bound to this site by the acetyl group (Figure 4.17). For ABS binding pockets, **93**, **107**, and **108** showed strong fit with the better binding interaction score to ABS2 than ABS1 approximately by -0.5 kcal/mol. These could suggest that the preferential binding site of these compounds **93**, **107**, and **108** was ABS2. Among these compounds, **107** revealed the strongest binding to ABS2 consistent with the experimental study with the sodium sulfate moiety binding with V294, A289, and S295. Both **93** and **108** revealed the similar binding to ABS1 and ABS2. However, the binding interaction score of **93** was slightly worse than **108** at ABS1 (Figure 4.17). This might be due to the different the core structure of **93** and **108**.

CHAPTER V

CONCLUSION

One hundred and eight chalcones and their analogues were synthesized using Claisen-Schmidt condensation. Thirty-three of two series chalcones including twenty-three 3',4',5'-trimethoxychalcones (**1-23**) and ten 3,4-dimethoxychalcones (**24-33**) were screened *in vitro* against A549 cancer cell lines. Seven compounds (**4, 5, 6, 11, 13, 15** and **20**) were disclosed as new potent candidates for lung cancer (A549) inhibitory activity. The structure-activity relationship displayed that electron donating groups including hydroxy and methoxy groups on the B ring, 3',4',5'-trimethoxyphenyl on the A ring and an enone part were crucial pharmacophores for the anti-cancer activity. Molecular docking suggested that hydrogen bonding, hydrophobic, and π -sulfur interaction be key parameters to stabilize the conformation in the pocket.

Forty-three chalcones were evaluated for cytotoxicity and twenty-seven was further investigated for anti-inflammatory in LPS-induced RAW 264.7 macrophage cells. Lead compounds including including 2'-hydroxychalcone (**34, 35, 42, 43, 45, and 48**) and 4'-aminochalcones (**54, 55, 57, 58, 59, 70**) exhibited high potent as anti-inflammatory without toxicity. The structure-activity relationships demonstrated that *para*-amino group on the A ring and electron donating group on the B ring played a key role to control anti-inflammatory activity including an enone part.

Thirty-six 4'-aminochalcones were tested for α -glucosidase inhibitory activity. *N*-monoalkyl substituent at *para*-position on the A ring and isovanillin part on the B ring (**89, 91, 92**) enhanced inhibitory activity against α -glucosidase. This result suggested that not only hydrogen bonding is involved to maintain the activity, but also hydrophobic interaction is occurred. Kinetic study of the best α -glucosidase inhibitory activity showed an uncompetitive manner. Therefore, the synthetic chalcones have a potency for type 2 diabetes mellitus (T2DM).

Twenty synthesized *E*-arylidene steroids were evaluated for α -glucosidase inhibitory activity. Three compounds (**107, 108, 110**) exhibited high α -glucosidase inhibitory activity. The structure-activity relationship demonstrated that methoxy at 2' position on the aryl moiety, double bond on endocyclic, and chiral center of hydroxy

group on the steroid structure are a key role to enhance α -glucosidase inhibitory activity. Moreover, the kinetic study revealed that those compounds exhibited uncompetitive, noncompetitive, and competitive inhibition mode, respectively. According to the molecular docking study, the second allosteric site (**ABS2**) exhibited high binding affinity with **93**, **107**, **108**, while **110** was bound with active site (**OBS**). A series of *E*-arylidene steroids could be the potent α -glucosidase inhibitory activity compared with acarbose.



REFERENCES



จุฬาลงกรณ์มหาวิทยาลัย
CHULALONGKORN UNIVERSITY

1. Zhou, B.; Xing, C., Diverse molecular targets for chalcones with varied bioactivities. *Med. Chem.* **2015**, *5*, 388.
2. Batovska, D. I.; Todorova, I. T., Trends in utilization of the pharmacological potential of chalcones. *Curr. Clin. Pharmacol.* **2010**, *5*, 1-29.
3. Singh, P.; Anand, A.; Kumar, V., Recent developments in biological activities of chalcones: A mini review. *Eur. J. Med. Chem.* **2014**, *85*, 758-777.
4. Zhuang, C.; Zhang, W.; Sheng, C.; Zhang, W.; Xing, C.; Miao, Z., Chalcone: a privileged structure in medicinal chemistry. *Chem.Rev.* **2017**, *117*, 7762-7810.
5. K Sahu, N.; S Balbhadra, S.; Choudhary, J.; V Kohli, D., Exploring pharmacological significance of chalcone scaffold: a review. *Curr. Med. Chem.* **2012**, *19*, 209-225.
6. Sebti, S. d.; Solhy, A.; Smahi, A.; Kossir, A.; Oumimoun, H., Dramatic activity enhancement of natural phosphate catalyst by lithium nitrate. An efficient synthesis of chalcones. *Catal. Commun.* **2002**, *3*, 335-339.
7. Gaonkar, S. L.; Vignesh, U., Synthesis and pharmacological properties of chalcones: a review. *Res. Chem. Intermed.* **2017**, *43*, 6043-6077.
8. Organization., W. H. Diabetes. <https://www.who.int/en/news-room/fact-sheets/detail/diabetes> (accessed November 24).
9. Bray, F.; Ferlay, J.; Soerjomataram, I.; Siegel, R. L.; Torre, L. A.; Jemal, A., Global cancer statistics 2018: GLOBOCAN estimates of incidence and mortality worldwide for 36 cancers in 185 countries. *CA Cancer J. Clin.* **2018**, *68*, 394-424.
10. Xu, G.; McLeod, H. L., Strategies for enzyme/prodrug cancer therapy. *Clin. Cancer Res.* **2001**, *7*, 3314-3324.
11. Fong, K. M.; Sekido, Y.; Minna, J. D., Molecular pathogenesis of lung cancer. *J. Thorac. Cardiovasc. Surg.* **1999**, *118*, 1136-1152.
12. Carcereny, E.; Morán, T.; Capdevila, L.; Cros, S.; Vilà, L.; de los Llanos Gil, M.; Remón, J.; Rosell, R., The epidermal growth factor receptor (EGFR) in lung cancer. *Transl. Respir. Med.* **2015**, *3*, 1-8.
13. Woll, P. J., New perspectives in lung cancer. 2. Growth factors and lung cancer. *Thorax.* **1991**, *46*, 924-929.

14. Ciardiello, F.; Tortora, G., Interactions between the epidermal growth factor receptor and type I protein kinase A: Biological significance and therapeutic implications. *Clin. Cancer Res.* **1998**, *4*, 821-828.
15. Woodburn, J., The epidermal growth factor receptor and its inhibition in cancer therapy. *Pharmacol. Ther.* **1999**, *82*, 241-250.
16. Ogiso, H.; Ishitani, R.; Nureki, O.; Fukai, S.; Yamanaka, M.; Kim, J.-H.; Saito, K.; Sakamoto, A.; Inoue, M.; Shirouzu, M., Crystal structure of the complex of human epidermal growth factor and receptor extracellular domains. *Cell* **2002**, *110*, 775-787.
17. Maemondo, M.; Inoue, A.; Kobayashi, K.; Sugawara, S.; Oizumi, S.; Isobe, H.; Gemma, A.; Harada, M.; Yoshizawa, H.; Kinoshita, I.; Fujita, Y.; Okinaga, S.; Hirano, H.; Yoshimori, K.; Harada, T.; Ogura, T.; Ando, M.; Miyazawa, H.; Tanaka, T.; Saijo, Y.; Hagiwara, K.; Morita, S.; Nukiwa, T., Gefitinib or chemotherapy for non-small-cell lung cancer with mutated EGFR. *N. Engl. J. Med.* **2010**, *362*, 2380-2388.
18. Ganjoo, K. N.; Wakelee, H., Review of erlotinib in the treatment of advanced non-small cell lung cancer. *Biol.: Targets Ther.* **2007**, *1*, 335.
19. Geyer, C. E.; Forster, J.; Lindquist, D.; Chan, S.; Romieu, C. G.; Pienkowski, T.; Jagiello-Gruszfeld, A.; Crown, J.; Chan, A.; Kaufman, B.; Skarlos, D.; Campone, M.; Davidson, N.; Berger, M.; Oliva, C.; Rubin, S. D.; Stein, S.; Cameron, D., Lapatinib plus capecitabine for HER2-positive advanced breast cancer. *N. Engl. J. Med.* **2006**, *355*, 2733-2743.
20. Li, D.; Ambrogio, L.; Shimamura, T.; Kubo, S.; Takahashi, M.; Chirieac, L. R.; Padera, R. F.; Shapiro, G. I.; Baum, A.; Himmelsbach, F.; Rettig, W. J.; Meyerson, M.; Solca, F.; Greulich, H.; Wong, K. K., BIBW2992, an irreversible EGFR/HER2 inhibitor highly effective in preclinical lung cancer models. *Oncogene* **2008**, *27*, 4702-4711.
21. Kalous, O.; Conklin, D.; Desai, A. J.; O'Brien, N. A.; Ginther, C.; Anderson, L.; Cohen, D. J.; Britten, C. D.; Taylor, I.; Christensen, J. G.; Slamon, D. J.; Finn, R. S., Dacomitinib (PF-00299804), an irreversible Pan-HER inhibitor, inhibits

- proliferation of HER2-amplified breast cancer cell lines resistant to Trastuzumab and Lapatinib. *Mol. Cancer Ther.* **2012**, *11*, 1978-1987.
22. Ávila, H. P.; Smânia, E. d. F. A.; Monache, F. D.; Smânia, A., Structure–activity relationship of antibacterial chalcones. *Bioorg. Med. Chem.* **2008**, *16*, 9790-9794.
 23. Cheng, J.-H.; Hung, C.-F.; Yang, S.-C.; Wang, J.-P.; Won, S.-J.; Lin, C.-N., Synthesis and cytotoxic, anti-inflammatory, and anti-oxidant activities of 2',5'-dialkoxylchalcones as cancer chemopreventive agents. *Bioorg. Med. Chem.* **2008**, *16*, 7270-7276.
 24. Rao, Y. K.; Fang, S.-H.; Tzeng, Y.-M., Synthesis and biological evaluation of 3',4',5'-trimethoxychalcone analogues as inhibitors of nitric oxide production and tumor cell proliferation. *Bioorg. Med. Chem.* **2009**, *17*, 7909-7914.
 25. Sortino, M.; Delgado, P.; Juárez, S.; Quiroga, J.; Abonía, R.; Insuasty, B.; Noguerras, M.; Rodero, L.; Garibotto, F. M.; Enriz, R. D.; Zacchino, S. A., Synthesis and antifungal activity of (Z)-5-arylidenerhodanines. *Bioorg. Med. Chem.* **2007**, *15*, 484-494.
 26. Vargas M, L. Y.; Castelli, M. a. V.; Kouznetsov, V. V.; Urbina G, J. M.; López, S. N.; Sortino, M.; Enriz, R. D.; Ribas, J. C.; Zacchino, S., In vitro antifungal activity of new series of homoallylamines and related compounds with inhibitory properties of the synthesis of fungal cell wall polymers. *Bioorg. Med. Chem.* **2003**, *11*, 1531-1550.
 27. Lopez, S. N.; Castelli, M. V.; Zacchino, S. A.; Dominguez, J. N.; Lobo, G.; Charris-Charris, J.; Cortés, J. C.; Ribas, J. C.; Devia, C.; Rodríguez, A. M., In vitro antifungal evaluation and structure–activity relationships of a new series of chalcone derivatives and synthetic analogues, with inhibitory properties against polymers of the fungal cell wall. *Bioorg. Med. Chem.* **2001**, *9*, 1999-2013.
 28. Katsori, A. M.; Hadjipavlou-Litina, D., Chalcones in cancer: understanding their role in terms of QSAR. *Curr. Med. Chem.* **2009**, *16*, 1062-1081.
 29. Achanta, G.; Modzelewska, A.; Feng, L.; Khan, S. R.; Huang, P., A boronic-chalcone derivative exhibits potent anticancer activity through inhibition of the proteasome. *Mol. Pharmacol.* **2006**, *70*, 426-433.

30. Modzelewska, A.; Pettit, C.; Achanta, G.; Davidson, N. E.; Huang, P.; Khan, S. R., Anticancer activities of novel chalcone and bis-chalcone derivatives. *Bioorg. Med. Chem.* **2006**, *14*, 3491-3495.
31. Kumar, S. K.; Hager, E.; Pettit, C.; Gurulingappa, H.; Davidson, N. E.; Khan, S. R., Design, synthesis, and evaluation of novel boronic-chalcone derivatives as antitumor agents. *J. Med. Chem.* **2003**, *46*, 2813-2815.
32. Edwards, M. L.; Stemerick, D. M.; Sunkara, P. S., Chalcones: a new class of antimetabolic agents. *J. Med. Chem.* **1990**, *33*, 1948-1954.
33. Venkataramana Reddy, P. O.; Hridhay, M.; Nikhil, K.; Khan, S.; Jha, P. N.; Shah, K.; Kumar, D., Synthesis and investigations into the anticancer and antibacterial activity studies of β -carboline chalcones and their bromide salts. *Bioorg. Med. Chem. Lett.* **2018**, *28*, 1278-1282.
34. Srinivasan, B.; Johnson, T. E.; Lad, R.; Xing, C., Structure-activity relationship studies of chalcone leading to 3-hydroxy-4,3',4',5'-tetramethoxychalcone and its analogues as potent nuclear factor κ B Inhibitors and their anticancer activities. *J. Med. Chem.* **2009**, *52*, 7228-7235.
35. Bandgar, B. P.; Gawande, S. S.; Bodade, R. G.; Totre, J. V.; Khobragade, C. N., Synthesis and biological evaluation of simple methoxylated chalcones as anticancer, anti-inflammatory and antioxidant agents. *Bioorg. Med. Chem.* **2010**, *18*, 1364-1370.
36. Bonesi, M.; Loizzo, M. R.; Statti, G. A.; Michel, S.; Tillequin, F.; Menichini, F., The synthesis and angiotensin converting enzyme (ACE) inhibitory activity of chalcones and their pyrazole derivatives. *Bioorg. Med. Chem. Lett.* **2010**, *20*, 1990-1993.
37. Wattenberg, L. W.; Coccia, J. B.; Galbraith, A. R., Inhibition of carcinogen-induced pulmonary and mammary carcinogenesis by chalcone administered subsequent to carcinogen exposure. *Cancer Lett.* **1994**, *83*, 165-169.
38. Wattenberg, L., Chalcones, myo-inositol and other novel inhibitors of pulmonary carcinogenesis. *J. Cell. Biochem.* **1995**, *59*, 162-168.

39. Yamazaki, S.; Morita, T.; Endo, H.; Hamamoto, T.; Baba, M.; Joichi, Y.; Kaneko, S.; Okada, Y.; Okuyama, T.; Nishino, H.; Tokue, A., Isoliquiritigenin suppresses pulmonary metastasis of mouse renal cell carcinoma. *Cancer Lett.* **2002**, *183*, 23-30.
40. Kanazawa, M.; Satomi, Y.; Mizutani, Y.; Ukimura, O.; Kawauchi, A.; Sakai, T.; Baba, M.; Okuyama, T.; Nishino, H.; Miki, T., Isoliquiritigenin Inhibits the Growth of Prostate Cancer. *Eur. Urol.* **2003**, *43*, 580-586.
41. Zi, X.; Simoneau, A. R., Flavokawain A, a Novel Chalcone from Kava Extract, Induces Apoptosis in Bladder Cancer Cells by Involvement of Bax Protein-Dependent and Mitochondria-Dependent Apoptotic Pathway and Suppresses Tumor Growth in Mice. *Cancer Res.* **2005**, *65*, 3479.
42. Yang, E. B.; Guo, Y. J.; Zhang, K.; Chen, Y. Z.; Mack, P., Inhibition of epidermal growth factor receptor tyrosine kinase by chalcone derivatives. *Biochim Biophys Acta Protein Struct Mol Enzymol.* **2001**, *1550*, 144-152.
43. Lee, R. M.; Gewirtz, D. A., Colchicine site inhibitors of microtubule integrity as vascular disrupting agents. *Drug Dev. Res.* **2008**, *69*, 352-358.
44. Pettit, G. R.; Singh, S. B.; Hamel, E.; Lin, C. M.; Alberts, D. S.; Garcia-Kendal, D., Isolation and structure of the strong cell growth and tubulin inhibitor combretastatin A-4. *Experientia* **1989**, *45*, 209-211.
45. Ma, M.; Sun, L.; Lou, H.; Ji, M., Synthesis and biological evaluation of Combretastatin A-4 derivatives containing a 3'-O-substituted carbonic ether moiety as potential antitumor agents. *Chem. Cent. J.* **2013**, *7*, 179.
46. Stefański, T.; Mikstacka, R.; Kurczab, R.; Dutkiewicz, Z.; Kucińska, M.; Murias, M.; Zielińska-Przyjemska, M.; Cichocki, M.; Teubert, A.; Kaczmarek, M., Design, synthesis, and biological evaluation of novel combretastatin A-4 thio derivatives as microtubule targeting agents. *Eur. J. Med. Chem.* **2018**, *144*, 797-816.
47. Sackett, D. L., Podophyllotoxin, steganacin and combretastatin: Natural products that bind at the colchicine site of tubulin. *Pharmacol. Ther.* **1993**, *59*, 163-228.
48. Romagnoli, R.; Baraldi, P. G.; Carrion, M. D.; Cara, C. L.; Cruz-Lopez, O.; Preti, D.; Tolomeo, M.; Grimaudo, S.; Di Cristina, A.; Zonta, N., Design, synthesis, and

- biological evaluation of thiophene analogues of chalcones. *Bioorg. Med. Chem.* **2008**, *16*, 5367-5376.
49. Lawrence, N. J.; McGown, A. T.; Ducki, S.; Hadfield, J. A., The interaction of chalcones with tubulin. *Anti-Cancer Drug Des.* **2000**, *15*, 135-141.
50. Salum, L. B.; Altei, W. F.; Chiaradia, L. D.; Cordeiro, M. N. S.; Canevarolo, R. R.; Melo, C. P. S.; Winter, E.; Mattei, B.; Daghestani, H. N.; Santos-Silva, M. C.; Creczynski-Pasa, T. B.; Yunes, R. A.; Yunes, J. A.; Andricopulo, A. D.; Day, B. W.; Nunes, R. J.; Vogt, A., Cytotoxic 3,4,5-trimethoxychalcones as mitotic arresters and cell migration inhibitors. *Eur. J. Med. Chem.* **2013**, *63*, 501-510.
51. Kumar, B.; Sharma, P.; Gupta, V. P.; Khullar, M.; Singh, S.; Dogra, N.; Kumar, V., Synthesis and biological evaluation of pyrimidine bridged combretastatin derivatives as potential anticancer agents and mechanistic studies. *Bioorg. Chem.* **2018**, *78*, 130-140.
52. Tuong, T. L.; Do, L. T. M.; Aree, T.; Wonganan, P.; Chavasiri, W., Tetrahydroxanthone–chromanone heterodimers from lichen *Usnea aciculifera* and their cytotoxic activity against human cancer cell lines. *Fitoterapia* **2020**, *147*, 104732.
53. Mahalapbutr, P.; Darai, N.; Panman, W.; Opasmahakul, A.; Kungwan, N.; Hannongbua, S.; Rungrotmongkol, T., Atomistic mechanisms underlying the activation of the G protein-coupled sweet receptor heterodimer by sugar alcohol recognition. *Sci. Rep.* **2019**, *9*, 10205.
54. Mahalapbutr, P.; Wonganan, P.; Charoenwongpaiboon, T.; Prousoontorn, M.; Chavasiri, W.; Rungrotmongkol, T., Enhanced solubility and anticancer potential of Mansonone G by β -cyclodextrin-based host-guest complexation: a computational and experimental study. *Biomolecules* **2019**, *9*, 545.
55. Frisch, M. J. T., G. W.; Schlegel, H. B.; Scuseria, G. E.; Robb, M. A.; Cheeseman, J. R.; Scalmani, G.; Barone, V.; Mennucci, B.; Petersson, G. A.; Nakatsuji, H.; Caricato, M.; Li, X.; Hratchian, H. P.; Izmaylov, A. F.; Bloino, J.; Zheng, G.; Sonnenberg, J. L.; Hada, M.; Ehara, M.; Toyota, K.; Fukuda, R.; Hasegawa, J.; Ishida, M.; Nakajima, T.; Honda, Y.; Kitao, O.; Nakai, H.; Vreven, T.; Montgomery Jr., J. A.; Peralta, J. E.; Ogliaro, F.; Bearpark, M. J.; Heyd, J.; Brothers, E. N.; Kudin, K. N.; Staroverov, V. N.;

- Kobayashi, R.; Normand, J.; Raghavachari, K.; Rendell, A. P.; Burant, J. C.; Iyengar, S. S.; Tomasi, J.; Cossi, M.; Rega, N.; Millam, N. J.; Klene, M.; Knox, J. E.; Cross, J. B.; Bakken, V.; Adamo, C.; Jaramillo, J.; Gomperts, R.; Stratmann, R. E.; Yazyev, O.; Austin, A. J.; Cammi, R.; Pomelli, C.; Ochterski, J. W.; Martin, R. L.; Morokuma, K.; Zakrzewski, V. G.; Voth, G. A.; Salvador, P.; Dannenberg, J. J.; Dapprich, S.; Daniels, A. D.; Farkas, Ö.; Foresman, J. B.; Ortiz, J. V.; Cioslowski, J.; Fox, D. J, Gaussian 09; Gaussian, Inc. *Wallingford, CT* **2009**, *32*, 5648-5652.
56. Wu, G.; Robertson, D. H.; Brooks III, C. L.; Vieth, M., Detailed analysis of grid-based molecular docking: a case study of CDOCKER-A CHARMM-based MD docking algorithm. *J. Comput. Chem.* **2003**, *24*, 1549-1562.
57. Batovska, D.; Parushev, S.; Stamboliyska, B.; Tsvetkova, I.; Ninova, M.; Najdenski, H., Examination of growth inhibitory properties of synthetic chalcones for which antibacterial activity was predicted. *Eur. J. Med. Chem.* **2009**, *44* (5), 2211-2218.
58. Aykul, S.; Martinez-Hackert, E., Determination of half-maximal inhibitory concentration using biosensor-based protein interaction analysis. *Anal. Biochem.* **2016**, *508*, 97-103.
59. Sharma, V. K.; Nandekar, P. P.; Sangamwar, A.; Pérez-Sánchez, H.; Agarwal, S. M., Structure guided design and binding analysis of EGFR inhibiting analogues of erlotinib and AEE788 using ensemble docking, molecular dynamics and MM-GBSA. *RSC adv.* **2016**, *6*, 65725-65735.
60. Bharathi, S.; Mahendiran, D.; Kumar, R. S.; Kim, Y. G.; Gajendiran, M.; Kim, K.; Rahiman, A. K., Biocompatibility, in Vitro Antiproliferative, and in Silico EGFR/VEGFR2 Studies of Heteroleptic Metal(II) Complexes of Thiosemicarbazones and Naproxen. *Chem. Res. Toxicol.* **2019**, *32*, 1554-1571.
61. Damodar, K.; Lee, J. T.; Kim, J.-K.; Jun, J.-G., Synthesis and in vitro evaluation of homoisoflavonoids as potent inhibitors of nitric oxide production in RAW-264.7 cells. *Bioorg. Med. Chem. Lett.* **2018**, *28*, 2098-2102.
62. Vong, L. B.; Nagasaki, Y., Nitric Oxide Nano-Delivery Systems for Cancer Therapeutics: Advances and Challenges. *Antioxidants* **2020**, *9*, 791.
63. Liu, T.; Zhang, L.; Joo, D.; Sun, S.-C., NF- κ B signaling in inflammation. *Signal Transduct. Target. Ther.* **2017**, *2*, 1-9.

64. Nathan, C. F.; Hibbs, J. B., Role of nitric oxide synthesis in macrophage antimicrobial activity. *Curr. Opin. Immunol.* **1991**, *3*, 65-70.
65. Lundberg, J. O. N.; Lundberg, J. M.; Alving, K.; Weitzberg, E., Nitric oxide and inflammation: The answer is blowing in the wind. *Nat. Med.* **1997**, *3*, 30-31.
66. Gotoh, T.; Terada, K.; Oyadomari, S.; Mori, M., hsp70-DnaJ chaperone pair prevents nitric oxide- and CHOP-induced apoptosis by inhibiting translocation of Bax to mitochondria. *Cell Death Differ.* **2004**, *11*, 390-402.
67. El-Gamal, M. I.; Bayomi, S. M.; El-Ashry, S. M.; Said, S. A.; Abdel-Aziz, A. A. M.; Abdel-Aziz, N. I., Synthesis and anti-inflammatory activity of novel (substituted)benzylidene acetone oxime ether derivatives: Molecular modeling study. *Eur. J. Med. Chem.* **2010**, *45*, 1403-1414.
68. Lee, S. H.; Kim, J. Y.; Seo, G. S.; Kim, Y. C.; Sohn, D. H., Isoliquiritigenin, from *Dalbergia odorifera*, up-regulates anti-inflammatory heme oxygenase-1 expression in RAW264.7 macrophages. *Inflamm. Res.* **2009**, *58*, 257-262.
69. Zheng, W.; Zhang, H.; Jin, Y.; Wang, Q.; Chen, L.; Feng, Z.; Chen, H.; Wu, Y., Butein inhibits IL-1 β -induced inflammatory response in human osteoarthritis chondrocytes and slows the progression of osteoarthritis in mice. *Int. Immunopharmacol.* **2017**, *42*, 1-10.
70. Furusawa, J.-i.; Funakoshi-Tago, M.; Mashino, T.; Tago, K.; Inoue, H.; Sonoda, Y.; Kasahara, T., Glycyrrhiza inflata-derived chalcones, Licochalcone A, Licochalcone B and Licochalcone D, inhibit phosphorylation of NF- κ B p65 in LPS signaling pathway. *Int. Immunopharmacol.* **2009**, *9*, 499-507.
71. Dhar, R.; Kimseng, R.; Chokchaisiri, R.; Hiransai, P.; Utaipan, T.; Suksamrarn, A.; Chunglok, W., 2',4-Dihydroxy-3',4',6'-trimethoxychalcone from *Chromolaena odorata* possesses anti-inflammatory effects via inhibition of NF- κ B and p38 MAPK in lipopolysaccharide-activated RAW 264.7 macrophages. *Immunopharmacol. Immunotoxicol.* **2018**, *40*, 43-51.
72. Prasad, Y. R.; Rao, A. S.; Rambabu, R., Synthesis of some 4'-amino chalcones and their antiinflammatory and antimicrobial activity. *Asian J. Chem* **2009**, *21*, 907-914.

73. Labib, M. B.; Sharkawi, S. M. Z.; El-Daly, M., Design, synthesis of novel isoindoline hybrids as COX-2 inhibitors: Anti-inflammatory, analgesic activities and docking study. *Bioorg. Chem.* **2018**, *80*, 70-80.
74. Bist, G.; Pun, N. T.; Magar, T. B. T.; Shrestha, A.; Oh, H. J.; Khakurel, A.; Park, P.-H.; Lee, E.-S., Inhibition of LPS-stimulated ROS production by fluorinated and hydroxylated chalcones in RAW 264.7 macrophages with structure-activity relationship study. *Bioorg. Med. Chem. Lett.* **2017**, *27*, 1205-1209.
75. Shrestha, A.; Shrestha, A.; Park, P.-H.; Lee, E.-S., Hydroxyl- and halogen-containing chalcones for the inhibition of LPS-stimulated ROS production in RAW 264.7 macrophages: Design, synthesis and structure-activity relationship study. *Bull. Korean Chem. Soc.* **2019**, *40*, 729-734.
76. Boshra, A. N.; Abdu-Allah, H. H. M.; Mohammed, A. F.; Hayallah, A. M., Click chemistry synthesis, biological evaluation and docking study of some novel 2'-hydroxychalcone-triazole hybrids as potent anti-inflammatory agents. *Bioorg. Chem.* **2020**, *95*, 103505.
77. Yang, Y.; Wei, Z.; Teichmann, A. T.; Wieland, F. H.; Wang, A.; Lei, X.; Zhu, Y.; Yin, J.; Fan, T.; Zhou, L.; Wang, C.; Chen, L., Development of a novel nitric oxide (NO) production inhibitor with potential therapeutic effect on chronic inflammation. *Eur. J. Med. Chem.* **2020**, *193*, 112216.
78. Sarigaputi, C.; Sangpech, N.; Palaga, T.; Pudhom, K., Suppression of inducible nitric oxide synthase pathway by 7-deacetylgedunin, a limonoid from *Xylocarpus* sp. *Planta Med.* **2015**, *81*, 312-319.
79. Green, L. C.; Wagner, D. A.; Glogowski, J.; Skipper, P. L.; Wishnok, J. S.; Tannenbaum, S. R., Analysis of nitrate, nitrite, and [15N] nitrate in biological fluids. *Anal. Biochem.* **1982**, *126*, 131-138.
80. Stoddart, M. J., Cell Viability Assays: Introduction. In *Mammalian Cell Viability: Methods and Protocols*, Stoddart, M. J., Ed. Humana Press: Totowa, NJ, 2011; pp 1-6.
81. Moore, K.; Howard, L.; Brownmiller, C.; Gu, I.; Lee, S.-O.; Mauromoustakos, A., Inhibitory effects of cranberry polyphenol and volatile extracts on nitric oxide

- production in LPS activated RAW 264.7 macrophages. *Food Funct.* **2019**, *10*, 7091-7102.
82. Baatar, D.; Siddiqi, M. Z.; Im, W. T.; Ul Khaliq, N.; Hwang, S. G., Anti-inflammatory effect of ginsenoside Rh2-mix on lipopolysaccharide-stimulated RAW 264.7 murine macrophage cells. *J. Med. Food.* **2018**, *21*, 951-960.
83. Shaker, O.; Ghallab, N. A.; Hamdy, E.; Sayed, S., Inducible nitric oxide synthase (iNOS) in gingival tissues of chronic periodontitis with and without diabetes: Immunohistochemistry and RT-PCR study. *Arch. Oral Biol.* **2013**, *58*, 1397-1406.
84. Taciak, B.; Białasek, M.; Braniewska, A.; Sas, Z.; Sawicka, P.; Kiraga, Ł.; Rygiel, T.; Król, M., Evaluation of phenotypic and functional stability of RAW 264.7 cell line through serial passages. *PLoS One* **2018**, *13*, e0198943-e0198943.
85. Wu, J.; Li, J.; Cai, Y.; Pan, Y.; Ye, F.; Zhang, Y.; Zhao, Y.; Yang, S.; Li, X.; Liang, G., Evaluation and discovery of novel synthetic chalcone derivatives as anti-inflammatory agents. *J. Med. Chem.* **2011**, *54*, 8110-8123.
86. Shiraki, T.; Kamiya, N.; Shiki, S.; Kodama, T. S.; Kakizuka, A.; Jingami, H., α , β -unsaturated ketone is a core moiety of natural ligands for covalent binding to peroxisome proliferator-activated receptor γ . *J. Biol. Chem.* **2005**, *280*, 14145-14153.
87. Funakoshi-Tago, M.; Nakamura, K.; Tsuruya, R.; Hatanaka, M.; Mashino, T.; Sonoda, Y.; Kasahara, T., The fixed structure of Licochalcone A by α , β -unsaturated ketone is necessary for anti-inflammatory activity through the inhibition of NF- κ B activation. *Int. Immunopharmacol.* **2010**, *10*, 562-571.
88. YAMAZAKI, Y.; KAWANO, Y.; NAGASHIMA, U., Structure-activity Relationship of α , β -Unsaturated Ketones for the Suppression of Tumor Necrosis Factor- α and Nitric Oxide Production in Lipopolysaccharide-stimulated Macrophages and Their Molecular Orbital Energies. *J. comput. chem., Jpn.* **2012**.
89. Cho, N.; Shaw, J.; Karuranga, S.; Huang, Y.; da Rocha Fernandes, J.; Ohlrogge, A.; Malanda, B., IDF Diabetes Atlas: Global estimates of diabetes prevalence for 2017 and projections for 2045. *Diabetes Res. Clin. Pract.* **2018**, *138*, 271-281.

90. Cai, C.-Y.; Rao, L.; Rao, Y.; Guo, J.-X.; Xiao, Z.-Z.; Cao, J.-Y.; Huang, Z.-S.; Wang, B., Analogues of xanthenes-chalcones and bis-chalcones as α -glucosidase inhibitors and anti-diabetes candidates. *Eur. J. Med. Chem.* **2017**, *130*, 51-59.
91. Burmaoglu, S.; Yilmaz, A. O.; Polat, M. F.; Kaya, R.; Gulcin, İ.; Algul, O., Synthesis and biological evaluation of novel tris-chalcones as potent carbonic anhydrase, acetylcholinesterase, butyrylcholinesterase and α -glycosidase inhibitors. *Bioorg. Chem.* **2019**, *85*, 191-197.
92. Hunziker, W.; Spiess, M.; Semenza, G.; Lodish, H. F., The sucrase-isomaltase complex: Primary structure, membrane-orientation, and evolution of a stalked, intrinsic brush border protein. *Cell* **1986**, *46*, 227-234.
93. Nichols, B. L.; Eldering, J.; Avery, S.; Hahn, D.; Quaroni, A.; Sterchi, E., Human small intestinal maltase-glucoamylase cDNA cloning: homology to sucrase-isomaltase. *J. Biol. Chem.* **1998**, *273*, 3076-3081.
94. Dahlqvist, A.; Auricchio, S.; Semenza, G.; Prader, A., Human intestinal disaccharidases and hereditary disaccharide intolerance. The hydrolysis of sucrose, isomaltose, palatinose (isomaltulose), and a 1, 6- α -oligosaccharide (isomalto-oligosaccharide) preparation. *J. Clin. Invest.* **1963**, *42*, 556-562.
95. SØRENSEN, S. H.; NORÉN, O.; SJÖSTRÖM, H.; DANIELSEN, E. M., Amphiphilic pig intestinal microvillus maltase/glucoamylase: structure and specificity. *Eur. J. Biochem.* **1982**, *126*, 559-568.
96. Semenza, G.; Auricchio, S.; Rubino, A., Multiplicity of human intestinal disaccharidases I. Chromatographic separation of maltases and of two lactases. *Biochim. Biophys. Acta, Nucleic Acids Protein Synth.* **1965**, *96*, 487-497.
97. Semenza, G., Small-intestinal disaccharidases. *the Metabolic and Molecular Bases of Inherited Disease* **1995**, 4451-4480.
98. Lee, B.-H.; Lin, A. H.-M.; Nichols, B. L.; Jones, K.; Rose, D. R.; Quezada-Calvillo, R.; Hamaker, B. R., Mucosal C-terminal maltase-glucoamylase hydrolyzes large size starch digestion products that may contribute to rapid postprandial glucose generation. *Mol. Nutr. Food Res.* **2014**, *58*, 1111-1121.

99. Gao, H.; Kawabata, J., α -Glucosidase inhibition of 6-hydroxyflavones. Part 3: Synthesis and evaluation of 2, 3, 4-trihydroxybenzoyl-containing flavonoid analogs and 6-aminoflavones as α -glucosidase inhibitors. *Bioorg. Med. Chem.* **2005**, *13*, 1661-1671.
100. Dong, Y.-s.; Yu, N.; Li, X.; Zhang, B.; Xing, Y.; Zhuang, C.; Xiu, Z.-l., Dietary 5, 6, 7-Trihydroxy-flavonoid aglycones and 1-deoxynojirimycin synergistically inhibit the recombinant maltase–glucoamylase subunit of α -glucosidase and lower postprandial blood glucose. *J. Agric. Food Chem.* **2020**, *68*, 8774-8787.
101. Bedekar, A.; Shah, K.; Koffas, M., Natural products for type II diabetes treatment. *Adv. Appl. Microbiol.* **2010**, *71*, 21-73.
102. Balfour, J. A.; McTavish, D., Acarbose. An update of its pharmacology and therapeutic use in diabetes mellitus. *Drugs* **1993**, *46*, 1025-1054.
103. Guo, H.; Wu, H.; Yang, J.; Xiao, Y.; Altenbach, H.-J.; Qiu, G.; Hu, H.; Wu, Z.; He, X.; Zhou, D., Synthesis, characterization and biological evaluation of some 16E-arylidene androstane derivatives as potential anticancer agents. *Steroids* **2011**, *76*, 709-723.
104. Bansal, R.; Guleria, S., Synthesis of 16E-[3-methoxy-4-(2-aminoethoxy)benzylidene] androstene derivatives as potent cytotoxic agents. *Steroids* **2008**, *73*, 1391-1399.
105. Banday, A. H.; Giri, A. K.; Parveen, R.; Bashir, N., Design and synthesis of D-ring steroidal isoxazolines and oxazolines as potential antiproliferative agents against LNCaP, PC-3 and DU-145 cells. *Steroids* **2014**, *87*, 93-98.
106. Yadav, M. R.; Barmade, M. A.; Tamboli, R. S.; Murumkar, P. R., Developing steroidal aromatase inhibitors-an effective armament to win the battle against breast cancer. *Eur. J. Med. Chem.* **2015**, *105*, 1-38.
107. Roy, J.; DeRoy, P.; Poirier, D., 2β -(N-substituted piperazino)- 5α -androstane- 3α , 17β -diols: parallel solid-phase synthesis and antiproliferative activity on human leukemia HL-60 cells. *J. Comb. Chem.* **2007**, *9*, 347-358.
108. Latham, K. A.; Zamora, A.; Drought, H.; Subramanian, S.; Matejuk, A.; Offner, H.; Rosloniec, E. F., Estradiol treatment redirects the isotype of the autoantibody

- response and prevents the development of autoimmune arthritis. *J. Immunol.* **2003**, *171*, 5820-5827.
109. Choudhary, M. I.; Shah, S. A. A.; Khan, S.-N.; Khan, M. T. H., Alpha-glucosidase and tyrosinase inhibitors from fungal hydroxylation of tibolone and hydroxytibolones. *Steroids* **2010**, *75*, 956-966.
110. Chen, T.; Kan, Y.-J.; Chou, G.-X.; Zhang, C.-G., A new highly oxygenated pregnane and two new 5-hydroxymethylfurfural derivatives from the water decoction of *Poria cocos*. *J. Asian Nat. Prod. Res.* **2018**, *20*, 1101-1107.
111. Paschou, S. A.; Papanas, N., Type 2 diabetes mellitus and menopausal hormone therapy: an update. *Diabetes Ther.* **2019**, *10*, 2313-2320.
112. Kamel, H. K.; Perry III, H. M.; Morley, J. E., Hormone replacement therapy and fractures in older adults. *J. Am. Geriatr. Soc.* **2001**, *49*, 179-187.
113. Crespo, C. J.; Smit, E.; Snelling, A.; Sempos, C. T.; Andersen, R. E., Hormone replacement therapy and its relationship to lipid and glucose metabolism in diabetic and nondiabetic postmenopausal women: results from the Third National Health and Nutrition Examination Survey (NHANES III). *Diabetes Care* **2002**, *25*, 1675-1680.
114. Seo, W. D.; Kim, J. H.; Kang, J. E.; Ryu, H. W.; Curtis-Long, M. J.; Lee, H. S.; Yang, M. S.; Park, K. H., Sulfonamide chalcone as a new class of α -glucosidase inhibitors. *Bioorg. Med. Chem. Lett.* **2005**, *15*, 5514-5516.
115. Liu, M.; Yin, H.; Liu, G.; Dong, J.; Qian, Z.; Miao, J., Xanthohumol, a prenylated chalcone from *beer hops*, acts as an α -glucosidase inhibitor in vitro. *J. Agric. Food Chem.* **2014**, *62*, 5548-5554.
116. Sun, H.; Li, Y.; Zhang, X.; Lei, Y.; Ding, W.; Zhao, X.; Wang, H.; Song, X.; Yao, Q.; Zhang, Y., Synthesis, α -glucosidase inhibitory and molecular docking studies of prenylated and geranylated flavones, isoflavones and chalcones. *Bioorg. Med. Chem. Lett.* **2015**, *25*, 4567-4571.
117. Bale, A. T.; Khan, K. M.; Salar, U.; Chigurupati, S.; Fasina, T.; Ali, F.; Wadood, A.; Taha, M.; Nanda, S. S.; Ghufuran, M., Chalcones and bis-chalcones: As potential

- α -amylase inhibitors; synthesis, in vitro screening, and molecular modelling studies. *Bioorg. Chem.* **2018**, *79*, 179-189.
118. Helal, I. E.; Elsbaey, M.; Zaghoul, A. M.; Mansour, E.-S. S., A unique C-linked chalcone-dihydrochalcone dimer from *Dracaena cinnabari* resin. *Nat. Prod. Res.* **2019**, 1-6.
119. Anto, R. J.; Sukumaran, K.; Kuttan, G.; Rao, M.; Subbaraju, V.; Kuttan, R., Anticancer and antioxidant activity of synthetic chalcones and related compounds. *Cancer Lett.* **1995**, *97*, 33-37.
120. Kumar, C.; Loh, W.-S.; Ooi, C. W.; Quah, C. K.; Fun, H.-K., Structural correlation of some heterocyclic chalcone analogues and evaluation of their antioxidant potential. *Molecules* **2013**, *18*, 11996-12011.
121. Nakamura, Y.; Watanabe, S.; Miyake, N.; Kohno, H.; Osawa, T., Dihydrochalcones: Evaluation as novel radical scavenging antioxidants. *J. Agric. Food Chem.* **2003**, *51*, 3309-3312.
122. Rammohan, A.; Bhaskar, B. V.; Venkateswarlu, N.; Gu, W.; Zyryanov, G. V., Design, synthesis, docking and biological evaluation of chalcones as promising antidiabetic agents. *Bioorg. Chem.* **2020**, *95*, 103527.
123. Acharjee, S.; Maity, T. K.; Samanta, S.; Mana, S.; Chakraborty, T.; Singha, T.; Mondal, A., Antihyperglycemic activity of chalcone based novel 1-{3-[3-(substituted phenyl) prop-2-enoyl] phenyl} thioureas. *Synth. Commun.* **2018**, *48*, 3015-3024.
124. Mai, C. W.; Yaeghoobi, M.; Abd-Rahman, N.; Kang, Y. B.; Pichika, M. R., Chalcones with electron-withdrawing and electron-donating substituents: Anticancer activity against TRAIL resistant cancer cells, structure-activity relationship analysis and regulation of apoptotic proteins. *Eur. J. Med. Chem.* **2014**, *77*, 378-387.
125. Romagnoli, R.; Baraldi, P. G.; Carrion, M. D.; Cruz-Lopez, O.; Cara, C. L.; Balzarini, J.; Hamel, E.; Canella, A.; Fabbri, E.; Gambari, R.; Basso, G.; Viola, G., Hybrid α -bromoacryloylamido chalcones. Design, synthesis and biological evaluation. *Bioorganic Med. Chem. Lett.* **2009**, *19*, 2022-2028.

126. Ku, B. M.; Ryu, H. W.; Lee, Y. K.; Ryu, J.; Jeong, J. Y.; Choi, J.; Cho, H. J.; Park, K. H.; Kang, S. S., 4'-Acetoamido-4-hydroxychalcone, a chalcone derivative, inhibits glioma growth and invasion through regulation of the tropomyosin 1 gene. *Biochem. Biophys. Res. Commun.* **2010**, *402*, 525-530.
127. Ren, J.-L.; Zhang, X.-Y.; Yu, B.; Wang, X.-X.; Shao, K.-P.; Zhu, X.-G.; Liu, H.-M., Discovery of novel AHLs as potent antiproliferative agents. *Eur. J. Med. Chem.* **2015**, *93*, 321-329.
128. Jha, A.; Mukherjee, C.; Rolle, A. J.; De Clercq, E.; Balzarini, J.; Stables, J. P., Cytostatic activity of novel 4'-aminochalcone-based imides. *Bioorganic Med. Chem. Lett.* **2007**, *17*, 4545-4550.
129. Pingaew, R.; Saekee, A.; Mandi, P.; Nantasenamat, C.; Prachayasittikul, S.; Ruchirawat, S.; Prachayasittikul, V., Synthesis, biological evaluation and molecular docking of novel chalcone-coumarin hybrids as anticancer and antimalarial agents. *Eur. J. Med. Chem.* **2014**, *85*, 65-76.
130. Tomar, V.; Bhattacharjee, G.; Kamaluddin; Rajakumar, S.; Srivastava, K.; Puri, S. K., Synthesis of new chalcone derivatives containing acridinyl moiety with potential antimalarial activity. *Eur. J. Med. Chem.* **2010**, *45*, 745-751.
131. Domínguez, J. N.; León, C.; Rodrigues, J.; Gamboa de Domínguez, N.; Gut, J.; Rosenthal, P. J., Synthesis and antimalarial activity of sulfonamide chalcone derivatives. *Il Farmaco* **2005**, *60*, 307-311.
132. Iqbal, H.; Prabhakar, V.; Sangith, A.; Chandrika, B.; Balasubramanian, R., Synthesis, anti-inflammatory and antioxidant activity of ring-A-monosubstituted chalcone derivatives. *Med Chem Res.* **2014**, *23*, 4383-4394.
133. Araico, A.; Terencio, M. C.; Alcaraz, M. J.; Domínguez, J. N.; León, C.; Ferrándiz, M. L., Phenylsulphonyl urenyl chalcone derivatives as dual inhibitors of cyclooxygenase-2 and 5-lipoxygenase. *Life Sci.* **2006**, *78*, 2911-2918.
134. Suwunwong, T.; Kobkeatthawin, T.; Chanawanno, K.; Saewan, N.; Wisitsak, P.; Chantrapromma, S., Tyrosinase Inhibitory Activity of Pyrazole Derivatives. *Adv Mat Res.* **2012**, *506*, 194-197.
135. Niu, C.; Li, G.; Madina, K.; Aisa, H., Synthesis and activity on tyrosinase of novel chalcone derivatives. *Chem. J. Chin. Univ.* **2014**, *35*, 1204-1211.

136. Gençer, N.; Bilen, Ç.; Demir, D.; Atahan, A.; Ceylan, M.; Küçükislamoğlu, M., In vitro inhibition effect of some chalcones on erythrocyte carbonic anhydrase I and II. *Artif Cells Nanomed Biotechnol.* **2013**, *41*, 384-388.
137. Bodiwala, H. S.; Sabde, S.; Gupta, P.; Mukherjee, R.; Kumar, R.; Garg, P.; Bhutani, K. K.; Mitra, D.; Singh, I. P., Design and synthesis of caffeoyl-anilides as portmanteau inhibitors of HIV-1 integrase and CCR5. *Bioorg. Med. Chem.* **2011**, *19*, 1256-1263.
138. Kang, J. E.; Cho, J. K.; Curtis-Long, M. J.; Ryu, H. W.; Kim, J. H.; Kim, H. J.; Yuk, H. J.; Kim, D. W.; Park, K. H., Inhibitory Evaluation of Sulfonamide Chalcones on β -Secretase and Acylcholinesterase. *Molecules* **2013**, *18*, 140-153.
139. Suwito, H.; Ni'matuzahroh; Kristanti, A. N.; Hayati, S.; Dewi, S. R.; Amalina, I.; Puspaningsih, N. N. T., Antimicrobial Activities and In silico Analysis of Methoxy Amino Chalcone Derivatives. *Procedia Chem.* **2016**, *18*, 103-111.
140. Tristão, T.; Campos-Buzzi, F.; Corrêa, R.; Cruz, R. B.; Cechinel Filho, V.; Cruz, A. B., Antimicrobial and cytotoxicity potential of acetamido, amino and nitrochalcones. *Arzneimittelforschung* **2012**, *62*, 590-594.
141. Ramadhan, R.; Phuwapraisirisan, P., New arylalkanones from *Horsfieldia macrobotrys*, effective antidiabetic agents concomitantly inhibiting α -glucosidase and free radicals. *Bioorg. Med. Chem. Lett.* **2015**, *25*, 4529-4533.
142. Tadera, K.; Minami, Y.; Takamatsu, K.; Matsuoka, T., Inhibition of α -glucosidase and α -amylase by flavonoids. *J. Nutr. Sci. Vitaminol.* **2006**, *52*, 149-153.
143. Zeng, L.; Zhang, G.; Lin, S.; Gong, D., Inhibitory mechanism of apigenin on α -glucosidase and synergy analysis of flavonoids. *J. Agric. Food Chem.* **2016**, *64*, 6939-6949.
144. Liu, D.; He, W.; Wang, Z.; Liu, L.; Wang, C.; Zhang, C.; Wang, C.; Wang, Y.; Tanabe, G.; Muraoka, O., Design, synthesis and biological evaluation of 3'-benzylated analogs of 3'-epi-neoponkoranol as potent α -glucosidase inhibitors. *Eur. J. Med. Chem.* **2016**, *110*, 224-236.

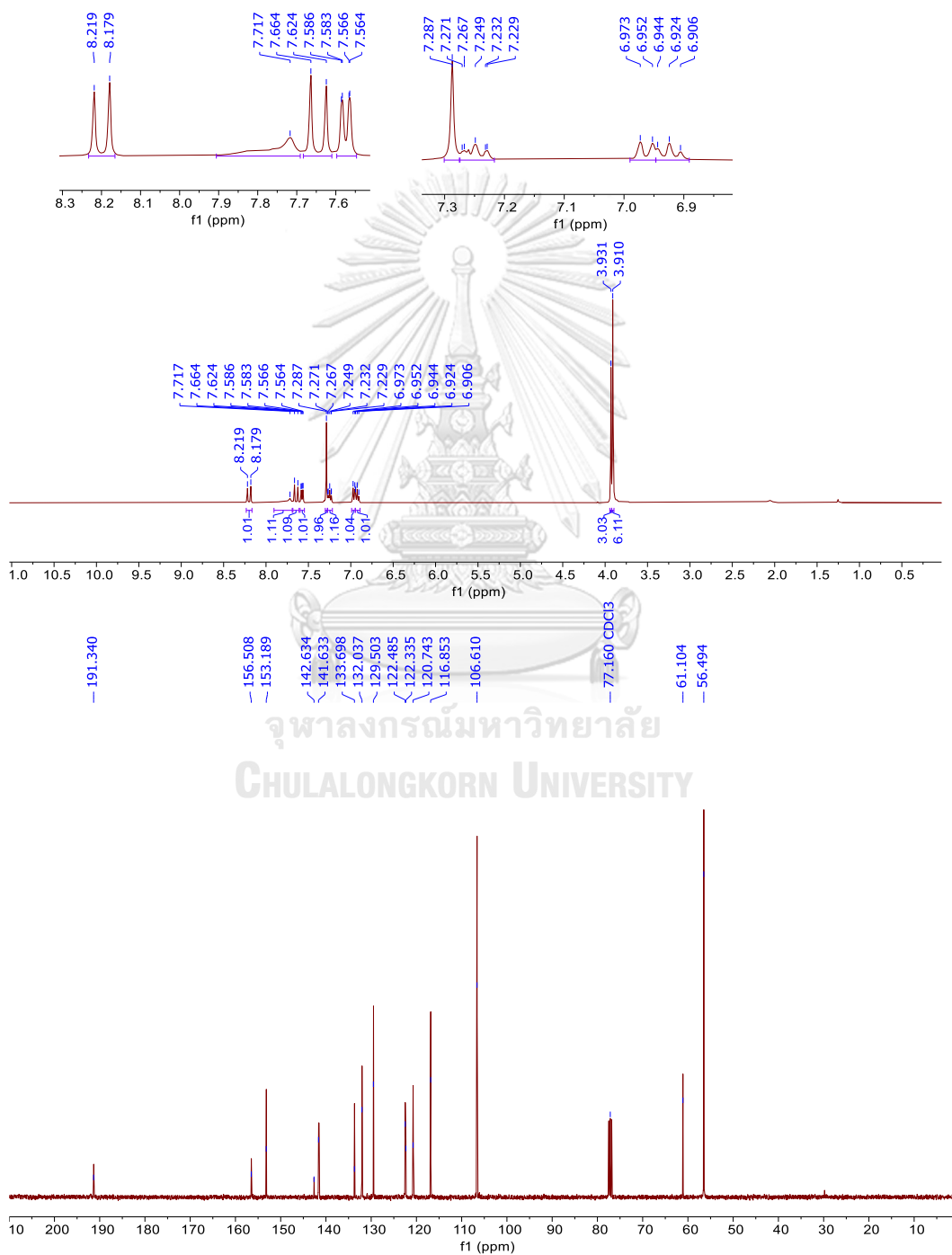
145. Gao, H.; Nishioka, T.; Kawabata, J.; Kasai, T., Structure-activity relationships for α -glucosidase inhibition of baicalein, 5, 6, 7-trihydroxyflavone: the effect of A-ring substitution. *Biosci. Biotechnol. Biochem.* **2004**, *68*, 369-375.
146. Gao, H.; Kawabata, J., Importance of the B ring and its substitution on the α -glucosidase inhibitory activity of baicalein, 5, 6, 7-trihydroxyflavone. *Biosci. Biotechnol. Biochem.* **2004**, *68*, 1858-1864.
147. Dan, W.-J.; Zhang, Q.; Zhang, F.; Wang, W.-W.; Gao, J.-M., Benzonate derivatives of acetophenone as potent α -glucosidase inhibitors: Synthesis, structure-activity relationship and mechanism. *J. Enzyme Inhib. Med. Chem.* **2019**, *34*, 937-945.
148. Yu, X.; Zhang, F.; Liu, T.; Liu, Z.; Dong, Q.; Li, D., Exploring efficacy of natural-derived acetylphenol scaffold inhibitors for α -glucosidase: Synthesis, in vitro and in vivo biochemical studies. *Bioorg. Med. Chem. Lett.* **2020**, *30*, 127528.
149. Yamamoto, K.; Miyake, H.; Kusunoki, M.; Osaki, S., Steric hindrance by 2 amino acid residues determines the substrate specificity of isomaltase from *Saccharomyces cerevisiae*. *Journal of Bioscience and Bioengineering* **2011**, *112*, 545-550.
150. Waterhouse, A.; Bertoni, M.; Bienert, S.; Studer, G.; Tauriello, G.; Gumienny, R.; Heer, F. T.; de Beer, T. A. P.; Rempfer, C.; Bordoli, L.; Lepore, R.; Schwede, T., SWISS-MODEL: homology modelling of protein structures and complexes. *Nucleic Acids Res* **2018**, *46*, W296-W303.
151. D.A. Case, K. B., I.Y. Ben-Shalom, S.R. Brozell, D.S. Cerutti, T.E. Cheatham, III, V.W.D. Cruzeiro, T.A. Darden, R.E. Duke, G. Giambasu, M.K. Gilson, H. Gohlke, A.W. Goetz, R. Harris, S. Izadi, S.A. Izmailov, K. Kasavajhala, A. Kovalenko, R. Krasny, T. Kurtzman, T.S. Lee, S. LeGrand, P. Li, C. Lin, J. Liu, T. Luchko, R. Luo, V. Man, K.M. Merz, Y. Miao, O. Mikhailovskii, G. Monard, H. Nguyen, A. Onufriev, F. Pan, S. Pantano, R. Qi, D.R. Roe, A. Roitberg, C. Sagui, S. Schott-Verdugo, J. Shen, C.L. Simmerling, N.R. Skrynnikov, J. Smith, J. Swails, R.C. Walker, J. Wang, L. Wilson, R.M. Wolf, X. Wu, Y. Xiong, Y. Xue, D.M. York and P.A. Kollman, *AMBER 2020*. University of California, San Francisco, 2020.

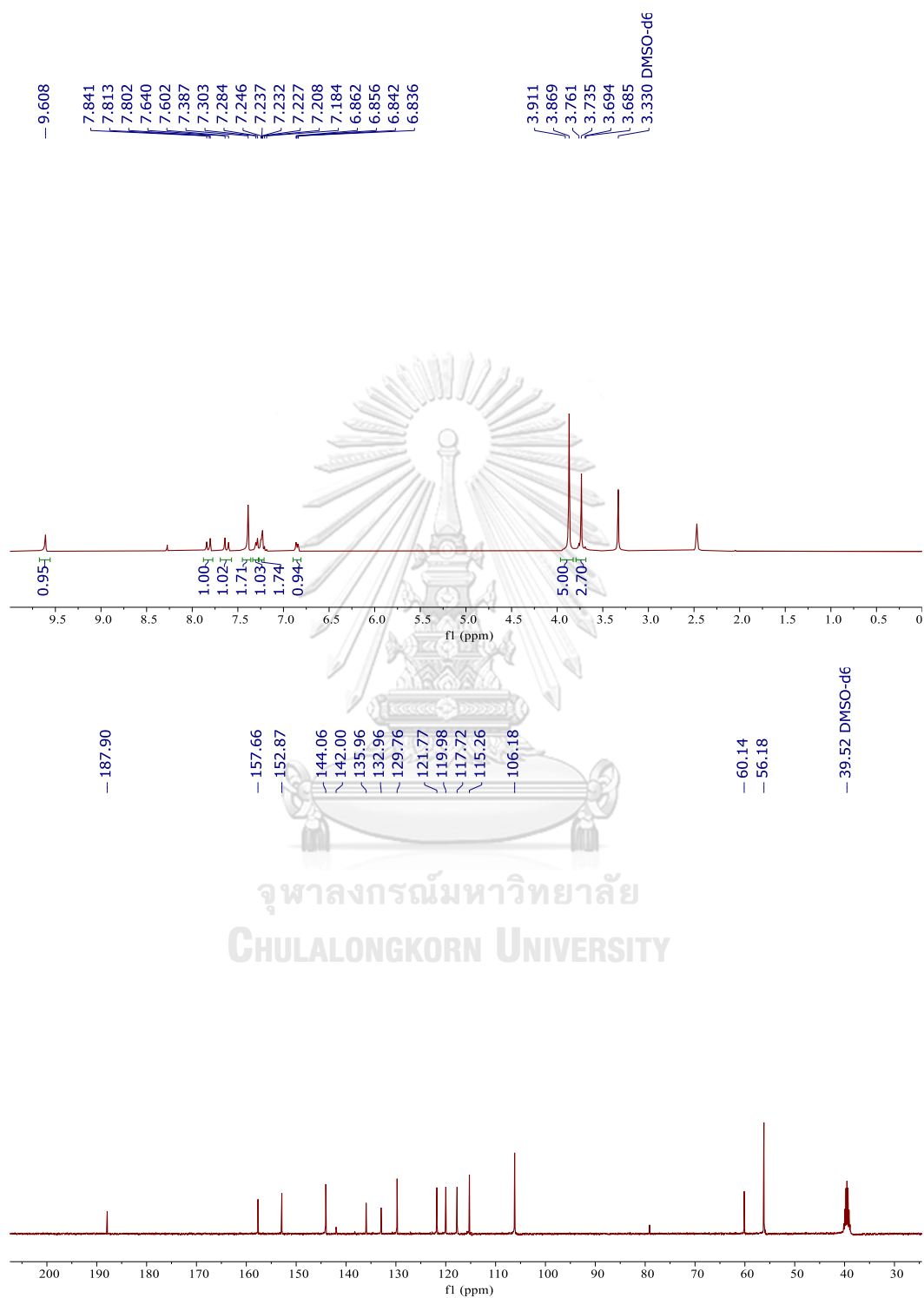
152. Trott, O.; Olson, A. J., AutoDock Vina: improving the speed and accuracy of docking with a new scoring function, efficient optimization and multithreading. *Journal of computational chemistry* **2010**, *31*, 455-461.
153. Morris, G. M.; Huey, R.; Lindstrom, W.; Sanner, M. F.; Belew, R. K.;Goodsell, D. S.; Olson, A. J., AutoDock4 and AutoDockTools4: Automated docking with selective receptor flexibility. *Journal of computational chemistry* **2009**, *30*, 2785-2791.
154. Yamamoto, K.; Miyake, H.; Kusunoki, M.; Osaki, S., Steric hindrance by 2 amino acid residues determines the substrate specificity of isomaltase from *Saccharomyces cerevisiae*. *J Biosci Bioeng* **2011**, *112*, 545-50.
155. Yu, J.; Zhou, Y.; Tanaka, I.; Yao, M., Roll: a new algorithm for the detection of protein pockets and cavities with a rolling probe sphere. *Bioinformatics* **2010**, *26*, 46-52.
156. Zafar, M.; Khan, H.; Rauf, A.; Khan, A.; Lodhi, M. A., In Silico Study of Alkaloids as α -Glucosidase Inhibitors: Hope for the Discovery of Effective Lead Compounds. *Front. Endocrinol.* **2016**, *7*, 153.
157. Kanchithalaivan, S.; Kumar, R. R.; Perumal, S., Synthesis of novel 16-spiro steroids: Spiro-7'-(aryl) tetrahydro-1H-pyrrolo [1, 2-c][1, 3] thiazolo-trans-androsterone hybrid heterocycles. *Steroids*. **2013**, *78*, 409-417.
158. Kanchithalaivan, S.; Kumar, R. R.; Perumal, S., Synthesis of novel 16-spiro steroids: Spiro-7'-(aryl) tetrahydro-1H-pyrrolo [1, 2-c][1, 3] thiazolo-trans-androsterone hybrid heterocycles. *Steroids*. **2013**, *78*, 409-417.
159. Jiang, F.-x.; Liu, Q.-z.; Zhao, D.; Luo, C.-t.; Guo, C.-p.; Ye, W.-c.; Luo, C.; Chen, H., A concise synthesis of N-substituted fagomine derivatives and the systematic exploration of their α -glycosidase inhibition. *Eur. J. Med. Chem.* **2014**, *77*, 211-222.
160. Şöhretoğlu, D.; Sari, S.; Özel, A.; Barut, B., α -Glucosidase inhibitory effect of *Potentilla astracana* and some isoflavones: Inhibition kinetics and mechanistic insights through in vitro and in silico studies. *International Journal of Biological Macromolecules* **2017**, *105*, 1062-1070.

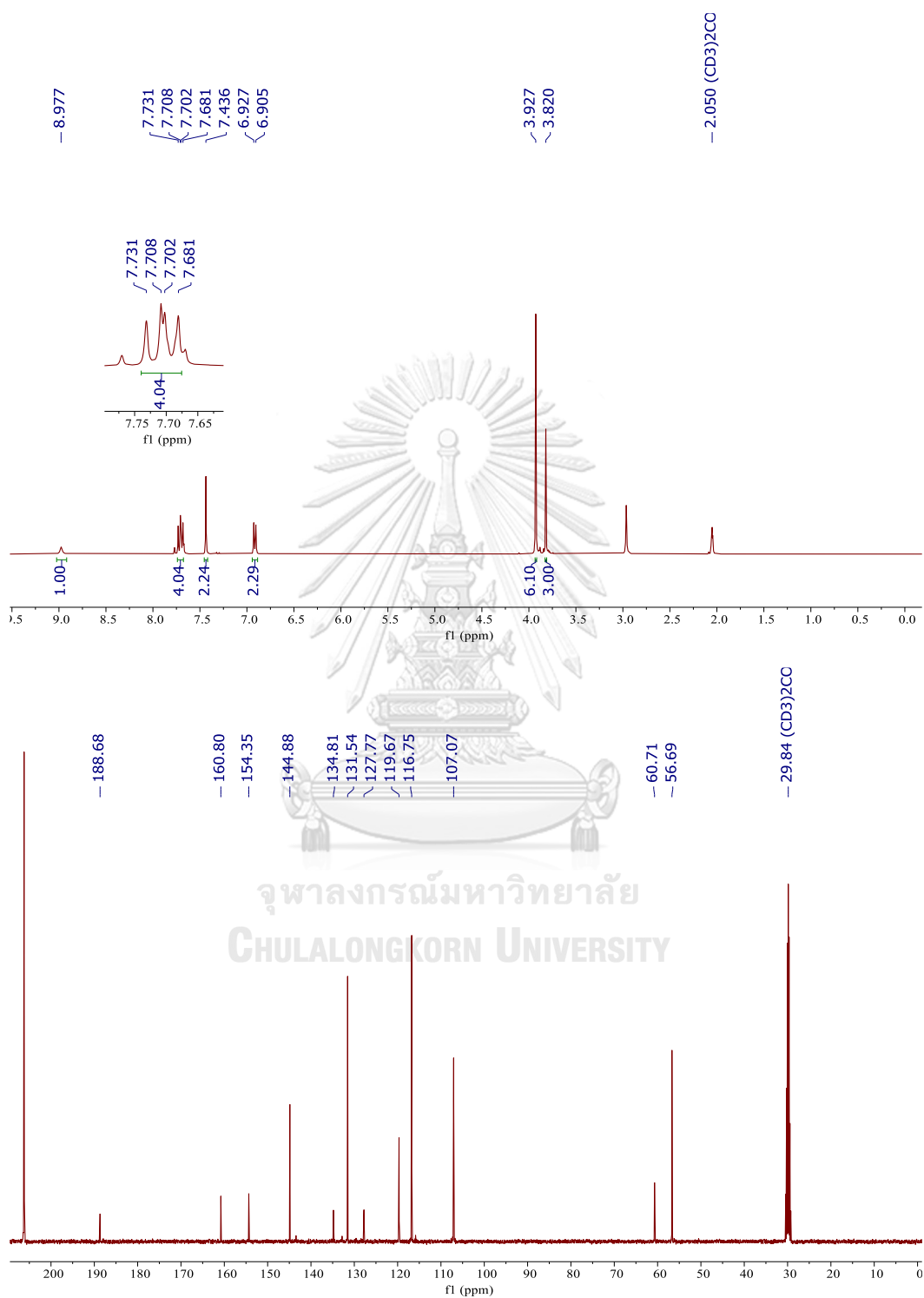
161. Kadziola, A.; Søgaard, M.; Svensson, B.; Haser, R., Molecular structure of a barley alpha-amylase-inhibitor complex: implications for starch binding and catalysis. *J Mol Biol* **1998**, *278*, 205-17.

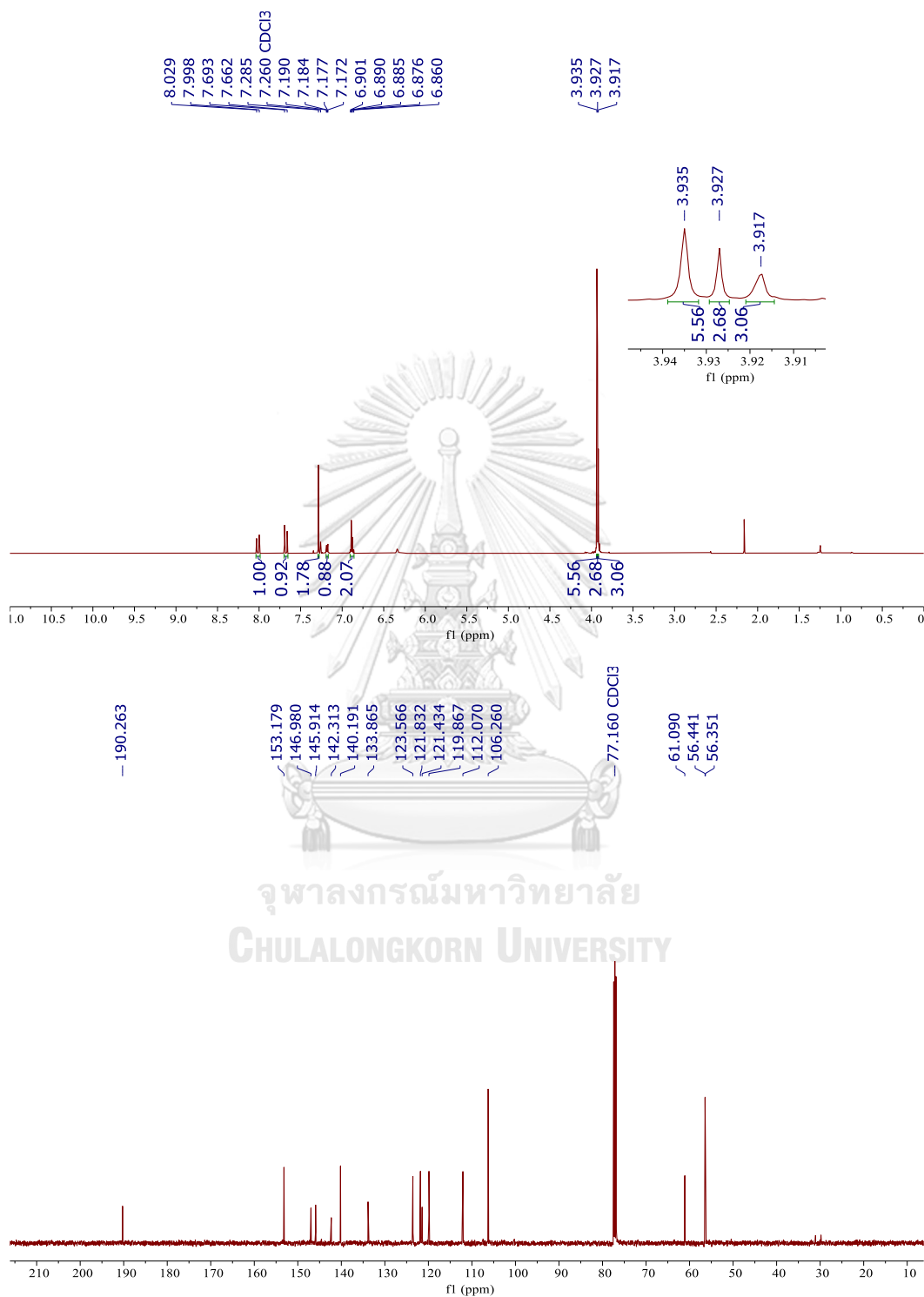


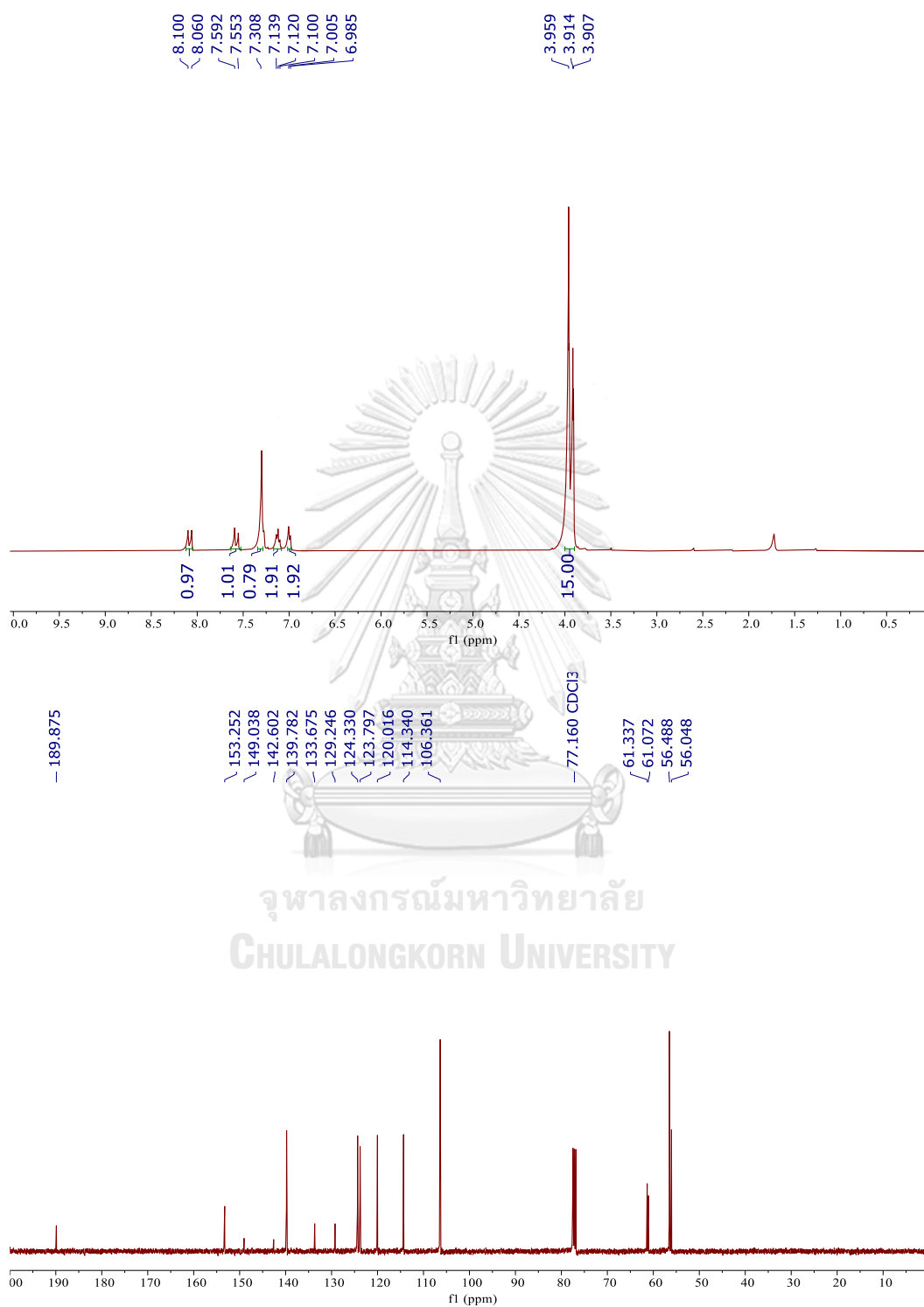
APPENDIX

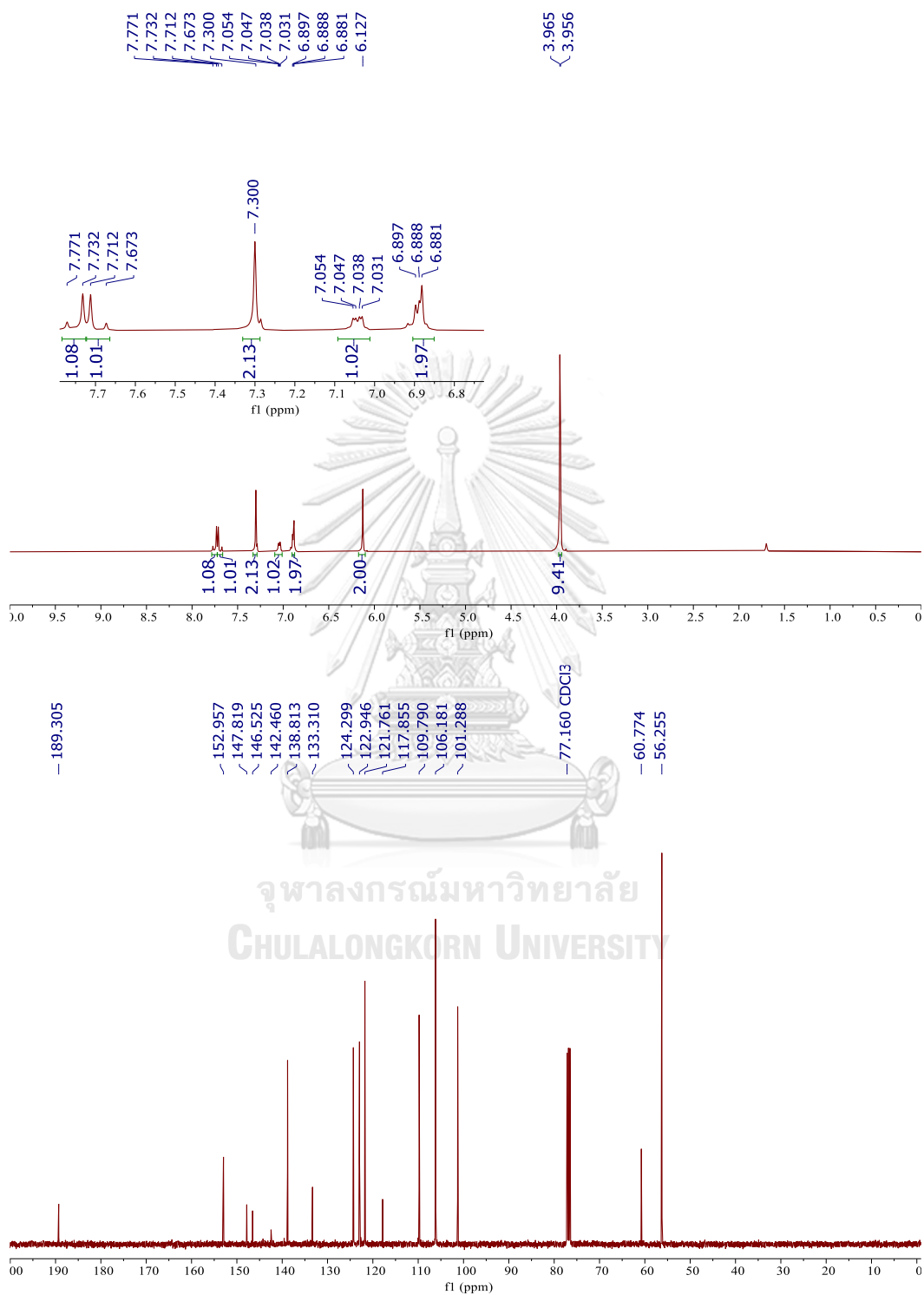
1. ^1H (400 MHz) and ^{13}C (100 MHz) NMR Spectra in CDCl_3 of **1**

2. ^1H (400 MHz) and ^{13}C (100 MHz) NMR Spectra in $\text{DMSO-}d_6$ of 2

3. ^1H (400 MHz) and ^{13}C (100 MHz) NMR Spectra in acetone- d_6 of **3**

4. ^1H (400 MHz) and ^{13}C (100 MHz) NMR Spectra in CDCl_3 of **4**

5. ^1H (400 MHz) and ^{13}C (100 MHz) NMR Spectra in CDCl_3 of 5

6. ^1H (400 MHz) and ^{13}C (100 MHz) NMR Spectra in CDCl_3 of **6** (new compound)

7. Mass Spectra of 6 (new compound)

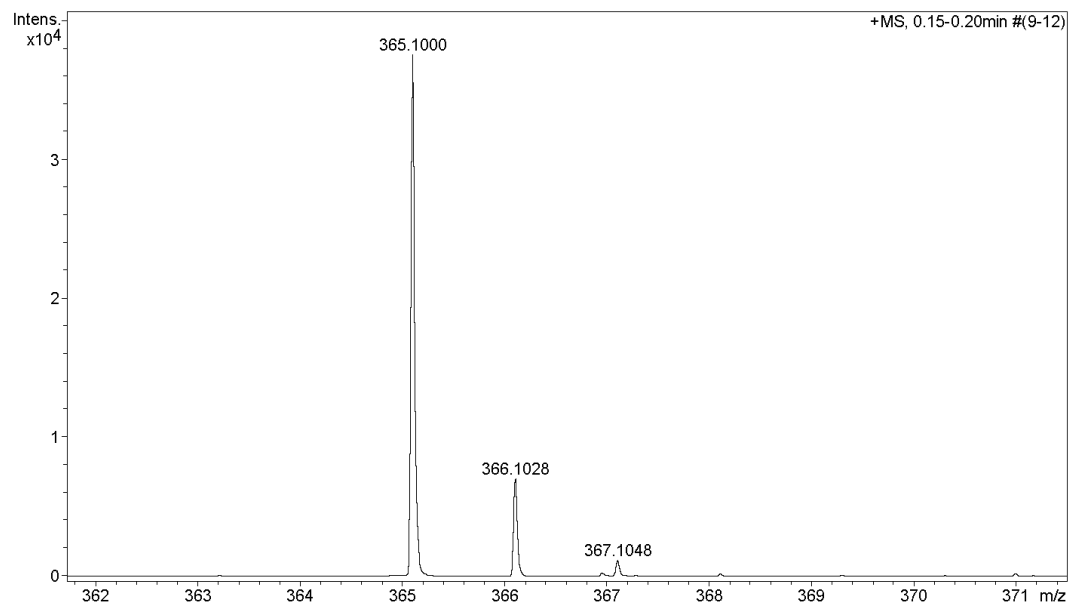
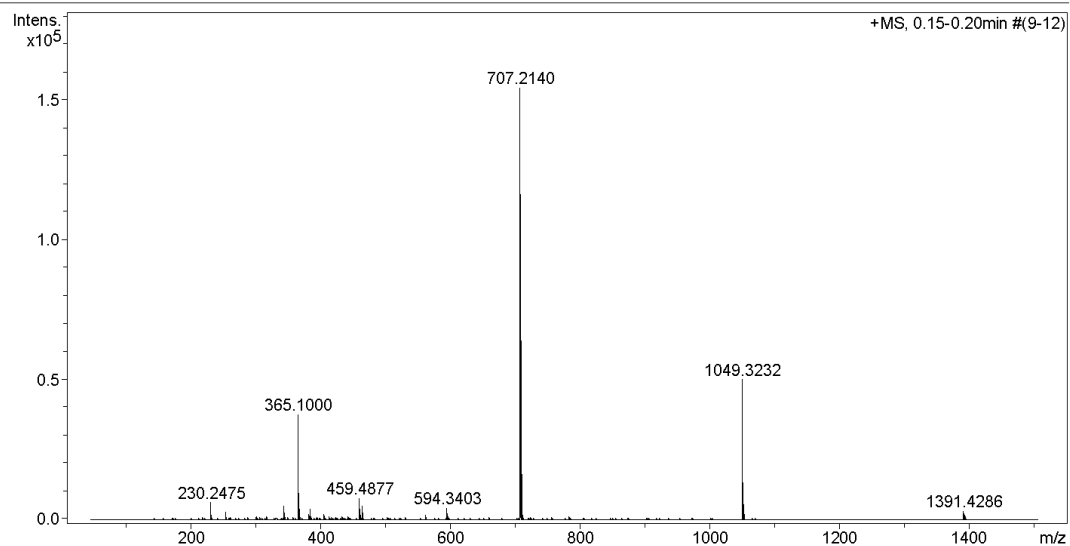
Generic Display Report

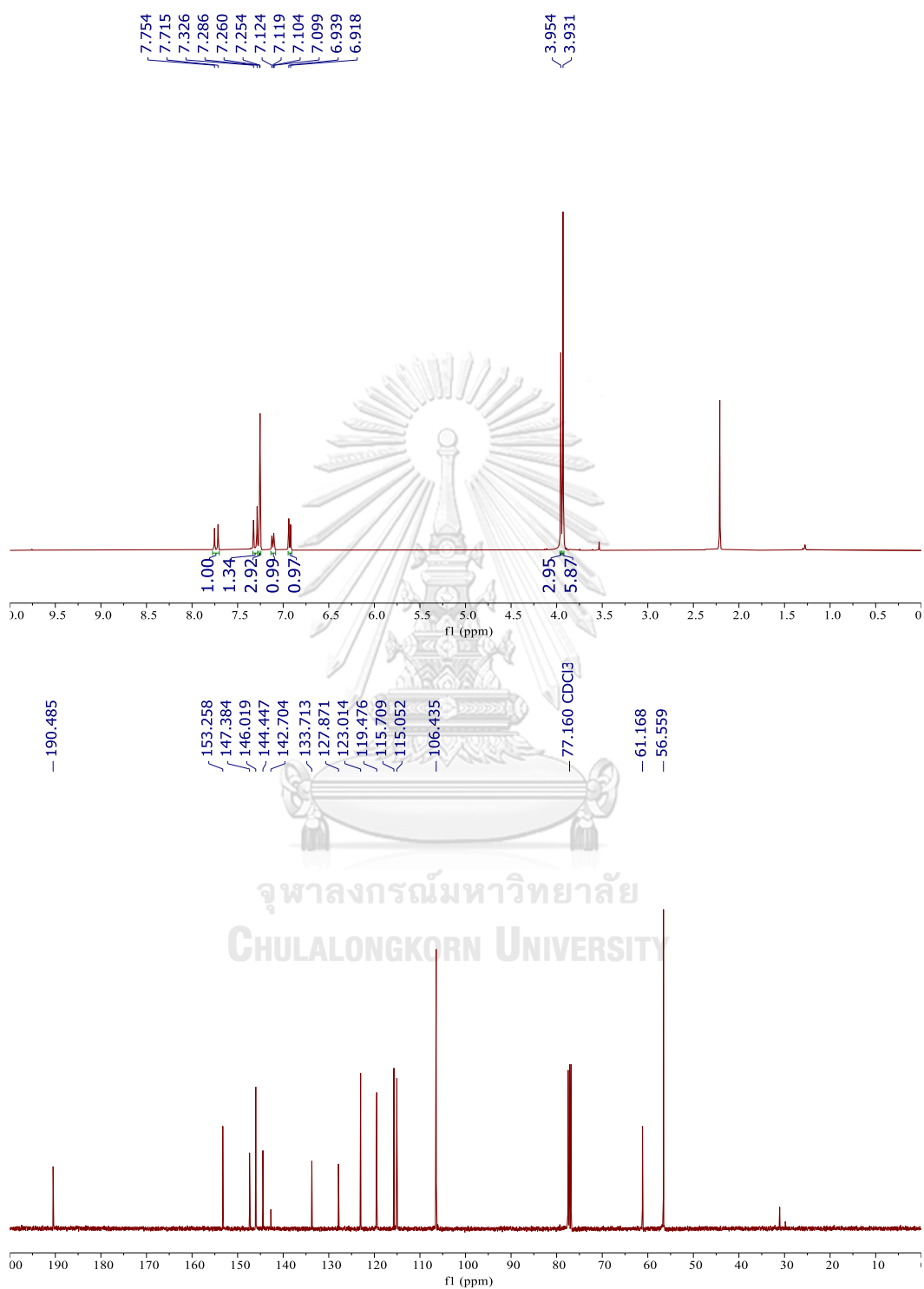
Analysis Info

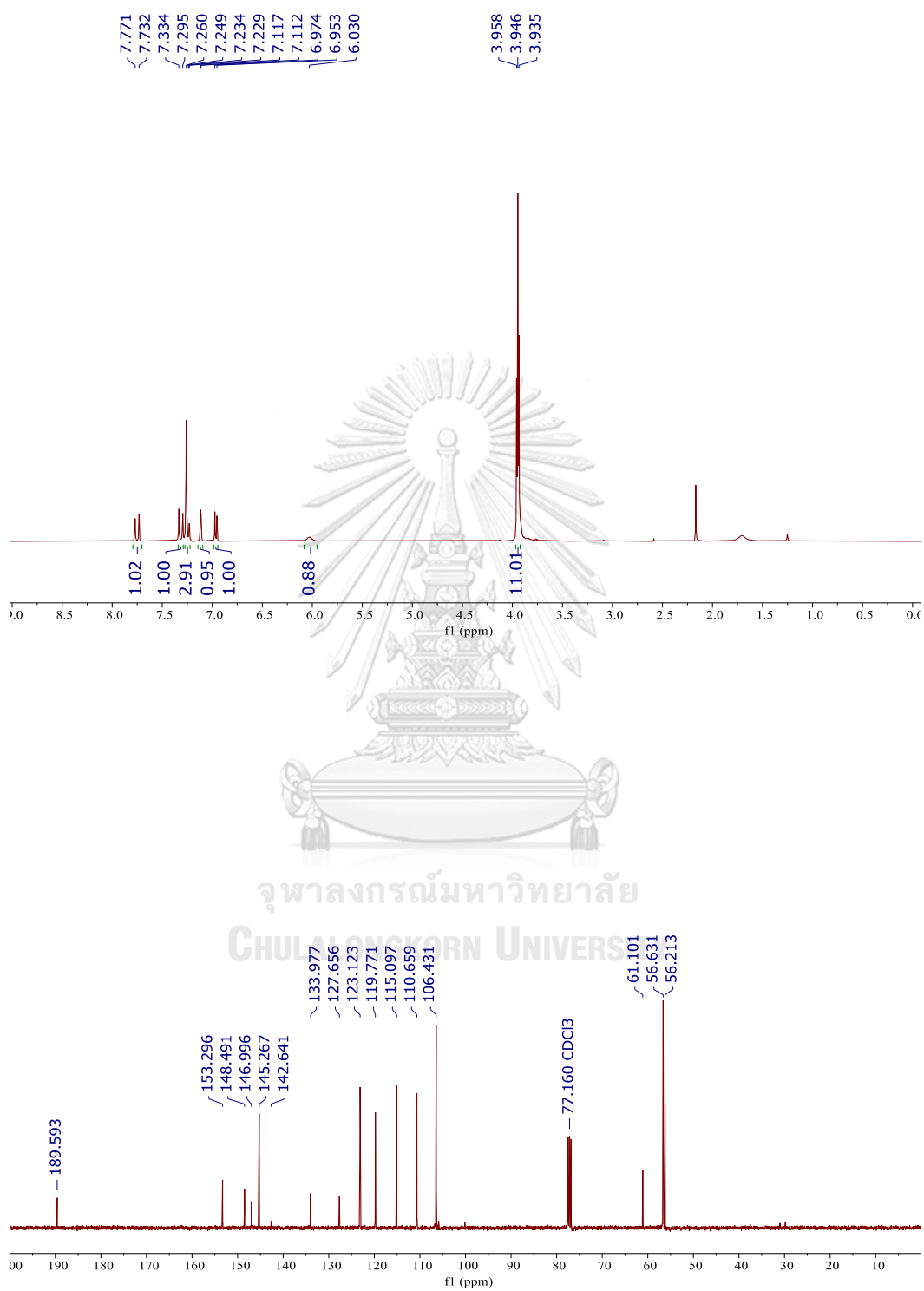
Analysis Name D:\Data\Data Service\191203\AD051_RA7_01_3518.d
Method nv_pos_6min_profile_wguardcol_50-1500_191021.m
Sample Name AD051
Comment

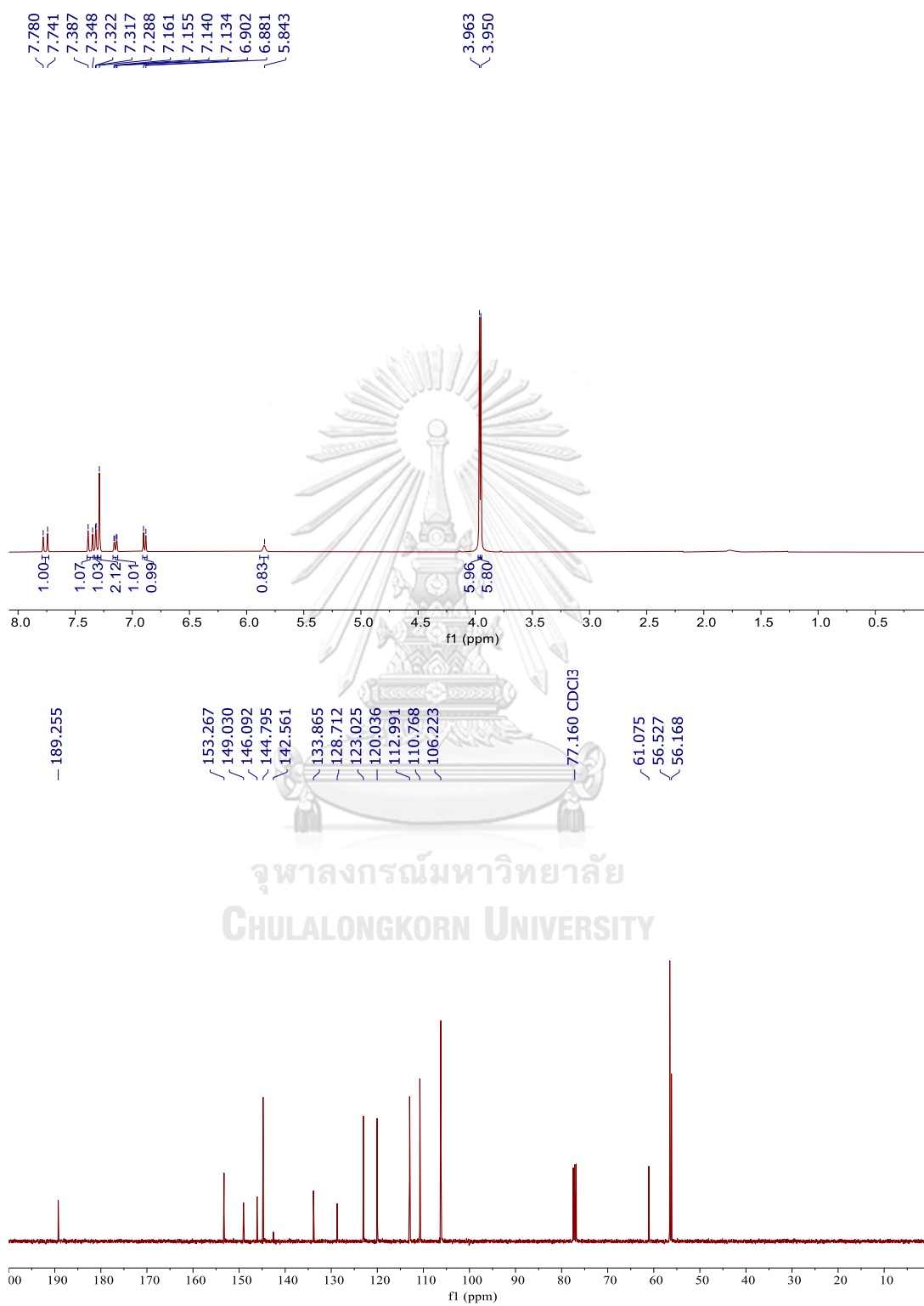
Acquisition Date 12/3/2019 5:10:20 PM

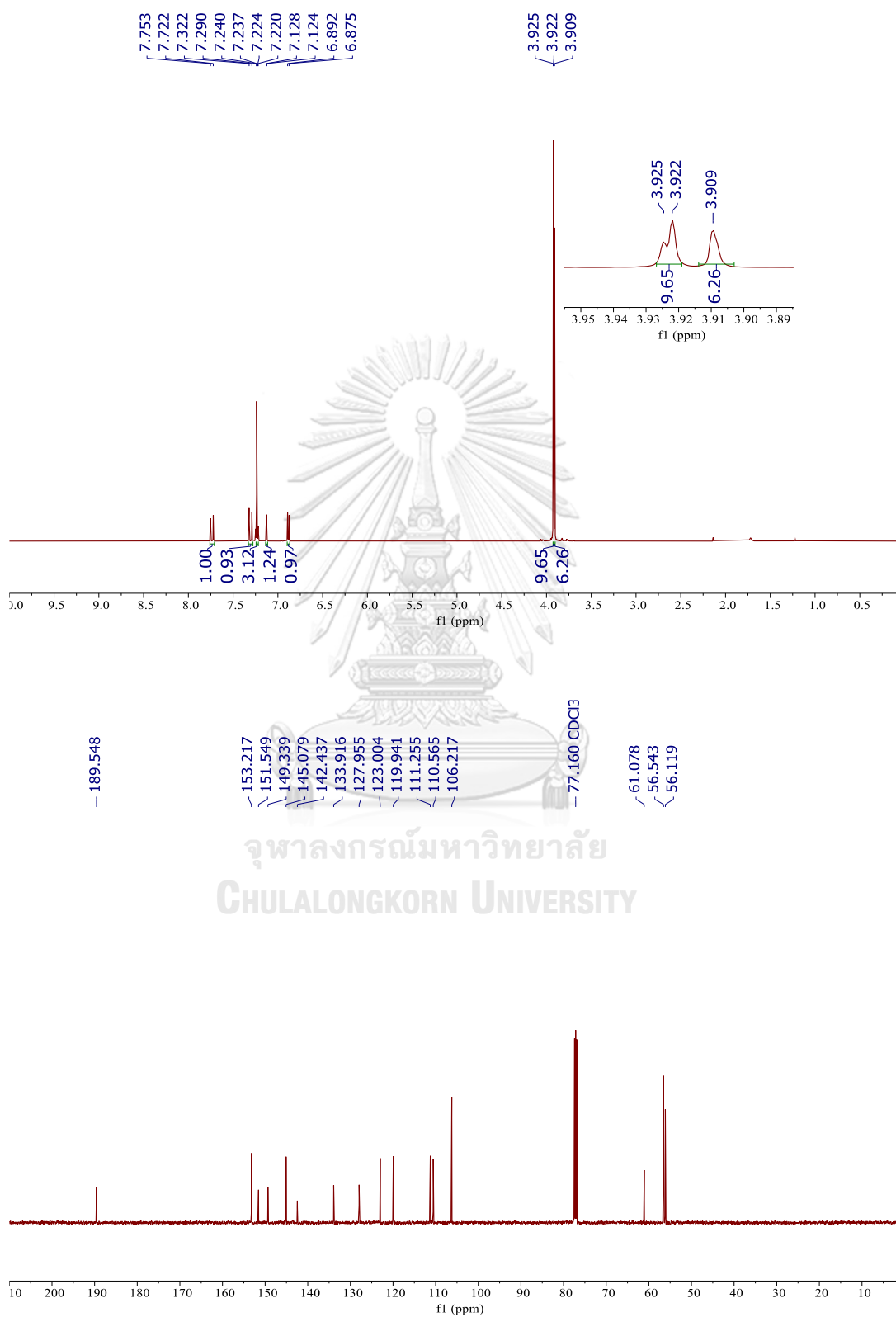
Operator CU.
Instrument microTOF-Q II

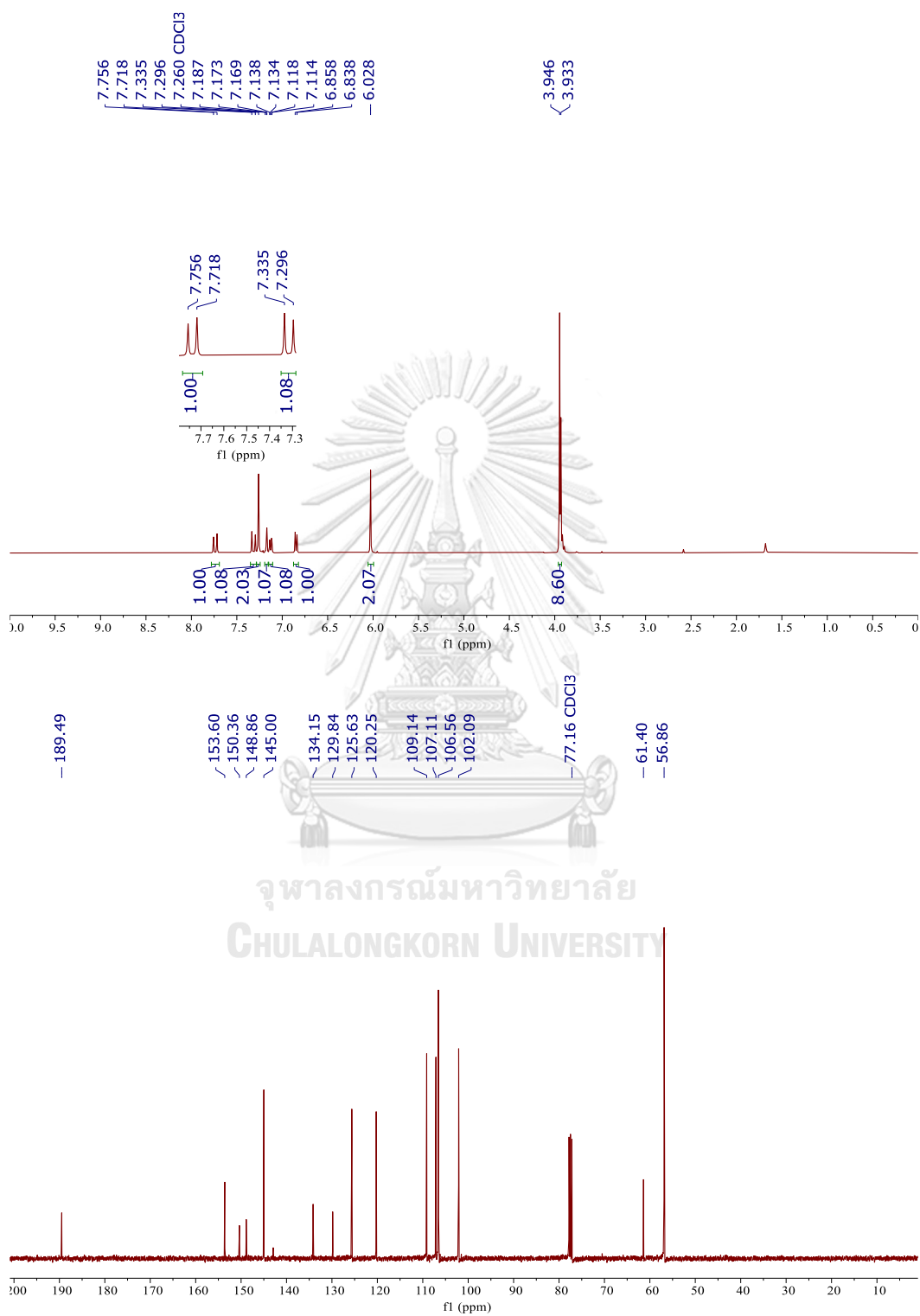


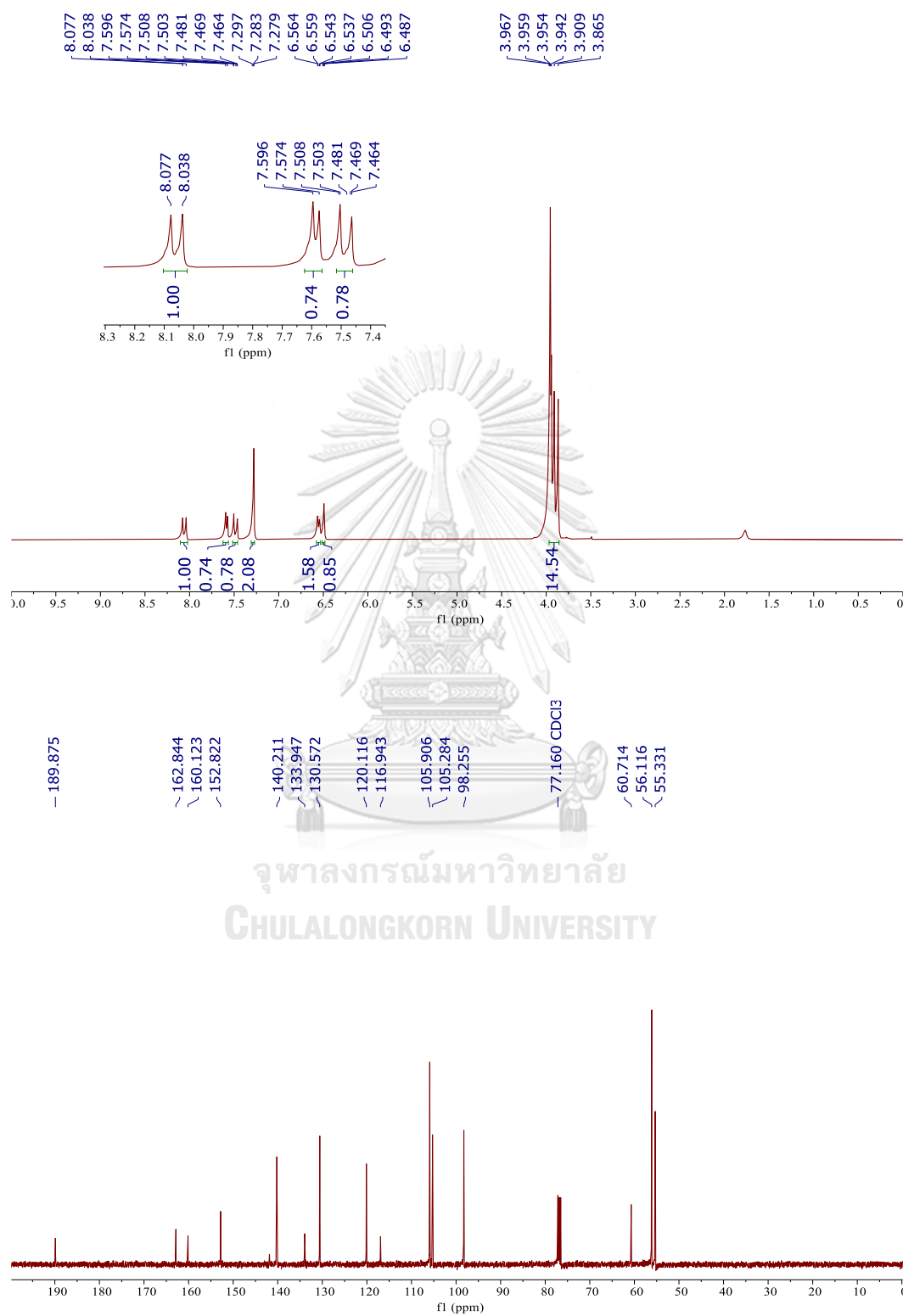
8. ^1H (400 MHz) and ^{13}C (100 MHz) NMR Spectra in CDCl_3 of 7

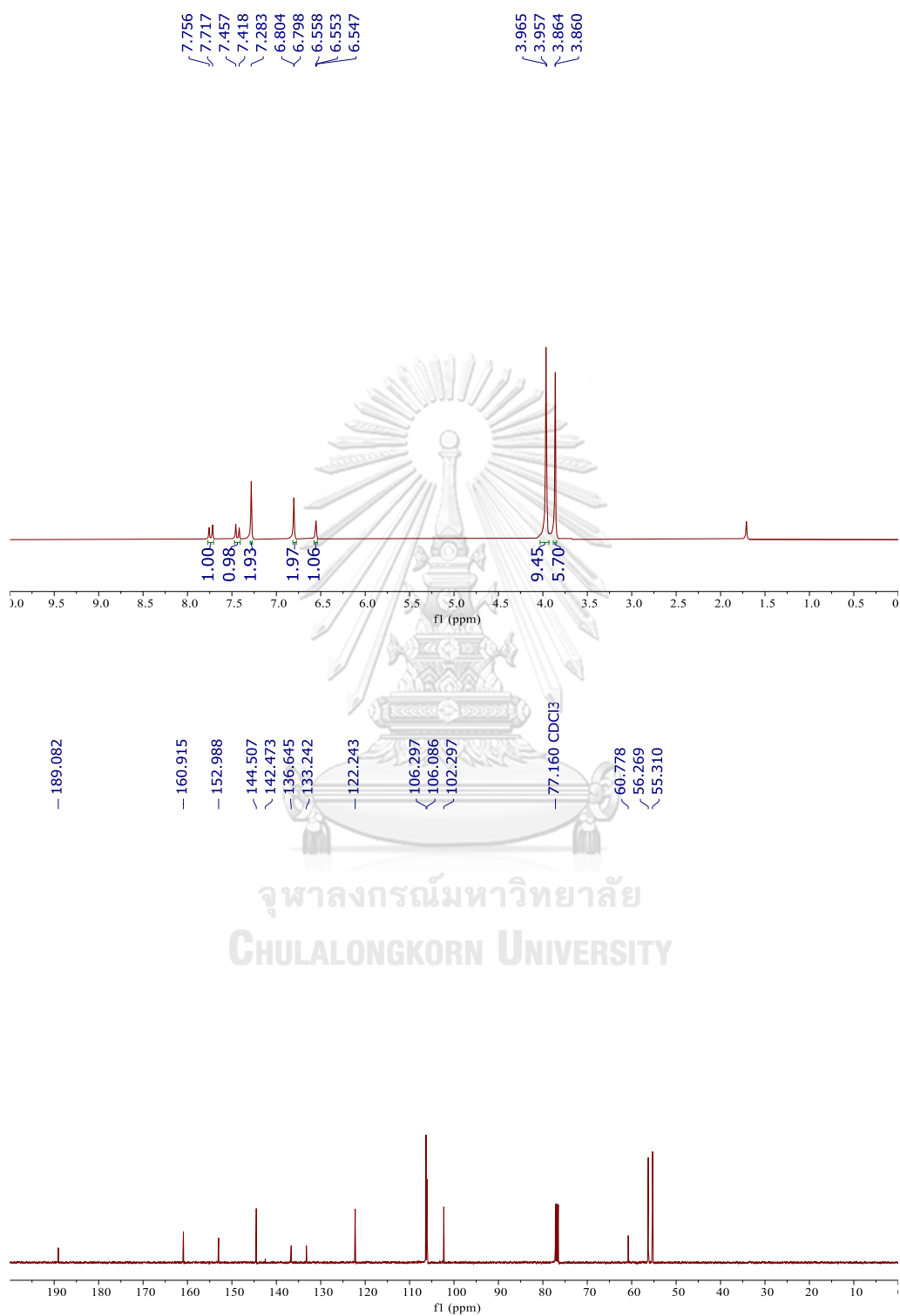
9. ^1H (400 MHz) and ^{13}C (100 MHz) NMR Spectra in CDCl_3 of **8**

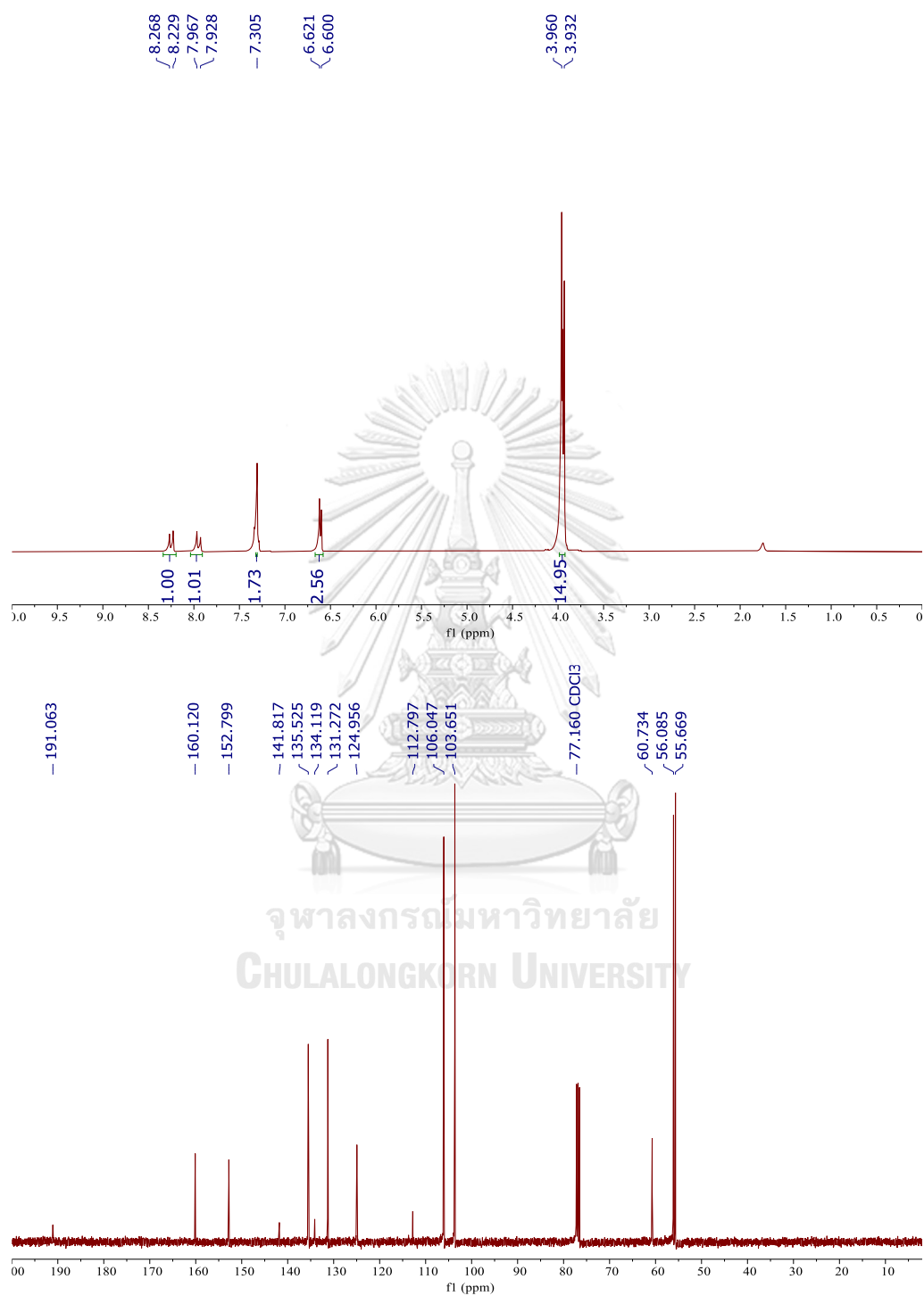
10. ^1H (400 MHz) and ^{13}C (100 MHz) NMR Spectra in CDCl_3 of **9**

11. ^1H (400 MHz) and ^{13}C (100 MHz) NMR Spectra in CDCl_3 of 10

12. ^1H (400 MHz) and ^{13}C (100 MHz) NMR Spectra in CDCl_3 of **11**

13. ^1H (400 MHz) and ^{13}C (100 MHz) NMR Spectra in CDCl_3 of 12

14. ^1H (400 MHz) and ^{13}C (100 MHz) NMR Spectra in CDCl_3 of **13**

15. ^1H (400 MHz) and ^{13}C (100 MHz) NMR Spectra in CDCl_3 of **14** (new compound)

16. Mass Spectra of 14 (new compound)

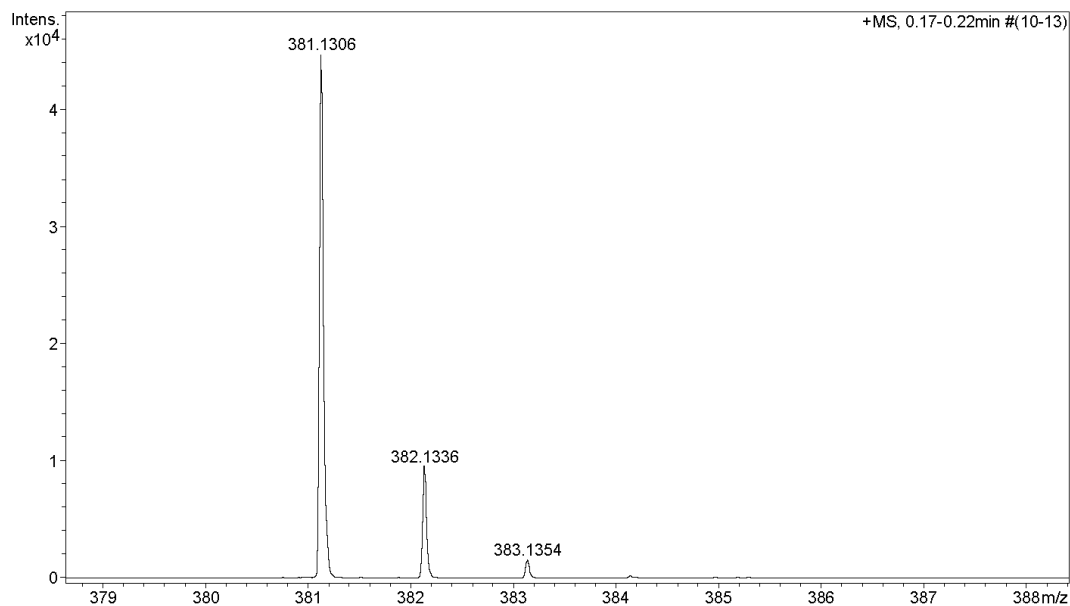
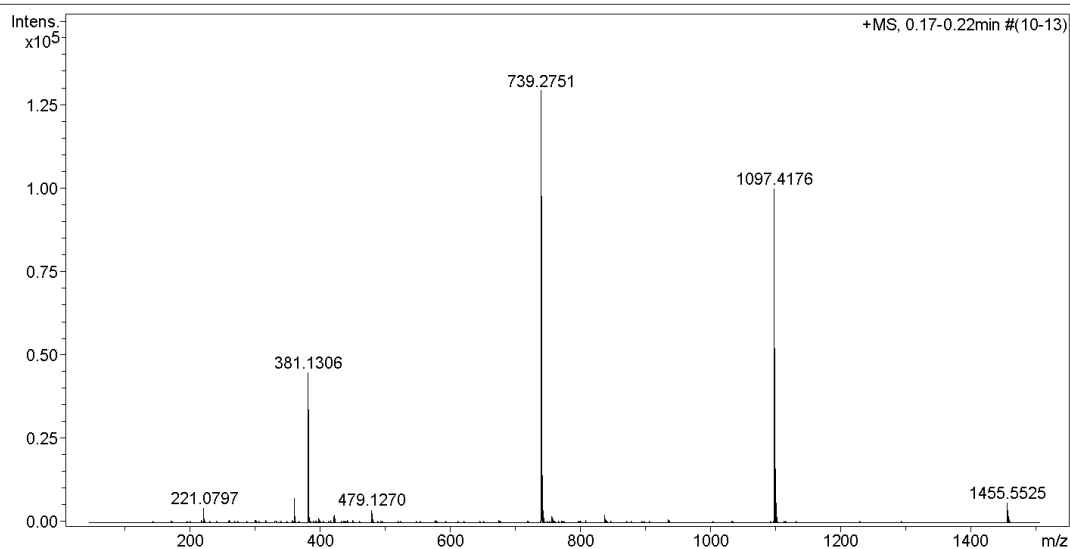
Generic Display Report

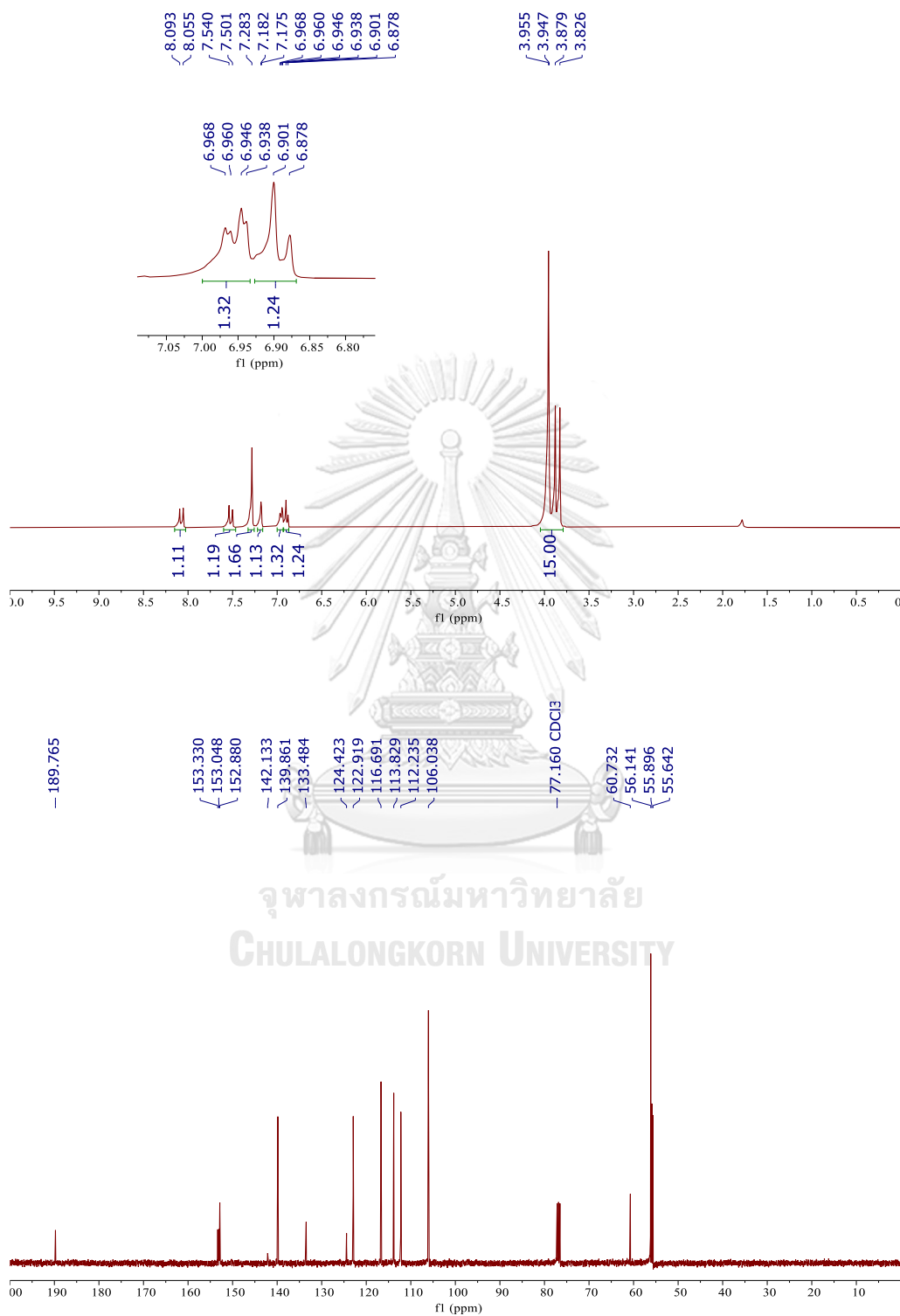
Analysis Info

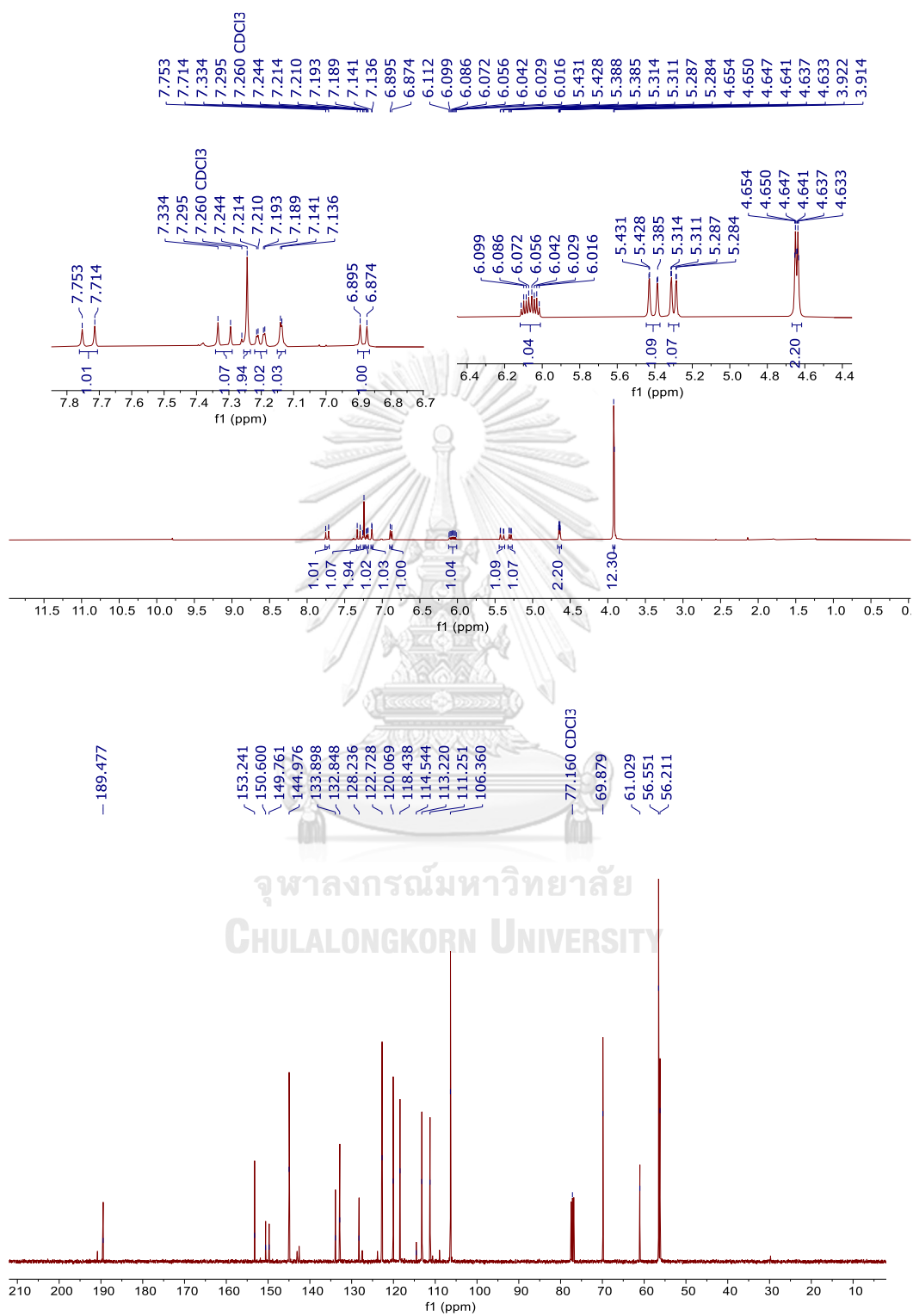
Analysis Name D:\Data\Data Service\191203\AD050_RA6_01_3517.d
Method nv_pos_6min_profile_wguardcol_50-1500_191021.m
Sample Name AD050
Comment

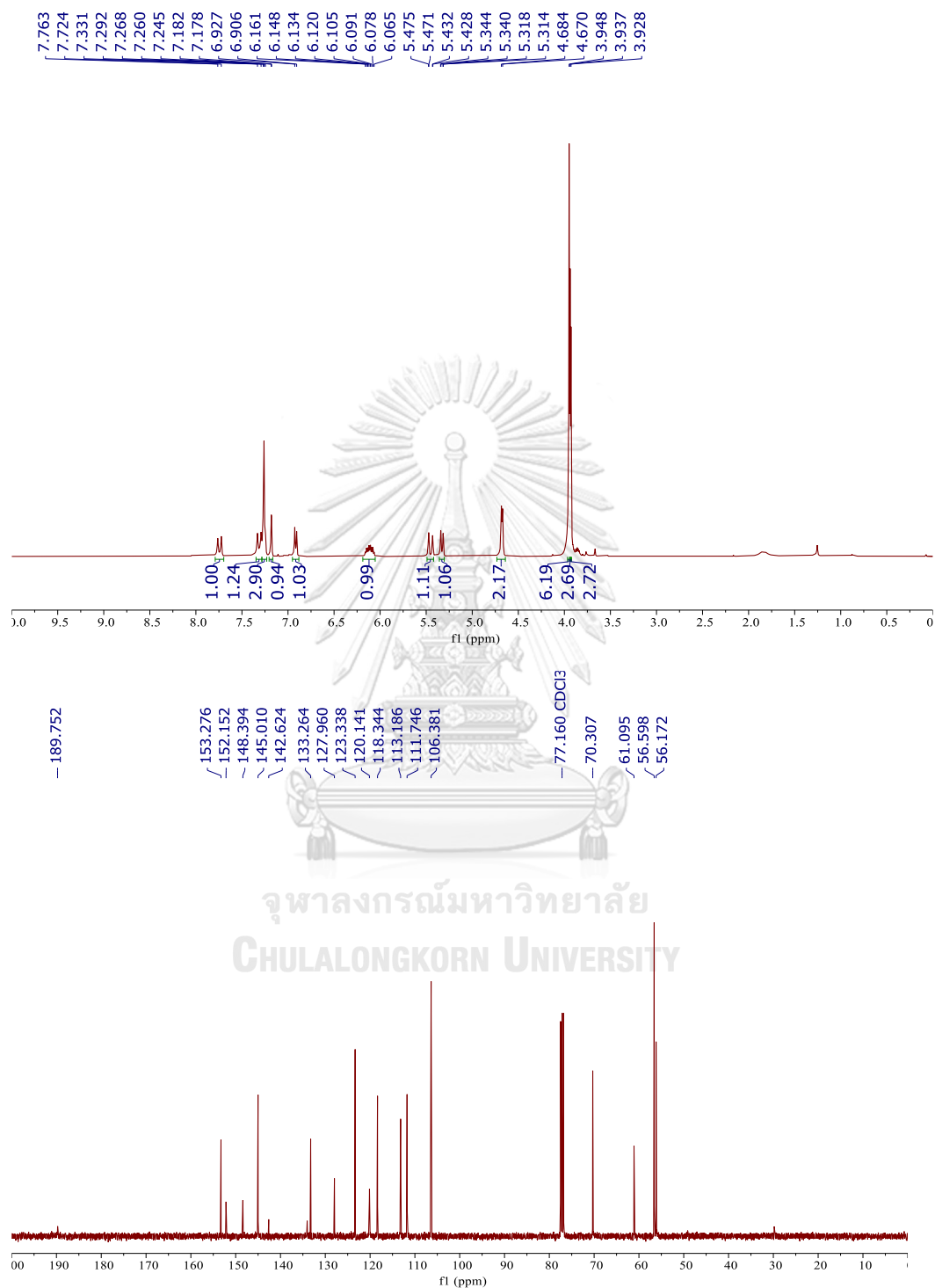
Acquisition Date 12/3/2019 5:03:53 PM

Operator CU.
Instrument micrOTOF-Q II



17. ^1H (400 MHz) and ^{13}C (100 MHz) NMR Spectra in CDCl_3 of 15

18. ^1H (400 MHz) and ^{13}C (100 MHz) NMR Spectra in CDCl_3 of 16

19. ^1H (400 MHz) and ^{13}C (100 MHz) NMR Spectra in CDCl_3 of **17** (new compound)

20. Mass Spectra of 17 (new compound)

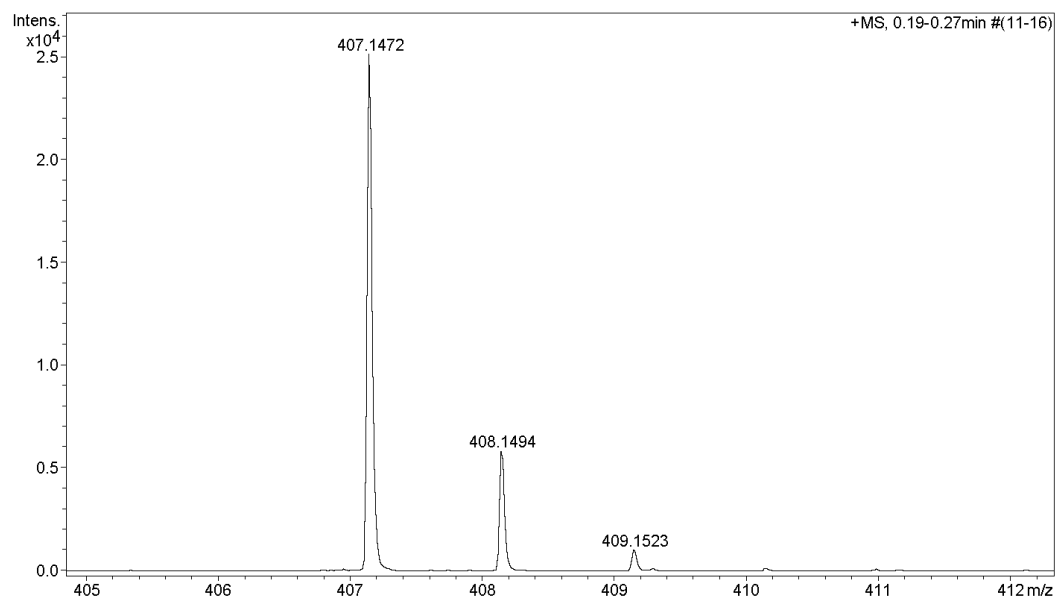
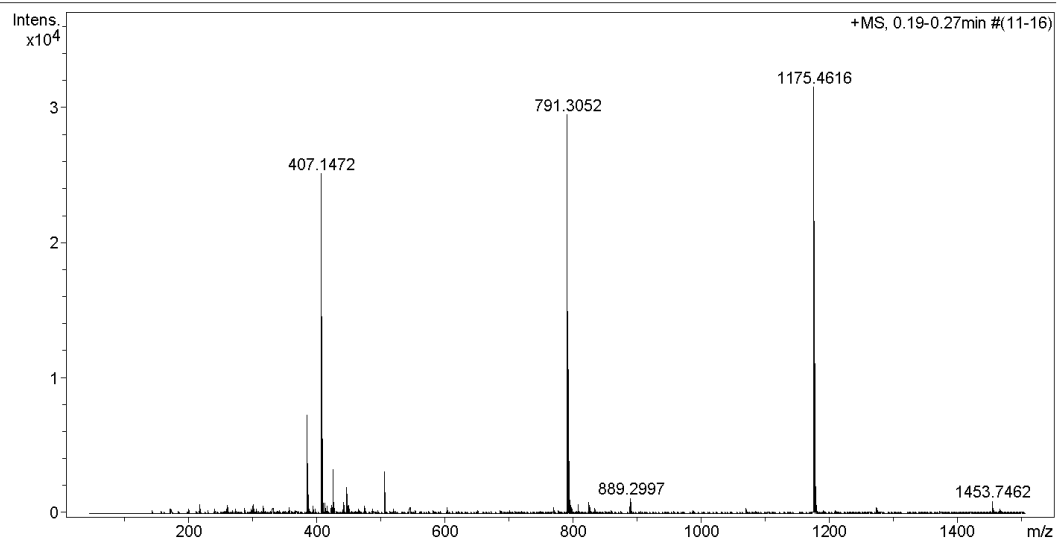
Generic Display Report

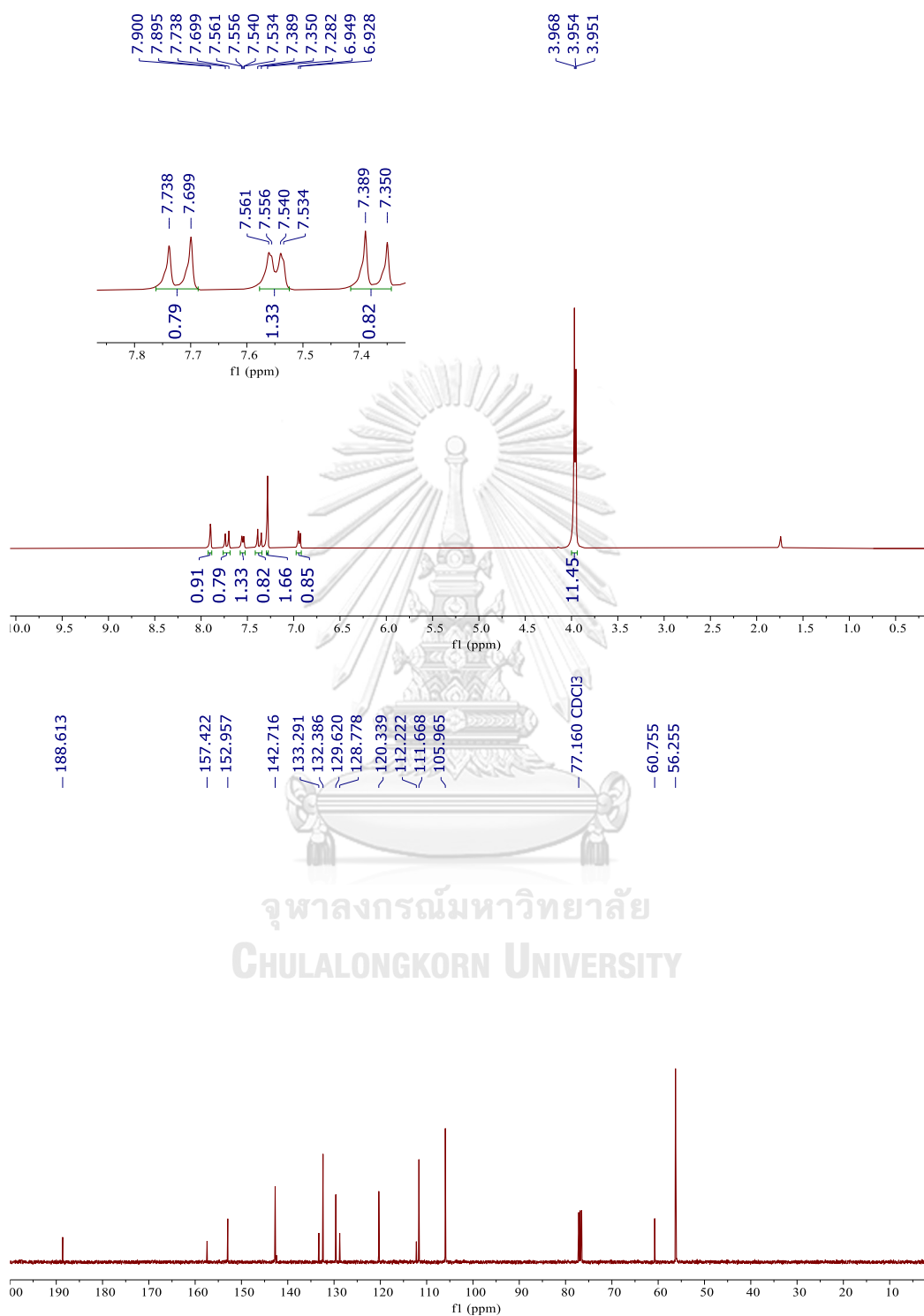
Analysis Info

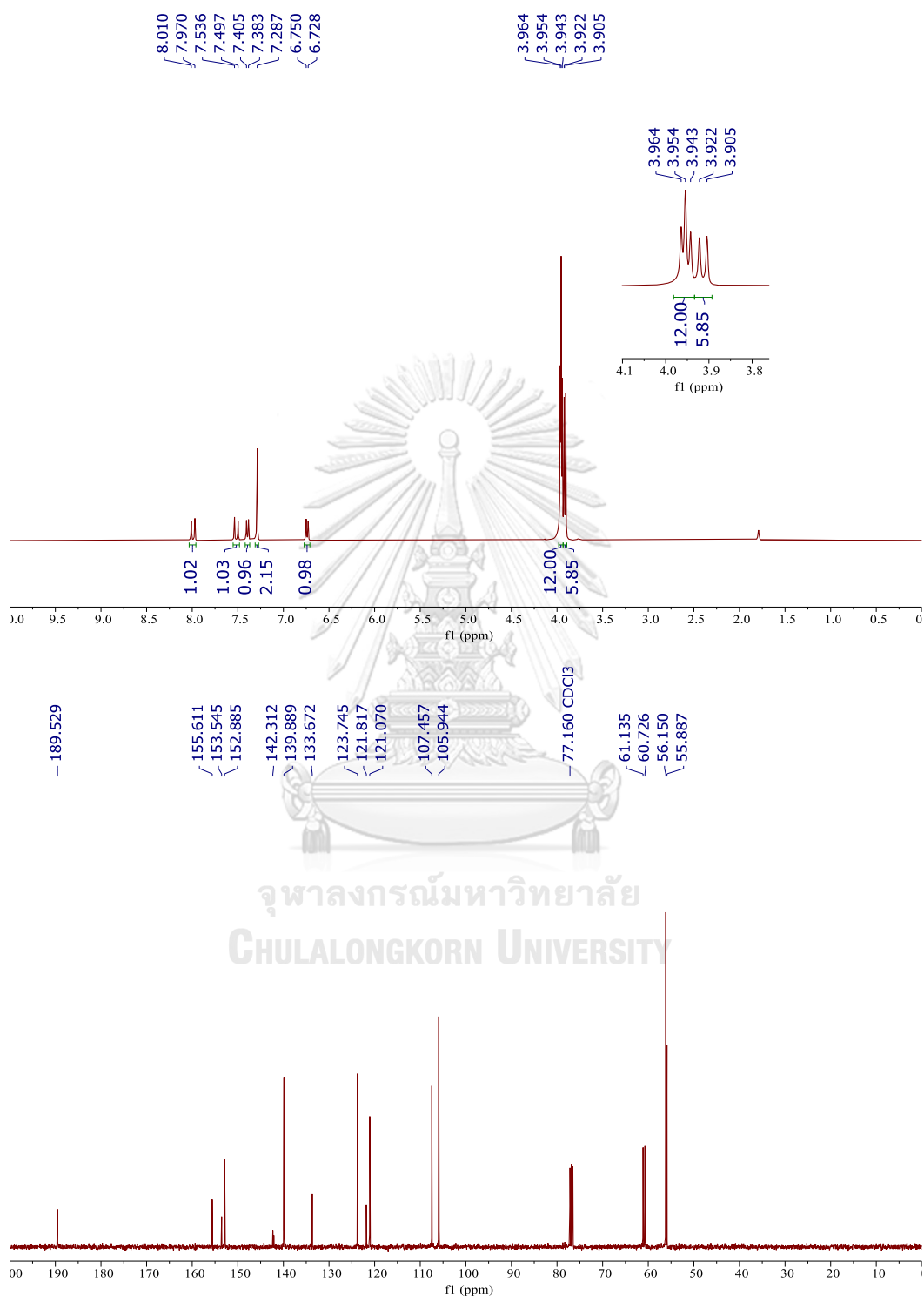
Analysis Name D:\Data\Data Service\191203\AD038_RA4_01_3515.d
Method nv_pos_6min_profile_wguardcol_50-1500_191021.m
Sample Name AD038
Comment

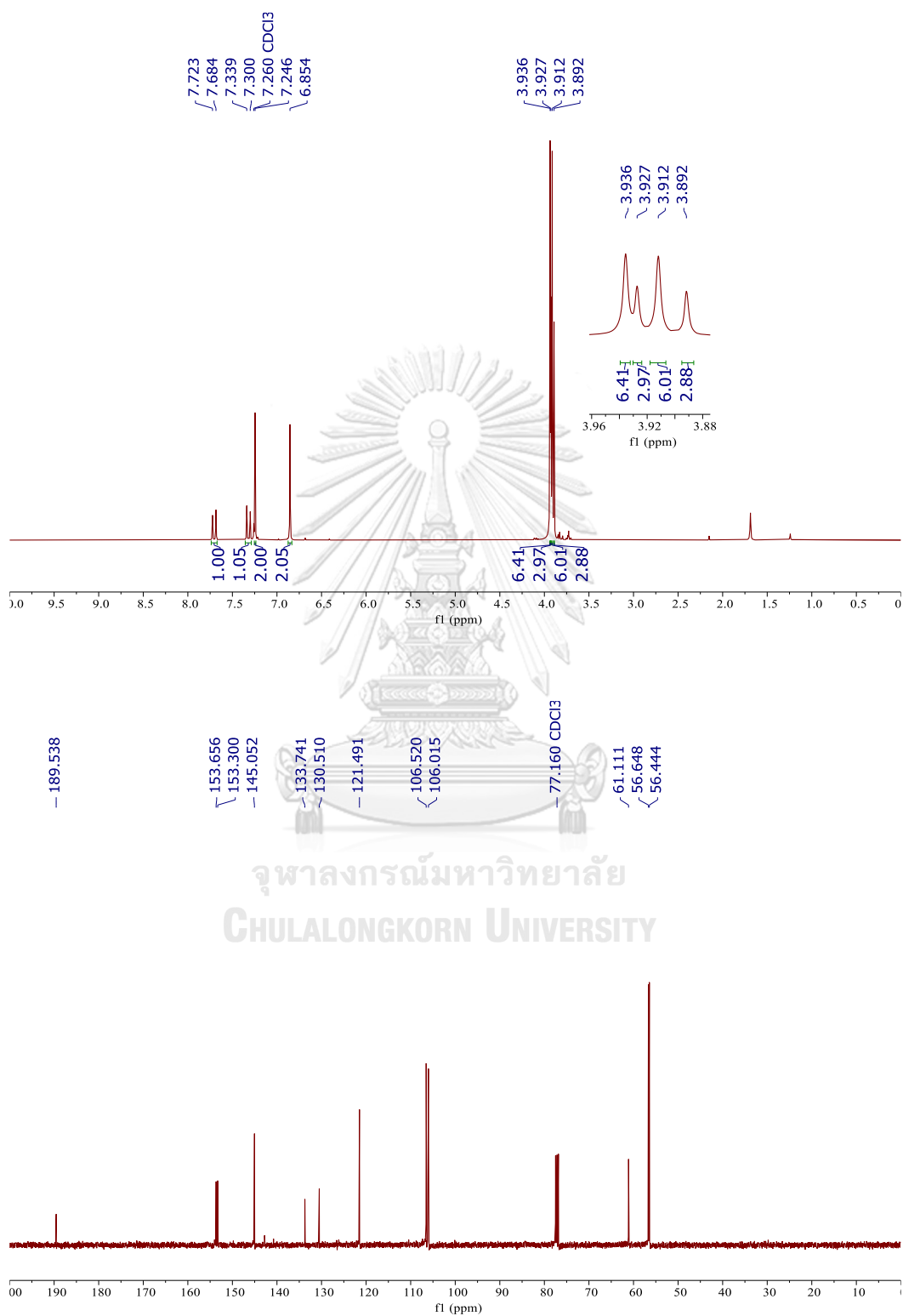
Acquisition Date 12/3/2019 4:51:02 PM

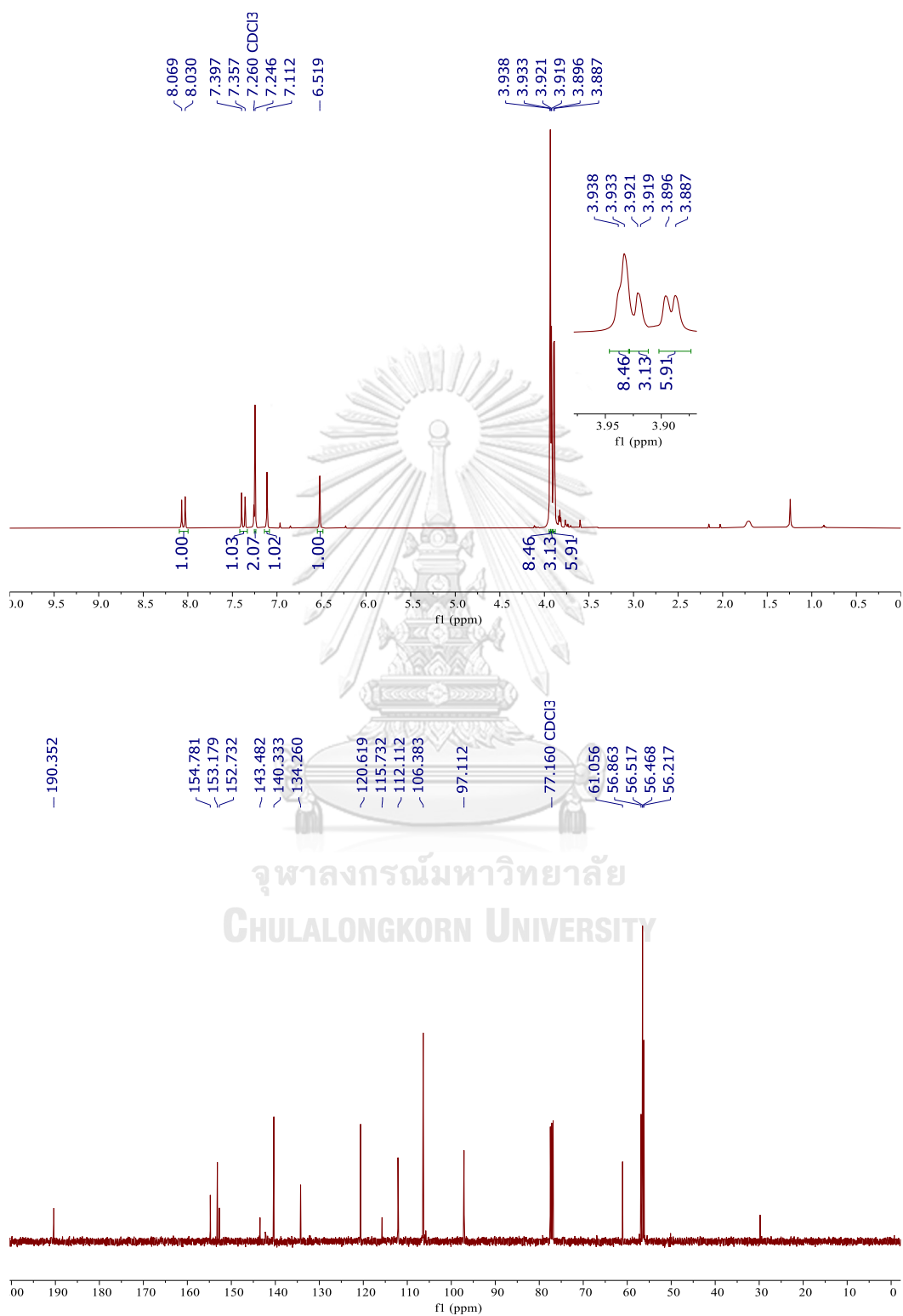
Operator CU.
Instrument micrOTOF-Q II



21. ^1H (400 MHz) and ^{13}C (100 MHz) NMR Spectra in CDCl_3 of **18**

22. ^1H (400 MHz) and ^{13}C (100 MHz) NMR Spectra in CDCl_3 of **19**

23. ^1H (400 MHz) and ^{13}C (100 MHz) NMR Spectra in CDCl_3 of 20

24. ^1H (400 MHz) and ^{13}C (100 MHz) NMR Spectra in CDCl_3 of **21** (new compound)

25. Mass Spectra of 21 (new compound)

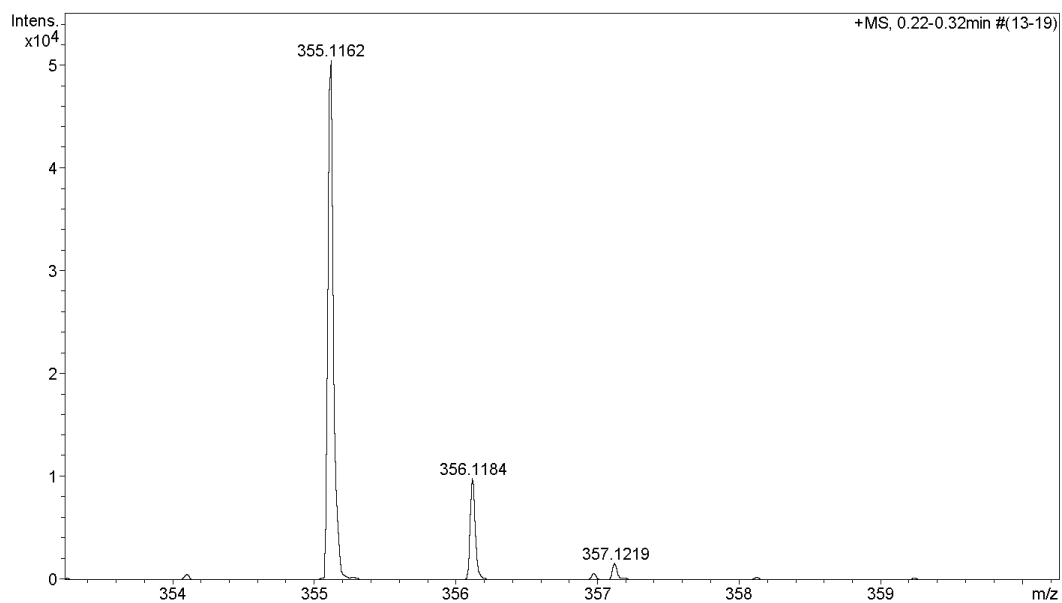
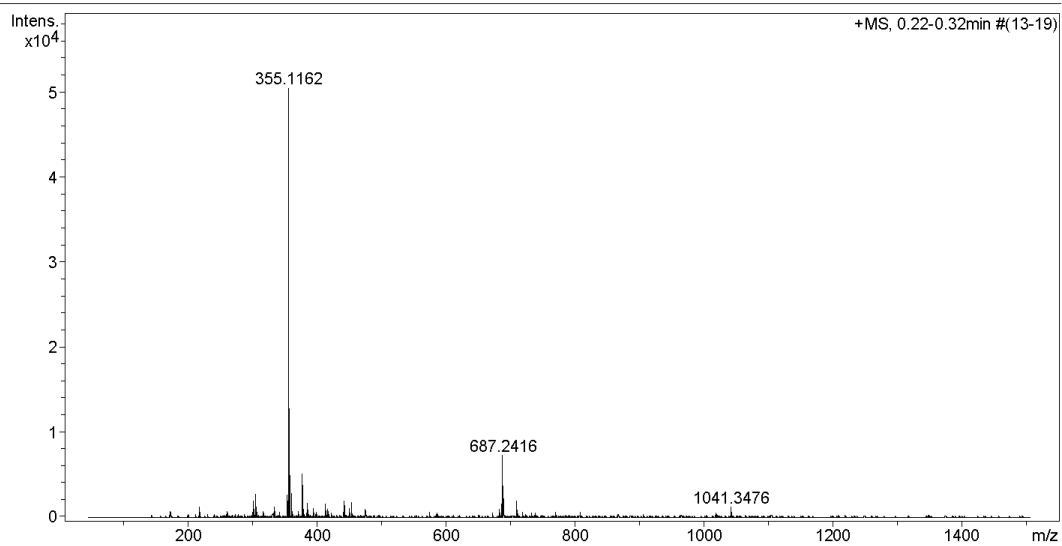
Generic Display Report

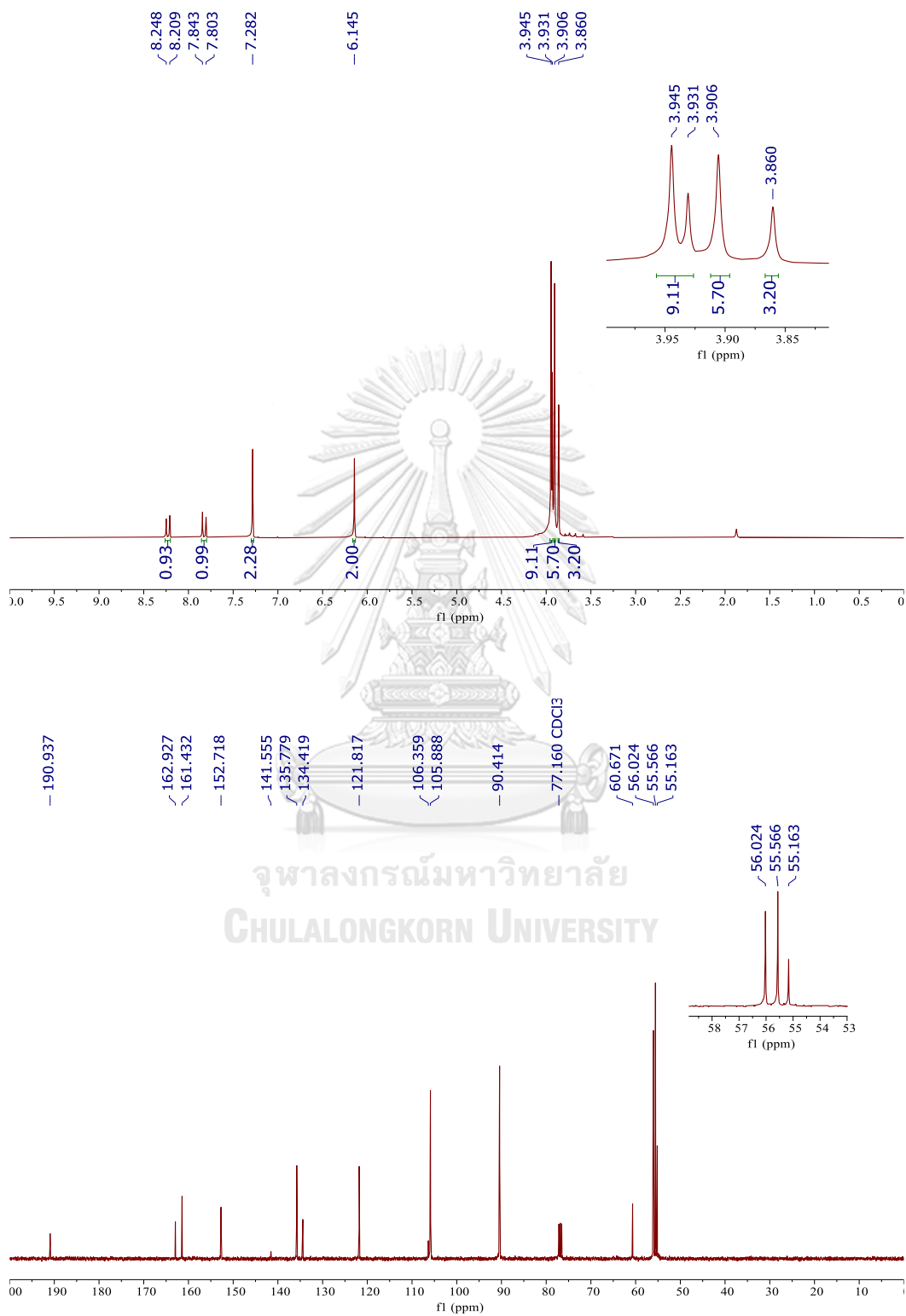
Analysis Info

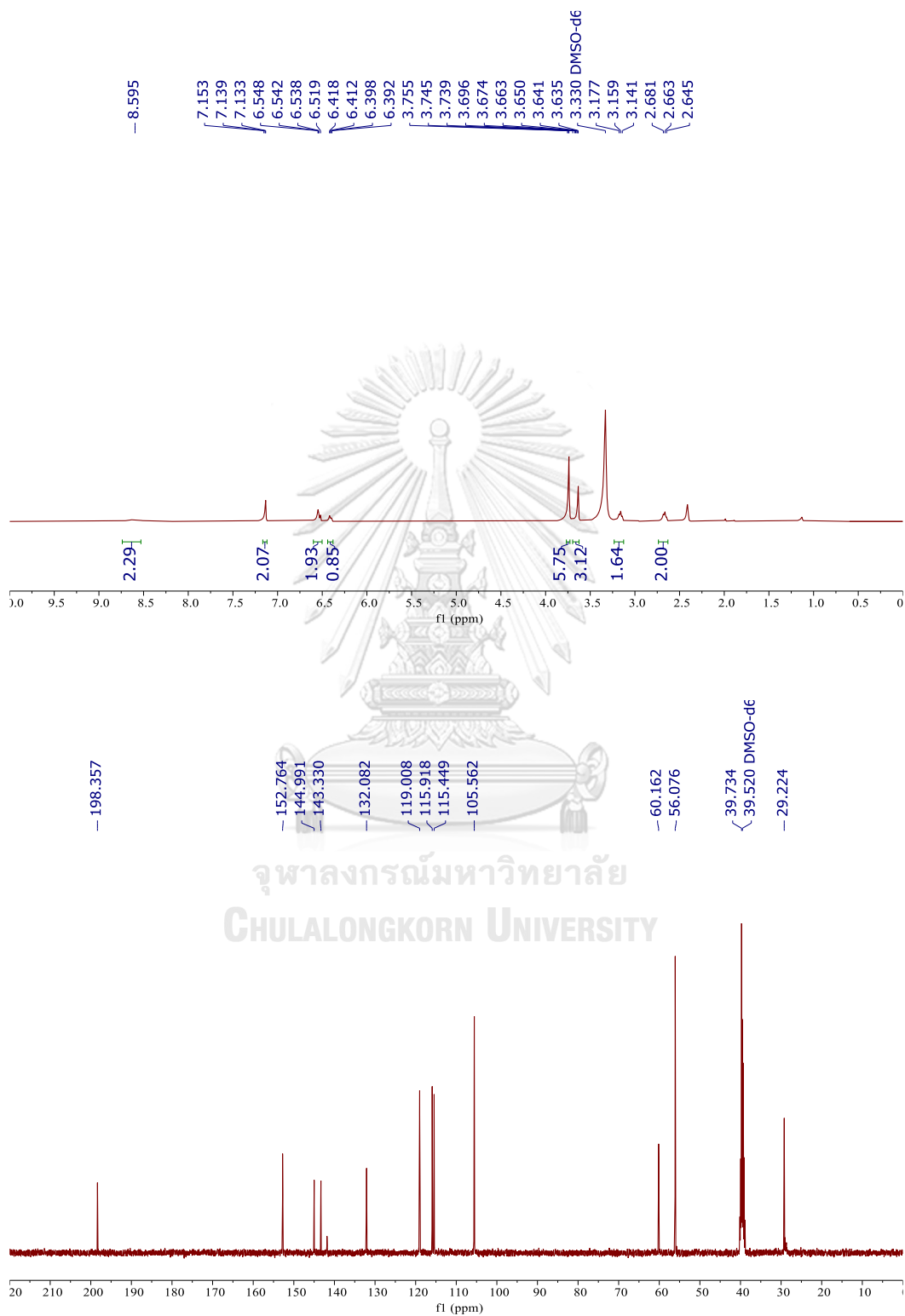
Analysis Name D:\Data\Data Service\191203\AD021_RA3_01_3514.d
Method nv_pos_6min_profile_wguardcol_50-1500_191021.m
Sample Name AD021
Comment

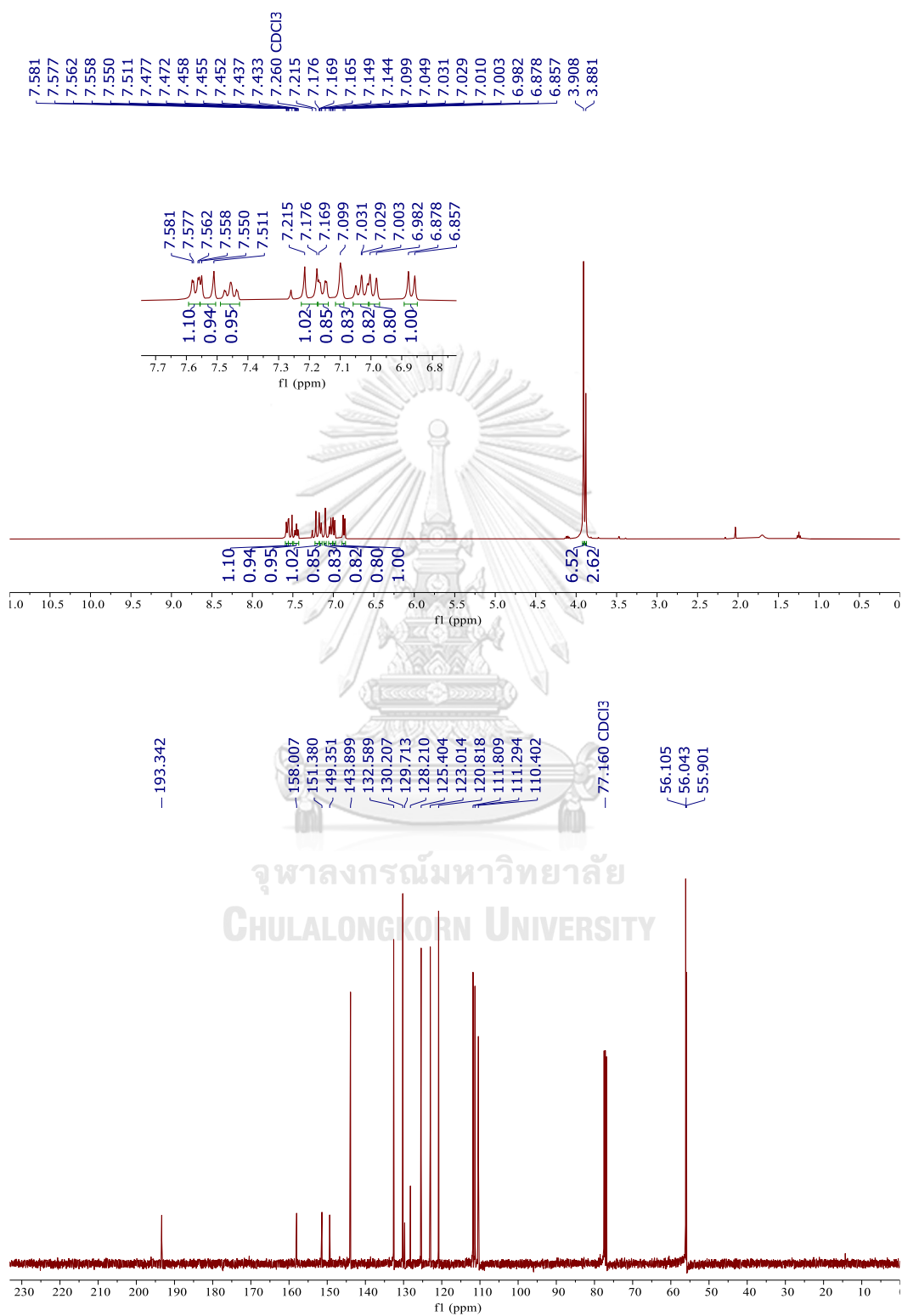
Acquisition Date 12/3/2019 4:44:38 PM

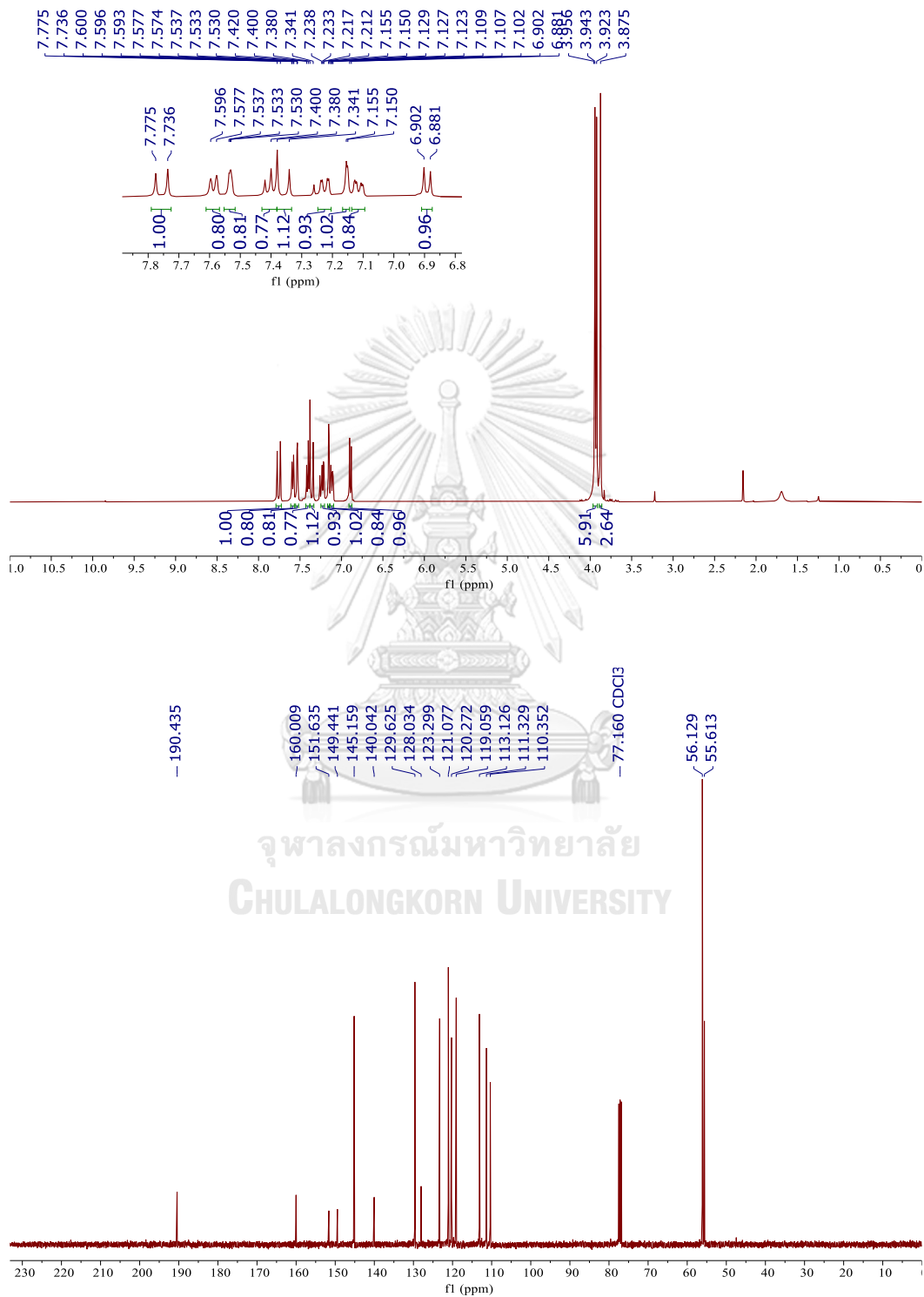
Operator CU.
Instrument micrOTOF-Q II

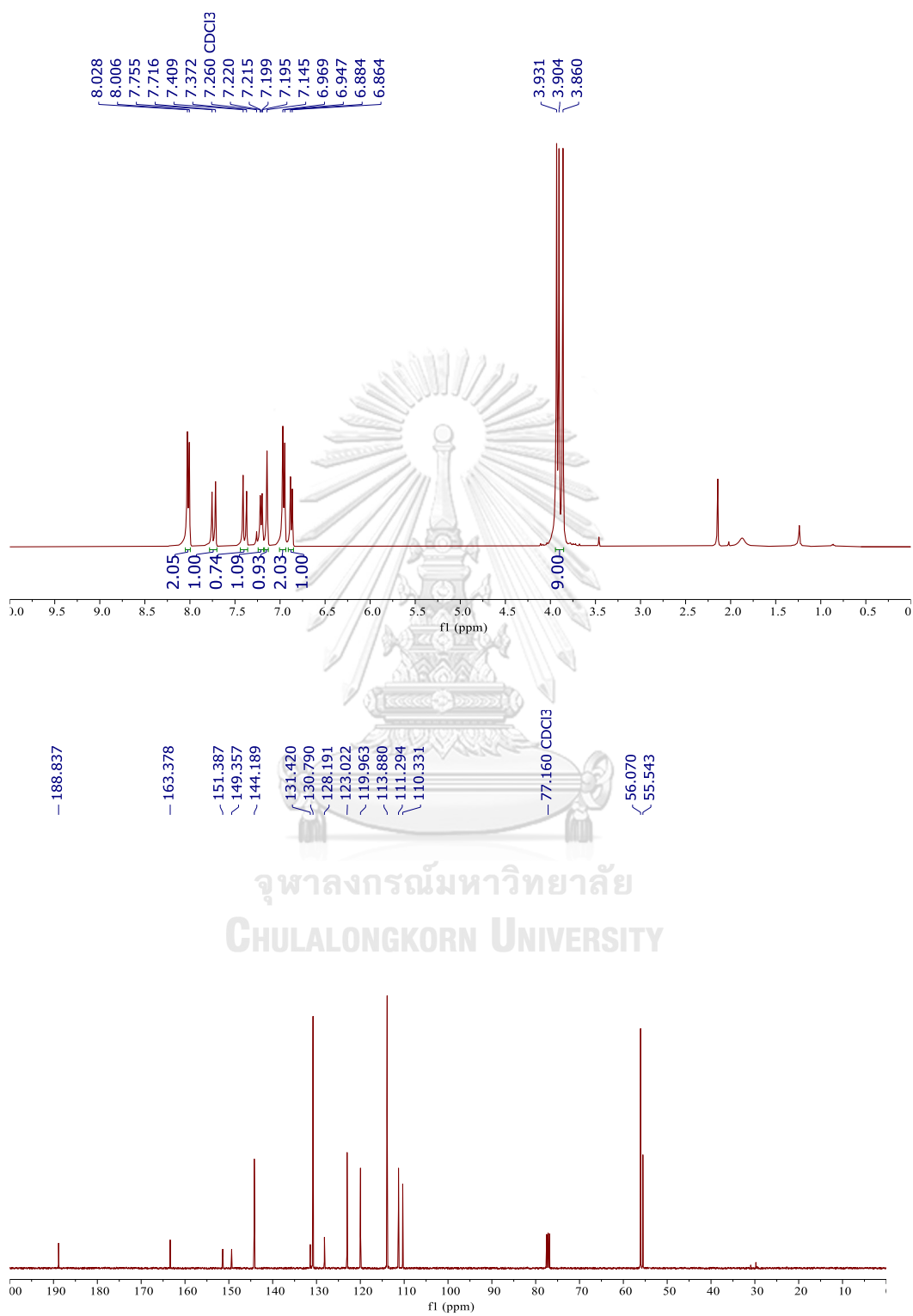


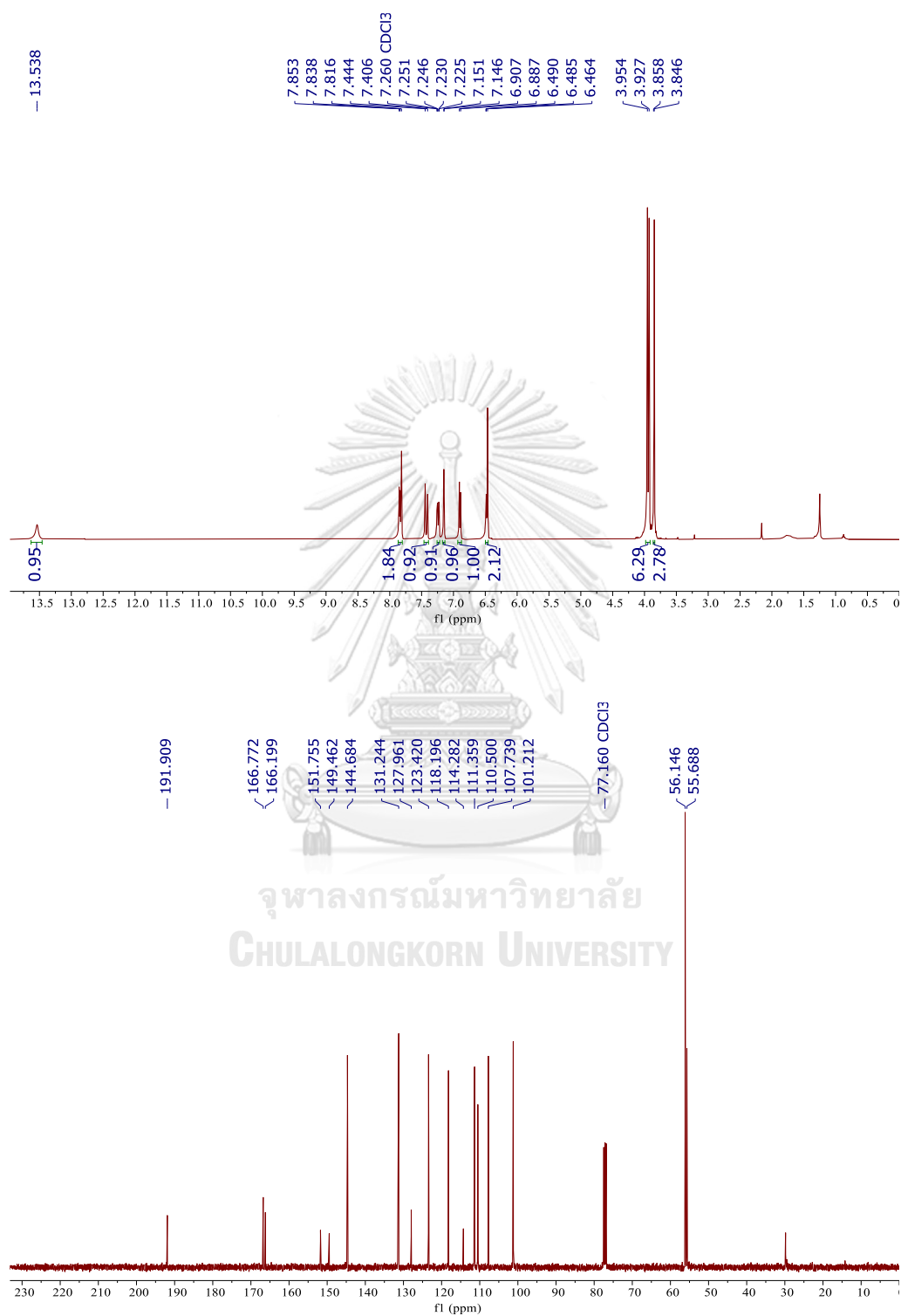
26. ^1H (400 MHz) and ^{13}C (100 MHz) NMR Spectra in CDCl_3 of 22

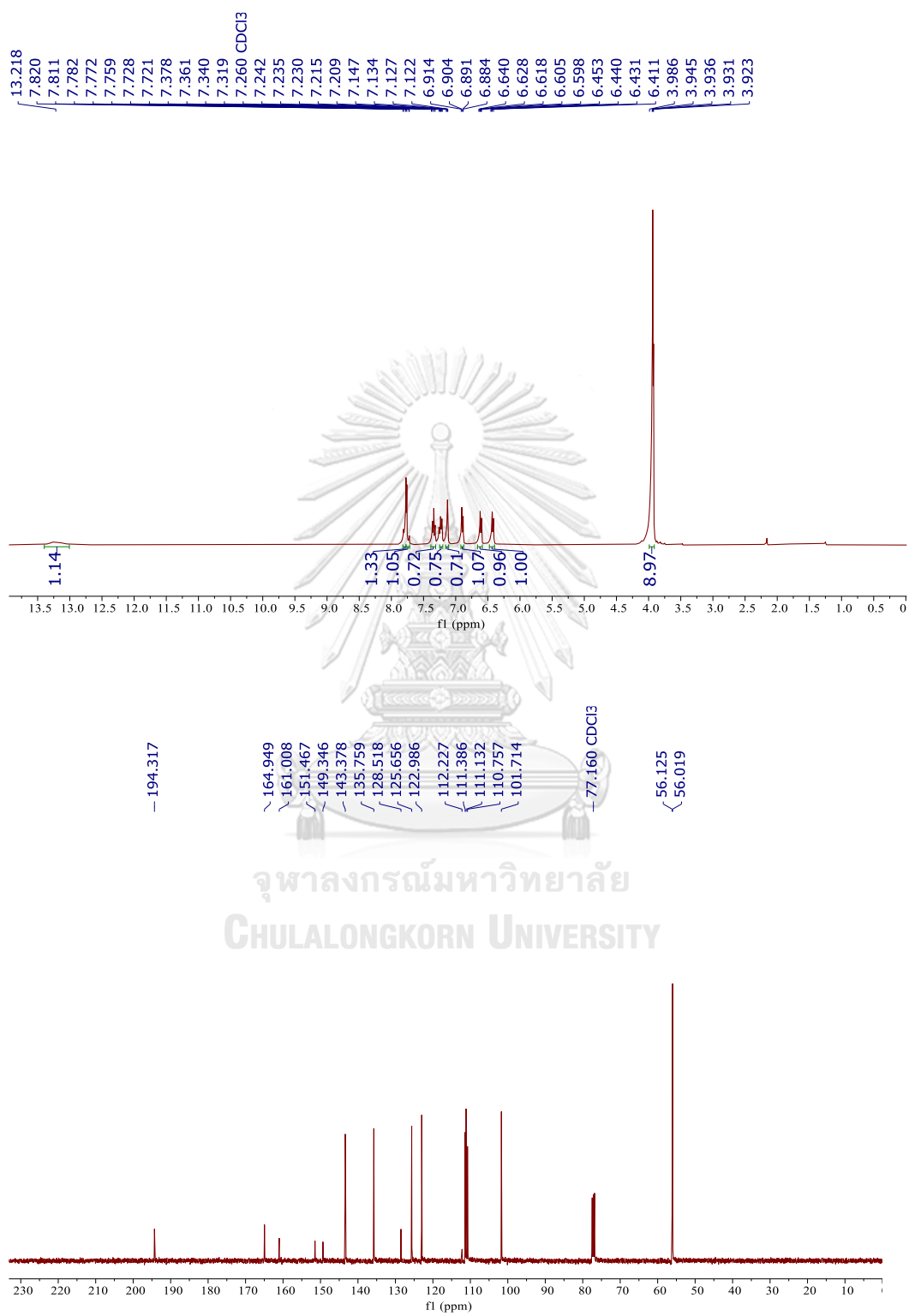
27. ^1H (400 MHz) and ^{13}C (100 MHz) NMR Spectra in $\text{DMSO-}d_6$ of **23**

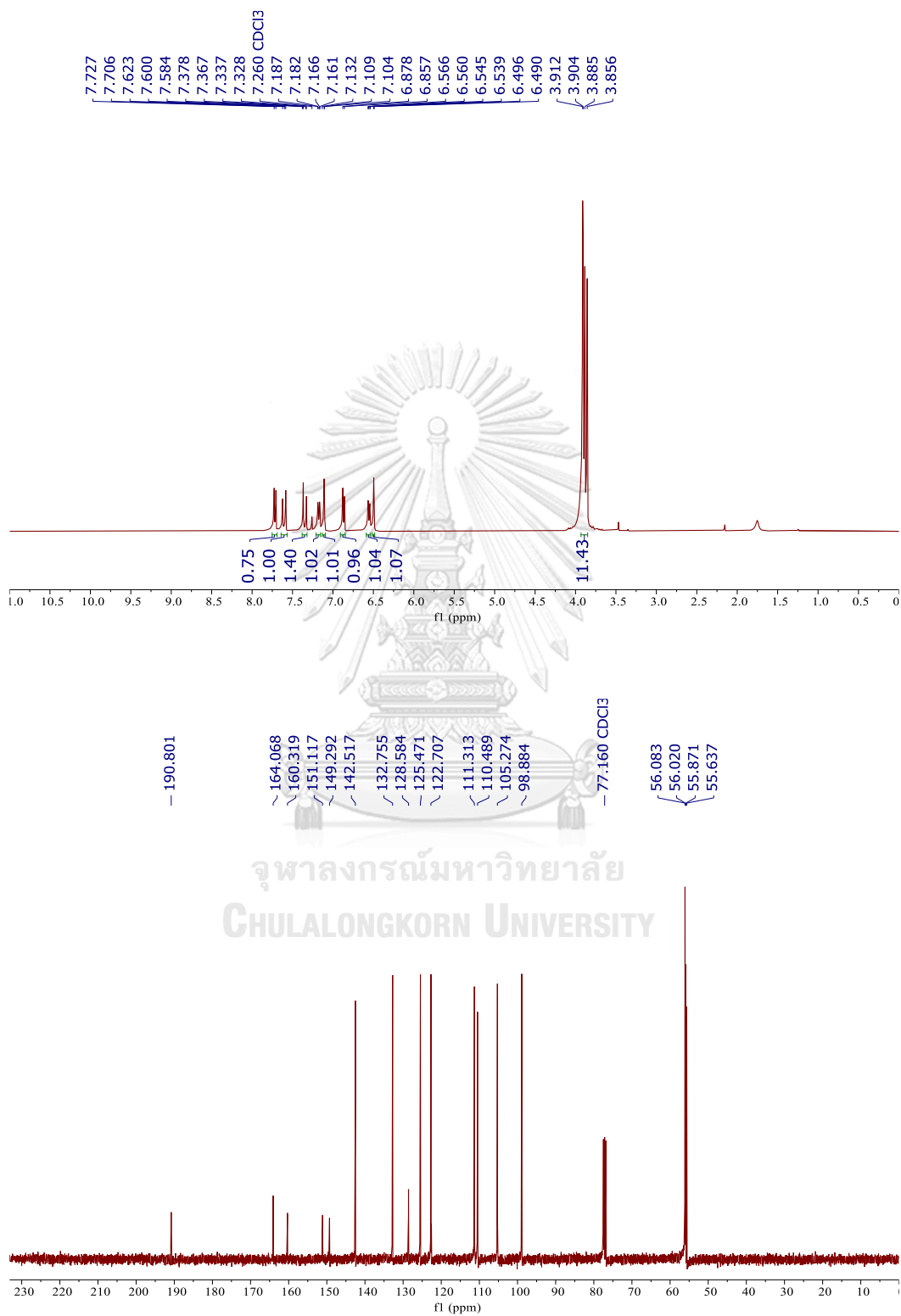
28. ^1H (400 MHz) and ^{13}C (100 MHz) NMR Spectra in CDCl_3 of 24

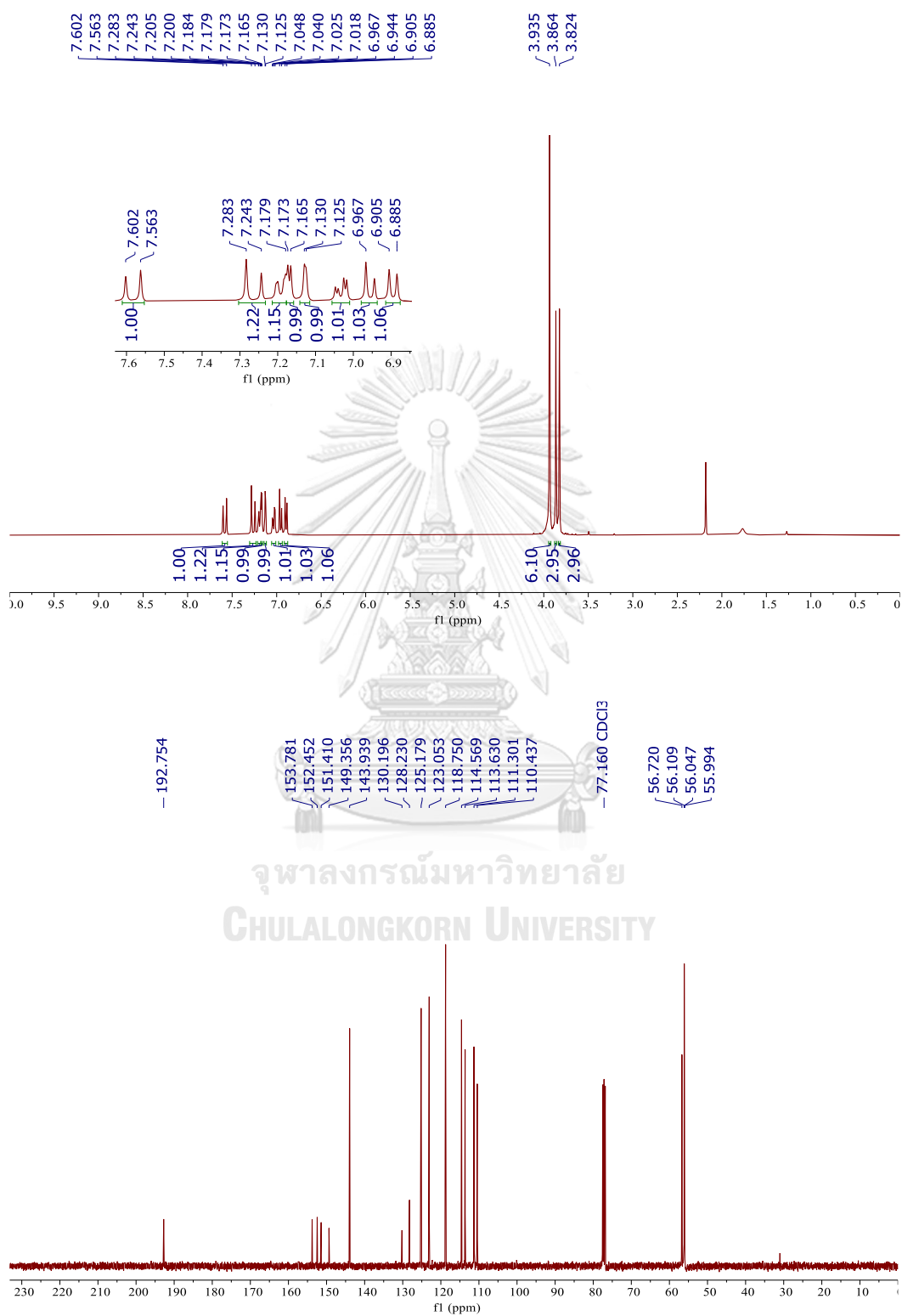
29. ^1H (400 MHz) and ^{13}C (100 MHz) NMR Spectra in CDCl_3 of 25

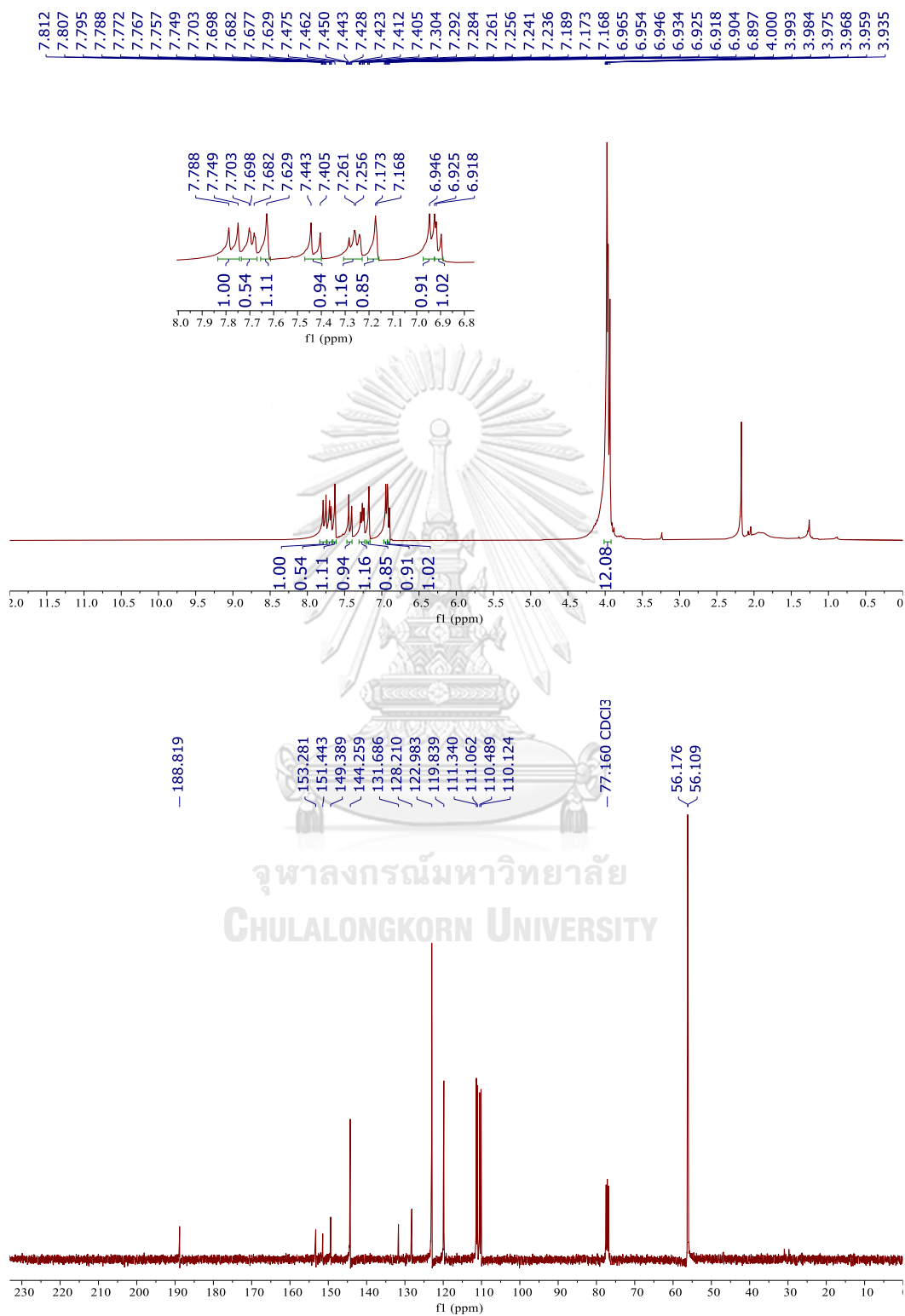
30. ^1H (400 MHz) and ^{13}C (100 MHz) NMR Spectra in CDCl_3 of 26

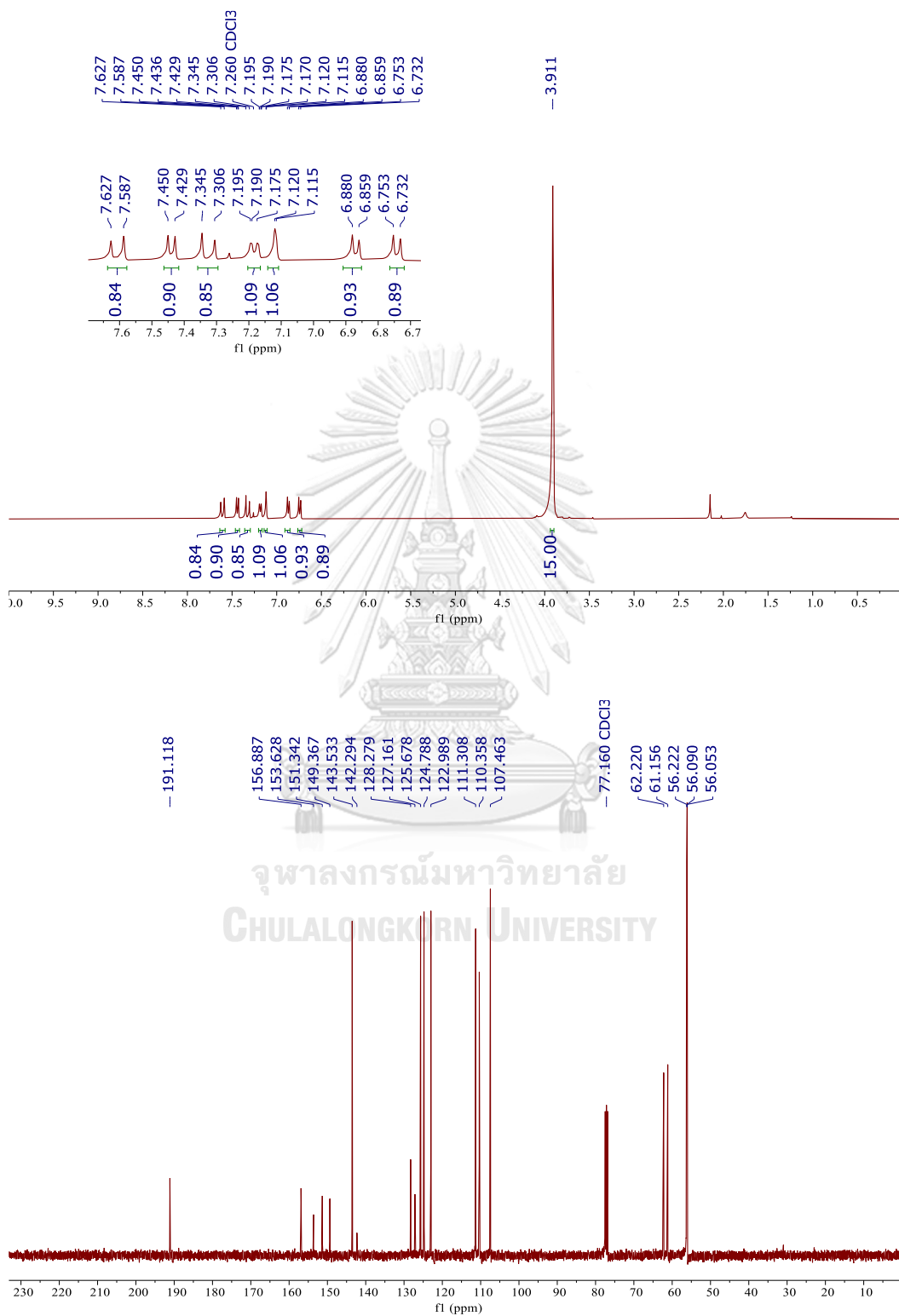
31. ^1H (400 MHz) and ^{13}C (100 MHz) NMR Spectra in CDCl_3 of 27

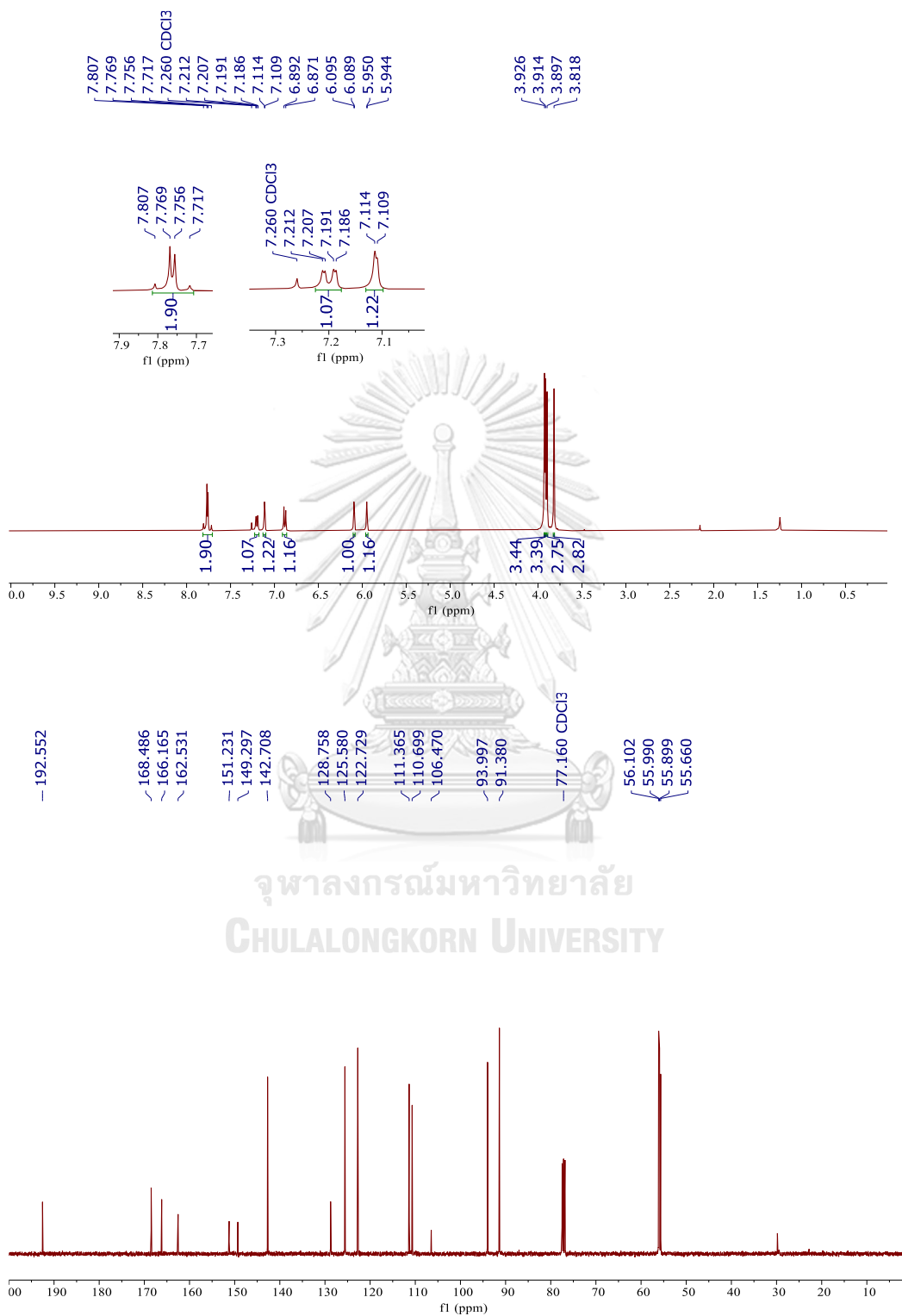
32. ^1H (400 MHz) and ^{13}C (100 MHz) NMR Spectra in CDCl_3 of 28

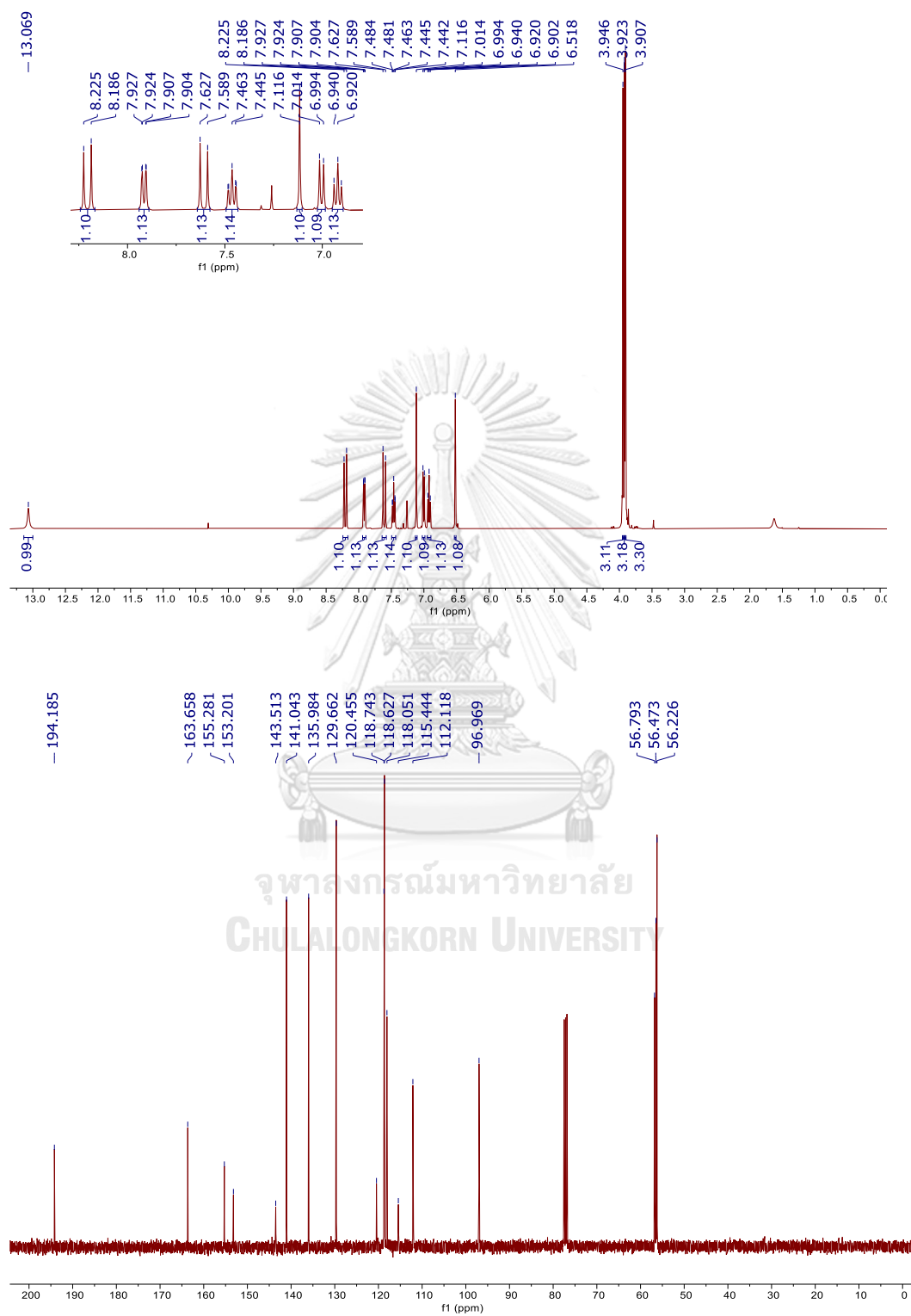
33. ^1H (400 MHz) and ^{13}C (100 MHz) NMR Spectra in CDCl_3 of **29**

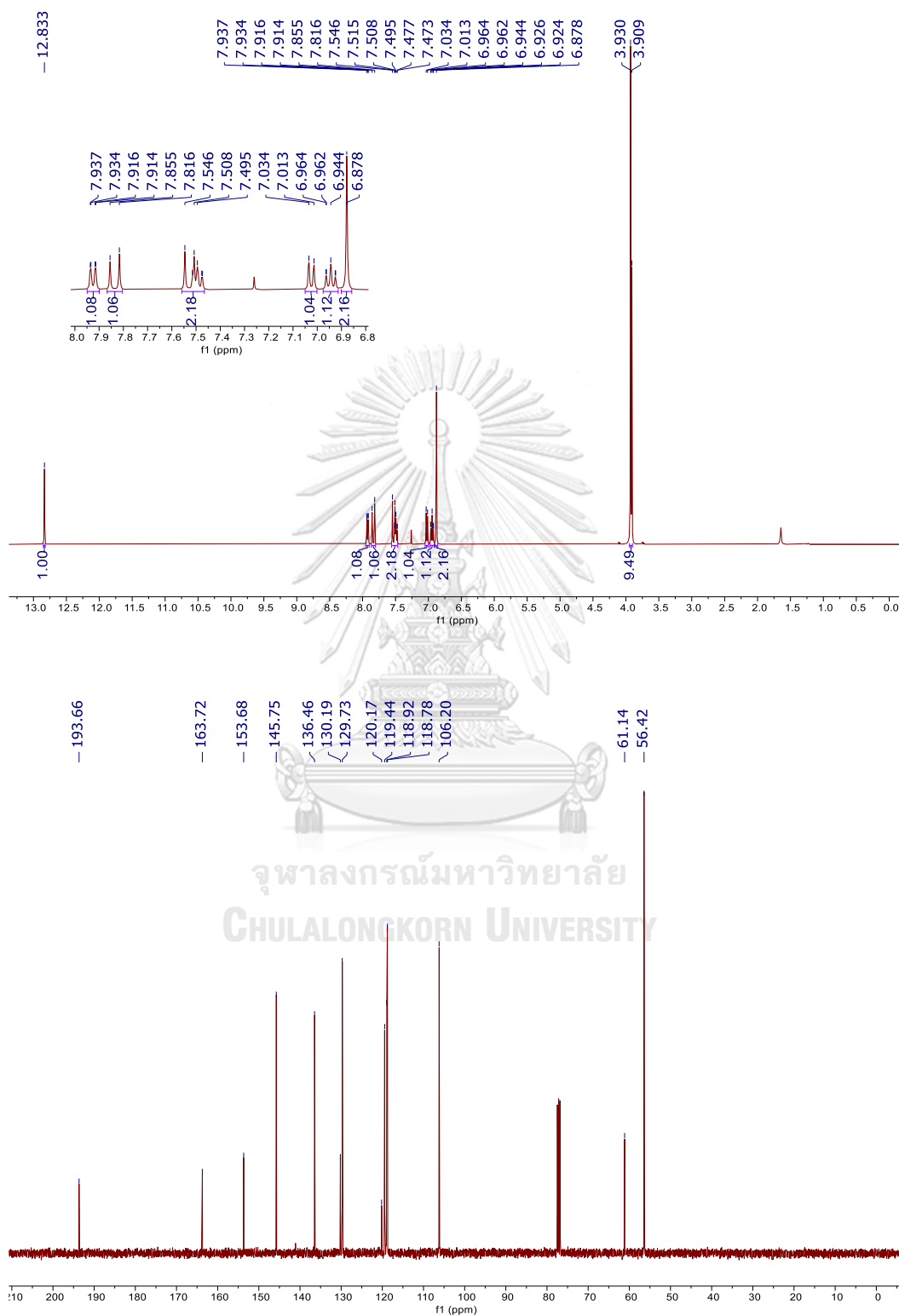
34. ^1H (400 MHz) and ^{13}C (100 MHz) NMR Spectra in CDCl_3 of 30

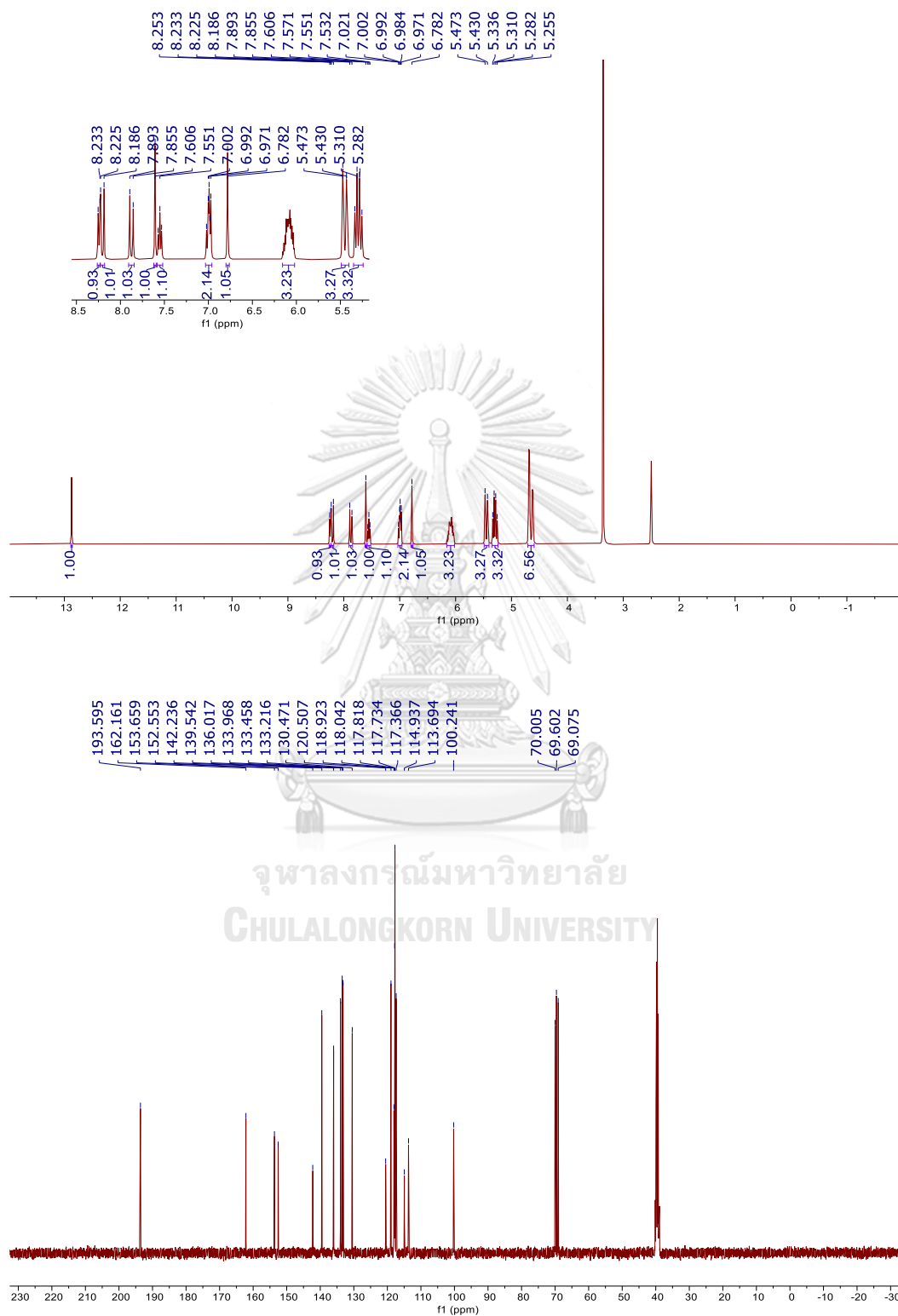
35. ^1H (400 MHz) and ^{13}C (100 MHz) NMR Spectra in CDCl_3 of **31**

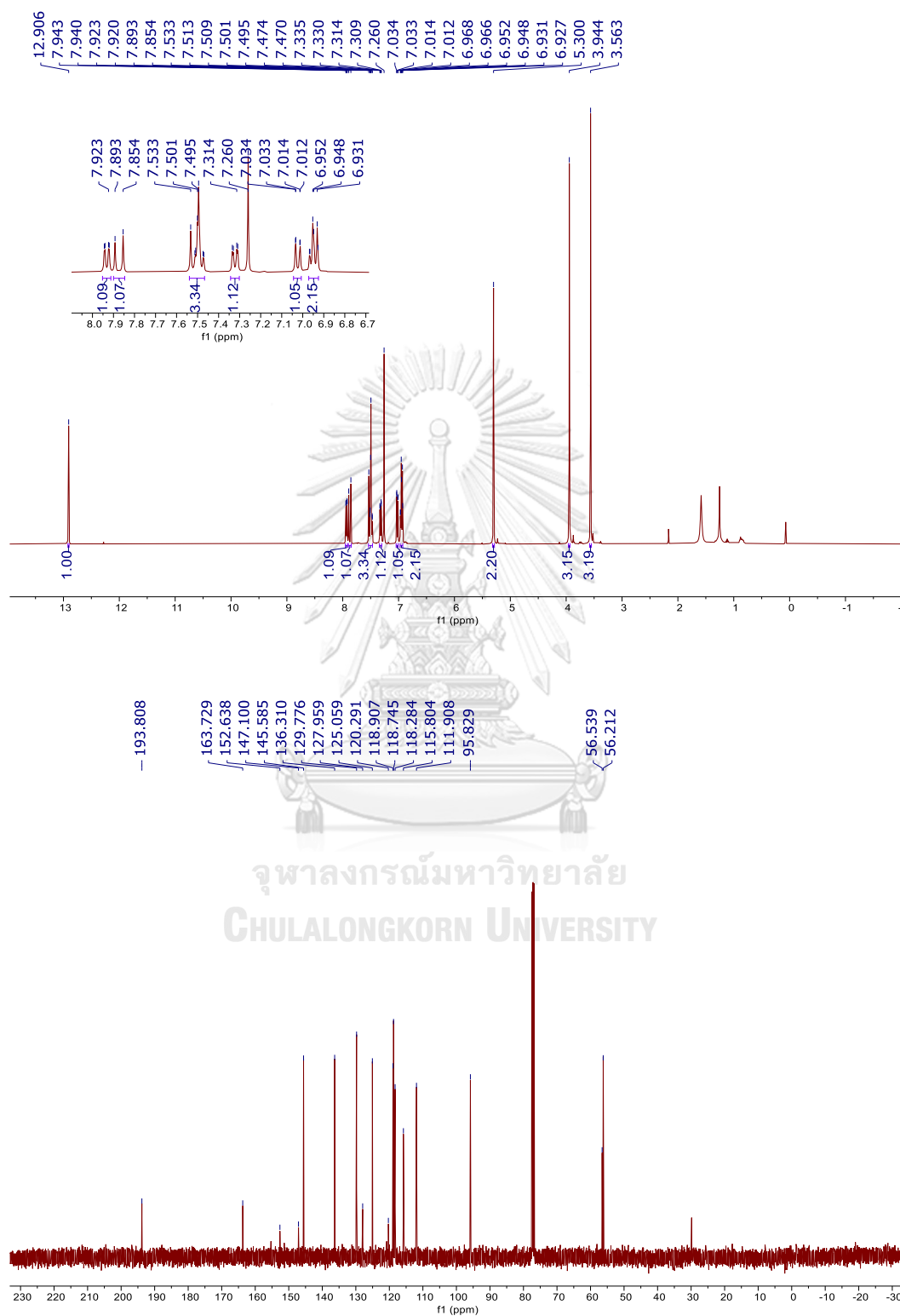
36. ^1H (400 MHz) and ^{13}C (100 MHz) NMR Spectra in CDCl_3 of 32

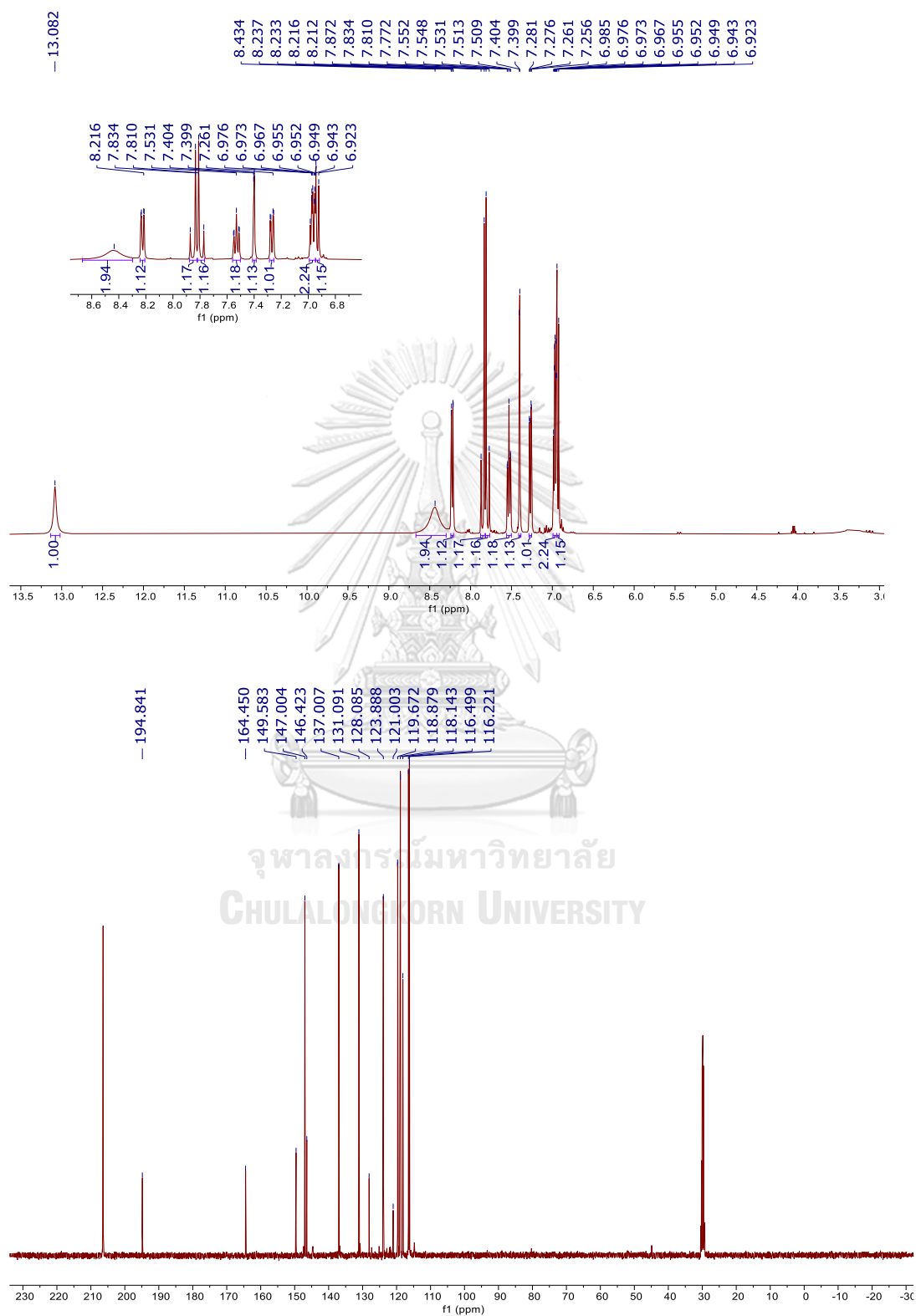
37. ^1H (400 MHz) and ^{13}C (100 MHz) NMR Spectra in CDCl_3 of 33

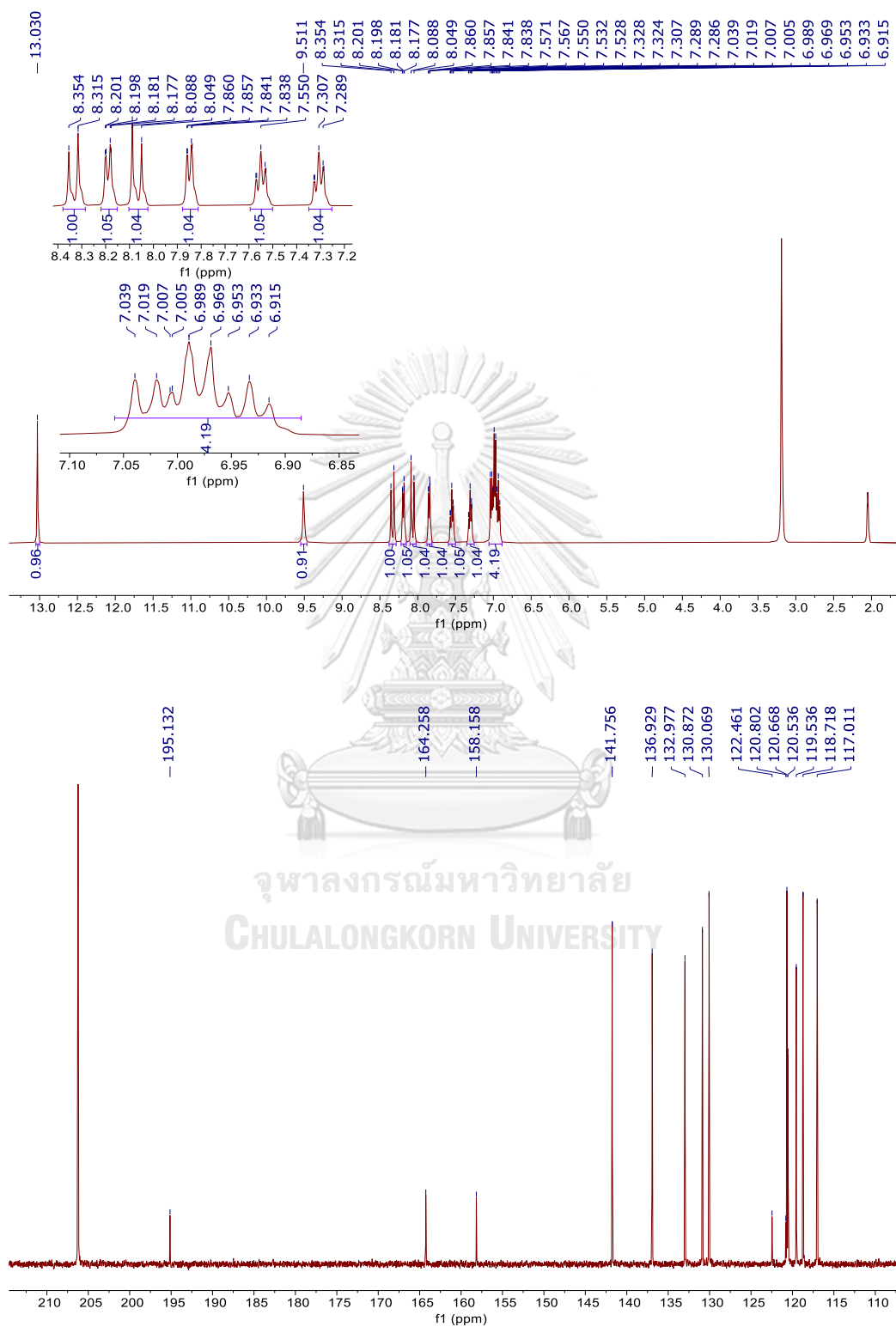
39. ^1H (400 MHz) and ^{13}C (100 MHz) NMR Spectra in CDCl_3 of 35

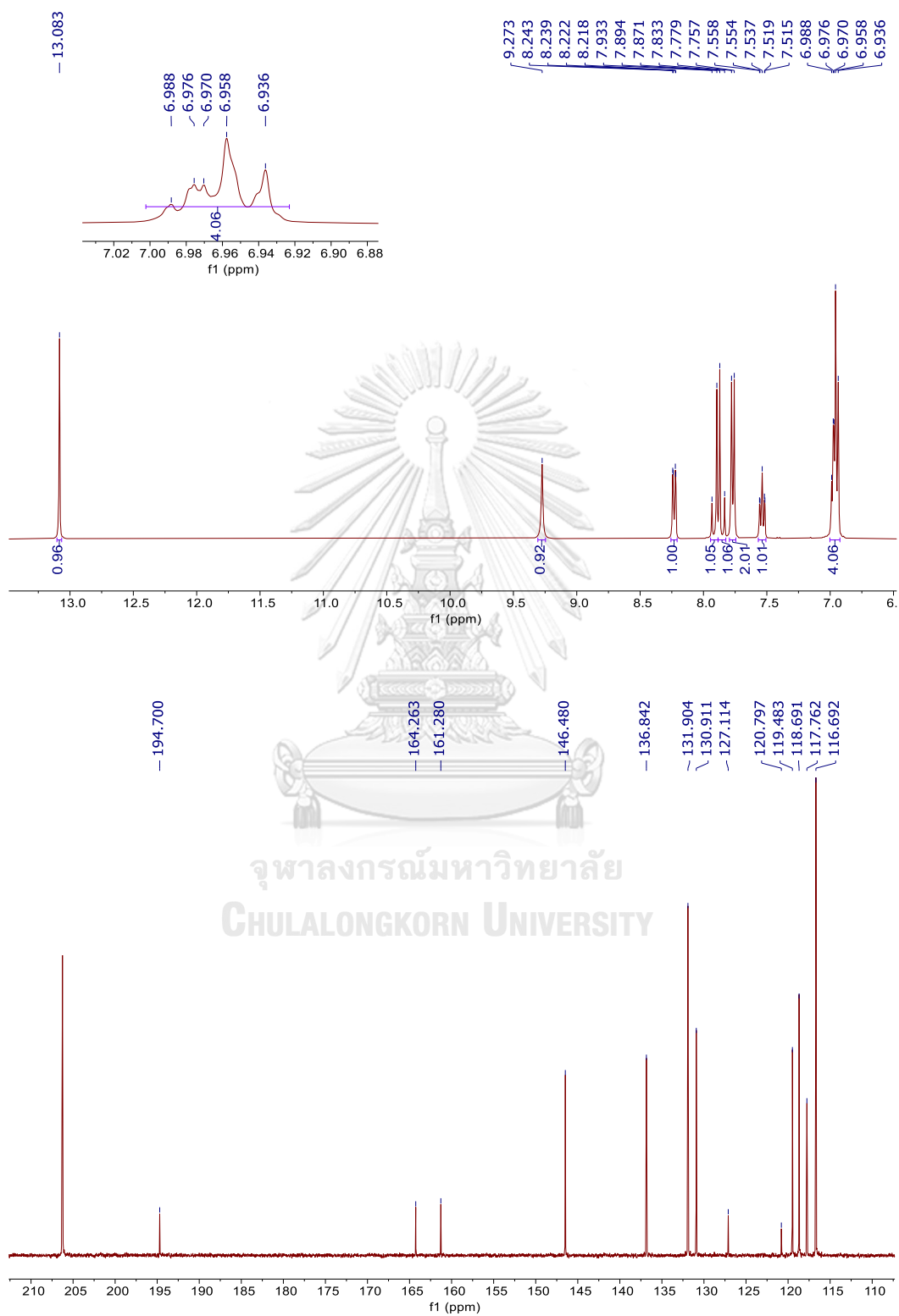
40. ^1H (400 MHz) and ^{13}C (100 MHz) NMR Spectra in CDCl_3 of **36**

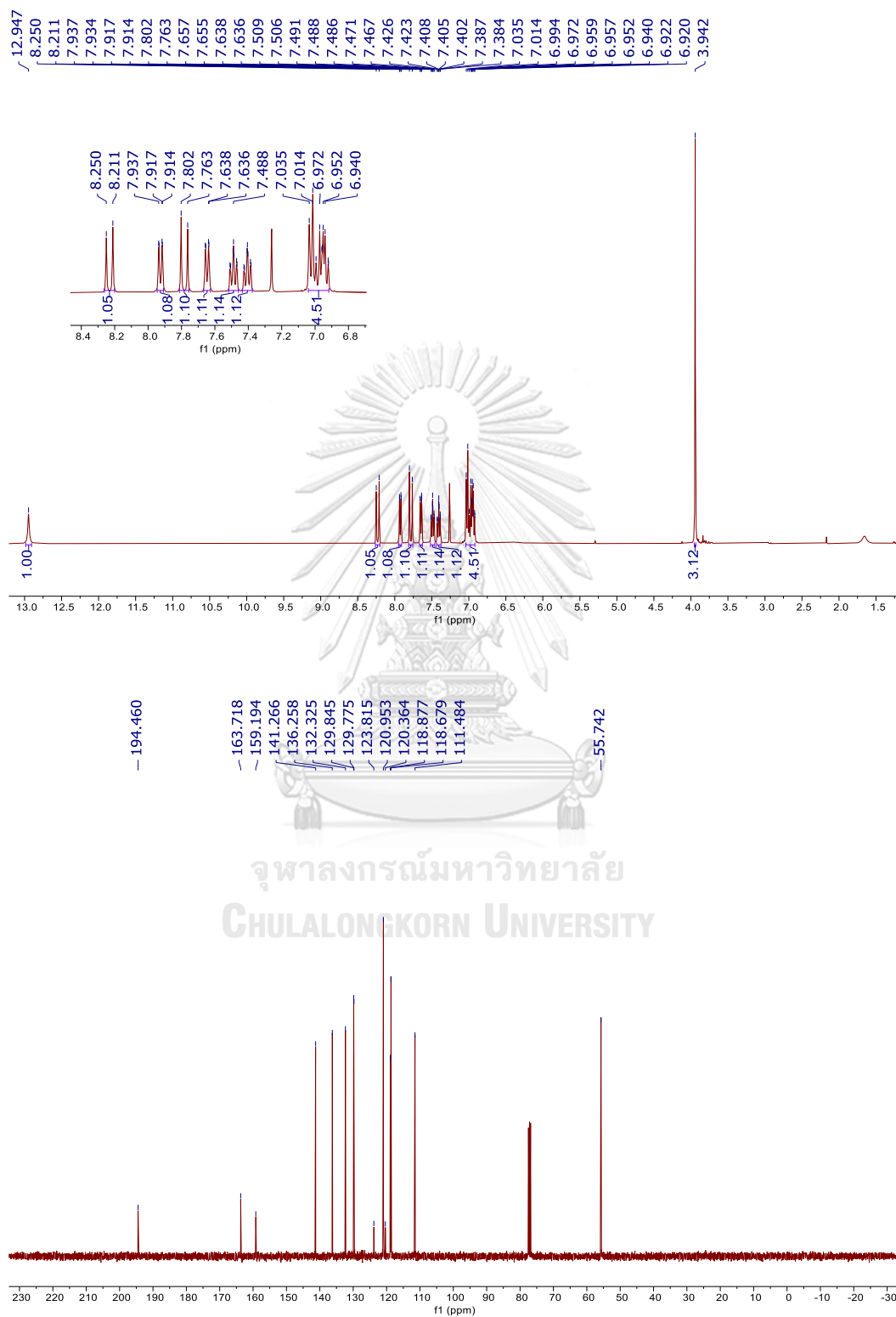
41. ^1H (400 MHz) and ^{13}C (100 MHz) NMR Spectra in CDCl_3 of 37

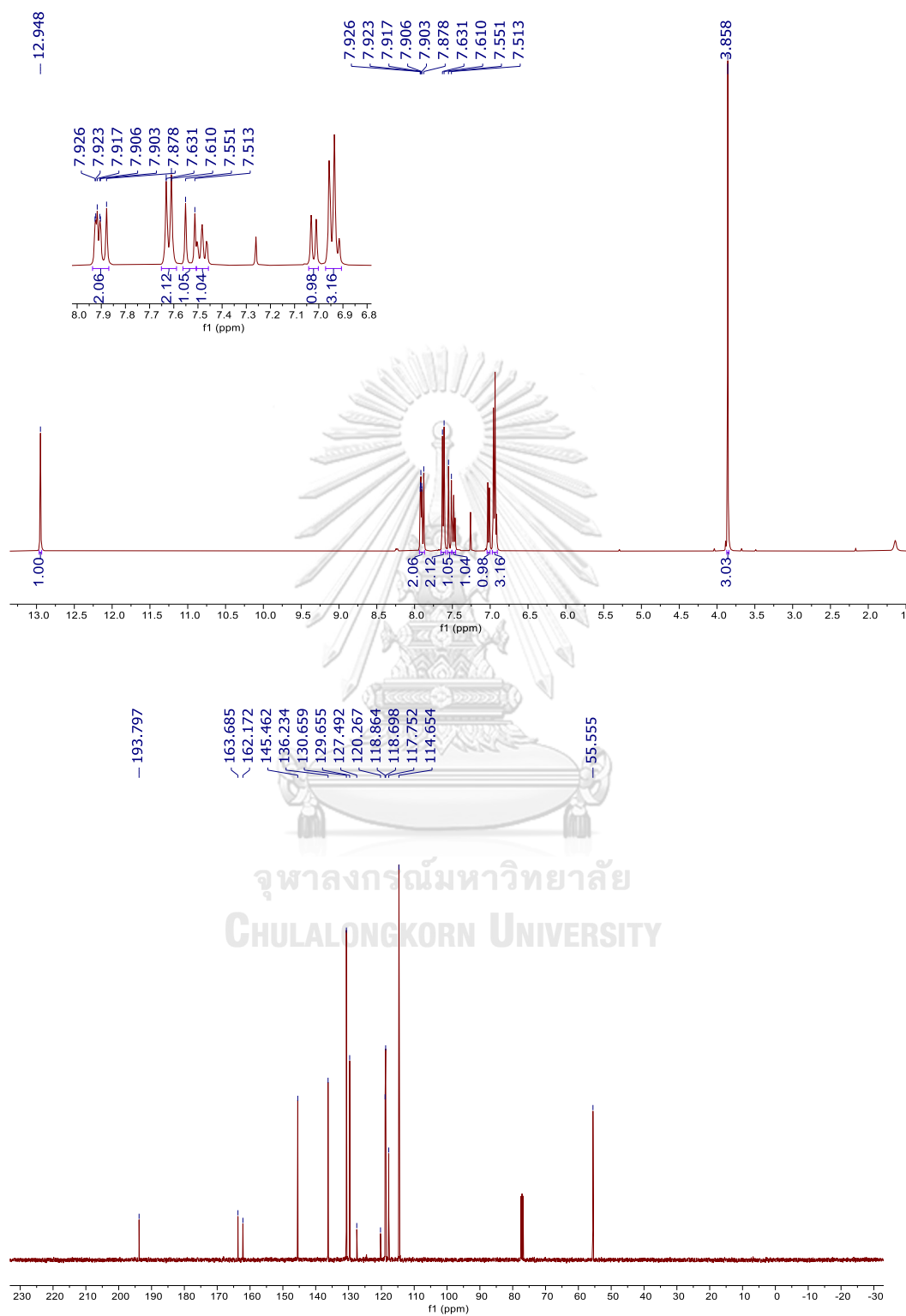
42. ^1H (400 MHz) and ^{13}C (100 MHz) NMR Spectra in CDCl_3 of 38

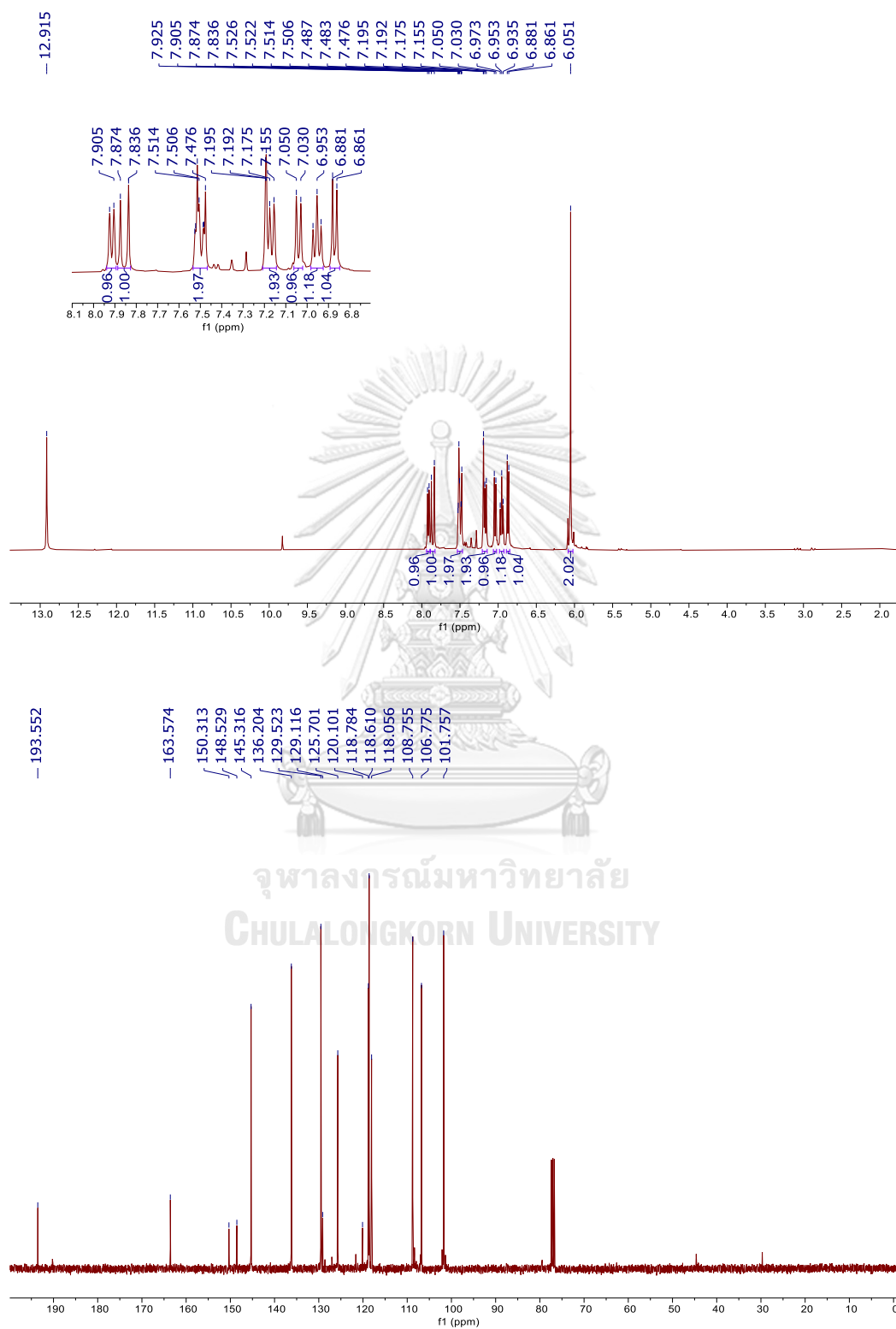
43. ^1H (400 MHz) and ^{13}C (100 MHz) NMR Spectra in acetone- d_6 of **39**

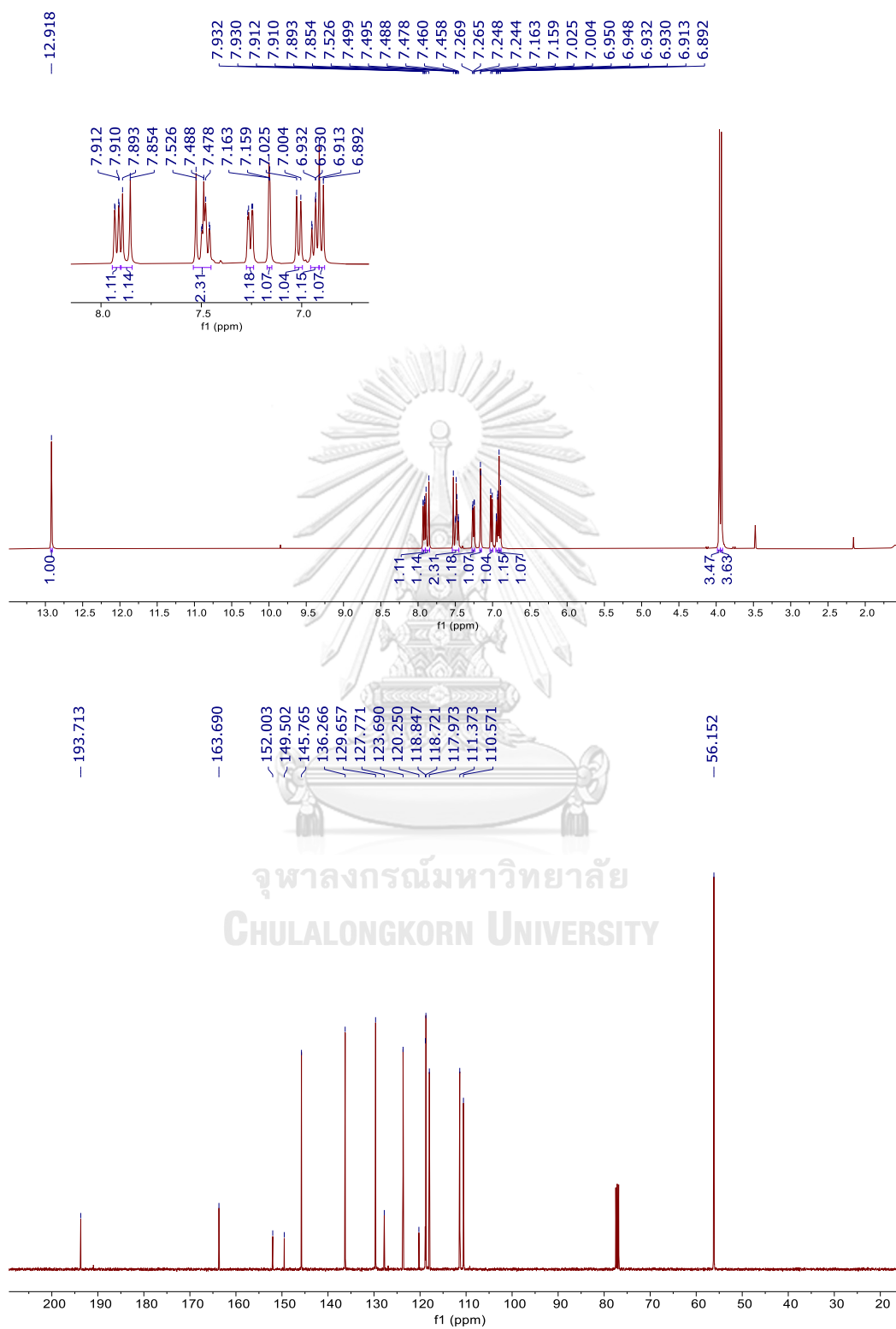
44. ^1H (400 MHz) and ^{13}C (100 MHz) NMR Spectra in acetone- d_6 of 40

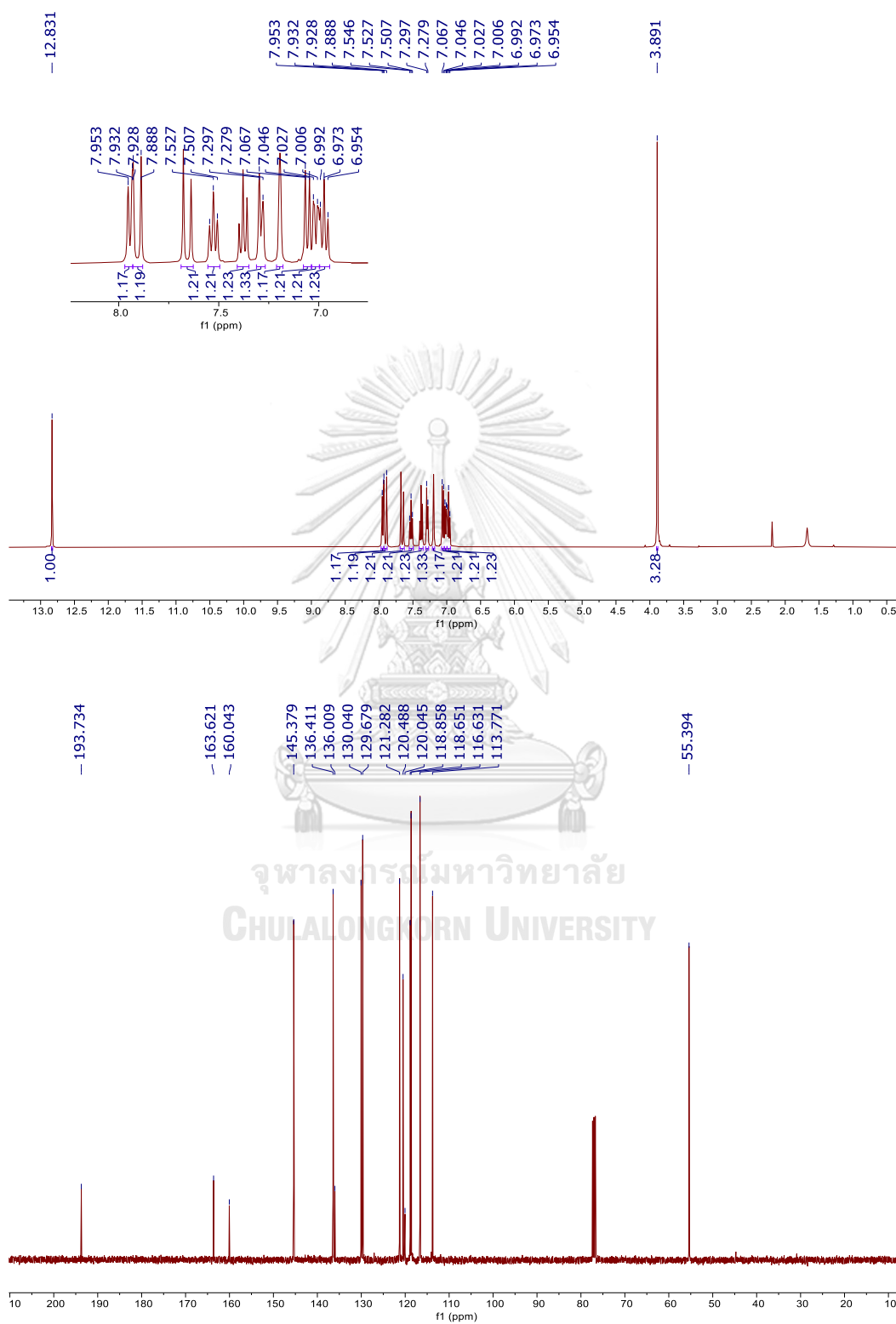
45. ^1H (400 MHz) and ^{13}C (100 MHz) NMR Spectra in acetone- d_6 of **41**

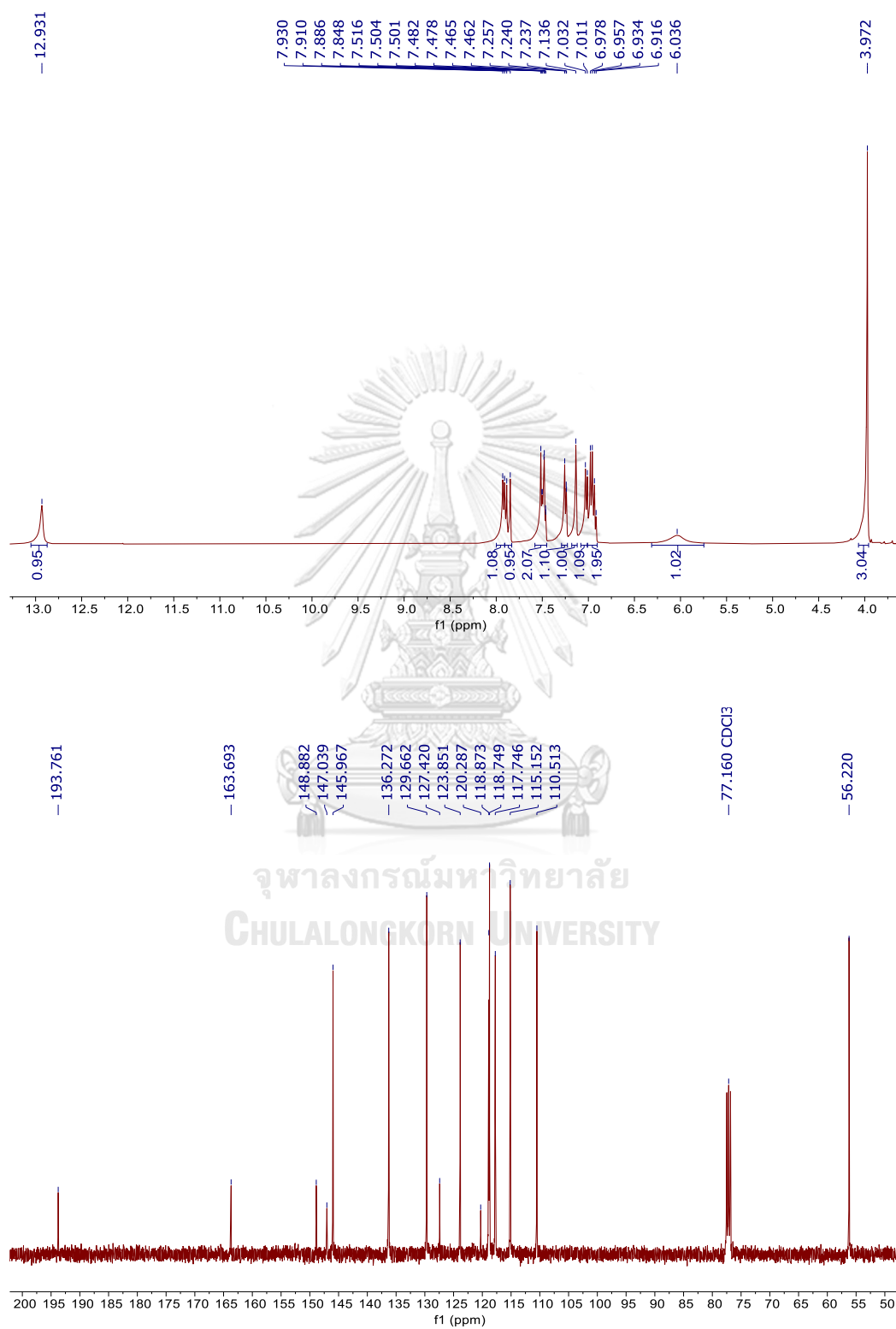
46. ^1H (400 MHz) and ^{13}C (100 MHz) NMR Spectra in CDCl_3 of **42**

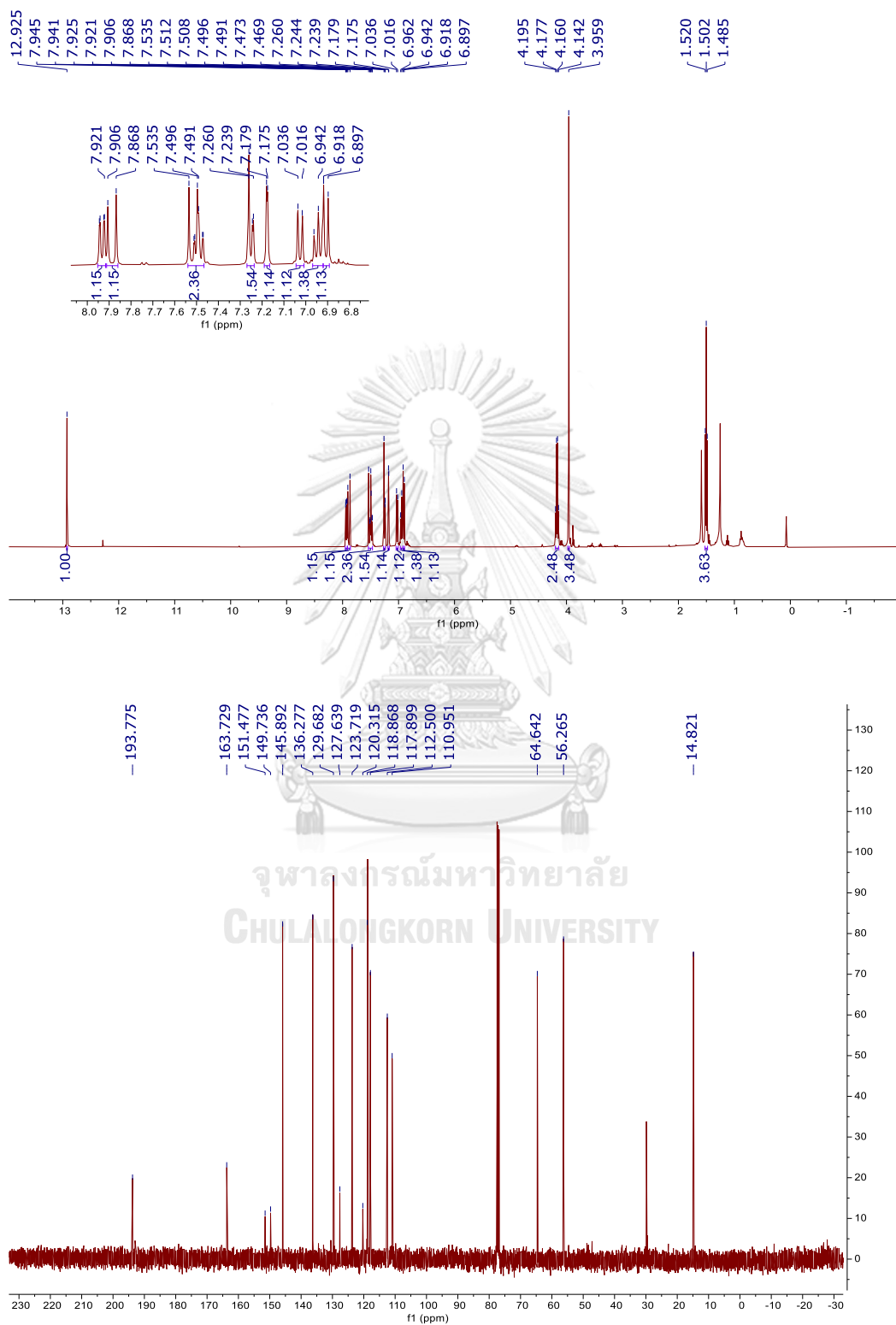
47. ^1H (400 MHz) and ^{13}C (100 MHz) NMR Spectra in CDCl_3 of **43**

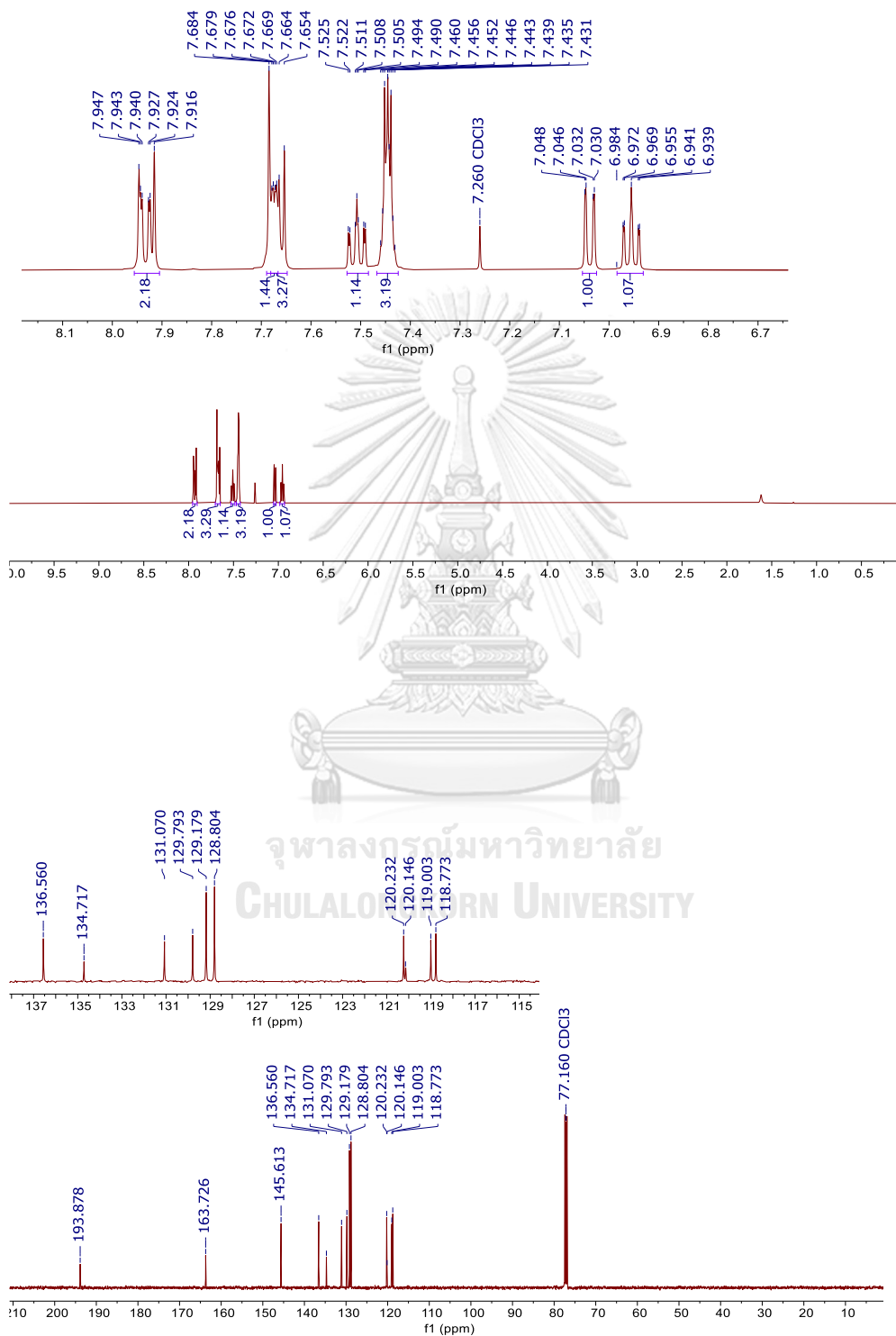
48. ^1H (400 MHz) and ^{13}C (100 MHz) NMR Spectra in CDCl_3 of **44**

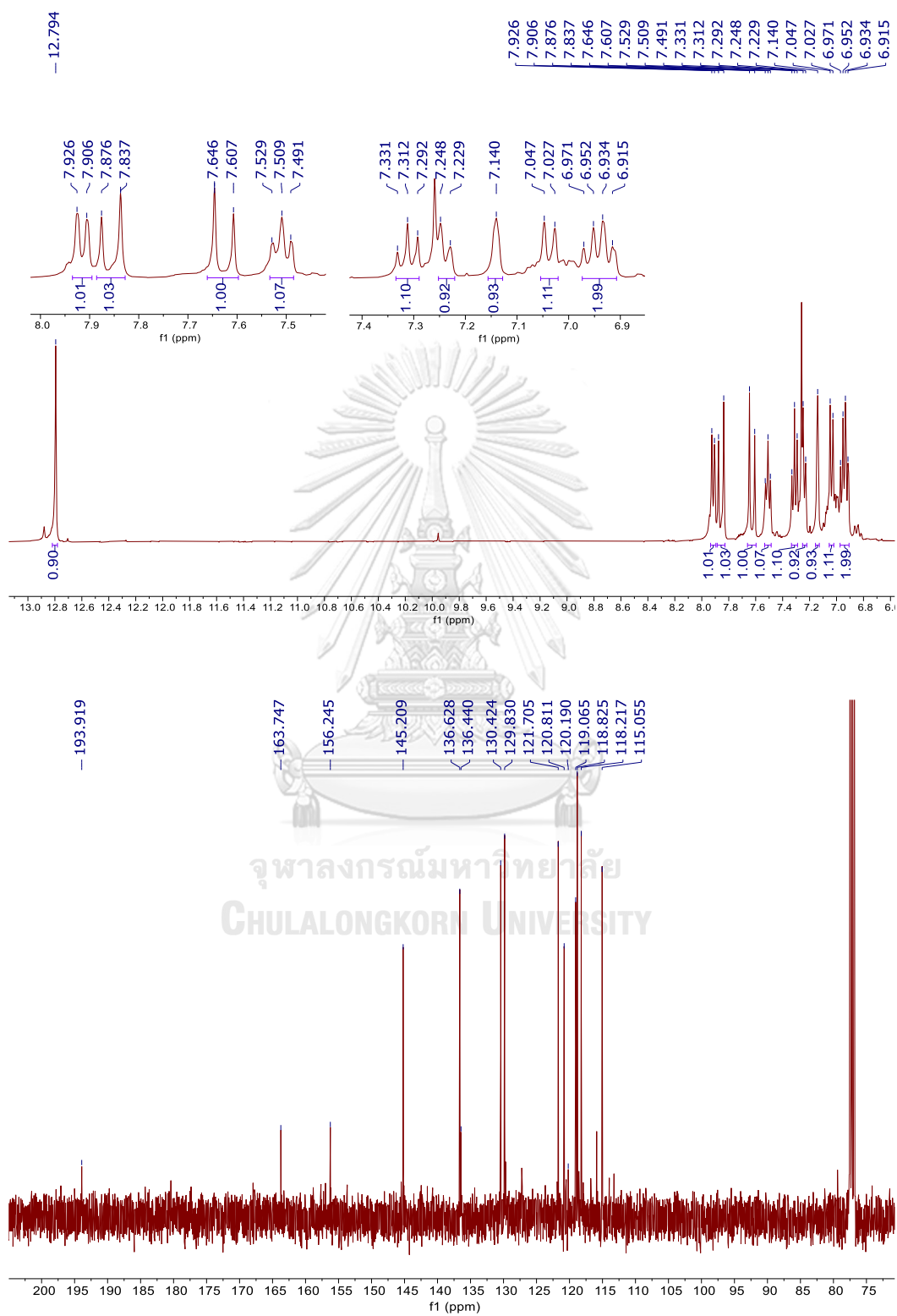
49. ^1H (400 MHz) and ^{13}C (100 MHz) NMR Spectra in CDCl_3 of 45

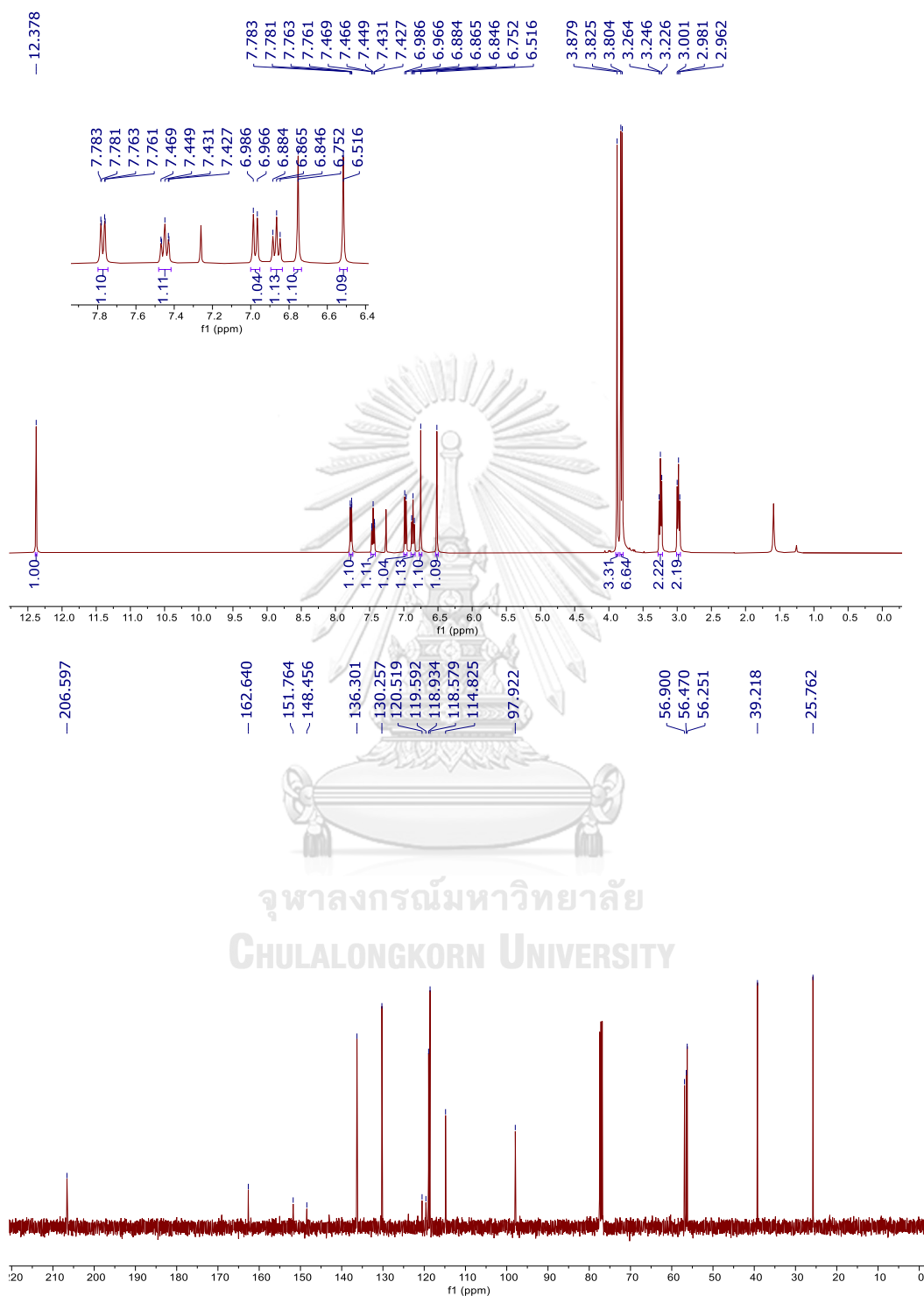
50. ^1H (400 MHz) and ^{13}C (100 MHz) NMR Spectra in CDCl_3 of **46**

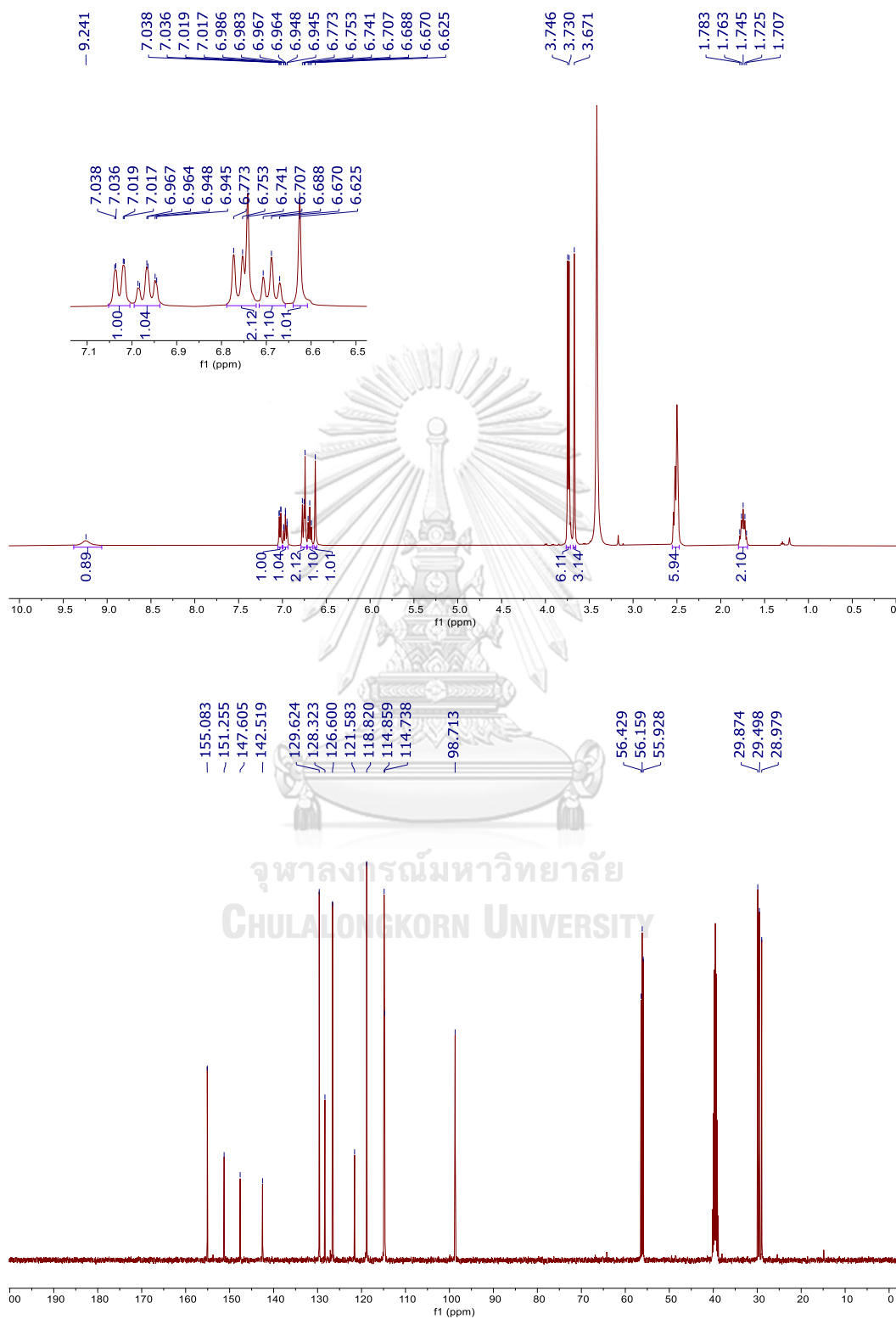
51. ^1H (400 MHz) and ^{13}C (100 MHz) NMR Spectra in CDCl_3 of 47

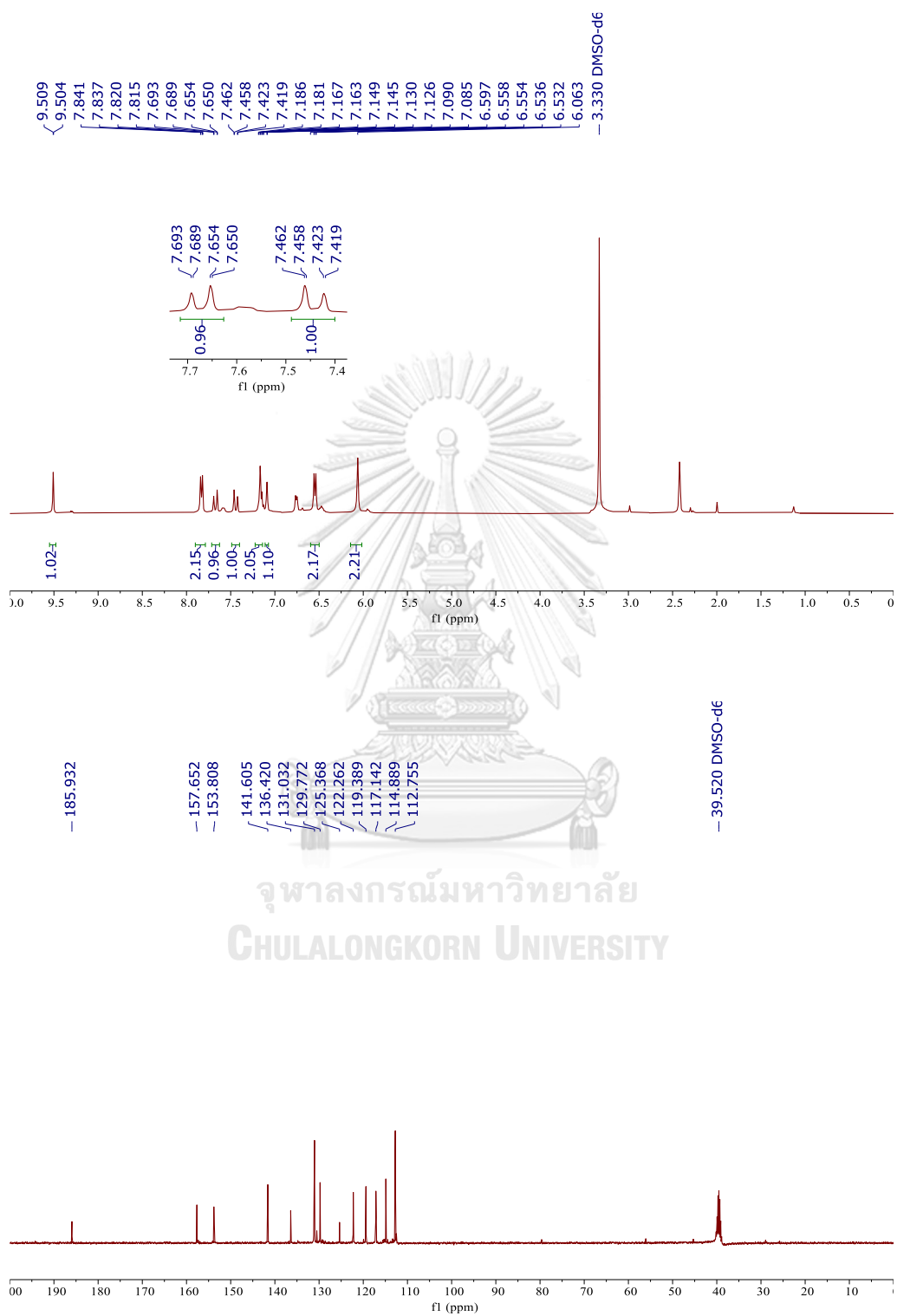
52. ^1H (400 MHz) and ^{13}C (100 MHz) NMR Spectra in CDCl_3 of 48

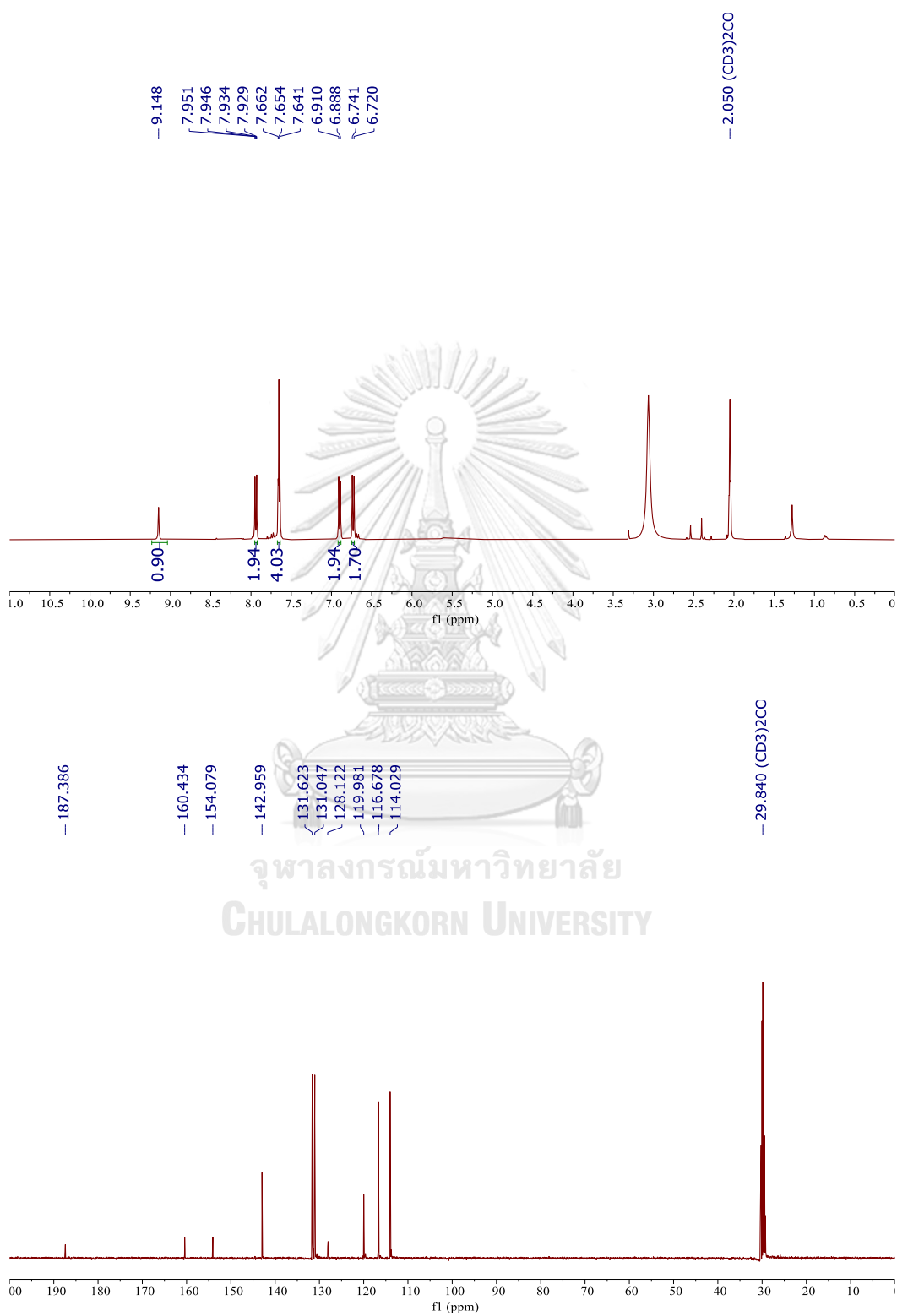
53. ^1H (500 MHz) and ^{13}C (125 MHz) NMR Spectra in CDCl_3 of **49**

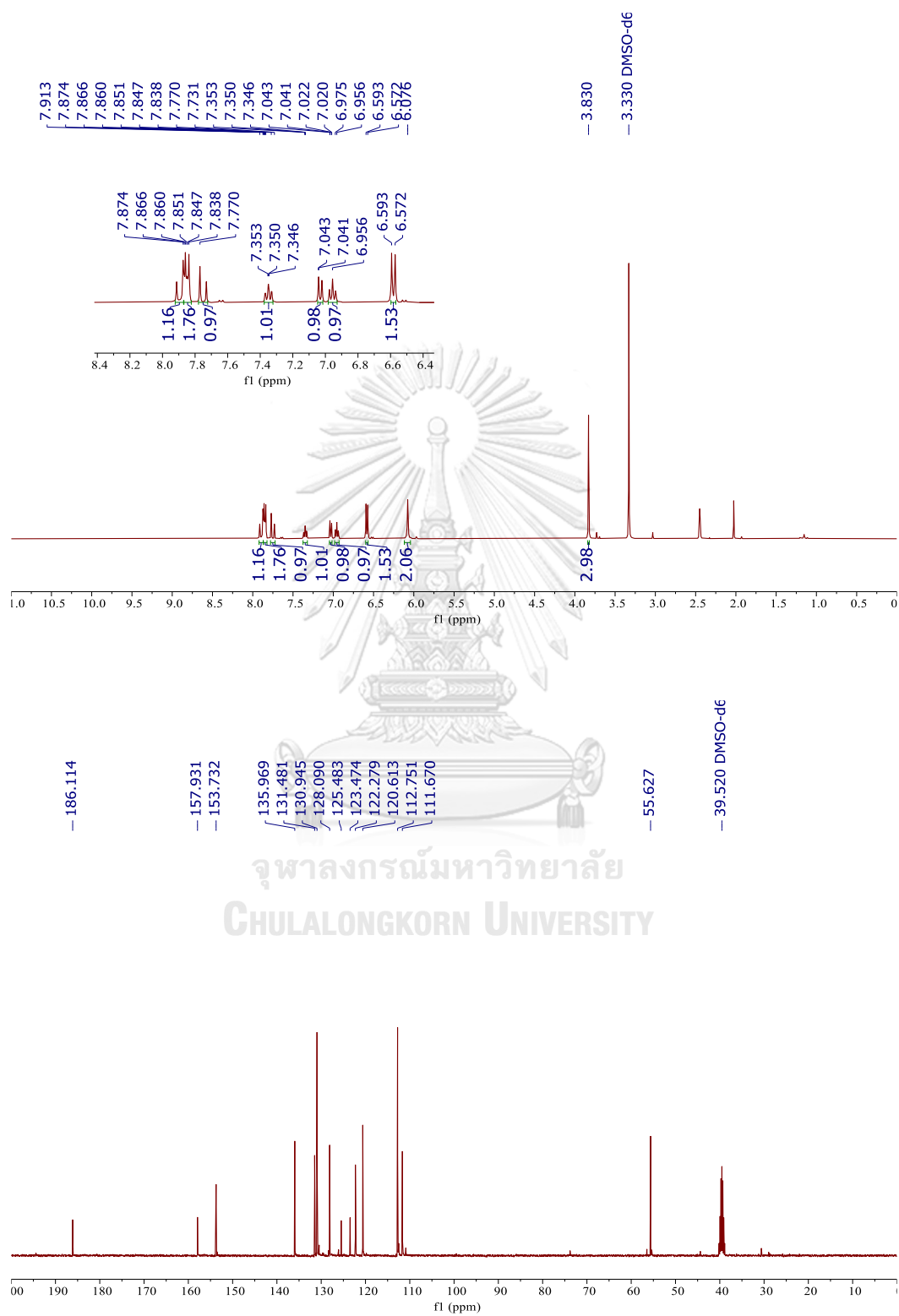
54. ^1H (400 MHz) and ^{13}C (100 MHz) NMR Spectra in CDCl_3 of 50

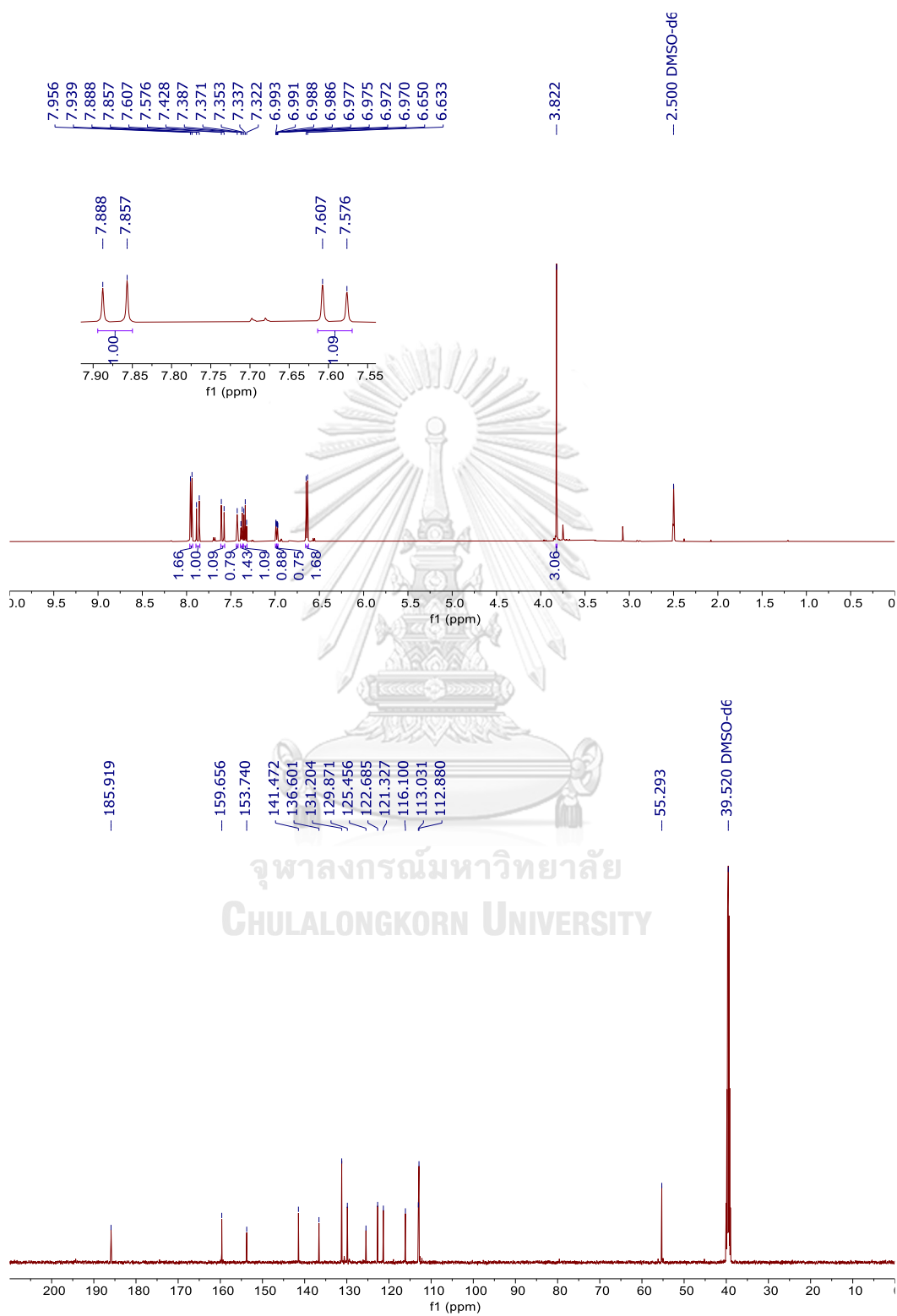
55. ^1H (400 MHz) and ^{13}C (100 MHz) NMR Spectra in CDCl_3 of 51

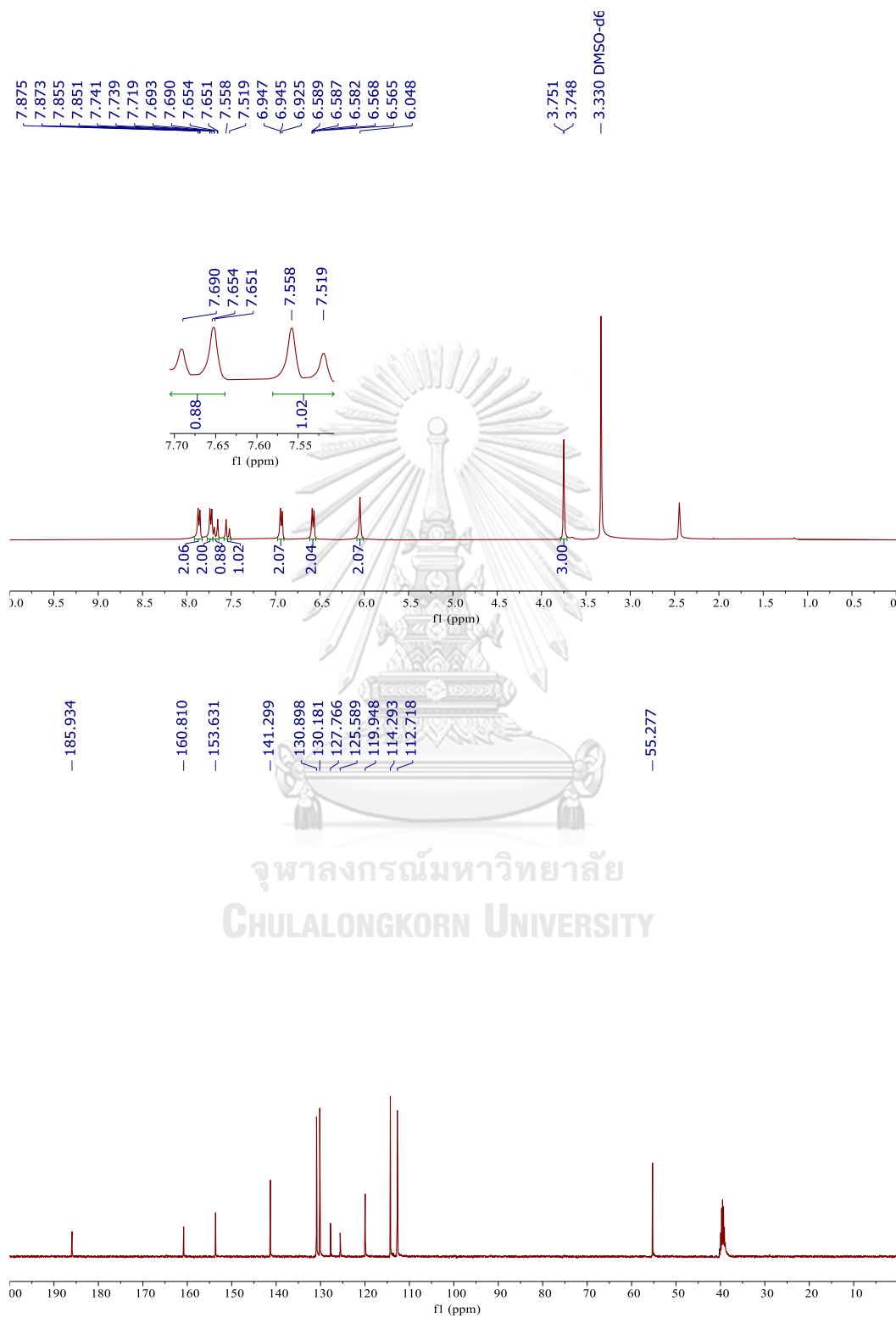
56. ^1H (400 MHz) and ^{13}C (100 MHz) NMR Spectra in $\text{DMSO-}d_6$ of 52

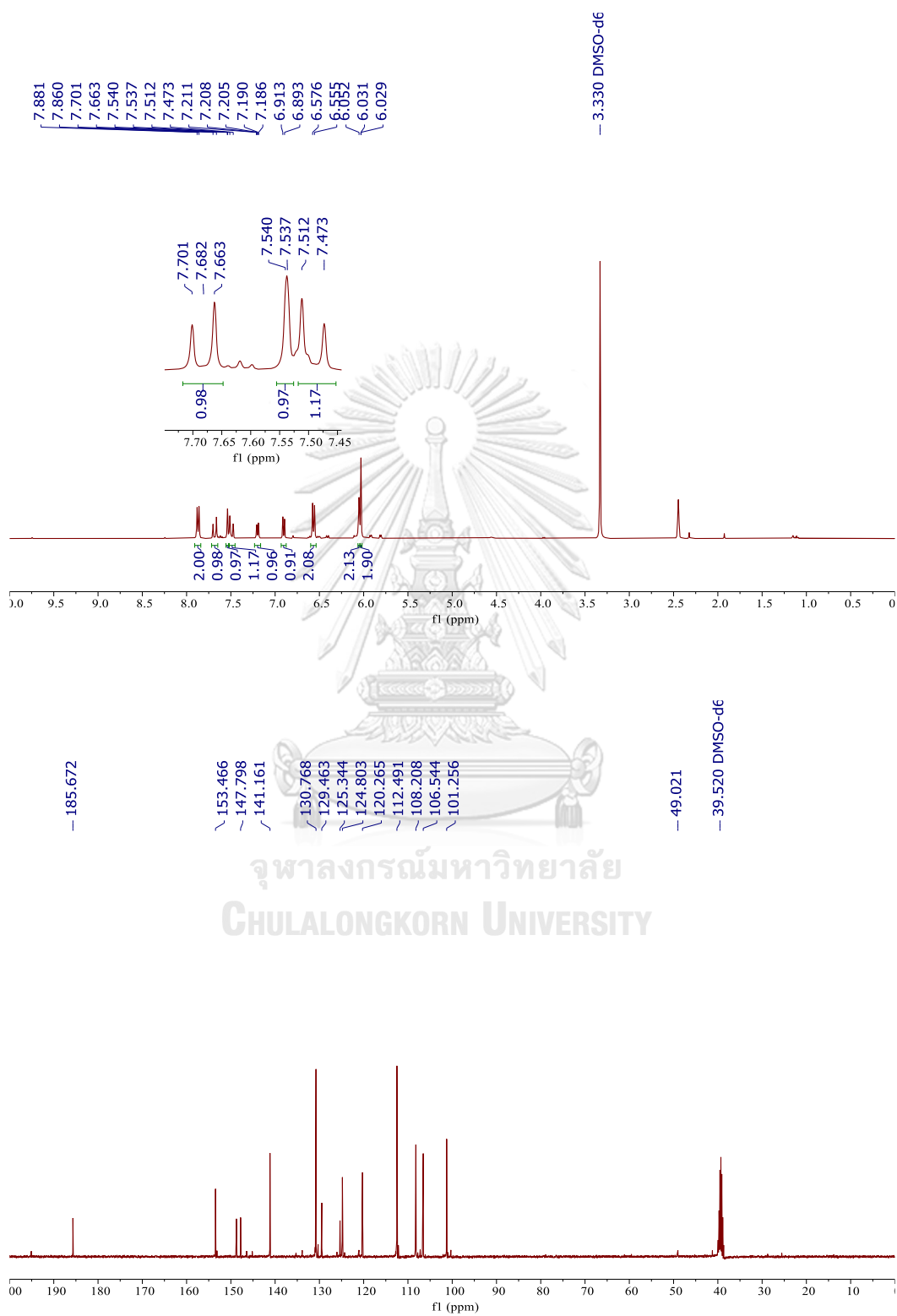
57. ^1H (400 MHz) and ^{13}C (100 MHz) NMR Spectra in $\text{DMSO-}d_6$ of **53**

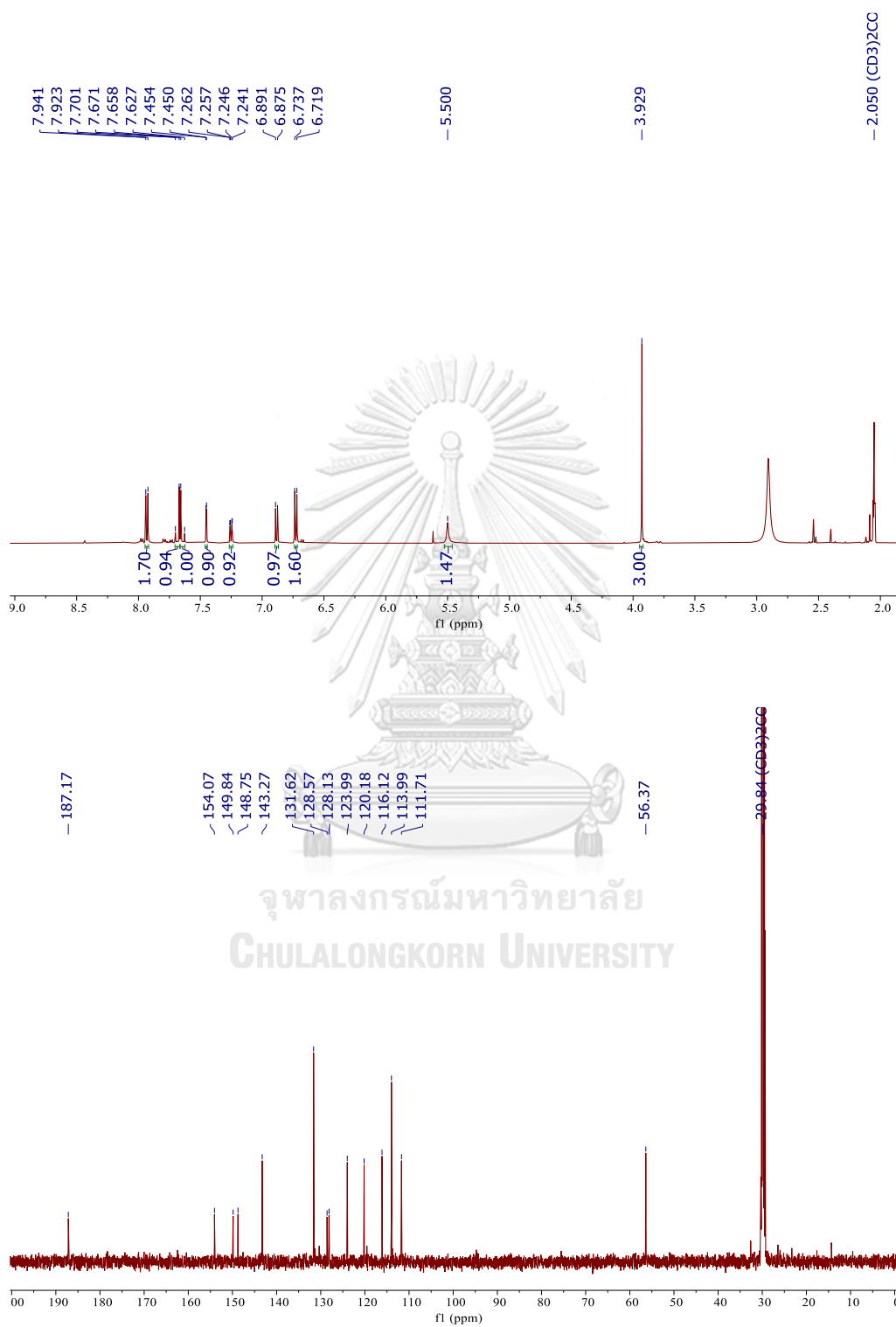
58. ^1H (400 MHz) and ^{13}C (100 MHz) NMR Spectra in acetone- d_6 of **54**

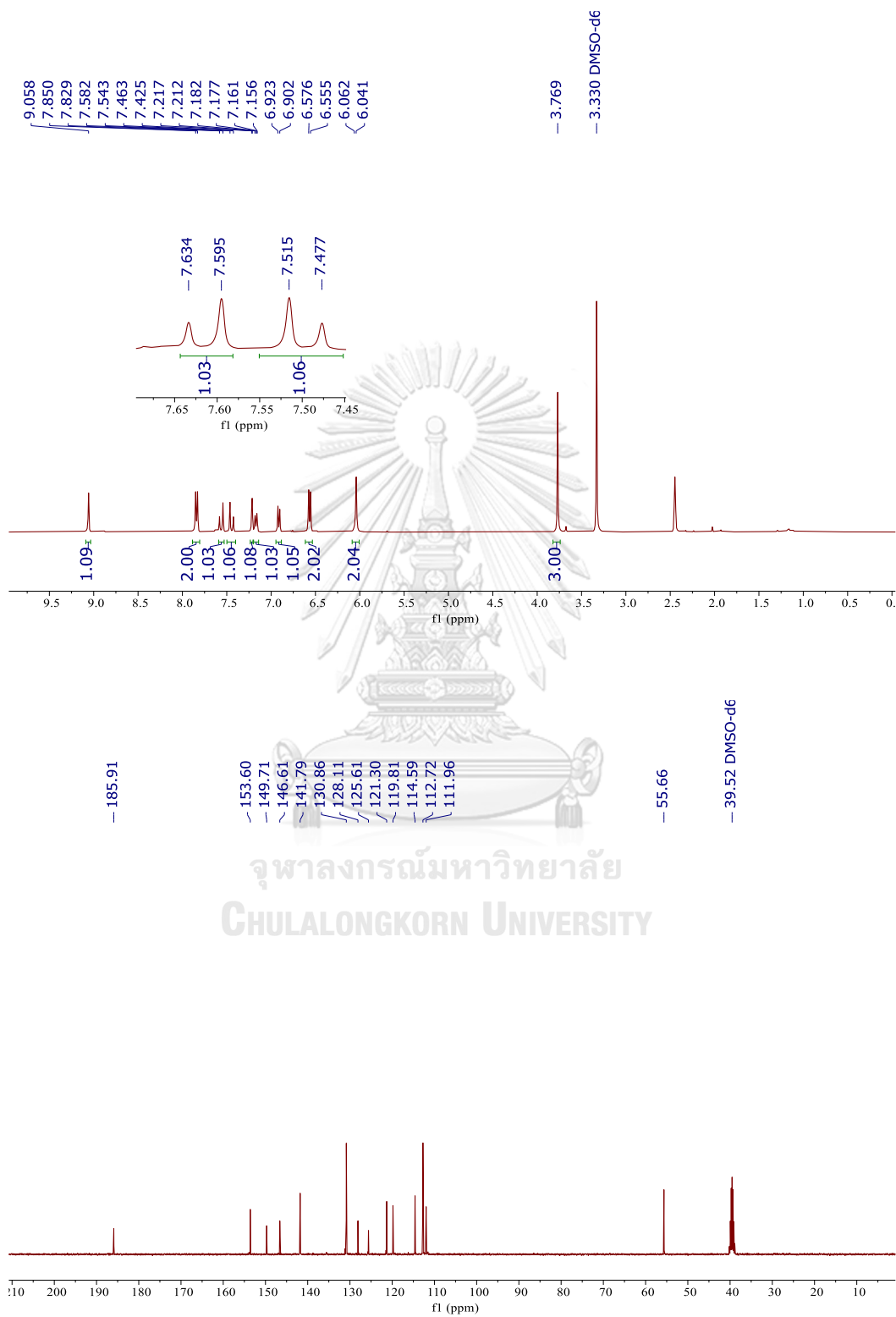
59. ^1H (400 MHz) and ^{13}C (100 MHz) NMR Spectra in $\text{DMSO-}d_6$ of 55

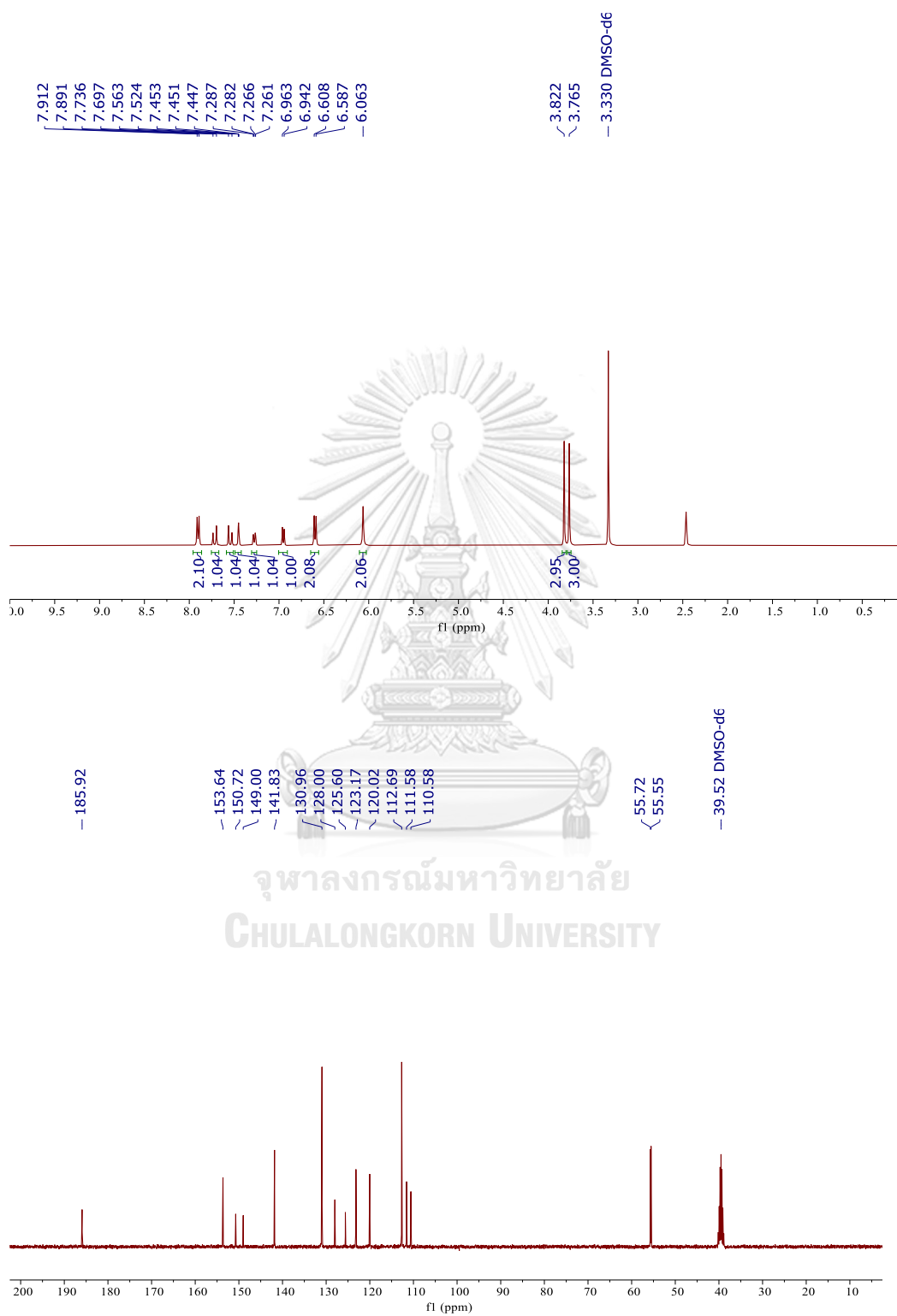
60. ^1H (500 MHz) and ^{13}C (125 MHz) NMR Spectra in $\text{DMSO-}d_6$ of **56**

61. ^1H (400 MHz) and ^{13}C (100 MHz) NMR Spectra in $\text{DMSO-}d_6$ of **57**

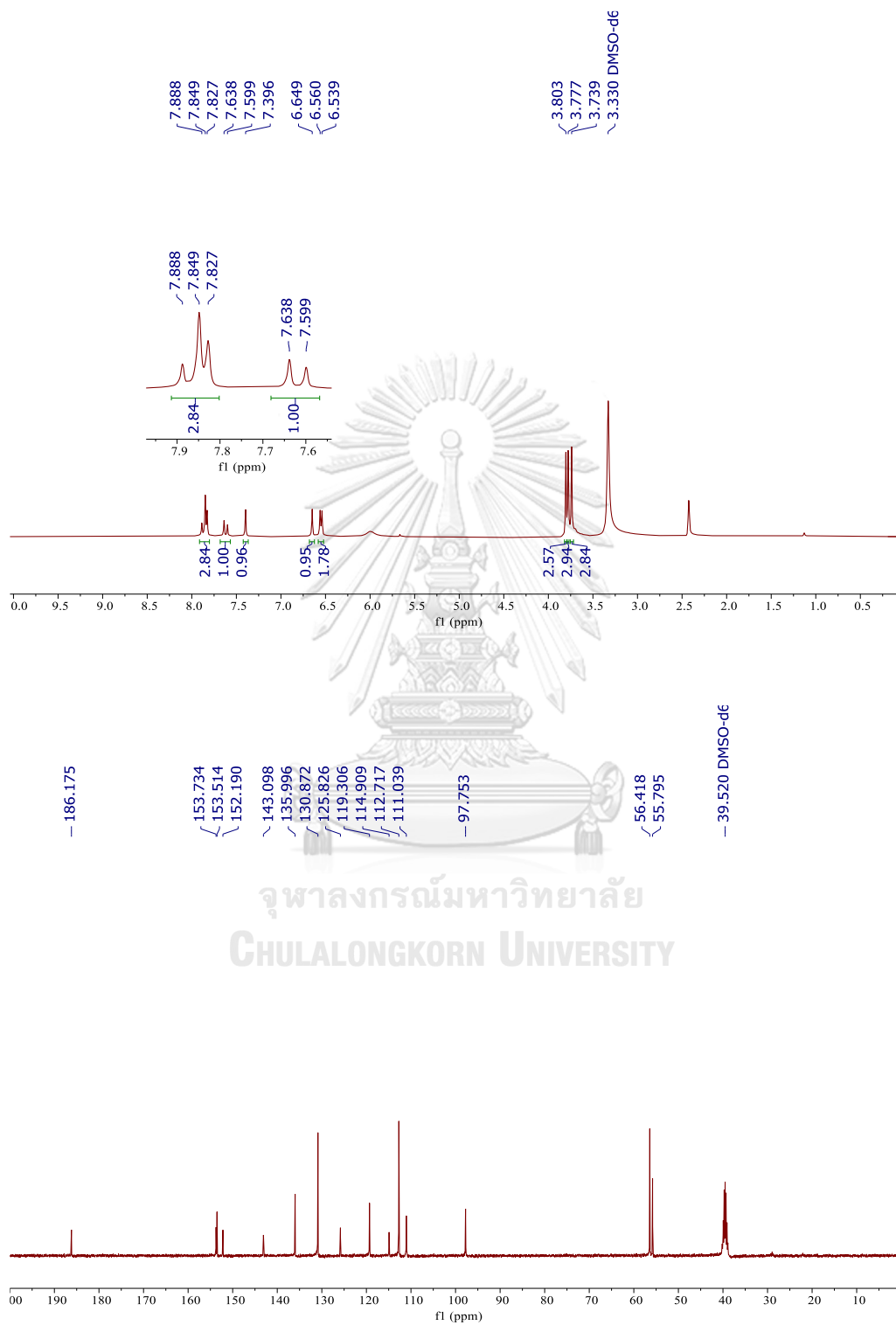
62. ^1H (400 MHz) and ^{13}C (100 MHz) NMR Spectra in $\text{DMSO-}d_6$ of **58**

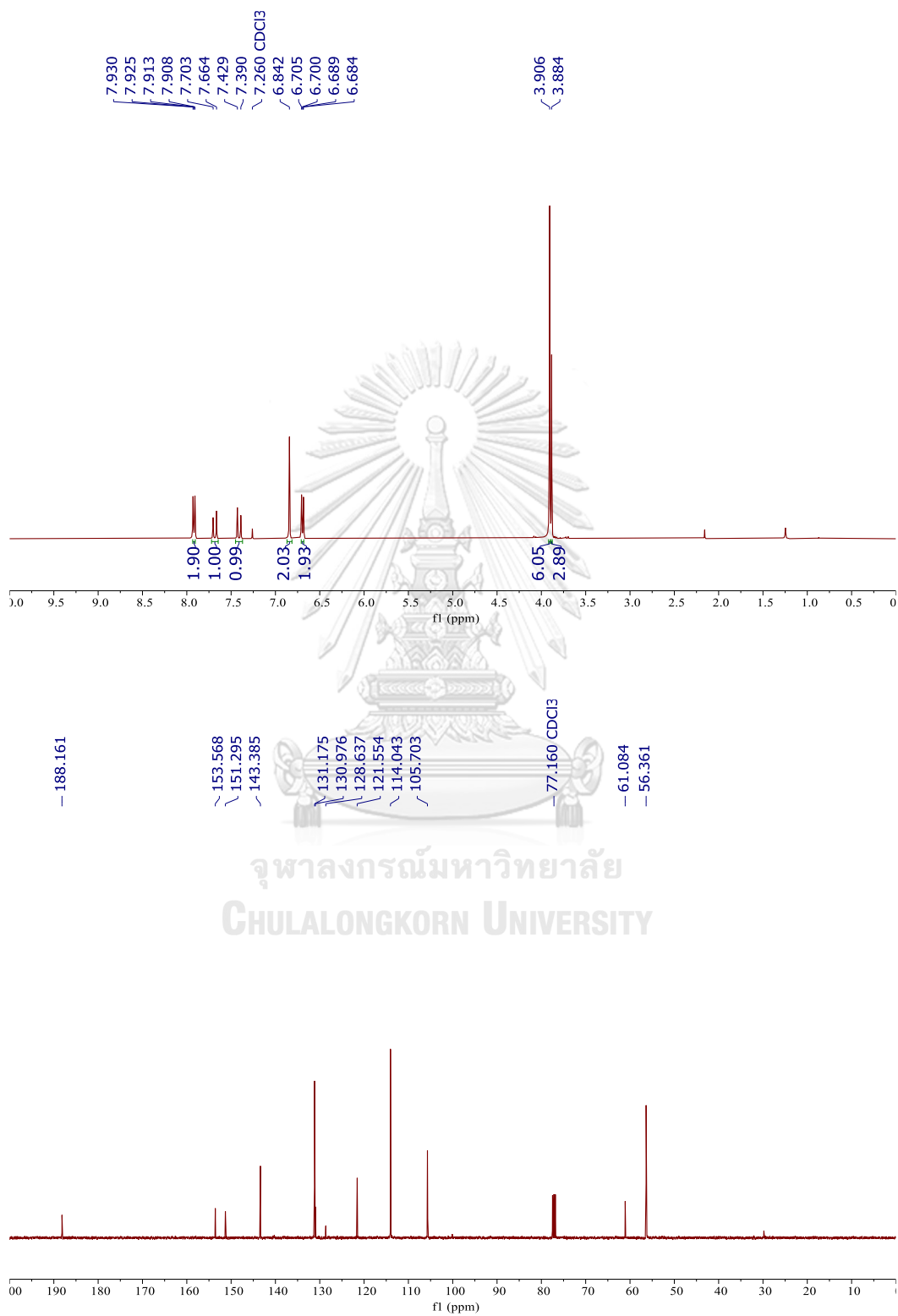
63. ^1H (500 MHz) and ^{13}C (125 MHz) NMR Spectra in acetone- d_6 of **59**

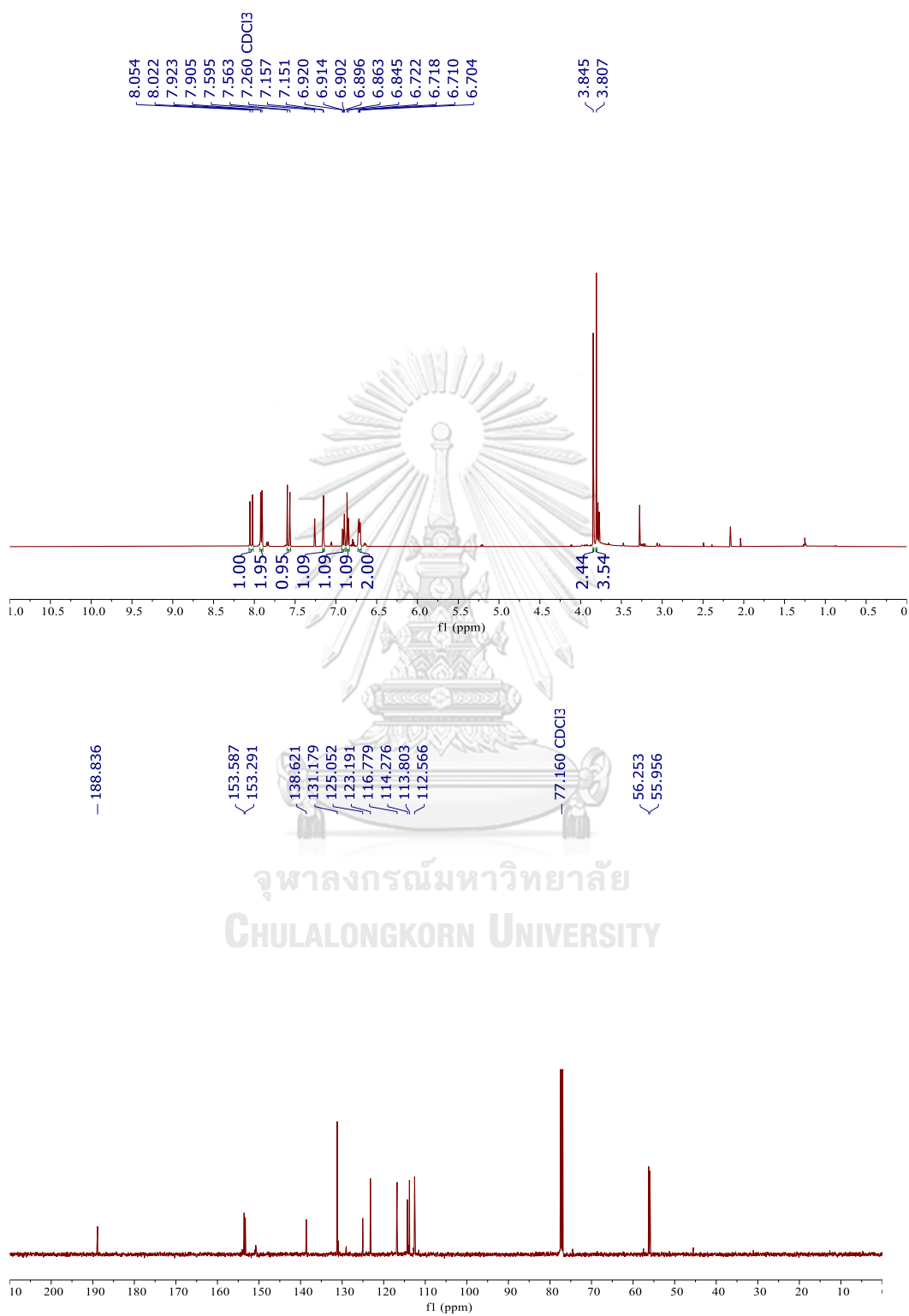
64. ^1H (400 MHz) and ^{13}C (100 MHz) NMR Spectra in $\text{DMSO-}d_6$ of **60**

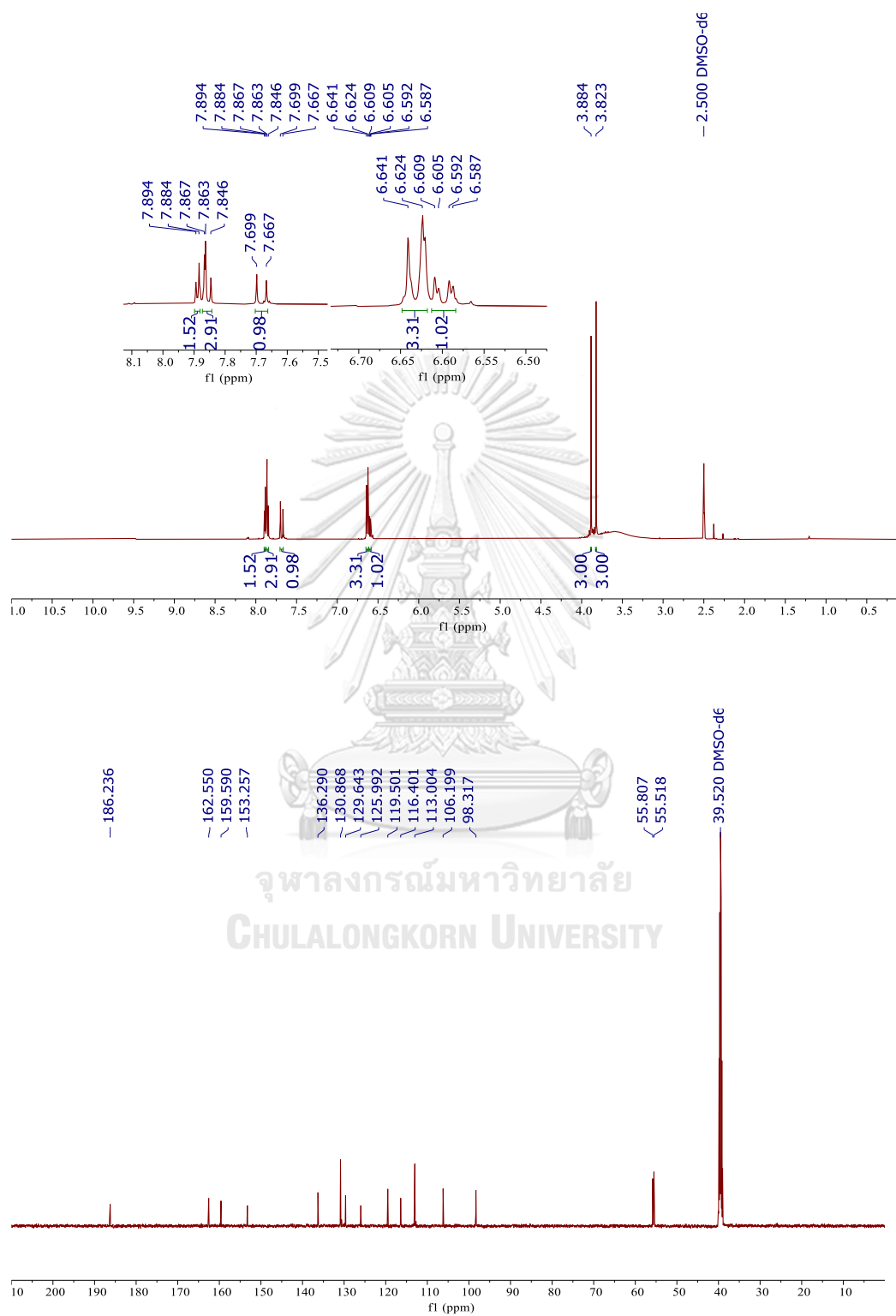
65. ^1H (400 MHz) and ^{13}C (100 MHz) NMR Spectra in $\text{DMSO-}d_6$ of **61**

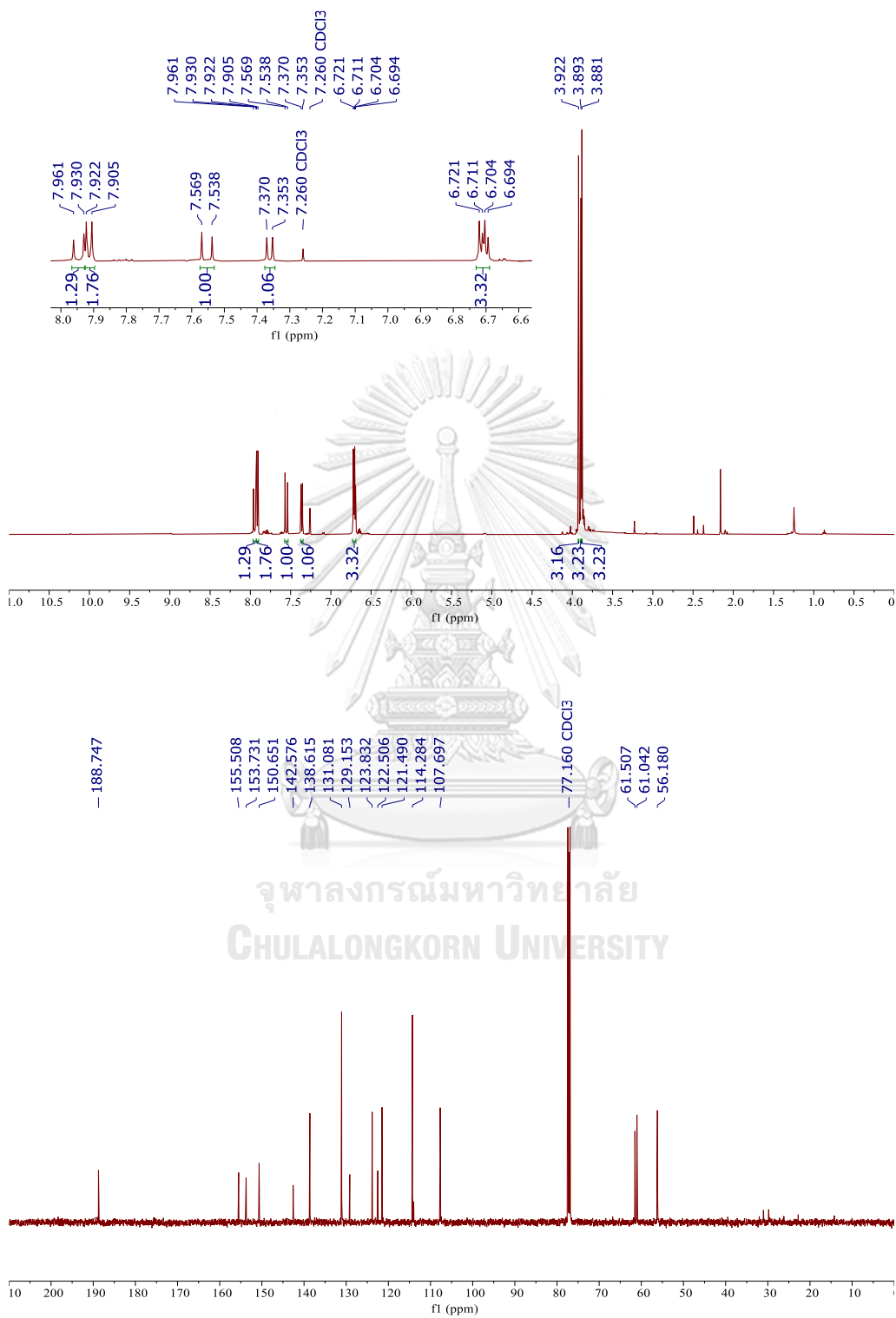
66. ^1H (400 MHz) and ^{13}C (100 MHz) NMR Spectra in $\text{DMSO-}d_6$ of **62**

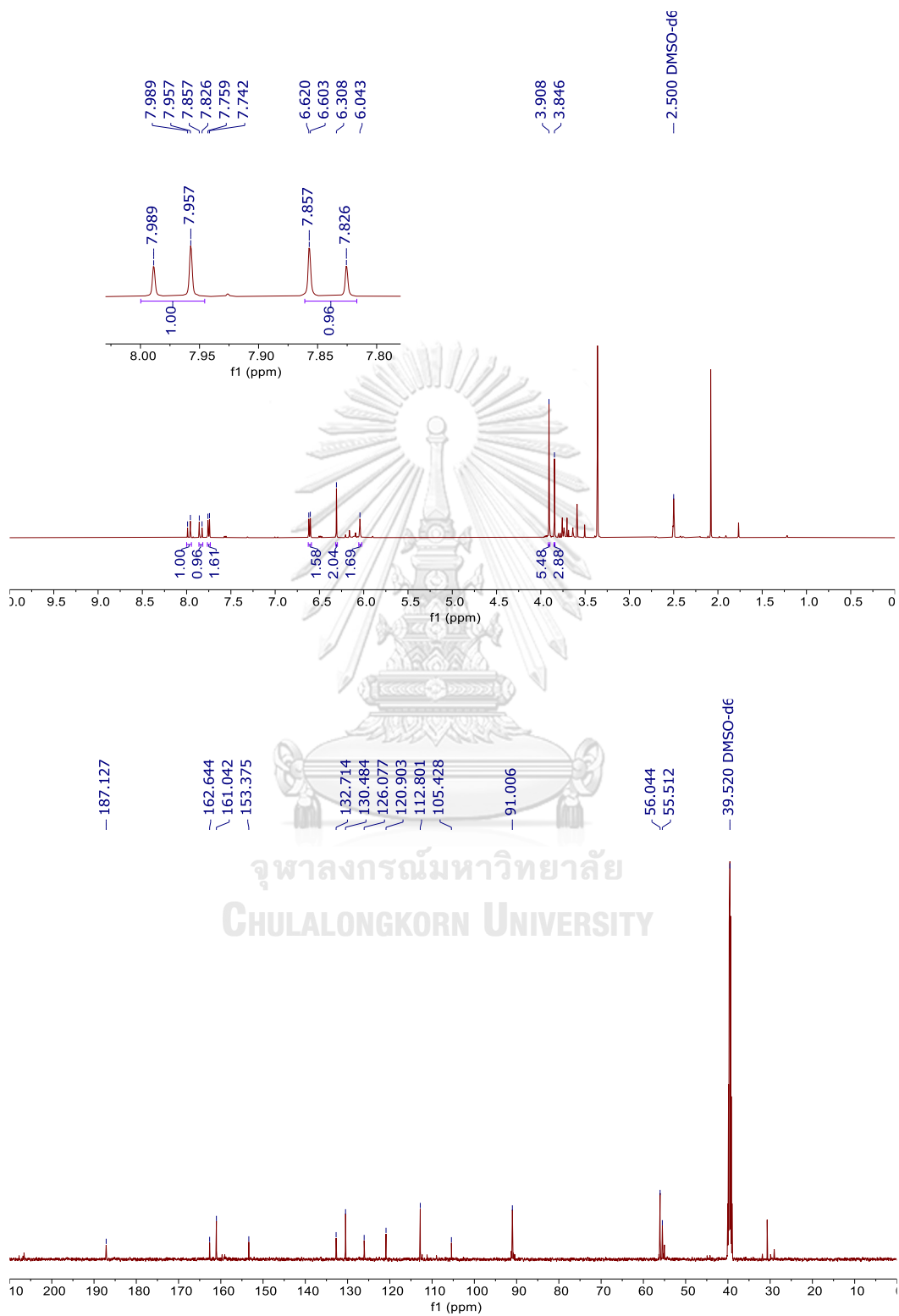


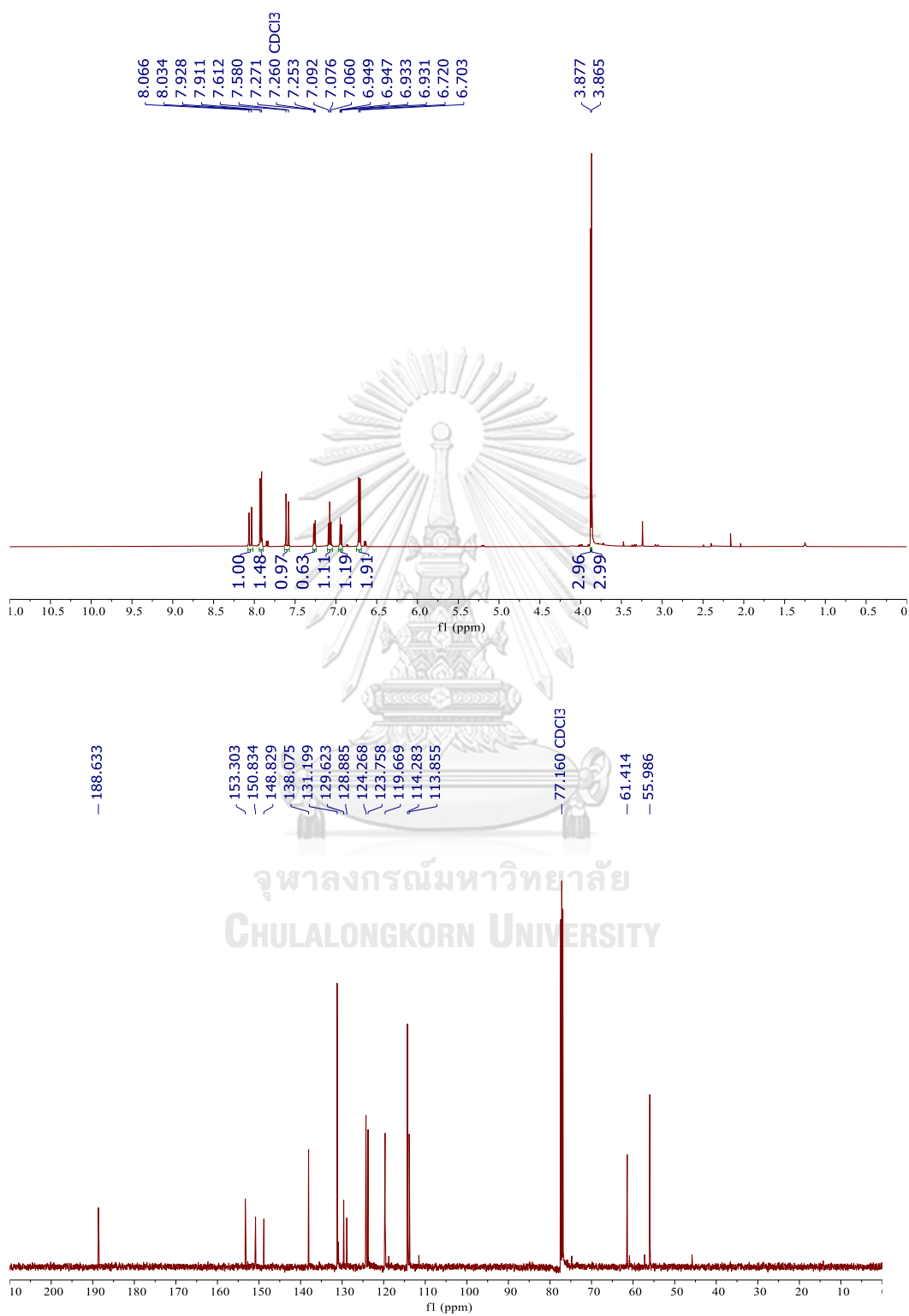
67. ^1H (400 MHz) and ^{13}C (100 MHz) NMR Spectra in CDCl_3 of **63**

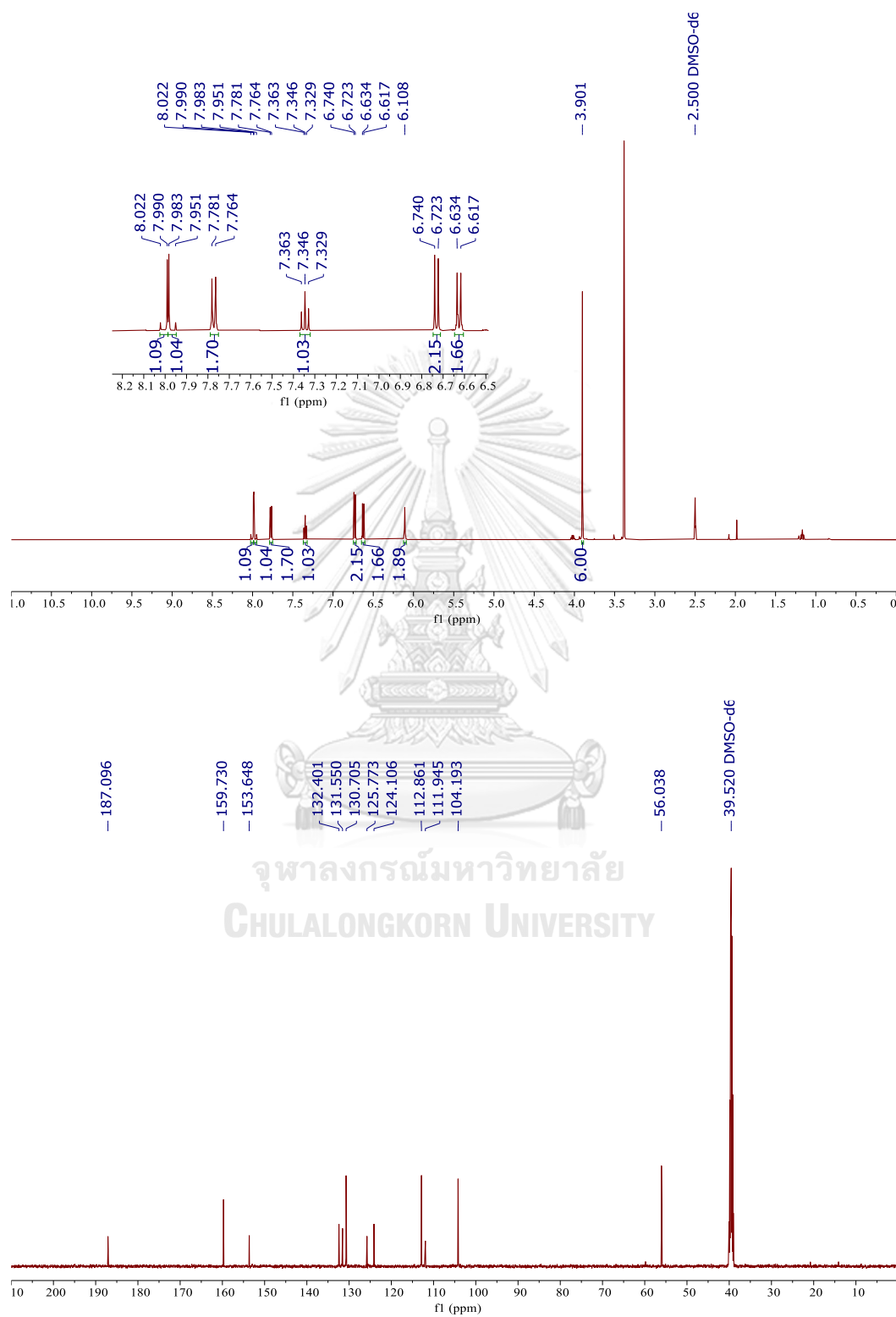
68. ^1H (500 MHz) and ^{13}C (125 MHz) NMR Spectra in CDCl_3 of **64**

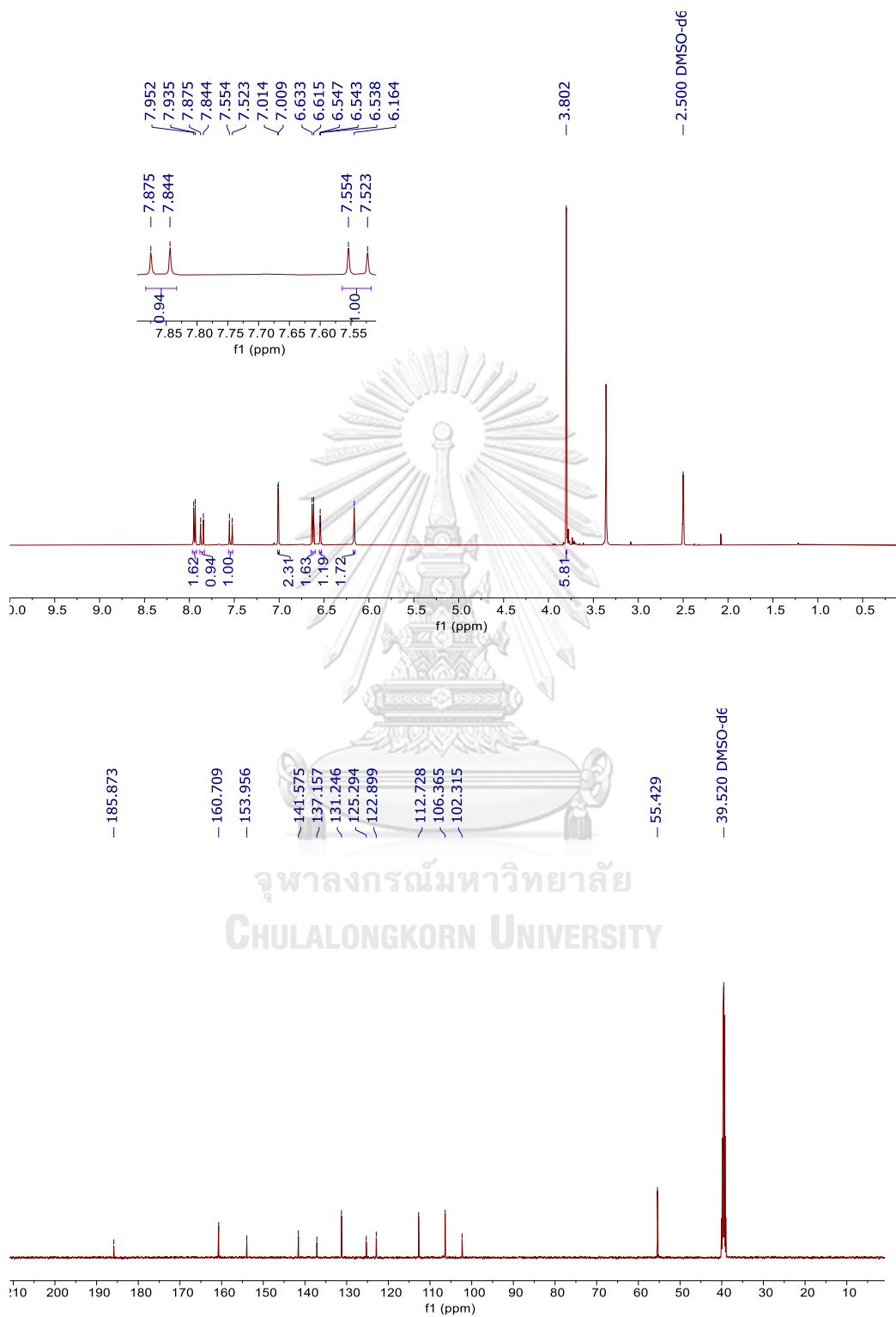
69. ^1H (500 MHz) and ^{13}C (125 MHz) NMR Spectra in $\text{DMSO-}d_6$ of **65**

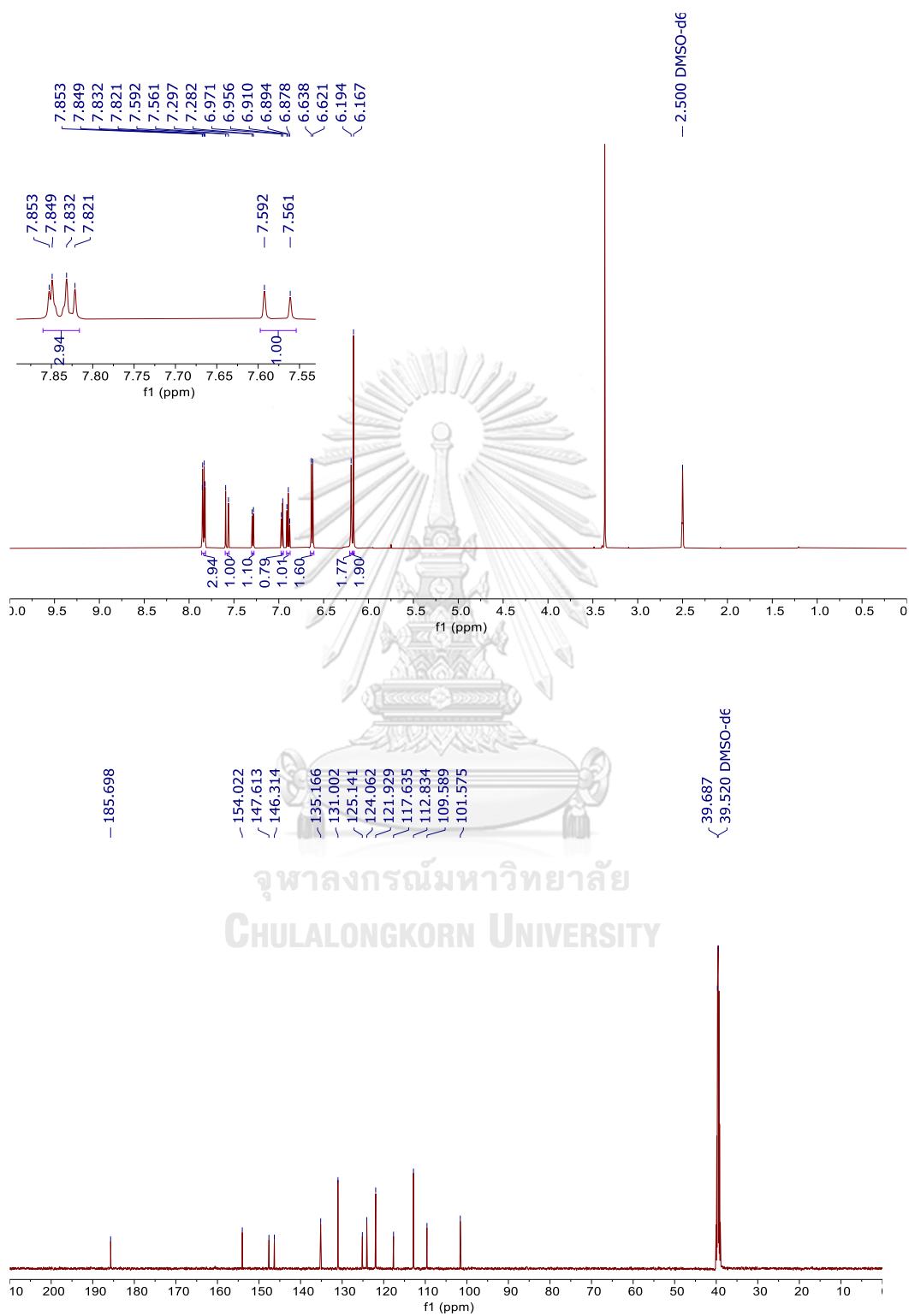
70. ^1H (500 MHz) and ^{13}C (125 MHz) NMR Spectra in CDCl_3 of **66**

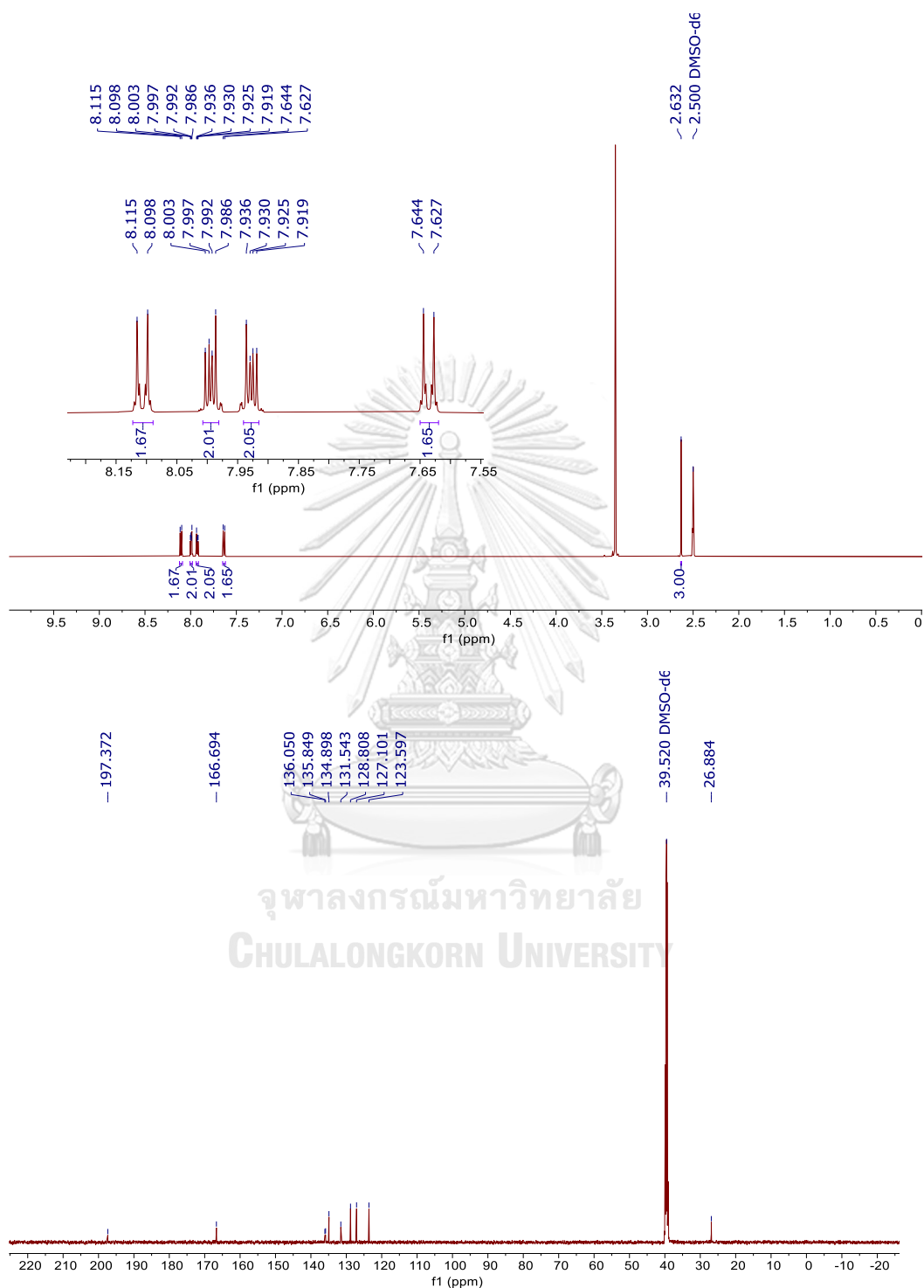
71. ^1H (500 MHz) and ^{13}C (125 MHz) NMR Spectra in $\text{DMSO-}d_6$ of **67**

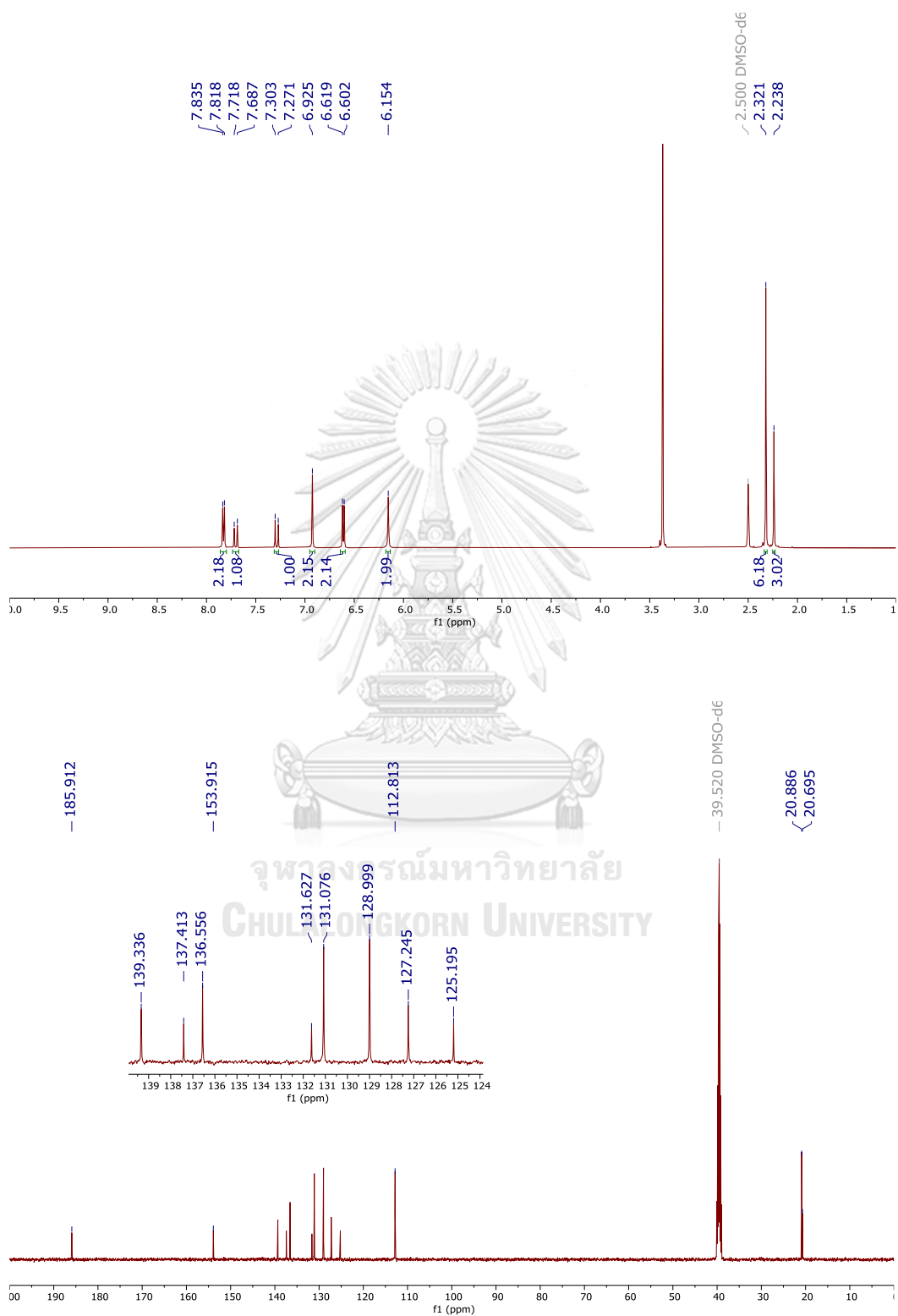
72. ^1H (500 MHz) and ^{13}C (125 MHz) NMR Spectra in CDCl_3 of **68**

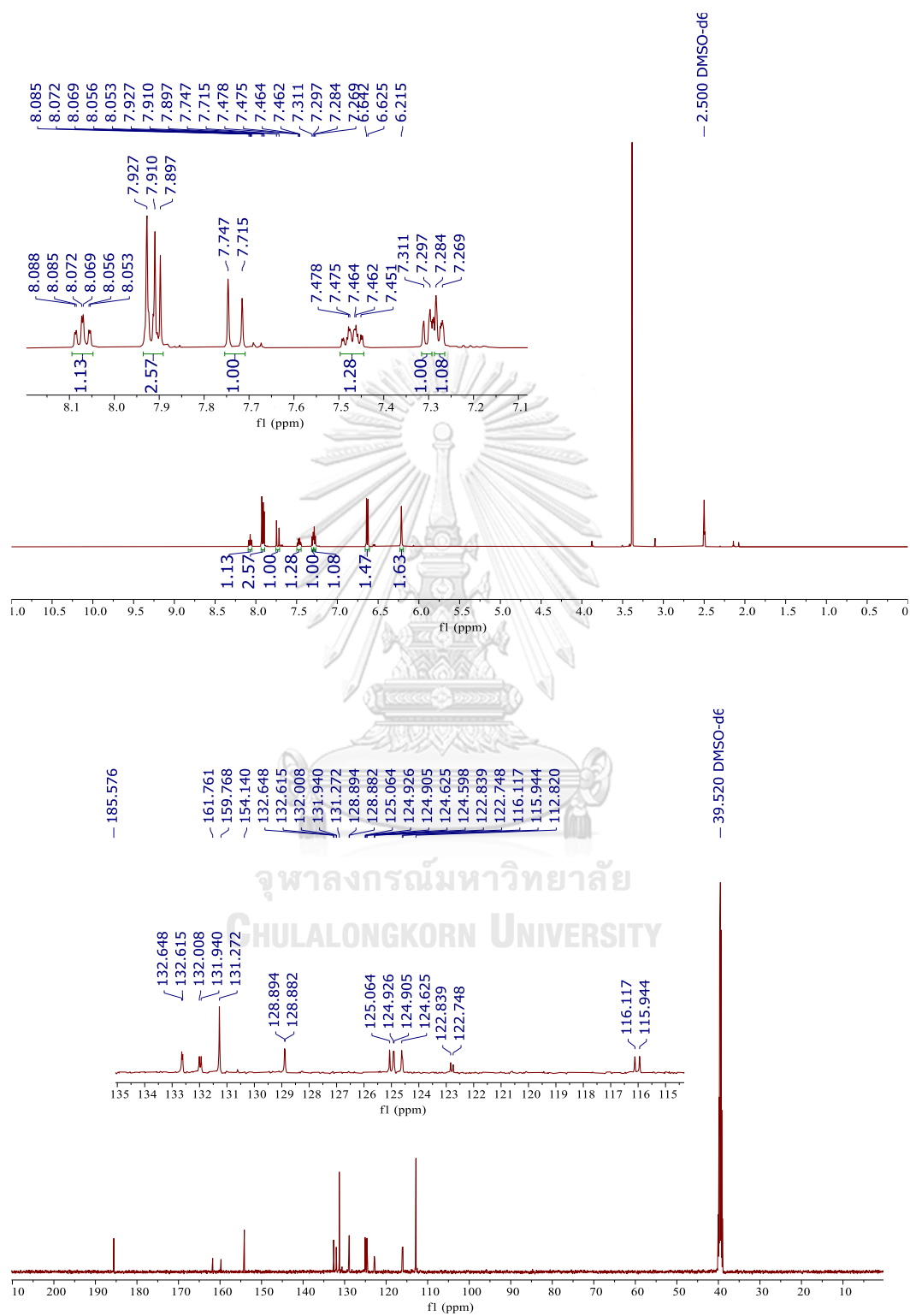
73. ^1H (500 MHz) and ^{13}C (125 MHz) NMR Spectra in $\text{DMSO-}d_6$ of **69**

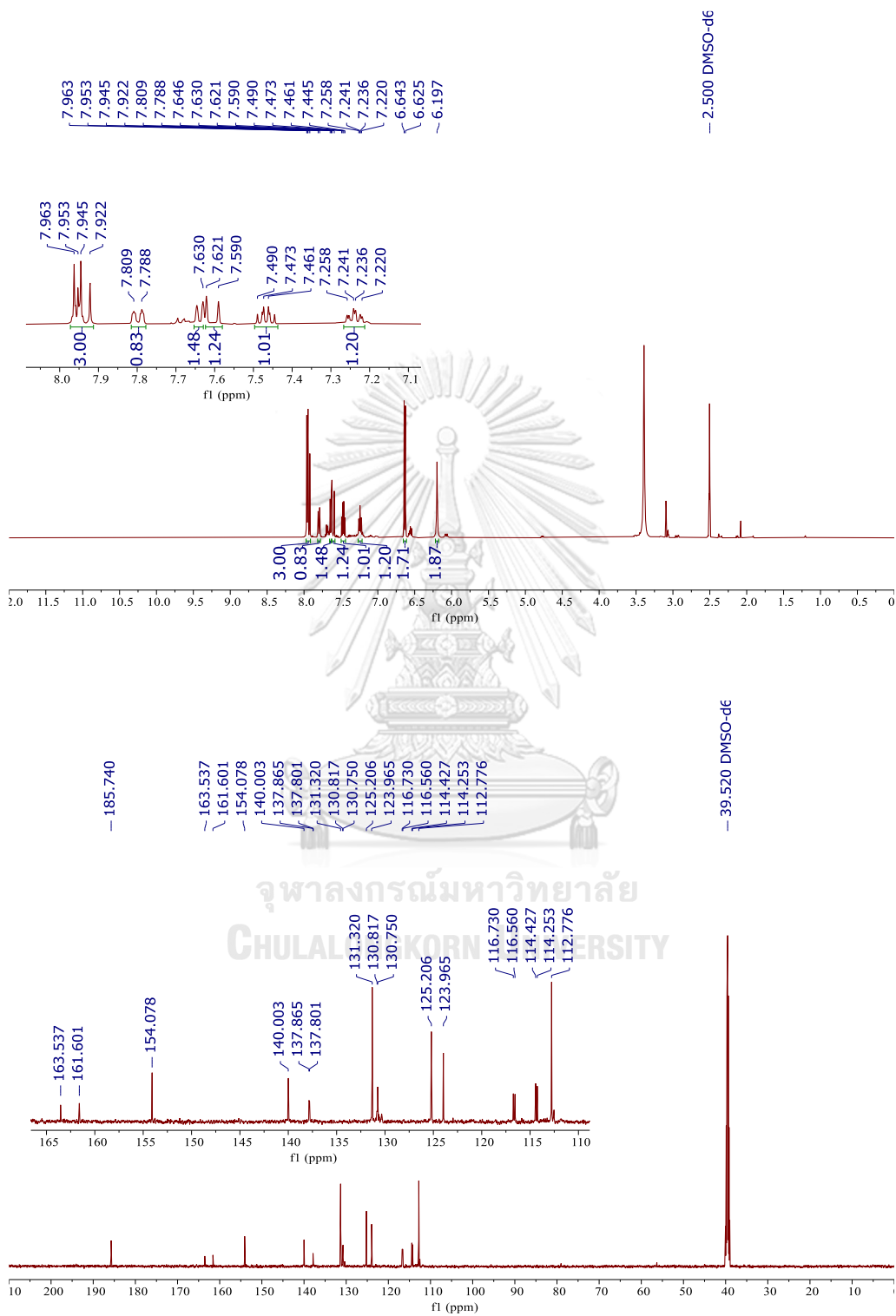
74. ^1H (500 MHz) and ^{13}C (125 MHz) NMR Spectra in $\text{DMSO-}d_6$ of 70

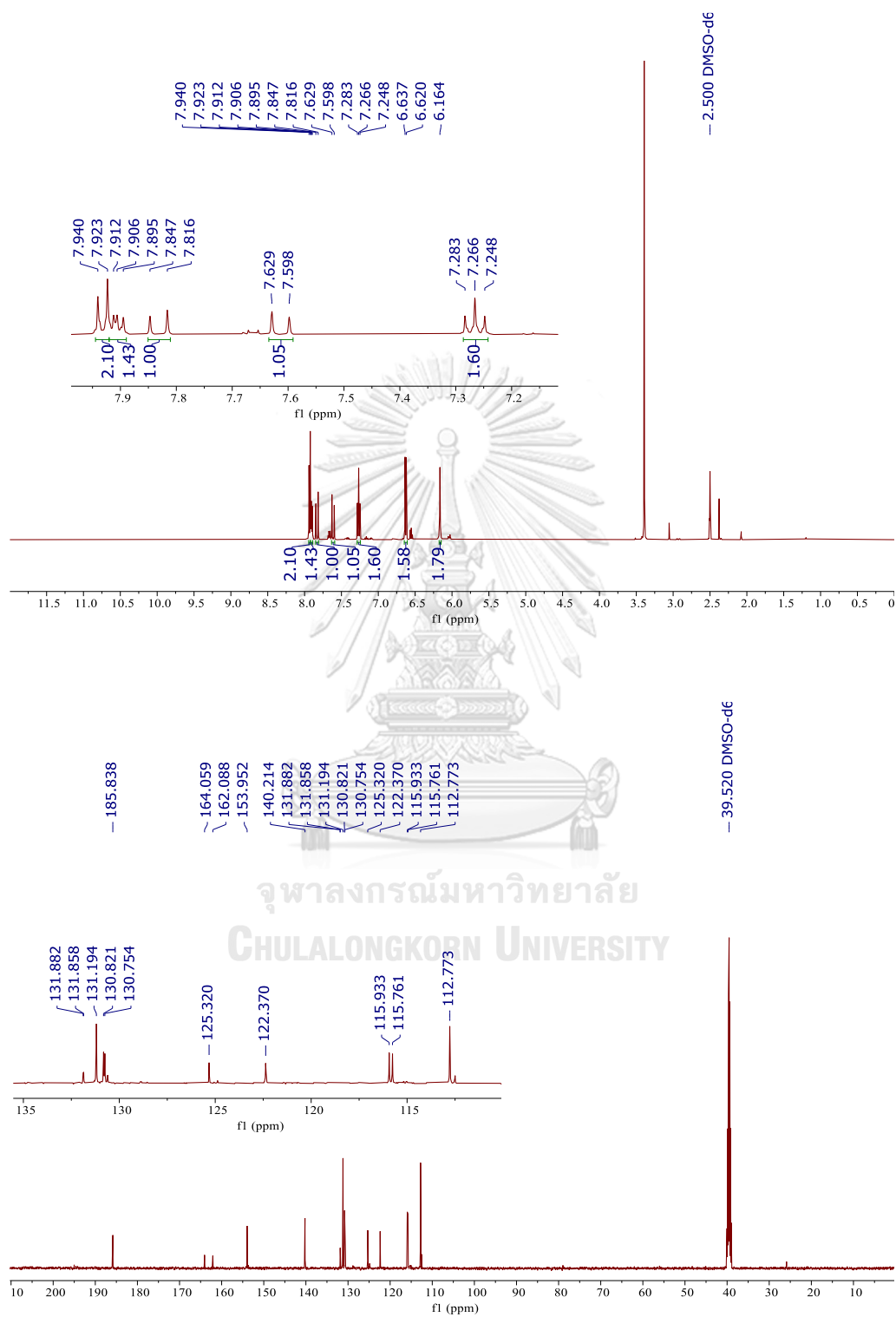
75. ^1H (500 MHz) and ^{13}C (125 MHz) NMR Spectra in $\text{DMSO-}d_6$ of **71**

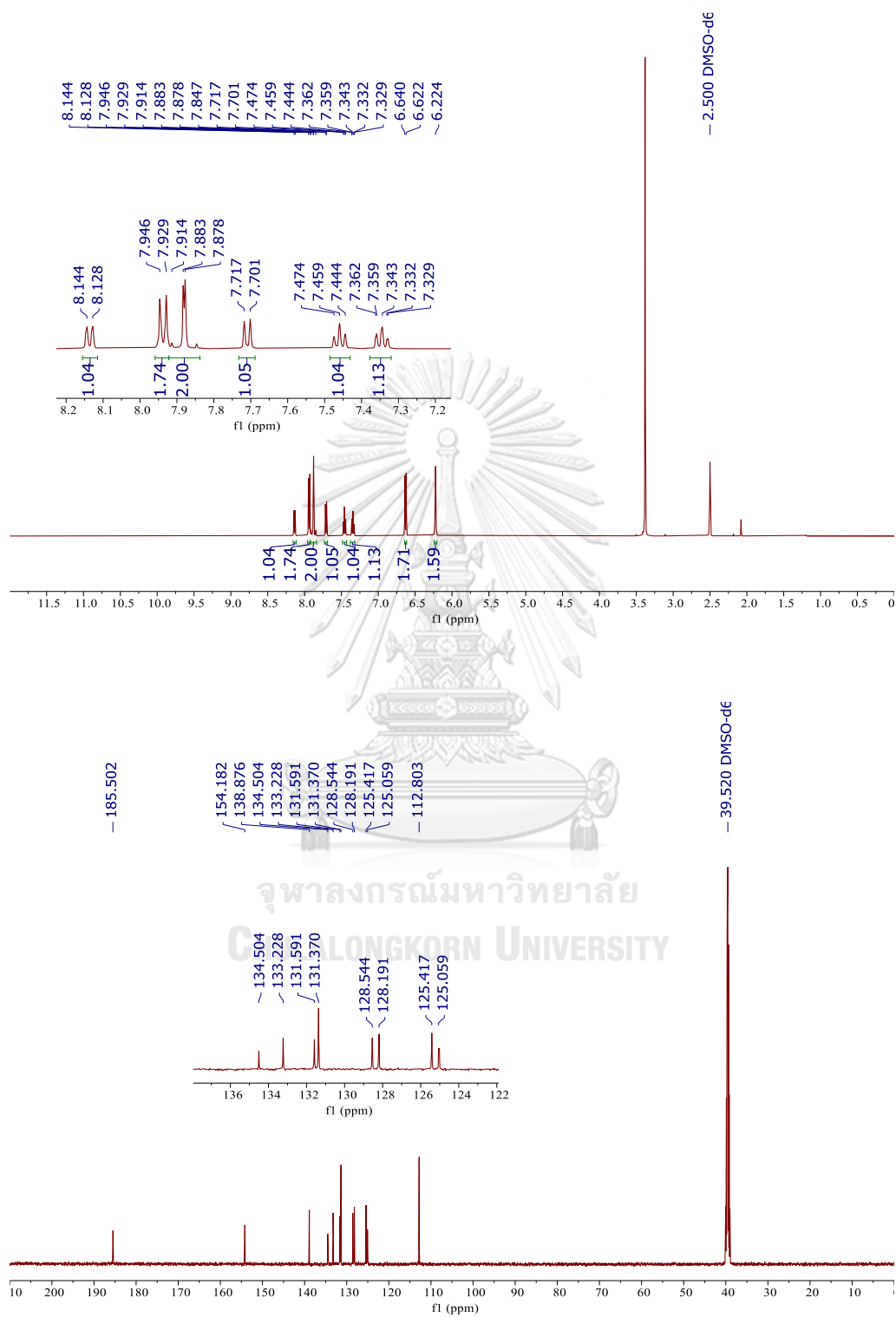
76. ^1H (500 MHz) and ^{13}C (125 MHz) NMR Spectra in $\text{DMSO-}d_6$ of 72

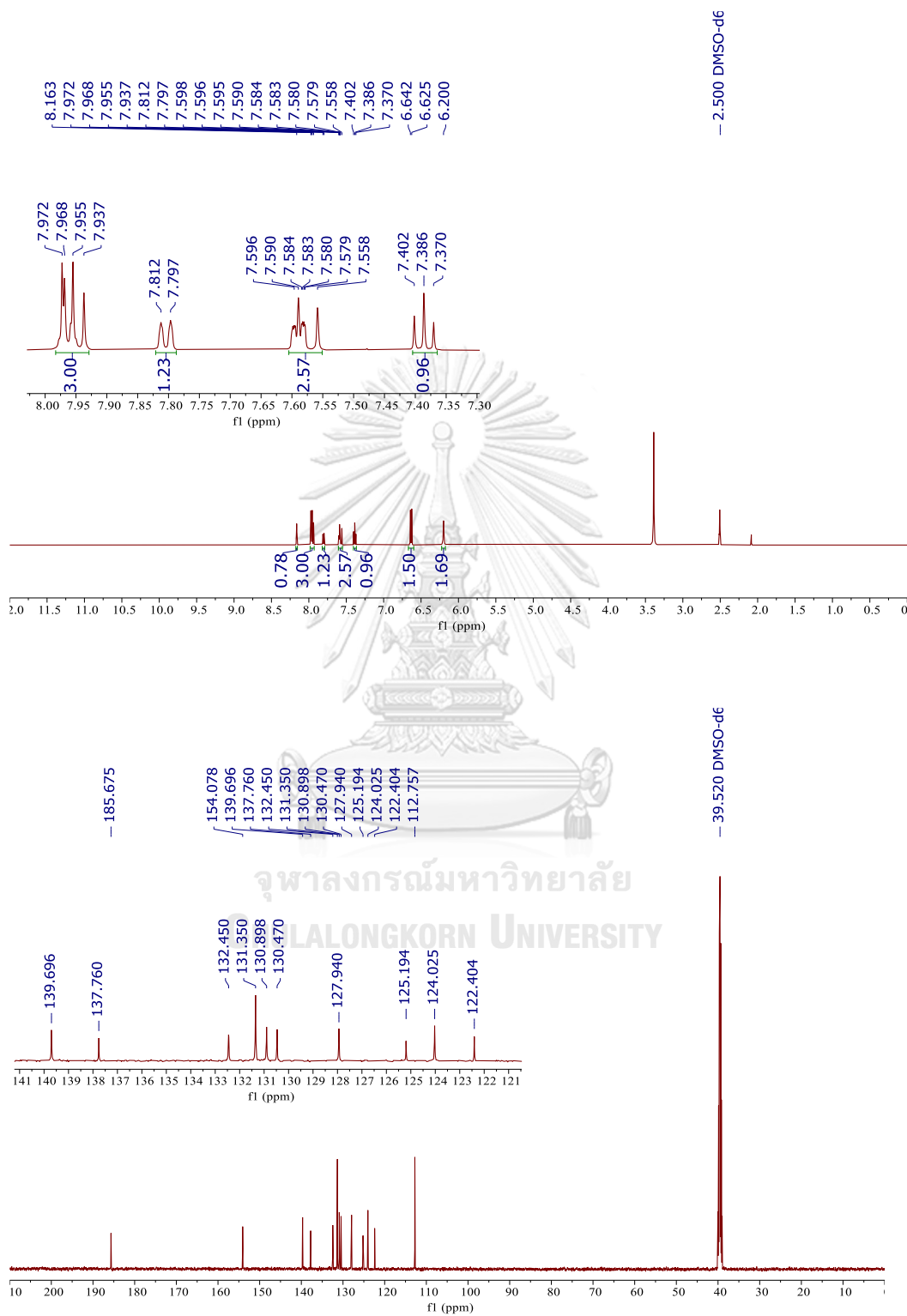
77. ^1H (500 MHz) and ^{13}C (125 MHz) NMR Spectra in $\text{DMSO-}d_6$ of **73**

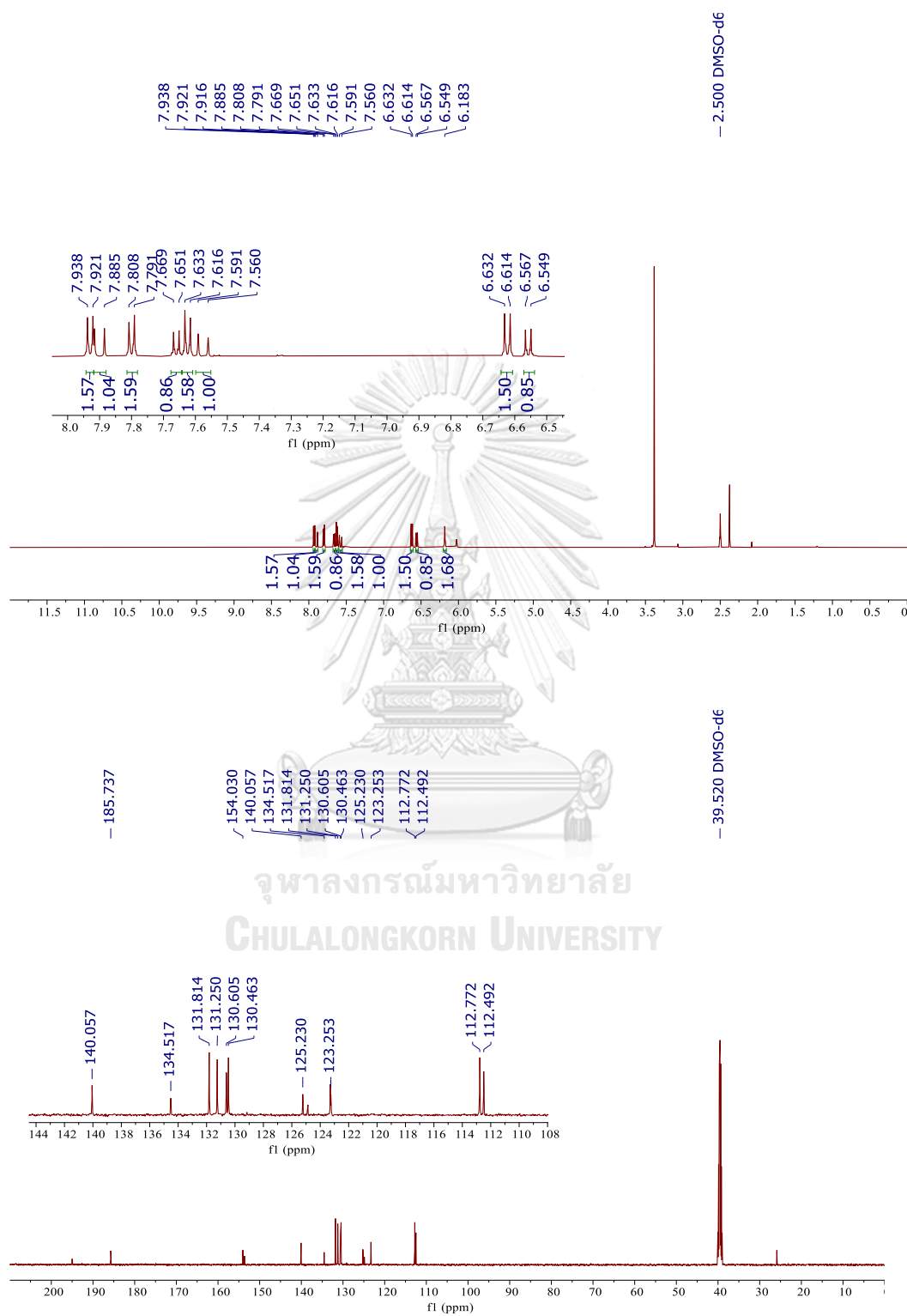
78. ^1H (500 MHz) and ^{13}C (125 MHz) NMR Spectra in $\text{DMSO-}d_6$ of 74

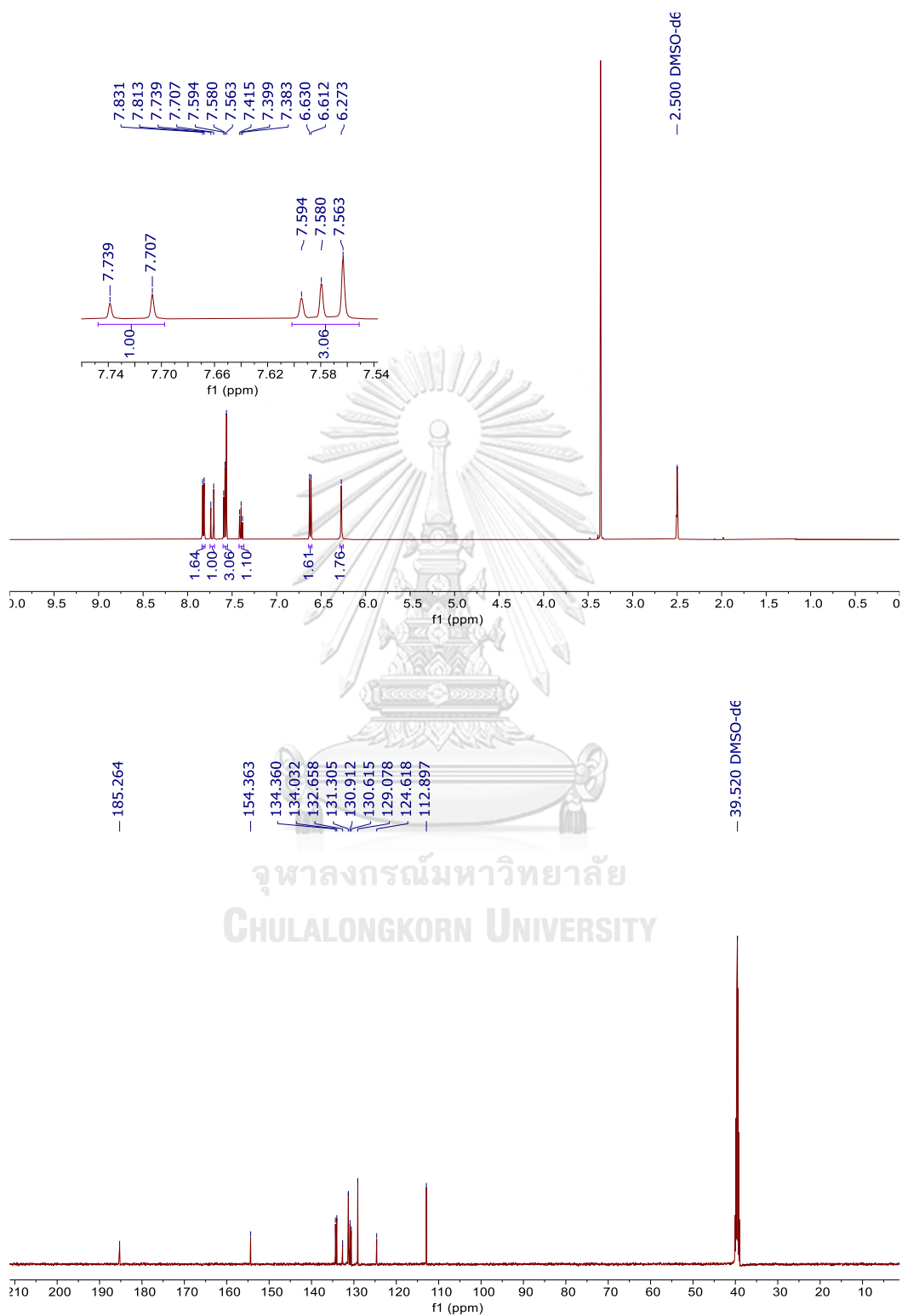
79. ^1H (500 MHz) and ^{13}C (125 MHz) NMR Spectra in $\text{DMSO-}d_6$ of 75

80. ^1H (500 MHz) and ^{13}C (125 MHz) NMR Spectra in $\text{DMSO-}d_6$ of **76**

81. ^1H (500 MHz) and ^{13}C (125 MHz) NMR Spectra in $\text{DMSO-}d_6$ of **77**

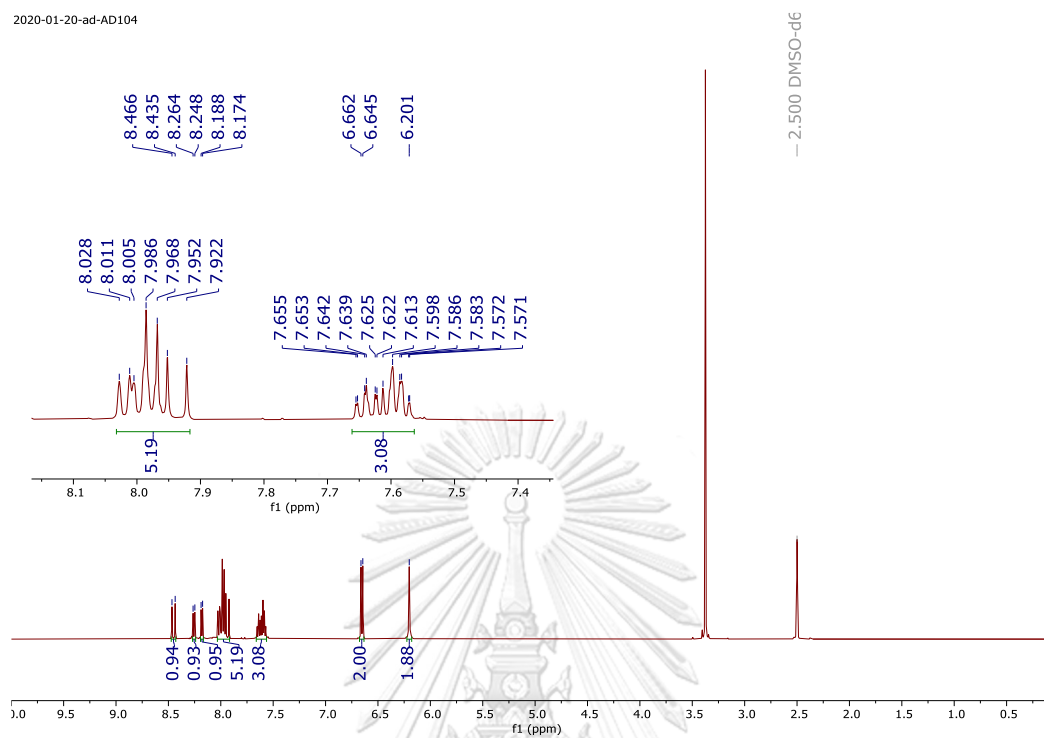
82. ^1H (500 MHz) and ^{13}C (125 MHz) NMR Spectra in $\text{DMSO-}d_6$ of **78**

83. ^1H (500 MHz) and ^{13}C (125 MHz) NMR Spectra in $\text{DMSO-}d_6$ of **79**

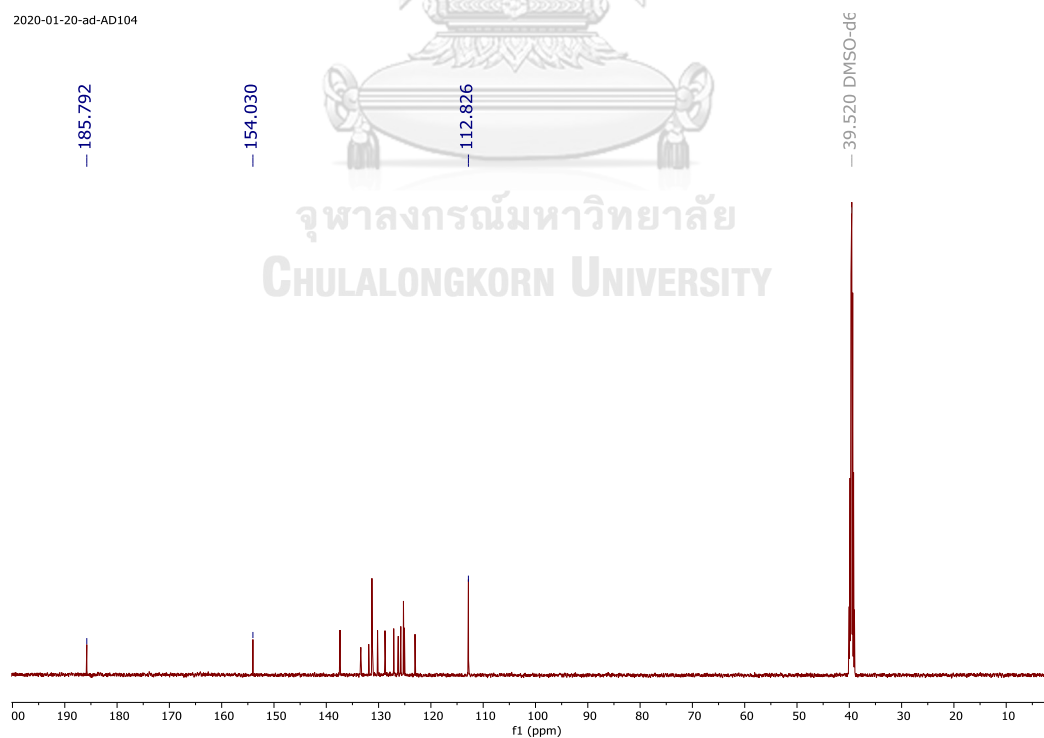
84. ^1H (500 MHz) and ^{13}C (125 MHz) NMR Spectra in $\text{DMSO-}d_6$ of **80**

85. ^1H (500 MHz) and ^{13}C (125 MHz) NMR Spectra in $\text{DMSO-}d_6$ of **81**

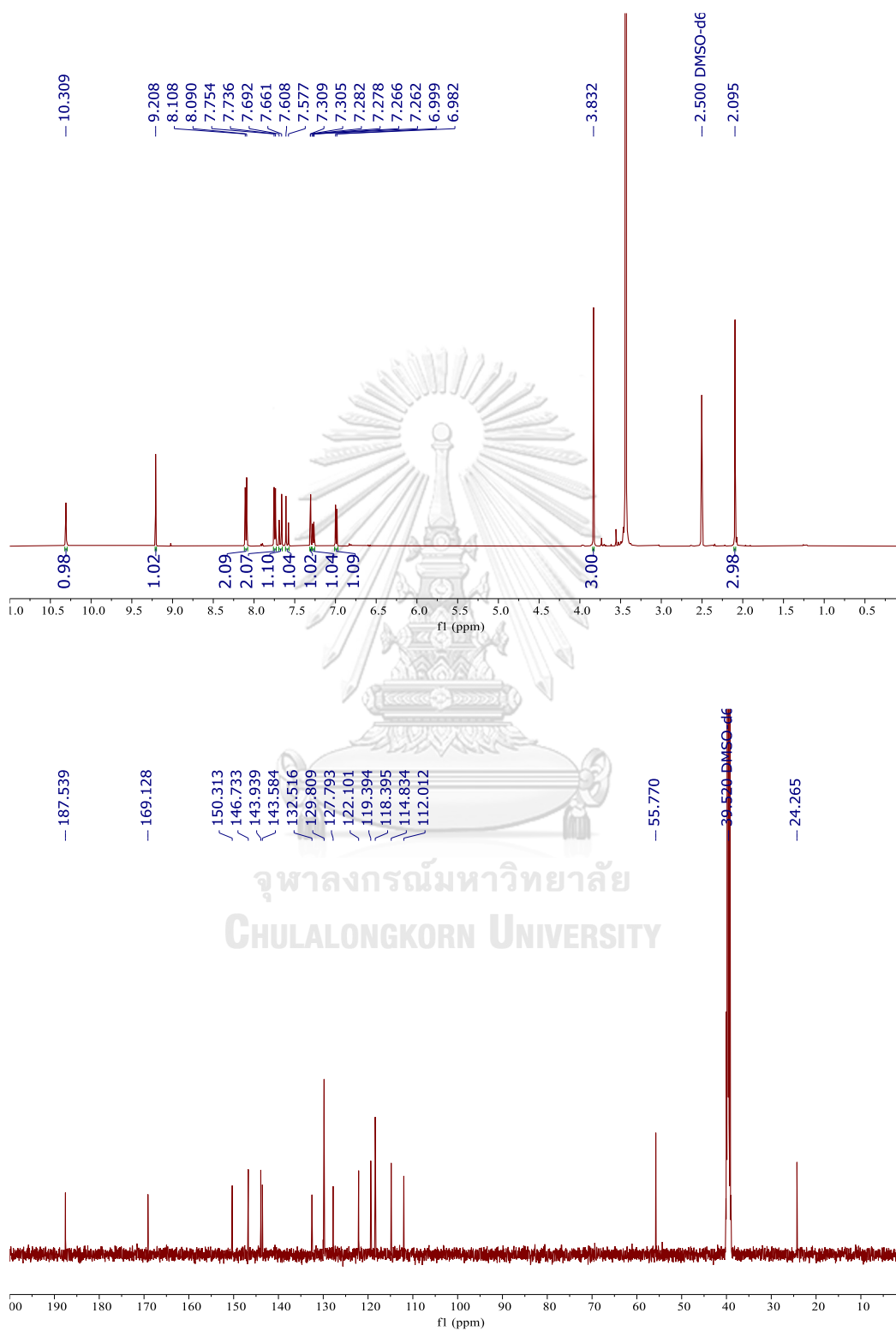
2020-01-20-ad-AD104



2020-01-20-ad-AD104



86. ^1H (500 MHz) and ^{13}C (125 MHz) NMR Spectra in $\text{DMSO-}d_6$ of **84** (new compound)



87. Mass Spectra of **84** (new compound)

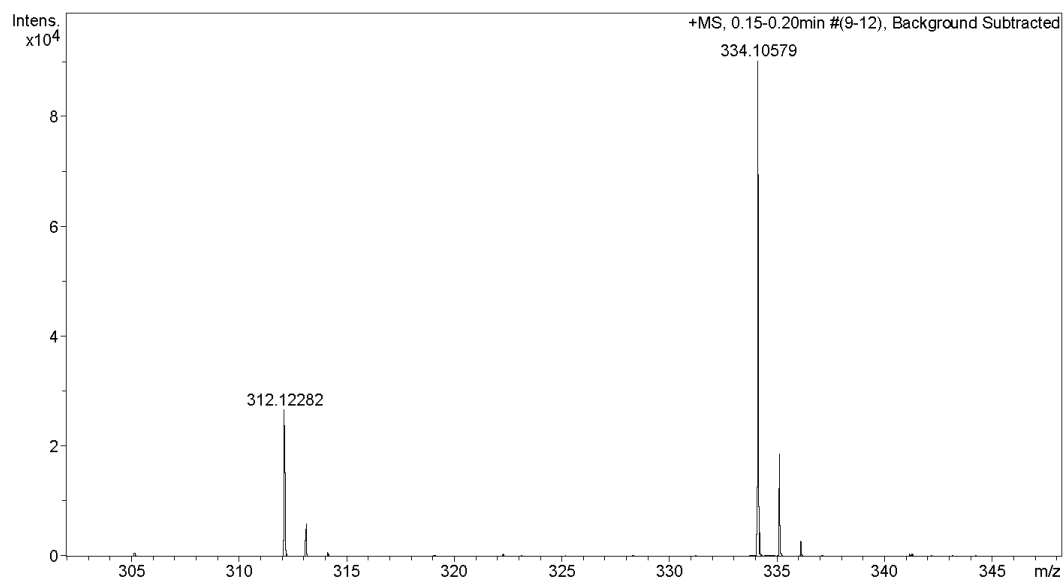
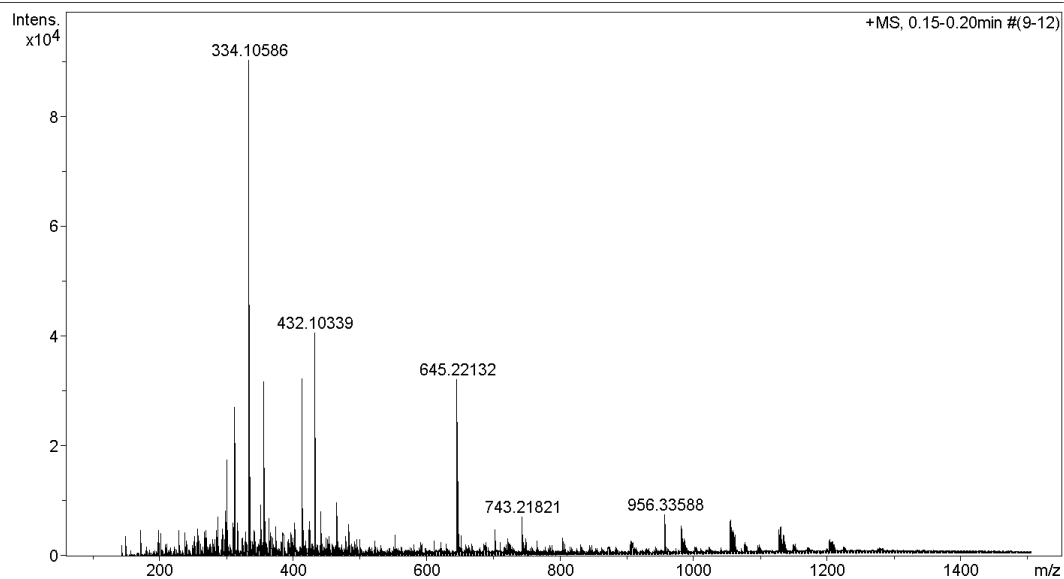
Generic Display Report

Analysis Info

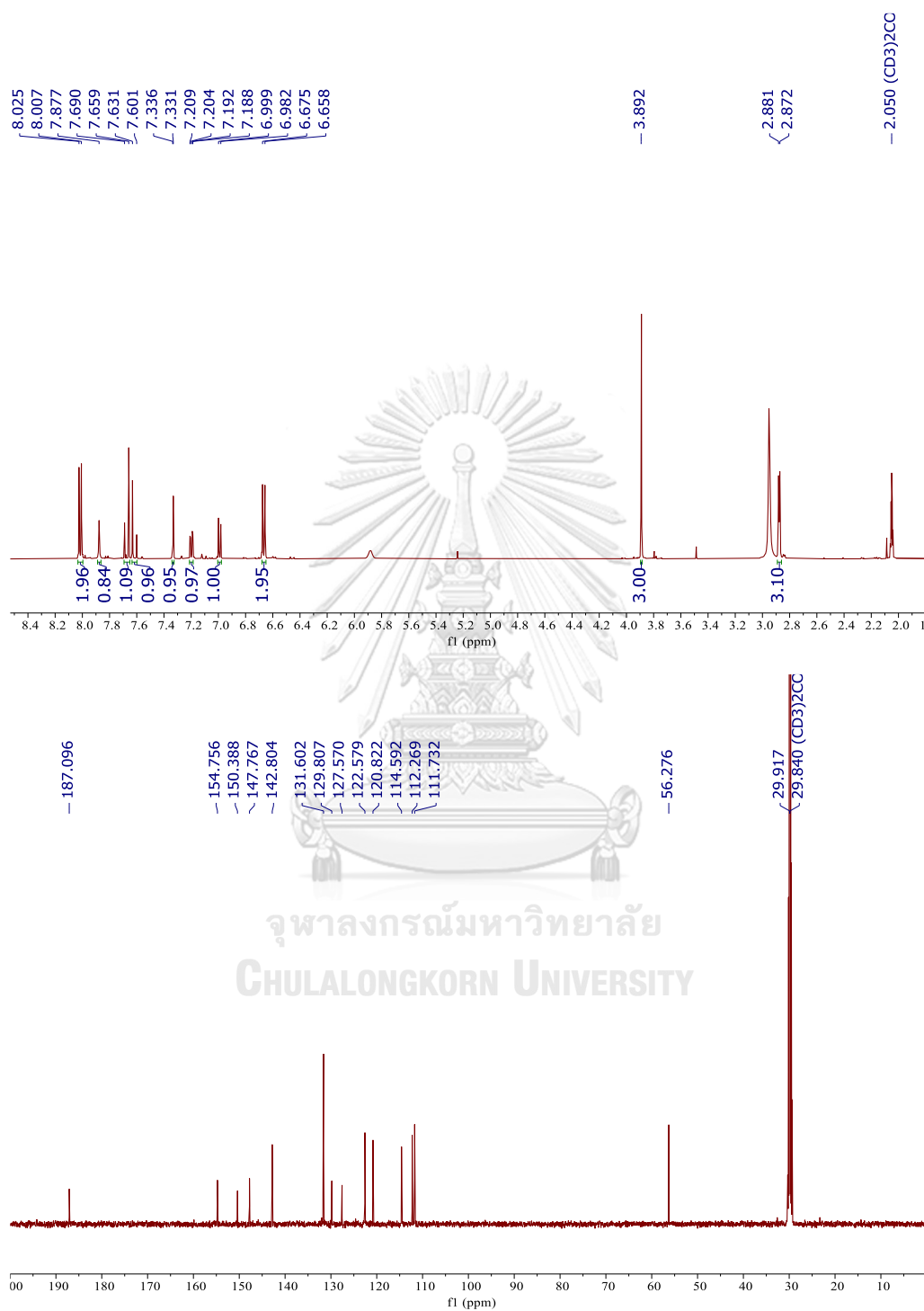
Analysis Name D:\Data\Data Service\201123\AAC_RA8_01_4890.d
Method nv_pos_5min_profile_190214.m
Sample Name AAC
Comment

Acquisition Date 11/23/2020 4:03:46 PM

Operator CU.
Instrument micrOTOF-Q II



88. ^1H (500 MHz) and ^{13}C (125 MHz) NMR Spectra in acetone- d_6 of **85** (new compound)



89. Mass Spectra of 85 (new compound)

Generic Display Report

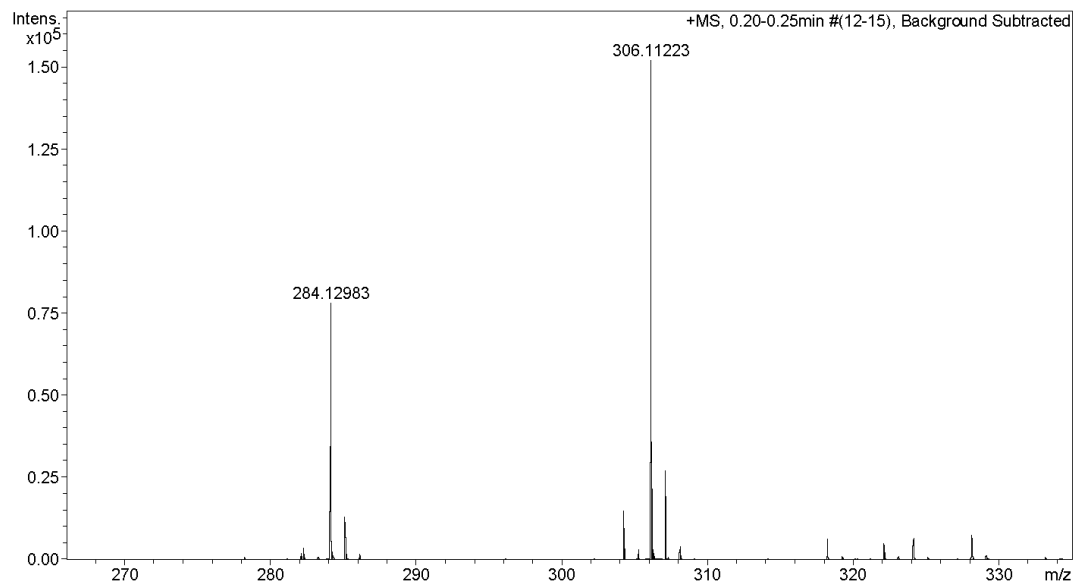
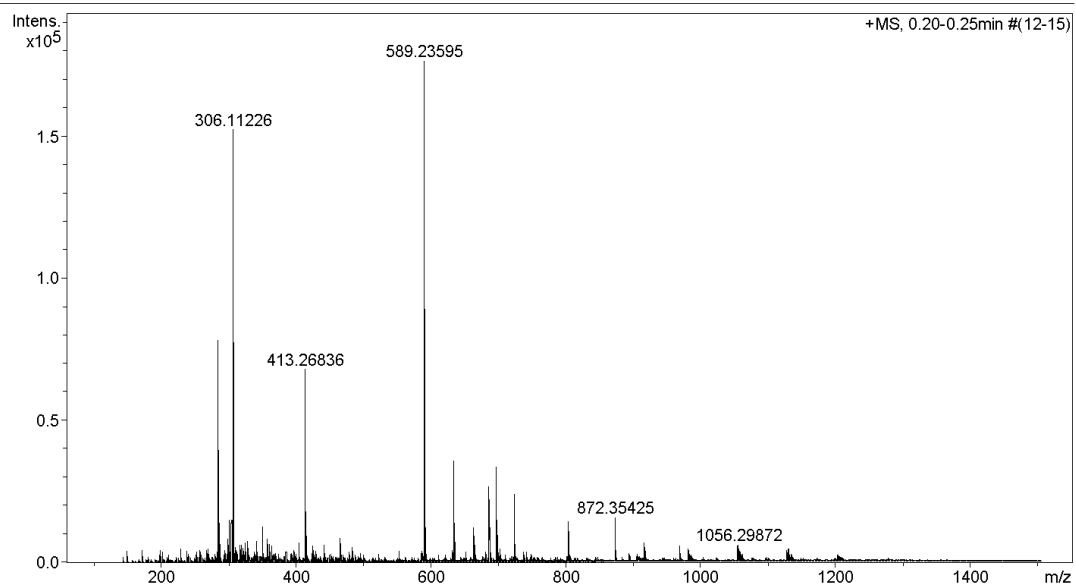
Analysis Info

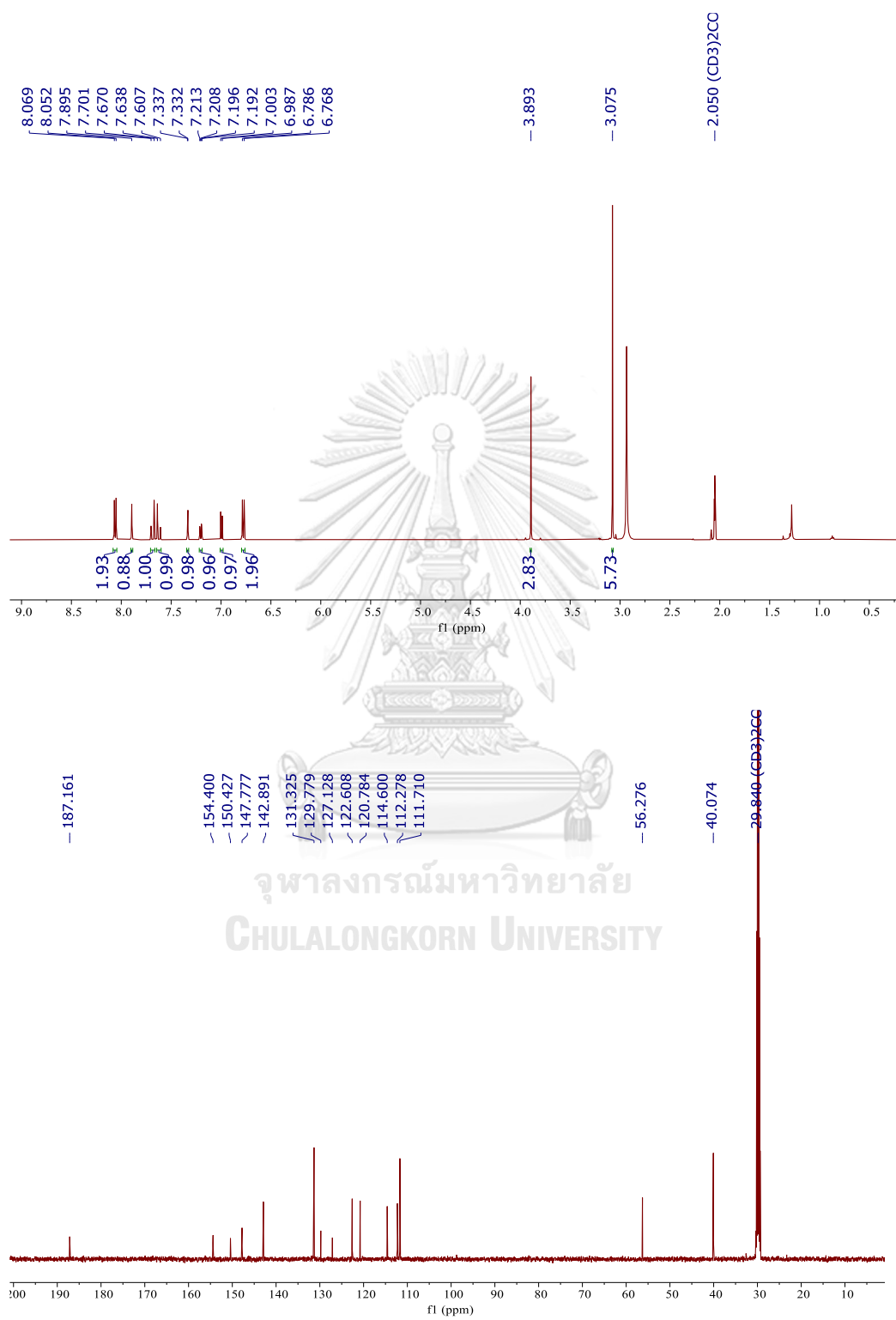
Analysis Name D:\Data\Data Service\2011123\MMAC_RA6_01_4888.d
Method nv_pos_5min_profile_190214.m
Sample Name MMAC
Comment

Acquisition Date 11/23/2020 3:50:57 PM

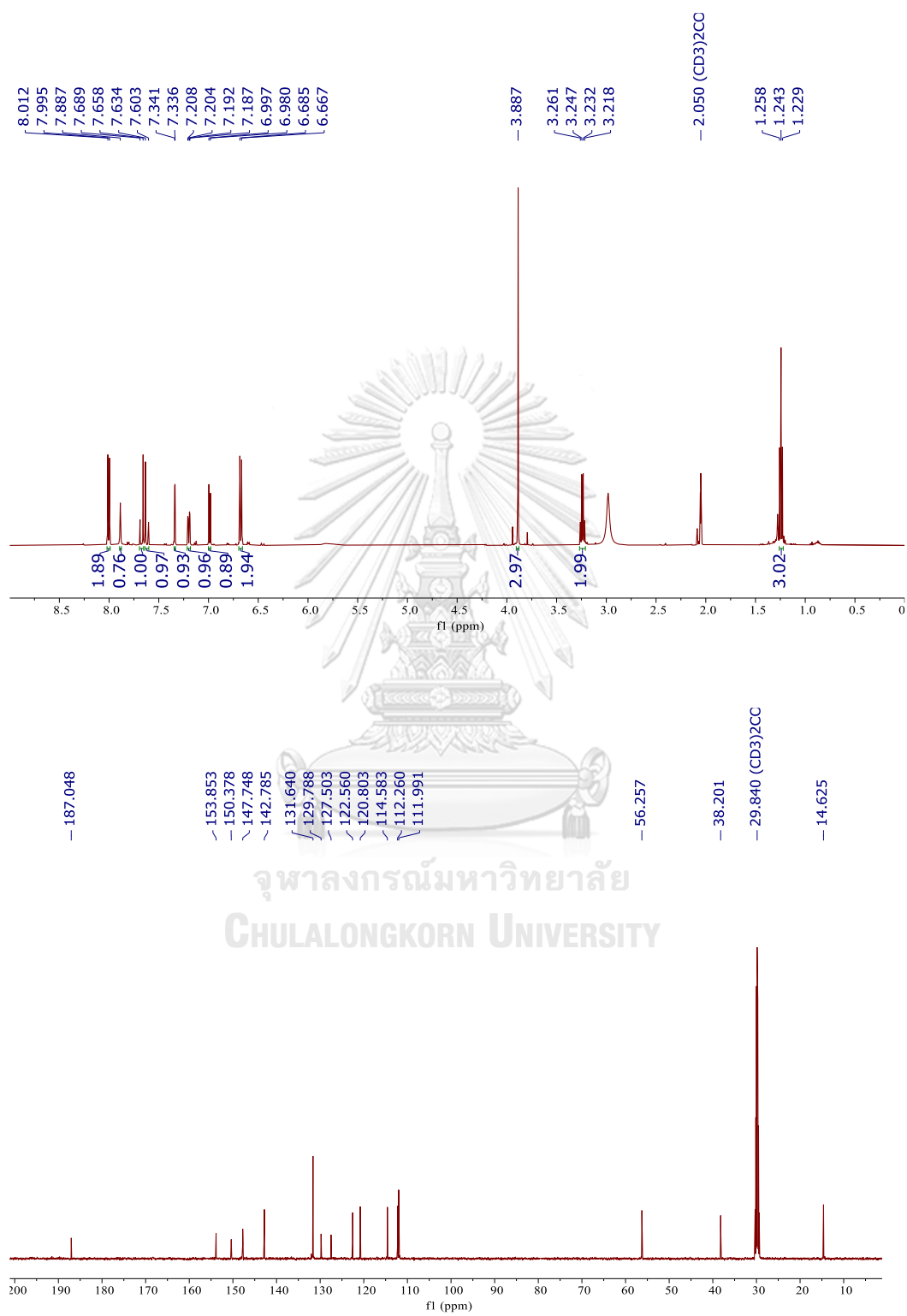
Operator CU.

Instrument micrOTOF-Q II



90. ^1H (500 MHz) and ^{13}C (125 MHz) NMR Spectra in acetone- d_6 of **86**

91. ^1H (500 MHz) and ^{13}C (125 MHz) NMR Spectra in acetone- d_6 of **89** (new compound)



92. Mass Spectra of 89 (new compound)

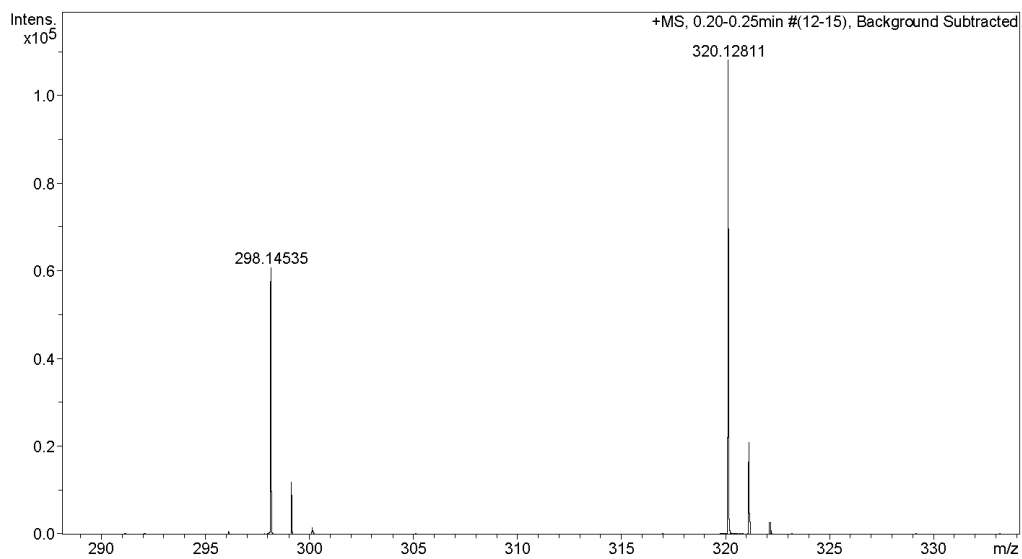
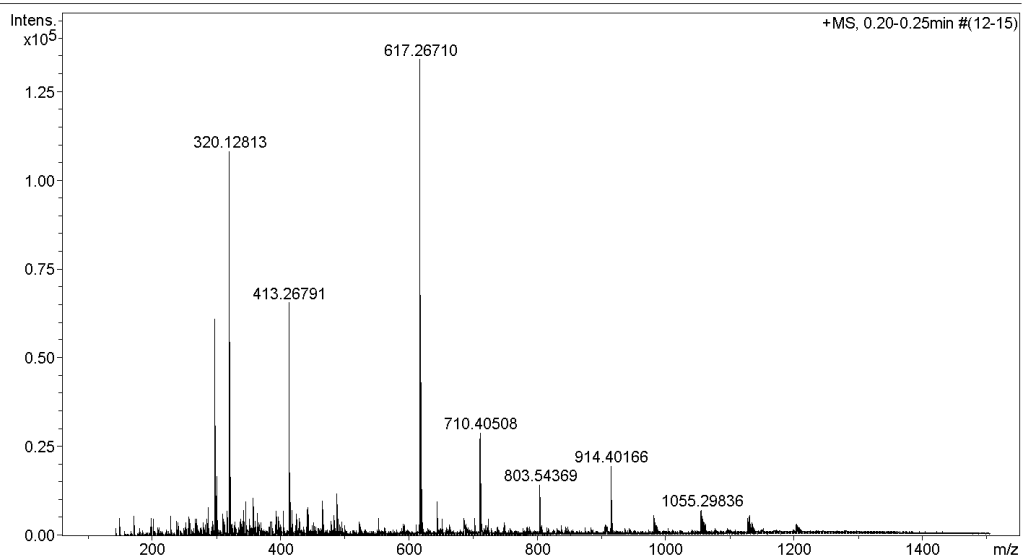
Generic Display Report

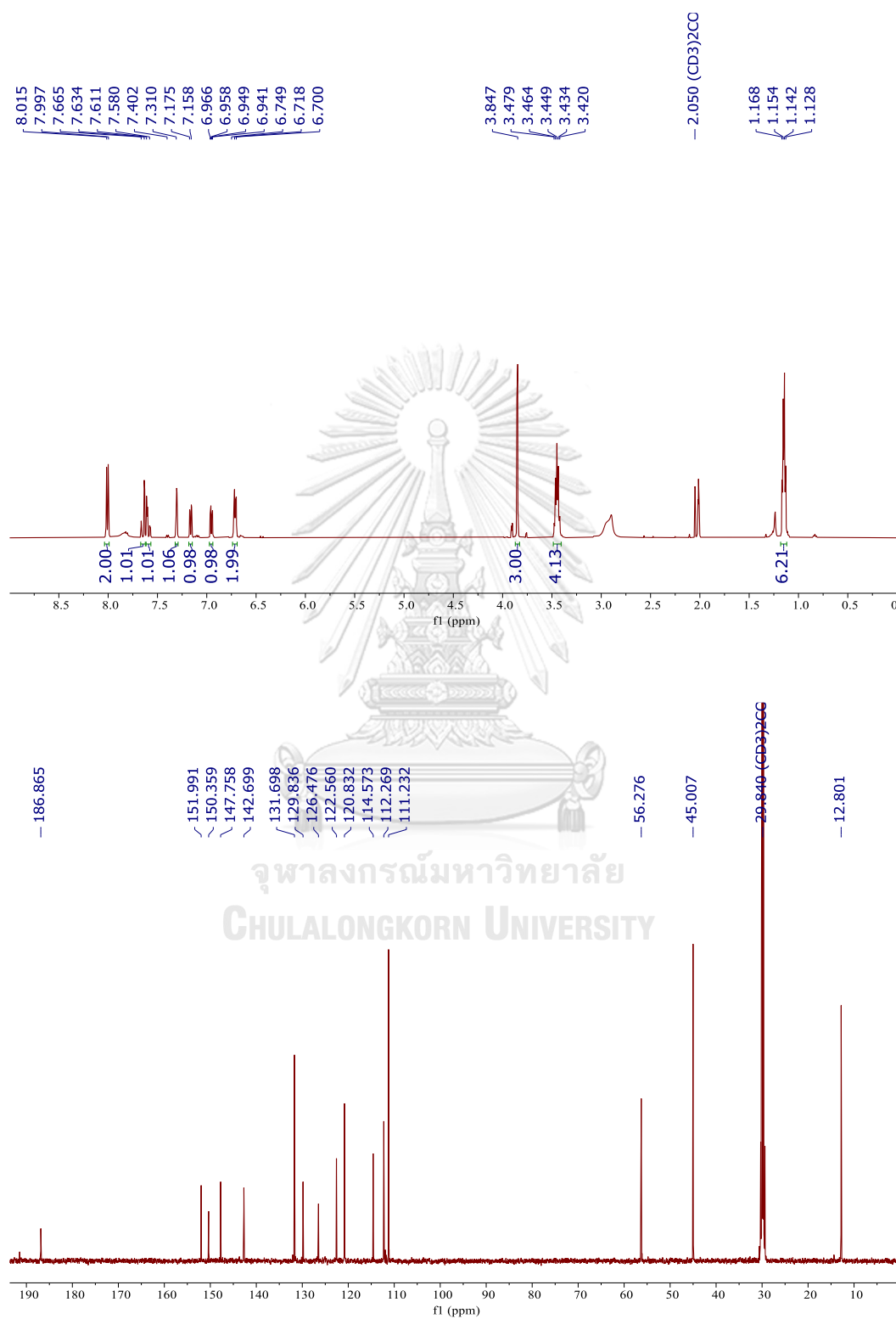
Analysis Info

Analysis Name D:\Data\Data Service\201123\MEAC_RA5_01_4887.d
Method nv_pos_5min_profile_190214.m
Sample Name MEAC
Comment

Acquisition Date 11/23/2020 3:44:37 PM

Operator CU.
Instrument micrOTOF-Q II



93. ^1H (500 MHz) and ^{13}C (125 MHz) NMR Spectra in acetone- d_6 of **90** (new compound)

94. Mass Spectra of 90 (new compound)

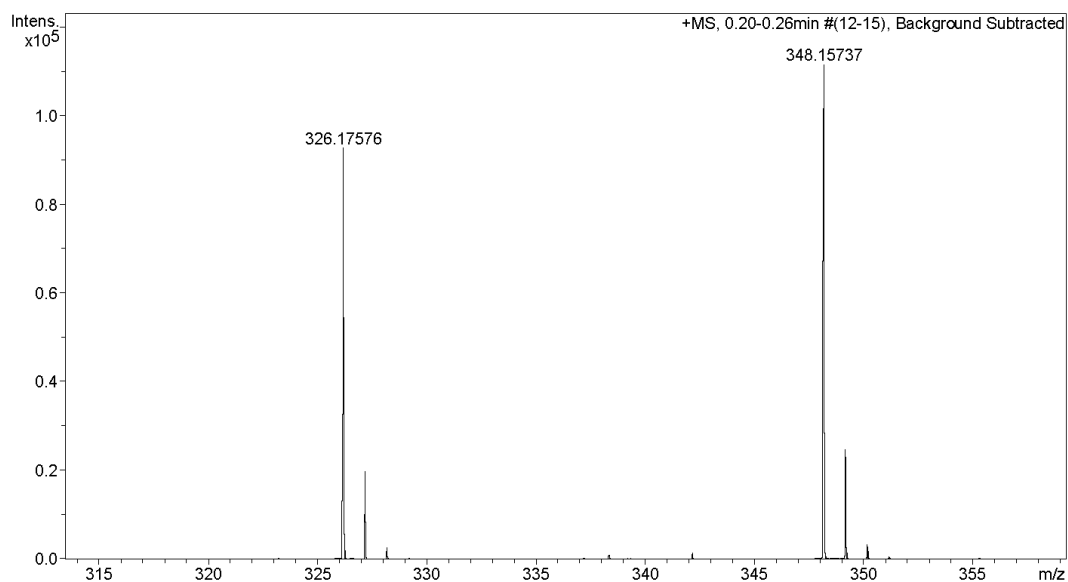
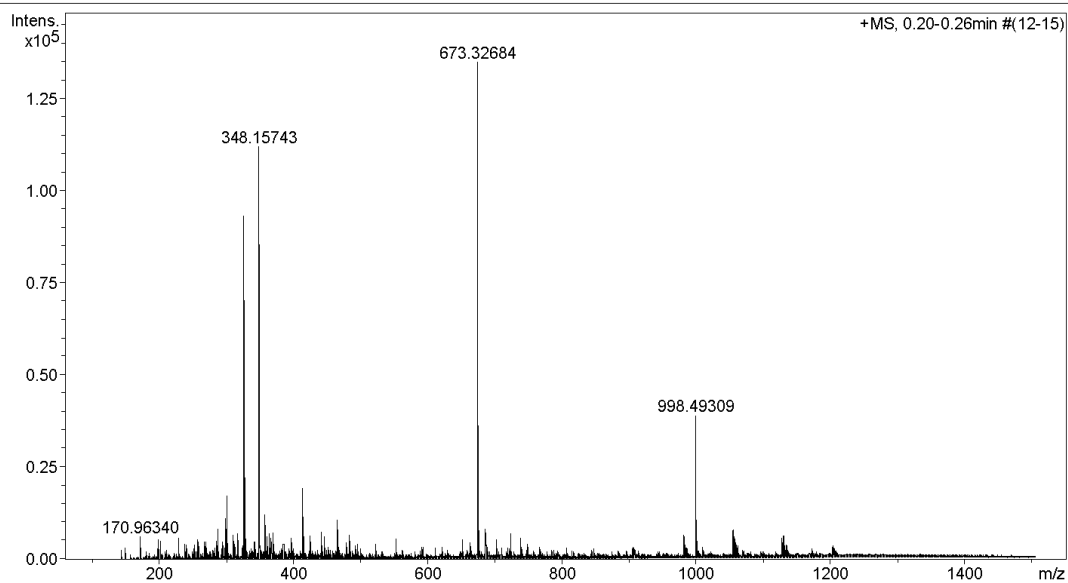
Generic Display Report

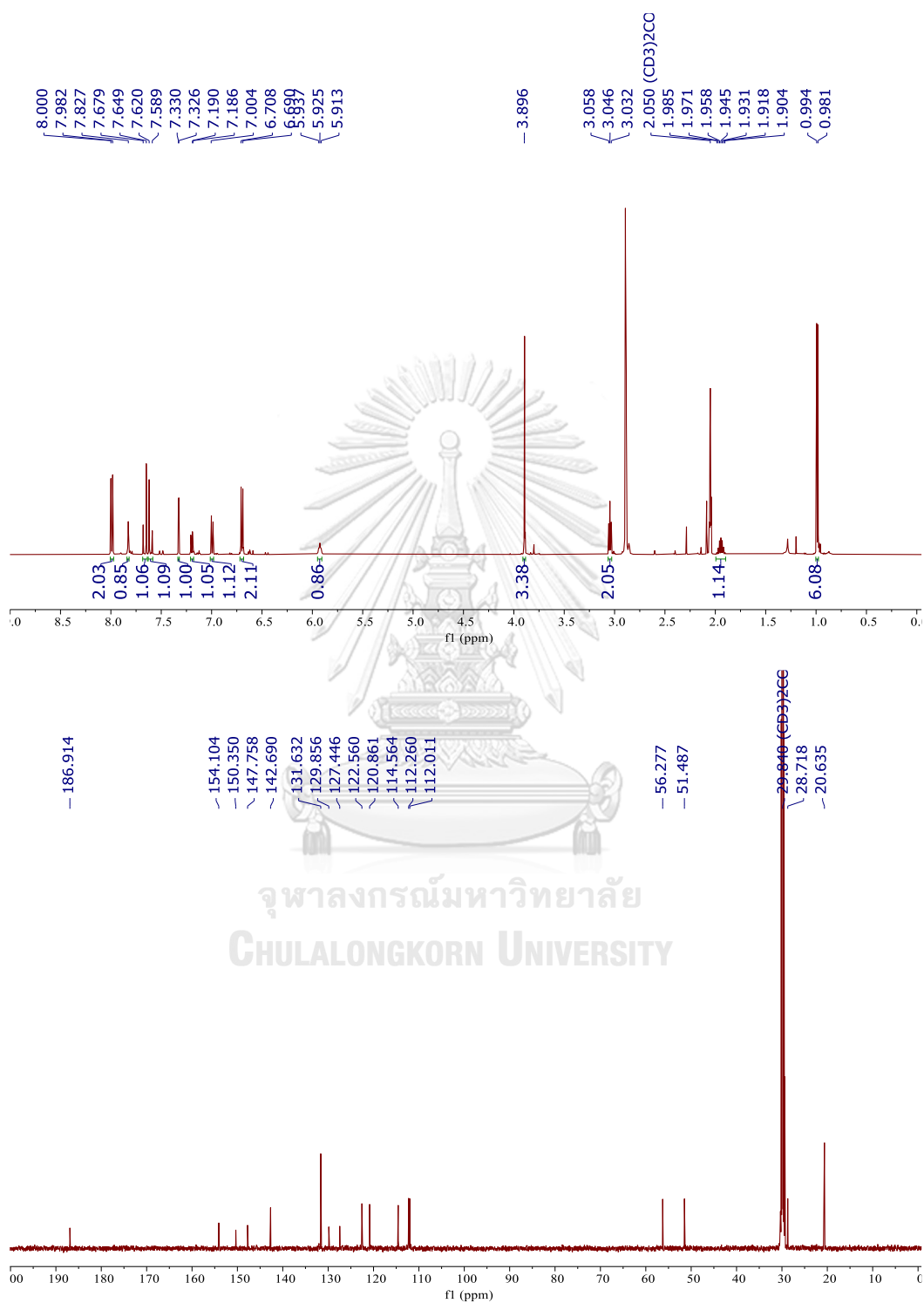
Analysis Info

Analysis Name D:\Data\Data Service\201123\DEAC_RA4_01_4885.d
Method nv_pos_5min_profile_190214.m
Sample Name DEAC
Comment

Acquisition Date 11/23/2020 3:31:22 PM

Operator CU.
Instrument micrOTOF-Q II



95. ^1H (500 MHz) and ^{13}C (125 MHz) NMR Spectra in acetone- d_6 of **91** (new compound)

96. Mass Spectra of 91 (new compound)

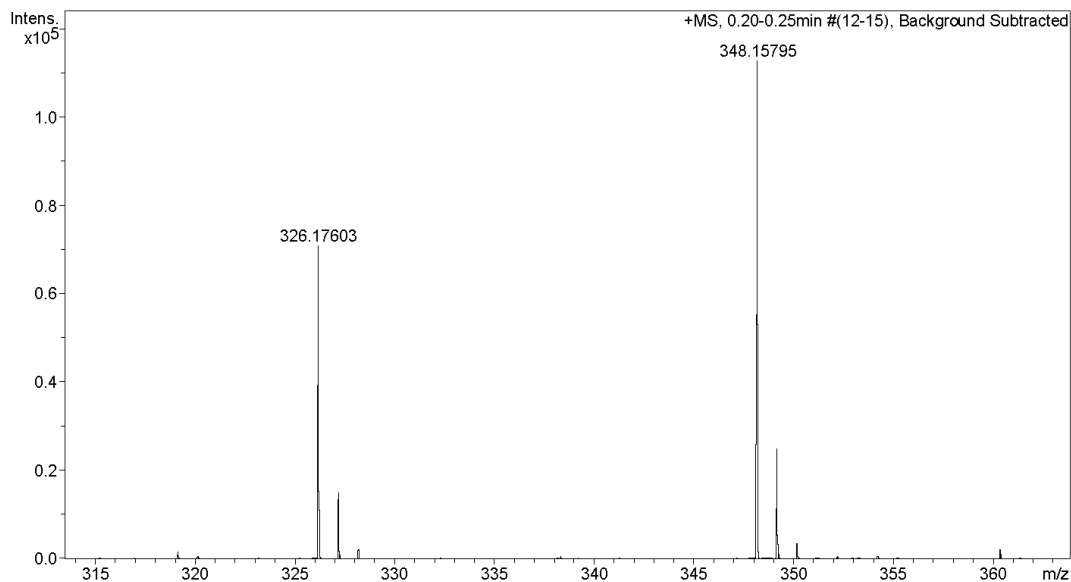
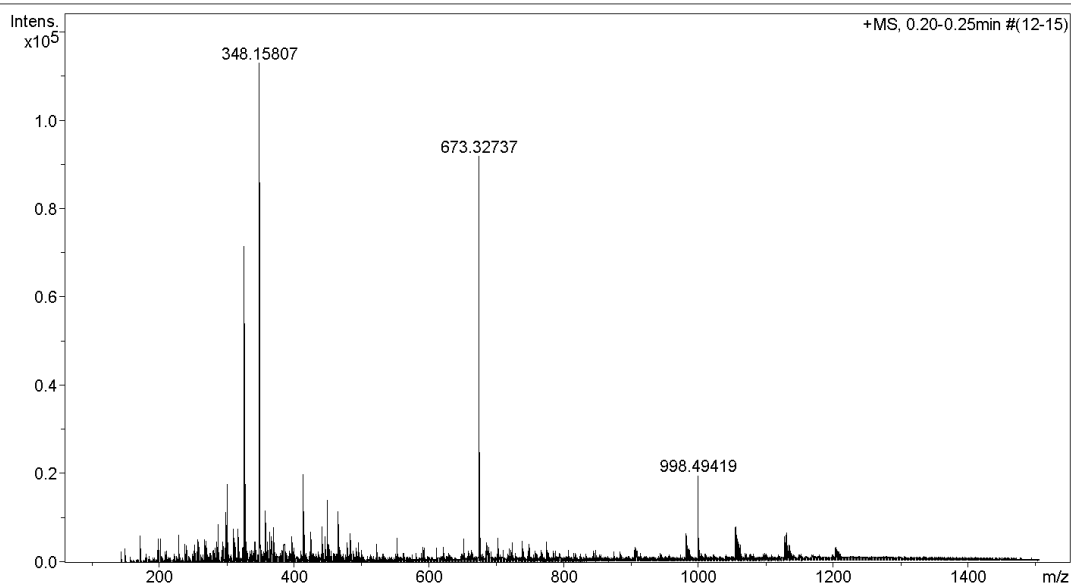
Generic Display Report

Analysis Info

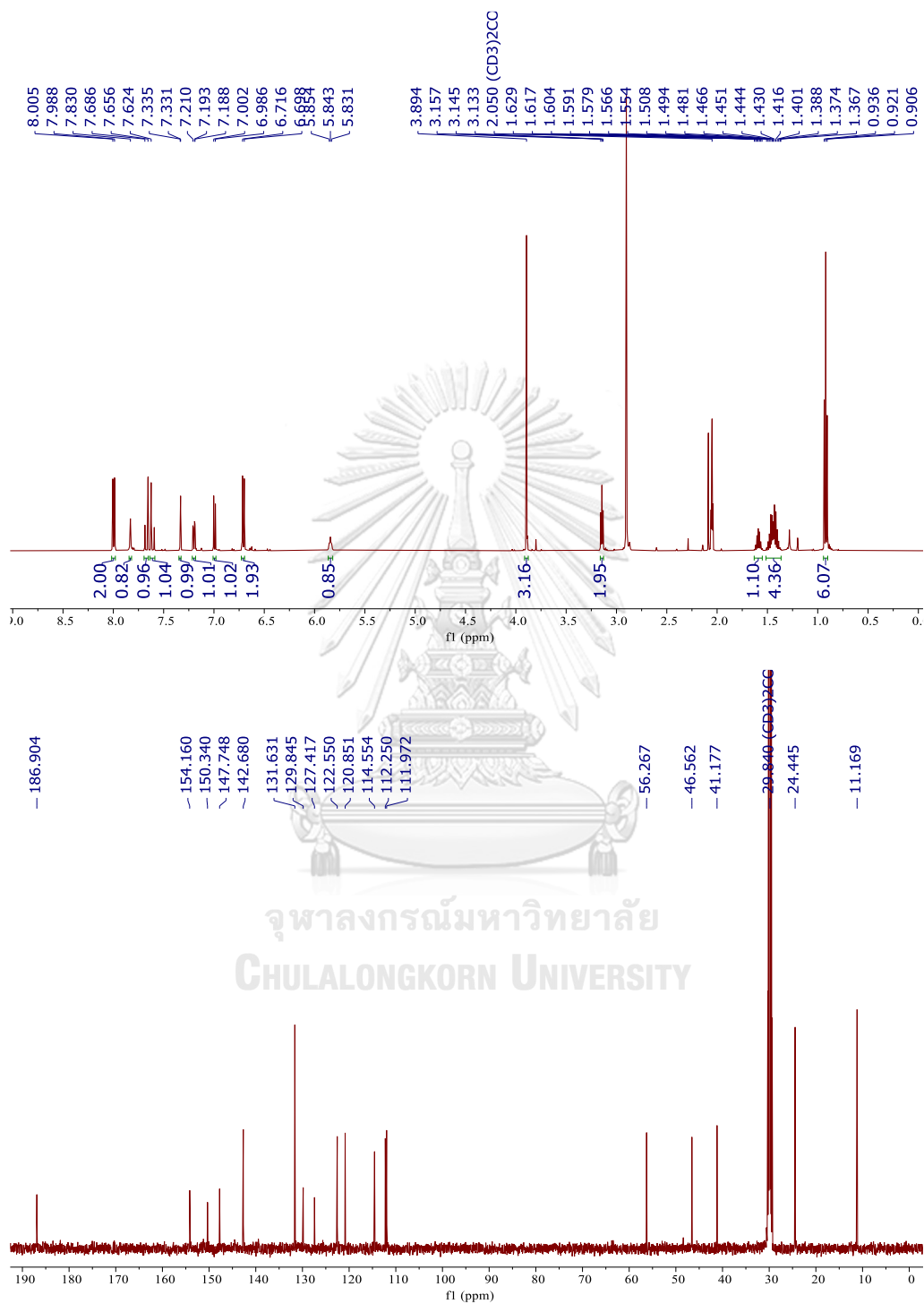
Analysis Name D:\Data\Data Service\201123\BAC_RA3_01_4884.d
Method nv_pos_5min_profile_190214.m
Sample Name IBAC
Comment

Acquisition Date 11/23/2020 3:25:04 PM

Operator CU.
Instrument micrOTOF-Q II



97. ^1H (500 MHz) and ^{13}C (125 MHz) NMR Spectra in acetone- d_6 of 92 (new compound)



98. Mass Spectra of 92 (new compound)

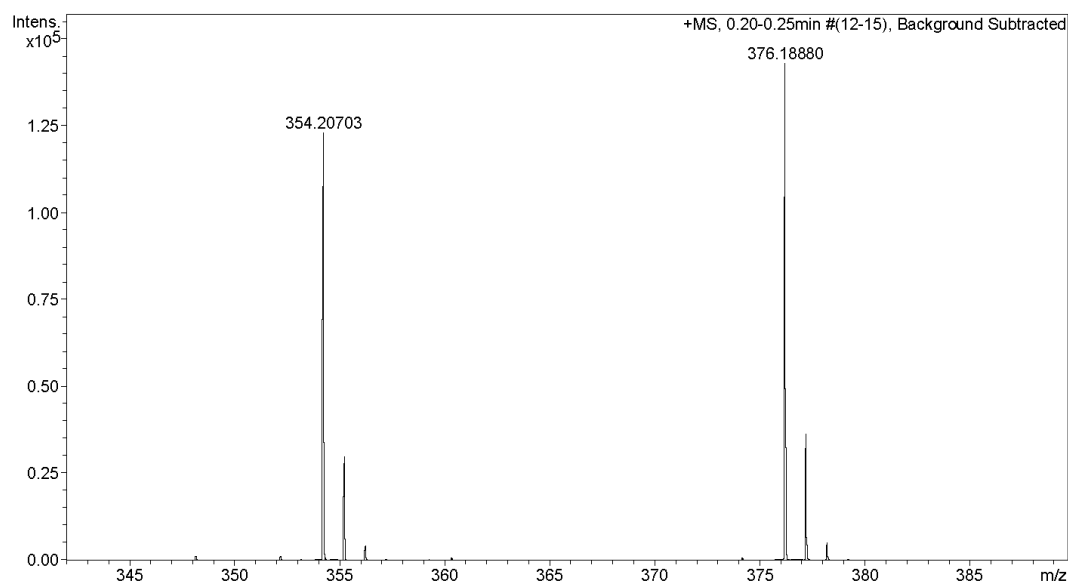
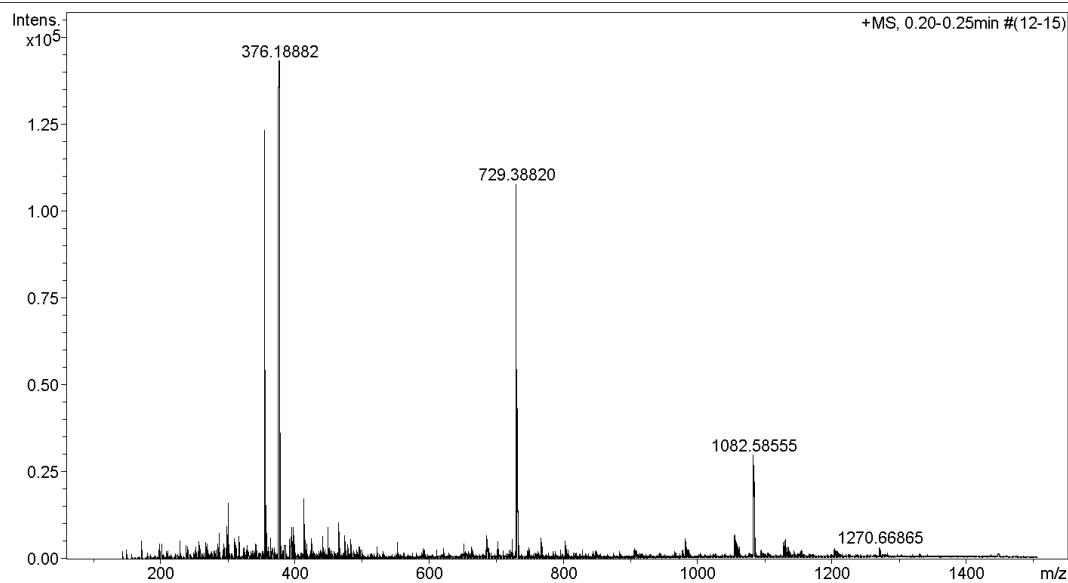
Generic Display Report

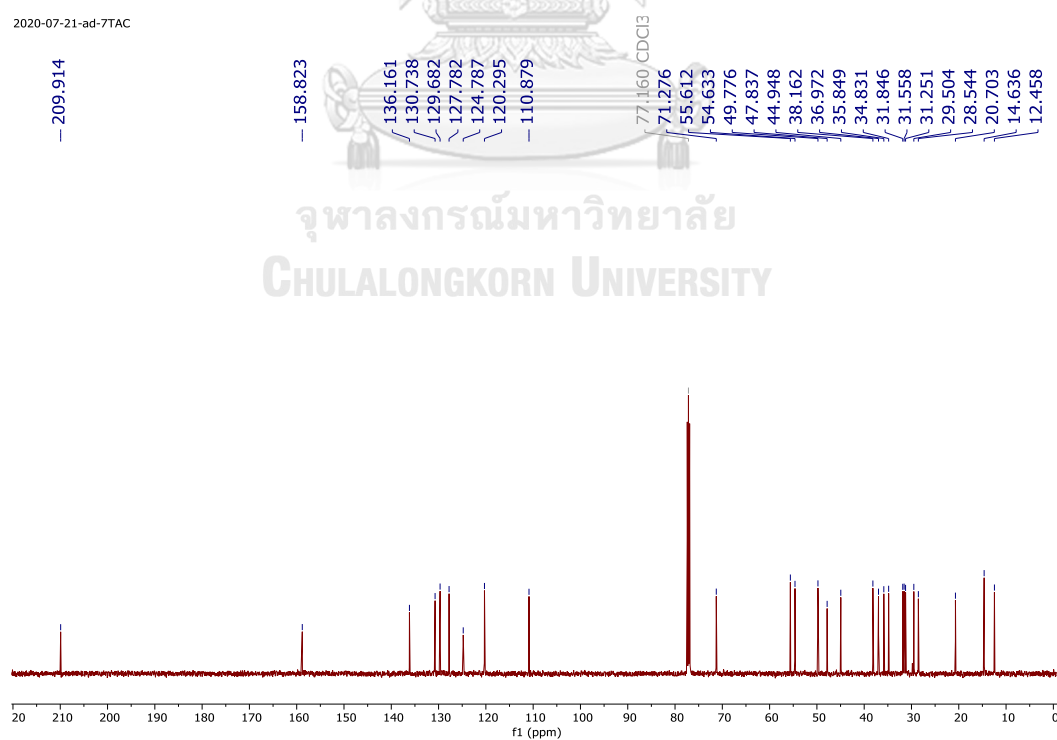
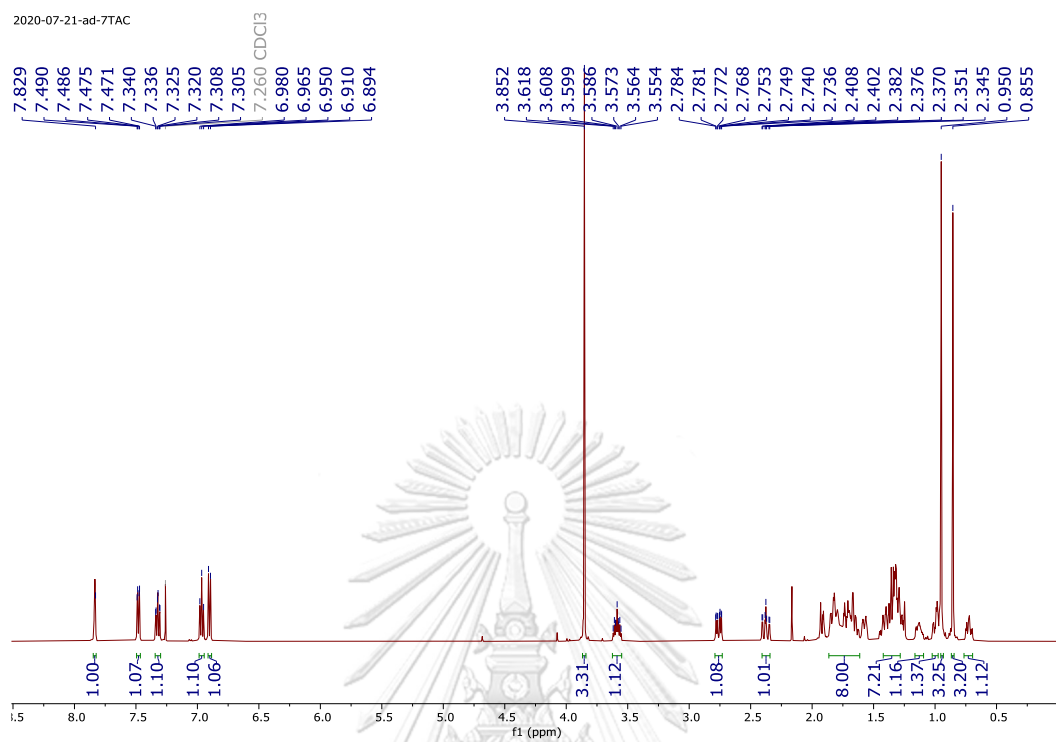
Analysis Info

Analysis Name D:\Data\Data Service\201123\EBAC_RA2_01_4883.d
Method nv_pos_5min_profile_190214.m
Sample Name EBAC
Comment

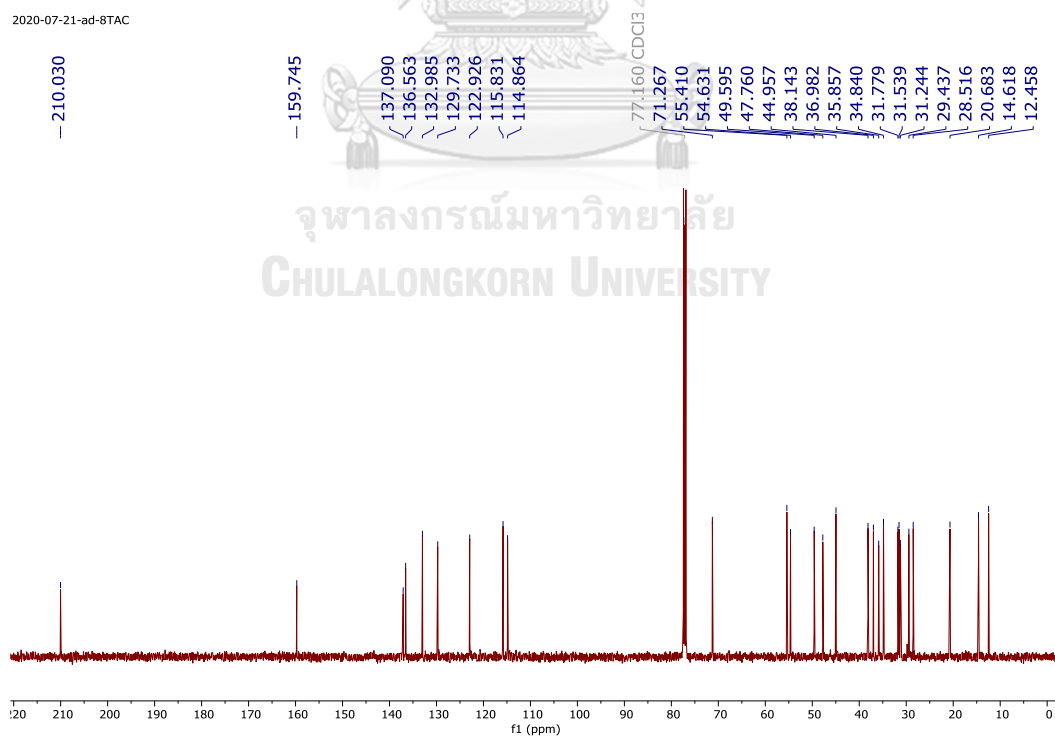
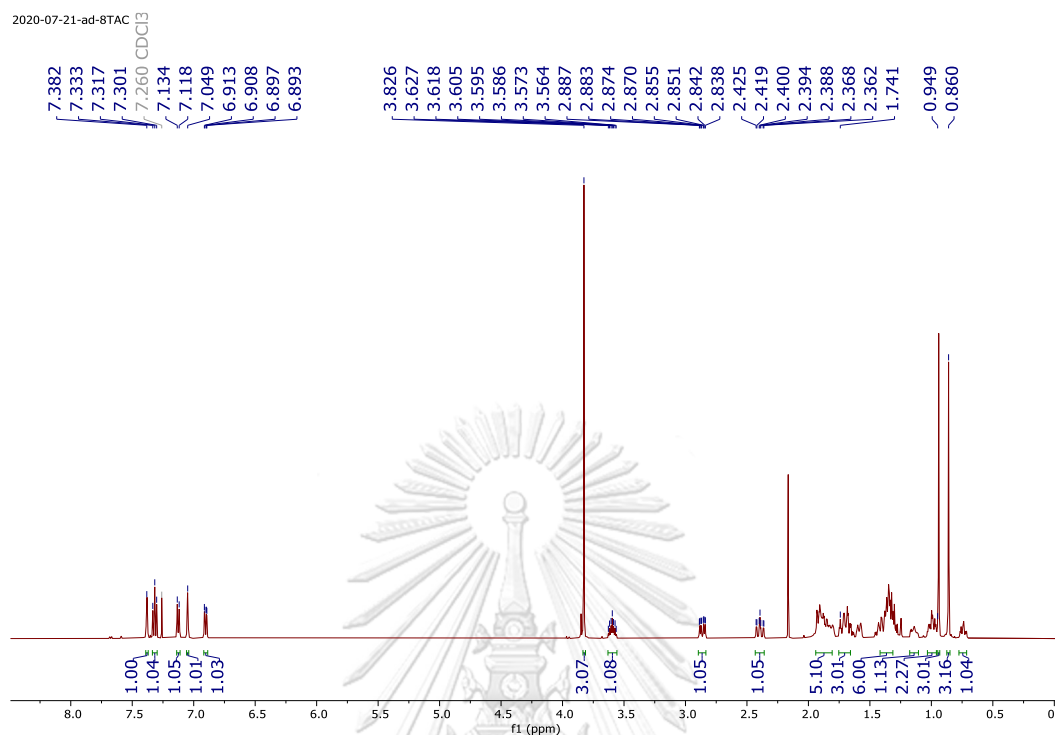
Acquisition Date 11/23/2020 3:18:46 PM

Operator CU.
Instrument micrOTOF-Q II



99. ^1H (500 MHz) and ^{13}C (125 MHz) NMR Spectra in CDCl_3 of 93

100. ^1H (500 MHz) and ^{13}C (125 MHz) NMR Spectra in CDCl_3 of **94** (new compound)



101. Mass Spectra of 94 (new compound)

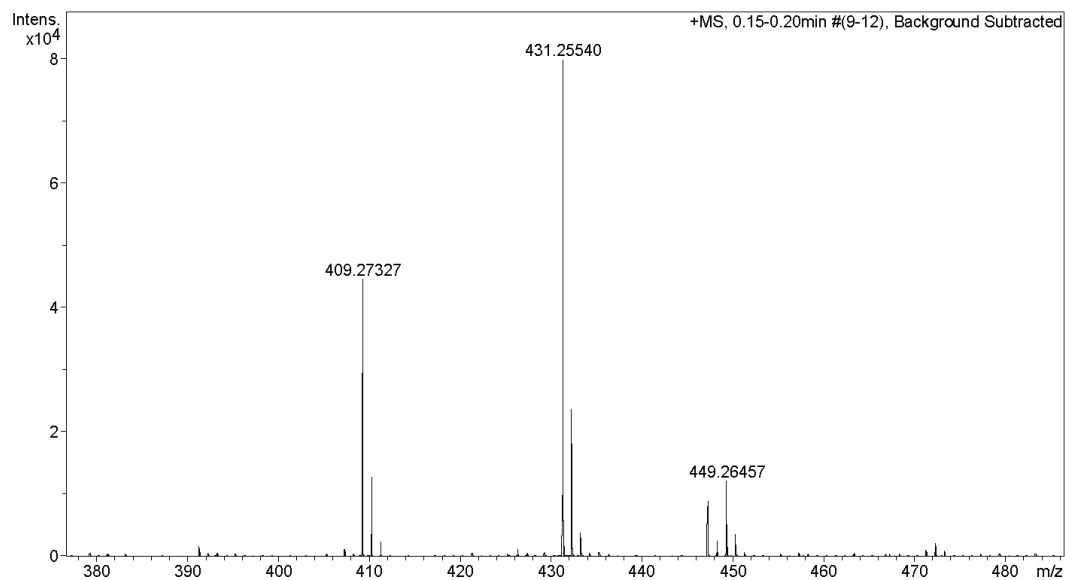
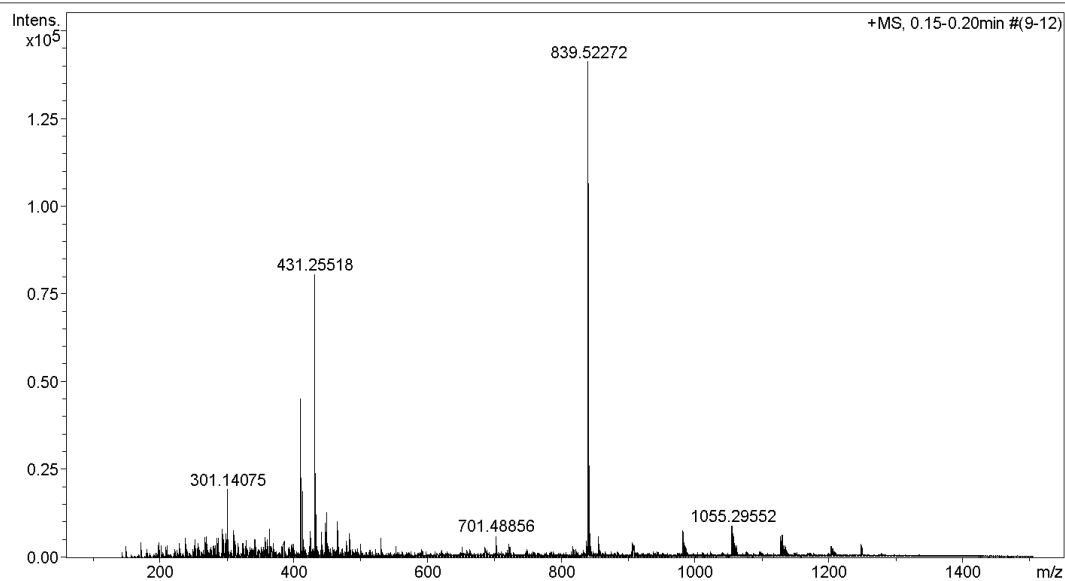
Generic Display Report

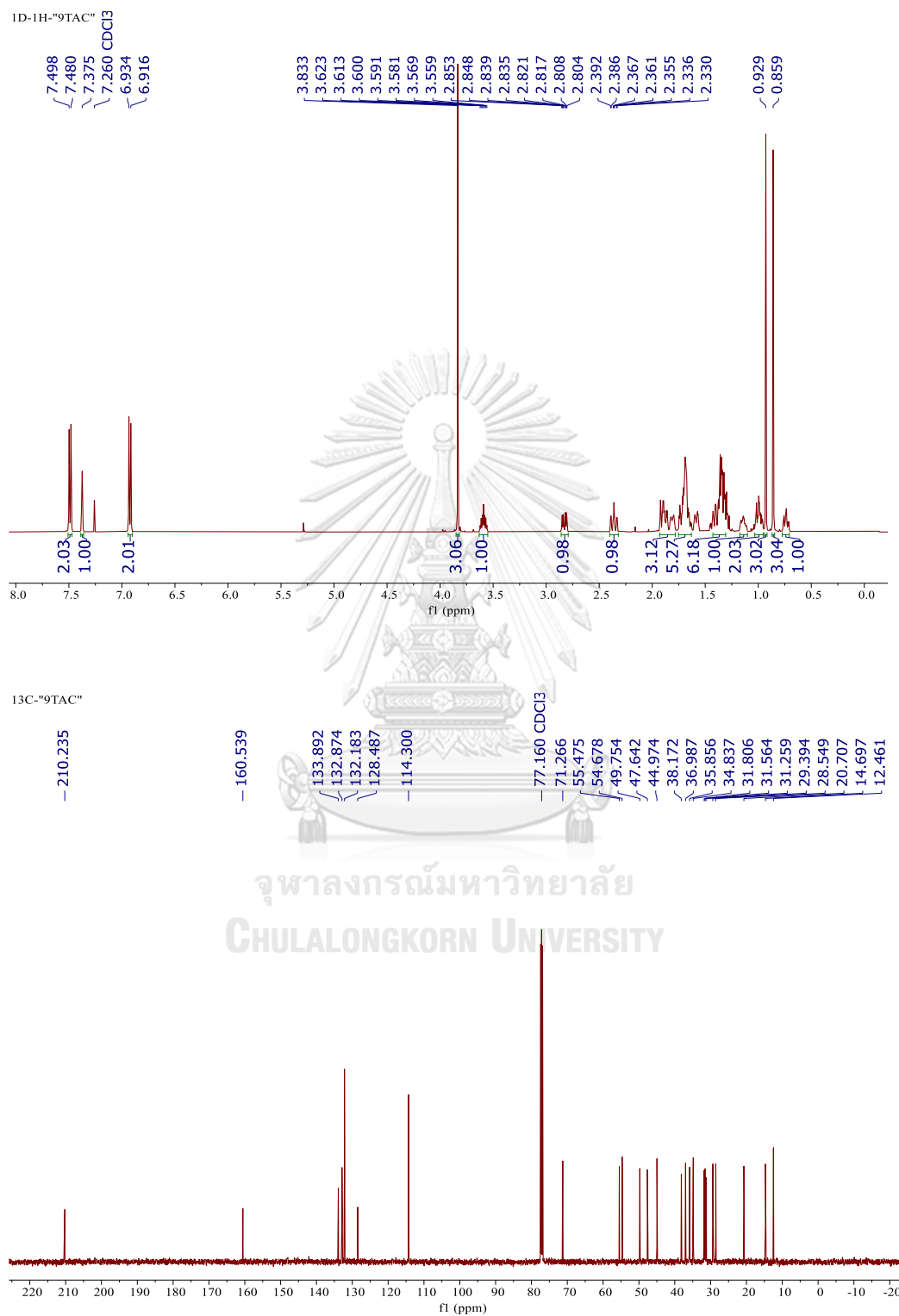
Analysis Info

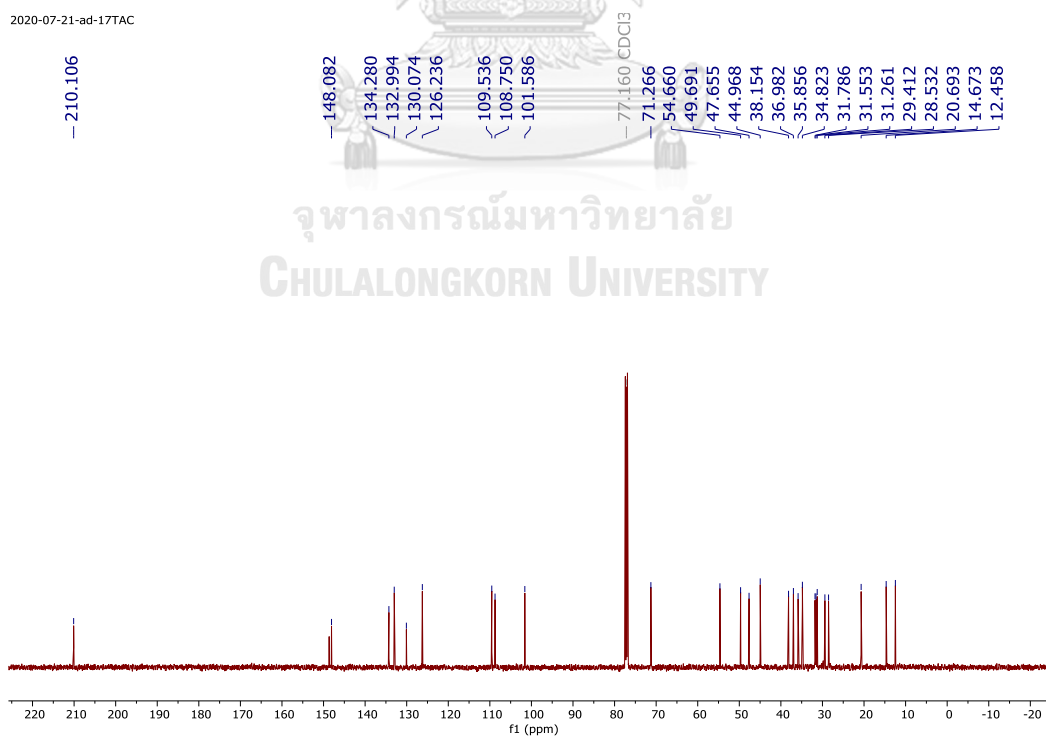
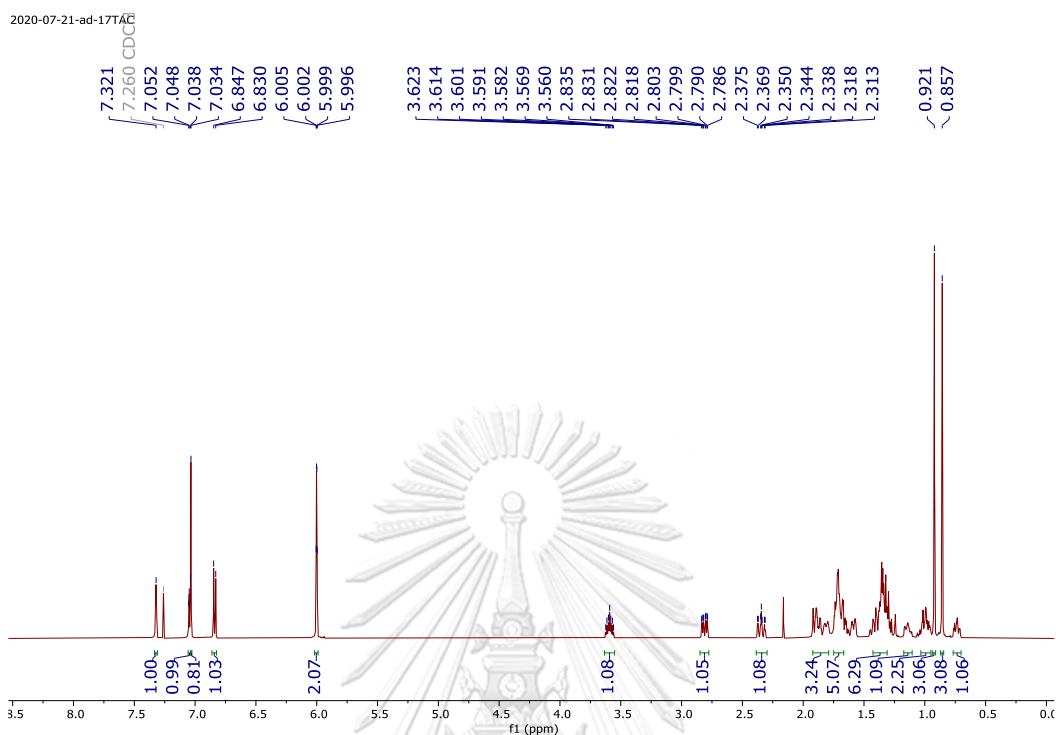
Analysis Name D:\Data\Data Service\201123\8TAC_RC7_01_4905.d
Method nv_pos_5min_profile_190214.m
Sample Name 8TAC
Comment

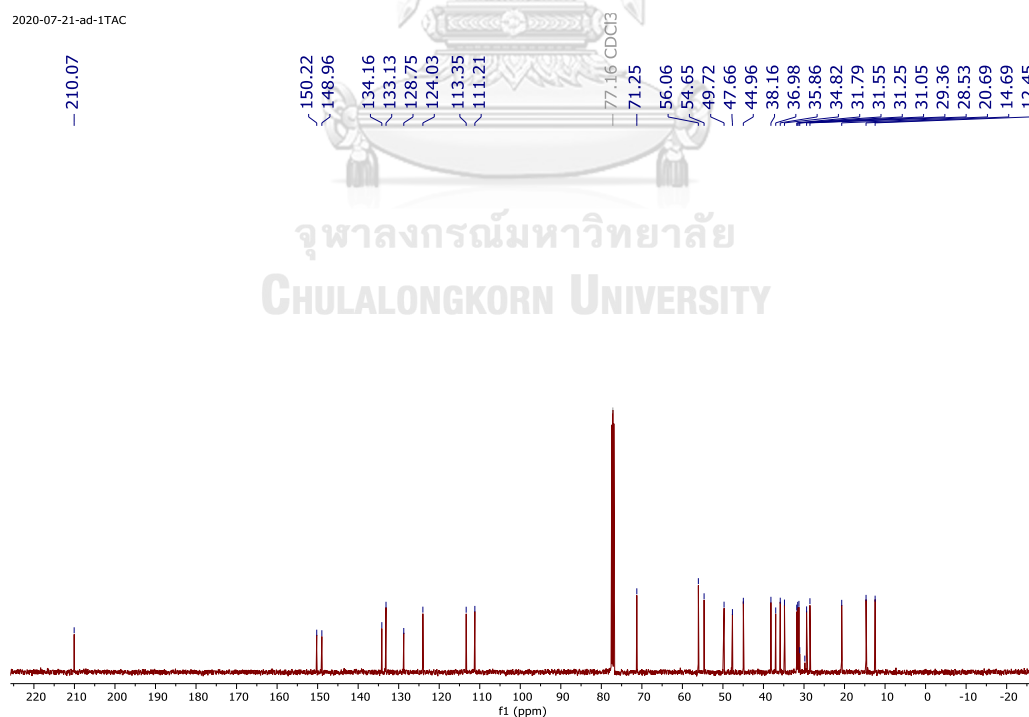
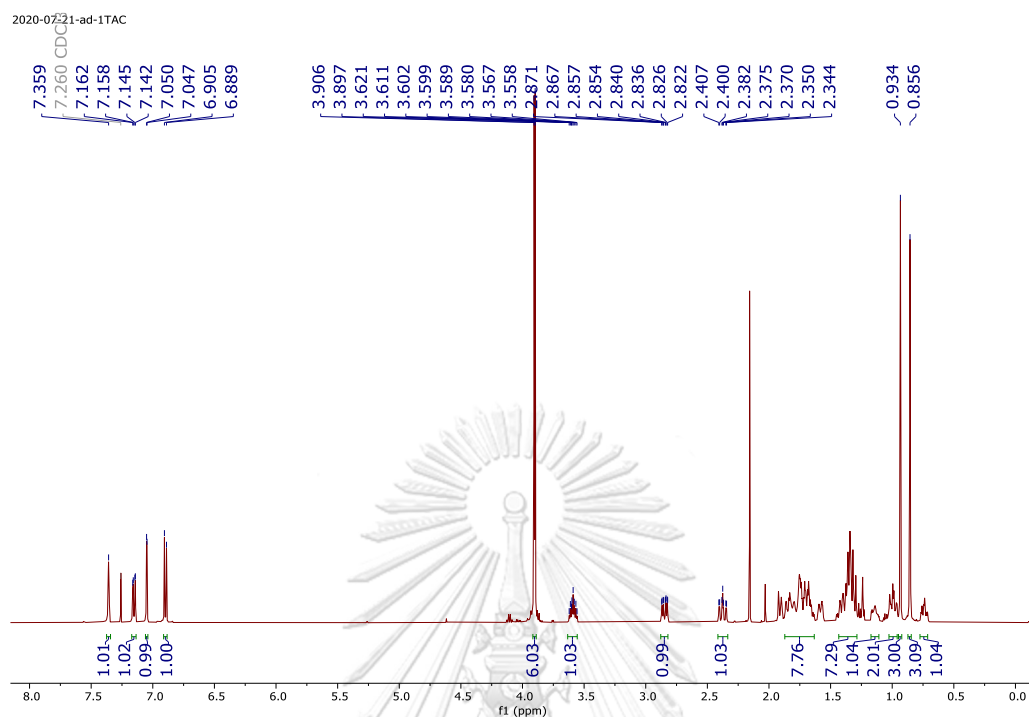
Acquisition Date 11/23/2020 5:39:55 PM

Operator CU.
Instrument micrOTOF-Q II



102. ^1H (500 MHz) and ^{13}C (125 MHz) NMR Spectra in CDCl_3 of **95**

103. ^1H (500 MHz) and ^{13}C (125 MHz) NMR Spectra in CDCl_3 of **96**

104. ^1H (500 MHz) and ^{13}C (125 MHz) NMR Spectra in CDCl_3 of **97** (new compound)

105. Mass Spectra of 97 (new compound)

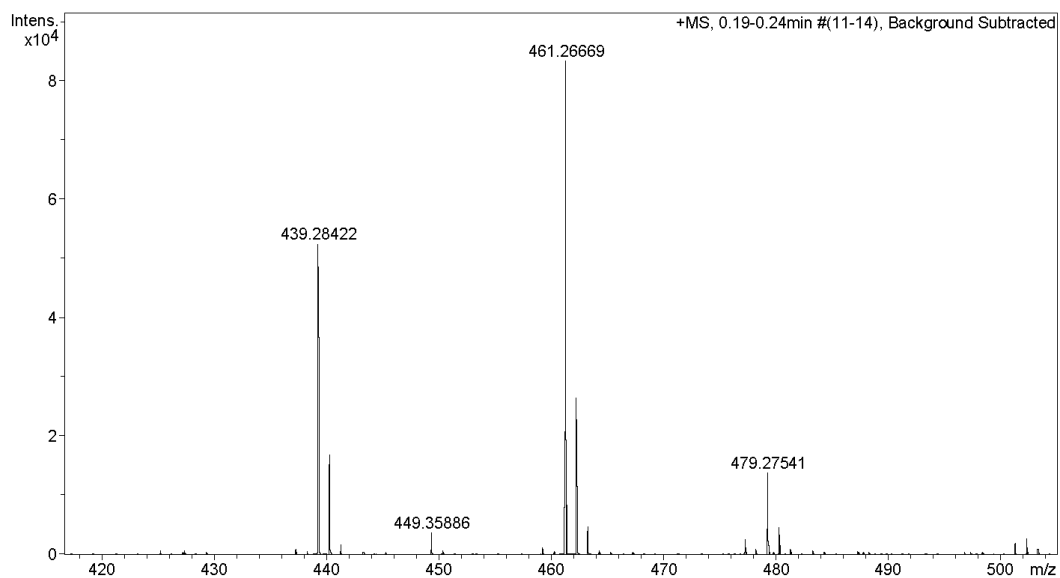
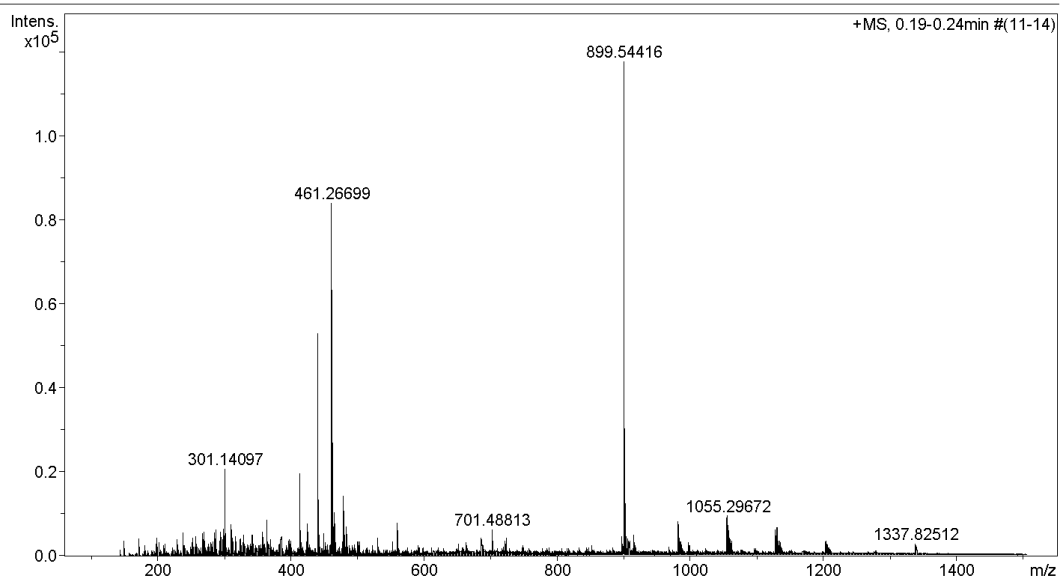
Generic Display Report

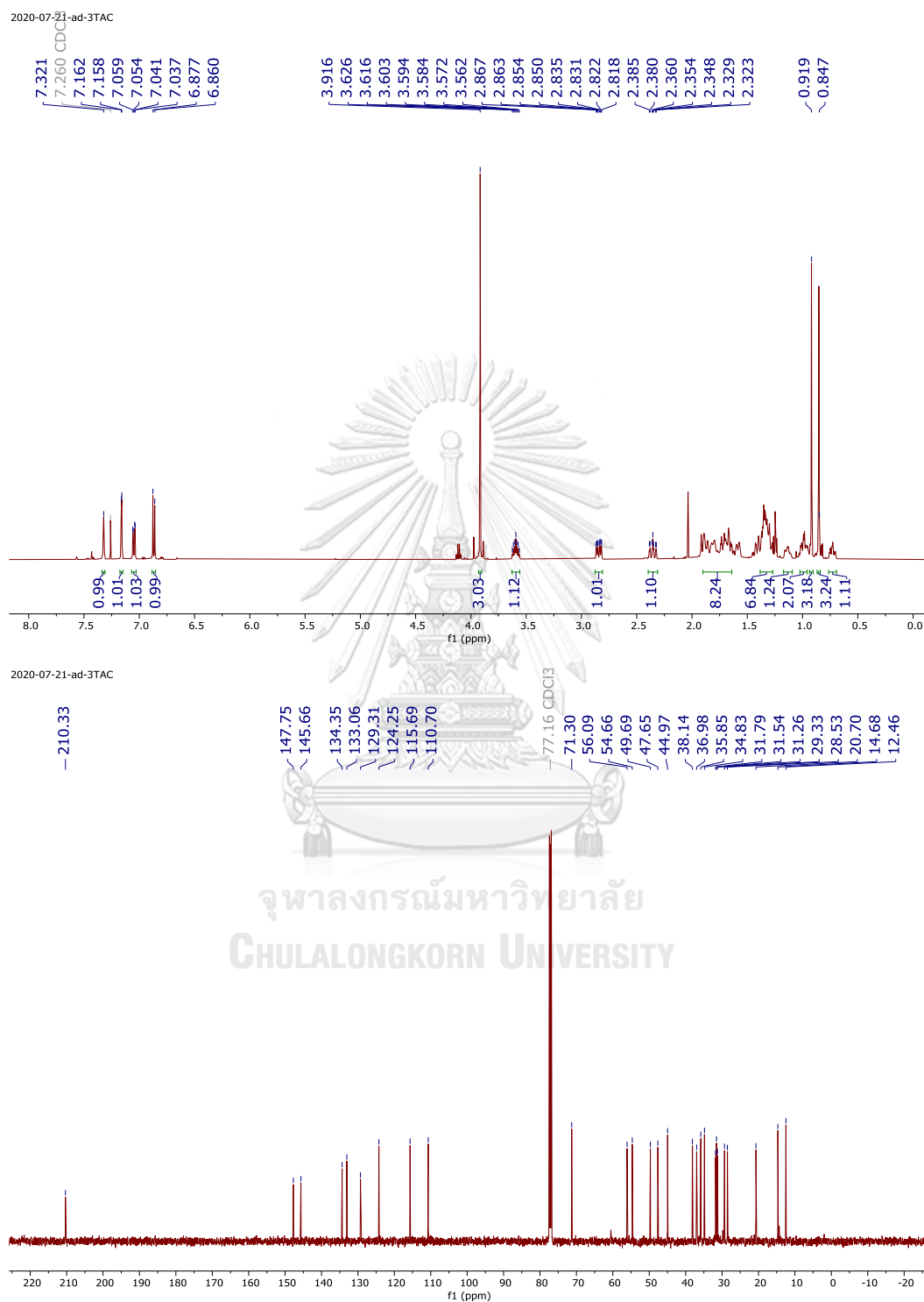
Analysis Info

Analysis Name D:\Data\Data Service\201123\1TAC_RC6_01_4904.d
Method nv_pos_5min_profile_190214.m
Sample Name 1TAC
Comment

Acquisition Date 11/23/2020 5:33:30 PM

Operator CU.
Instrument micrOTOF-Q II



106. ^1H (500 MHz) and ^{13}C (125 MHz) NMR Spectra in CDCl_3 of **98** (new compound)

107. Mass Spectra of 98 (new compound)

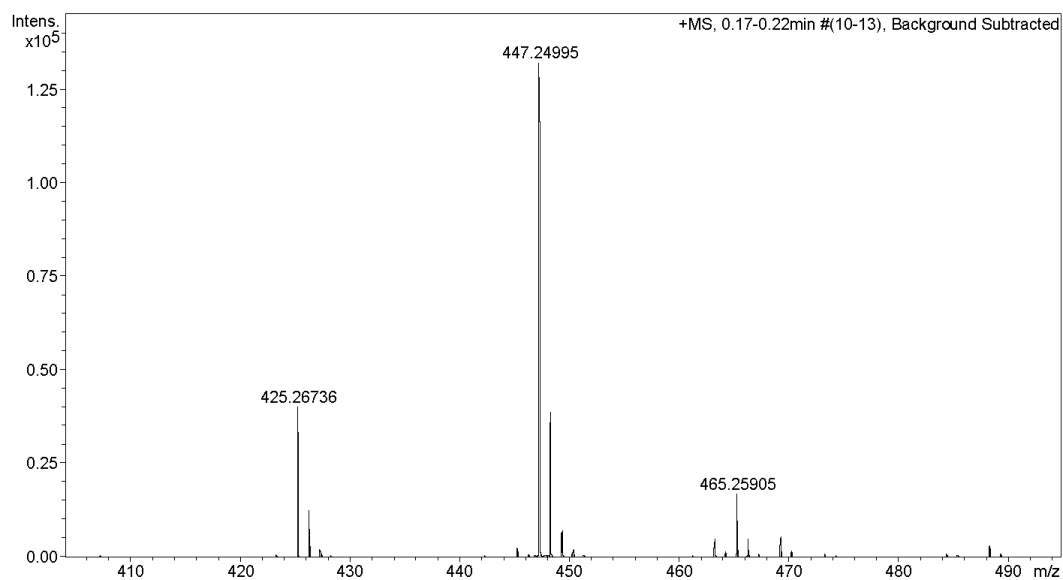
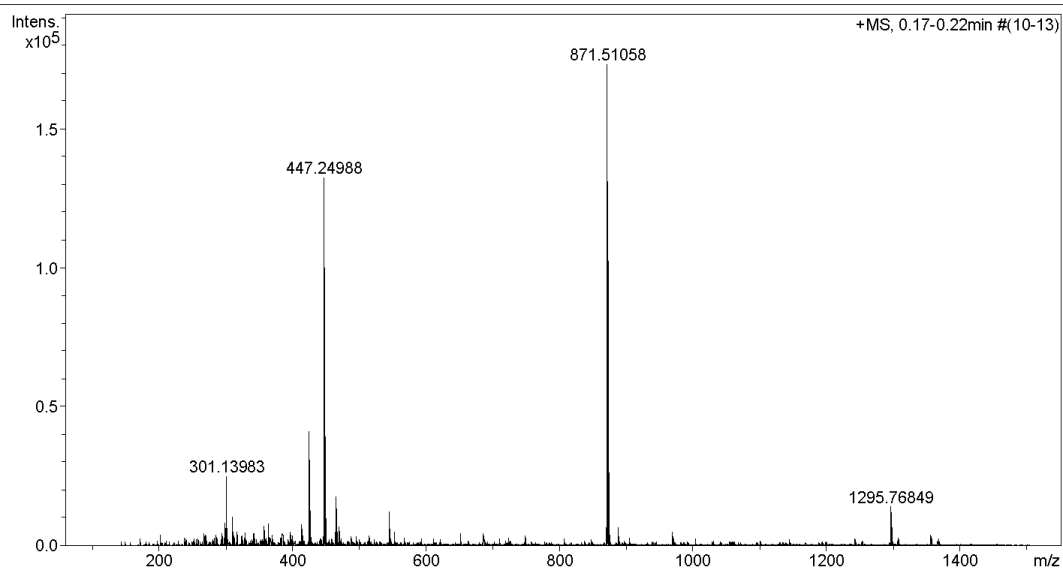
Generic Display Report

Analysis Info

Analysis Name D:\Data\Data Service\201221\3TAC_RA6_01_5077.d
Method nv_pos_5min_profile_190214.m
Sample Name 3TAC
Comment

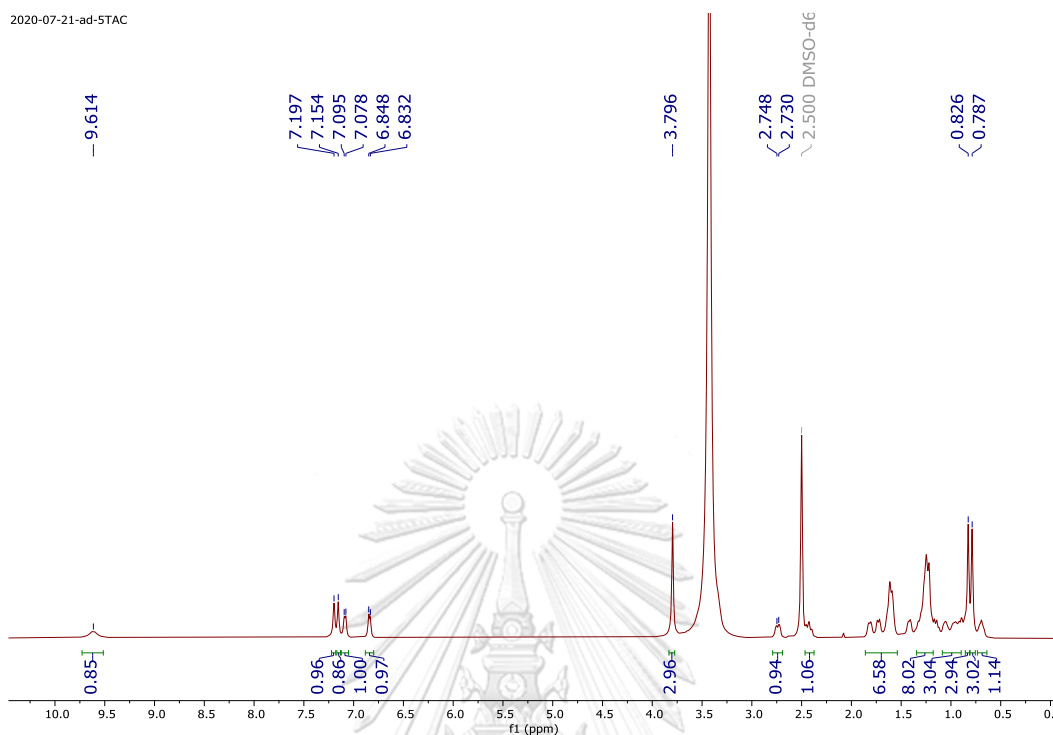
Acquisition Date 12/21/2020 2:08:30 PM

Operator CU.
Instrument micrOTOF-Q II

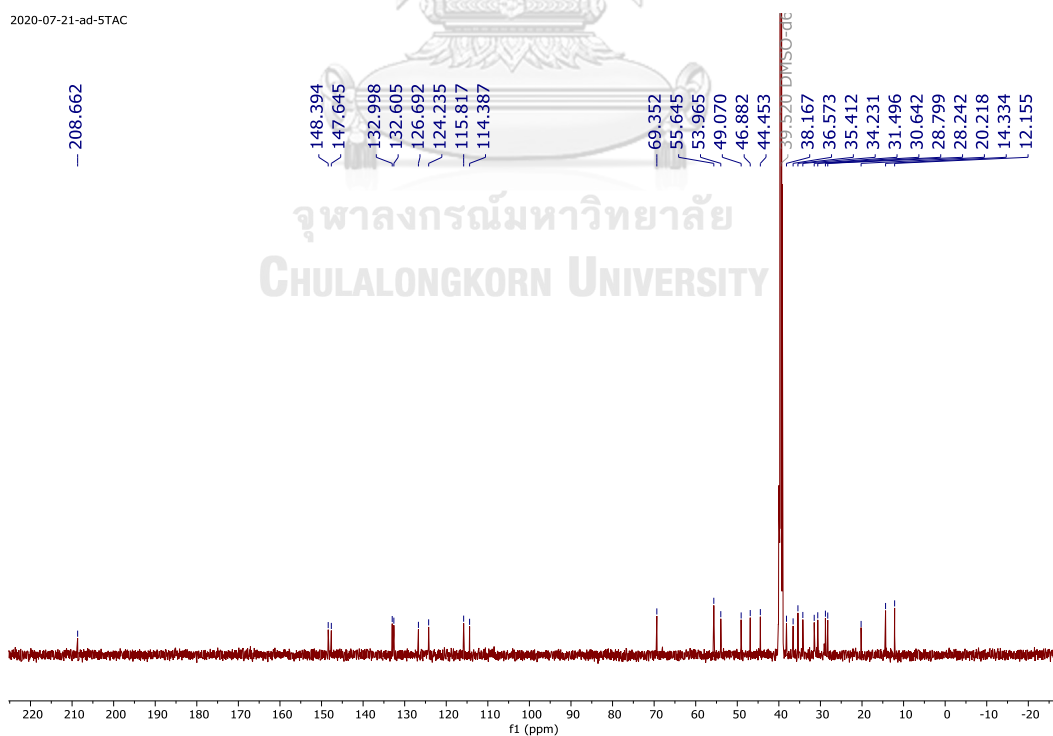


108. ^1H (500 MHz) and ^{13}C (125 MHz) NMR Spectra in DMSO- d_6 of **99**

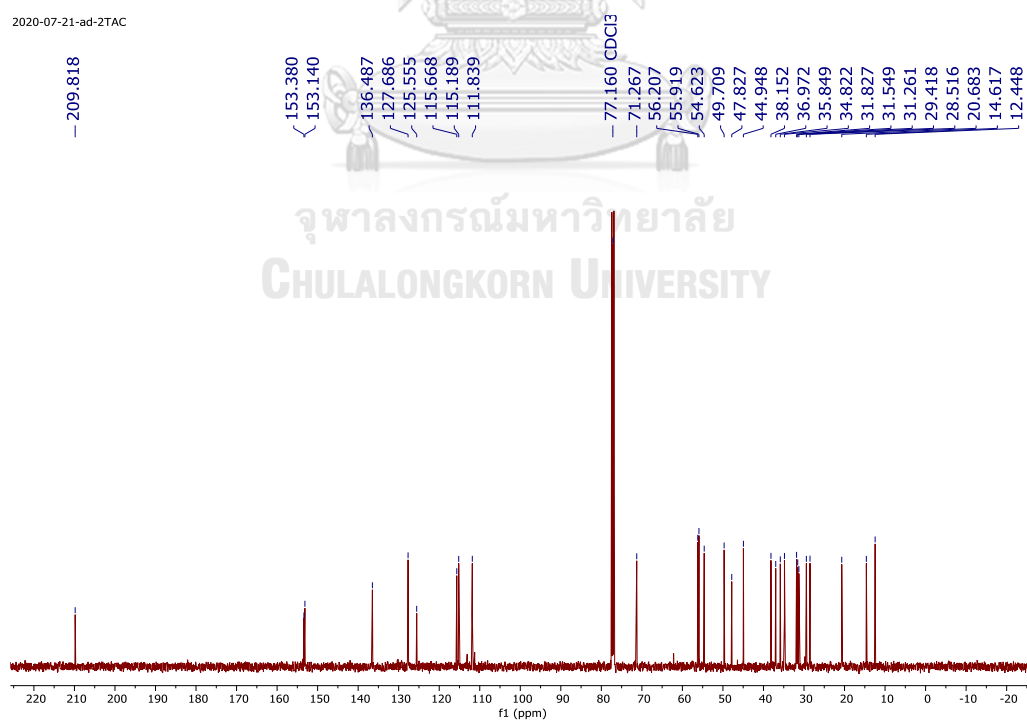
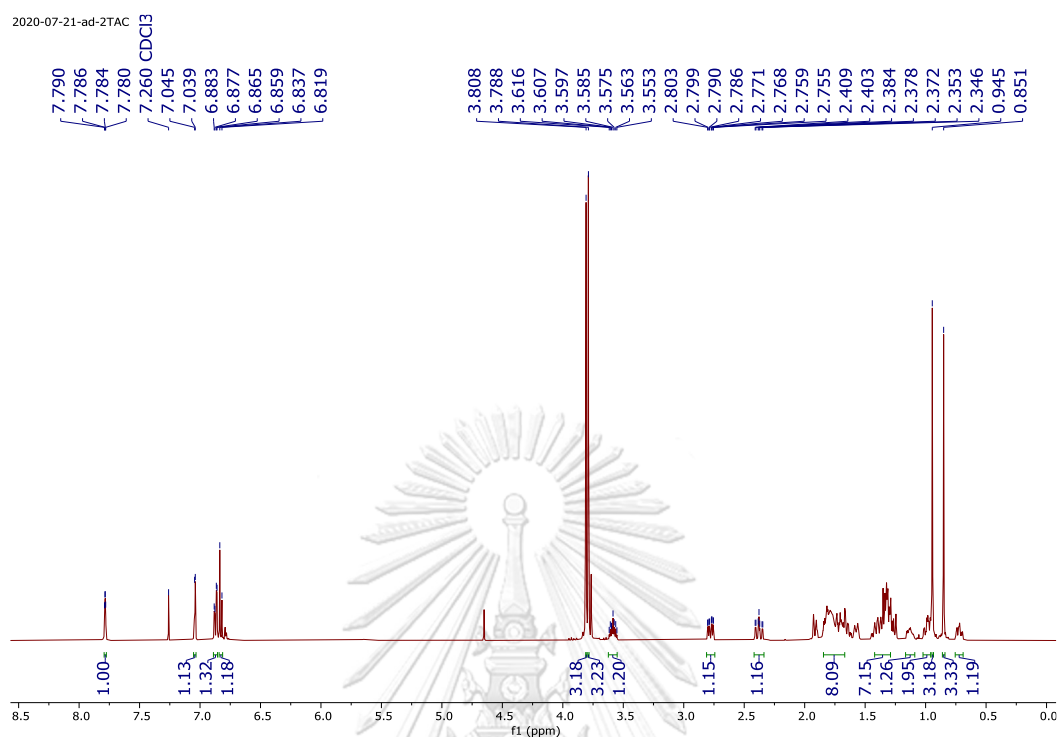
2020-07-21-ad-5TAC



2020-07-21-ad-5TAC



จุฬาลงกรณ์มหาวิทยาลัย
CHULALONGKORN UNIVERSITY

109. ^1H (500 MHz) and ^{13}C (125 MHz) NMR Spectra in CDCl_3 of **100** (new compound)

110. Mass Spectra of 100 (new compound)

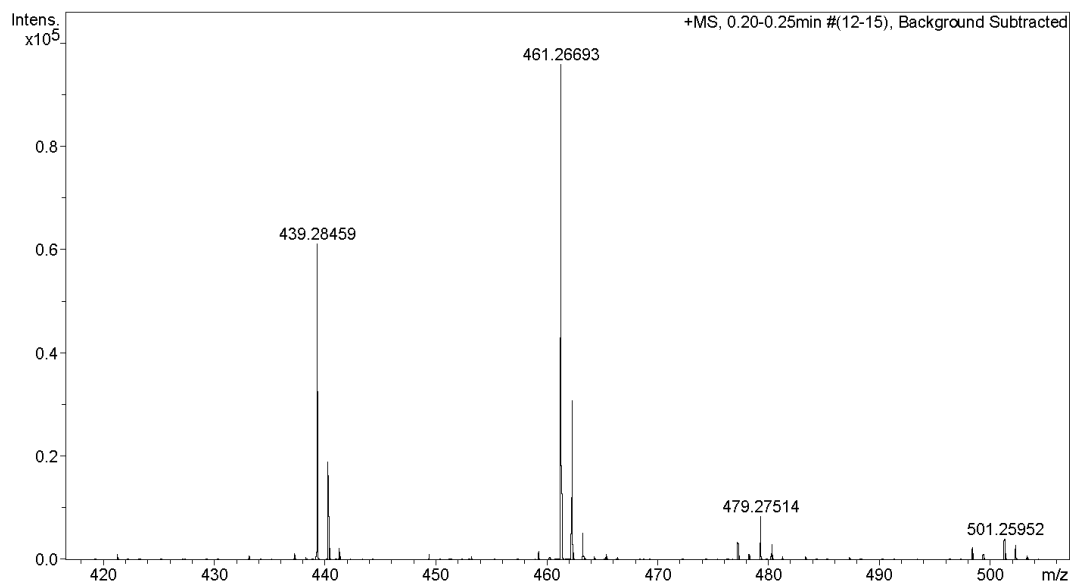
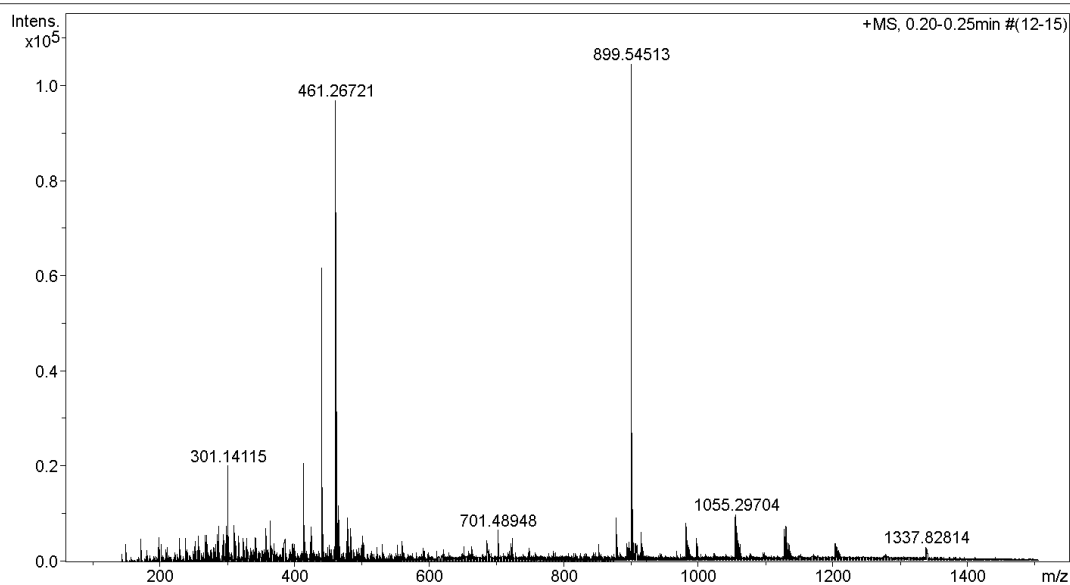
Generic Display Report

Analysis Info

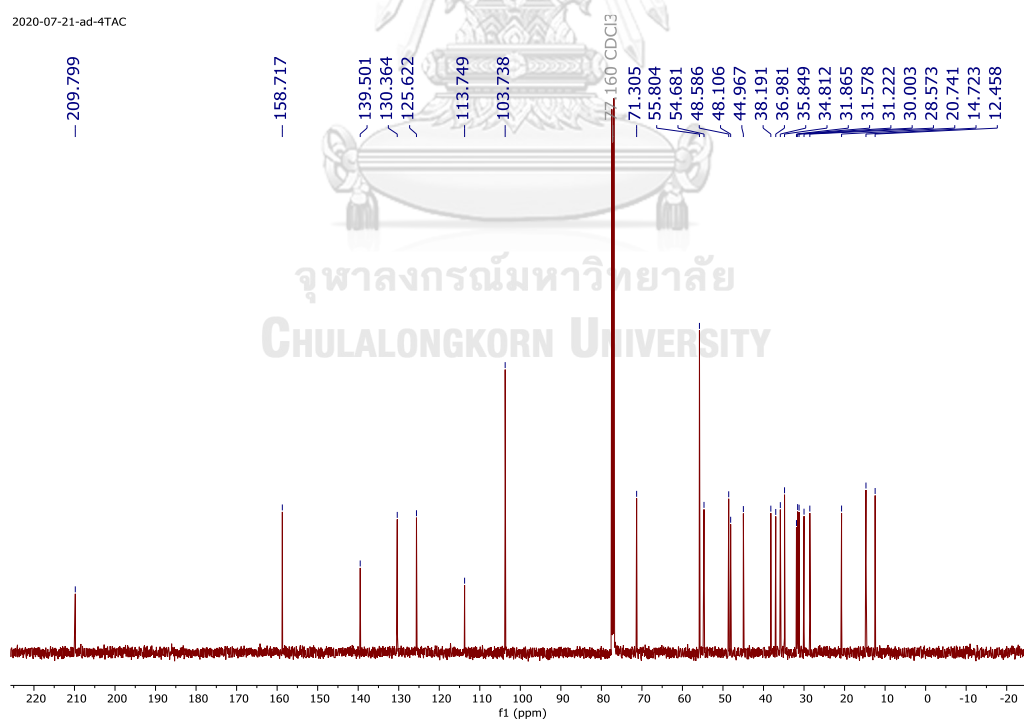
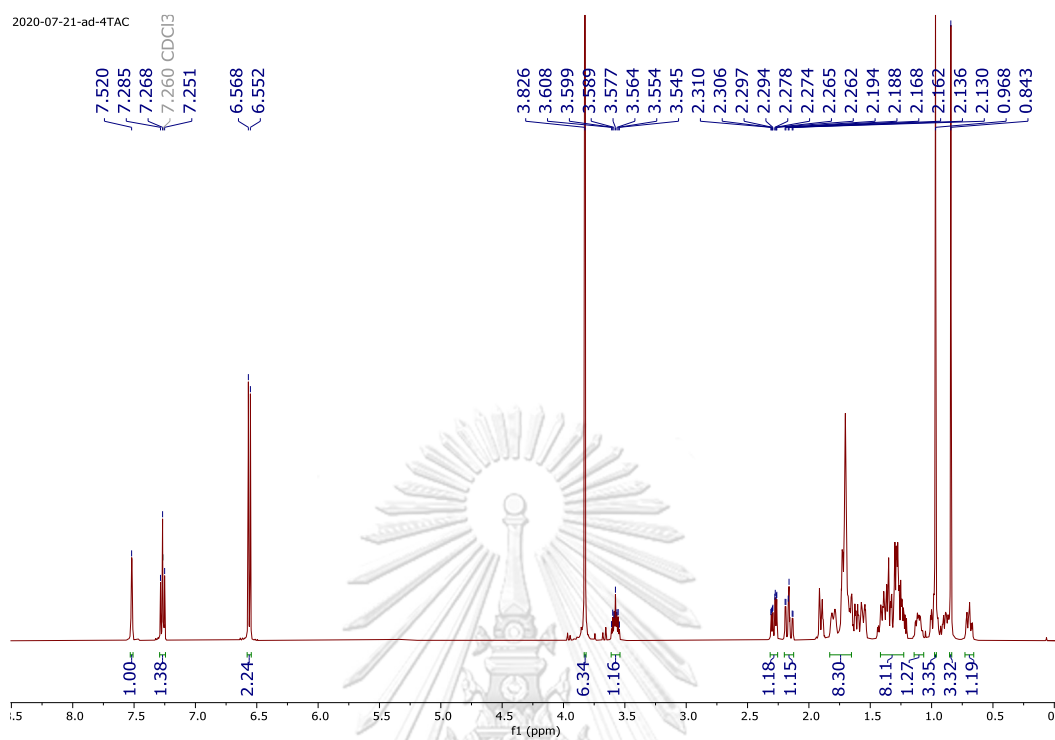
Analysis Name D:\Data\Data Service\201123\2TAC_RC5_01_4903.d
Method nv_pos_5min_profile_190214.m
Sample Name 2TAC
Comment

Acquisition Date 11/23/2020 5:27:05 PM

Operator CU.
Instrument micrOTOF-Q II



111. ^1H (500 MHz) and ^{13}C (125 MHz) NMR Spectra in CDCl_3 of **101** (new compound)



112. Mass Spectra of 101 (new compound)

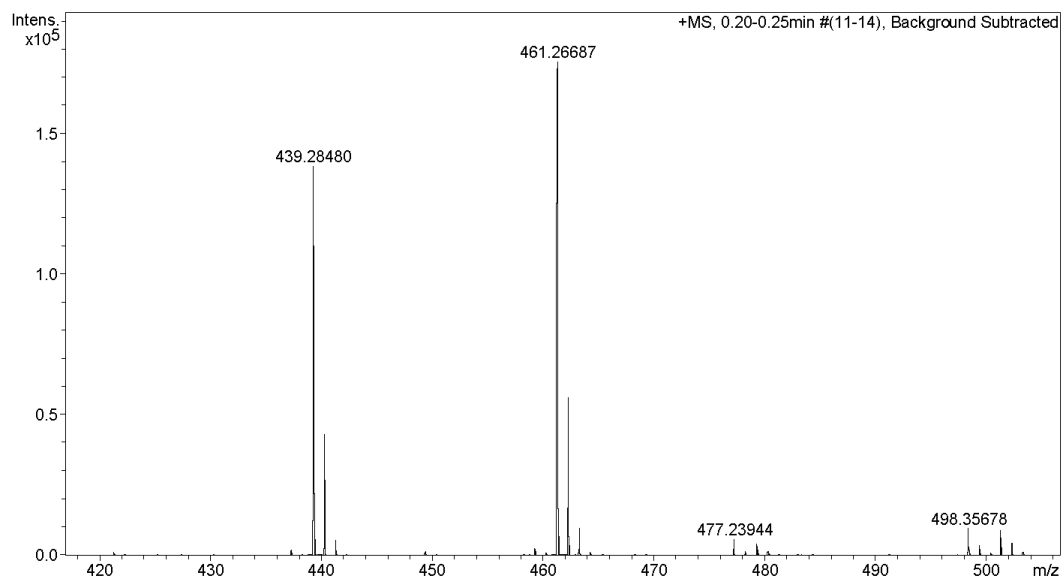
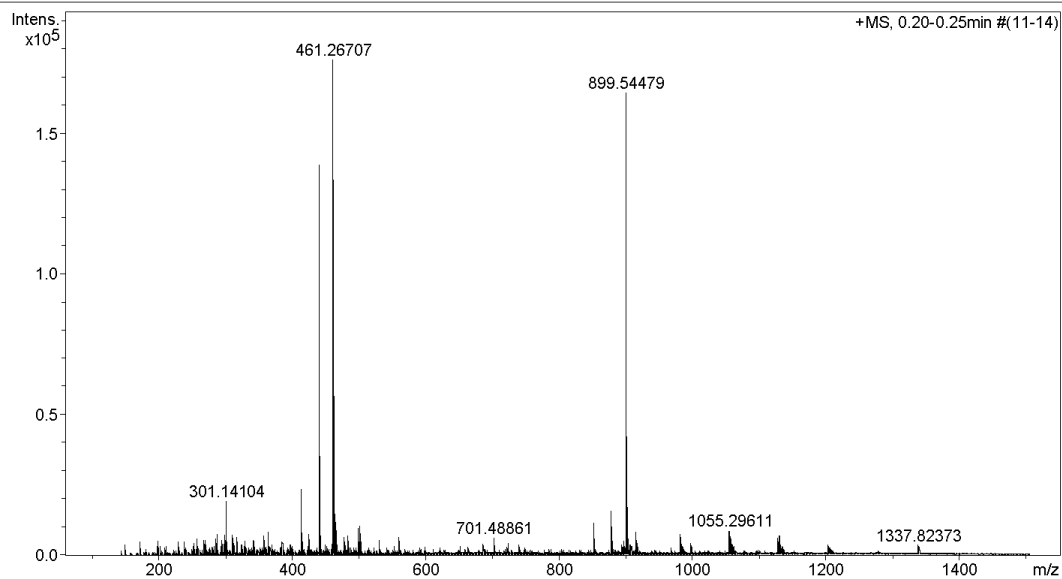
Generic Display Report

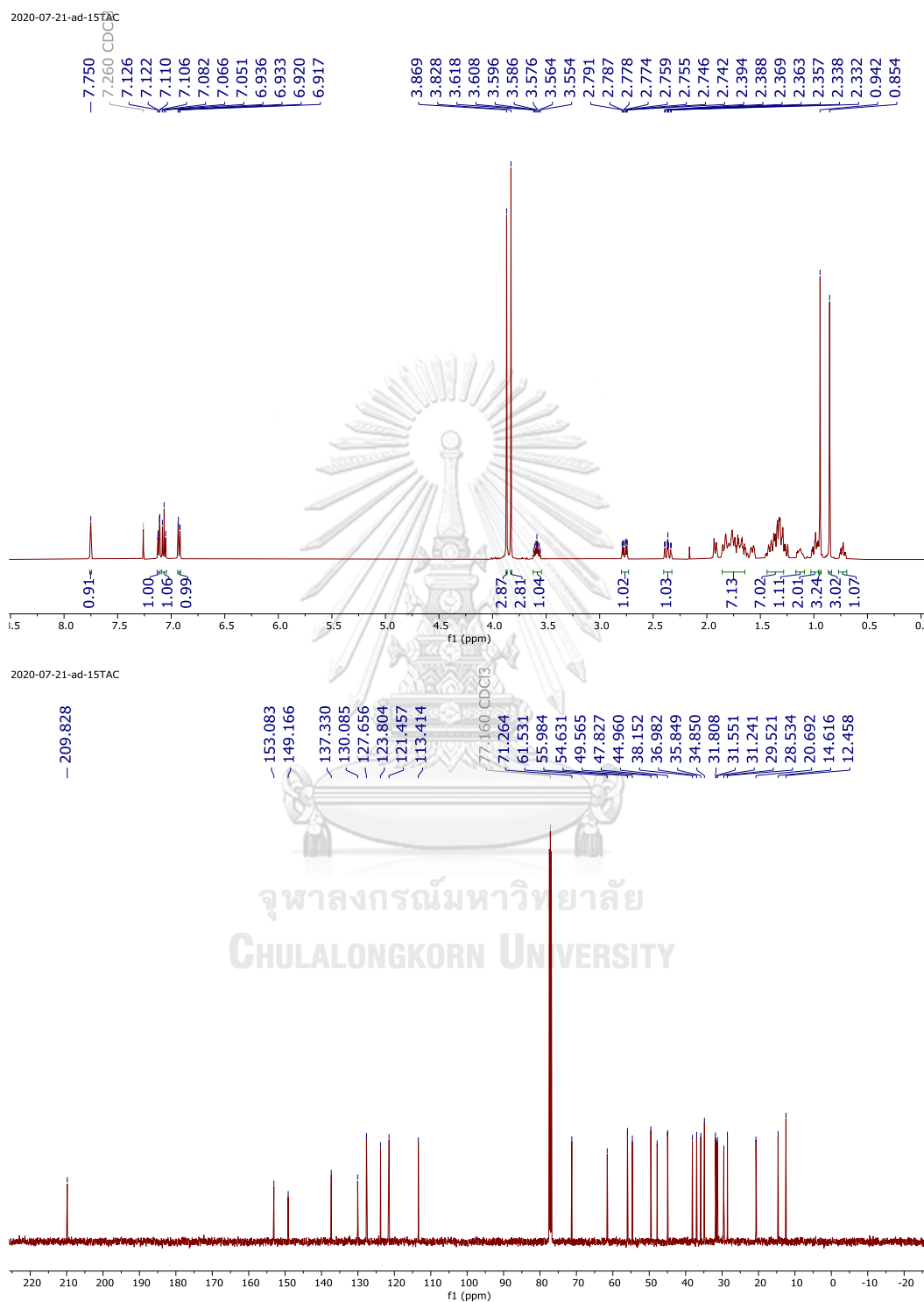
Analysis Info

Analysis Name D:\Data\Data Service\201123\4TAC_RC4_01_4902.d
Method nv_pos_5min_profile_190214.m
Sample Name 4TAC
Comment

Acquisition Date 11/23/2020 5:20:41 PM

Operator CU.
Instrument micrOTOF-Q II



113. ^1H (500 MHz) and ^{13}C (125 MHz) NMR Spectra in CDCl_3 of **102** (new compound)

114. Mass Spectra of 102 (new compound)

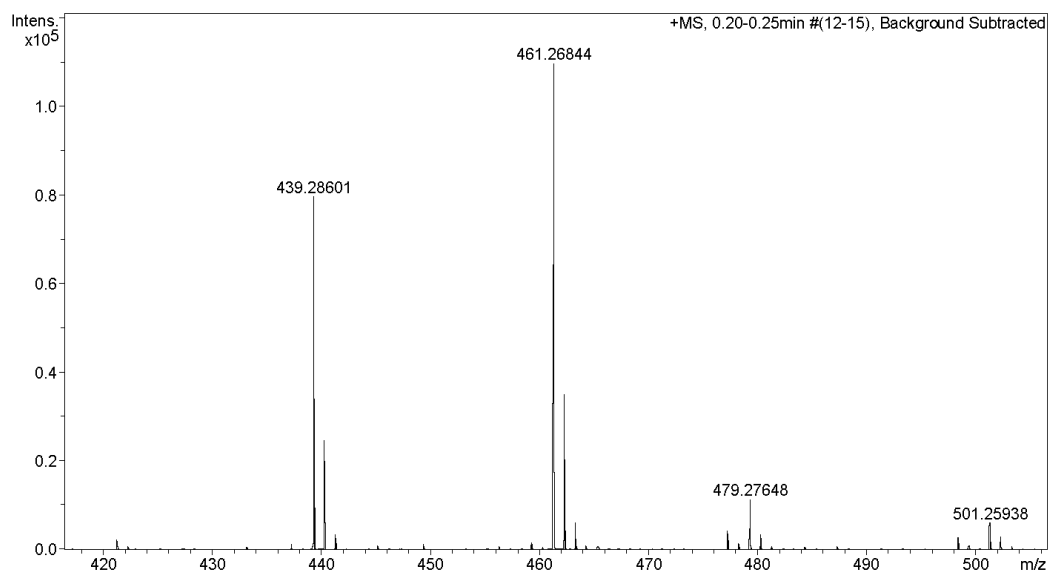
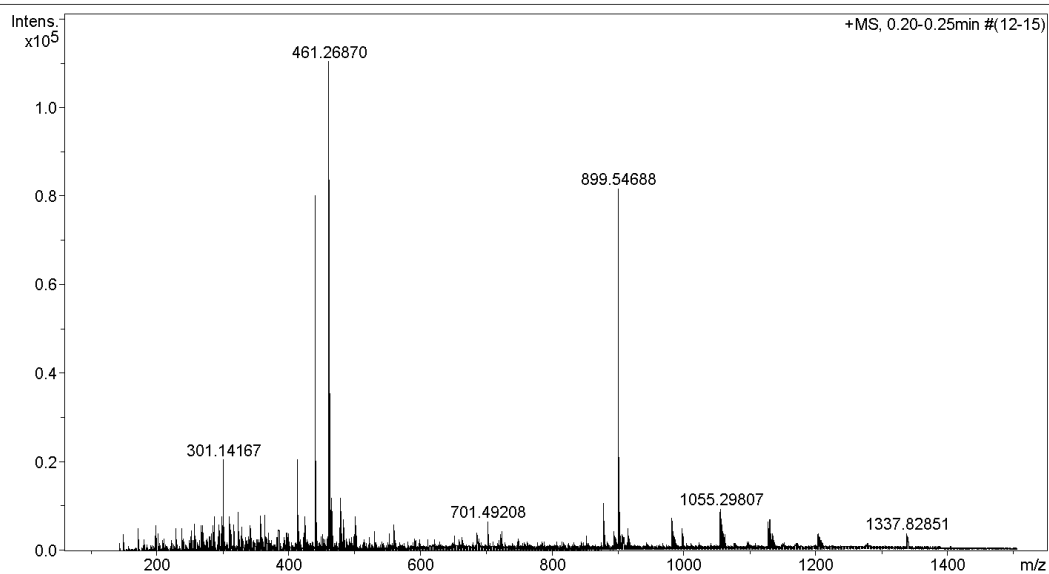
Generic Display Report

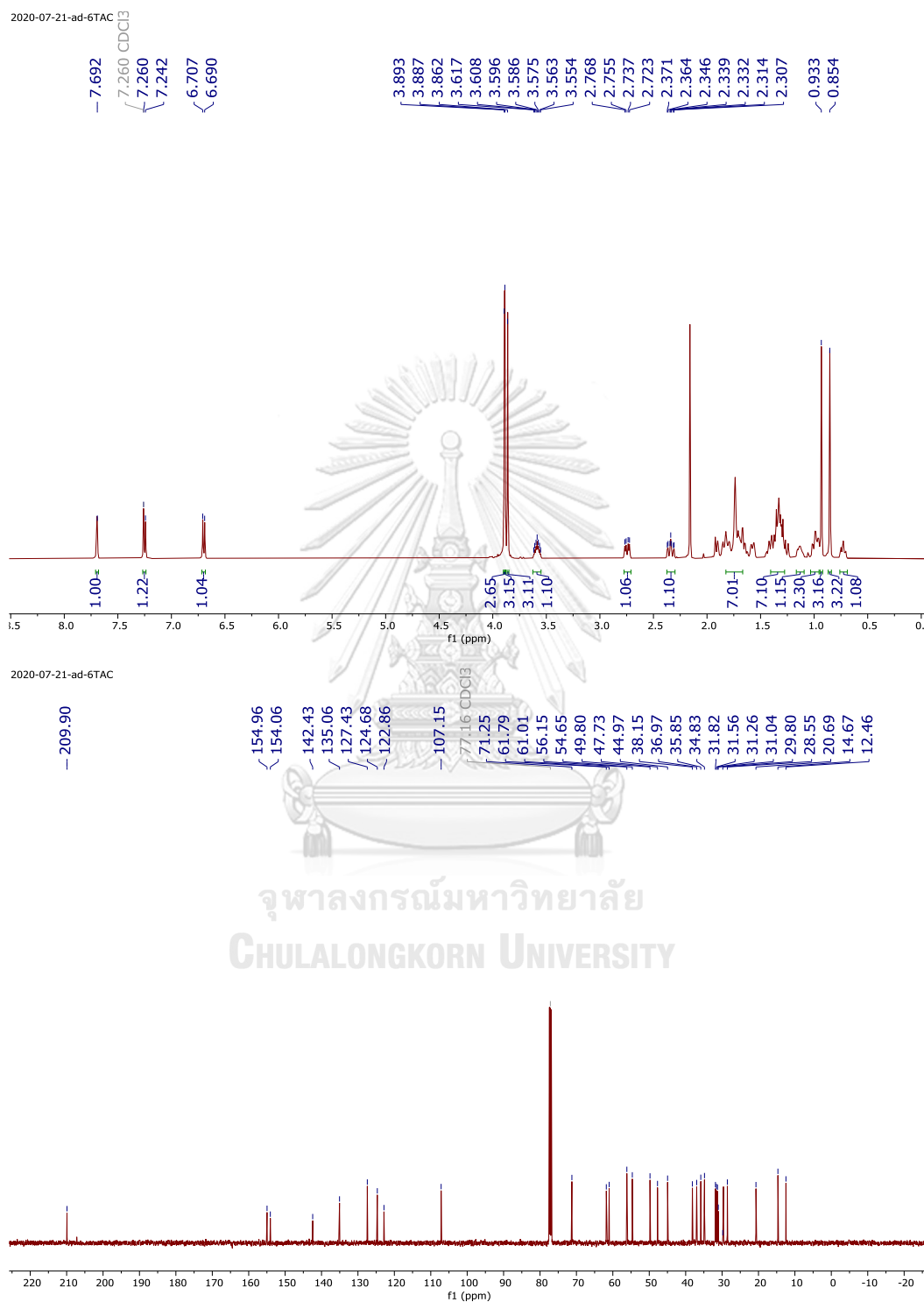
Analysis Info

Analysis Name D:\Data\Data Service\201123\15TAC_RC3_01_4901.d
Method nv_pos_5min_profile_190214.m
Sample Name 15TAC
Comment

Acquisition Date 11/23/2020 5:14:16 PM

Operator CU.
Instrument micrOTOF-Q II



115. ^1H (500 MHz) and ^{13}C (125 MHz) NMR Spectra in CDCl_3 of **103** (new compound)

116. Mass Spectra of 103 (new compound)

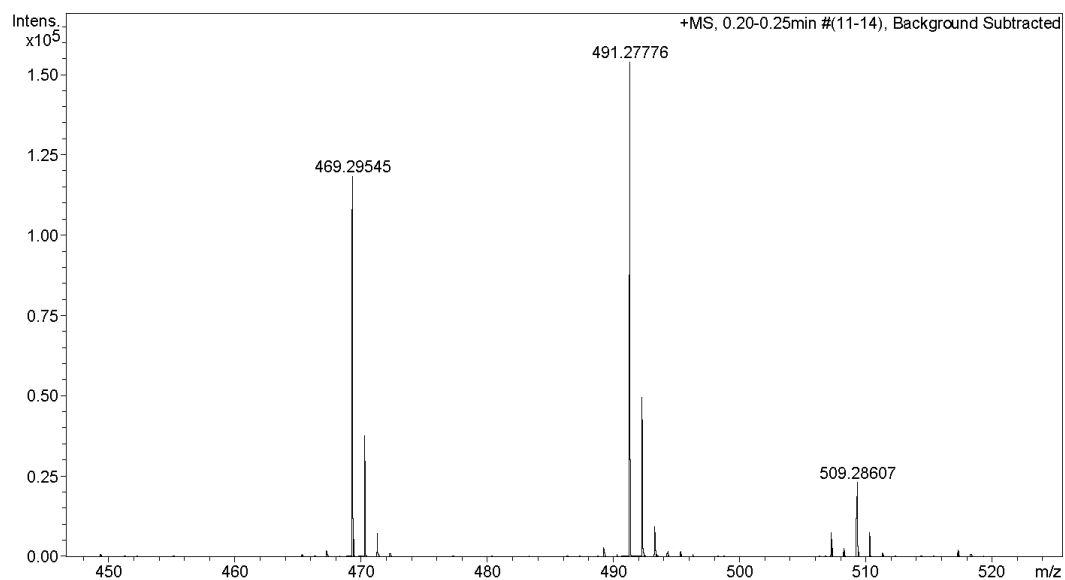
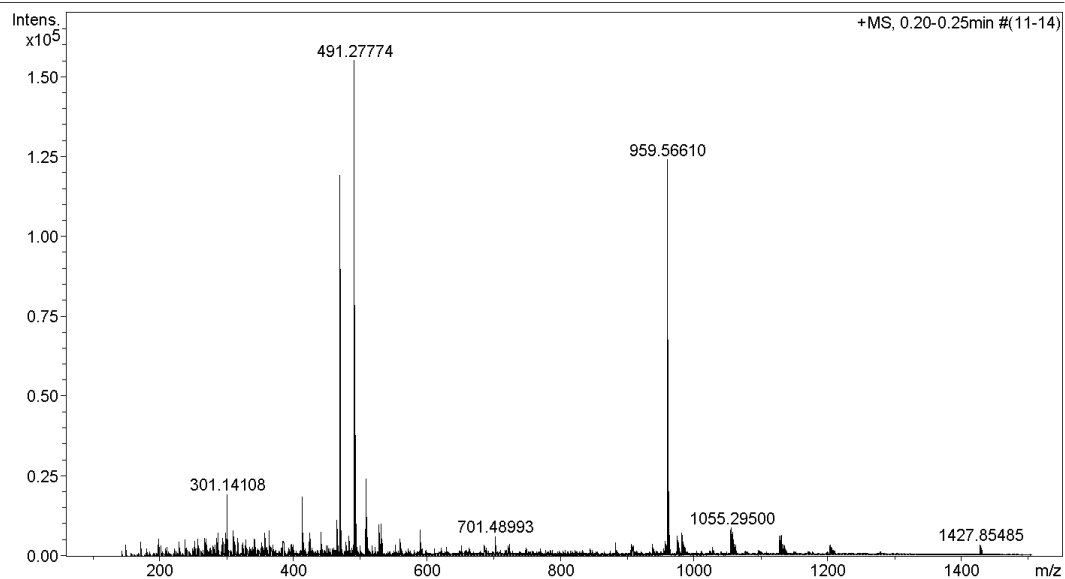
Generic Display Report

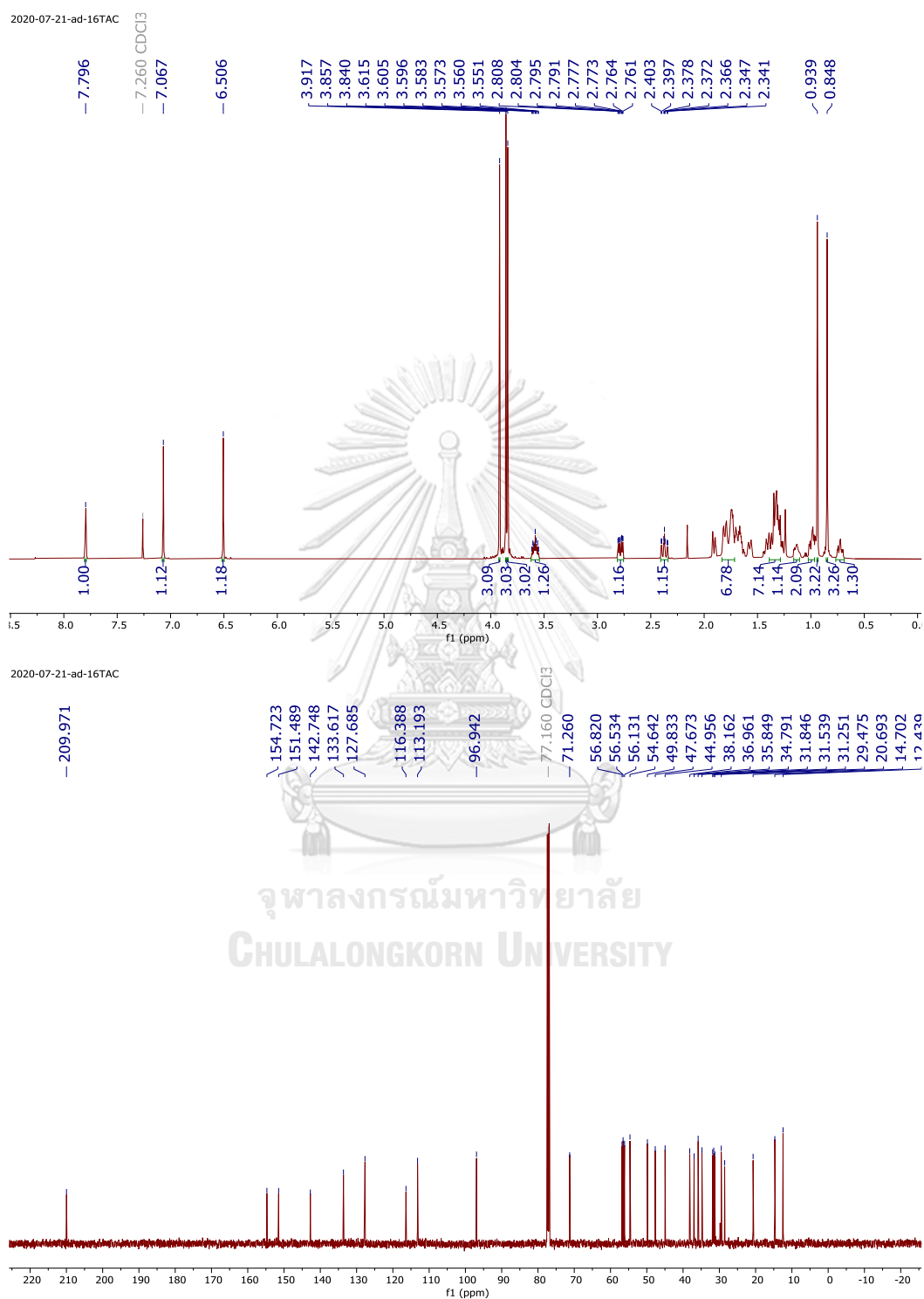
Analysis Info

Analysis Name D:\Data\Data Service\201123\6TAC_RC2_01_4900.d
Method nv_pos_5min_profile_190214.m
Sample Name 6TAC
Comment

Acquisition Date 11/23/2020 5:07:52 PM

Operator CU.
Instrument micrOTOF-Q II



117. ^1H (500 MHz) and ^{13}C (125 MHz) NMR Spectra in CDCl_3 of **104** (new compound)

118. Mass Spectra of 104 (new compound)

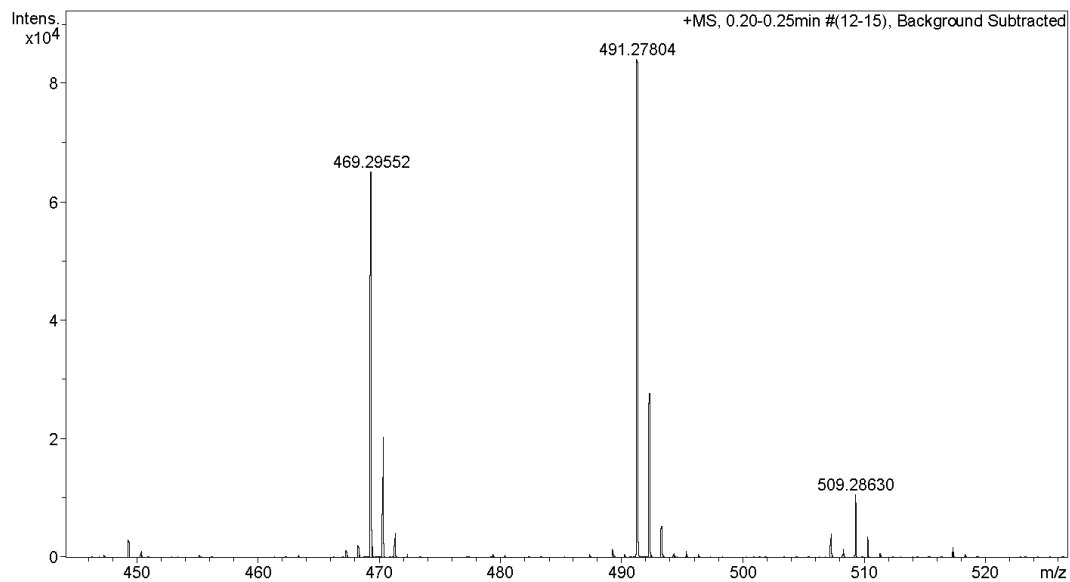
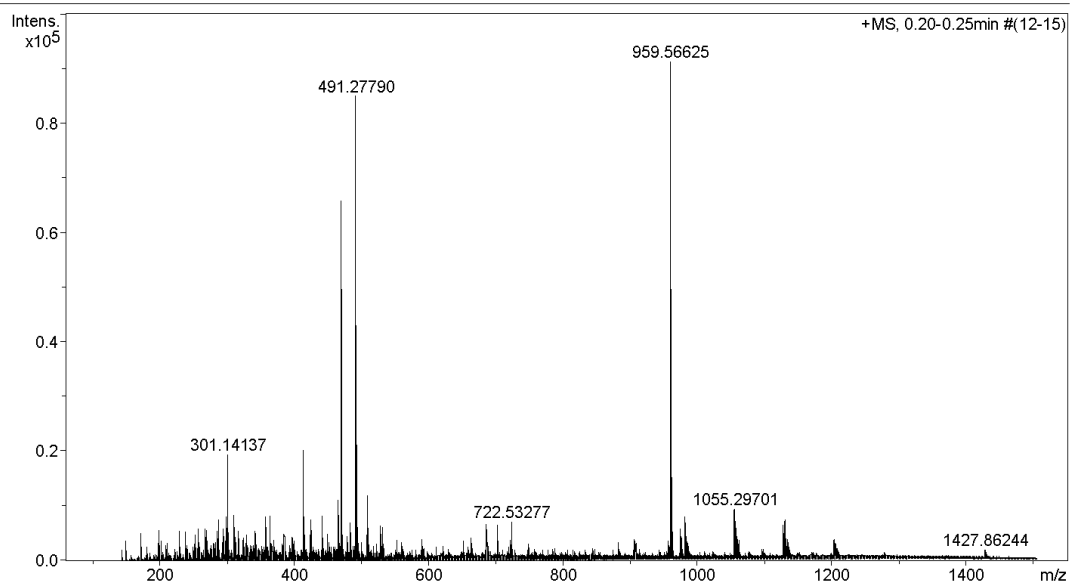
Generic Display Report

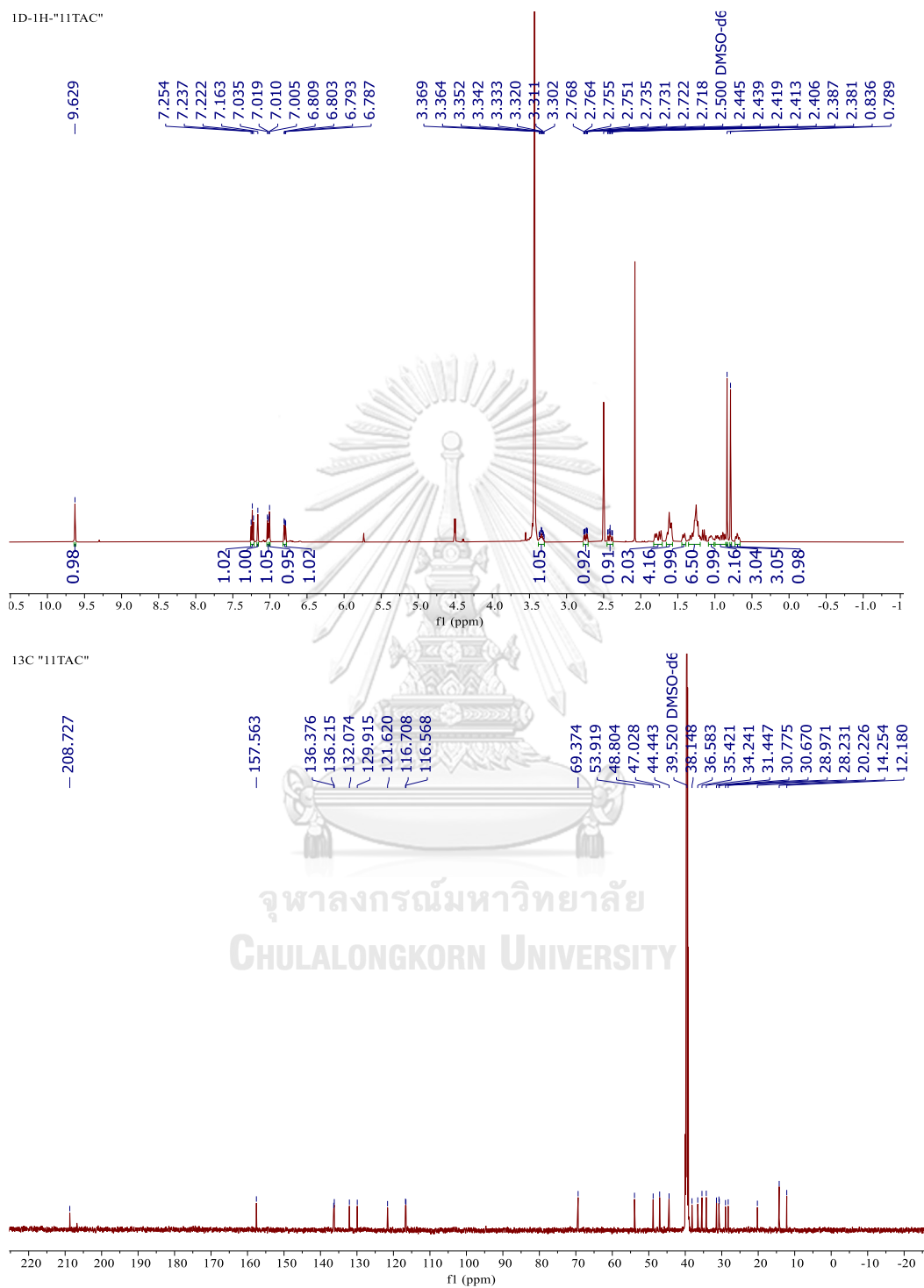
Analysis Info

Analysis Name D:\Data\Data Service\201123\16TAC_RC1_01_4899.d
Method nv_pos_5min_profile_190214.m
Sample Name 16TAC
Comment

Acquisition Date 11/23/2020 5:01:26 PM

Operator CU.
Instrument micrOTOF-Q II



119. ^1H (500 MHz) and ^{13}C (125 MHz) NMR Spectra in $\text{DMSO-}d_6$ of **105** (new compound)

120. Mass Spectra of 105 (new compound)

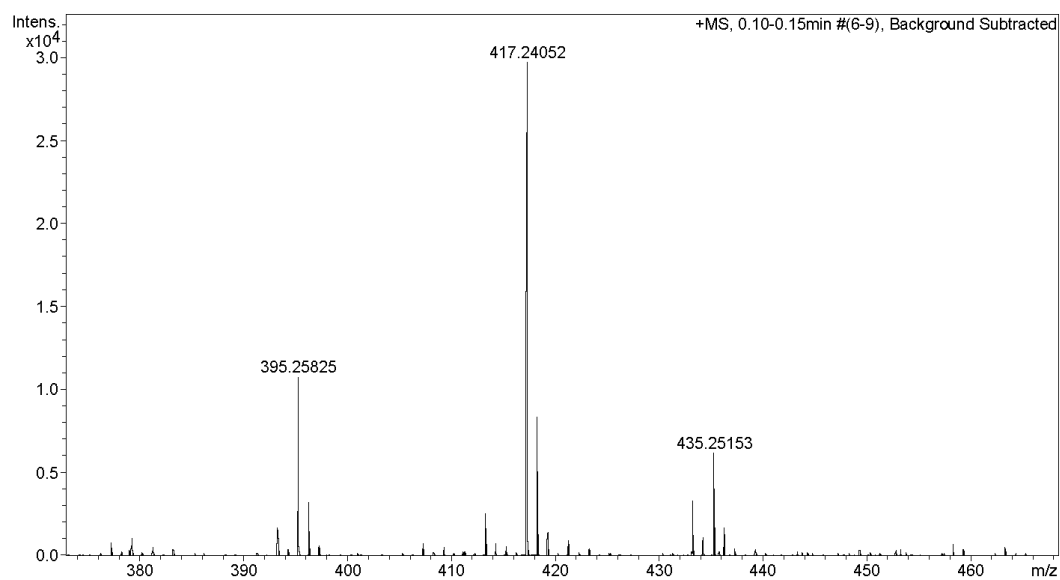
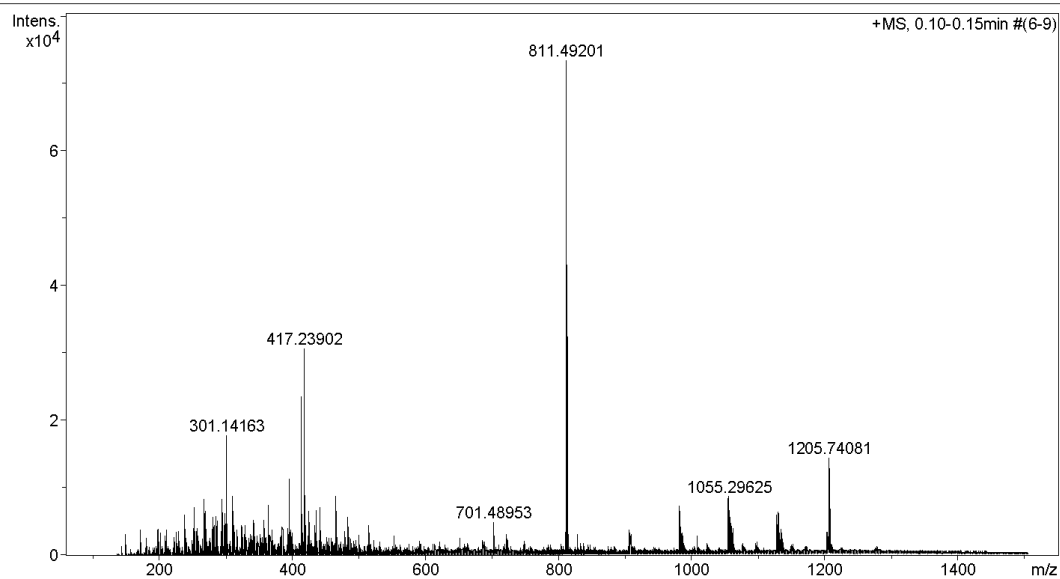
Generic Display Report

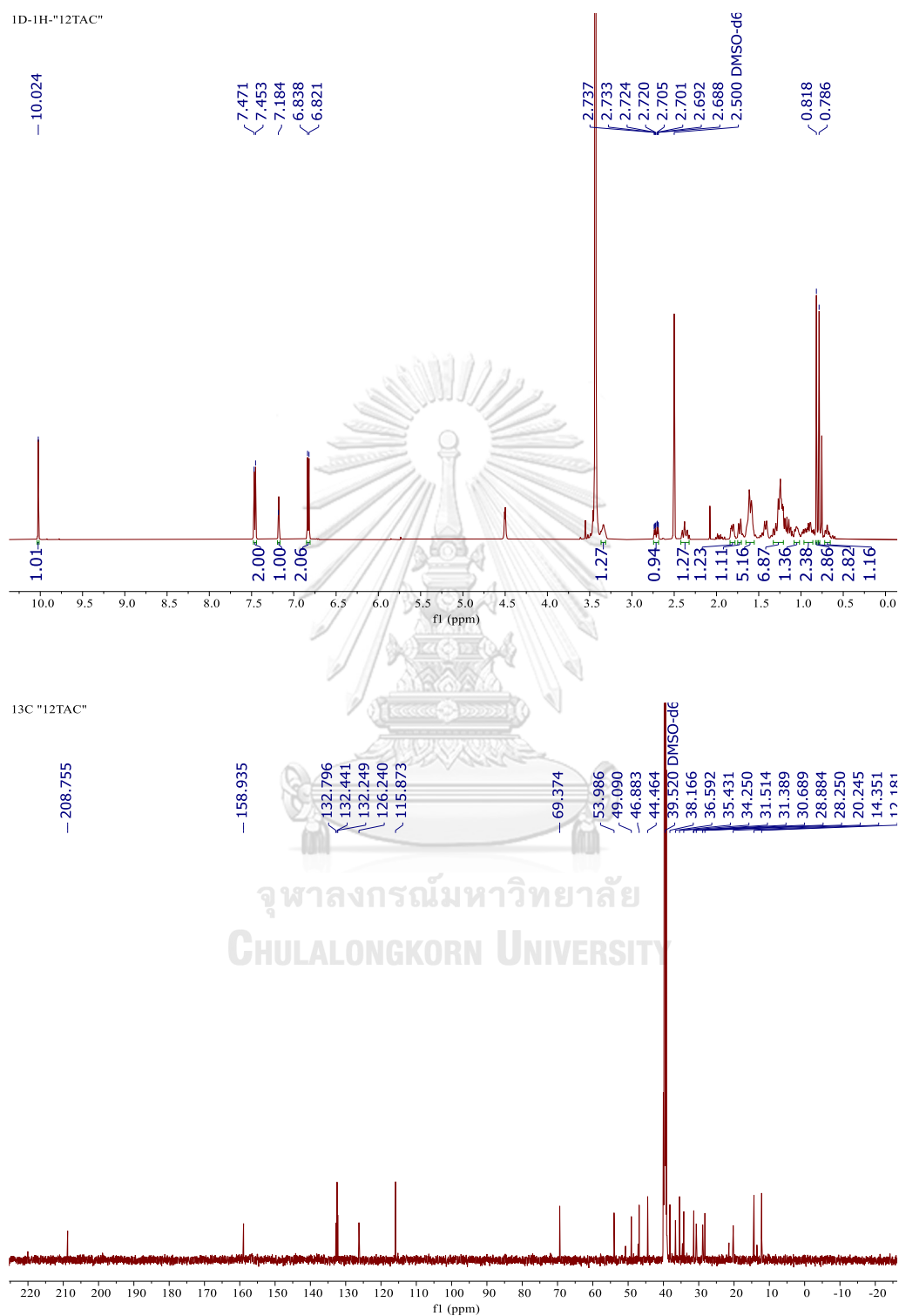
Analysis Info

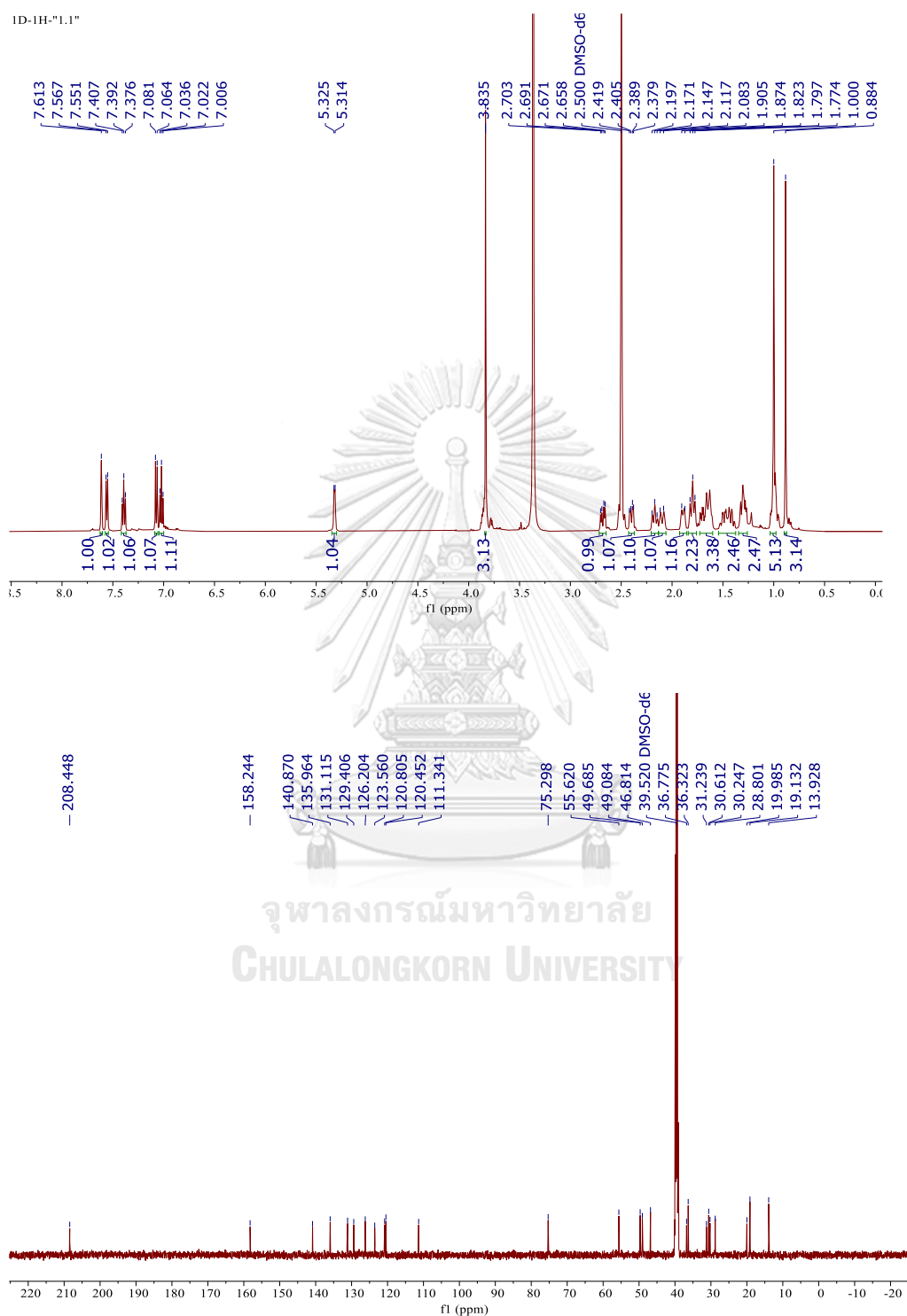
Analysis Name D:\Data\Data Service\201123\11TAC_RB8_01_4907.d
Method nv_pos_5min_profile_190214.m
Sample Name 11TAC
Comment

Acquisition Date 11/23/2020 5:52:34 PM

Operator CU.
Instrument micrOTOF-Q II



121. ^1H (500 MHz) and ^{13}C (125 MHz) NMR Spectra in $\text{DMSO-}d_6$ of **106**

122. ^1H (500 MHz) and ^{13}C (125 MHz) NMR Spectra in $\text{DMSO-}d_6$ of **107** (new compound)

123. Mass Spectra of 107 (new compound)

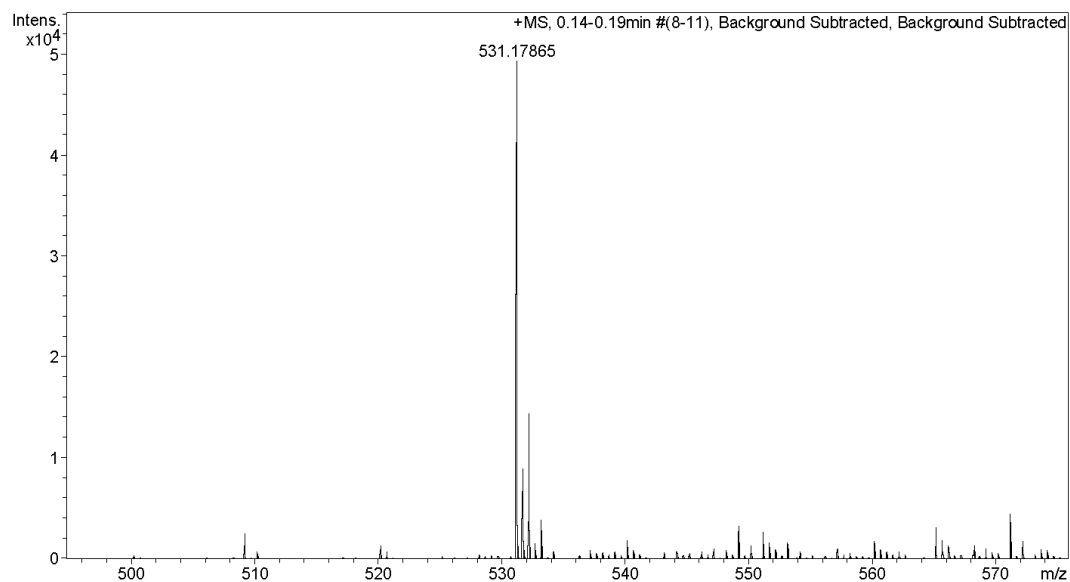
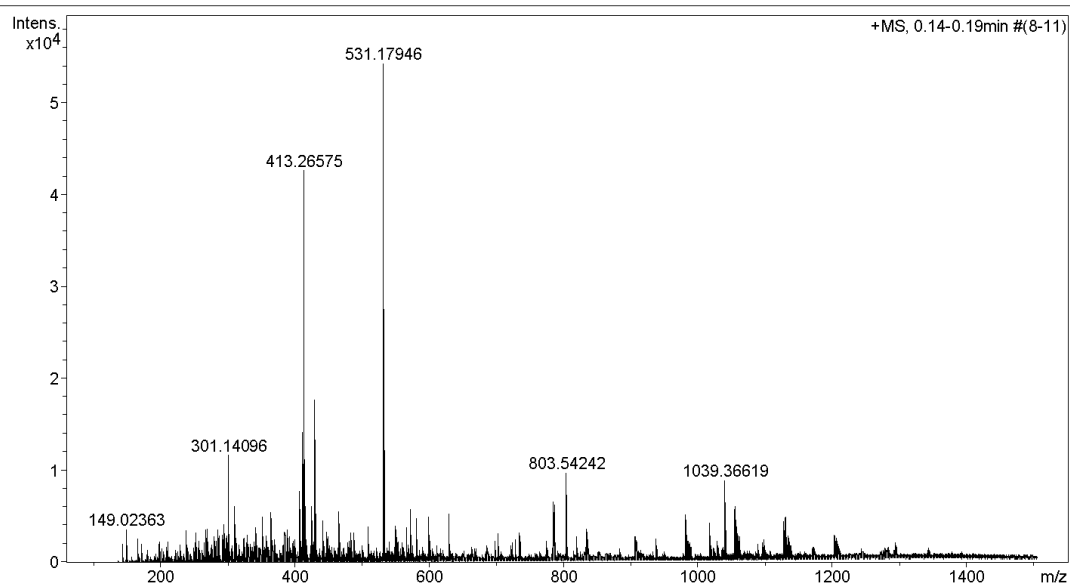
Generic Display Report

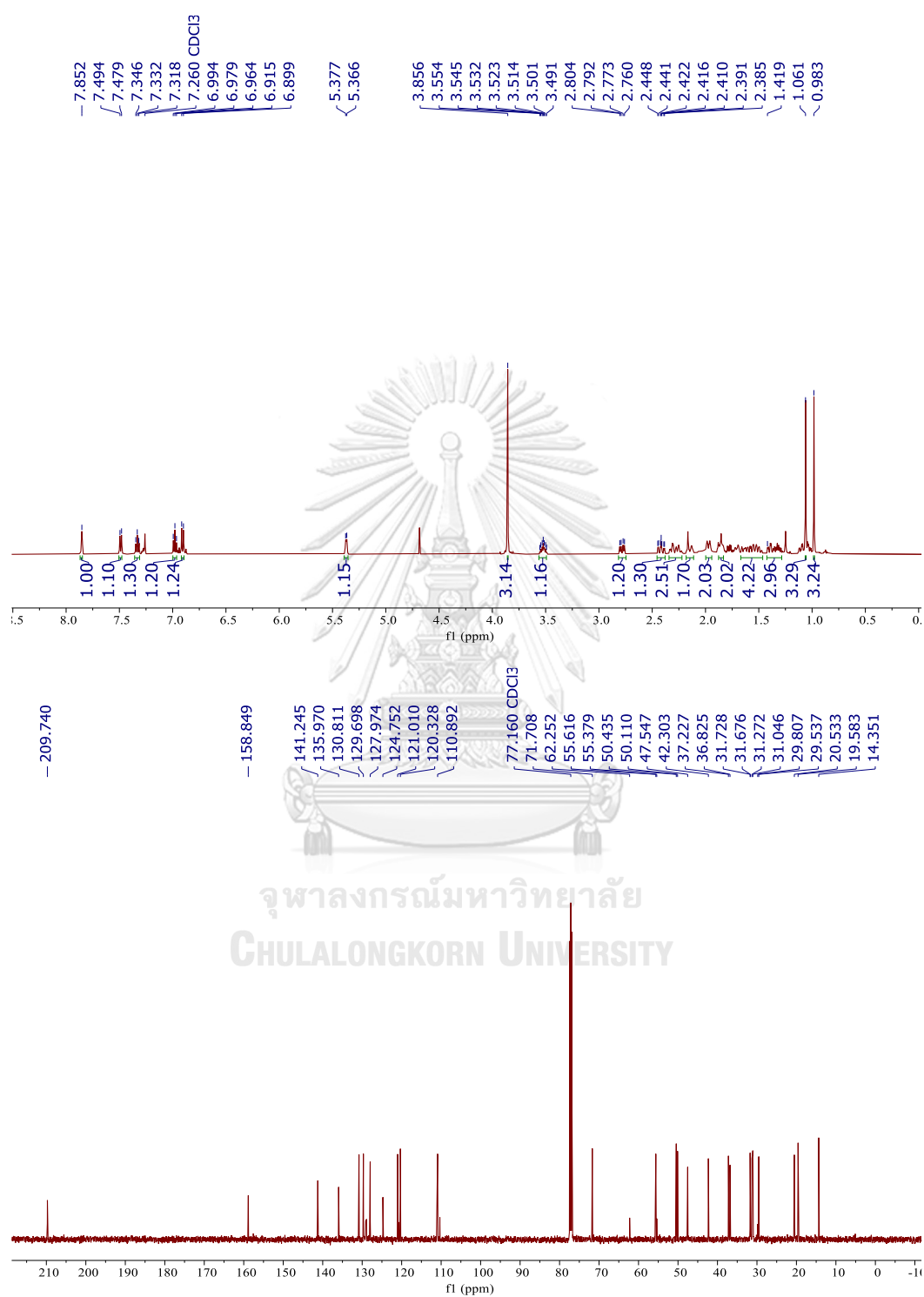
Analysis Info

Analysis Name D:\Data\Data Service\201123\1.1_RB7_01_4906.d
Method nv_pos_5min_profile_190214.m
Sample Name 1.1
Comment

Acquisition Date 11/23/2020 5:46:16 PM

Operator CU.
Instrument micrOTOF-Q II



124. ^1H (500 MHz) and ^{13}C (125 MHz) NMR Spectra in CDCl_3 of **108** (new compound)

125. Mass Spectra of 108 (new compound)

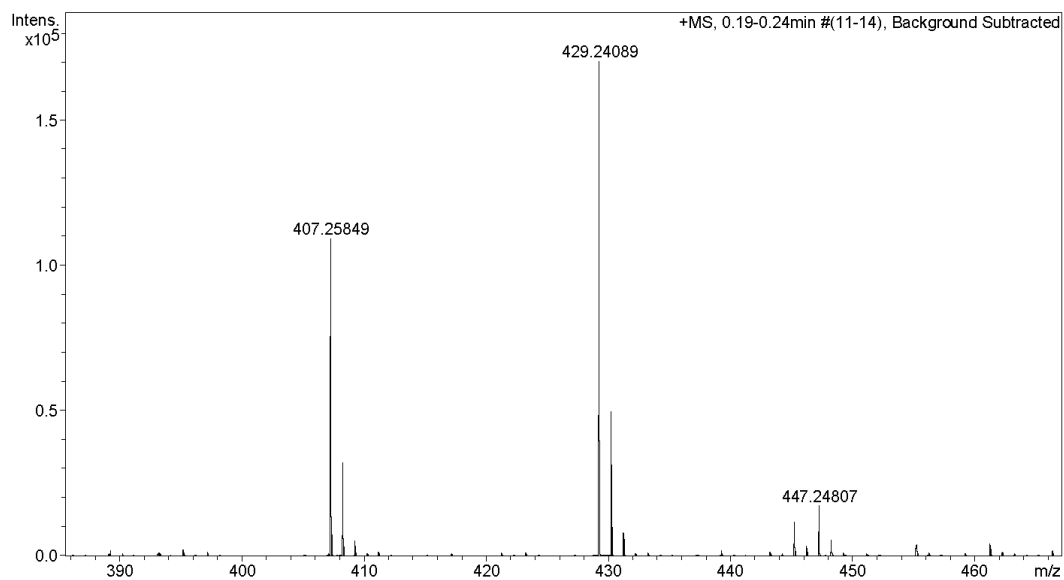
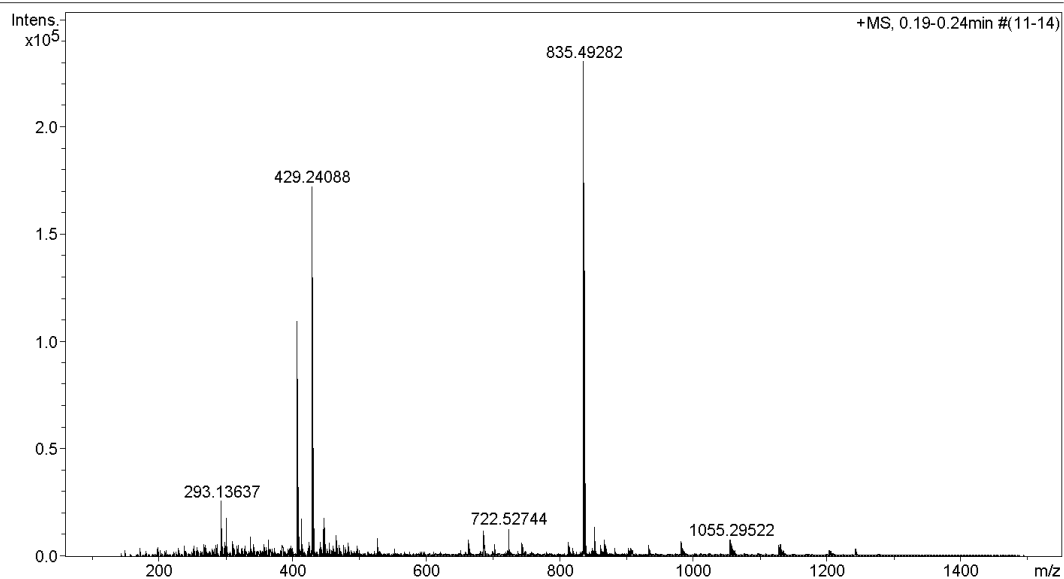
Generic Display Report

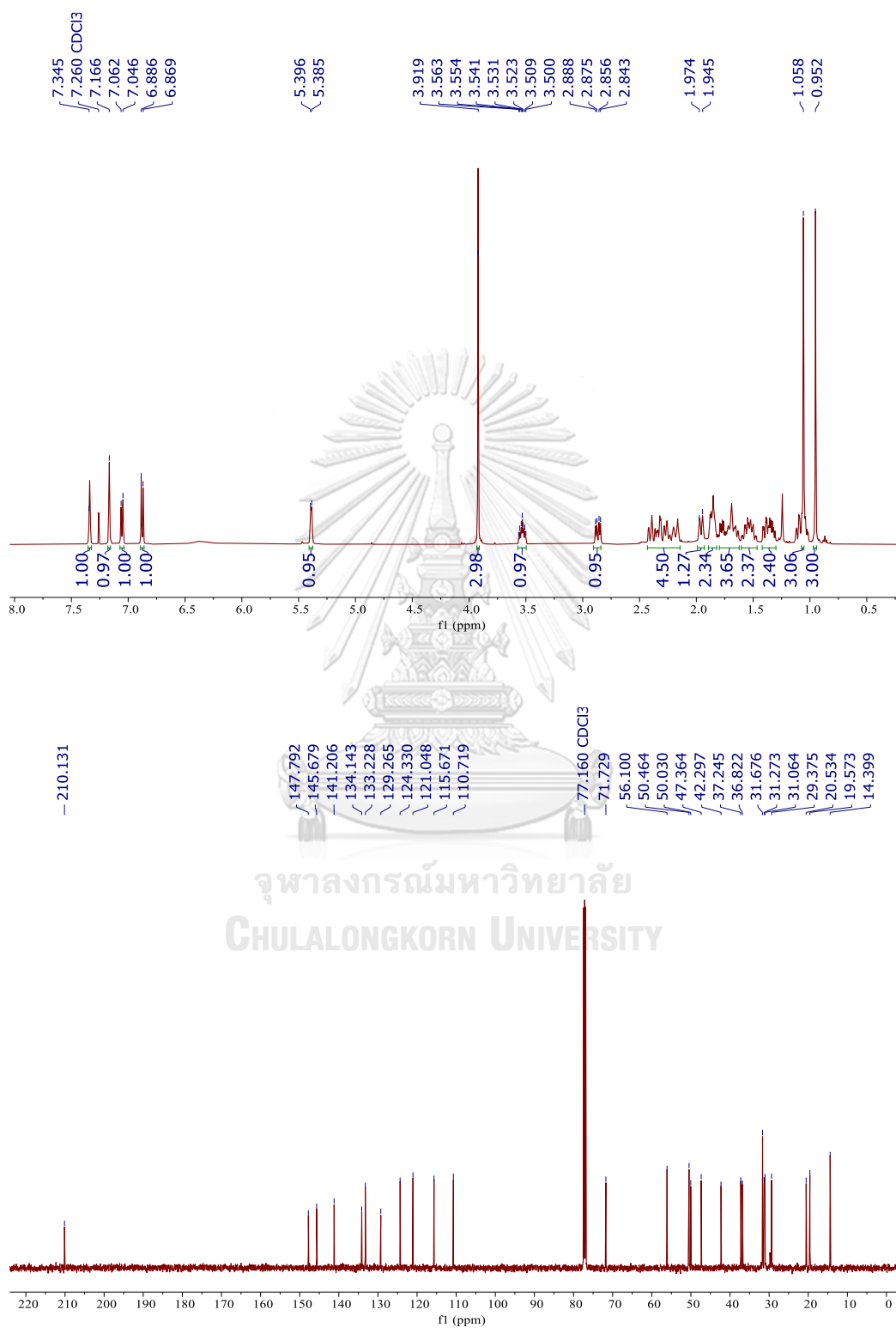
Analysis Info

Analysis Name D:\Data\Data Service\201123\2.1_RB6_01_4896.d
Method nv_pos_5min_profile_190214.m
Sample Name 2.1
Comment

Acquisition Date 11/23/2020 4:42:13 PM

Operator CU.
Instrument micrOTOF-Q II



126. ^1H (500 MHz) and ^{13}C (125 MHz) NMR Spectra in CDCl_3 of **109** (new compound)

127. Mass Spectra of 109 (new compound)

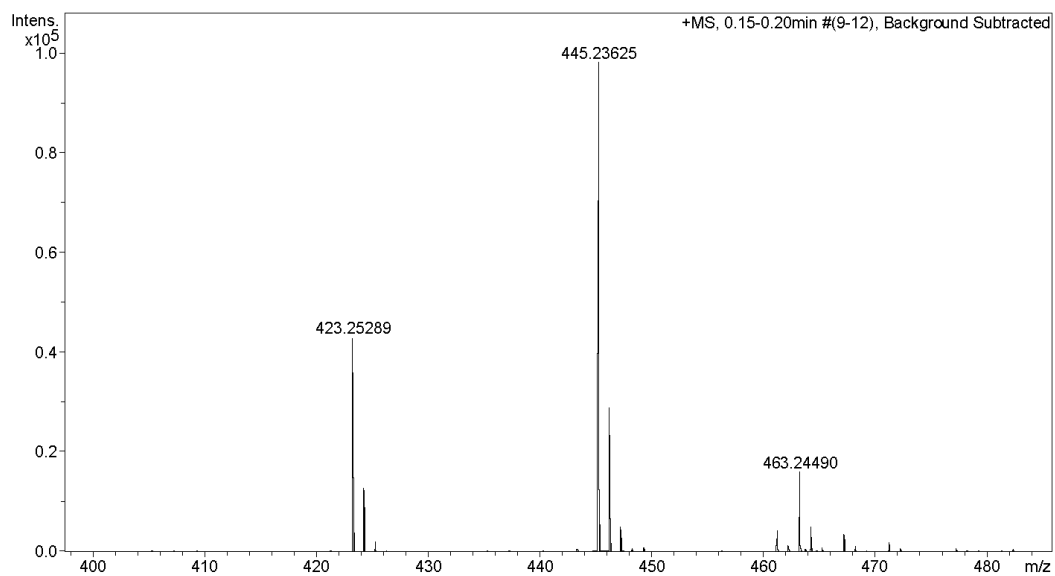
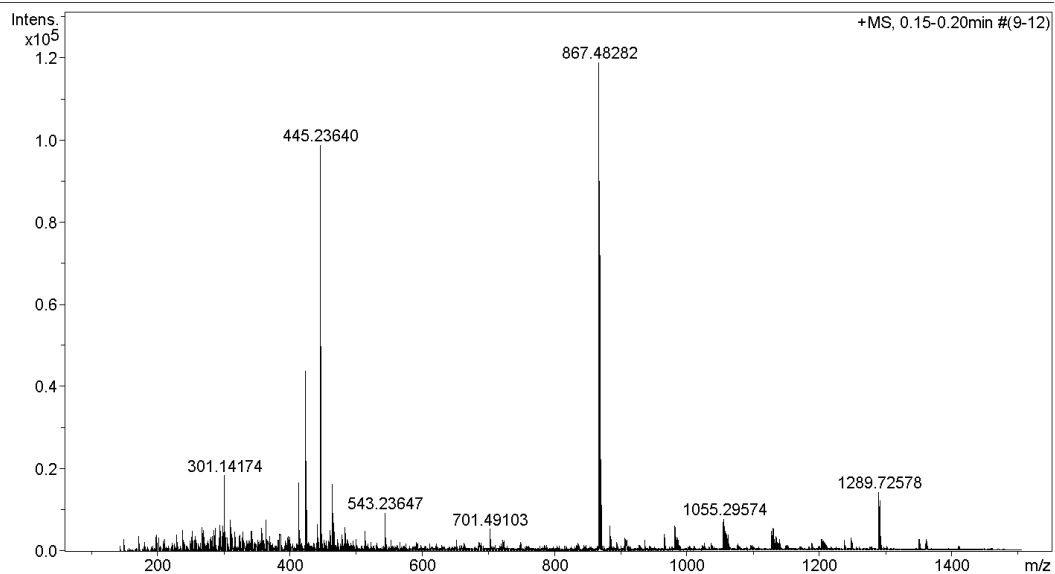
Generic Display Report

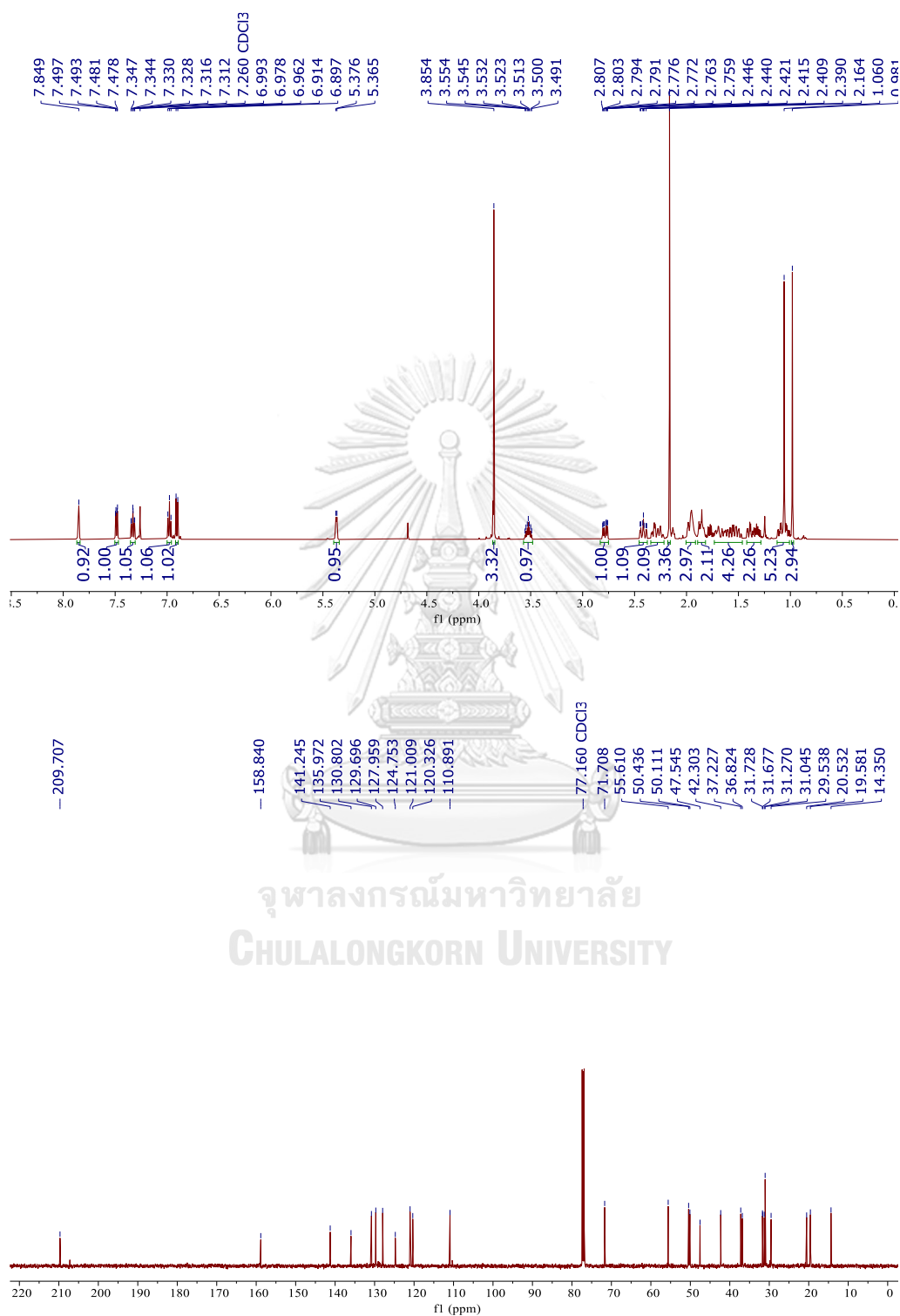
Analysis Info

Analysis Name D:\Data\Data Service\201123\2.2_RB5_01_4895.d
Method nv_pos_5min_profile_190214.m
Sample Name 2.2
Comment

Acquisition Date 11/23/2020 4:35:48 PM

Operator CU.
Instrument micrOTOF-Q II



128. ^1H (500 MHz) and ^{13}C (125 MHz) NMR Spectra in CDCl_3 of **110** (new compound)

129. Mass Spectra of 110 (new compound)

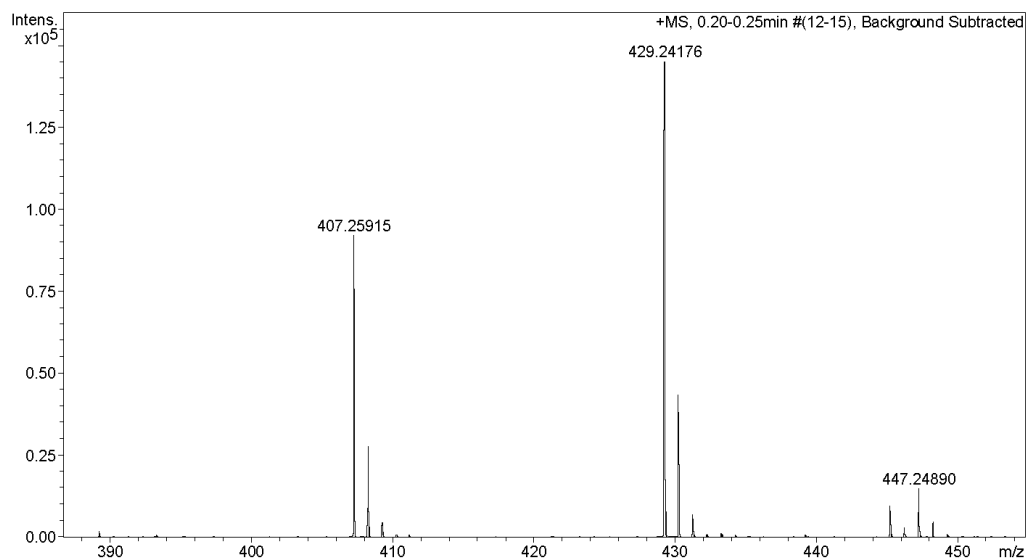
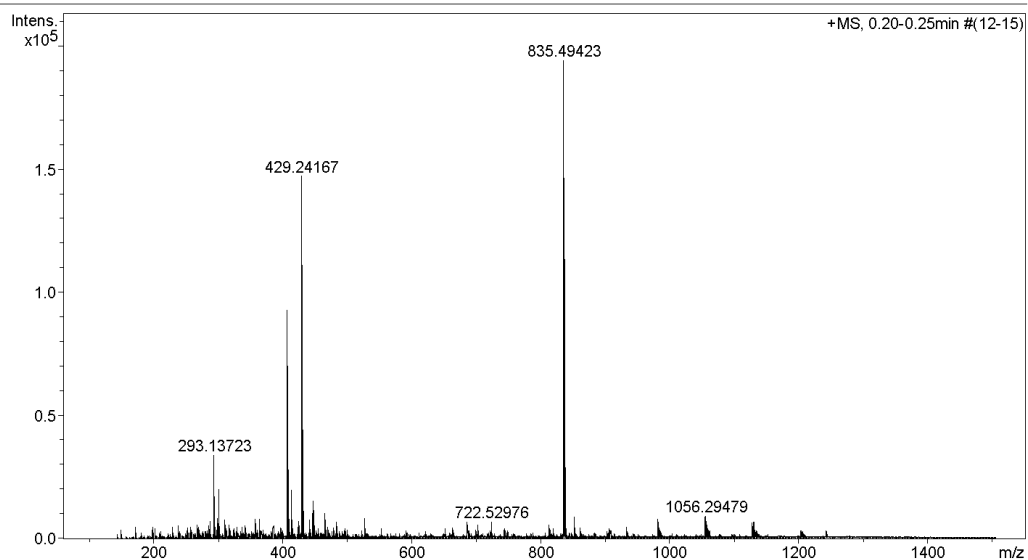
Generic Display Report

Analysis Info

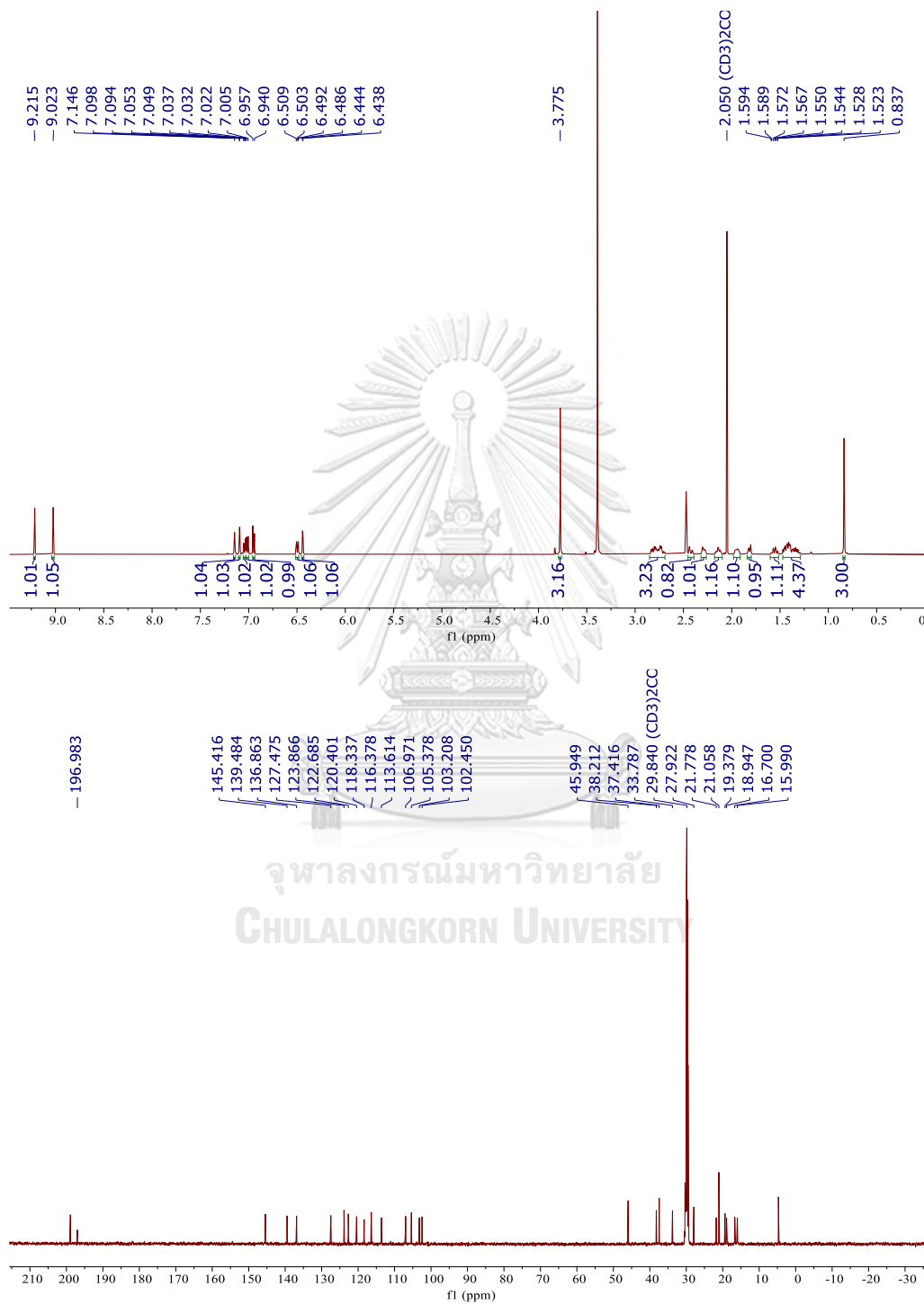
Analysis Name D:\Data\Data Service\201123\4.1_RB4_01_4894.d
Method nv_pos_5min_profile_190214.m
Sample Name 4.1
Comment

Acquisition Date 11/23/2020 4:29:24 PM

Operator CU.
Instrument micrOTOF-Q II



130. ^1H (500 MHz) and ^{13}C (125 MHz) NMR Spectra in acetone- d_6 of **111** (new compound)



131. Mass Spectra of 111 (new compound)

Generic Display Report

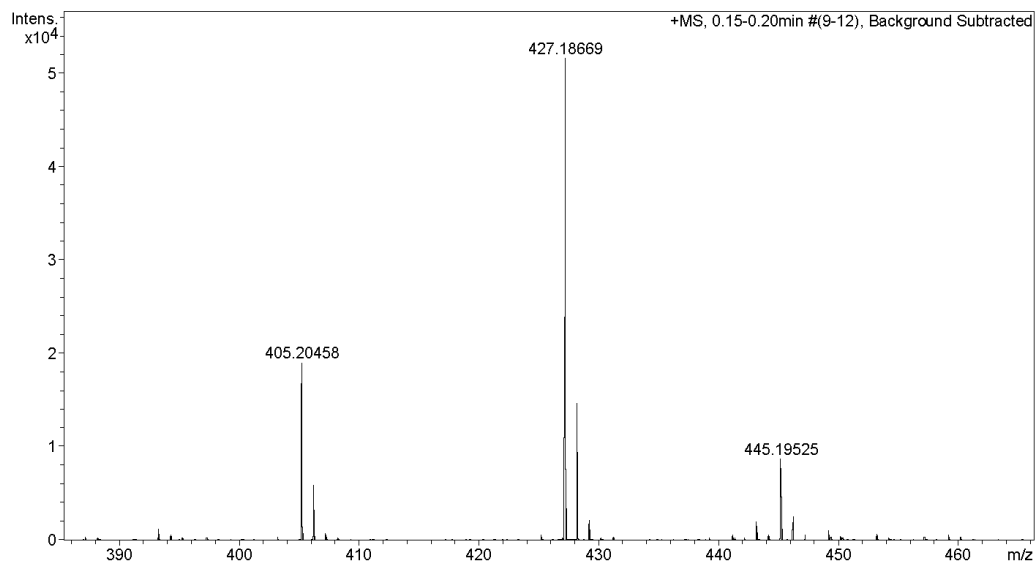
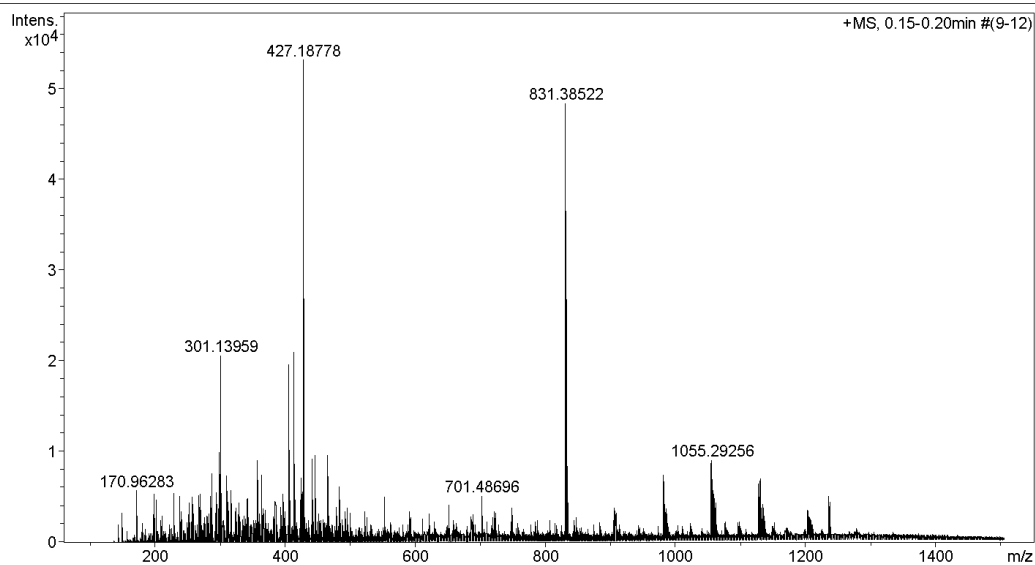
Analysis Info

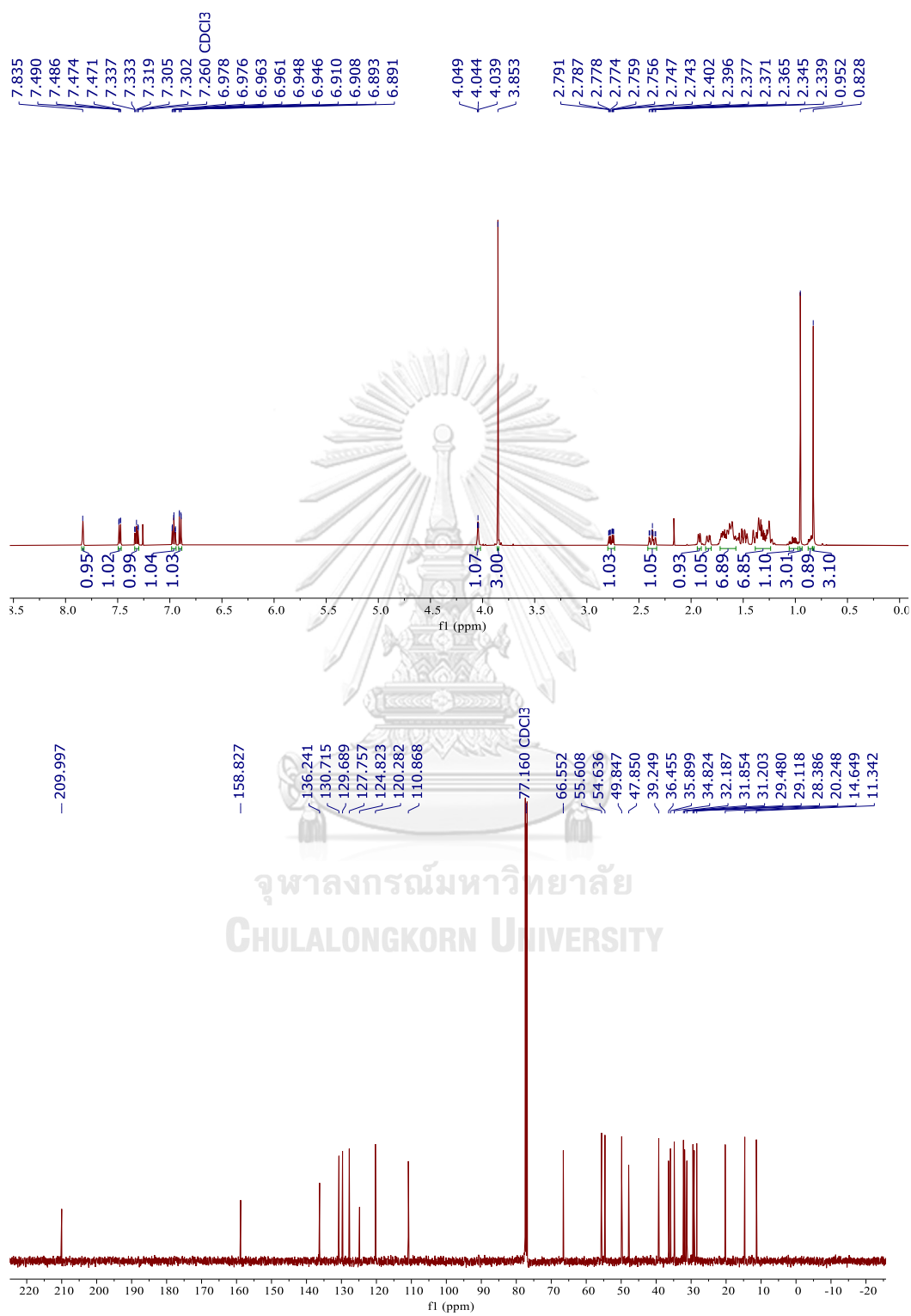
Analysis Name D:\Data\Data Service\201123\4AEC_RB1_01_4891.d
Method nv_pos_5min_profile_190214.m
Sample Name 4AEC
Comment

Acquisition Date 11/23/2020 4:10:11 PM

Operator CU.

Instrument micrOTOF-Q II



132. ^1H (500 MHz) and ^{13}C (125 MHz) NMR Spectra in CDCl_3 of **112** (new compound)

133. Mass Spectra of 112 (new compound)

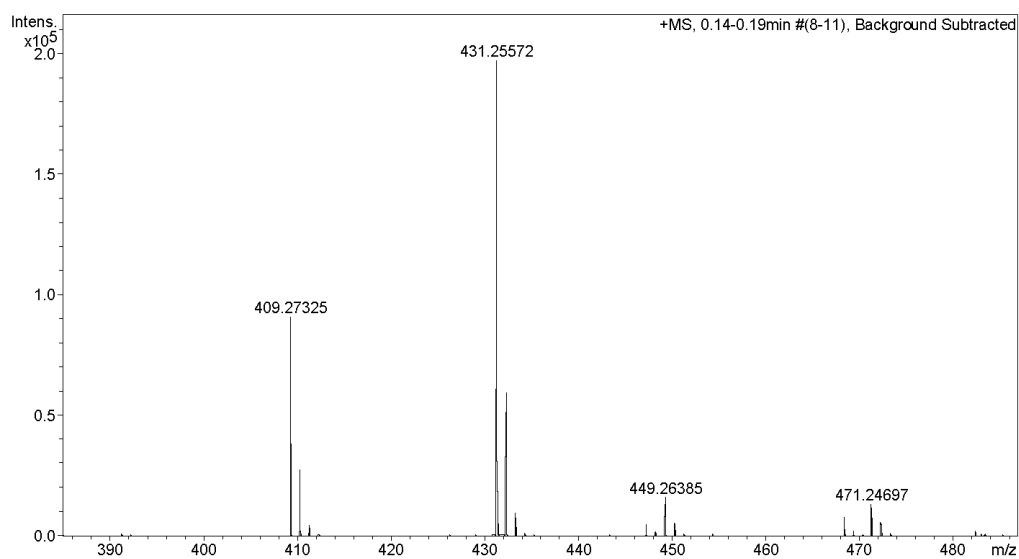
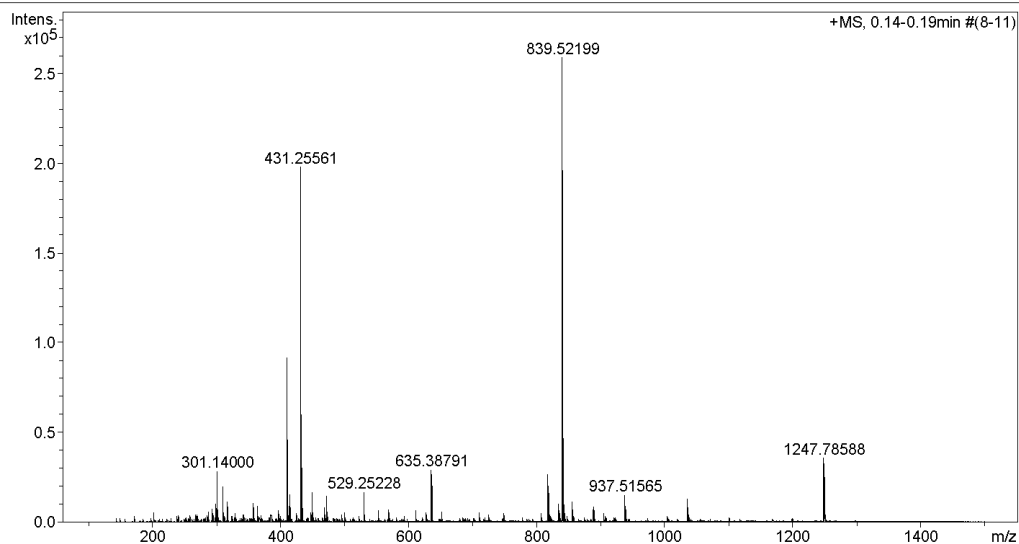
Generic Display Report

Analysis Info

Analysis Name D:\Data\Data Service\201221\5.1 andro-c_RA5_01_5076.d
Method nv_pos_5min_profile_190214.m
Sample Name 5.1 andro-c
Comment

Acquisition Date 12/21/2020 2:02:05 PM

Operator CU.
Instrument micrOTOF-Q II



VITA

NAME Ade Danova
DATE OF BIRTH 12 December 1992
PLACE OF BIRTH Majalengka, West Java, Indonesia
INSTITUTIONS ATTENDED B.Sc. in Chemistry, Faculty of Mathematics and Natural Sciences, Mulawarman University, Indonesia
M.Sc. in Chemistry, Faculty of Mathematics and Natural Sciences, Institut Teknologi Bandung, Indonesia
HOME ADDRESS Adia Street, No. 2, Pagandon (Village), Kadipaten (Sub-district), Majalengka (District), West Java (Province), Indonesia, 45452
PUBLICATION 1) Linh, N. T. T., Danova, A., Truong, T. L., Chavasiri, W., Phung, N. K. P., & Chi, H. B. L. (2020). Chemical constituents of chloroform extract from the lichen *Ramalina peruviana* Arch (Ramalinaceae). *Vietnam Journal of Chemistry*, 58(2), 231-236.
2) Sukanadi, I. P., Danova, A., & Chavasiri, W. (2021). Synthesis of Sulfonamide Chalcones as α -Glucosidase Inhibitors. *RSU International Research Conference 2021 on Science and Technology*, 6, 604-615.
3) Duong, T. H., Nguyen, H. T., Nguyen, C. H., Tran, N. M. A., Danova, A., Tran, T. M. D., Vu-Huynh, K.L., Musa, V., Jutakanoke, R., Nguyen, N.H. & Sichaem, J. (2021). Identification of Highly Potent α -Glucosidase Inhibitors from *Artocarpus integer* and Molecular Docking Studies. *Chemistry & biodiversity*, e2100499.